nutrients

Special Issue Reprint

Effects of Plant Extracts on Human Health

2nd Edition

Edited by
Fátima Regina Mena Barreto Silva and Diana Marcela Aragon Novoa

mdpi.com/journal/nutrients

MDPI

Effects of Plant Extracts on Human Health—2nd Edition

Effects of Plant Extracts on Human Health—2nd Edition

Guest Editors

Fátima Regina Mena Barreto Silva
Diana Marcela Aragon Novoa

MDPI

Basel • Beijing • Wuhan • Barcelona • Belgrade • Novi Sad • Cluj • Manchester

Guest Editors

Fátima Regina Mena Barreto Silva
Departament of Biochemistry
Federal University of Santa Catarina
Florianópolis
Brazil

Diana Marcela Aragon Novoa
Departamento de Farmácia
Universidad Nacional de Colombia
Bogotá
Colombia

Editorial Office
MDPI AG
Grosspeteranlage 5
4052 Basel, Switzerland

This is a reprint of the Special Issue, published open access by the journal *Nutrients* (ISSN 2072-6643), freely accessible at: https://www.mdpi.com/journal/nutrients/special_issues/3H28397R01.

For citation purposes, cite each article independently as indicated on the article page online and as indicated below:

Lastname, A.A.; Lastname, B.B. Article Title. *Journal Name* **Year**, *Volume Number*, Page Range.

ISBN 978-3-7258-7262-6 (Hbk)
ISBN 978-3-7258-7263-3 (PDF)
https://doi.org/10.3390/books978-3-7258-7263-3

© 2026 by the authors. Articles in this reprint are Open Access and distributed under the Creative Commons Attribution (CC BY) license. The reprint as a whole is distributed by MDPI under the terms and conditions of the Creative Commons Attribution-NonCommercial-NoDerivs (CC BY-NC-ND) license (https://creativecommons.org/licenses/by-nc-nd/4.0/).

Contents

About the Editors . . . . . **vii**

Fátima Regina Mena Barreto Silva and Marcela Aragón Novoa
Effects of Plant Extracts on Human Health—2nd Edition
Reprinted from: *Nutrients* **2026**, *18*, 732, https://doi.org/10.3390/nu18050732 . . . . . **1**

Giuseppina Malcangi, Angelo Michele Inchingolo, Lucia Casamassima, Irma Trilli, Laura Ferrante, Francesco Inchingolo, Andrea Palermo, et al.
Effectiveness of Herbal Medicines with Anti-Inflammatory, Antimicrobial, and Antioxidant Properties in Improving Oral Health and Treating Gingivitis and Periodontitis: A Systematic Review
Reprinted from: *Nutrients* **2025**, *17*, 762, https://doi.org/10.3390/nu17050762 . . . . . **4**

Marisa Jadna Silva Frederico, Paola Miranda Sulis, Landerson Lopes Pereira, Diana Rey, Marcela Aragón and Fátima Regina Mena Barreto Silva
Potential Effect of Cinnamaldehyde on Insulin Resistance Is Mediated by Glucose and Lipid Homeostasis
Reprinted from: *Nutrients* **2025**, *17*, 297, https://doi.org/10.3390/nu17020297 . . . . . **24**

Hammad Ullah, Marco Dacrema, Daniele Giuseppe Buccato, Marwa A. A. Fayed, Lorenza Francesca De Lellis, Maria Vittoria Morone, et al.
A Narrative Review on Plant Extracts for Metabolic Syndrome: Efficacy, Safety, and Technological Advances
Reprinted from: *Nutrients* **2025**, *17*, 877, https://doi.org/10.3390/nu17050877 . . . . . **34**

Carmen Altomare, Roberta Macrì, Maria Serra, Sara Ussia, Giovanna Ritorto, Jessica Maiuolo, et al.
The Potential of Nutraceutical Supplementation in Counteracting Cancer Development and Progression: A Pathophysiological Perspective
Reprinted from: *Nutrients* **2025**, *17*, 2354, https://doi.org/10.3390/nu17142354 . . . . . **59**

Ana Guzmán-Carrasco, Cristina Mesas, Kevin Doello, Jesús M. Porres, Alejandro García-Beltrán, Rosario Martínez, et al.
The Antioxidant and Chemopreventive Activity of a Nutraceutical Derived from *Brassicaceae* Seed Extracts for Colorectal Cancer
Reprinted from: *Nutrients* **2025**, *17*, 1358, https://doi.org/10.3390/nu17081358 . . . . . **100**

Wen Duan, Bisheng Zheng, Tong Li and Rui Hai Liu
Effects of Polyphenols from Oat and Oat Bran on Anti-Inflammatory Activity and Intestinal Barrier Function in Raw264.7 and Caco-2 Models
Reprinted from: *Nutrients* **2025**, *17*, 1962, https://doi.org/10.3390/nu17121962 . . . . . **122**

Shirley Arbizu, Susanne U. Mertens-Talcott, Stephen Talcott, Aaron Riviere, Steven E. Riechman and Giuliana D. Noratto
Assessing the Role of Dark Sweet Cherry (*Prunus avium* L.) Consumption on Cognitive Function, Neuropeptides, and Circadian Rhythm in Obesity: Results from a Randomized Controlled Trial
Reprinted from: *Nutrients* **2025**, *17*, 784, https://doi.org/10.3390/nu17050784 . . . . . **141**

Hemalata Deshmukh, Roberto Mendóza, Julianna M. Santos, Sathish Sivaprakasam, Moamen M. Elmassry, Jonathan M. Miranda, et al.
Effect of Peanut Shell Extract and Luteolin on Gut Microbiota and High-Fat Diet-Induced Sequelae of the Inflammatory Continuum in a Metabolic Syndrome-like Murine Model
Reprinted from: *Nutrients* **2025**, *17*, 2290, https://doi.org/10.3390/nu17142290 . . . . . **158**

Lorenza Francesca De Lellis, Hammad Ullah, Maria Vittoria Morone, Daniele Giuseppe Buccato, Alessandra Baldi, Alessandro Di Minno, et al.
Efficacy and Satisfaction of a Chemically Characterized *Malva sylvestris* L. Extract-Based Food Supplement for Functional Constipation in Healthy Consumers: Preliminary Results of a Questionnaire-Based Survey
Reprinted from: *Nutrients* **2025**, *17*, 77, https://doi.org/10.3390/nu17010077 . . . . . **181**

Sarmistha Mitra, Raju Dash, Md Abul Bashar, Kishor Mazumder and Il Soo Moon
Neuroprotective and Neurotrophic Potential of *Flammulina velutipes* Extracts in Primary Hippocampal Neuronal Culture
Reprinted from: *Nutrients* **2025**, *17*, 3107, https://doi.org/10.3390/nu17193107 . . . . . **198**

Wei Lu, Yujie Li, Xinyuan Liao, Han Hu, Bolin Zhang, Lisong Liang and Haina Gao
From Microbiota to Metabolomics: How *Corylus heterophylla* Fisch. Male Flower Extract Shields Mice from Cognitive Decline
Reprinted from: *Nutrients* **2025**, *17*, 3958, https://doi.org/10.3390/nu17243958 . . . . . **218**

Wen Xin Janice Lim, Rachel A. Page, Cheryl S. Gammon and Paul J. Moughan
The Hypoglycaemic Effects of the New Zealand Pine Bark Extract on Sucrose Uptake and Glycaemic Responses in Healthy Adults—A Single-Blind, Randomised, Placebo-Controlled, Crossover Trial
Reprinted from: *Nutrients* **2025**, *17*, 2277, https://doi.org/10.3390/nu17142277 . . . . . **247**

Taehoon Oh, Chan Hee Cho, Su Cheol Baek, Mun Seok Jo, Woo Bong Kang, Yun Seok Kang, et al.
Bioactive Phenolics from Vinegar–Egg Accelerates Acute Wound Healing by Activation of Focal Adhesion and Mitogen-Activated Protein Kinase Signaling
Reprinted from: *Nutrients* **2025**, *17*, 2584, https://doi.org/10.3390/nu17162584 . . . . . **262**

Binyan Zhang, Kun Xu, Baibing Mi, Hong Yan, Duolao Wang, Shaonong Dang and Ke Men
Maternal Dietary Anthocyanidin, Dietary Inflammatory Potential, and Risk of Small-for-Gestational-Age in China
Reprinted from: *Nutrients* **2025**, *17*, 3187, https://doi.org/10.3390/nu17203187 . . . . . **276**

Zhaomin Liu, Minmin Li, Yuming Chen, Cheng Wang, Jianyin Chen, Huanhuan Long, et al.
Purified Anthocyanins Indicated No Significant Effect on Arterial Stiffness, Four-Limb Blood Pressures and Cardiovascular Risk—A 12-Week Dose–Response Trial in Chinese Middle-Aged and Elderly Adults with Hyperglycemia
Reprinted from: *Nutrients* **2026**, *18*, 112, https://doi.org/10.3390/nu18010112 . . . . . **291**

About the Editors

Fátima Regina Mena Barreto Silva

Fátima Regina Mena Barreto Silva is a full professor of Chemistry at the Universidade Federal de Santa Catarina in Florianópolis, Brazil and a coordinator of the "Instituto de Bioeletricidade Celular (IBIOCEL): Ciência & Saúde". She has participated in several projects related to diabetes, male fertility and cancer. Her research focus is on characterizing intracellular pathways mediated by hormones, toxicants, natural and synthetic compounds involving different programs and countries as follows: an international cooperation program with UNICAEN, projects for undergraduate and graduate (Master, PhD and Post-Doctoral) exchange students among UNICAEN and UFSC, and international projects in collaboration with the University of Guelph/Canada Sorbonne Universités; the University of California, Riverside; the Universidad Nacional de Colombia, Bogota; De Montfort University, Leicester, UK; the University of Coimbra; and the University of Porto. She has been a fellowship student of the Japan International Cooperation Agency, Japan, a Visiting Scientist at UCR/USA and at UNICAEN, and an Invited Professor at UNICAEN/France in undergraduate and graduation Biology courses. As a researcher, she has developed studies in Pharmacy related to Pharmacognosy, Medicinal Chemistry and Precision Medicine. Keywords: Electrophysiology; Diagnostic strategies; Pathophysiology; Drug development; Diabetes; Infertility; Cancer.

Diana Marcela Aragon Novoa

Diana Marcela Aragon Novoa is a pharmacist with a PhD in Pharmaceutical Science and a full professor at the National University of Colombia. She has experience in the research and development of new drug delivery systems, extract standardization, and the study of the pharmacokinetic and biopharmaceutical properties of different active pharmaceutical agents. She has supervised more than 25 Master's and PhD theses and has published more than 60 scientific papers, 10 scientific book chapters, and a book about the role of women in science. Her PhD thesis was awarded as a "Meritorious Thesis". She has been awarded for her performance as a researcher at the National University of Colombia and has been named a senior researcher by the Ministry of Science of Colombia. She has led research projects funded by different organizations with Colombian and foreign participants and has been an invited researcher at different foreign universities. She is a member of the Ibero-American Pharmacometrics Network (RedIF) and the Organization for Women in Science for the Developing World (OWSD-Colombia).

nutrients

MDPI

Editorial

Effects of Plant Extracts on Human Health—2nd Edition

Fátima Regina Mena Barreto Silva [1,*] and Marcela Aragón Novoa [1,2,*]

[1] Instituto de Bioeletricidade Celular (IBIOCEL): Ciência & Saúde, Departamento de Bioquímica, Universidade Federal de Santa Catarina, Florianópolis 88049-900, SC, Brazil
[2] Departamento de Farmacia, Universidad Nacional de Colombia, Av. Carrera 30 # 45-03 Edif 450, Bogotá 111321, Colombia
* Correspondence: mena.barreto@ufsc.br (F.R.M.B.S.); dmaragonn@unal.edu.co (M.A.N.)

Plant extracts and their bioactive components have garnered increasing scientific interest due to their diverse chemical profiles and potential impacts on human health. From antioxidant and anti-inflammatory activity to metabolic and neuroprotective effects, botanicals continue to be explored across nutritional, physiological, and clinical domains. The Special Issue "Effects of Plant Extracts on Human Health—2nd Edition" in *Nutrients* assembles a multidisciplinary collection of articles that collectively advance our understanding of these complex interactions and highlight emerging directions in plant extract research.

A core theme that emerges from this Special Issue is the investigation of plant extracts in the context of metabolic health. Several contributions examine how specific botanical extracts influence lipid metabolism, glycemic control, and weight management, offering insights into mechanisms that may complement traditional dietary and pharmacological interventions. These studies underscore the importance of standardized extract characterization and appropriate dosimetry in assessing physiological outcomes, and they point toward the need for rigorous human trials to substantiate preclinical findings.

Another significant strand of research in this Special Issue focuses on the neuroprotective potential of plant-derived compounds. Evidence from both cellular and animal models suggests that specific phytochemicals can modulate signaling pathways associated with neuronal survival, oxidative stress, and inflammation. These findings contribute to a growing body of literature that positions certain plant extracts as candidates for mitigating age-related cognitive decline and supporting neural health, although translation to clinical contexts remains a challenge.

The Special Issue also includes contributions that explore the bioactive diversity of lesser-studied plant species and their unique phytochemical profiles. Such work expands the botanical landscape beyond commonly studied extracts, illuminating novel chemical entities and complex mixtures with promising bioactivity. This trend aligns with the broader objective of diversifying the sources and structural motifs under investigation, and it highlights the value of integrating advanced analytical technologies to map extract composition with biological function.

Across multiple contributions, several articles identify challenges associated with variable extract composition and inconsistent reporting practices, reinforcing calls for harmonized analytical protocols. These methodological considerations are essential for making meaningful comparisons across studies and for advancing plant extract research toward effective human applications.

Despite notable progress, several knowledge gaps remain. A limited number of well-powered clinical trials means that evidence for many putative health effects is still preliminary. Furthermore, uncertainties about optimal dosing regimens, long-term safety,

and interactions with conventional therapies highlight the need for careful translational research. The complexity of plant extracts—often comprising hundreds of compounds with potential synergistic interactions—adds an additional layer of challenge that warrants integrative biological and computational approaches.

Looking forward, the collection of work published in this Special Issue suggests several promising directions for future research. Studies that bridge pharmacokinetics, systems biology, metabolomics, and clinical nutrition are likely to yield deeper mechanistic insights and facilitate personalized approaches to botanical interventions. Additionally, an expanded focus on bioavailability enhancement strategies and targeted delivery systems may improve the efficacy and consistency of plant-derived bioactives in human populations.

"Effects of Plant Extracts on Human Health—2nd Edition" provides a timely overview of contemporary research exploring the multifaceted roles of plant extracts in human health. The breadth of topics covered—ranging from metabolic modulation to neuroprotection and extract characterization—reflects the dynamic nature of the field and underscores the potential of plant-based approaches to contribute to nutritional and therapeutic strategies. We hope that this Special Issue will stimulate further research, foster interdisciplinary collaboration, and support the responsible translation of botanical insights into health-promoting applications.

Author Contributions: Writing—original draft, M.A.N.; revision and editing, F.R.M.B.S. and M.A.N. All authors have read and agreed to the published version of the manuscript.

Funding: The authors thank to FAPESC 2024TR000070 by supporting part of the experimental procedures.

Conflicts of Interest: The authors declare no conflicts of interest.

List of Contributions:

1. Malcangi, G.; Inchingolo, A.M.; Casamassima, L.; Trilli, I.; Ferrante, L.; Inchingolo, F.; Palermo, A.; Inchingolo, A.D.; Dipalma, G. Effectiveness of Herbal Medicines with Anti-Inflammatory, Antimicrobial, and Antioxidant Properties in Improving Oral Health and Treating Gingivitis and Periodontitis: A Systematic Review. *Nutrients* **2025**, *17*, 762. https://doi.org/10.3390/nu17050762.
2. Ullah, H.; Dacrema, M.; Buccato, D.G.; Fayed, M.A.A.; De Lellis, L.F.; Morone, M.V.; Di Minno, A.; Baldi, A.; Daglia, M. A Narrative Review on Plant Extracts for Metabolic Syndrome: Efficacy, Safety, and Technological Advances. *Nutrients* **2025**, *17*, 877. https://doi.org/10.3390/nu17050877.
3. Altomare, C.; Macrì, R.; Serra, M.; Ussia, S.; Ritorto, G.; Maiuolo, J.; Muscoli, C.; Perri, E.; Mollace, V. The Potential of Nutraceutical Supplementation in Counteracting Cancer Development and Progression: A Pathophysiological Perspective. *Nutrients* **2025**, *17*, 2354. https://doi.org/10.3390/nu17142354.
4. Lellis, L.F.D.; Ullah, H.; Morone, M.V.; Buccato, D.G.; Baldi, A.; Minno, A.D.; Larsen, D.S.; Sacchi, R.; Daglia, M. Efficacy and Satisfaction of a Chemically Characterized *Malva sylvestris* L. Extract-Based Food Supplement for Functional Constipation in Healthy Consumers: Preliminary Results of a Questionnaire-Based Survey. *Nutrients* **2025**, *17*, 77. https://doi.org/10.3390/nu17010077.
5. Frederico, M.J.S.; Sulis, P.M.; Pereira, L.L.; Rey, D.; Aragón, M.; Silva, F.R.M.B. Potential Effect of Cinnamaldehyde on Insulin Resistance Is Mediated by Glucose and Lipid Homeostasis. *Nutrients* **2025**, *17*, 297. https://doi.org/10.3390/nu17020297.
6. Arbizu, S.; Mertens-Talcott, S.U.; Talcott, S.; Riviere, A.; Riechman, S.E.; Noratto, G.D. Assessing the Role of Dark Sweet Cherry (*Prunus avium* L.) Consumption on Cognitive Function, Neuropeptides, and Circadian Rhythm in Obesity: Results from a Randomized Controlled Trial. *Nutrients* **2025**, *17*, 784. https://doi.org/10.3390/nu17050784.
7. Guzmán-Carrasco, A.; Mesas, C.; Doello, K.; Porres, J.M.; García-Beltrán, A.; Martínez, R.; Bermúdez, F.; Peña, M.; Melguizo, C.; Prados, J. The Antioxidant and Chemopreventive Activity of a Nutraceutical Derived from *Brassicaceae* Seed Extracts for Colorectal Cancer. *Nutrients* **2025**, *17*, 1358. https://doi.org/10.3390/nu17081358.

8. Duan, W.; Zheng, B.; Li, T.; Liu, R.H. Effects of Polyphenols from Oat and Oat Bran on Anti-Inflammatory Activity and Intestinal Barrier Function in Raw264.7 and Caco-2 Models. *Nutrients* **2025**, *17*, 1962. https://doi.org/10.3390/nu17121962.
9. Lim, W.X.J.; Page, R.A.; Gammon, C.S.; Moughan, P.J. The Hypoglycaemic Effects of the New Zealand Pine Bark Extract on Sucrose Uptake and Glycaemic Responses in Healthy Adults—A Single-Blind, Randomised, Placebo-Controlled, Crossover Trial. *Nutrients* **2025**, *17*, 2277. https://doi.org/10.3390/nu17142277.
10. Deshmukh, H.; Mendóza, R.; Santos, J.M.; Sivaprakasam, S.; Elmassry, M.M.; Miranda, J.M.; Pham, P.Q.; Driver, Z.; Bender, M.; Dufour, J.M.; et al. Effect of Peanut Shell Extract and Luteolin on Gut Microbiota and High-Fat Diet-Induced Sequelae of the Inflammatory Continuum in a Metabolic Syndrome-like Murine Model. *Nutrients* **2025**, *17*, 2290. https://doi.org/10.3390/nu17142290.
11. Oh, T.; Cho, C.H.; Baek, S.C.; Jo, M.S.; Kang, W.B.; Kang, Y.S.; Ko, S.-K.; Kim, K.H. Bioactive Phenolics from Vinegar–Egg Accelerates Acute Wound Healing by Activation of Focal Adhesion and Mitogen-Activated Protein Kinase Signaling. *Nutrients* **2025**, *17*, 2584. https://doi.org/10.3390/nu17162584.
12. Mitra, S.; Dash, R.; Bashar, M.A.; Mazumder, K.; Moon, I.S. Neuroprotective and Neurotrophic Potential of *Flammulina velutipes* Extracts in Primary Hippocampal Neuronal Culture. *Nutrients* **2025**, *17*, 3107. https://doi.org/10.3390/nu17193107.
13. Zhang, B.; Xu, K.; Mi, B.; Yan, H.; Wang, D.; Dang, S.; Men, K. Maternal Dietary Anthocyanidin, Dietary Inflammatory Potential, and Risk of Small-for-Gestational-Age in China. *Nutrients* **2025**, *17*, 3187. https://doi.org/10.3390/nu17203187.
14. Lu, W.; Li, Y.; Liao, X.; Hu, H.; Zhang, B.; Liang, L.; Gao, H. From Microbiota to Metabolomics: How *Corylus heterophylla* Fisch. Male Flower Extract Shields Mice from Cognitive Decline. *Nutrients* **2025**, *17*, 3958. https://doi.org/10.3390/nu17243958.
15. Liu, Z.; Li, M.; Chen, Y.; Wang, C.; Chen, J.; Long, H.; Liu, R.; Chiou, J.; Chen, C. Purified Anthocyanins Indicated No Significant Effect on Arterial Stiffness, Four-Limb Blood Pressures and Cardiovascular Risk—A 12-Week Dose–Response Trial in Chinese Middle-Aged and Elderly Adults with Hyperglycemia. *Nutrients* **2026**, *18*, 112. https://doi.org/10.3390/nu18010112.

Disclaimer/Publisher's Note: The statements, opinions and data contained in all publications are solely those of the individual author(s) and contributor(s) and not of MDPI and/or the editor(s). MDPI and/or the editor(s) disclaim responsibility for any injury to people or property resulting from any ideas, methods, instructions or products referred to in the content.

nutrients

MDPI

Systematic Review

Effectiveness of Herbal Medicines with Anti-Inflammatory, Antimicrobial, and Antioxidant Properties in Improving Oral Health and Treating Gingivitis and Periodontitis: A Systematic Review

Giuseppina Malcangi [1,†], Angelo Michele Inchingolo [1,*,†], Lucia Casamassima [1], Irma Trilli [1], Laura Ferrante [1], Francesco Inchingolo [1,*], Andrea Palermo [2], Alessio Danilo Inchingolo [1,‡] and Gianna Dipalma [1,‡]

[1] Department of Interdisciplinary Medicine, University of Bari "Aldo Moro", 70121 Bari, Italy; giuseppinamalcangi@libero.it (G.M.); lucia.casamassima@uniba.it (L.C.); irmatrilli@hotmail.com (I.T.); lauraferrante79@virgilio.it (L.F.); alessiodanilo.inchingolo@uniba.it (A.D.I.); giannadipalma@uniba.it (G.D.)
[2] Department of Experimental Medicine, University of Salento, 73100 Lecce, Italy; andreapalermo@unisalento.it
* Correspondence: angeloinchingolo@gmail.com (A.M.I.); francesco.inchingolo@uniba.it (F.I.)
† These authors contributed equally to this work.
‡ These authors also contributed equally to this work.

Abstract

Objectives: This systematic review investigates the effectiveness of natural extracts with anti-inflammatory properties for improving oral health, particularly in managing gingivitis and periodontal disease (PD). With PD being a major global health issue, exacerbated by microbial dysbiosis and oxidative stress, the integration of phytochemicals and herbal formulations into periodontal therapy offers a promising avenue for adjunctive treatments. Methods: A systematic review was conducted following PRISMA guidelines and registered under the International Prospective Register of Systematic Reviews (ID: 641944). Databases, including PubMed, Scopus, and Web of Science, were searched between 18–24 December 2024, using Boolean keywords combining terms such as "herbal medicine", "plant extracts", "anti-inflammatory", and "periodontal therapy". Studies involving animal models, in vitro data, or non-peer-reviewed articles were excluded. Results: Seventeen studies met inclusion criteria. Polyherbal formulations and single-component extracts (e.g., *Camellia sinensis*, *Punica granatum*, *Zingiber officinale*, and *Rosmarinus officinalis*) demonstrated comparable efficacy to conventional agents like chlorhexidine (CHX). Polyherbal rinses, *camellia sinensis* gels, and extracts like *Punica granatum* reduced inflammation, improved gingival health, and showed antimicrobial properties, offering effective natural alternatives. Conclusions: Natural products, including single extracts and polyherbal formulations, provide effective and safe alternatives for managing gingivitis and PD. Their anti-inflammatory, antimicrobial, and antioxidant properties support their adjunctive role alongside with scaling and root planning therapy (SRP) in periodontal therapy. However, further large-scale, long-term studies are needed to standardize formulations and establish optimal protocols.

Keywords: herbal medicine; plant extracts; essential oils; phytochemicals; antibacterial activity; gingivitis; periodontitis; anti-inflammatory activity; dentistry oral health; periodontal therapy

1. Introduction

Dental caries (DC) and periodontal disease (PD) continue to be the most prevalent public health problems in the world. Although recent surveys show a decrease in the incidence and severity of carious lesions, PD remains the sixth most common disease worldwide, with 10% of the population affected by severe PD [1–7].

PD is a degenerative inflammatory disease of the periodontium caused by an altered oral microbiota associated with a reduced immune response of the body [8–10].

It involves the production of pro-inflammatory cytokines, particularly IL-1β, PGE2 (linked to bone resorption and PD severity), and MMPs (especially MMP-8 and MMP-9), which degrade collagen and contribute to periodontal tissue destruction [11–17]. Other metabolic, neurodegenerative, autoimmune, and oncological diseases are often associated with PD [18–20]. The potential link between PD and systemic diseases has led to research into new treatment options and a greater emphasis on periodontal treatment and control, as well as early diagnosis [21,22].

PD is diagnosed by assessing the plaque index (PI), bleeding on probing (BOP), the depth of the periodontal pocket, and the extent of gingival recession, and by testing for biomarkers (MMP-8 and MMP-9, PGE2 and IL-1β) that are detectable in the crevicular fluid [23–26].

To assess the therapeutic efficacy of natural products in periodontal health, various clinical parameters and biomarkers are commonly evaluated. The primary indicators include the Plaque Index (PI) and Bleeding on Probing (BOP), which provide insights into plaque accumulation and gingival inflammation. Additionally, reductions in periodontal pocket depth (PPD) and gingival recession (GR) are used to measure improvements in periodontal structure. At a molecular level, changes in biomarkers such as matrix metalloproteinases (MMP-8 and MMP-9), prostaglandin E2 (PGE2), and interleukin-1β (IL-1β) in gingival crevicular fluid (GCF) serve as objective indicators of inflammation modulation. In several clinical studies, the efficacy of plant-derived mouthwashes and gels has been confirmed through these parameters, showing significant reductions in inflammatory markers and improvements in periodontal health compared to conventional treatments. PD management typically involves specialist visits, home hygiene, CHX mouthrinses, and antibiotics like metronidazole. However, prolonged CHX use may cause mucosal and dental staining, taste loss, irritation, and antibiotic resistance [27–30].

In recent years, the scientific community has developed an interest in the use of natural products, rich in bioactive substances with antimicrobial, bacteriostatic, immunomodulatory, and restorative properties, known since ancient times, capable of slowing down, controlling, or preventing PD [31–33]. About 35,000 medicinal plants are known, but only 20% are analyzed phytochemically, and of these, only 10% are biologically screened to ensure quality and non-toxicity [34–39]. Extracts, concentrated forms of phytochemicals known as nutraceuticals, have received particular attention [40,41].

There are many ways to extract substances from plants, from long boiling to cold infusion, or by using alcohol, vinegar, hot water, or other solvents such as acetone and chloroform [42–44].

Nutraceuticals are bioactive substances that can be used as main therapeutic agents or as a basis for the synthesis of other drugs (e.g., morphine from opium, extracted from *Papaver somniferum*) [45–47].

Many natural substances have been the subject of research for the treatment of oral cavity inflammation. The use of herbal extracts alone or in combination with other natural herbal extracts (triphala, sage, green tea, tulsi patra, jyestiamadh, neem, clove oil, pudina, ajwain, ginger, calendula, aloe vera, propolis, mangosteen extract complex, elderberry) in the form of mouthwashes, gels, and toothpastes (Figure 1) have been scientifically tested

for various oral health problems: gingivitis, bleeding, bad breath, soft-tissue ulcers, infections, and prevention of the onset of DC [8,48–53]. These benefits are largely attributed to bioactive compounds such as polyphenols, flavonoids, tannins, and terpenoids, which exhibit anti-inflammatory, antimicrobial, and antioxidant properties. The active ingredients of phytotherapeutic products have the advantage that they have no side effects and are not harmful even in the medium and long term. In addition, all natural herbal mouthwashes do not contain sugar and/or alcohol, which are present in the vast majority of over-the-counter oral hygiene products, and can be a good substrate for the development of microorganisms [54–57]. Herbs from the *Lythraceae* family have high phytotherapeutic properties, including *Punica granatum* (pomegranate) and *Lawsonia inermis* (henna), whose extracts have shown remarkable anti-inflammatory properties [58–61]. Both extracts were used as mouthwashes, and the reduction in gingival and periodontal inflammatory status was correlated to the decrease in salivary enzyme activity of aspartate aminotransferase (AST), alanine aminotransferase (ALT), and lactate dehydrogenase (LDH), with a greater reduction with *Punica granatum* mouthwash [34,62,63]. Pomegranate extract owes its beneficial effects to the presence of punicalin, phenols, flavonoids, and triterpenoids, which are mainly found in the rind. The bioactive components reduce inflammatory mediators, stimulate collagen production, and angiogenesis and reduce bacterial proliferation. *Lawsonia inermis* owes its antibacterial properties to the presence of 2-hydroxynaphthoquinone, saponins, and xanthones. *Punica granatum* extract, rich in punicalin, phenols, flavonoids, and triterpenoids, reduces inflammation, promotes collagen production, and inhibits bacterial growth. Similarly, other bioactive compounds such as tannins, terpenoids, and saponins found in medicinal plants contribute to oral health improvement by modulating inflammatory responses and reducing microbial adhesion. *Lawsonia inermis*' antibacterial effects stem from 2-hydroxynaphthoquinone, saponins, and xanthones [64–67]. Polyherbal mouthwashes based on extracts of rosemary (*Rosmarinus officinalis Lamiaceae*), *Zingiber officinale*, and marigold (*Calendula officinalis*) have been produced which have shown efficacy in the treatment and prophylaxis of gingivitis comparable to that of CHX mouthwash without adverse effects [68–72]. Rosemary extract is a spice. It belongs to the *Lamiaceae* family and is also used in medicine for its many therapeutic properties and high antioxidant and antibacterial activity, thanks to the presence of active compounds: phenolic diterpenes (carnosic acid, but also carnosol, rosmanol and epi- and isorosmanol), flavonoids, and terpenoids. The healing of oral ulcers and gingivitis has been improved by its use in dentistry. *Rosmarinus* extract, a Lamiaceae spice with strong antioxidant and antibacterial properties, aids oral ulcer and gingivitis healing due to its phenolic diterpenes, flavonoids, and terpenoids. [73–81]. Ginger, *Zingiber officinale Roscoe*, a culinary spice, is widely used in phytotherapy. It has antimicrobial, antifungal, and pharmaceutical properties due to the presence of gingerol *zingiber* [82–85]. The mechanisms by which ginger *zingiber* inhibits the growth of oral bacteria that contribute to PD are still poorly understood [34,73–76,86,87]. However, it was found that ginger reduces PR synthesis and that two highly alkylated extracts in particular inhibit three anaerobic Gram-negative bacteria that cause PD: *Porphyromonas gingivalis* ATCC (American Type Culture Collection) 53978, *Porphyromonas endodontalis* ATCC 35406, and *Prevotella intermedia* ATCC 25611 at low doses (6–30 μg/mL). It involves the production of pro-inflammatory cytokines, particularly IL-1β, PGE2 (linked to bone resorption and PD severity), and MMPs (especially MMP-8 and MMP-9), which degrade collagen and contribute to periodontal tissue destruction [77–81,88–95]. The triterpenoids in the CO_2 (carbon dioxide) extract of calendula flowers, including faradiol monoester, demonstrated predominant anti-inflammatory activity [96–106]. A 2% gel based on *Calendula officinalis* flowers is also used as an individual treatment for inflammation of the oral mucosa and oropharyngeal mucositis caused by radiotherapy and chemotherapy [62,77,107–112]. The

combined extract of *propolis* and *Propolis* and *Mangosteen Extract Complex* (*PMEC*) was used to treat patients with advanced gingivitis and PD [113–122]. The results showed a strong therapeutic response with reduction of all biomarkers present in GCF (IL-1β: 57.9%, PGE2: 51.1%, MMP-8: 46.3%, and MMP-9: 54.4%), including macrophages, gingival fibroblasts, and neutrophils, resulting in improved osteogenesis, decreased osteoclastic activity, and reduced alveolar bone resorption. However, the use of PMEC found little short-term clinical improvement due to its inability to prevent direct invasion of the gingival tissue by periodontal pathogens. It reduced GCF biomarkers and improved osteogenesis, but *PMEC* had limited short-term clinical benefits due to persistent pathogen invasion [123–125]. Mouthwashes with natural herbs (*neem*, *tulsi*, *pudina*, *clove* oil, *camellia sinensis* green tea, *aloe vera*, *ajwain*, *triphala* and many others) have been formulated to treat bleeding gums, bad breath, and mouth ulcers, and to prevent tooth decay. Herbal and essential oil mouthwashes have been used [49,126–129]. This study provides a novel perspective by systematically evaluating not only the anti-inflammatory properties of herbal formulations in periodontal therapy but also their antimicrobial and antioxidant effects, highlighting their potential as comprehensive adjuncts to conventional treatments.

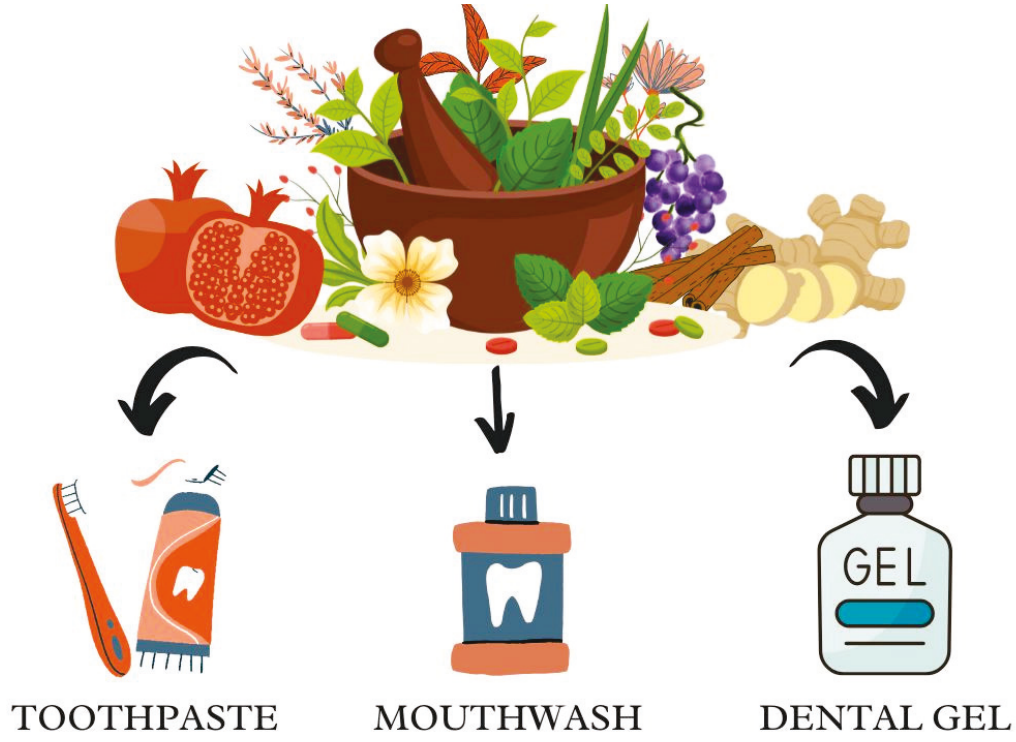

Figure 1. This image illustrates using extracts from natural ingredients (such as *punica granatum*, *flowers*, *zingiber*, *grapes*, and *cinnamon*) in oral care products. It shows the transformation of these natural components into three different types of dental products: toothpaste, mouthwash, and dental gel, highlighting a herbal approach to dental hygiene.

2. Materials and Methods

2.1. Search Processing

The current systematic review followed the PRISMA (Preferred Reporting Items for Systematic reviews and Meta-Analyses) guidelines and International Prospective Register of Systematic Review Registry procedures (full ID: 641944). The databases PubMed, Web of Science, and Scopus were examined from 18 December 2024 to 24 December 2024 to search articles of the last 10 years (Table S1). The search strategy was created by combining terms relevant to the study's purpose. The following Boolean keyword search was applied:

("herbal medicine" OR "plant extracts" OR "essential oils" OR "phytochemicals") AND ("anti-inflammatory" OR "anti-inflammatory activity") AND ("dentistry" OR "oral health" OR "periodontal therapy" OR "gingivitis" OR "periodontitis")).

2.2. Inclusion and Exclusion Criteria

The reviewers worked in groups to assess all relevant studies that evaluated or compared the effectiveness of natural extracts with anti-inflammatory properties in improving oral health and treating gingivitis and PD, following the inclusion criteria below:

- Studies with open access written in English.
- Studies that did the research "in vivo" or in "humans".
- Case-control studies, cohort studies, randomized controlled trials (RCTs).
- Studies that were published in the last 10 years.
- Articles related to adult studies.

Studies that fulfilled at least one of the following exclusion criteria were excluded: reviews, case reports and series, letters to the authors, animal models, and in vitro studies.

2.3. PICo Question

The PICo format is a framework used in qualitative research to structure clinical research questions. The PICo addressed the question: *"What is the effectiveness of herbal medicine with anti-inflammatory properties in improving oral health or treating gingivitis and periodontitis in adult patients?"*

I. P (Population): Adult patients with gingivitis or periodontitis.
II. I (Phenomenon of Interest): Effectiveness of herbal medicine with anti-inflammatory properties.
III. Co (Context): It applies to improving oral health or treating gingivitis and periodontitis.

2.4. Data Processing

Four independent reviewers (L.C., L.F., I.T., and G.M.) assessed the included studies' quality using criteria such as selection criteria, methods of outcome evaluation, and data analysis. This enhanced 'risk of bias' tool additionally provides quality standards for selection, performance, detection, reporting, and other biases. All differences were settled through conversation or collaboration with other researchers (G.D., A.D.M., and A.M.I.). The reviewers screened the records according to the inclusion and exclusion criteria. The 301 selected articles were downloaded into "Zotero 6.0.36" for organization and analysis.

3. Results

3.1. Selection and Characteristics of the Study

A total of 301 publications were identified through online databases: PubMed (n = 43), Scopus (n = 185), and Web of Science (n = 73). No additional studies were identified through manual research. After removing 2 duplicate records, 299 studies remained and were screened by title and abstract.

Following a detailed eligibility assessment of the 100 reports, 83 were excluded for not meeting the criteria, leaving 17 studies for qualitative analysis. The selection process and summary of included records are illustrated in Figure 2.

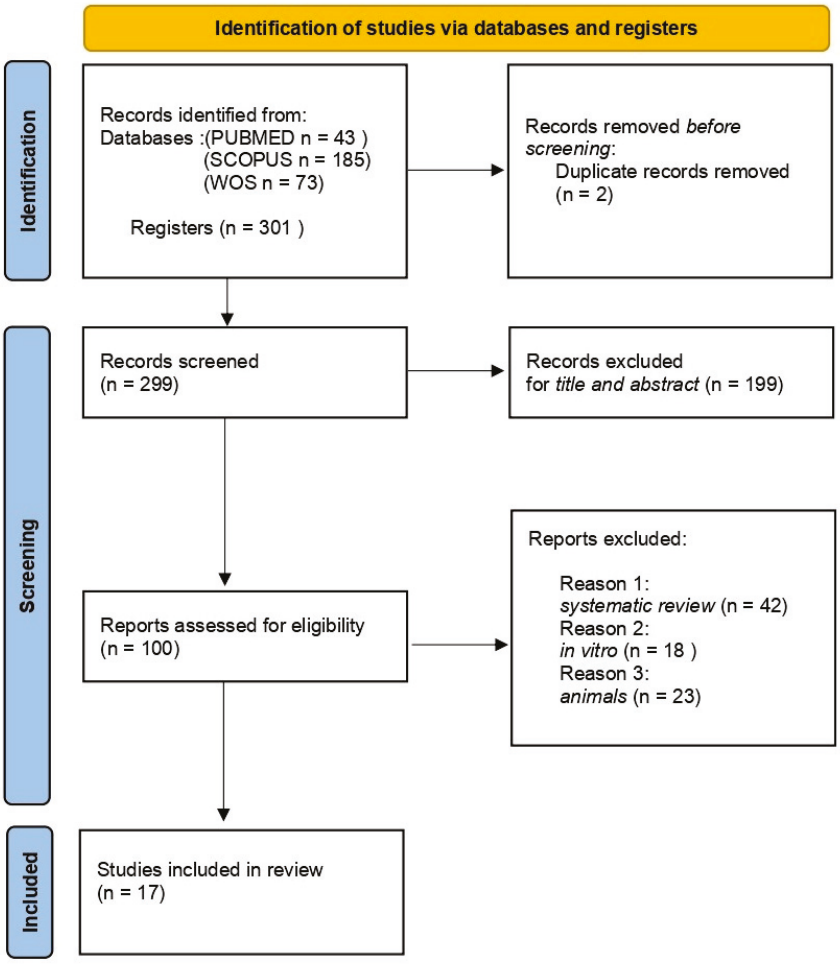

Figure 2. PRISMA flowchart.

3.2. Key Results and Summary

The primary outcomes considered for each study included plaque index (PI), gingival index (GI), bleeding index (BI), bleeding on probing percentage (BOP%), and clinical attachment level (CAL).

A summary of key findings from selected studies is provided below, while the full dataset is available in Table S2:

- *Camellia sinensis*-based dentifrice significantly reduced gingival inflammation and increased antioxidant activity in gingival crevicular fluid.
- Polyherbal mouthwash (*Zingiber* officinale, *Rosmarinus* officinalis, *Calendula* officinalis) showed comparable efficacy to chlorhexidine (CHX) in reducing gingivitis.
- Locally delivered *Camellia sinensis* gel provided clinical benefits in periodontitis management but had no significant long-term superiority over SRP alone.
- *Grape* seed extract gel (2%) improved GI and PI but showed no significant differences in probing depth (PoD).
- Cinnamon extract as an ultrasonic coolant effectively reduces bacterial contamination in aerosols, offering a cost-effective alternative to CHX.
- *Rhizoma chuanxiong* and *Rhizoma imperatae* toothpaste improved GI, BI, and BOP% significantly after 12 weeks.
- *Podila* extract toothpaste showed sustained improvement in PI, GI, BI, and BOP%, with no significant adverse effects.
- Sage-containing mouthwash had no superior effect over placebo in reducing Sulcus Bleeding Index (SBI) and PI.

- *Punica granatum* and *Lawsonia inermis* mouthwashes significantly reduced salivary inflammation markers, with *Punica granatum* showing superior efficacy.

These results emphasize the potential of herbal medicine in oral health care, particularly in reducing gingival inflammation, plaque accumulation, and bacterial load, with some extracts offering comparable efficacy to conventional treatments like CHX.

3.3. Quality Assessment and Risk of Bias of Included Articles

The quality assessment and risk of bias evaluation using the "Risk of Bias in Non-Randomized Studies of Interventions" (ROBINS-I) tool included 17 studies, as reported in Table S3. This evaluation assessed six domains (D1–D6) across multiple studies. Bias due to confounding (D1): all studies effectively controlled for potential confounding factors by implementing strategies such as randomization, and clearly defined inclusion and exclusion criteria. This ensured that the results were reliable and attributable to the interventions being tested. Bias arising from measurement of the exposure (D2): the measurement process was consistently standardized across the studies, resulting in a low risk of bias in this domain. Bias in the selection of participants (D3): most studies maintained a low risk by employing proper selection processes. However, a few studies showed some concerns, suggesting minor issues in participant recruitment or allocation. Bias due to post-exposure interventions (D4): all studies effectively standardized post-exposure interventions, resulting in a consistently low risk of bias in this domain. Bias due to missing data (D5): some studies were flagged for missing data, leading to some concerns. This highlights areas where dropouts or incomplete data handling could potentially influence the outcomes. Bias arising from the measurement of the outcome (D6): most studies demonstrated low risk in this domain, utilizing validated and objective outcome measures. However, a few instances of some concerns were noted.

The majority of the studies demonstrated a low overall risk of bias, reflecting methodological rigor and reliable findings. Nonetheless, a few areas with some concerns, particularly regarding missing data and participant selection, highlight opportunities for improved reporting and data handling in future research.

4. Discussion

PD and gingivitis represent chronic inflammatory conditions primarily caused by microbial dysbiosis and exacerbated by oxidative stress [130–134]. Conventional treatments, including SRP, are often augmented with chemotherapeutics or antioxidants to enhance outcomes. The integration of natural and plant-based products as adjunctive therapies has gained substantial attention due to their antimicrobial, antioxidant, and anti-inflammatory properties. This review synthesizes findings from 17 studies investigating the efficacy of various natural compounds and formulations in managing periodontal conditions [135–146]. To provide a clearer overview of the bioactive components responsible for the beneficial effects of natural products in oral health, Table S4 summarizes the key plant species included in this review along with their main active compounds and associated therapeutic properties. Summary of plant-based products with their effects on oral cavity is represented in Table S5.

4.1. Camellia sinensis-Based Interventions

T. S. Hrishi et al. (2016) explored the adjunctive role of *Camellia sinensis*-based dentifrice in treating mild-to-moderate PD. Their randomized clinical trial with 30 patients compared outcomes between a test group using *Camellia sinensis* dentifrice and a control group using commercial toothpaste [147]. The clinical parameters GI, PI, probing PoD, and CAL—along with antioxidant markers in GCF, were evaluated over four weeks. While both groups

improved due to SRP, the *Camellia sinensis* group showed significantly greater reductions in gingival inflammation and enhanced antioxidant activity. This suggests the potential of *Camellia sinensis* as a beneficial adjunct, though larger-scale studies are warranted [147–152]. Similarly, Kanyawat Rattanasuwan et al. (2016) investigated a locally delivered *Camellia sinensis* gel in chronic PD. Forty-two participants underwent SRP, followed by application of either *Camellia sinensis* gel or placebo. While both groups showed significant clinical improvements, the *Camellia sinensis* gel demonstrated superior anti-inflammatory effects at three months, though its impact on long-term periodontal outcomes was inconclusive. The study emphasized the need for larger trials to determine optimal protocols and long-term efficacy [153].

4.2. Polyherbal Mouthwashes

Saman Mahyari et al. (2016) evaluated a polyherbal mouthwash containing extracts of *Zingiber* officinale, *Rosmarinus* officinalis, and *Calendula officinalis* in gingivitis management [68]. Sixty participants were divided into polyherbal, CHX, and placebo groups, with assessments over 14 days. Both the polyherbal and CHX mouthwashes significantly improved clinical indices, demonstrating comparable efficacy. Polyherbal formulation had no adverse effects, suggesting it as a viable alternative to synthetic products [51,68,154–156]. In 2019, Scilla Sparabombe et al. examined another polyherbal mouthwash containing *propolis*, *plantago lanceolata*, *salvia officinalis* and essential oils. Over three months, the mouthwash significantly reduced inflammation (FMBS) and plaque accumulation (FMPS), particularly in moderate-to-severe PD cases, without adverse effects. The findings underscore its potential as a safe and effective alternative to conventional CHX mouthwash [157].

4.3. Herbal Toothpastes

He (2019) conducted a double-blind trial assessing toothpaste containing *Rhizoma Chuanxiong* and *Rhizoma Imperatae* extracts. Over 12 weeks, 120 participants showed significant reductions in GI, BI, and BOP in the test group compared to controls. The herbal toothpaste demonstrated no adverse effects, highlighting its efficacy and safety for managing gingivitis [158]. Li Cheng et al. (2019) tested *Pudilan* extract-containing toothpaste, composed of flavonoids, alkaloids, and organic acids, over a 12-week period. Significant improvements in PI, GI, BI, and BOP were observed in the experimental group compared to placebo. The gradual improvement over time suggests potential long-term benefits of *Pudilan* extract in chronic gingivitis management [159]. In 2020, Zaira F. Kharaeva explored a toothpaste combining sodium monofluorophosphate, xylitol, and Swiss herbal extracts, including Chamomilla recutita and Salvia officinalis. Results indicated significant reductions in inflammation, plaque presence, and early signs of PD compared to controls [160]. The study highlighted the synergistic effects of chemical and plant-derived antibacterials in managing PD [160–164].

4.4. Alternative Herbal Agents in Gingivitis and Periodontitis

Mohammad Rayyan et al. (2018) assessed a 2% mucoadhesive *Grape* Seed Extract (*GSE*) gel in chronic PD [165]. Over six months, the *GSE* group showed significant reductions in GI and PI compared to controls, though PoD improvements were limited. The authors suggested that higher *GSE* concentrations might yield better results [165–168]. Alefiya Shabbir Mamajiwala et al. (2018) compared CHX and cinnamon extract as ultrasonic coolant agents during scaling. Both significantly reduced bacterial contamination in aerosols, with cinnamon extract demonstrating comparable efficacy without side effects like staining. This positions cinnamon extract as a cost-effective alternative for low-resource settings [169]. Eltay et al. (2021) studied a solution containing 5% *Punica granatum* extract as a supplement to non-surgical therapy for chronic gingivitis. Over four weeks, *Punica*

granatum significantly reduced PI, GI, and IL-1β levels compared to placebo, demonstrating potent anti-inflammatory and antimicrobial properties without adverse effects. These findings support its potential for safe and natural periodontal therapy [170]. Takkella et al. (2021) compared mouthwashes containing *Punica granatum* and *Lawsonia inermis*. Both reduced salivary enzymes linked to inflammation and tissue damage, with *punica granatum* showing superior efficacy due to its bioactive compounds promoting collagen synthesis and reducing bacterial proliferation. The study recommended herbal mouthwashes as safe alternatives to alcohol-based formulations [58].

4.5. Propolis and Other Natural Extracts

Jaber Yaghini et al. (2019) compared *aloe vera camellia sinensis*, matrica, and CHX mouthwashes in plaque-induced gingivitis. *Aloe vera camellia sinensis* was as effective as CHX in reducing plaque and gingival inflammation while causing less dental staining. The findings highlight its promise as an alternative to conventional chemical mouthwashes [171]. Hendrik Jünger et al. (2020) investigated a sage-based mouthwash in elderly patients receiving supportive periodontal care. Although improvements in gingival inflammation were observed, they were not statistically significant compared to placebo. The study suggested that the antimicrobial properties of alcohol and mint oil in the placebo might have confounded results. Future research without alcohol-based controls was recommended [172]. Jung et al. (2024) evaluated a *PMEC* compound for moderate-to-severe gingivitis. Over eight weeks, *PMEC* significantly reduced inflammatory biomarkers in GCF, including IL-1β and PGE2, though clinical improvements in GI and BOP were modest. The authors demonstrated the significant reductions in gingival crevicular fluid biomarkers, by explaining the mechanism of inhibition that the *PMEC* complex explicates on the expression of pro-inflammatory cytokines (IL-1β and PGE2) and metalloproteases (MMP-8 and MMP-9) in periodontal tissue cells infected with oral bacteria, including neutrophils, macrophages, and gingival fibroblasts; such inhibition, in fact, reduces the process of osteoclastogenesis and conversely promotes the osteogenetic one, thereby reducing alveolar bone destruction. However, *PMEC* does not prevent the direct invasion of periodontal pathogens into gingival tissue cells or the subsequent release of lipopolysaccharide (LPS) and exotoxins into the gingival capillaries, which is why the study still shows a discrepancy between results of clinical parameters in *PMEC*-treated and placebo-treated groups. The study highlighted *PMEC*'s potential anti-inflammatory effects and called for longer-term trials [173].

4.6. Innovative Approaches and Phytocompounds

Aslan Kh. Sheregov et al. (2021) assessed *standardized fermented papaya* gel (*SFPG*) in moderate chronic PD associated with orthodontic treatment. *SFPG* significantly reduced inflammation and cytokine levels, emphasizing its antioxidant and antimicrobial properties as a topical adjunct to conventional therapy [174]. Young Park et al. (2021) evaluated *PMEC* capsules in early gingivitis and PD. Over two months, *PMEC* reduced GI and IL-6 levels in GCF, indicating anti-inflammatory benefits. However, improvements in clinical parameters like periodontal depth were not statistically significant. The study highlighted the potential for systemic phytocompounds in periodontal therapy [175]. Yu Rin Kim et al. (2022) examined a Sambucus williamsii var. coreana-based mouthwash. Significant reductions in periodontal indices and pathogenic bacteria were observed, showcasing the mouthwash's immediate and progressive antibacterial effects. The study underscored the potential of natural alternatives to prevent and treat dental diseases [176]. The reviewed studies collectively emphasize the potential of natural and herbal compounds in managing gingivitis and PD. Products like *Camellia sinensis*, *Polyherbal mouthwashes, GSE* and *Punica granatum* demonstrate significant anti-inflammatory, antioxidant, and antimicrobial

properties. While many natural agents show promise as safe alternatives to conventional treatments like CHX, limitations include small sample sizes, short follow-up periods, and variations in study design. Further large-scale, long-term studies are necessary to validate their clinical efficacy and establish standardized protocols for integration into periodontal care. Nonetheless, these findings pave the way for innovative, plant-based solutions that address oral health challenges while minimizing side effects associated with synthetic agents [177–179].

4.7. Clinical Implications of Structure–Activity Correlations

The therapeutic efficacy of plant-derived compounds in managing periodontal diseases is largely determined by their chemical structure, which governs their bioavailability and biological activity. Understanding these structure–activity relationships can help elucidate the mechanisms through which natural compounds exert their antimicrobial, anti-inflammatory, and antioxidant effects in periodontal therapy.

Polyphenols (e.g., catechins from *Camellia sinensis*): the presence of multiple hydroxyl groups enables metal ion chelation and free radical neutralization, reducing oxidative stress in periodontal tissues. Additionally, catechins interact with bacterial membrane proteins, inhibiting bacterial adhesion and biofilm formation.

Ellagitannins (e.g., punicalagins from *Punica granatum*): These tannins act as potent MMP inhibitors, preventing the degradation of collagen and extracellular matrix components. They also suppress IL-1β and TNF-α production, thereby modulating inflammatory responses and limiting tissue destruction.

Terpenoids (e.g., carnosic acid from *Rosmarinus officinalis*): Due to their lipophilic nature, terpenoids integrate into bacterial membranes, increasing their permeability and leading to cell lysis. This mechanism underlies their broad-spectrum antimicrobial properties.

Flavonoids (e.g., quercetin from *Cinnamomum verum* and *Zingiber officinale*): Flavonoids regulate NF-κB signaling pathways, thereby reducing the transcription of pro-inflammatory cytokines such as IL-1β, TNF-α, and PGE2. This anti-inflammatory action helps control gingival inflammation and periodontal tissue damage.

Polysaccharides (e.g., acemannan from *Aloe vera*): These compounds stimulate fibroblast proliferation and enhance collagen synthesis, promoting tissue regeneration and wound healing. Additionally, acemannan exhibits immune-modulatory effects, reducing inflammatory mediator release [160–164].

These structure–activity correlations highlight the pharmacological potential of phytochemicals in periodontal therapy. By targeting key molecular pathways involved in oxidative stress, bacterial proliferation, and inflammation, plant-based compounds serve as valuable adjuncts to conventional periodontal treatments. However, further studies are needed to standardize formulations, optimize bioavailability, and confirm long-term clinical efficacy.

5. Conclusions

This systematic review collects various clinical studies that explore the use of natural remedies and supplements as complementary treatments for PD, including gingivitis and PD. The conclusions of this systematic review are as follows:

- Potential of Plant-Based Remedies: Natural extracts like *Camellia sinensis*, cinnamon, *aloe vera* and *rosmarinus* show promise in reducing inflammation, plaque, and bleeding in PD.
- Effectiveness Compared to Conventional Treatments: While these remedies offer benefits, they often do not surpass conventional options like CHX or antibiotic gels.

- Safer Alternative with Fewer Side Effects: Some plant-based treatments, such as cinnamon, have performed similarly to CHX but without side effects like dental staining.
- Temporary and Variable Effects: The benefits of these natural remedies are often short-lived, and results vary across studies, highlighting the need for standardization.

Overall, this review supports the idea that some natural extracts could be a valuable aid in the management of PD, but further investigations, with larger sample sizes and longer follow-ups, are necessary to determine their definitive role as first-line treatments or as supplements to existing therapies.

Supplementary Materials: The following supporting information can be downloaded at: https://www.mdpi.com/article/10.3390/nu17050762/s1.

Author Contributions: Conceptualization, I.T., L.C., L.F., A.M.I., A.D.I., G.D. and L.F.; methodology, L.F., G.D., A.M.I., A.D.I., L.C., G.M. and F.I.; software, A.D.I., L.C. and G.D.; validation, A.M.I. and L.C.; formal analysis, F.I.; resources, I.T. and L.F.; data curation, G.D.; writing—original draft preparation, I.T., A.M.I., A.P., G.D. and G.M.; writing—review and editing, A.P., G.D., F.I. and A.D.I.; visualization, G.M.; supervision, F.I.; project administration, G.M. All authors have read and agreed to the published version of the manuscript.

Funding: This research received no external funding.

Conflicts of Interest: The authors declare no conflicts of interest.

Abbreviations

ALT	Alanine Aminotransferase
AST	Aspartate Aminotransferase
ATCC	American Type Culture Collection
BI	Bleeding Index
BOP	Bleeding on Probing
CAL	Clinical Attachment Level
CHX	Chlorhexidine
CO2	Carbon Dioxide
CTP	Control Toothpaste
DC	Dental Caries
DW	Distilled Water
FMBS	Full Mouth Bleeding Score
FMPS	Full Mouth Plaque Score
GCF	Gingival Crevicular Fluid
GBI	Gingival Bleeding Index
GI	Gingival Index
GSE	Grape Seed Extract
IL	Interleukin
IL-6	Interleukin-6
LDH	Lactate Dehydrogenase
MGI	Modified Gingival Index
MMPs	Metalloproteinases
MQH	Modified Quigley-Hein Index
PD	Periodontal Disease
PoD	Pocket Depth
PI	Plaque Index
PMEC	*Propolis-Mangosteen* Extract Complex
PPD	Probing Pocket Depth

PR	Prostaglandin
PROMs	Patient-Reported Outcomes Measures
RCT	Randomized Controlled Trial
SBI	Sulcus Bleeding Index
SFPG	Fermented Papaya Gel
SRP	Scaling and Root Planing

References

1. Frencken, J.E.; Sharma, P.; Stenhouse, L.; Green, D.; Laverty, D.; Dietrich, T. Global Epidemiology of Dental Caries and Severe Periodontitis-a Comprehensive Review. *J. Clin. Periodontol.* **2017**, *44* (Suppl. 18), S94–S105. [CrossRef] [PubMed]
2. Cazzato, G.; Massaro, A.; Colagrande, A.; Lettini, T.; Cicco, S.; Parente, P.; Nacchiero, E.; Lospalluti, L.; Cascardi, E.; Giudice, G.; et al. Dermatopathology of Malignant Melanoma in the Era of Artificial Intelligence: A Single Institutional Experience. *Diagnostics* **2022**, *12*, 1972. [CrossRef]
3. Arezzo, F.; Loizzi, V.; La Forgia, D.; Moschetta, M.; Tagliafico, A.S.; Cataldo, V.; Kawosha, A.A.; Venerito, V.; Cazzato, G.; Ingravallo, G.; et al. Radiomics Analysis in Ovarian Cancer: A Narrative Review. *Appl. Sci.* **2021**, *11*, 7833. [CrossRef]
4. Ballini, A.; Santacroce, L.; Cantore, S.; Bottalico, L.; Dipalma, G.; Topi, S.; Saini, R.; De Vito, D.; Inchingolo, F. Probiotics Efficacy on Oxidative Stress Values in Inflammatory Bowel Disease: A Randomized Double-Blinded Placebo-Controlled Pilot Study. *Endocr. Metab. Immune Disord. Drug Targets* **2019**, *19*, 373–381. [CrossRef] [PubMed]
5. Jepsen, S.; Blanco, J.; Buchalla, W.; Carvalho, J.C.; Dietrich, T.; Dörfer, C.; Eaton, K.A.; Figuero, E.; Frencken, J.E.; Graziani, F.; et al. Prevention and Control of Dental Caries and Periodontal Diseases at Individual and Population Level: Consensus Report of Group 3 of Joint EFP/ORCA Workshop on the Boundaries between Caries and Periodontal Diseases. *J. Clin. Periodontol.* **2017**, *44* (Suppl. 18), S85–S93. [CrossRef] [PubMed]
6. Tonetti, M.S.; Bottenberg, P.; Conrads, G.; Eickholz, P.; Heasman, P.; Huysmans, M.-C.; López, R.; Madianos, P.; Müller, F.; Needleman, I.; et al. Dental Caries and Periodontal Diseases in the Ageing Population: Call to Action to Protect and Enhance Oral Health and Well-Being as an Essential Component of Healthy Ageing-Consensus Report of Group 4 of the Joint EFP/ORCA Workshop on the Boundaries between Caries and Periodontal Diseases. *J. Clin. Periodontol.* **2017**, *44* (Suppl. 18), S135–S144. [CrossRef] [PubMed]
7. Bonamonte, D.; Filoni, A.; De Marco, A.; Lospalluti, L.; Nacchiero, E.; Ronghi, V.; Colagrande, A.; Giudice, G.; Cazzato, G. Squamous Cell Carcinoma in Patients with Inherited Epidermolysis Bullosa: Review of Current Literature. *Cells* **2022**, *11*, 1365. [CrossRef]
8. Choi, Y.J.; Lee, Y.C.; Kim, J.M.; Kim, J.I.; Moon, J.S.; Lim, Y.J.; Baik, G.H.; Son, B.K.; Lee, H.L.; Kim, K.O.; et al. Triple Therapy-Based on Tegoprazan, a New Potassium-Competitive Acid Blocker, for First-Line Treatment of Helicobacter Pylori Infection: A Randomized, Double-Blind, Phase III, Clinical Trial. *Gut Liver* **2022**, *16*, 535–546. [CrossRef]
9. Lee, J. Role of Tegoprazan in Helicobacter Pylori Eradication Therapy. *Gut Liver* **2022**, *16*, 493–494. [CrossRef]
10. Cho, Y.K.; Choi, M.-G.; Choi, S.C.; Lee, K.M.; Kim, T.O.; Park, S.-H.; Moon, J.S.; Lim, Y.J.; Kang, D.H.; Cheon, G.J.; et al. Randomised Clinical Trial: Tegoprazan, a Novel Potassium-Competitive Acid Blocker, or Lansoprazole in the Treatment of Gastric Ulcer. *Aliment. Pharmacol. Ther.* **2020**, *52*, 789–797. [CrossRef]
11. Mandriani, B.; Pellè, E.; Mannavola, F.; Palazzo, A.; Marsano, R.M.; Ingravallo, G.; Cazzato, G.; Ramello, M.C.; Porta, C.; Strosberg, J.; et al. Development of Anti-Somatostatin Receptors CAR T Cells for Treatment of Neuroendocrine Tumors. *J. Immunother. Cancer* **2022**, *10*, e004854. [CrossRef] [PubMed]
12. Hernández, M.; Baeza, M.; Räisänen, I.T.; Contreras, J.; Tervahartiala, T.; Chaparro, A.; Sorsa, T.; Hernández-Ríos, P. Active MMP-8 Quantitative Test as an Adjunctive Tool for Early Diagnosis of Periodontitis. *Diagnostics* **2021**, *11*, 1503. [CrossRef] [PubMed]
13. Luchian, I.; Goriuc, A.; Sandu, D.; Covasa, M. The Role of Matrix Metalloproteinases (MMP-8, MMP-9, MMP-13) in Periodontal and Peri-Implant Pathological Processes. *Int. J. Mol. Sci.* **2022**, *23*, 1806. [CrossRef] [PubMed]
14. Sorsa, T.; Ding, Y.; Salo, T.; Lauhio, A.; Teronen, O.; Ingman, T.; Ohtani, H.; Andoh, N.; Takeha, S.; Konttinen, Y.T. Effects of Tetracyclines on Neutrophil, Gingival, and Salivary Collagenases. A Functional and Western-Blot Assessment with Special Reference to Their Cellular Sources in Periodontal Diseases. *Ann. N. Y Acad. Sci.* **1994**, *732*, 112–131. [CrossRef] [PubMed]
15. Isacco, C.G.; Ballini, A.; De Vito, D.; Nguyen, K.C.D.; Cantore, S.; Bottalico, L.; Quagliuolo, L.; Boccellino, M.; Di Domenico, M.; Santacroce, L.; et al. Rebalancing the Oral Microbiota as an Efficient Tool in Endocrine, Metabolic and Immune Disorders. *Endocr. Metab. Immune Disord. Drug Targets* **2021**, *21*, 777–784. [CrossRef]
16. Li, J.; Hu, F.B. Research Digest: Reshaping the Gut Microbiota. *Lancet Diabetes Endocrinol.* **2019**, *7*, 671. [CrossRef]

17. Baeza, M.; Garrido, M.; Hernández-Ríos, P.; Dezerega, A.; García-Sesnich, J.; Strauss, F.; Aitken, J.P.; Lesaffre, E.; Vanbelle, S.; Gamonal, J.; et al. Diagnostic Accuracy for Apical and Chronic Periodontitis Biomarkers in Gingival Crevicular Fluid: An Exploratory Study. *J. Clin. Periodontol.* **2016**, *43*, 34–45. [CrossRef]
18. Baimuratova, M.; Shertayeva, A.; Madraimov, N.; Erkebay, R.; Diusebayev, E. Diseases of Periodontal Tissues: Modern Challenges of the Time. *Georgian Med. News* **2023**, *336*, 126–131.
19. Romito, G.A.; Feres, M.; Gamonal, J.; Gomez, M.; Carvajal, P.; Pannuti, C.; Duque Duque, A.; Romanelli, H.; Rösing, C.K.; Aranguiz Freyhofer, V.; et al. Periodontal Disease and Its Impact on General Health in Latin America: LAOHA Consensus Meeting Report. *Braz. Oral. Res.* **2020**, *34*, e027. [CrossRef]
20. Botero, J.E.; Rösing, C.K.; Duque, A.; Jaramillo, A.; Contreras, A. Periodontal Disease in Children and Adolescents of Latin America. *Periodontol. 2000* **2015**, *67*, 34–57. [CrossRef]
21. Hajishengallis, G. Interconnection of Periodontal Disease and Comorbidities: Evidence, Mechanisms, and Implications. *Periodontol. 2000* **2022**, *89*, 9–18. [CrossRef] [PubMed]
22. Hajishengallis, G.; Chavakis, T. Local and Systemic Mechanisms Linking Periodontal Disease and Inflammatory Comorbidities. *Nat. Rev. Immunol.* **2021**, *21*, 426–440. [CrossRef] [PubMed]
23. Wan, L.; Tian, W.; Li, N.; Chen, D.; Xu, Q.; Li, H.; He, J.; Lu, J. Hydrophilic Porous PVDF Membrane Embedded with BaTiO3 Featuring Controlled Oxygen Vacancies for Piezocatalytic Water Cleaning. *Nano Energy* **2022**, *94*, 106930. [CrossRef]
24. Zhou, A.; Jiang, L.; Yue, J.; Tong, Y.; Zhang, Q.; Lin, Z.; Liu, B.; Wu, C.; Suo, L.; Hu, Y.-S.; et al. Water-in-Salt Electrolyte Promotes High-Capacity FeFe(CN)6 Cathode for Aqueous Al-Ion Battery. *ACS Appl. Mater. Interfaces* **2019**, *11*, 41356–41362. [CrossRef]
25. Hu, L.; Zeng, X.; Wei, X.; Wang, H.; Wu, Y.; Gu, W.; Shi, L.; Zhu, C. Interface Engineering for Enhancing Electrocatalytic Oxygen Evolution of NiFe LDH/NiTe Heterostructures. *Appl. Catal. B Environ.* **2020**, *273*, 119014. [CrossRef]
26. Feng, W.; Yuan, J.; Gao, F.; Weng, B.; Hu, W.; Lei, Y.; Huang, X.; Yang, L.; Shen, J.; Xu, D.; et al. Piezopotential-Driven Simulated Electrocatalytic Nanosystem of Ultrasmall MoC Quantum Dots Encapsulated in Ultrathin N-Doped Graphene Vesicles for Superhigh H2 Production from Pure Water. *Nano Energy* **2020**, *75*, 104990. [CrossRef]
27. Lazar, V.; Saviuc, C.-M.; Chifiriuc, M.C. Periodontitis and Periodontal Disease-Innovative Strategies for Reversing the Chronic Infectious and Inflammatory Condition by Natural Products. *Curr. Pharm. Des.* **2016**, *22*, 230–237. [CrossRef]
28. Samuels, N.; Grbic, J.T.; Saffer, A.J.; Wexler, I.D.; Williams, R.C. Effect of an Herbal Mouth Rinse in Preventing Periodontal Inflammation in an Experimental Gingivitis Model: A Pilot Study. *Compend. Contin. Educ. Dent.* **2012**, *33*, 204–206, 208–211.
29. Witt, J.J.; Walters, P.; Bsoul, S.; Gibb, R.; Dunavent, J.; Putt, M. Comparative Clinical Trial of Two Antigingivitis Mouthrinses. *Am. J. Dent.* **2005**, *18*, 15A–17A.
30. Carabotti, M.; Scirocco, A.; Maselli, M.A.; Severi, C. The Gut-Brain Axis: Interactions between Enteric Microbiota, Central and Enteric Nervous Systems. *Ann. Gastroenterol.* **2015**, *28*, 203–209.
31. Amruthesh, S. Dentistry and Ayurveda-III (Basics-Ama, Immunity, Ojas, Rasas, Etiopathogenesis and Prevention). *Indian J. Dent. Res.* **2007**, *18*, 112–119. [CrossRef] [PubMed]
32. Amruthesh, S. Dentistry and Ayurveda-IV: Classification and Management of Common Oral Diseases. *Indian J. Dent. Res.* **2008**, *19*, 52–61. [CrossRef] [PubMed]
33. Wiseman, M. Palliative Care Dentistry: Focusing on Quality of Life. *Compend. Contin. Educ. Dent.* **2017**, *38*, 529–534; quiz 535. [PubMed]
34. Breijyeh, Z.; Karaman, R. Antibacterial Activity of Medicinal Plants and Their Role in Wound Healing. *Future J. Pharm. Sci.* **2024**, *10*, 68. [CrossRef]
35. Obodozie, O.O. Pharmacokinetics and Drug Interactions of Herbal Medicines: A Missing Critical Step in the Phytomedicine/Drug Development Process. In *Readings in Advanced Pharmacokinetics-Theory, Methods and Applications*; IntechOpen: London, UK, 2012; ISBN 978-953-51-0533-6.
36. Gargiulo Isacco, C.; Ballini, A.; De Vito, D.; Michele Inchingolo, A.; Cantore, S.; Paduanelli, G.; Cao Diem Nguyen, K.; Danilo Inchingolo, A.; Dipalma, G.; Inchingolo, F. Probiotics in Health and Immunity: A First Step toward Understanding the Importance of Microbiota System in Translational Medicine. In *Prebiotics and Probiotics-Potential Benefits in Nutrition and Health*; Franco-Robles, E., Ramírez-Emiliano, J., Eds.; IntechOpen: London, UK, 2020; ISBN 978-1-78985-921-8.
37. Campanella, V.; Syed, J.; Santacroce, L.; Saini, R.; Ballini, A.; Inchingolo, F. Oral Probiotics Influence Oral and Respiratory Tract Infections in Pediatric Population: A Randomized Double-Blinded Placebo-Controlled Pilot Study. *Eur. Rev. Med. Pharmacol. Sci.* **2018**, *22*, 8034–8041. [CrossRef]
38. Casu, C.; Mosaico, G.; Natoli, V.; Scarano, A.; Lorusso, F.; Inchingolo, F. Microbiota of the Tongue and Systemic Connections: The Examination of the Tongue as an Integrated Approach in Oral Medicine. *Hygiene* **2021**, *1*, 56–68. [CrossRef]
39. Atanasov, A.G.; Waltenberger, B.; Pferschy-Wenzig, E.-M.; Linder, T.; Wawrosch, C.; Uhrin, P.; Temml, V.; Wang, L.; Schwaiger, S.; Heiss, E.H.; et al. Discovery and Resupply of Pharmacologically Active Plant-Derived Natural Products: A Review. *Biotechnol. Adv.* **2015**, *33*, 1582–1614. [CrossRef]

40. Shikov, A.N.; Mikhailovskaya, I.Y.; Narkevich, I.A.; Flisyuk, E.V.; Pozharitskaya, O.N. Chapter 35-Methods of Extraction of Medicinal Plants. In *Evidence-Based Validation of Herbal Medicine*, 2nd ed.; Mukherjee, P.K., Ed.; Elsevier: Amsterdam, The Netherlands, 2022; pp. 771–796. ISBN 978-0-323-85542-6.
41. Bisht, A.; Sahu, S.C.; Kumar, A.; Maqsood, S.; Barwant, M.M.; Jaiswal, S.G. Recent Advances in Conventional and Innovative Extraction Techniques for Recovery of High-Added Value Compounds for Food Additives and Nutraceuticals. *Food Physics* **2025**, *2*, 100047. [CrossRef]
42. Wachtel-Galor, S.; Benzie, I.F.F. Herbal Medicine: An Introduction to Its History, Usage, Regulation, Current Trends, and Research Needs. In *Herbal Medicine: Biomolecular and Clinical Aspects*; Benzie, I.F.F., Wachtel-Galor, S., Eds.; CRC Press/Taylor & Francis: Boca Raton, FL, USA, 2011; ISBN 978-1-4398-0713-2.
43. McCurdy, C.R.; Scully, S.S. Analgesic Substances Derived from Natural Products (Natureceuticals). *Life Sci.* **2005**, *78*, 476–484. [CrossRef]
44. Villa, F.A.; Gerwick, L. Marine Natural Product Drug Discovery: Leads for Treatment of Inflammation, Cancer, Infections, and Neurological Disorders. *Immunopharmacol. Immunotoxicol.* **2010**, *32*, 228–237. [CrossRef]
45. Kumar, A.; Nirmal, P.; Kumar, M.; Jose, A.; Tomer, V.; Oz, E.; Proestos, C.; Zeng, M.; Elobeid, T.; Sneha, K.; et al. Major Phytochemicals: Recent Advances in Health Benefits and Extraction Method. *Molecules* **2023**, *28*, 887. [CrossRef] [PubMed]
46. Rusu, M.E.; Gheldiu, A.-M.; Mocan, A.; Moldovan, C.; Popa, D.-S.; Tomuta, I.; Vlase, L. Process Optimization for Improved Phenolic Compounds Recovery from Walnut (Juglans Regia L.) Septum: Phytochemical Profile and Biological Activities. *Molecules* **2018**, *23*, 2814. [CrossRef] [PubMed]
47. Pop, A.; Fizeșan, I.; Vlase, L.; Rusu, M.E.; Cherfan, J.; Babota, M.; Gheldiu, A.-M.; Tomuta, I.; Popa, D.-S. Enhanced Recovery of Phenolic and Tocopherolic Compounds from Walnut (Juglans Regia L.) Male Flowers Based on Process Optimization of Ultrasonic Assisted-Extraction: Phytochemical Profile and Biological Activities. *Antioxidants* **2021**, *10*, 607. [CrossRef] [PubMed]
48. Corriero, A.; Giglio, M.; Soloperto, R.; Inchingolo, F.; Varrassi, G.; Puntillo, F. Microbial Symphony: Exploring the Role of the Gut in Osteoarthritis-Related Pain. A Narrative Review. *Pain. Ther.* **2024**, *13*, 409–433. [CrossRef]
49. Malhotra, R.; Grover, V.; Kapoor, A.; Saxena, D. Comparison of the Effectiveness of a Commercially Available Herbal Mouthrinse with Chlorhexidine Gluconate at the Clinical and Patient Level. *J. Indian Soc. Periodontol.* **2011**, *15*, 349–352. [CrossRef]
50. Singh, A.; Daing, A.; Dixit, J. The Effect of Herbal, Essential Oil and Chlorhexidine Mouthrinse on de Novo Plaque Formation. *Int. J. Dent. Hyg.* **2013**, *11*, 48–52. [CrossRef]
51. Kanu, J.E.; Soldera, J. Treatment of Helicobacter Pylori with Potassium Competitive Acid Blockers: A Systematic Review and Meta-Analysis. *World J. Gastroenterol.* **2024**, *30*, 1213–1223. [CrossRef]
52. Santacroce, L.; Sardaro, N.; Topi, S.; Pettini, F.; Bottalico, L.; Cantore, S.; Cascella, G.; Del Prete, R.; Dipalma, G.; Inchingolo, F. The Pivotal Role of Oral Microbiota in Health and Disease. *J. Biol. Regul. Homeost. Agents* **2020**, *34*, 733–737. [CrossRef]
53. Pacifici, A.; Pacifici, L.; Nuzzolese, M.; Cascella, G.; Ballini, A.; Santacroce, L.; Dipalma, G.; Aiello, E.; Amantea, M.; Saini, R.; et al. The Alteration of Stress-Related Physiological Parameters after Probiotics Administration in Oral Surgeons with Different Degrees of Surgical Experience. *Clin. Ter.* **2020**, *171*, e197–e208. [CrossRef]
54. Matsumoto, H.; Shiotani, A.; Katsumata, R.; Fujita, M.; Nakato, R.; Murao, T.; Ishii, M.; Kamada, T.; Haruma, K.; Graham, D.Y. Helicobacter Pylori Eradication with Proton Pump Inhibitors or Potassium-Competitive Acid Blockers: The Effect of Clarithromycin Resistance. *Dig. Dis. Sci.* **2016**, *61*, 3215–3220. [CrossRef]
55. Inchingolo, F.; Santacroce, L.; Cantore, S.; Ballini, A.; Del Prete, R.; Topi, S.; Saini, R.; Dipalma, G.; Arrigoni, R. Probiotics and EpiCor® in Human Health. *J. Biol. Regul. Homeost. Agents* **2019**, *33*, 1973–1979. [CrossRef] [PubMed]
56. Ballini, A.; Cantore, S.; Saini, R.; Pettini, F.; Fotopoulou, E.A.; Saini, S.R.; Georgakopoulos, I.P.; Dipalma, G.; Gargiulo Isacco, C.; Inchingolo, F. Effect of Activated Charcoal Probiotic Toothpaste Containing Lactobacillus Paracasei and Xylitol on Dental Caries: A Randomized and Controlled Clinical Trial. *J. Biol. Regul. Homeost. Agents* **2019**, *33*, 977–981. [PubMed]
57. Cantore, S.; Ballini, A.; De Vito, D.; Abbinante, A.; Altini, V.; Dipalma, G.; Inchingolo, F.; Saini, R. Clinical Results of Improvement in Periodontal Condition by Administration of Oral Probiotics. *J. Biol. Regul. Homeost. Agents* **2018**, *32*, 1329–1334. [PubMed]
58. Takkella, B.K.; Venkata Anusha, N.; Lokanathan Balaji, D.; Prabhat, M.V.; Sarat, G.; Polepalle, T.; Naffizuddin, M.; Ramsunil, C.; Sujana, V.; Chaitanya Krishna, T. The Comparison of the Anti-Inflammatory Efficacy of Phytochemical Extracts in Punica Granatum and Lawsonia Inermis Among Patients Diagnosed With Chronic Periodontitis. *Cureus* **2023**, *15*, e47557. [CrossRef] [PubMed]
59. Ballini, A.; Cantore, S.; Scacco, S.; Perillo, L.; Scarano, A.; Aityan, S.K.; Contaldo, M.; Cd Nguyen, K.; Santacroce, L.; Syed, J.; et al. A Comparative Study on Different Stemness Gene Expression between Dental Pulp Stem Cells vs. Dental Bud Stem Cells. *Eur. Rev. Med. Pharmacol. Sci.* **2019**, *23*, 1626–1633. [CrossRef]
60. Contaldo, M.; Lajolo, C.; Di Petrillo, M.; Ballini, A.; Inchingolo, F.; Serpico, R.; Romano, A. Analysis of Lip Pigmentations by Reflectance Confocal Microscopy: Report of Two Cases. *J. Biol. Regul. Homeost. Agents* **2019**, *33*, 19–25, DENTAL SUPPLEMENT.
61. Inchingolo, A.M.; Patano, A.; De Santis, M.; Del Vecchio, G.; Ferrante, L.; Morolla, R.; Pezzolla, C.; Sardano, R.; Dongiovanni, L.; Inchingolo, F.; et al. Comparison of Different Types of Palatal Expanders: Scoping Review. *Children* **2023**, *10*, 1258. [CrossRef]

62. Neukirch, H.; D'Ambrosio, M.; Dalla Via, J.; Guerriero, A. Simultaneous Quantitative Determination of Eight Triterpenoid Monoesters from Flowers of 10 Varieties of Calendula Officinalis L. and Characterisation of a New Triterpenoid Monoester. *Phytochem. Anal.* **2004**, *15*, 30–35. [CrossRef]
63. Youl, O.; Konaté, S.; Sombié, E.N.; Boly, R.; Kaboré, B.; Koala, M.; Zoungrana, A.; Savadogo, S.; Tahita, C.M.; Valea, I.; et al. Phytochemical Analysis and Antimicrobial Activity of *Lawsonia Inermis* Leaf Extracts from Burkina Faso. *Am. J. Plant Sci.* **2024**, *15*, 552–576. [CrossRef]
64. Hossain, T.J. Methods for Screening and Evaluation of Antimicrobial Activity: A Review of Protocols, Advantages, and Limitations. *Eur. J. Microbiol. Immunol. (Bp)* **2024**, *14*, 97–115. [CrossRef]
65. Lima, P.G.; Oliveira, J.T.A.; Amaral, J.L.; Freitas, C.D.T.; Souza, P.F.N. Synthetic Antimicrobial Peptides: Characteristics, Design, and Potential as Alternative Molecules to Overcome Microbial Resistance. *Life Sci.* **2021**, *278*, 119647. [CrossRef] [PubMed]
66. Chen, Z.; Yang, X.; Liu, Z.; Zeng, L.; Lee, W.; Zhang, Y. Two Novel Families of Antimicrobial Peptides from Skin Secretions of the Chinese Torrent Frog, Amolops Jingdongensis. *Biochimie* **2012**, *94*, 328–334. [CrossRef] [PubMed]
67. De Vrese, M.; Schrezenmeir, J. Probiotics, Prebiotics, and Synbiotics. *Adv. Biochem. Eng. Biotechnol.* **2008**, *111*, 1–66. [CrossRef] [PubMed]
68. Mahyari, S.; Mahyari, B.; Emami, S.A.; Malaekeh-Nikouei, B.; Jahanbakhsh, S.P.; Sahebkar, A.; Mohammadpour, A.H. Evaluation of the Efficacy of a Polyherbal Mouthwash Containing Zingiber Officinale, Rosmarinus Officinalis and Calendula Officinalis Extracts in Patients with Gingivitis: A Randomized Double-Blind Placebo-Controlled Trial. *Complement. Ther. Clin. Pract.* **2016**, *22*, 93–98. [CrossRef] [PubMed]
69. Batista, D.G.; Sganzerla, W.G.; da Silva, L.R.; Vieira, Y.G.S.; Almeida, A.R.; Dominguini, D.; Ceretta, L.; Pinheiro, A.C.; Bertoldi, F.C.; Becker, D.; et al. Antimicrobial and Cytotoxic Potential of Eucalyptus Essential Oil-Based Nanoemulsions for Mouthwashes Application. *Antibiotics* **2024**, *13*, 942. [CrossRef]
70. Kim, T.-H.; Heo, S.-Y.; Chandika, P.; Kim, Y.-M.; Kim, H.-W.; Kang, H.W.; Je, J.-Y.; Qian, Z.-J.; Kim, N.; Jung, W.-K. A Literature Review of Bioactive Substances for the Treatment of Periodontitis: In Vitro, in Vivo and Clinical Studies. *Heliyon* **2024**, *10*, e24216. [CrossRef]
71. Inchingolo, A.D.; Inchingolo, A.M.; Malcangi, G.; Avantario, P.; Azzollini, D.; Buongiorno, S.; Viapiano, F.; Campanelli, M.; Ciocia, A.M.; De Leonardis, N.; et al. Effects of Resveratrol, Curcumin and Quercetin Supplementation on Bone Metabolism-A Systematic Review. *Nutrients* **2022**, *14*, 3519. [CrossRef]
72. De Gabriele, O.; Dallatana, G.; Riva, R.; Vasudavan, S.; Wilmes, B. The Easy Driver for Placement of Palatal Mini-Implants and a Maxillary Expander in a Single Appointment. *J. Clin. Orthod.* **2017**, *51*, 728–737.
73. Wink, M. Modes of Action of Herbal Medicines and Plant Secondary Metabolites. *Medicines* **2015**, *2*, 251–286. [CrossRef]
74. Inchingolo, A.D.; Malcangi, G.; Inchingolo, A.M.; Piras, F.; Settanni, V.; Garofoli, G.; Palmieri, G.; Ceci, S.; Patano, A.; De Leonardis, N.; et al. Benefits and Implications of Resveratrol Supplementation on Microbiota Modulations: A Systematic Review of the Literature. *Int. J. Mol. Sci.* **2022**, *23*, 4027. [CrossRef]
75. Borsani, E.; Bonazza, V.; Buffoli, B.; Nocini, P.F.; Albanese, M.; Zotti, F.; Inchingolo, F.; Rezzani, R.; Rodella, L.F. Beneficial Effects of Concentrated Growth Factors and Resveratrol on Human Osteoblasts In Vitro Treated with Bisphosphonates. *BioMed Res. Int.* **2018**, *2018*, 1–13. [CrossRef] [PubMed]
76. Inchingolo, F.; Martelli, F.S.; Gargiulo Isacco, C.; Borsani, E.; Cantore, S.; Corcioli, F.; Boddi, A.; Nguyễn, K.C.D.; De Vito, D.; Aityan, S.K.; et al. Chronic Periodontitis and Immunity, Towards the Implementation of a Personalized Medicine: A Translational Research on Gene Single Nucleotide Polymorphisms (SNPs) Linked to Chronic Oral Dysbiosis in 96 Caucasian Patients. *Biomedicines* **2020**, *8*, 115. [CrossRef] [PubMed]
77. Babaee, N.; Moslemi, D.; Khalilpour, M.; Vejdani, F.; Moghadamnia, Y.; Bijani, A.; Baradaran, M.; Kazemi, M.T.; Khalilpour, A.; Pouramir, M.; et al. Antioxidant Capacity of Calendula Officinalis Flowers Extract and Prevention of Radiation Induced Oropharyngeal Mucositis in Patients with Head and Neck Cancers: A Randomized Controlled Clinical Study. *Daru* **2013**, *21*, 18. [CrossRef] [PubMed]
78. Valero-Mendoza, A.G.; Meléndez-Rentería, N.P.; Chávez-González, M.L.; Flores-Gallegos, A.C.; Wong-Paz, J.E.; Govea-Salas, M.; Zugasti-Cruz, A.; Ascacio-Valdés, J.A. The Whole Pomegranate (*Punica granatum*. L.), Biological Properties and Important Findings: A Review. *Food Chem. Adv.* **2023**, *2*, 100153. [CrossRef]
79. Siddiqui, S.A.; Singh, S.; Nayik, G.A. Bioactive Compounds from Pomegranate Peels-Biological Properties, Structure–Function Relationships, Health Benefits and Food Applications–A Comprehensive Review. *J. Funct. Foods* **2024**, *116*, 106132. [CrossRef]
80. Luzardo-Ocampo, I.; Rebollo-Hernanz, M. Journal of Functional Foods Special Issue: Phenolic Compounds and Their Impact on the Gut-Brain Axis. *J. Funct. Foods* **2024**, *116*, 106171. [CrossRef]
81. Oudmaijer, C.A.J.; de Bruin, R.W.F.; Ooms, L.S.S.; Selten, J.W.; van Straalen, E.; Ambagtsheer, G.; Terkivatan, T.; IJzermans, J.N.M. Preoperative Dietary Intake of Low-Dose Sulforaphane Induces No Clinically Significant Effect in Living Donor Kidney Transplantation. *J. Funct. Foods* **2024**, *116*, 106161. [CrossRef]

82. Bai, N.; He, K.; Roller, M.; Lai, C.-S.; Shao, X.; Pan, M.-H.; Ho, C.-T. Flavonoids and Phenolic Compounds from Rosmarinus Officinalis. *J. Agric. Food Chem.* **2010**, *58*, 5363–5367. [CrossRef]
83. He, X.; Liu, R.H. Phytochemicals of Apple Peels: Isolation, Structure Elucidation, and Their Antiproliferative and Antioxidant Activities. *J. Agric. Food Chem.* **2008**, *56*, 9905–9910. [CrossRef]
84. He, X.; Liu, R.H. Cranberry Phytochemicals: Isolation, Structure Elucidation, and Their Antiproliferative and Antioxidant Activities. *J. Agric. Food Chem.* **2006**, *54*, 7069–7074. [CrossRef]
85. Dong, M.; He, X.; Liu, R.H. Phytochemicals of Black Bean Seed Coats: Isolation, Structure Elucidation, and Their Antiproliferative and Antioxidative Activities. *J. Agric. Food Chem.* **2007**, *55*, 6044–6051. [CrossRef] [PubMed]
86. Inchingolo, A.D.; Cazzolla, A.P.; Di Cosola, M.; Greco Lucchina, A.; Santacroce, L.; Charitos, I.A.; Topi, S.; Malcangi, G.; Hazballa, D.; Scarano, A.; et al. The Integumentary System and Its Microbiota between Health and Disease. *J. Biol. Regul. Homeost. Agents* **2021**, *35*, 303–321. [CrossRef] [PubMed]
87. Xutian, S.; Zhang, J.; Louise, W. New Exploration and Understanding of Traditional Chinese Medicine. *Am. J. Chin. Med.* **2009**, *37*, 411–426. [CrossRef] [PubMed]
88. Lin, D.; Fu, X.; Li, B.; Huo, Y.; Xie, M.; Li, T.; Zhu, P.; Li, G.; Huang, F. Integrating Untargeted and Oxylipins-Targeted Metabolomics to Reveal the Anti-Obesity and Hypolipidemic Mechanism of Conjugated Linoleic Acid in High-Fat Diet Rats. *J. Funct. Foods* **2024**, *116*, 106182. [CrossRef]
89. Zeng, J.; Xu, C.; Chen, L.; Li, M.; Yang, J.; Nie, L.; Zhang, M.; Zhang, X.; Zhang, E. Anti-Glioma Effect of *Buthus Martensii Karsch* (*BmK*) Scorpion by Inhibiting Myeloid-Derived Suppressor Cells and Activating T Cells in Tumor Microenvironment. *J. Funct. Foods* **2024**, *116*, 106163. [CrossRef]
90. D'Ambrosio, M.; Bigagli, E.; Cinci, L.; Cipriani, G.; Niccolai, A.; Biondi, N.; Rodolfi, L.; Zambelli, F.; Gencarelli, M.; Laurino, A.; et al. *Arthrospira platensis* F&M-C265 Reduces Cardiometabolic Risk Factors in Rats Fed a High Fat Diet. *J. Funct. Foods* **2024**, *116*, 106150. [CrossRef]
91. Li, Z.; Wang, H.; Sun, S.; Shao, Z.; Lv, C.; Dong, X.; Wang, L.; Wang, W. Ellagitannins from Pomegranate (*Punica Granatum* L.) Flower with Xanthine Oxidase and α-Glucosidase Inhibitory Activities. *J. Funct. Foods* **2024**, *116*, 106153. [CrossRef]
92. Xu, Y.; Zhang, H.; Yang, H.; Liu, C.; Song, C.; Cheng, Y.; He, C.; Zou, Z.; Zhou, D.; Wu, G.; et al. Eicosapentaenoic Acid and Docosahexaenoic Acid Suppress Colonic Tumorigenesis in Obese Mice. *J. Funct. Foods* **2024**, *116*, 106164. [CrossRef]
93. Gargiulo Isacco, C.; Inchingolo, A.D.; Nguyen Cao, K.D.; Malcangi, G.; Paduanelli, G.; Pham Hung, V.; Tran Cong, T.; Bordea, I.R.; Scarano, A.; Laforgia, A.; et al. The Bad Relationship, Osteo-Decay and Diabetes Type 2 Searching for a Link: A Literature Review. *J. Biol. Regul. Homeost. Agents* **2021**, *35*, 253–269. [CrossRef]
94. Di Cosola, M.; Cazzolla, A.P.; Charitos, I.A.; Ballini, A.; Inchingolo, F.; Santacroce, L. Candida Albicans and Oral Carcinogenesis. A Brief Review. *J Fungi* **2021**, *7*, 476. [CrossRef]
95. Gargiulo Isacco, C.; Balzanelli, M.G.; Garzone, S.; Lorusso, M.; Inchingolo, F.; Nguyen, K.C.D.; Santacroce, L.; Mosca, A.; Del Prete, R. Alterations of Vaginal Microbiota and Chlamydia Trachomatis as Crucial Co-Causative Factors in Cervical Cancer Genesis Procured by HPV. *Microorganisms* **2023**, *11*, 662. [CrossRef] [PubMed]
96. Sharma, G.; Garg, N.; Hasan, S.; Shirodkar, S. Prevotella: An Insight into Its Characteristics and Associated Virulence Factors. *Microb. Pathog.* **2022**, *169*, 105673. [CrossRef] [PubMed]
97. Ye, X.; Paul, B.; Mo, J.; Reynolds, E.C.; Ghosal, D.; Veith, P.D. Ultrastructural and Glycoproteomic Characterization of Prevotella Intermedia: Insights into O-glycosylation and Outer Membrane Vesicles. *Microbiologyopen* **2024**, *13*, e1401. [CrossRef] [PubMed]
98. Hashimoto, M.; Asai, Y.; Tamai, R.; Jinno, T.; Umatani, K.; Ogawa, T. Chemical Structure and Immunobiological Activity of Lipid A from Prevotella Intermedia ATCC 25611 Lipopolysaccharide. *FEBS Lett.* **2003**, *543*, 98–102. [CrossRef]
99. Sawada, N.; Ogawa, T.; Asai, Y.; Makimura, Y.; Sugiyama, A. Toll-like Receptor 4-Dependent Recognition of Structurally Different Forms of Chemically Synthesized Lipid As of Porphyromonas Gingivalis. *Clin. Exp. Immunol.* **2007**, *148*, 529–536. [CrossRef]
100. Kumada, H.; Haishima, Y.; Watanabe, K.; Hasegawa, C.; Tsuchiya, T.; Tanamoto, K.; Umemoto, T. Biological Properties of the Native and Synthetic Lipid A of Porphyromonas Gingivalis Lipopolysaccharide. *Oral. Microbiol. Immunol.* **2008**, *23*, 60–69. [CrossRef]
101. Tanamoto, K.; Azumi, S.; Haishima, Y.; Kumada, H.; Umemoto, T. The Lipid A Moiety of Porphyromonas Gingivalis Lipopolysaccharide Specifically Mediates the Activation of C3H/HeJ Mice. *J. Immunol.* **1997**, *158*, 4430–4436. [CrossRef]
102. Darveau, R.P.; Pham, T.-T.T.; Lemley, K.; Reife, R.A.; Bainbridge, B.W.; Coats, S.R.; Howald, W.N.; Way, S.S.; Hajjar, A.M. Porphyromonas Gingivalis Lipopolysaccharide Contains Multiple Lipid A Species That Functionally Interact with Both Toll-like Receptors 2 and 4. *Infect. Immun.* **2004**, *72*, 5041–5051. [CrossRef]
103. West, T.E.; Ernst, R.K.; Jansson-Hutson, M.J.; Skerrett, S.J. Activation of Toll-like Receptors by Burkholderia Pseudomallei. *BMC Immunol.* **2008**, *9*, 46. [CrossRef]
104. Sengyee, S.; Yoon, S.H.; Paksanont, S.; Yimthin, T.; Wuthiekanun, V.; Limmathurotsakul, D.; West, T.E.; Ernst, R.K.; Chantratita, N. Comprehensive Analysis of Clinical Burkholderia Pseudomallei Isolates Demonstrates Conservation of Unique Lipid A Structure and TLR4-Dependent Innate Immune Activation. *PLoS Negl. Trop. Dis.* **2018**, *12*, e0006287. [CrossRef]

105. Sengyee, S.; Yoon, S.H.; West, T.E.; Ernst, R.K.; Chantratita, N. Lipopolysaccharides from Different Burkholderia Species with Different Lipid A Structures Induce Toll-Like Receptor 4 Activation and React with Melioidosis Patient Sera. *Infect. Immun.* **2019**, *87*, e00692-19. [CrossRef] [PubMed]
106. Contaldo, M.; Boccellino, M.; Zannini, G.; Romano, A.; Sciarra, A.; Sacco, A.; Settembre, G.; Coppola, M.; Di Carlo, A.; D'Angelo, L.; et al. Sex Hormones and Inflammation Role in Oral Cancer Progression: A Molecular and Biological Point of View. *J. Oncol.* **2020**, *2020*, 9587971. [CrossRef] [PubMed]
107. Della Loggia, R.; Tubaro, A.; Sosa, S.; Becker, H.; Saar, S.; Isaac, O. The Role of Triterpenoids in the Topical Anti-Inflammatory Activity of Calendula Officinalis Flowers. *Planta Med.* **1994**, *60*, 516–520. [CrossRef] [PubMed]
108. Neukirch, H.; D'Ambrosio, M.; Sosa, S.; Altinier, G.; Della Loggia, R.; Guerriero, A. Improved Anti-Inflammatory Activity of Three New Terpenoids Derived, by Systematic Chemical Modifications, from the Abundant Triterpenes of the Flowery Plant Calendula Officinalis. *Chem. Biodivers.* **2005**, *2*, 657–671. [CrossRef] [PubMed]
109. Aghamohammadi, A.; Moslemi, D.; Akbari, J.; Ghasemi, A.; Azadbakht, M.; Asgharpour, A.; Hosseinimehr, S.J. The Effectiveness of Zataria Extract Mouthwash for the Management of Radiation-Induced Oral Mucositis in Patients: A Randomized Placebo-Controlled Double-Blind Study. *Clin. Oral. Investig.* **2018**, *22*, 2263–2272. [CrossRef]
110. Maier, T. Oral Microbiome in Health and Disease: Maintaining a Healthy, Balanced Ecosystem and Reversing Dysbiosis. *Microorganisms* **2023**, *11*, 1453. [CrossRef]
111. Kilian, M.; Chapple, I.L.C.; Hannig, M.; Marsh, P.D.; Meuric, V.; Pedersen, A.M.L.; Tonetti, M.S.; Wade, W.G.; Zaura, E. The Oral Microbiome-an Update for Oral Healthcare Professionals. *Br. Dent. J.* **2016**, *221*, 657–666. [CrossRef]
112. Pathak, J.L.; Yan, Y.; Zhang, Q.; Wang, L.; Ge, L. The Role of Oral Microbiome in Respiratory Health and Diseases. *Respir. Med.* **2021**, *185*, 106475. [CrossRef]
113. Yen, S.-H.; Wang, L.-W.; Lin, Y.-H.; Jen, Y.-M.; Chung, Y.-L. Phenylbutyrate Mouthwash Mitigates Oral Mucositis during Radiotherapy or Chemoradiotherapy in Patients with Head-and-Neck Cancer. *Int. J. Radiat. Oncol. Biol. Phys.* **2012**, *82*, 1463–1470. [CrossRef]
114. Ertekin, M.V.; Koç, M.; Karslioglu, I.; Sezen, O. Zinc Sulfate in the Prevention of Radiation-Induced Oropharyngeal Mucositis: A Prospective, Placebo-Controlled, Randomized Study. *Int. J. Radiat. Oncol. Biol. Phys.* **2004**, *58*, 167–174. [CrossRef]
115. Jiang, C.; Wang, H.; Xia, C.; Dong, Q.; Chen, E.; Qiu, Y.; Su, Y.; Xie, H.; Zeng, L.; Kuang, J.; et al. A Randomized, Double-Blind, Placebo-Controlled Trial of Probiotics to Reduce the Severity of Oral Mucositis Induced by Chemoradiotherapy for Patients with Nasopharyngeal Carcinoma. *Cancer* **2019**, *125*, 1081–1090. [CrossRef] [PubMed]
116. Wu, H.G.; Song, S.Y.; Kim, Y.S.; Oh, Y.T.; Lee, C.G.; Keum, K.C.; Ahn, Y.C.; Lee, S. Therapeutic Effect of Recombinant Human Epidermal Growth Factor (RhEGF) on Mucositis in Patients Undergoing Radiotherapy, with or without Chemotherapy, for Head and Neck Cancer: A Double-Blind Placebo-Controlled Prospective Phase 2 Multi-Institutional Clinical Trial. *Cancer* **2009**, *115*, 3699–3708. [CrossRef] [PubMed]
117. Mantovani, G.; Massa, E.; Astara, G.; Murgia, V.; Gramignano, G.; Lusso, M.R.; Camboni, P.; Ferreli, L.; Mocci, M.; Perboni, S.; et al. Phase II Clinical Trial of Local Use of GM-CSF for Prevention and Treatment of Chemotherapy- and Concomitant Chemoradiotherapy-Induced Severe Oral Mucositis in Advanced Head and Neck Cancer Patients: An Evaluation of Effectiveness, Safety and Costs. *Oncol. Rep.* **2003**, *10*, 197–206. [CrossRef]
118. Ryu, J.K.; Swann, S.; LeVeque, F.; Scarantino, C.W.; Johnson, D.; Chen, A.; Fortin, A.; Pollock, J.; Kim, H.; Ang, K.K. The Impact of Concurrent Granulocyte Macrophage-Colony Stimulating Factor on Radiation-Induced Mucositis in Head and Neck Cancer Patients: A Double-Blind Placebo-Controlled Prospective Phase III Study by Radiation Therapy Oncology Group 9901. *Int. J. Radiat. Oncol. Biol. Phys.* **2007**, *67*, 643–650. [CrossRef] [PubMed]
119. Veness, M.J.; Foroudi, F.; Gebski, V.; Timms, I.; Sathiyaseelan, Y.; Cakir, B.; Tiver, K.W. Use of Topical Misoprostol to Reduce Radiation-Induced Mucositis: Results of a Randomized, Double-Blind, Placebo-Controlled Trial. *Australas. Radiol.* **2006**, *50*, 468–474. [CrossRef]
120. Contaldo, M.; Luzzi, V.; Ierardo, G.; Raimondo, E.; Boccellino, M.; Ferati, K.; Bexheti-Ferati, A.; Inchingolo, F.; Di Domenico, M.; Serpico, R.; et al. Bisphosphonate-Related Osteonecrosis of the Jaws and Dental Surgery Procedures in Children and Young People with Osteogenesis Imperfecta: A Systematic Review. *J. Stomatol. Oral. Maxillofac. Surg.* **2020**, *121*, 556–562. [CrossRef]
121. Bernardi, S.; Mummolo, S.; Varvara, G.; Marchetti, E.; Continenza, M.A.; Marzo, G.; Macchiarelli, G. Bio-Morphological Evaluation of Periodontal Ligament Fibroblasts on Mineralized Dentin Graft: An in Vitro Study. *J. Biol. Regul. Homeost. Agents* **2019**, *33*, 275–280.
122. Su, C.K.; Mehta, V.; Ravikumar, L.; Shah, R.; Pinto, H.; Halpern, J.; Koong, A.; Goffinet, D.; Le, Q.-T. Phase II Double-Blind Randomized Study Comparing Oral Aloe Vera versus Placebo to Prevent Radiation-Related Mucositis in Patients with Head-and-Neck Neoplasms. *Int. J. Radiat. Oncol. Biol. Phys.* **2004**, *60*, 171–177. [CrossRef]
123. Inchingolo, A.D.; Di Cosola, M.; Inchingolo, A.M.; Greco Lucchina, A.; Malcangi, G.; Pettini, F.; Scarano, A.; Bordea, I.R.; Hazballa, D.; Lorusso, F.; et al. Correlation between Occlusal Trauma and Oral Microbiota: A Microbiological Investigation. *J. Biol. Regul. Homeost. Agents* **2021**, *35*, 295–302. [CrossRef]

124. Dipalma, G.; Inchingolo, A.D.; Inchingolo, F.; Charitos, I.A.; Di Cosola, M.; Cazzolla, A.P. Focus on the Cariogenic Process: Microbial and Biochemical Interactions with Teeth and Oral Environment. *J. Biol. Regul. Homeost. Agents* **2021**, *35*, 429–440. [CrossRef]
125. Sędzikowska, A.; Szablewski, L. Human Gut Microbiota in Health and Selected Cancers. *Int. J. Mol. Sci.* **2021**, *22*, 13440. [CrossRef] [PubMed]
126. Paraskevas, S.; Rosema, N.A.M.; Versteeg, P.; Van der Velden, U.; Van der Weijden, G.A. Chlorine Dioxide and Chlorhexidine Mouthrinses Compared in a 3-Day Plaque Accumulation Model. *J. Periodontol.* **2008**, *79*, 1395–1400. [CrossRef] [PubMed]
127. Li, Z.; Huang, Q.; Wang, Z.; Huang, L.; Gu, L. Effects of Porphyromonas Gingivalis and Aggregatibacter Actinomycetemcomitans on Modeling Subgingival Microbiome and Impairment of Oral Epithelial Barrier. *J. Infect. Dis.* **2024**, *229*, 262–272. [CrossRef] [PubMed]
128. Grover, V.; Kapoor, A.; Malhotra, R.; Battu, V.S.; Bhatia, A.; Sachdeva, S. To Assess the Effectiveness of a Chlorhexidine Chip in the Treatment of Chronic Periodontitis: A Clinical and Radiographic Study. *J. Indian Soc. Periodontol.* **2011**, *15*, 139–146. [CrossRef]
129. Jose, K.A.; Ambooken, M.; Mathew, J.J.; Issac, A.V.; Kunju, A.P.; Parameshwaran, R.A. Management of Chronic Periodontitis Using Chlorhexidine Chip and Diode Laser-A Clinical Study. *J. Clin. Diagn. Res.* **2016**, *10*, ZC76-80. [CrossRef]
130. Martínez-García, M.; Hernández-Lemus, E. Periodontal Inflammation and Systemic Diseases: An Overview. *Front. Physiol.* **2021**, *12*, 709438. [CrossRef]
131. Aarabi, G.; Zeller, T.; Seedorf, H.; Reissmann, D.R.; Heydecke, G.; Schaefer, A.S.; Seedorf, U. Genetic Susceptibility Contributing to Periodontal and Cardiovascular Disease. *J. Dent. Res.* **2017**, *96*, 610–617. [CrossRef]
132. Bochenek, G.; Häsler, R.; El Mokhtari, N.-E.; König, I.R.; Loos, B.G.; Jepsen, S.; Rosenstiel, P.; Schreiber, S.; Schaefer, A.S. The Large Non-Coding RNA ANRIL, Which Is Associated with Atherosclerosis, Periodontitis and Several Forms of Cancer, Regulates ADIPOR1, VAMP3 and C11ORF10. *Hum. Mol. Genet.* **2013**, *22*, 4516–4527. [CrossRef]
133. Schaefer, A.S.; Bochenek, G.; Jochens, A.; Ellinghaus, D.; Dommisch, H.; Güzeldemir-Akçakanat, E.; Graetz, C.; Harks, I.; Jockel-Schneider, Y.; Weinspach, K.; et al. Genetic Evidence for PLASMINOGEN as a Shared Genetic Risk Factor of Coronary Artery Disease and Periodontitis. *Circ. Cardiovasc. Genet.* **2015**, *8*, 159–167. [CrossRef]
134. Munz, M.; Chen, H.; Jockel-Schneider, Y.; Adam, K.; Hoffman, P.; Berger, K.; Kocher, T.; Meyle, J.; Eickholz, P.; Doerfer, C.; et al. A Haplotype Block Downstream of Plasminogen Is Associated with Chronic and Aggressive Periodontitis. *J. Clin. Periodontol.* **2017**, *44*, 962–970. [CrossRef]
135. Di Stefano, M.; Polizzi, A.; Santonocito, S.; Romano, A.; Lombardi, T.; Isola, G. Impact of Oral Microbiome in Periodontal Health and Periodontitis: A Critical Review on Prevention and Treatment. *Int. J. Mol. Sci.* **2022**, *23*, 5142. [CrossRef] [PubMed]
136. Hashim, A.; Alsam, A.; Payne, M.A.; Aduse-Opoku, J.; Curtis, M.A.; Joseph, S. Loss of Neutrophil Homing to the Periodontal Tissues Modulates the Composition and Disease Potential of the Oral Microbiota. *Infect. Immun.* **2021**, *89*, e0030921. [CrossRef] [PubMed]
137. Curtis, M.A.; Diaz, P.I.; Van Dyke, T.E. The Role of the Microbiota in Periodontal Disease. *Periodontol. 2000* **2020**, *83*, 14–25. [CrossRef] [PubMed]
138. Kinane, D.F. Causation and Pathogenesis of Periodontal Disease. *Periodontol. 2000* **2001**, *25*, 8–20. [CrossRef]
139. Magnusson, I.; Runstad, L.; Nyman, S.; Lindhe, J. A Long Junctional Epithelium—A Locus Minoris Resistentiae in Plaque Infection? *J. Clin. Periodontol.* **1983**, *10*, 333–340. [CrossRef]
140. Wennström, J.; Lindhe, J.; Nyman, S. The Role of Keratinized Gingiva in Plaque-Associated Gingivitis in Dogs. *J. Clin. Periodontol.* **1982**, *9*, 75–85. [CrossRef]
141. Hadavi, F.; Caffesse, R.G.; Charbeneau, G.T. A Study of the Gingival Response to Polished and Unpolished Amalgam Restorations. *J. Can. Dent. Assoc.* **1986**, *52*, 211–214.
142. Smales, R.J.; Nixon, K.C.; Joyce, K.P. Effects of Subgingival Restorations in Beagle Dogs. Part II: Gingivitis. *J. Prosthet. Dent.* **1979**, *41*, 522–527. [CrossRef]
143. Konradsson, K.; van Dijken, J.W.V. Effect of a Novel Ceramic Filling Material on Plaque Formation and Marginal Gingiva. *Acta Odontol. Scand.* **2002**, *60*, 370–374. [CrossRef]
144. van Dijken, J.W.; Sjöström, S. The Effect of Glass Ionomer Cement and Composite Resin Fillings on Marginal Gingiva. *J. Clin. Periodontol.* **1991**, *18*, 200–203. [CrossRef]
145. Van Dijken, J.W.; Sjöström, S.; Wing, K. The Effect of Different Types of Composite Resin Fillings on Marginal Gingiva. *J. Clin. Periodontol.* **1987**, *14*, 185–189. [CrossRef] [PubMed]
146. Heintze, S.D.; Rousson, V.; Hickel, R. Clinical Effectiveness of Direct Anterior Restorations—A Meta-Analysis. *Dent. Mater.* **2015**, *31*, 481–495. [CrossRef] [PubMed]
147. Hrishi, T.S.; Kundapur, P.P.; Naha, A.; Thomas, B.S.; Kamath, S.; Bhat, G.S. Effect of Adjunctive Use of Green Tea Dentifrice in Periodontitis Patients-A Randomized Controlled Pilot Study. *Int. J. Dent. Hyg.* **2016**, *14*, 178–183. [CrossRef] [PubMed]
148. Simpson, J. Does the Adjunctive Use of Green Tea Improve Periodontal Indices in Patients Undergoing Non-Surgical Periodontal Treatment? *BDJ Team* **2022**, *9*, 10–13. [CrossRef]

149. Mazur, M.; Ndokaj, A.; Jedlinski, M.; Ardan, R.; Bietolini, S.; Ottolenghi, L. Impact of Green Tea (*Camellia sinensis*) on Periodontitis and Caries. Systematic Review and Meta-Analysis. *Jpn. Dent. Sci. Rev.* **2021**, *57*, 1–11. [CrossRef]
150. Kushiyama, M.; Shimazaki, Y.; Murakami, M.; Yamashita, Y. Relationship Between Intake of Green Tea and Periodontal Disease. *J. Periodontol.* **2009**, *80*, 372–377. [CrossRef]
151. Clarke, N.G.; Hirsch, R.S. Personal Risk Factors for Generalized Periodontitis. *J. Clin. Periodontol.* **1995**, *22*, 136–145. [CrossRef]
152. Wolff, L.; Dahlén, G.; Aeppli, D. Bacteria as Risk Markers for Periodontitis. *J. Periodontol.* **1994**, *65*, 498–510. [CrossRef]
153. Rattanasuwan, K.; Rassameemasmaung, S.; Sangalungkarn, V.; Komoltri, C. Clinical Effect of Locally Delivered Gel Containing Green Tea Extract as an Adjunct to Non-Surgical Periodontal Treatment. *Odontology* **2016**, *104*, 89–97. [CrossRef]
154. Pradeep, A.R.; Suke, D.K.; Martande, S.S.; Singh, S.P.; Nagpal, K.; Naik, S.B. Triphala, a New Herbal Mouthwash for the Treatment of Gingivitis: A Randomized Controlled Clinical Trial. *J. Periodontol.* **2016**, *87*, 1352–1359. [CrossRef]
155. Gunjal, S.; Pateel, D.G.S. Comparative Effectiveness of Propolis with Chlorhexidine Mouthwash on Gingivitis-a Randomized Controlled Clinical Study. *BMC Complement. Med. Ther.* **2024**, *24*, 154. [CrossRef] [PubMed]
156. Niazi, F.H.; Kamran, M.A.; Naseem, M.; AlShahrani, I.; Fraz, T.R.; Hosein, M. Anti-Plaque Efficacy of Herbal Mouthwashes Compared to Synthetic Mouthwashes in Patients Undergoing Orthodontic Treatment: A Randomised Controlled Trial. *Oral. Health Prev. Dent.* **2018**, *16*, 409–416. [CrossRef] [PubMed]
157. Sparabombe, S.; Monterubbianesi, R.; Tosco, V.; Orilisi, G.; Hosein, A.; Ferrante, L.; Putignano, A.; Orsini, G. Efficacy of an All-Natural Polyherbal Mouthwash in Patients With Periodontitis: A Single-Blind Randomized Controlled Trial. *Front. Physiol.* **2019**, *10*, 632. [CrossRef]
158. He, J.; Deng, Y.; Zhu, F.; Zhong, T.; Luo, N.; Lei, L.; Cheng, L.; Hu, T. The Efficacy and Safety of a Herbal Toothpaste in Reducing Gingivitis: A Double-Blind, Randomized, Placebo-Controlled, Parallel Allocation Clinical Trial. *Evid. Based Complement. Alternat Med.* **2019**, *2019*, 3764936. [CrossRef] [PubMed]
159. Cheng, L.; Liu, W.; Zhang, T.; Xu, T.; Shu, Y.-X.; Yuan, B.; Yang, Y.-M.; Hu, T. Evaluation of the Effect of a Toothpaste Containing Pudilan Extract on Inhibiting Plaques and Reducing Chronic Gingivitis: A Randomized, Double-Blinded, Parallel Controlled Clinical Trial. *J. Ethnopharmacol.* **2019**, *240*, 111870. [CrossRef]
160. Kharaeva, Z.F.; Mustafaev, M.S.; Khazhmetov, A.V.; Gazaev, I.H.; Blieva, L.Z.; Steiner, L.; Mayer, W.; Luca, C.D.; Korkina, L.G. Anti-Bacterial and Anti-Inflammatory Effects of Toothpaste with Swiss Medicinal Herbs towards Patients Suffering from Gingivitis and Initial Stage of Periodontitis: From Clinical Efficacy to Mechanisms. *Dent. J.* **2020**, *8*, 10. [CrossRef]
161. Kiger, R.D.; Nylund, K.; Feller, R.P. A Comparison of Proximal Plaque Removal Using Floss and Interdental Brushes. *J. Clin. Periodontol.* **1991**, *18*, 681–684. [CrossRef]
162. Bergenholtz, A.; Olsson, A. Efficacy of Plaque-Removal Using Interdental Brushes and Waxed Dental Floss. *Eur. J. Oral. Sci.* **1984**, *92*, 198–203. [CrossRef]
163. Graziani, F.; Palazzolo, A.; Gennai, S.; Karapetsa, D.; Giuca, M.; Cei, S.; Filice, N.; Petrini, M.; Nisi, M. Interdental Plaque Reduction after Use of Different Devices in Young Subjects with Intact Papilla: A Randomized Clinical Trial. *Int. J. Dent. Hyg.* **2018**, *16*, 389–396. [CrossRef]
164. Santacroce, L.; Inchingolo, F.; Topi, S.; Del Prete, R.; Di Cosola, M.; Charitos, I.A.; Montagnani, M. Potential Beneficial Role of Probiotics on the Outcome of COVID-19 Patients: An Evolving Perspective. *Diabetes Metab. Syndr.* **2021**, *15*, 295–301. [CrossRef]
165. Rayyan, M.; Terkawi, T.; Abdo, H.; Abdel Azim, D.; Khalaf, A.; AlKhouli, Z.; Meziad, M.; Alshamma'a, M.; Abu Naim, H. Efficacy of Grape Seed Extract Gel in the Treatment of Chronic Periodontitis: A Randomized Clinical Study. *J. Investig. Clin. Dent.* **2018**, *9*, e12318. [CrossRef] [PubMed]
166. Agarwal, E.; Pradeep, A.R.; Bajaj, P.; Naik, S.B. Efficacy of Local Drug Delivery of 0.5% Clarithromycin Gel as an Adjunct to Non-Surgical Periodontal Therapy in the Treatment of Current Smokers with Chronic Periodontitis: A Randomized Controlled Clinical Trial. *J. Periodontol.* **2012**, *83*, 1155–1163. [CrossRef] [PubMed]
167. Das, M.; Das, A.C.; Panda, S.; Greco Lucchina, A.; Mohanty, R.; Manfredi, B.; Rovati, M.; Giacomello, M.S.; Colletti, L.; Mortellaro, C.; et al. Clinical Efficacy of Grape Seed Extract as an Adjuvant to Scaling and Root Planing in Treatment of Periodontal Pockets. *J. Biol. Regul. Homeost. Agents* **2021**, *35*, 89–96. [CrossRef] [PubMed]
168. Apatzidou, D.A.; Kinane, D.F. Quadrant Root Planing versus Same-Day Full-Mouth Root Planing. I. Clinical Findings. *J. Clin. Periodontol.* **2004**, *31*, 132–140. [CrossRef]
169. Mamajiwala, A.S.; Sethi, K.S.; Raut, C.P.; Karde, P.A.; Khedkar, S.U. Comparative Evaluation of Chlorhexidine and Cinnamon Extract Used in Dental Unit Waterlines to Reduce Bacterial Load in Aerosols during Ultrasonic Scaling. *Indian J. Dent. Res.* **2018**, *29*, 749–754. [CrossRef]
170. Eltay, E.G.; Gismalla, B.G.; Mukhtar, M.M.; Awadelkarim, M.O.A. Punica Granatum Peel Extract as Adjunct Irrigation to Nonsurgical Treatment of Chronic Gingivitis. *Complement. Ther. Clin. Pract.* **2021**, *43*, 101383. [CrossRef]
171. Yaghini, J.; Naghsh, N.; Sadeghi, S.M.; Soltani, S. Gingival Inflammatory Indices and Dental Stain Index after Using Aloe Vera-Green Tea Mouthwash, Matrica Mouthwash, or 0.2% Chlorhexidine Mouthwash Compared with Placebo in Patients with Gingival Inflammation. *Open Dent. J.* **2019**, *13*, 214–220. [CrossRef]

172. Jünger, H.; Jaun-Ventrice, A.; Guldener, K.; Ramseier, C.A.; Reissmann, D.R.; Schimmel, M. Anti-Inflammatory Potential of an Essential Oil-Containing Mouthwash in Elderly Subjects Enrolled in Supportive Periodontal Therapy: A 6-Week Randomised Controlled Clinical Trial. *Clin. Oral. Investig.* **2020**, *24*, 3203–3211. [CrossRef]
173. Jung, J.-S.; Choi, G.-H.; Lee, H.; Ko, Y.; Ji, S. The Clinical Effect of a Propolis and Mangosteen Extract Complex in Subjects with Gingivitis: A Randomized, Double-Blind, and Placebo-Controlled Clinical Trial. *Nutrients* **2024**, *16*, 3000. [CrossRef]
174. Sheregov, A.K.; Kharaeva, Z.F.; Mustafaev, M.S.; Korkina, L.G.; Batyrbekova, F.R.; Agnokova, T.K. Effectiveness Of Using Fermented Herbal Preparation In Complex Therapy Of Periodontitis Developed As An Orthodontic Treatment Complication. *Russ. Open Med. J.* **2021**, *10*, e0425. [CrossRef]
175. Park, J.-Y.; Ko, K.-A.; Lee, J.-Y.; Oh, J.-W.; Lim, H.-C.; Lee, D.-W.; Choi, S.-H.; Cha, J.-K. Clinical and Immunological Efficacy of Mangosteen and Propolis Extracted Complex in Patients with Gingivitis: A Multi-Centered Randomized Controlled Clinical Trial. *Nutrients* **2021**, *13*, 2604. [CrossRef] [PubMed]
176. Kim, Y.-R.; Nam, S.-H. A Randomized, Placebo-Controlled Clinical Trial Evaluating of a Mouthwash Containing Sambucus Williamsii Var. Coreana Extract for Prevention of Gingivitits. *Sci. Rep.* **2022**, *12*, 11250. [CrossRef] [PubMed]
177. Poswal, F.S.; Russell, G.; Mackonochie, M.; MacLennan, E.; Adukwu, E.C.; Rolfe, V. Herbal Teas and Their Health Benefits: A Scoping Review. *Plant Foods Hum. Nutr.* **2019**, *74*, 266–276. [CrossRef] [PubMed]
178. Fu, Y.; Yang, J.-C.; Cunningham, A.B.; Towns, A.M.; Zhang, Y.; Yang, H.-Y.; Li, J.-W.; Yang, X.-F. A Billion Cups: The Diversity, Traditional Uses, Safety Issues and Potential of Chinese Herbal Teas. *J. Ethnopharmacol.* **2018**, *222*, 217–228. [CrossRef]
179. Wang, K.; Wu, K.; Li, N. Insect Tea Originated from Ethnic Minority Regions in Southwest China: A Review on the Types, Traditional Uses, Nutrients, Chemistry and Pharmacological Activities. *J. Ethnopharmacol.* **2023**, *309*, 116340. [CrossRef]

Disclaimer/Publisher's Note: The statements, opinions and data contained in all publications are solely those of the individual author(s) and contributor(s) and not of MDPI and/or the editor(s). MDPI and/or the editor(s) disclaim responsibility for any injury to people or property resulting from any ideas, methods, instructions or products referred to in the content.

nutrients

MDPI

Article

Potential Effect of Cinnamaldehyde on Insulin Resistance Is Mediated by Glucose and Lipid Homeostasis

Marisa Jadna Silva Frederico [1,2], Paola Miranda Sulis [1], Landerson Lopes Pereira [1], Diana Rey [1,3], Marcela Aragón [3] and Fátima Regina Mena Barreto Silva [1,*]

[1] Instituto de Bioeletricidade Celular (IBIOCEL): Ciência & Saúde, Departamento de Bioquímica, Centro de Ciências Biológicas, Universidade Federal de Santa Catarina, Rua João Pio Duarte Silva, 241, Sala G 301, Florianópolis 88038-000, SC, Brazil; marisafrederico@ufc.br (M.J.S.F.); pasulis@hotmail.com (P.M.S.); landersonplopes@gmail.com (L.L.P.); dprey@unal.edu.co (D.R.)

[2] Laboratório de Bioquímica e Farmacologia, Departamento de Farmacologia e Fisiologia, Núcleo de Pesquisa e Desenvolvimento de Medicamentos, Escola de Medicina, Universidade Federal do Ceará, Rua Coronel Nunes de Melo, Fortaleza 60430-275, CE, Brazil

[3] Departamento de Farmacia, Universidad Nacional de Colombia, Av. Carrera 30 # 45-03 Edif. 450, Bogotá 111321, Colombia; dmaragonn@unal.edu.co

* Correspondence: mena.barreto@ufsc.br; Tel.: +55-(48)-3721-6159

Abstract

Diabetes mellitus is a metabolic syndrome that has grown globally to become a significant public health challenge. Hypothesizing that the plasma membrane protein, transient receptor potential ankyrin-1, is a pivotal target in insulin resistance, we investigated the mechanism of action of cinnamaldehyde (CIN), an electrophilic TRPA1 agonist, in skeletal muscle, a primary insulin target. Specifically, we evaluated the effect of CIN on insulin resistance, hepatic glycogen accumulation and muscle and adipose tissue glucose uptake. Furthermore, the in vitro role of CIN in glucose uptake and intracellular signaling was determined in insulin-resistant rats whose calcium influx was analyzed. Moreover, the serum lipid profile was assessed following short-term CIN treatment in rats, and lipid tolerance was analyzed. The effects of CIN on insulin resistance were mediated by TRPA1, with downstream signaling involving the activation of PI3-K, MAPK, PKC, as well as extracellular calcium and calcium release from intracellular stores. Additionally, cytoskeleton integrity was required for the complete action of CIN on glucose uptake in muscle. CIN also ameliorated the serum lipid profile and improved triglyceride tolerance following acute vivo exposure.

Keywords: cinnamaldehyde; insulin resistant; skeletal muscle; adipose tissue; glucose uptake; glycogen; lipids

1. Introduction

Diabetes mellitus (DM) is a public health disease, prompting governments to allocate yearly budgets based on an alarming estimate for 2045 [1]. Type 1 diabetes is a metabolic syndrome caused by an imbalance of glucose, lipid and proteins, due to a lack of insulin synthesis by β-cells, or the production of insufficient insulin for the regulation of intermediate metabolism. In contrast, type 2 diabetes features by insulin resistance and β-cell dysfunction, as the result of high and persistent glycemia (hyperglycemia) [2]. Although maintaining physiological levels of glycated hemoglobin (HbA1c) is important for preventing macro- and microvascular complications [3,4], a balance between glucose and plasma lipids is essential for the control of diabetes. As such, long-term therapies that can sustain

glycemic control and blood lipid homeostasis, while improving insulin resistance and β-cell function, are highly sought.

Transient receptor potential ankyrin-1, a channel that is permeable to sodium (Na^+) and calcium (Ca^{2+}), has gained attention as a potential target for drug development, particularly for glucose and lipid metabolism pathways ([5]. The binding of electrophilic agonists, such as cinnamaldehyde (CIN), to TRPA1 may induce structural modifications that keep it open. Alternatively, the channel can be activated by non-electrophilic ligands through classical orthosteric ligand/receptor binding [6,7]. We previously described a role for TRPA-1 in prompt effects of CIN on insulin secretion by pancreatic islets and in its in vitro effects on glucagon-like peptide -1 release in the intestine [8]. Building on our previous studies of CIN, an electrophilic TRPA-1 agonist, we further explored its TRPA-1-dependent mechanism of action in an insulin-target tissue, namely skeletal muscle, from insulin-resistant rats. The present investigation evaluated the effects of short-term in vivo CIN administration, in rats, on insulin tolerance, hepatic glycogen accumulation, and muscle and adipose tissue glucose uptake. In addition, the in vitro intracellular signaling that transduces CIN pathways on glucose uptake was studied and calcium influx was analyzed. Furthermore, the lipid profile was assessed after short-term administration of CIN, and its acute effects were observed in vitro.

2. Materials and Methods

2.1. Rats

Adult male Wistar rats were kept with pelleted food (Nuvital, Nuvilab CR1, Curitiba, PR, Brazil) and tap water was available ad libitum. Fasting rats were deprived of food for 12 h but were handled in accordance with the ethical recommendations of the local Ethical Committee for Animal Use (Protocol CEUA/UFSC/PP00398/749).

2.2. Effect of Cinnamaldehyde on Insulin Resistance

To perform tests with the insulin-resistance model, rats were treated for 5 days and separated as follows: a control group, which received saline solution (0.9% sodium chloride solution, i.p. and v.o.); a Dexamethasone group, which received an intraperitoneal (s.c.) and saline (v.o.); a Dexamethasone + CIN group, which received an injection of dexamethasone (1 mg/kg/d) and CIN (20 mg/kg, v.o.); and a CIN group, which received saline (i.p.) and CIN (20 mg/kg v.o.) [9].

2.3. Cinnamaldehyde on Glycogen Content in Insulin-Resistant Rats

To determine glycogen, slices of liver tissue from insulin-resistant rats and rats treated with CIN (20/mg/kg) were removed at the end of the glucose tolerance curve. They were divided into four groups: Control (vehicle), dexamethasone, dexamethasone + CIN and CIN groups. Glycogen was quantified and the results were expressed as mg/dL of glycogen per mg of liver [10,11].

2.4. Signaling Pathway of Cinnamaldehyde on Glucose Uptake in Insulin-Resistant Rats

To evaluate the action of CIN on glucose uptake in skeletal muscle tissue and epididymal adipose tissue, tissues were collected from rats induced to insulin resistance and treated with dexamethasone and with CIN for 5 days. After the dissection and fragmentation of the respective tissues, they were preincubated (30 min) and then incubated (60 min) and total protein was quantified [12]. The glucose uptake results are expressed as nmol glucose/mg of protein. 14C-DG was measured in a liquid scintillator spectrometer (model LS 6500; Multi-Purpose Scintillation Counter-Beckman, Boston, MA, USA).

2.5. Action of Cinnamaldehyde on ^{14}C-Glucose Uptake in Insulin-Resistant Rats

Slices of soleus muscle from normoglycaemic rats were allocated to the control and treated groups (four slices for each group). The muscles were dissected, preincubated (30 min) and then incubated (60 min) at 37 °C in O_2/CO_2 (95%: 5%, *v*/*v*), with pH 7.4 in Krebs Ringer-bicarbonate buffer (KRb) without (control) or with CIN (100 μM CIN). CIN was added to the incubation medium (60 min) in the presence or absence of 300 nM of capsaiscin, 100 μM of alil-isotiocianato (AITC), 100 nM of wortmannin, 10 μM of SB239063, 1 μM of Nifedipine, 50 μM of BAPTA-AM, 1 μM of colchicine, 10 μM of chytocalasin and 50 μM of RO-310432. 14C-DG (0.1 μCi/mL; 0.12 nM) was added to all samples throughout the incubation period, The glucose uptake results are expressed as nmol glucose/mg of protein. 14C-DG was measured in a liquid scintillator spectrometer (model LS 6500; Multi-Purpose Scintillation Counter-Beckman, Boston, MA, USA).

2.6. Role of Cinnamaldehyde on $^{45}Ca^{2+}$ Influx

Slices of soleus muscle were pre-incubated for 30 min in an incubator in KRb-HEPES buffer with 5.6 mM of glucose and 0.1 μCi/mL $^{45}Ca^{2+}$ concentrations. [8]. Subsequently, muscles were incubated in the absence (control) or presence of CIN in KRb-HEPES. In some assays, an intracellular calcium chelator or a blocker of L-type voltage-dependent calcium channels was added during the last 60 min of incubation, prior to treatment, and maintained throughout the incubation period. Drugs used included 50 μM of BAPTA-AM and 1 μM of nifedipine and these were processed according the work of Batra et al. [13].

2.7. Effect of Cinnamaldehyde on Serum Lipid Profile of Insulin-Resistant Rats

To evaluate the effect of CIN on lipid profile, blood samples from rats induced to insulin resistance by dexamethasone, from control and treated rats, were collected after euthanasia, and the concentrations of triacylglycerol, total cholesterol, low density lipoprotein and high density lipoprotein were determined using kits (Biotécnica, Varginha, Brazil) and expressed as mg/dL [14].

2.8. Role of Cinnamaldehyde on the Oral Triglyceride Tolerance Test

Fasted rats (12 h) were separated into groups of six: Group 1 received 6 mL of saline (v.o.); Group 2 received the emulsion (6 mL of corn oil, 80 mg of cholic acid, 2 g of chloestryloleate plus 6 mL of saline) and Group 3 received 20 mg/kg CIN (i.p.) plus lipid emulsion 30 min later. Blood was analyzed at zero time (before the administration of saline, emulsion or CIN) and at 1, 2, 3, 4, 5 and 6 h after emulsion overload. The triglycerides were determined in the blood by a kit from Gold analyses (Belo Horizonte, MG, Brazil).

2.9. Statistical Analysis

Data are expressed as means ± standard errors of the mean. One-way analysis of variance and Bonferroni post hoc test or unpaired Student's *t*-test were used. Differences of $p \leq 0.05$ were considered as significant using GraphPad Prism@ 5 program.

3. Results

3.1. Cinnamaldehyde and Insulin Tolerance

The synthetic glucocorticoid, dexamethasone, is widely used as a tool to induce insulin-resistance in experimental model rats [9,11]. The present study shows that dexamethasone (0.1 mg/kg; subcutaneously injected for 5 days) was able to induce insulin resistance in rats, compared with the control. Furthermore, the treatment of insulin-resistant rats with CIN (20 mg/kg by intraperitoneal injection, for 5 days) significantly improved insulin-resistance, as shown in Figure 1.

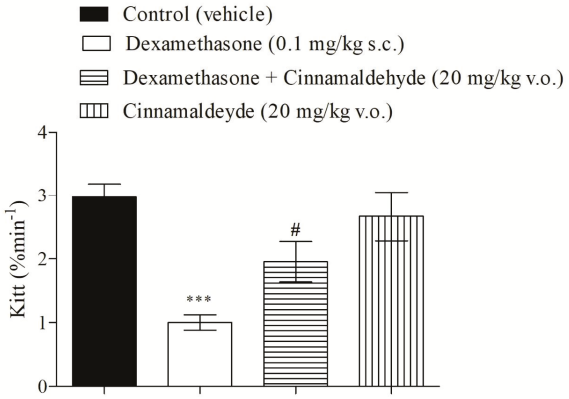

Figure 1. Effect of CIN (5 days, 20 mg/kg) on the insulin-tolerance test in insulin-resistant rats. N = 5, *** $p \leq 0.001$ compared to control (vehicle); # $p \leq 0.05$ compared to dexamethasone group.

3.2. Cinnamaldehyde on Hepatic Glycogen Accumulation

CIN, an essential oil extracted from cinnamon, exhibits several biological effects. Among these effects, CIN achieves carbohydrate balance by inducing insulin and glucagon-like peptide-1 secretion, the inhibition of intestinal disaccharidases, and, consequently, improves glucose tolerance. Figure 2 shows that following in vivo treatment with CIN (20 mg/kg), hepatic glycogen levels in insulin-resistant rats were restored to normal, as compared with control groups.

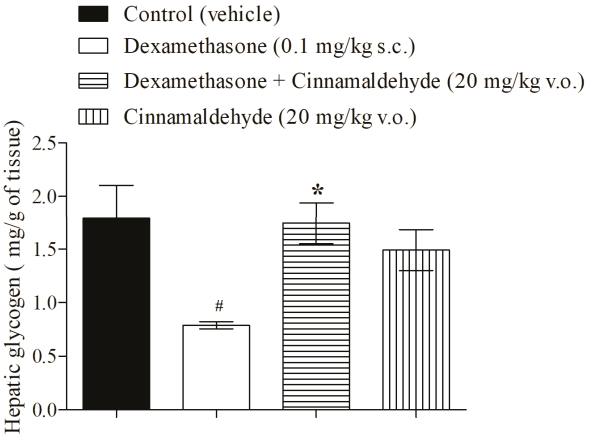

Figure 2. Action of CIN on hepatic glycogen accumulation in insulin-resistant rats, after 5 days of in vivo treatment. N = 5, # $p \leq 0.05$ compared with control (vehicle); * $p \leq 0.05$ compared with the dexamethasone group.

3.3. Effect of Cinnamaldehyde on ^{14}C-Glucose Uptake

As previously demonstrated, CIN is an insulin and GLP-1 secretagogue. As such, we investigated the action of CIN on glucose uptake in the soleus and adipose tissue of insulin-resistant rats. Figure 3A,B show that, in both insulin-target tissues, CIN reversed the effect of insulin resistance on glucose uptake.

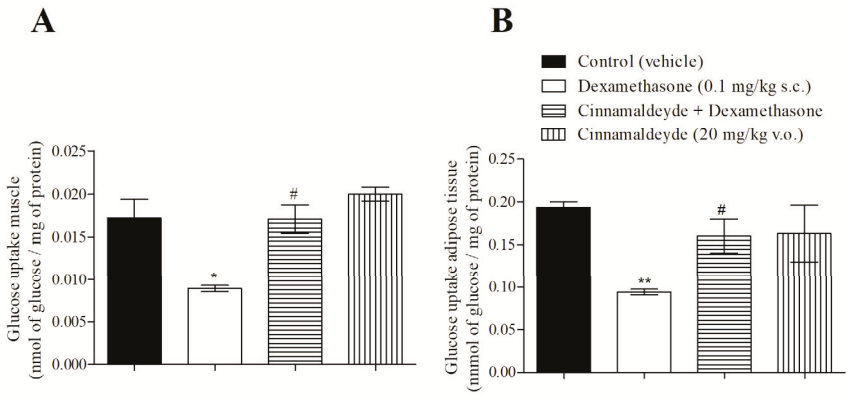

Figure 3. Effect of CIN on [^{14}C]-glucose uptake in (**A**) soleus skeletal muscle and (**B**) adipose tissue from insulin-resistant rats, treated for 5 days. N = 5, * $p \leq 0.05$ and ** $p \leq 0.01$ compared with control (vehicle); $^{\#}$ $p \leq 0.05$ compared with dexamethasone group.

3.4. Mechanism of Action of Cinnamaldehyde on ^{14}C-Glucose Uptake

One desirable effect sought in compounds in development for diabetes therapy is their insulin-mimetic action, to rapidly improve glycemic control. Based on our previous studies of calcium influx in β-cells, the concentration of 100 μM of CIN was assayed to investigate the mechanism by which CIN affects glucose uptake in the soleus muscle. Figure 4A shows that CIN (acute effect) has a stimulatory effect on glucose uptake in insulin-resistant. In addition, capsaicin, an agonist of TRPV1, as well as the combination of 300 nM of capsaicin plus CIN, similarly increased glucose uptake to the level observed for the CIN group. Furthermore, a non-electrophilic agonist of TRPA1 (100 μM of AITC) increased glucose uptake, similar to that observed when muscle was incubated with both (CIN + AITC). Figure 4B shows that the action of CIN was significantly reduced (by approximately 40%) in the presence of 100 nM of wortmannin, an inhibitor of PI3-K, and when co-incubated with 10 μM of SB 239063, an inhibitor of p38 MAPK. To investigate the influence of calcium in the mechanism of CIN on glucose uptake, an inhibitor of voltage-dependent calcium channels, 1 μM of nifedine, and an intracellular calcium chelating agent, 50 μM of BAPTA-AM, were added into the medium. Figure 4C shows that the stimulatory effect of CIN was reduced by 45%.

The integrity of the cell cytoskeleton was investigated using an inhibitor of microtubules polymerization, colchicine. When the polymerization of microtubules was interrupted by colchicine, the action of CIN on glucose uptake was blocked around 37%. However, 10 μM of cytochalasin D, an inhibitor of actin association/dissociation, did not alter CIN-induced glucose uptake (Figure 4D). Finally, the influence of protein kinase C (PKC) in the effect of CIN on glucose uptake was investigated using a PKC inhibitor, 50 μM of RO-310432. This drug reduced the effect of CIN on glucose uptake by 30% (Figure 4E).

3.5. Effect of Cinnamaldehyde on $^{45}Ca^{2+}$ Influx in Skeletal Muscle

As calcium is mandatory for triggering the trafficking of vesicles for exocytosis, among other mechanisms [15], the role that calcium plays in the stimulatory effect of CIN on glucose uptake was evaluated. Figure 5 shows that both calcium from intracellular stores and extracellular calcium participate in the intracellular signaling of CIN on skeletal muscle, since the presence of BAPTA-AM and nifedipine significantly decreased the CIN-induced calcium influx.

3.6. In Vivo Effect of Cinnamaldehyde on Serum Lipid Profile

As expected, the lipid profile behaved in line with the effects of dexamethasone (0.1 mg/kg) after 5 days of subcutaneous injection. Surprisingly, CIN significantly diminished triglycerides, cholesterol and LDL, while improving HDL, thereby ameliorating the total serum lipid profile in insulin-resistant rats after in vivo treatment (Figure 6).

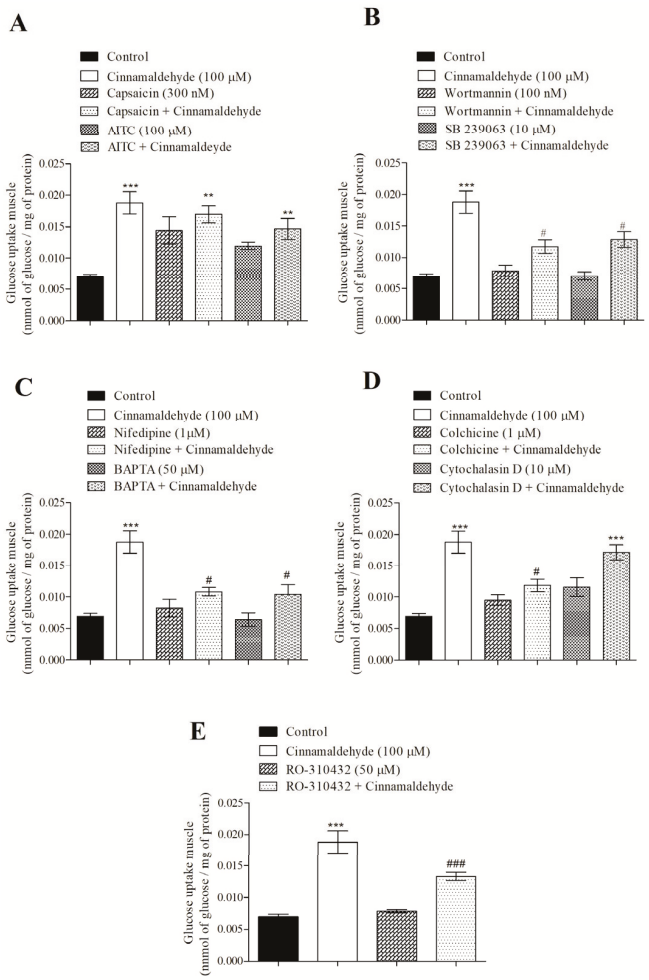

Figure 4. Mechanism of action by which CIN induces [^{14}C]-glucose uptake in skeletal muscle from insulin-resistant rats. Involvement of TRPV1 (capsaicin) and TRPA1 (AITC) (**A**); PI3-K (wortmannin) and p38 MAPK (SB 239063) (**B**); L-type VDCC (nifedipine) and calcium from stores (BAPTA-AM) (**C**); cytoskeleton (colchicine) and actin (cytochalasin) (**D**); and PKC (RO-3104320) (**E**). Pre-incubation time = 30 min; incubation time = 60 min. N = 6 for each group. *** $p \leq 0.001$ and ** $p \leq 0.01$ compared to control group. ### $p \leq 0.001$ and # $p \leq 0.05$ compared to CIN group.

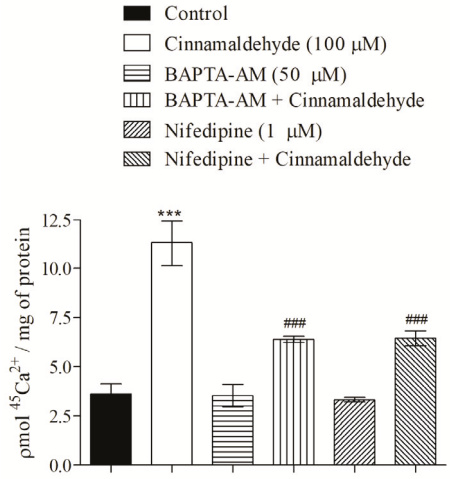

Figure 5. Mechanism of action of CIN on $^{45}Ca^{2+}$ influx in skeletal muscle. Involvement of calcium from intracellular stores (BAPTA-AM) and extracellular calcium by L-type VDCC (nifedipine). Pre-incubation time = 30 min; incubation time = 60 min. N = 6 for each group. *** $p \leq 0.001$, compared to control group and ### $p \leq 0.001$, compared to CIN group.

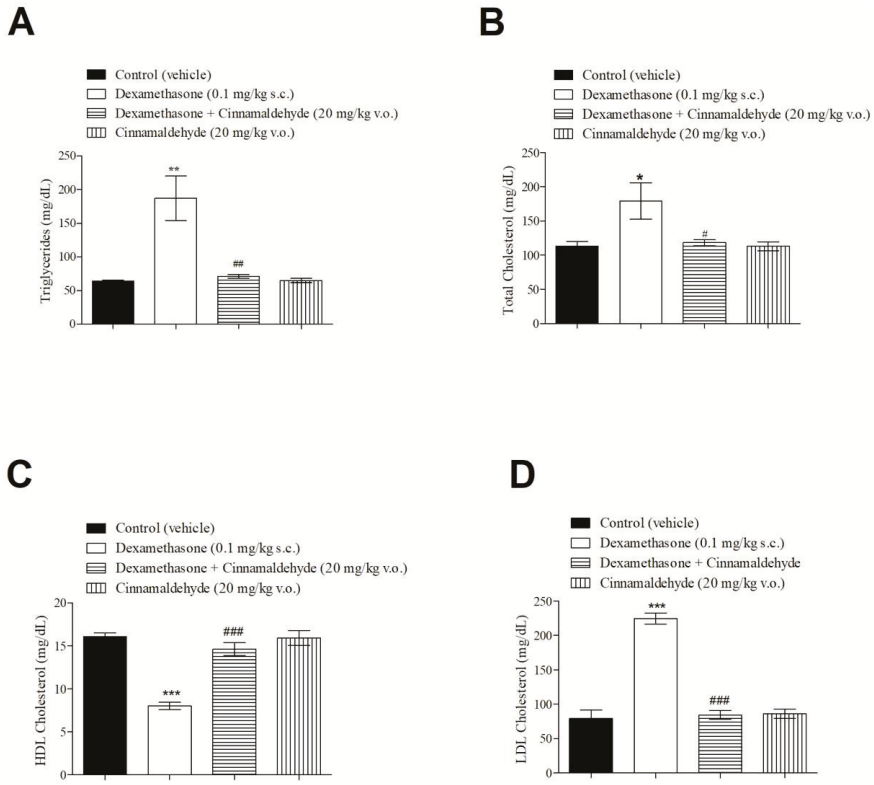

Figure 6. Effect of CIN on (**A**) triglycerides, (**B**) total cholesterol, (**C**) HDL cholesterol and (**D**) LDL cholesterol in insulin-resistant rats after 5 days of treatment with dexamethasone. N = 6 for each group. *** $p \leq 0.001$; ** $p \leq 0.01$ and * $p \leq 0.05$, compared to the control group. ### $p \leq 0.001$; ## $p \leq 0.01$ and # $p \leq 0.05$, compared to the dexamethasone group.

3.7. Effect of Cinnamaldehyde on Oral Triglyceride Tolerance Test

The acute effect of CIN on triglyceride tolerance was evaluated from 1 h to 6 h in normal rats overloaded with a fat-enriched emulsion, as shown in Figure 7. The progressive increase in serum triglycerides observed in the lipid-enriched emulsion-overloaded group was significantly reduced by CIN (20 mg/kg i.p.) from 2 h to 6 h (Figure 7).

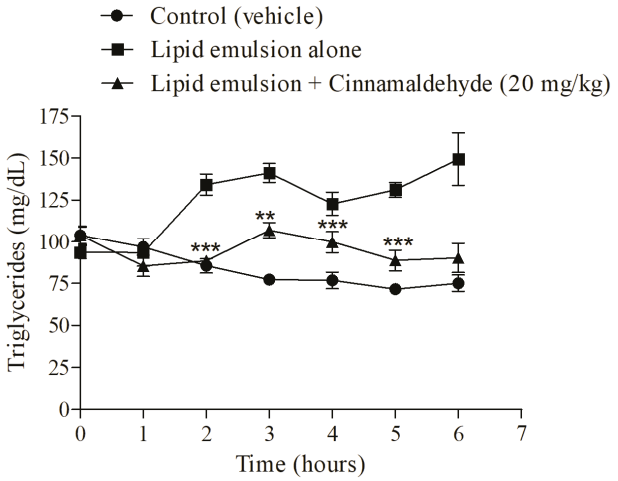

Figure 7. Acute effect of CIN on the oral triglyceride tolerance test in normal rats overloaded with an enriched lipid emulsion, at 0 to 6 h. N = 6. *** $p \leq 0.001$ and ** $p \leq 0.01$, compared to the respective value for the lipid emulsion group.

4. Discussion

An insulin receptor can detect high glucose and activates intracellular downstream signaling pathways to regulate glycemia [16]. This augments glucose uptake, particularly in insulin-target tissues, through the action of increased glucose transporter-4 (GLUT-4). The pleiotropic insulin receptor depends on intracellular substrates to trigger specific mechanisms to increase GLUT-4 at the plasma membrane, such as that mediated by PI3-K. In the present study, CIN, an electrophilic agonist of TRPA1, improved insulin tolerance after 5 days of in vivo treatment. This is in line with reports in the literature that suggest several therapeutic effects of TRPA1, including increased glucose uptake, improved glucose insulin sensitivity and heart protection [17]. Furthermore, the effect of CIN on insulin sensitivity tissues may contribute to its ability to improve insulin-resistance, as reported by Zhu et al. [18]. Our findings further support the ability of CIN to improve insulin resistance, as shown by analyzing hepatic glycogen accumulation and glucose uptake in muscle and adipose tissue. In diabetic rats, CIN has been reported to increase glucose uptake and improve insulin sensitivity in adipose and muscle, increase glycogen synthesis in the liver, restore pancreatic cell function, delay gastric emptying and improve diabetic renal and brain disorders through multiple methods [17,18].

We also investigated how CIN modulated glucose uptake in insulin-resistant muscle using ^{14}C-glucose. Results indicate that CIN may increase glucose uptake via a TRPA1-mediated mechanism and through TRPV1. In addition, the participation of PI3-K, p38 MAPK and PKC is crucial for the complete stimulatory effect of this compound on glucose uptake in skeletal muscle. Zhu et al. [18] reported that PI3-K and p38 MAPK participate in the CIN-induced signaling pathway that increases glucose uptake in diabetic rats, both in muscle and in adipose tissue, through the TRPA1/ghrelin receptor. Among the various phosphorylation events that are mediated by PKC, the activity ionic channels are regulated by a family of kinases, including the T-type VDCC, and the transient receptor potential melastatin family (TRPM) [19].

We also studied the ionic influence on the stimulatory effect of CIN on glucose uptake. Incubation of tissues with nifedipine, and with BAPTA-AM, demonstrated a primary signaling role for calcium (extracellular and intracellularly stored calcium) in CIN-induced glucose uptake. A major PKC family is calcium dependent or calcium-calmodulin dependent, coordinating the activity of ionic channels to trigger several physiological events [19–21].

The cytoskeleton supports and organizes the trafficking of organelles and vesicles. The cytoskeleton and actin movement are essential for the intracellular displacement of vesicles and the distribution or secretion of proteins intra- and inter-cellularly [22,23]. When CIN was co-incubated with colchicine, a microtubule disruptor, the stimulatory effect of the compound was significantly diminished. However, under similar experimental conditions, cytochalasin D, an inhibitor of actin polymerization, did not affect glucose uptake. As currently discussed in the literature, the functional integrity (polymerization/depolymerization cycle) of microtubules and actin is essential to vesicle trafficking. Mendes et al. [14] showed that the integrity of the microtubule network is necessary for the translocation of insulin vesicles from the cytosol to the plasma membrane in pancreatic islets. Similarly, in other systems, such as the central nervous system, the integrity of the cytoskeleton (microtubule or actin network) is essential for the recycling of synaptic vesicles [24].

Insulin resistance is associated with a metabolic condition that leads to lipid and carbohydrate homeostasis impairment. Significant diminution in triglycerides and LDL was detected in insulin-resistant rats treated with CIN for 5 days. This occurred in association with an augment in HDL, demonstrating effects of CIN on lipid homeostasis. Additionally, acute CIN exposure significantly improved triglyceride tolerance, with the effect lasting

for 2 h to 6 h after lipid overloading. Our findings of improvements in lipids after CIN treatment support the data discussed by Jamali et al. [25], Allen et al. [26] in studies from type 2 diabetic patients, and Li et al. [27] in db/db mice. However, these data are conflicting and require further mechanistic investigation.

5. Conclusions

The effect of cinnamaldehyde on insulin resistance is mediated by TRPA1, with downstream signaling involving the activation of PI3-K, MAPK, PKC, as well as extracellular and stored calcium. Complete cytoskeleton integrity is required for its full stimulatory effect on glucose uptake in soleus muscle. Additionally, cinnamaldehyde ameliorates the lipid profile and improves triglyceride tolerance following acute in vivo exposure.

Author Contributions: Conceptualization, M.J.S.F. and F.R.M.B.S.; methodology, D.R., M.J.S.F., L.L.P. and P.M.S.; software, M.A. and M.J.S.F.; validation, M.J.S.F., M.A. and F.R.M.B.S.; formal analysis, M.J.S.F. and F.R.M.B.S.; investigation, M.J.S.F., L.L.P. and D.R.; resources, F.R.M.B.S.; data curation, M.J.S.F. and M.A.; writing—original draft preparation, F.R.M.B.S. and P.M.S.; writing—review and editing, M.J.S.F., M.A. and D.R.; visualization, M.J.S.F. and P.M.S.; supervision, F.R.M.B.S. and M.A.; project administration, F.R.M.B.S.; funding acquisition, F.R.M.B.S. All authors have read and agreed to the published version of the manuscript.

Funding: This research was funded by CNPq, grant number 305892; FAPESC number 2024TR000070 and CAPES PPG-BQA/PNPD 2018/2019.

Institutional Review Board Statement: The study was conducted in accordance with the Declaration of Helsinki and approved by the Committee for Ethics in Animal Research of the UFSC (protocol code PP00749 approved 11 September 2017).

Informed Consent Statement: Not applicable.

Data Availability Statement: All data in this study are contained within the article.

Acknowledgments: We thank the UFSC for the use of the LAMEB/CCB-UFSC equipment.

Conflicts of Interest: The authors declare no conflicts of interest.

References

1. Sun, H.; Saeedi, P.; Karuranga, S.; Pinkepank, M.; Ogurtsova, K.; Duncan, B.B.; Stein, C.; Basit, A.; Chan, J.C.; Mbanya, J.C.; et al. IDF Diabetes Atlas: Global, regional and country-level diabetes prevalence estimates for 2021 and projections for 2045. *Diabetes Res. Clin. Pract.* **2022**, *183*, 109119. [CrossRef] [PubMed]
2. Punthakee, Z.; Goldenberg, R.; Katz, P. Definition, Classification and Diagnosis of Diabetes, Prediabetes and Metabolic Syndrome. *Can. J. Diabetes* **2018**, *42* (Suppl. 1), S10–S15. [CrossRef] [PubMed]
3. Duckworth, W.; Abraira, C.; Moritz, T.; Reda, D.; Emanuele, N.; Reaven, P.D.; Zieve, F.J.; Marks, J.; Davis, S.N.; Hayward, R.; et al. Glucose control and vascular complications in veterans with type 2 diabetes. *N. Engl. J. Med.* **2009**, *360*, 129–139. [CrossRef] [PubMed]
4. Taylor, S.I.; Yazdi, Z.S.; Beitelshees, A.L. Pharmacological treatment of hyperglycemia in type 2 diabetes. *J. Clin. Investig.* **2021**, *131*, e142243. [CrossRef] [PubMed]
5. Sodhi, R.K.; Kumar, H.; Singh, R.; Bansal, Y.; Singh, Y.; Kondepudi, K.K.; Bishnoi, M.; Kuhad, A. Allyl isothiocyanate, a TRPA1 agonist, protects against olanzapine-induced hypothalamic and hepatic metabolic aberrations in female mice. *Biochem. Pharmacol.* **2024**, *222*, 116074. [CrossRef]
6. Bautista, D.M.; Movahed, P.; Hinman, A.; Axelsson, H.E.; Sterner, O.; Högestätt, E.D.; Julius, D.; Jordt, S.-E.; Zygmunt, P.M. Pungent products from garlic activate the sensory ion channel TRPA1. *Proc. Natl. Acad. Sci. USA* **2005**, *102*, 12248–12252. [CrossRef] [PubMed]
7. Bautista, D.M.; Jordt, S.-E.; Nikai, T.; Tsuruda, P.R.; Read, A.J.; Poblete, J.; Yamoah, E.N.; Basbaum, A.I.; Julius, D. TRPA1 mediates the inflammatory actions of environmental irritants and proalgesic agents. *Cell* **2006**, *124*, 1269–1282. [CrossRef]
8. Frederico, M.J.S.; Cipriani, A.; Heim, J.B.A.; Mendes, A.K.B.; Aragón, M.; Gaspar, J.M.; De Alencar, N.M.N.; Silva, F.R.M.B. Electrophilic Agonists Modulate the Transient Receptor Potential Ankyrin-1 Channels Mediated by Insulin and Glucagon-like Peptide-1 Secretion for Glucose Homeostasis. *Pharmaceuticals* **2023**, *16*, 1167. [CrossRef] [PubMed]

9. Tzeng, C.-Y.; Lee, Y.-C.; Chung, J.-J.; Tsai, J.-C.; Chen, Y.-I.; Hsu, T.-H.; Lin, J.-G.; Lee, K.-R.; Chang, S.-L. 15 Hz electroacupuncture at ST36 improves insulin sensitivity and reduces free fatty acid levels in rats with chronic dexamethasone-induced insulin resistance. *Acupunct. Med. J. Br. Med. Acupunct. Soc.* **2016**, *34*, 296–301. [CrossRef]
10. Kappel, V.D.; Pereira, D.F.; Cazarolli, L.H.; Guesser, S.M.; da Silva, C.H.B.; Schenkel, E.P.; Reginatto, F.G.; Silva, F.R.M.B. Short and long-term effects of *Baccharis articulata* on glucose homeostasis. *Molecules* **2012**, *17*, 6754–6768. [CrossRef]
11. Krisman, C.R. A method for the colorimetric estimation of glycogen with lodine. *Anal. Biochem.* **1962**, *4*, 17–23. [CrossRef] [PubMed]
12. Lowry, O.H.; Rosebrough, N.J.; Randall, R.J.; Farr, L. Protein measurement with the folin phenol reagent. *J. Biol. Chem.* **1951**, *193*, 265–275. [CrossRef]
13. Batra, S.; Sjogren, C. Effect of estrogen treatment of calcium uptake by the rat uterine smooth muscle. *Life Sci.* **1983**, *32*, 315–319. [CrossRef] [PubMed]
14. Mendes, A.K.B.; Sulis, P.M.; Cavalari, F.C.; Padilla, D.P.R.; Aragón, M.; Gaspar, J.M.; Silva, F.R.M.B. 1α,25-$(OH)_2$ Vitamin D3 prevents insulin resistance and regulates coordinated exocytosis and insulin secretion. *J. Nutr. Biochem.* **2021**, *99*, 108864. [CrossRef] [PubMed]
15. Rey, D.; Sulis, P.M.; Fernandes, T.A.; Gonçalves, R.; Frederico, M.J.S.; Costa, G.M.; Aragon, M.; Ospina, L.F.; Silva, F.R.M.B. Astragalin augments basal calcium influx and insulin secretion in rat pancreatic islets. *Cell Calcium* **2019**, *80*, 56–62. [CrossRef] [PubMed]
16. Concepción, B.D.l.C.; Cortez, Y.A.F.; Bonilla, M.I.B.; Bello, J.M.M.; Rojo, M.E. Insulin: A connection between pancreatic β cells and the hypothalamus. *World J. Diabetes* **2023**, *14*, 76–91. [CrossRef]
17. Guo, J.; Yan, S.; Jiang, X.; Su, Z.; Zhang, F.; Xie, J.; Hao, E.; Yao, C. Advances in pharmacological effects and mechanism of action of cinnamaldehyde. *Front. Pharmacol.* **2024**, *15*, 1365949. [CrossRef] [PubMed]
18. Zhu, R.; Liu, H.; Liu, C.; Wang, L.; Ma, R.; Chen, B.; Li, L.; Niu, J.; Fu, M.; Zhang, D.; et al. Cinnamaldehyde in diabetes: A review of pharmacology, pharmacokinetics and safety. *Pharmacol. Res.* **2017**, *122*, 78–89. [CrossRef] [PubMed]
19. Shan, H.Q.; Smith, T.; Klorig, D.C.; Godwin, D.W. Protein kinase C epsilon-mediated modulation of T-type calcium channels underlies alcohol withdrawal hyperexcitability in the midline thalamus. *Alcohol. Clin. Exp. Res.* **2024**, *48*, 1278–1288. [CrossRef]
20. Nmarneh, A.; Priel, A. TRPM5 activation depends on a synergistic effect of calcium and PKC phosphorylation. *Commun. Biol.* **2024**, *7*, 1–10. [CrossRef]
21. Xing, H.; Sabe, S.A.; Shi, G.; Harris, D.D.; Liu, Y.; Sellke, F.W.; Feng, J. Role of Protein Kinase C in Metabolic Regulation of Coronary Endothelial Small Conductance Calcium-Activated Potassium Channels. *J. Am. Hear. Assoc.* **2024**, *13*, e031028. [CrossRef] [PubMed]
22. Zaninello, M.; Bean, C. Highly Specialized Mechanisms for Mitochondrial Transport in Neurons: From Intracellular Mobility to Intercellular Transfer of Mitochondria. *Biomolecules* **2023**, *13*, 938. [CrossRef]
23. Smyth, J.W.; Vogan, J.M.; Buch, P.J.; Zhang, S.-S.; Fong, T.S.; Hong, T.-T.; Shaw, R.M. Actin Cytoskeleton rest stops regulate anterograde traffic of connexin 43 vesicles to the plasma membrane. *Circ. Res.* **2012**, *110*, 978–989. [CrossRef] [PubMed]
24. Parkes, M.; Landers, N.L.; Gramlich, M.W. Recently recycled synaptic vesicles use multi-cytoskeletal transport and differential presynaptic capture probability to establish a retrograde net flux during ISVE in central neurons. *Front. Cell Dev. Biol.* **2023**, *11*, 1286915. [CrossRef] [PubMed]
25. Jamali, N.; Kazemi, A.; Saffari-Chaleshtori, J.; Samare-Najaf, M.; Mohammadi, V.; Clark, C.C. The effect of cinnamon supplementation on lipid profiles in patients with type 2 diabetes: A systematic review and meta-analysis of clinical trials. *Complement. Ther. Med.* **2020**, *55*, 102571. [CrossRef] [PubMed]
26. Allen, R.W.; Schwartzman, E.; Baker, W.L.; Coleman, C.I.; Phung, O.J. Cinnamon use in type 2 diabetes: An updated systematic review and meta-analysis. *Ann. Fam. Med.* **2013**, *11*, 452–459. [CrossRef] [PubMed]
27. Li, J.-E.; Futawaka, K.; Yamamoto, H.; Kasahara, M.; Tagami, T.; Liu, T.-H.; Moriyama, K. Cinnamaldehyde Contributes to Insulin Sensitivity by Activating PPARδ, PPARγ, and RXR. *Am. J. Chin. Med.* **2015**, *43*, 879–892. [CrossRef]

Disclaimer/Publisher's Note: The statements, opinions and data contained in all publications are solely those of the individual author(s) and contributor(s) and not of MDPI and/or the editor(s). MDPI and/or the editor(s) disclaim responsibility for any injury to people or property resulting from any ideas, methods, instructions or products referred to in the content.

nutrients

MDPI

Review

A Narrative Review on Plant Extracts for Metabolic Syndrome: Efficacy, Safety, and Technological Advances

Hammad Ullah [1,2,*], Marco Dacrema [1], Daniele Giuseppe Buccato [1], Marwa A. A. Fayed [3], Lorenza Francesca De Lellis [1], Maria Vittoria Morone [4], Alessandro Di Minno [1,5], Alessandra Baldi [1] and Maria Daglia [1,6,*]

1 Department of Pharmacy, University of Napoli Federico II, Via D. Montesano 49, 80131 Naples, Italy; marcodacrema1991@gmail.com (M.D.); d.buccato@gmail.com (D.G.B.); lo.delellis2@gmail.com (L.F.D.L.); alessandro.diminno@unina.it (A.D.M.); alessandra.baldi.alimenti@gmail.com (A.B.)
2 School of Medicine, Xi'an International University, Xi'an 710077, China
3 Department of Pharmacognosy, Faculty of Pharmacy, University of Sadat City, Sadat 32897, Egypt; marwa.fayed@fop.usc.edu.eg
4 Department of Experimental Medicine, Section of Microbiology and Clinical Microbiology, University of Campania "L. Vanvitelli", 80138 Naples, Italy; mariavittoria.morone@unicampania.it
5 CEINGE-Biotecnologie Avanzate, Via Gaetano Salvatore 486, 80145 Naples, Italy
6 International Research Center for Food Nutrition and Safety, Jiangsu University, Zhenjiang 212013, China
* Correspondence: hammad.ullah@unina.it (H.U.); maria.daglia@unina.it (M.D.)

Abstract

Metabolic syndrome, a global health concern, is characterized by visceral obesity, hyperglycemia, dyslipidemia, hypertension, and chronic low-grade inflammation. Current therapeutic options are limited by their varying efficacy and significantly adverse side effects, fueling interest in natural products, particularly plant extracts, as potential preventive interventions for high-risk individuals. This review examines the role of plant extracts in mitigating metabolic syndrome risk factors, addressing safety concerns and exploring associated technological advancements. The literature indicates that plant extracts hold promise for addressing the pathophysiology of metabolic dysfunction. However, challenges such as safety concerns, a lack of standardized regulation, and potential drug–plant interactions currently limit their clinical application. Rigorous, long-term clinical trials are necessary to confirm the efficacy and safety of plant extracts before they can be established as a preventive strategy for managing metabolic syndrome.

Keywords: plant extracts; functional foods; metabolic syndrome; efficacy; safety; technological advancements

1. Introduction

Metabolic syndrome is a complex cluster of conditions, including obesity, hyperglycemia, hypertension, dyslipidemia, and a chronic pro-inflammatory state [1,2]. These factors significantly increase the risk of cardiovascular disease, type 2 diabetes mellitus (T2DM), and cerebrovascular accidents. Also known as Reaven's syndrome, Syndrome X, the deadly quartet, or insulin resistance syndrome, its precise definition and diagnostic criteria vary across organizations like the World Health Organization (WHO), the National Cholesterol Education Program's Adult Treatment Panel III (NCEP ATP III), and the International Diabetes Federation (IDF) [3–5]. However, all definitions emphasize the importance of visceral obesity, dyslipidemia, hypertension, and hyperglycemia.

The prevalence of metabolic syndrome has risen globally in recent decades, particularly among urban populations in developing countries [6]. A recent meta-analysis of data from 28 million individuals estimated a global adult prevalence of 12.5–31.4%, depending on diagnostic criteria [7], with significantly higher rates observed in the Eastern Mediterranean Region and the Americas. Prevalence rates for individual components are as follows: 45.1% for ethnicity-specific central obesity, 42.6% for elevated blood pressure (systolic $\geq$130 mmHg and/or diastolic $\geq$85 mmHg), 40.2% for reduced HDL-cholesterol (<1.03 mmol/L for men or <1.29 mmol/L for women), 28.9% for elevated triglycerides ($\geq$1.7 mmol/L), and 24.5% for elevated fasting plasma glucose ($\geq$5.6 mmol/L) [7]. The WHO has also reported alarmingly high global figures for obesity (890 million), diabetes (422 million), and hypertension (1.28 billion) [8–10].

Risk factors for developing metabolic syndrome include female sex, an age of over 50 years, a sedentary lifestyle, a family history of metabolic syndrome, low socioeconomic status, illiteracy, unemployment, an omnivore diet, stress, insomnia, and a high body mass index (BMI) [11]. Untreated or poorly managed metabolic syndrome can lead to serious health complications, including coronary heart disease (CHD), heart failure, stroke, hepatic steatosis, and liver failure, presenting a major challenge to global healthcare systems [12,13]. Current management strategies primarily involve lifestyle modifications (aerobic exercise and dietary changes) and pharmacological interventions targeting individual components of the syndrome [14–16]. However, the numerous and potentially severe adverse drug reactions (ADRs) associated with these treatments, including lactic acidosis (metformin), congestive heart failure (thiazolidinediones), renal toxicities and hyperkalemia (RAAS inhibitors), peptic ulcers (aspirin), and myopathies (hypolipidemics), often outweigh the benefits [17–20].

Natural products from marine and terrestrial sources offer significant potential for promoting human health and managing challenging diseases [21]. The growing global market for natural substances reflects a rising consumer preference for preventative healthcare [22]. Indeed, a 2014 report indicated that over 80% of the world's population utilizes botanical products for primary healthcare [23]. Herbal products have demonstrated efficacy in randomized controlled trials for reducing metabolic syndrome risk factors by positively influencing blood pressure, serum glucose levels, waist circumference, and lipid levels [24], suggesting that they may provide valuable alternative treatment options.

This review examines the efficacy and safety of plant extracts in mitigating metabolic syndrome risk factors. We consider the challenges and opportunities presented by current extraction and encapsulation techniques and aim to achieve the following: (i) assess the evidence on the efficacy of plant extracts in managing metabolic syndrome risk factors; (ii) evaluate their safety profiles based on existing data; and (iii) assess technological advancements in extract preparation and delivery methods relevant to clinical applications. This review synthesizes information from 139 articles identified through a comprehensive literature search in PubMed, Scopus, Web of Science, and the Cochrane Library. Plant extracts were included based on their documented efficacy in managing metabolic disorders. Articles focusing on extracts with limited or inconclusive metabolic effects were excluded. Additionally, studies addressing safety, bioavailability, or technological advancements related to plant extracts were prioritized.

2. Plant Extracts as Functional Food Ingredients

A diverse range of fruits and vegetables are rich in bioactive compounds such as polyphenols (flavonoids, phenolic acids, and stilbenes), carotenoids, organosulfur compounds, and dietary fibers, which offers a promising approach to mitigating metabolic syndrome risk factors. Polyphenols and carotenoids can reduce oxidative stress, improve

insulin sensitivity, and enhance glucose metabolism. Organosulfur compounds may improve glucose and lipid metabolism and reduce systemic inflammation, while dietary fibers are best known for their role in regulating gut microbiota, enhancing satiety, and improving insulin sensitivity [25,26]. These foods demonstrate potential benefits in improving glucose and lipid homeostasis, reducing ectopic lipid deposition, lowering inflammatory markers, and modulating the gut microbiome. Furthermore, bioactive compounds within these foods can modulate multiple signaling pathways, affecting enzyme activity, gene expression, epigenetic regulation, and protein expression [27]. The incorporation of plant extracts and their bioactive components into functional foods and supplements presents a novel strategy for preventing metabolic syndrome, particularly among high-risk individuals. Figure 1 illustrates the factors contributing to metabolic syndrome and the potential targets of medicinal plants in mitigating its risk factors.

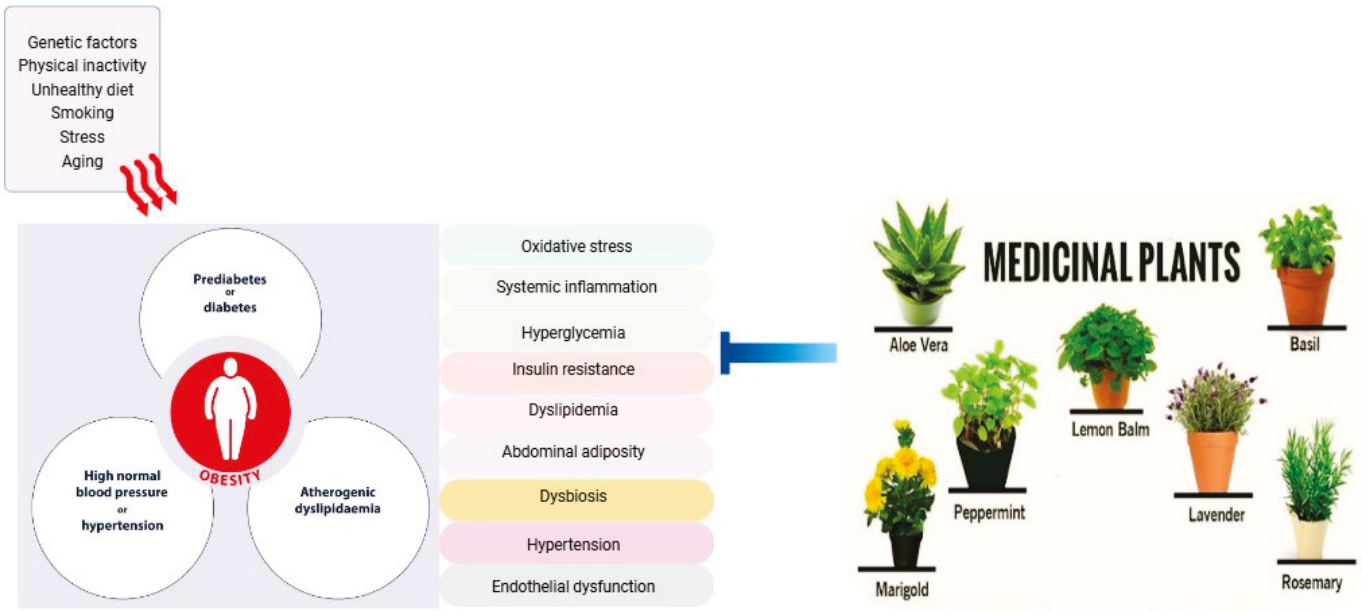

Figure 1. Factors contributing to metabolic syndrome and potential targets of medicinal plants in mitigating risk factors.

2.1. Obesity and Hyperglycemia

Obesity is characterized by excessive body fat accumulation and is accompanied by adverse alterations in adipose tissue, including reduced lipid turnover and increased infiltration of inflammatory macrophages [28]. Visceral and abdominal adipose tissue, in particular, negatively impacts metabolic and insulin signaling pathways, contributing to the pathogenesis of obesity and other metabolic syndrome risk factors [29]. Chronic hyperglycemia, resulting from impaired insulin secretion and/or action, can progress silently to T2DM, leading to potentially severe complications including retinopathy, neuropathy, nephropathy, atherosclerosis, peripheral arterial disease, and cerebrovascular accidents [30–32]. In most cases, both insulin resistance and impaired insulin secretion contribute to the metabolic disturbances affecting carbohydrate, protein, and lipid metabolism.

Several studies highlight the potential of specific plant extracts in addressing obesity and hyperglycemia. A study by Ullah et al. [33] demonstrated that a polyphenol-rich hydroethanolic extract of *Prunus domestica* L. inhibited key enzymes involved in glucose and lipid metabolism (α-amylase, α-glucosidase, HMG-CoA reductase, and pancreatic lipase) in vitro. Supplementation with *Prunus persica* (L.) Stokes flower extract (0.2% or 0.6%) for eight weeks significantly reduced body weight, visceral fat mass, and serum levels of glucose, alanine aminotransferase (ALT), and aspartate aminotransferase (AST) in a high-

fat, diet-induced, obesity mouse model [34]. These effects were linked to improved hepatic lipid metabolism. *Berberis* species, rich in berberine, have demonstrated anti-diabetic effects in in vitro, in vivo, and clinical studies [35]. Berberine's mechanism involves promoting glucose uptake, inhibiting gluconeogenesis through SIRT3 inhibition, and mimicking insulin-sensitizing effects via protein tyrosine 1B downregulation [36–39]. *Hibiscus sabdariffa* L., *Vigna unguiculata* L. Walp., and *Solanum nigrum* L. extracts significantly reduced fasting blood glucose levels in a high-fat, diet-streptozotocin-induced, diabetic rat model [40].

A randomized, placebo-controlled, crossover trial showed that consuming Queen Garnet plum juice for 28 days significantly decreased body weight, BMI, and leptin levels, and increased adiponectin levels in healthy participants [41]. Another randomized, placebo-controlled, crossover trial demonstrated that soluble fiber-rich brewer's spent grain significantly reduced postprandial glycemia and insulinemia in healthy individuals with slightly impaired glucose tolerance [42]. The extensive literature has reported the pronounced health benefits of a Mediterranean diet rich in olive oil (containing monounsaturated fatty acids and polyphenols), particularly on metabolic health [43,44]. A randomized clinical trial showed an attenuation of the early postprandial glycemic response in type 1 diabetic patients who consumed extra-virgin olive oil mixed with a high-glycemic index meal [45]. Another study demonstrated a significant reduction in fasting blood glucose, total cholesterol (TC), low-density lipoprotein (LDL), and triglycerides in diabetic subjects who consumed olive oil (30 mL/day) for four weeks [46]. In addition, high-density lipoprotein (HDL) levels were considerably increased with olive oil consumption. The oral administration of olive leaf extract (500 mg/day) for 14 weeks significantly decreased HbA1c and fasting insulin levels in diabetic subjects in a randomized, placebo-controlled trial [47].

Additional studies using fenugreek seeds [48–50] and green tea extract [51–53] are also described. Gupta et al. [48] observed significant improvements in the area under the curve of glucose and insulin sensitivity in diabetic patients supplemented either with fenugreek seeds (1 g/day) or a placebo for two months, though no significant differences were noted in fasting blood glucose levels or an oral glucose tolerance test among these groups. Another study with a cross-over design showed a considerable decrease in fasting blood glucose levels and an improvement in an oral glucose tolerance test in diabetic subjects supplemented with a diet containing fenugreek seeds (100 g/day) for 10 days [49]. The supplementation of diabetic subjects with fenugreek seeds (15 g/day) soaked in water resulted in a significant reduction in postprandial glucose levels [50]. Green tea, one of the most common beverages in the world used for maintaining a normal body weight and glucose metabolism, showed controversial results in clinical trials. A randomized, placebo-controlled study exhibited a significant decrease in HbA1c levels with no considerable effects on the fasting blood glucose levels of healthy subjects who consumed a packet of green tea extract (containing 544 mg polyphenols) daily for two months [51]. A combination of exercise and green tea extract (containing 890 mg polyphenols) resulted in a significant decrease in the area under the curve for insulin, with an increase in insulin sensitivity in healthy subjects [52]. Conversely, another study showed no effects on fasting blood glucose and HbA1c levels, insulin sensitivity and secretion, and glucose tolerance in healthy subjects supplemented with epigallo-catechin-3-gallate (800 mg/day) for eight weeks [53]. A study by Wang et al. [54] compared the beneficial effects of Qinggan Jiangtang and Glucophage tablets in patients with metabolic syndrome through a randomized, controlled, double-blind clinical trial. The results demonstrated that both treatments significantly reduced blood glucose levels, lipid profiles, blood pressure, and insulin resistance. However, no statistically significant differences were observed between the two interventions in terms of their overall efficacy. While assessing the potential benefits of grape seed extract (rich

in resveratrol and procyanidins) against insulin resistance in Iranian adolescents with metabolic syndrome, Mohammed et al. [55] observed significant improvements in insulin concentration and insulin resistance after supplementing participants with grape seed extract (100 mg/day) for eight weeks.

2.2. Dyslipidemia

Dyslipidemia, a key risk factor for atherosclerosis and subsequent cardiovascular events, is characterized by abnormal lipid profiles: elevated levels of TC, LDL, very-low-density lipoprotein (VLDL), and triglycerides (TGs), coupled with low levels of high-density lipoprotein (HDL) [54,55]. Dyslipidemia is strongly associated with obesity and/or T2DM [56,57], and risk factors include smoking, excessive alcohol consumption, obesity, T2DM, and certain medications (e.g., steroids) [58]. The Mediterranean diet, rich in fruits, vegetables, legumes, complex carbohydrates, unsaturated fatty acids, moderate wine consumption, and fish, while limiting red meat and dairy, has demonstrated significant protective effects against dyslipidemia [59,60].

Numerous studies have investigated the effects of various plant extracts on dyslipidemia. Extracts from the fruits, leaves, and bark of *Zanthoxylum armatum* DC (500 mg/kg) demonstrated significant hypolipidemic effects in mice treated for 15 days. A reduction in TC, TG, and LDL levels was observed [61]. A novel herbal formula (Schisandrae Fructus, milk thistle, hawthorn, and bitter melon) demonstrated efficacy in ameliorating diet-induced metabolic syndrome [62]. In vitro studies indicated the potent inhibitory effects of the formula's components on adipocyte differentiation, cholesterol uptake, and hepatic lipid accumulation. In vivo studies demonstrated reduced body weight, fat pad mass, and liver weight, and improved lipid profiles. Fixed oils from spices (*Alpinia galanga* (L.) Willd., *Cinnamomum zeylanicum* var. cassia, *Trigonella foenum-graecum* L., *Foeniculum vulgare* Mill., and *Myristica fragrans* Houtt.) showed an in vitro reduction in accumulated lipid droplets in 3T3-L1 cell lines, and an in vivo improvement of lipid profiles, anti-oxidant enzymes, and reduced droplets in liver and adipose tissues in C57BL/6 mice [63]. Another study showed a significant decrease in TC, LDL, TG, and the atherogenic index, and an increase in HDL levels in diet-induced dyslipidemia in Wistar rats treated with *Mangifera indica* L. leaf extract [64]. An interventional study by Venturini et al. [65] demonstrated a significant decrease in oxidative capacity and an improvement in cholesterol parameters (TC, LDL, and HDL) in subjects with metabolic syndrome, co-supplemented with fish oil (3 g/day) and extra-virgin olive oil (10 mL/day) for three months.

De Lellis et al. [66] observed the hypolipidemic effects of food supplements based on monacolins, γ-oryzanol, and γ-aminobutyric acid (bioactive ingredients from rice fermented with the *Monascus purpureus*) in participants with mild dyslipidemia. In a randomized, double-blind, placebo-controlled trial, enrolled subjects were treated either with a supplement or a placebo for three months, and the results indicated a significant decrease in TC and LDL and an increase in HDL levels in the supplement-treated group. The daily consumption of prunes (100 g) for eight weeks resulted in a significant reduction in serum LDL levels and fecal bile concentration of lithocholic acid as compared to grape juice (control) in a cross-over study [67]. A randomized clinical study demonstrated a considerable improvement of TC, TG, LDL, and HDL in hyperlipidemic subjects treated with lettuce seed extract (1000 mg/day) for 12 weeks [68]. Eight weeks of intake of a nutraceutical supplement based on bergamot extract (120 mg flavonoids), vitamin C, phytosterols, and chlorogenic acid from dry artichoke extract significantly improved the levels of TC, TG, LDL, non-HDL cholesterol, high sensitivity C-reactive protein (hs-CRP), and tumor necrosis factor-alpha (TNF-α) in a three-arm, placebo-controlled trial in dyslipidemic, overweight subjects [69]. A three-times daily intake of bitter melon extract (100 mg) for 30 days significantly reduced

LDL levels as compared to a placebo in Japanese adults, though no significant difference was observed among the groups in TC, TG, and blood glucose levels [70]. A participant-blinded, randomized, placebo-controlled, crossover trial showed a significant improvement in fat distribution and lipid profiles in healthy adolescents supplemented with psyllium fibers (6 g/day) for six weeks [71].

2.3. Hypertension, Endothelial Dysfunction, and Pro-Inflammatory State

The etiology of hypertension in metabolic syndrome is multifactorial, involving insulin resistance, obesity, hyperglycemia, and dyslipidemia [72–74]. Hypertension is a major risk factor for cardiovascular and cerebrovascular complications. A substantial body of evidence supports dietary modifications as effective strategies for preventing or managing hypertension [75]. Diets rich in fruits, vegetables, whole grains, and low-fat dairy products, while minimizing sodium intake, are particularly beneficial. Furthermore, reducing inflammation and improving endothelial function are crucial components of metabolic syndrome therapy in order to prevent or delay the onset of chronic complications [76].

Polyphenol-rich diets (e.g., those including tea, red wine, fruits, and vegetables) modulate vascular tone by upregulating the nitric oxide–cyclic guanosine monophosphate (NO-cGMP) pathway, and they mitigate oxidative stress by reducing the production of endogenous reactive oxygen species (ROS) such as NADPH oxidase [25]. Luna-Vazquez et al. [77] demonstrated that a chemically characterized black cherry fruit extract (300 mg/kg/day), rich in polyphenols (chlorogenic acid and anthocyanins), significantly reduced oxidative stress markers and systolic blood pressure in an L-NAME-induced, hypertensive rat model. Similarly, treatment with a methanolic extract of *Adansonia digitata* L. (200 mg/kg and 400 mg/kg/day) dose-dependently reduced systolic and diastolic blood pressure, mean arterial pressure, and heart rate to normal physiological levels [78]. Furthermore, *A. digitata* extract reduced biomarkers associated with endothelial dysfunction (angiotensin-converting enzyme activity), inflammation (C-reactive protein and IL-1β), oxidative stress (malondialdehyde), and cardiac injury (creatine kinase-MB and lactate dehydrogenase).

Kim et al. [79] studied the vasorelaxant effects of *Prunus persica* extract on endothelium-denuded aortic rings from a rat thoracic aorta using concentrations ranging from 0.5 to 20 μg/mL. They found that the extract's vasorelaxation involved the nitric oxide–soluble guanylate cyclase–cyclic guanosine monophosphate (NO-sGC-cGMP) pathway, vascular prostacyclin, and muscarinic receptor transduction. Additionally, the extract reduced calcium-induced vasoconstriction via inositol triphosphate receptors (IP3Rs) in the endoplasmic reticulum membrane. A randomized, controlled, cross-over clinical trial showed a significant reduction in systolic blood pressure in adults with mildly elevated blood pressure who consumed cruciferous vegetables (300 g/day) as compared to root and squash vegetables [80]. The supplementation of subjects with mild hypertension with *Nigella sativa* L. seed extracts (200 and 400 mg per day) for eight weeks resulted in a significant reduction in systolic and diastolic blood pressure in a randomized, placebo-controlled clinical trial [81]. The consumption of garlic may enhance nitric oxide production, improve endothelial function, and reduce oxidative stress, thereby improving blood pressure [82]. A double-blind, randomized, placebo-controlled clinical trial showed that the supplementation of hypertensive subjects with aged garlic extract (960 mg/day, containing 2.4 mg S-allylcysteine) for 12 weeks reduced systolic blood pressure in treated patients with uncontrolled hypertension [83].

Supplementation with anthocyanin-rich Queen Garnet plum juice alleviates platelet aggregation via reduced P-selectin expression of activated de-granulated platelets, increased activated partial thromboplastin clotting time, and decreased blood levels of fibrinogen and malondialdehyde in healthy volunteers in a randomized, placebo-controlled

clinical trial [84,85]. An experimental study designed to verify the potential of dietary berries (*Viburnum trilobum* Marshall, *Amelanchier alnifolia*, *Shepherdia argentea* (Pursh) Nutt., and *Prunus virginiana* L.) in alleviating diabetic microvascular complications and pro-inflammatory gene expression showed the potent inhibition of aldose reductase with a nonpolar fraction (rich in carotenoids) and the strong inhibition of IL-1β and COX-2 gene expression with polar fraction (rich in anthocyanins, phenolic acids, and proanthocyanidins) [86]. The aldose reductase enzyme is reportedly involved in the pathogenesis of diabetic microvascular complications.

The potential effects of plant extracts on metabolic syndrome risk factors from in vitro, in vivo, and clinical studies are summarized in Table 1.

Table 1. Effects of plant extracts on metabolic syndrome risk factors.

Plant Extract	Study Model	Concentration/Dose	Outcomes	References
Prunus domestica L. fruit pulp	In vitro	-	↓ α-amylase, α-glucosidase, HMG-CoA reductase, and pancreatic lipase enzymes ↓ nitrate, PGE_2, and IL-1β	[33]
Prunus persica (L.) Stokes flower	In vivo	0.2% or 0.6% extract mixed with diet for 8 weeks	↓ body weight, visceral fat mass, and serum levels of glucose, ALT, and AST	[34]
Hibiscus sabdariffa L., *Vigna unguiculata* L. Walp., and *Solanum nigrum* L. extracts	In vivo	200 mg/kg/day for 12 days	↓ FBG levels	[40]
Prunus salicina Lindl. (Queen Garnet plum juice)	Randomized, double-blinded, placebo-controlled, cross-over trial	200 mL/day for 4 weeks	↓ body weight, BMI, leptin levels, and increased adiponectin levels in healthy participants	[41]
Soluble fiber-rich brewer's spent grain (rich in soluble fibers and ferulic acid)	Randomized, placebo-controlled, double-blind, cross-over clinical trial	4.25 g of extract before OGTT in cross-over design	↓ postprandial glycemia and insulinemia in healthy individuals with slightly impaired glucose tolerance	[42]
Extra-virgin olive oil	Randomized, controlled, cross-over clinical trial	Olive oil consumed as meal	↓ postprandial glycemic response in type 1 diabetic patients	[45]
Olive oil	Interventional study	30 mL/day for 4 weeks	↓ FBG, TC, LDL, and TGs in diabetic patients ↑ HDL	[46]
Olive leaf extract	Randomized, placebo-controlled, clinical trial	500 mg/day for 14 weeks	↓ HbA1c and fasting insulin levels in diabetic patients	[47]
Fenugreek seeds	Randomized, double-blind, placebo-controlled, clinical trial	1 g/day for 2 months	Improvement of glucose and insulin in diabetic patients Non-significant effects on FBG and OGTT	[48]
Fenugreek seeds	Randomized, placebo-controlled, cross-over clinical trial	100 g/day for 10 days	↓ FBG and improvement in OGTT in diabetic patients	[49]
Fenugreek seeds	Interventional study	15 g/day	↓ postprandial glucose levels in diabetic patients	[50]
Green tea extract	Randomized, placebo-controlled, cross-over clinical trial	Packet of green tea extract (containing 544 mg polyphenols) for 2 months	↓ HbA1c levels in healthy subjects No effects on FBG	[51]
Exercise and green tea extract	Randomized, placebo-controlled, cross-over clinical trial	Green tea extract (containing 890 mg polyphenols)	↓ AUC for insulin in healthy subjects ↑ insulin sensitivity	[52]

Table 1. *Cont.*

Plant Extract	Study Model	Concentration/Dose	Outcomes	References
Epigallo-catechin-3-gallate (800 mg/day)	Randomized, double-blind, clinical trial	Epigallo-catechin-3-gallate (800 mg/day) for 8 weeks	No significant effects on FBG, HbA1c, insulin sensitivity, insulin secretion, and glucose tolerance	[53]
Qinggan Jiangtang tablets	Randomized, controlled, double-blind clinical trial	Three tablets twice a day for 1 month	↓ blood glucose levels, lipid profiles, blood pressure, and insulin resistance in patients with metabolic syndrome	[54]
Grape seed extract (rich in resveratrol and procyanidins)	Randomized, placebo-controlled, clinical trial	100 mg/day for 8 weeks	Improvement of insulin concentration and resistance in adolescents with metabolic syndrome.	[55]
Zanthoxylum armatum DC (fruits, leaves, and bark extracts)	In vivo	500 mg/kg/day for 15 days	↓ TC, TG, LGL levels	[61]
Schisandrae Fructus, milk thistle, hawthorn, and bitter melon	In vitro / In vivo	0–1000 μg/mL (in vitro); 2–4 % herbal formula for 12 weeks (in vivo)	↓ adipocyte differentiation, cholesterol uptake, and hepatic lipid accumulation. ↓ body weight, fat pad mass, liver weight, and improved lipid profiles.	[62]
Fixed oils from spices (*Alpinia galanga* (L.) Willd., *Cinnamomum zeylanicum* var. cassia, *Trigonella foenum-graecum* L., *Foeniculum vulgare* Mill., and *Myristica fragrans* Houtt.)	In vitro / In vivo	12.5–100 μg/mL (in vitro); 2.5–12.5% fixed oils mixed with diet (in vivo)	↓ accumulated lipid droplets in 3T3-L1 cell lines. Improvement of lipid profiles and antioxidant enzymes. ↓ droplets in liver and adipose tissues.	[63]
Mangifera indica L. leaves extract	In vivo	400 mg/kg for 32 days	↓ TC, TG, LDL, atherogenic index ↑ HDL levels	[64]
Extra-virgin olive oil plus fish oil	Interventional study	Extra-virgin olive oil (10 mL/day) and fish oil (3 g/day) for 3 months	↓ TC, LDL, and oxidative capacity ↑ HDL levels	[65]
Monascus purpureus	Randomized, double-blind, placebo-controlled trial	Standardized food supplement (2.8 mg of monacolins) for 3 months	↓ TC and LDL levels ↑ HDL levels	[66]
Prunes	Randomized, placebo-controlled, crossover, clinical trial	100 g for 8 weeks	↓ serum LDL levels and fecal lithocholic acid	[67]
Lettuce seed extract	Randomized, double-blind, placebo-controlled, pilot trial	1000 mg/day for 12 weeks	↓ TC, TG, and LDL levels ↑ HDL levels	[68]
Bergamot extract (120 mg flavonoids), vitamin C, phytosterols, and chlorogenic acid from dry artichoke extract	Randomized, double-blind, placebo-controlled trial	Two pills of food supplement for 8 weeks	↓ TC, TG, LDL, and non-HDL cholesterol levels. ↓ hs-CRP and TNF-α.	[69]
Bitter melon extract	Randomized, placebo-controlled, clinical trial	100 mg for 30 days	↓ LDL levels. No significant effects on TC, TG, and blood glucose levels	[70]

Table 1. *Cont.*

Plant Extract	Study Model	Concentration/Dose	Outcomes	References
Psyllium fibers	Randomized, placebo-controlled, crossover, clinical trial	6 g/day for 6 weeks	Improvement of fat distribution and lipid profile in healthy adolescents	[71]
Black cherry fruit extract	In vivo	300 mg/kg/day for 4 weeks	↓ oxidative stress markers and systolic blood pressure	[77]
Adansonia digitata L.	In vivo	200 mg/kg and 400 mg/kg/day for 3 weeks	Dose-dependent reduction in systolic and diastolic blood pressure, mean arterial pressure, and heart rate. ↓ ACE activity, CRP, IL-1β, malondialdehyde, creatine kinase-MB, and lactate dehydrogenase	[78]
Prunus persica (L.) Stokes extract	In vitro	0.5 to 20 µg/mL	Enhanced vasorelaxation by targeting NO-sGC-cGMP and IP3R pathways	[79]
Cruciferous vegetables	Randomized, placebo-controlled, cross-over clinical trial	300 g/day for 2 weeks	↓ systolic blood pressure	[80]
Nigella sativa L. seed extract	Randomized, double-blind, placebo-controlled, clinical trial	200 and 400 mg/day for 8 weeks	↓ systolic and diastolic blood pressure	[81]
Garlic extract	Randomized, double-blind, placebo-controlled, clinical trial	960 mg/day (containing 2.4 mg S-allylcysteine) for 12 weeks	↓ systolic blood pressure	[83]
Anthocyanin-rich Queen Garnet plum juice	Randomized, double-blind, placebo-controlled, cross-over trial	200 mL/day for 28 days	↓ ADP-induced platelet aggregation and platelet activation-dependent P-selectin expression. Prolonged activated-partial thromboplastin clotting time. ↓ plasma-fibrinogen and malondialdehyde levels.	[84,85]
Viburnum trilobum Marshall, *Amelanchier alnifolia, Shepherdia argentea* (Pursh) Nutt., and *Prunus virginiana* L.	In vitro	-	↓ aldose reductase. ↓ IL-1β and COX-2 gene expression.	[86]

Increase (↑), decrease (↓), prostaglandin E2 (PGE2), interleukin-1β (IL-1β); alanine aminotransferase (ALT), aspartate aminotransferase (AST), fasting blood glucose (FBG), body mass index (BMI), oral glucose tolerance test (OGTT), total cholesterol (TC), low-density lipoprotein (LDL), high-density lipoprotein (HDL), triglycerides (TGs), glycated hemoglobin (HbA1c), area under curve (AUC), high sensitivity C-reactive protein (hs-CRP), tumor necrosis factor-α (TNF-α), angiotensin-converting enzyme (ACE), nitric oxide–soluble guanylate cyclase–cyclic guanosine monophosphate pathway (NO-sGC-cGMP), inositol triphosphate receptors (IP3R), cyclooxygenase (COX-2).

3. Safety Concerns

The safety of plant extracts and their bioactive constituents is paramount when considering their use in dietary supplements or functional foods. Although generally considered safe, thorough evaluation is crucial to ensure human safety, as many plant extracts lack systematic toxicity testing [87]. A significant number of plants used traditionally as food or medicine have demonstrated potential toxicity, mutagenicity, or carcinogenicity [87]. Adewunmi and Ojewole [88] identified several potentially toxic compounds found in com-

plementary and alternative medicines: lectins, viscotoxins, aristolochic acids, pyrrolizidine alkaloids, benzophenanthrine alkaloids, saponins, diterpenes, cyanogenic glycosides, and furanocoumarins.

Unlike conventional pharmaceuticals, dose-dependent toxicity data and long-term safety evaluations for plant extracts are often limited, especially for novel or high-potency formulations [89]. Several commonly used plant extracts, for example, *Curcuma longa* L., *Camellia sinensis* (L.) Kuntze, *Withania somnifera* (L.) Dunal, *Garcinia gummi-gutta* (L.) N. Robson, *Monascus purpureus*, and *Actaea racemosa* L., have been associated with increased hepatotoxicity risk [89].

Additional safety concerns arise from microbial or heavy metal contamination during the harvesting, processing, and storage of plant materials [90]. Heavy metal contamination, resulting from various industrial, agricultural, and technological sources, is often found in herbal products at concentrations exceeding permitted limits [91]. These heavy metals are known carcinogens and can cause internal organ toxicity affecting the brain, heart, lungs, liver, and kidneys [91]. The WHO emphasizes the need for international standards and procedures for assessing the safety and efficacy of traditional medicines [92]. Although pharmacological and toxicological data are crucial for drug development, such data for plant extracts are far less abundant than reports of their purported therapeutic benefits [93–96]. Rigorous in vivo safety and efficacy studies, using appropriate animal models and well-designed, randomized, placebo-controlled clinical trials, are essential [92,97]. Comprehensive long-term safety evaluations are critical for the development of standardized herbal medicines and their adoption by healthcare providers.

Finally, drug–botanical interactions pose a growing concern [98]. These interactions may be pharmacokinetic (affecting drug absorption, distribution, metabolism, and elimination) or pharmacodynamic (producing antagonistic, synergistic, or additive effects). Grapefruit products, for instance, inhibit intestinal cytochrome P450 3A4 (due to furanocoumarins) and modulate P-glycoprotein and drug transporters (due to flavonoids), altering the bioavailability of many drugs, including calcium channel blockers, statins, antihistamines, and immunosuppressants [99]. American ginseng and cranberry juice can affect warfarin metabolism, impacting coagulation and bleeding risk [100,101]. Similarly, ginkgo products can interfere with P-glycoprotein-mediated drug transport, reducing blood and tissue concentrations of several drugs, such as colchicine, doxorubicin, digoxin, quinidine, tacrolimus, verapamil, and rosuvastatin [98].

Regulations governing the use of plant extracts for managing risk factors associated with metabolic syndrome vary significantly across countries. In the United States, plant extracts are regulated by the Food and Drug Administration (FDA) under the Dietary Supplement Health and Education Act (DSHEA). This framework ensures that these products are safe for consumption and are accurately labeled. However, unlike pharmaceutical drugs, plant extracts do not require pre-market approval. In contrast, within the European Union, plant extracts are regulated by the European Medicines Agency (EMA) and are classified either as food supplements or medicinal products, depending on their intended use. Regardless of the regulatory framework, plant extracts intended for the management of metabolic syndrome risk factors must meet stringent efficacy and safety standards to ensure their therapeutic potential and minimize health risks [102].

4. Technological Aspects

Plant extracts have a long history of use as preventive and therapeutic agents for managing metabolic syndrome risk factors [103]. Rich in bioactive compounds, these extracts offer promising potential for mitigating obesity, hyperglycemia, hypertension, and dyslipidemia. However, widespread clinical application requires a thorough understanding of the

technological aspects of their production, stabilization, and delivery. Recent advancements in extraction and processing techniques have significantly improved the stability, bioavailability, efficacy, and safety of bioactive compounds, enhancing their effectiveness in both supplements and pharmaceutical formulations [104,105].

The technological aspects of plant extract utilization are multifaceted, ranging from selecting optimal extraction methods to developing innovative delivery systems. Emerging technologies, including ultrasound-assisted extraction, supercritical fluid extraction, and encapsulation, offer significant advantages over traditional methods: enhanced efficiency, higher yields, improved compound stability, and reduced environmental impact. This section will explore the technological aspects of plant extract processing, focusing on extraction techniques, delivery systems, stability enhancement strategies, formulation approaches, and industrial-scale production.

4.1. Extraction Techniques

Extraction is the initial step in isolating and purifying bioactive compounds from botanical and food sources. Soluble compounds are generally easier to extract than insoluble secondary metabolites such as flavonoids and phenolic acids. While Soxhlet, maceration, and heat reflux are established methods, their equipment requirements vary. Optimal extraction technologies prioritize product quality, efficiency, cost-effectiveness, and sustainability [104]. The food industry is actively exploring novel extraction methods to meet consumer demand for chemical-free, sustainably produced products. Cutting-edge techniques such as ultrasound-assisted extraction (UAE), enzyme-assisted extraction, microwave-assisted extraction (MAE), pressurized liquid extraction (PLE), and supercritical fluid extraction (SFE) are rapidly replacing traditional methods [106]. These innovative approaches often result in higher yields, improved extraction rates, reduced energy consumption, and better preservation of thermosensitive compounds [106]. Figure 2 summarizes these techniques.

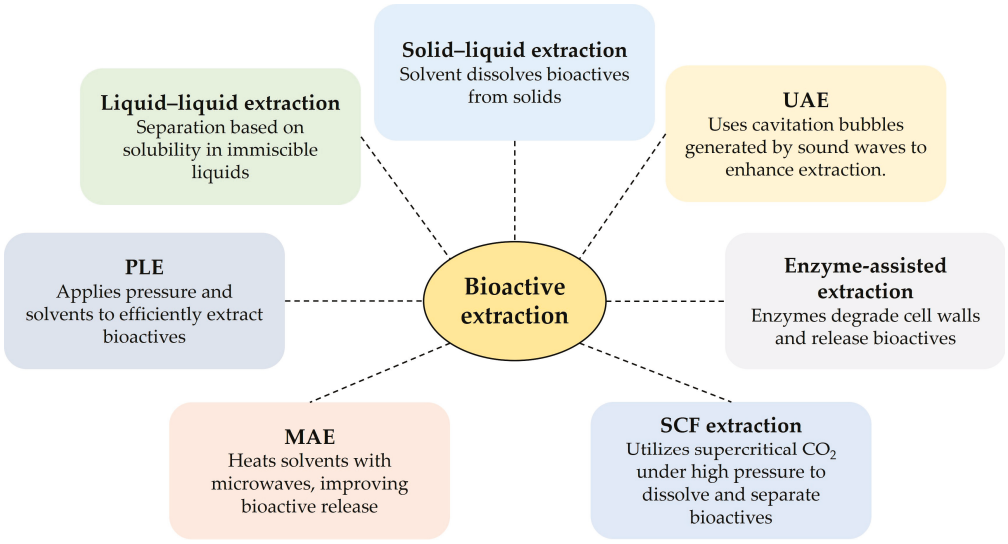

Figure 2. Extraction techniques and their basic principles. Ultrasound-assisted extraction (UAE); microwave-assisted extraction (MAE); pressurized liquid extraction (PLE); and super critical fluid (SCF).

Traditional methods, such as liquid–liquid extraction, solid-phase extraction, and solid-phase microextraction, have also been used. Liquid–liquid extraction utilizes two immiscible solvents (e.g., aqueous and organic solvents) to partition the analyte based on its relative solubility in each solvent [107]. Solid-phase extraction uses a solid stationary

phase to selectively adsorb or extract analytes from a liquid sample [108]. Solid-phase microextraction exposes a sample to a solid phase coated with an extracting phase for a defined period, followed by analysis using gas chromatography or high-performance liquid chromatography (HPLC). This method is particularly useful for detecting trace amounts of bioactive compounds [109].

UAE utilizes ultrasonic frequencies (18–100 kHz), inaudible to humans, to enhance mass transfer and disrupt cellular matrices, thereby increasing extraction yields [110,111]. Enzyme-assisted extraction employs enzymes to break down cell walls, improving solvent access to bioactive compounds [112]. MAE uses microwave energy for both the internal and external heating of the sample matrix, avoiding thermal gradients and enhancing extraction efficiency [113]. PLE applies pressure to maintain the liquid state of the solvent at elevated temperatures (50–200 °C), increasing extraction efficiency [114]. SFE utilizes supercritical fluids (e.g., CO2) whose properties can be finely tuned by adjusting the temperature and pressure to achieve optimal selectivity and efficiency [115].

Using ultrasound energy to extract tea solids from dried leaves with water increased the extraction yield by 20%. Using several solvents, such as ethanol, ethyl acetate, and butanone, UAE also demonstrated superior carnosic acid extraction and decreased extraction time [116]. Jadhav et al. [117] demonstrated the enhanced extraction of vanillin in a shorter time period for different solvents using UAE technique as compared to the Soxhlet method. Cho et al. [118] showed UAE as being very effective method for extracting resveratrol from grapes, where the degradation of resveratrol during extraction process was negligible within a specified time period. When compared to maceration and Soxhlet extraction, UAE provides the maximum extraction yield of some flavonoids, including tectoridin, iristectorin B, iristectorin A, tectorigenin, iris-tectorigenin A, and total isoflavones, in a shorter amount of time [119]. MAE, an alternate method for extracting tanshinones from the root of *Saliva miltiorrhiza* Bunge, yields higher extraction efficiency in less time [120]. A kinetic analysis of the impact of the solvent composition, the solvent volume, the extraction temperature, and matrix properties on the MAE of peppermint and rosemary leaves showed that using pure, microwave-transparent solvents like hexane could lead to the quick extraction of essential oil components from sample matrices that contain water. This resulted from the direct contact of microwaves with the cell's free water molecules, which ruptured the cell and released the essential oil into the hexane [121]. The MAE-prepared extract had the highest scavenging activity and the highest phenolic and tannin concentration. MAE was found to be more effective than UAE in terms of extraction efficiency, especially when it came to extracting the phenolic and tannin content. Additionally, a notable 20% increase in antioxidant activity was seen [122].

SFE is used to extract volatile or aromatic chemicals from plant materials, including caffeine and essential oils. Several variables are crucial for extraction by SFE, including temperature, pressure, sample volume, cosolvent addition, and flow and pressure control [116]. Hexane, pentane, butane, nitrous oxide, sulfur hexafluoride, and fluorinated hydrocarbons are among the solvents that can be utilized for SFE, with CO_2 being the most widely used extraction solvent [123]. There are several benefits to using SFE with CO_2 for grape seed oil extraction in terms of both process efficiency and extracted oil quality. Supercritical CO_2 extraction produces oil devoid of organic solvents, and it also takes less processing time than traditional solvent extraction techniques. Today's oil technology requires the extract to be completely free of organic solvents; otherwise, it takes a lot of time and effort [124]. Kothari et al. [125] conducted a comparative analysis of different extraction techniques for extracting phenolic and antibacterial components from plant seeds (*Annona squamosa*, *Manilkara zapota*, *Phoenix sylvestris*, *Syzygium cumini*, and *Tamarindus indica*). These techniques included the Soxhlet method, UAE, extraction by continuous

shaking at room temperature, and MAE, both with and without intermittent cooling. The Soxhlet technique was more effective in terms of higher extraction efficiency and phenolic compound extraction. MAE with intermittent cooling, room temperature extraction by shaking, and UAE showed promising effects in extracting antibacterial components from plant seeds.

4.2. Encapsulation and Delivery Systems

Despite their wide range of health benefits, the application of plant extracts and their bioactive compounds in functional foods and supplements has been limited by their low bioaccessibility and bioavailability [126–130]. This is often due to several factors, including limited release from the matrix, poor solubility in gastrointestinal fluids, low permeability across epithelial cells, and susceptibility to degradation during gastrointestinal transit [126–130]. Many bioactive compounds are also sensitive to environmental factors such as oxygen and heat, further reducing their effectiveness.

Encapsulation and advanced delivery systems offer innovative solutions to these challenges, improving the stability and bioavailability of plant extracts [131,132]. Encapsulation involves coating an active compound or mixture with a polymeric material to protect it from environmental degradation and to control the release of the bioactive compounds at specific sites [133]. Encapsulation can also mask unpleasant odors or tastes, improving the overall sensory appeal of the product [134]. Given the often-limited bioavailability of plant-derived bioactives, encapsulation is a promising strategy to protect these compounds during gastrointestinal transit and to enhance their delivery to the target site of action. Figure 3 illustrates various factors that affect the stability and bioavailability of botanical extracts, as well as the different encapsulation techniques used to protect against these factors, thereby improving both stability and bioavailability.

Encapsulation techniques are classified by capsule size as nano-encapsulation (<1 μm) or microencapsulation (3–800 μm) [135,136]. Various methods are currently being explored, including spray drying, freeze drying, extrusion, emulsification, coacervation, molecular inclusion, and ionic gelation (Table 2).

Table 2. Encapsulation techniques, their definitions, uses, advantages, and disadvantages [131].

Encapsulation Technique	Definition	Uses	Advantages	Disadvantages
Spray-drying	A method where active ingredients are mixed with a wall material, atomized in a hot chamber, and dried into powder.	Used for shelf-life enhancement and the encapsulation of various active compounds.	Low cost, easy scalability, and improved product stability.	A limited number of wall materials can be used.
Freeze-drying	Freezing active materials to form ice, followed by sublimation in a vacuum to create porous, powdered products.	Encapsulation of temperature-sensitive materials like aromas and volatile oils.	Simple process, preserves sensitive compounds effectively.	Time-consuming and high energy costs.
Extrusion	Polymer solution-containing active material is extruded through a nozzle into a gel solution.	Used for encapsulating both hydrophilic and hydrophobic compounds.	Simple, laboratory-friendly, and produces high shelf-life capsules.	Difficult and expensive to scale up.
Emulsification	Involves creating emulsions of two immiscible liquids (water and oil) stabilized by emulsifiers.	Encapsulation of oil-soluble compounds like dietary fats and sterols.	Provides both liquid and powder encapsulation options.	Requires specific emulsifiers for stabilization.

Table 2. *Cont.*

Encapsulation Technique	Definition	Uses	Advantages	Disadvantages
Coacervation	Separation of phases leading to the formation of encapsulated materials within polymeric walls.	High-efficiency encapsulation with controlled release properties.	High encapsulation efficiency and control over material release.	Capsules are often unstable and the production cost is high.
Molecular inclusion	Based on hydrogen bonding and electrostatic interactions between polar molecules.	Encapsulation of polar molecules, commonly using cyclodextrins.	Compatible with a wide range of polar compounds.	Limited use outside of specific polar interactions.
Ionic gelation	Encapsulation using microbeads in biopolymer gels, formed by methods like spraying or extrusion.	Commonly used for suspending active materials in polymer solutions.	Simple and adaptable to various active materials.	Limited by the biopolymer's properties and stability in different environments.

Several encapsulation techniques are employed to enhance the stability and bioavailability of plant extracts. Spray drying, a cost-effective and scalable method, atomizes a mixture of wall material and active ingredients in a hot chamber, causing the solvent to evaporate and the active compound to solidify into a powder [137]. Freeze drying, suitable for temperature-sensitive compounds, freezes the mixture and then removes the ice through sublimation under vacuum, resulting in a porous powder [137]. Extrusion involves forcing a gel solution (often using sodium alginate as the wall material) through a nozzle to create capsules in a hardening bath (e.g., calcium chloride solution) [138]. Emulsification combines two immiscible liquids (e.g., oil and water) stabilized by an emulsifier, producing either a liquid or solid final product [137]. Coacervation involves separating polyelectrolyte phases to encapsulate the active compounds, with cross-linking agents often used to improve stability [136]. Molecular inclusion utilizes cyclodextrins or similar compounds to encapsulate polar molecules through non-covalent interactions [139,140]. Finally, ionic gelation employs biopolymer-based microbeads to encapsulate active compounds, often using calcium alginate [139].

Numerous studies have demonstrated the benefits of encapsulation in improving the delivery and efficacy of plant-derived compounds. Ezzat et al. [141] and Peng et al. [142] reported increased oral bioavailability of encapsulated tea polyphenols in rats. Similarly, coacervated fisetin showed enhanced bioavailability and increased peak plasma concentrations in C57BL/6 mice [143]. Nano-formulated tea extracts demonstrated anti-obesity effects in rats via the modulation of the AMPK/Sirt-1/Glut-4 and PPAR-γ pathways [144]. Freeze-dried mulberry fruit extract improved various metabolic parameters (body weight, adiposity index, glucose intolerance, lipid profiles, atherogenic index, and oxidative stress) in a menopausal, metabolic syndrome animal model [145]. Andean blueberry anthocyanin niosomes reduced fasting blood glucose and insulin levels, glucose intolerance, and body weight [146]. The ionic gelation of black carrot anthocyanin extract reduced lipid peroxidation, increased antioxidant enzyme activity, and decreased lipogenesis [147]. Spray-dried peanut skin extract reduced postprandial glucose spikes [148]. Finally, 14-day toxicity studies in animal models demonstrated the safety of encapsulated extracts from green coffee fruit, polyherbal formulations (PHFs), and *Moringa oleifera* leaf polyphenols [149–151]. The encapsulation of cocoa polyphenol extract significantly improved the delivery of flavanols to the gut in a randomized, cross-over clinical trial, thereby enhancing their bioaccessibility and bioavailability [152]. Another study showed increased bioavailability of encapsulated almond skin polyphenols (flavan-3-ols, flavonols, and flavanones) in a single-blind, placebo-controlled, and randomized trial [153]. These studies strongly suggest the safety and potential benefits of using encapsulated plant extracts.

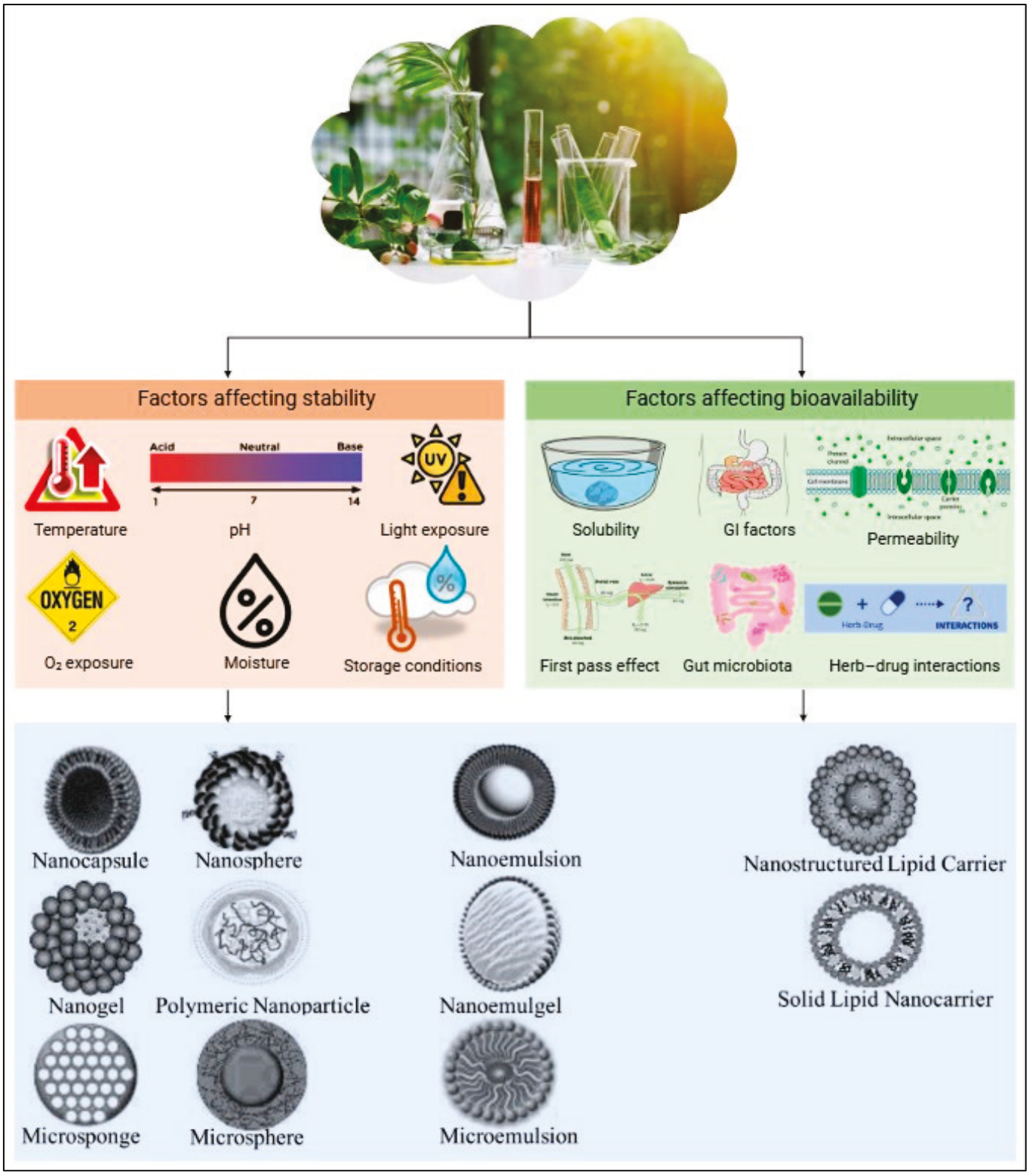

Figure 3. Factors influencing stability and bioavailability of botanical extracts and encapsulation techniques for enhancement.

4.3. Stabilization and Shelf-Life Improvement

Maintaining the shelf life of plant extracts in functional foods presents a significant challenge. Bioactive compounds, such as phenols and carotenoids, are susceptible to degradation from environmental factors like oxygen, heat, and light, resulting in reduced

bioactivity [154,155]. Several technologies, including encapsulation, spray drying, and freeze drying, along with the use of natural stabilizers and antioxidants, are crucial for extending shelf life and maintaining functionality [154,155].

For example, microencapsulation via extrusion extends the shelf life of oxidation-sensitive flavor compounds, such as citrus oils, by creating a nearly impermeable barrier against oxygen diffusion through the hydrophilic glassy matrix [156]. Extruded citrus oils can remain stable for up to five years, compared to one year for spray-dried oils and only a few months for unencapsulated oils [156]. The spray drying of *Euterpe oleracea* Mart. powder reduced moisture content and improved stability, inhibiting microbial growth and chemical degradation [157]. Similarly, the spray drying of grape skin phenolic extracts decreased moisture content and water activity, while freeze drying reduced hygroscopicity [158].

4.4. Formulation into Functional Foods, Scalability, and Industrial Applications

The incorporation of plant extracts into functional foods has gained significant attention as a preventative strategy to combat the rising prevalence of metabolic disorders and their associated health consequences. However, several challenges exist. The characteristics of plant extracts may change as production scales up, potentially affecting the flavor, texture, and nutritional value of the final product [159]. Moreover, the inherent instability of many bioactive compounds leads to degradation during processing and storage, reducing efficacy and health benefits [160].

Meeting the growing demand for functional foods necessitates scaling up production, a complex process requiring careful planning and execution. Simple quantity increases are insufficient; several factors change as production scales from small to large volumes. Maintaining desired effects require the careful consideration of bioactive compounds' interactions within the food matrix, as their behavior can differ significantly at higher concentrations [161]. For example, bioactives such as polyphenols, carotenoids, phytosterols, and peptides, while enhancing nutritional value, may lose bioactivity during processing and storage [161]. Changes in taste and stability can also arise, potentially creating incompatibilities with existing food manufacturing processes. Challenges include adapting sourcing and processing, modifying formulations, and addressing potential operational complications [159,161]. Encapsulation techniques, such as spray drying, freeze drying, and coacervation, are commonly used to overcome these challenges and effectively incorporate bioactive compounds into functional foods [162,163].

5. Conclusions

This review underscores the considerable potential of plant extracts in mitigating risk factors associated with metabolic syndrome. Current evidence highlights their ability to regulate glucose and lipid metabolism, improve vascular function, and counteract oxidative stress. Integrating plant extracts into functional foods and supplements presents a promising strategy for enhancing the health-promoting properties of these products and potentially preventing chronic diseases. However, several limitations exist within the body of research investigating the beneficial effects of plant extracts on metabolic syndrome, revealing critical gaps in the literature:

i. Limited clinical translation: The majority of studies are based on in vitro and animal models, which may not fully reflect clinical effects in human populations.
ii. Variability in bioactive composition: The composition and concentration of bioactive compounds in plant extracts can vary due to multiple factors, including plant sources, environmental conditions, and extraction methods. This variability complicates the establishment of consistent efficacy and safety profiles.

iii. Confounding variables in study design: Many studies do not adequately control for lifestyle factors such as diet and physical activity. Consequently, observed effects may be influenced by external variables rather than the plant extracts alone.
iv. Short study durations and small sample sizes: Clinical trials investigating the effects of plant extracts on metabolic syndrome often have limited durations, small sample populations, and insufficient long-term follow-up, restricting the generalizability of findings and their broader clinical application. Large-scale, long-term, randomized controlled trials are essential to establish both efficacy and safety for widespread use.
v. Underrepresentation of pediatric and adolescent populations: While metabolic syndrome is predominantly associated with adults and older individuals, its prevalence is increasing among children and adolescents. However, research on the potential benefits of plant extracts in these younger populations remains limited.
vi. Lack of direct comparisons with conventional therapies: Most clinical studies utilize placebo-controlled designs, with relatively few directly comparing plant extracts to conventional pharmaceutical treatments. Future research should emphasize comparative studies to draw more definitive conclusions regarding the therapeutic potential of plant extracts relative to standard medical interventions.
vii. Limited investigation into bioavailability: Bioavailability is a crucial determinant of the physiological effects of both pharmacological drugs and plant extracts. However, in contrast to pharmaceutical compounds, the bioavailability of plant-derived extracts in human subjects remains largely unexplored.
viii. Regulatory and interaction challenges: The absence of standardized regulatory frameworks and the potential for interactions between plant extracts and pharmaceutical drugs present additional challenges that must be addressed to ensure safe and effective use.
ix. Stability and commercial viability: While the stability and shelf-life of plant extracts have been extensively studied, their evaluation within commercially available products is limited. Further research is needed to optimize formulations for real-world applications.

To fully harness the therapeutic potential of plant extracts, rigorous, well-designed clinical trials are essential to confirm their efficacy, safety, and long-term benefits. Addressing these research gaps will facilitate the integration of plant-based interventions into mainstream healthcare and functional food industries.

Author Contributions: Conceptualization, H.U. and M.D. (Maria Daglia); methodology, H.U., M.D. (Marco Dacrema) and A.D.M.; validation, M.D. (Marco Dacrema), D.G.B. and L.F.D.L.; formal analysis, D.G.B., M.A.A.F., L.F.D.L. and A.B.; resources, M.A.A.F., M.V.M. and A.B.; data curation, D.G.B. and A.B.; writing—original draft preparation, H.U., M.D. (Marco Dacrema) and M.A.A.F.; writing—review and editing, H.U., L.F.D.L., M.V.M., A.D.M. and M.D. (Maria Daglia); visualization, A.D.M. and M.D. (Maria Daglia); supervision, H.U. and M.D. (Maria Daglia). All authors have read and agreed to the published version of the manuscript.

Funding: This research received no external funding.

Institutional Review Board Statement: Not applicable.

Informed Consent Statement: Not applicable.

Conflicts of Interest: Author Alessandro Di Minno was employed by the company CEINGE-Biotecnologie Avanzate. The remaining authors declare that the research was conducted in the absence of any commercial or financial relationships that could be construed as a potential conflict of interest.

Abbreviations

ADRs	adverse drug reactions
ALT	alanine aminotransferase
AST	aspartate aminotransferase
BMI	body mass index
CHD	coronary heart disease
DSHEA	Dietary Supplement Health and Education Act
EMA	European Medicines Agency
FDA	Food and Drug Administration
HbA1c	glycated hemoglobin
HDL	high-density lipoprotein
HPLC	high-performance liquid chromatography
hs-CRP	high sensitivity C-reactive protein
IDF	International Diabetes Federation
LDL	low-density lipoprotein
MAE	microwave-assisted extraction
NCEP ATP III	National Cholesterol Education Program's Adult Treatment Panel III
NO-cGMP	nitric oxide–cyclic guanosine monophosphate pathway
NO-sGC-cGMP	nitric oxide–soluble guanylate cyclase–cyclic guanosine monophosphate pathway
PLE	pressurized liquid extraction
ROS	reactive oxygen species
SFE	supercritical fluid extraction
T2DM	type 2 diabetes mellitus
TC	total cholesterol
TGs	triglycerides
UAE	ultrasound-assisted extraction
VLDL	very-low-density lipoprotein
WHO	World Health Organization

References

1. Costa, L.A.; Canani, L.H.; Lisboa, H.R.K.; Tres, G.S.; Gross, J.L. Aggregation of features of the metabolic syndrome is associated with increased prevalence of chronic complications in Type 2 diabetes. *Diabet. Med.* **2004**, *21*, 252–255. [CrossRef] [PubMed]
2. McCracken, E.; Monaghan, M.; Sreenivasan, S. Pathophysiology of the metabolic syndrome. *Clin. Dermatol.* **2018**, *36*, 14–20. [CrossRef]
3. Alberti, K.G.M.M.; Zimmet, P.Z. Definition, diagnosis and classification of diabetes mellitus and its complications. Part 1: Diagnosis and classification of diabetes mellitus. Provisional report of a WHO consultation. *Diabet. Med.* **1998**, *15*, 539–553. [CrossRef]
4. Expert Panel on Detection, E. Executive summary of the third report of the National Cholesterol Education Program (NCEP) expert panel on detection, evaluation, and treatment of high blood cholesterol in adults (Adult Treatment Panel III). *JAMA* **2001**, *285*, 2486.
5. IDF. International Diabetes Federation: The IDF Consensus Worldwide Definition of the Metabolic Syndrome. 2005. Available online: https://idf.org/media/uploads/2023/05/attachments-30.pdf (accessed on 9 August 2024).
6. Zhang, H.; Zhou, X.D.; Shapiro, M.D.; Lip, G.Y.; Tilg, H.; Valenti, L.; Somers, V.K.; Byrne, C.D.; Targher, G.; Yang, W.; et al. Global burden of metabolic diseases, 1990–2021. *Metabolism* **2024**, *160*, 155999. [CrossRef] [PubMed]
7. Noubiap, J.J.; Nansseu, J.R.; Lontchi-Yimagou, E.; Nkeck, J.R.; Nyaga, U.F.; Ngouo, A.T.; Tounouga, D.N.; Tianyi, F.L.; Foka, A.J.; Ndoadoumgue, A.L.; et al. Geographic distribution of metabolic syndrome and its components in the general adult population: A meta-analysis of global data from 28 million individuals. *Diabetes Res. Clin. Pract.* **2022**, *188*, 109924. [CrossRef] [PubMed]
8. WHO. Obesity and Overweight. 2018. Available online: https://www.who.int/news-room/fact-sheets/detail/obesity-and-overweight (accessed on 9 August 2024).
9. WHO. Diabetes. 2019. Available online: https://www.who.int/news-room/fact-sheets/detail/diabetes (accessed on 9 August 2024).
10. WHO. Hypertension. 2019. Available online: https://www.who.int/news-room/fact-sheets/detail/hypertension (accessed on 9 August 2024).

11. Kaur, J. Assessment and screening of the risk factors in metabolic syndrome. *Med. Sci.* **2014**, *2*, 140–152. [CrossRef]
12. Åberg, F.; Helenius-Hietala, J.; Puukka, P.; Färkkilä, M.; Jula, A. Interaction between alcohol consumption and metabolic syndrome in predicting severe liver disease in the general population. *Hepatology* **2018**, *67*, 2141–2149. [CrossRef]
13. Mongraw-Chaffin, M.; Foster, M.C.; Anderson, C.A.; Burke, G.L.; Haq, N.; Kalyani, R.R.; Ouyang, P.; Sibley, C.T.; Tracy, R.; Woodward, M.; et al. Metabolically healthy obesity, transition to metabolic syndrome, and cardiovascular risk. *J. Am. Coll. Cardiol.* **2018**, *71*, 1857–1865. [CrossRef]
14. Prasad, H.; Ryan, D.A.; Celzo, M.F.; Stapleton, D. Metabolic syndrome: Definition and therapeutic implications. *Postgrad. Med.* **2012**, *124*, 21–30. [CrossRef]
15. Rask Larsen, J.; Dima, L.; Correll, C.U.; Manu, P. The pharmacological management of metabolic syndrome. *Expert Rev. Clin. Pharmacol.* **2018**, *11*, 397–410. [CrossRef]
16. Matfin, G. Developing therapies for the metabolic syndrome: Challenges, opportunities, and... the unknown. *Ther. Adv. Endocrinol. Metab.* **2010**, *1*, 89–94. [CrossRef] [PubMed]
17. Behzad, M.; Negah, R.; Suveer, B.; Neda, R. A review of thiazolidinediones and metformin in the treatment of type 2 diabetes with focus on cardiovascular complications. *Vasc. Health Risk Manag.* **2007**, *3*, 967–973.
18. Cheung, K.S.; Chan, E.W.; Wong, A.Y.; Chen, L.; Seto, W.K.; Wong, I.C.; Leung, W.K. Aspirin and risk of gastric cancer after Helicobacter pylori eradication: A territory-wide study. *J. Natl. Cancer Inst.* **2018**, *110*, 743–749. [CrossRef]
19. Pasnoor, M.; Barohn, R.J.; Dimachkie, M.M. Toxic myopathies. *Curr. Opin. Neurol.* **2018**, *31*, 575–582. [CrossRef] [PubMed]
20. Weir, M.R.; Bakris, G.L.; Bushinsky, D.A.; Mayo, M.R.; Garza, D.; Stasiv, Y.; Wittes, J.; Christ-Schmidt, H.; Berman, L.; Pitt, B. Patiromer in patients with kidney disease and hyperkalemia receiving RAAS inhibitors. *N. Engl. J. Med.* **2015**, *372*, 211–221. [CrossRef]
21. Guo, Z. The modification of natural products for medical use. *Acta Pharm. Sin. B* **2017**, *7*, 119–136. [CrossRef]
22. Williamson, E.M.; Liu, X.; Izzo, A.A. Trends in use, pharmacology, and clinical applications of emerging herbal nutraceuticals. *Br. J. Pharmacol.* **2020**, *177*, 1227–1240. [CrossRef]
23. Ekor, M. The growing use of herbal medicines: Issues relating to adverse reactions and challenges in monitoring safety. *Front. Pharmacol.* **2014**, *4*, 177. [CrossRef] [PubMed]
24. Jang, S.; Jang, B.H.; Ko, Y.; Sasaki, Y.; Park, J.S.; Hwang, E.H.; Song, Y.K.; Shin, Y.C.; Ko, S.G. Herbal medicines for treating metabolic syndrome: A systematic review of randomized controlled trials. *Evid. Based Complement. Alternat. Med.* **2016**, *2016*, 5936402. [CrossRef]
25. Ullah, H.; De Filippis, A.; Khan, H.; Xiao, J.; Daglia, M. An overview of the health benefits of Prunus species with special reference to metabolic syndrome risk factors. *Food Chem. Toxicol.* **2020**, *144*, 111574. [CrossRef] [PubMed]
26. Ullah, H.; Daglia, M. Phytonutrients in the management of glucose metabolism. In *The Role of Phytonutrients in Metabolic Disorders*; Khan, H., Akkol, E., Daglia, M., Eds.; Academic Press: Cambridge, UK, 2022; pp. 163–193.
27. Ullah, H.; De Filippis, A.; Santarcangelo, C.; Daglia, M. Epigenetic regulation by polyphenols in diabetes and related complications. *Med. J. Nutrition. Metab.* **2020**, *13*, 289–310. [CrossRef]
28. Sam, S.; Mazzone, T. Adipose tissue changes in obesity and the impact on metabolic function. *Transl. Res.* **2014**, *164*, 284–292. [CrossRef] [PubMed]
29. Blüher, M.; Paschke, R. Visceral adipose tissue and metabolic syndrome. *Dtsch. Med. Wochenschr.* **2003**, *128*, 2319–2323.
30. Lotfy, M.; Adeghate, J.; Kalasz, H.; Singh, J.; Adeghate, E. Chronic complications of diabetes mellitus: A mini review. *Curr. Diabetes Rev.* **2017**, *13*, 3–10. [CrossRef]
31. Gandhi, J.; Dagur, G.; Warren, K.; Smith, N.L.; Khan, S.A. Genitourinary complications of diabetes mellitus: An overview of pathogenesis, evaluation, and management. *Curr. Diabetes Rev.* **2017**, *13*, 498–518. [CrossRef]
32. Ozougwu, J.; Obimba, K.; Belonwu, C.; Unakalamba, C. The pathogenesis and pathophysiology of type 1 and type 2 diabetes mellitus. *J. Physiol. Pathophysiol.* **2013**, *4*, 46–57. [CrossRef]
33. Ullah, H.; Sommella, E.; Santarcangelo, C.; D'Avino, D.; Rossi, A.; Dacrema, M.; Minno, A.D.; Di Matteo, G.; Mannina, L.; Campiglia, P.; et al. Hydroethanolic extract of *Prunus domestica* L.: Metabolite profiling and in vitro modulation of molecular mechanisms associated to cardiometabolic diseases. *Nutrients* **2022**, *14*, 340. [CrossRef]
34. Song, J.; Kim, Y.S.; Kim, L.; Park, H.J.; Lee, D.; Kim, H. Anti-obesity effects of the flower of Prunus persica in high-fat diet-induced obese mice. *Nutrients* **2019**, *11*, 2176. [CrossRef] [PubMed]
35. Belwal, T.; Bisht, A.; Devkota, H.P.; Ullah, H.; Khan, H.; Pandey, A.; Bhatt, I.D.; Echeverría, J. Phytopharmacology and clinical updates of *Berberis* species against diabetes and other metabolic diseases. *Front. Pharmacol.* **2020**, *11*, 41. [CrossRef] [PubMed]
36. Zhang, B.; Pan, Y.; Xu, L.; Tang, D.; Dorfman, R.G.; Zhou, Q.; Yin, Y.; Li, Y.; Zhou, L.; Zhao, S.; et al. Berberine promotes glucose uptake and inhibits gluconeogenesis by inhibiting deacetylase SIRT3. *Endocrine* **2018**, *62*, 576–587. [CrossRef] [PubMed]
37. Chen, C.; Zhang, Y.; Huang, C. Berberine inhibits PTP1B activity and mimics insulin action. *Biochem. Biophys. Res. Commun.* **2010**, *397*, 543–547. [CrossRef]

38. Ko, B.-S.; Choi, S.B.; Park, S.K.; Jang, J.S.; Kim, Y.E.; Park, S. Insulin sensitizing and insulinotropic action of berberine from *Cortidis rhizoma*. *Biol. Pharm. Bull.* **2005**, *28*, 1431–1437. [CrossRef] [PubMed]
39. Sun, Y.; Xia, M.; Yan, H.; Han, Y.; Zhang, F.; Hu, Z.; Cui, A.; Ma, F.; Liu, Z.; Gong, Q.; et al. Berberine attenuates hepatic steatosis and enhances energy expenditure in mice by inducing autophagy and fibroblast growth factor 21. *Br. J. Pharmacol.* **2018**, *175*, 374–387. [CrossRef] [PubMed]
40. Asekenye, C.; Alele, P.E.; Ogwang, P.E.; Olet, E.A. Hypoglycemic effect of leafy vegetables from Ankole and Teso sub-regions of Uganda: Preclinical evaluation using a high fat diet-streptozotocin model. *Res. Sq.* 2024, *online ahead of print*. [CrossRef]
41. Tucakovic, L.; Colson, N.; Santhakumar, A.B.; Kundur, A.R.; Shuttleworth, M.; Singh, I. The effects of anthocyanins on body weight and expression of adipocyte's hormones: Leptin and adiponectin. *J. Funct. Foods* **2018**, *45*, 173–180. [CrossRef]
42. Ullah, H.; Esposito, C.; Piccinocchi, R.; De Lellis, L.F.; Santarcangelo, C.; Minno, A.D.; Baldi, A.; Buccato, D.G.; Khan, A.; Piccinocchi, G.; et al. Postprandial glycemic and insulinemic response by a Brewer's spent grain extract-based food supplement in subjects with slightly impaired glucose tolerance: A monocentric, randomized, cross-over, double-blind, placebo-controlled clinical trial. *Nutrients* **2022**, *14*, 3916. [CrossRef]
43. Perez-Martinez, P.; Garcia-Rios, A.; Delgado-Lista, J.; Perez-Jimenez, F.; Lopez-Miranda, J. Mediterranean diet rich in olive oil and obesity, metabolic syndrome and diabetes mellitus. *Curr. Pharm. Des.* **2011**, *17*, 769–777. [CrossRef]
44. Soriguer, F.; Rojo-Martínez, G.; de Fonseca, F.R.; García-Escobar, E.; García Fuentes, E.; Olveira, G. Obesity and the metabolic syndrome in Mediterranean countries: A hypothesis related to olive oil. *Mol. Nutr. Food Res.* **2007**, *51*, 1260–1267. [CrossRef]
45. Bozzetto, L.; Alderisio, A.; Giorgini, M.; Barone, F.; Giacco, A.; Riccardi, G.; Rivellese, A.A.; Annuzzi, G. Extra-virgin olive oil reduces glycemic response to a high–glycemic index meal in patients with type 1 diabetes: A randomized controlled trial. *Diabetes Care* **2016**, *39*, 518–524. [CrossRef]
46. Al Jamal, A.R.; Ibrahim, A. Effects of olive oil on lipid profiles and blood glucose in type2 diabetic patients. *Int. J. Diabetes Metab.* **2011**, *19*, 19–22. [CrossRef]
47. Wainstein, J.; Ganz, T.; Boaz, M.; Bar Dayan, Y.; Dolev, E.; Kerem, Z.; Madar, Z. Olive leaf extract as a hypoglycemic agent in both human diabetic subjects and in rats. *J. Med. Food* **2012**, *15*, 605–610. [CrossRef]
48. Gupta, A.; Gupta, R.; Lal, B. Effect of Trigonella foenum-graecum (fenugreek) seeds on glycaemic control and insulin resistance in type 2 diabetes mellitus: A double blind placebo controlled study. *J. Assoc. Physicians India* **2001**, *49*, 1057–1061.
49. Sharma, R.D.; Raghuram, T.C. Hypoglycaemic effect of fenugreek seeds in non-insulin dependent diabetic subjects. *Nutr. Res.* **1990**, *10*, 731–739. [CrossRef]
50. Madar, Z.; Abel, R.; Samish, S.; Arad, J. Glucose-lowering effect of fenugreek in non-insulin dependent diabetics. *Eur. J. Clin. Nutr.* **1988**, *42*, 51–54. [PubMed]
51. Fukino, Y.; Ikeda, A.; Maruyama, K.; Aoki, N.; Okubo, T.; Iso, H. Randomized controlled trial for an effect of green tea-extract powder supplementation on glucose abnormalities. *Eur. J. Clin. Nutr.* **2008**, *62*, 953–960. [CrossRef]
52. Venables, M.C.; Hulston, C.J.; Cox, H.R.; Jeukendrup, A.E. Green tea extract ingestion, fat oxidation, and glucose tolerance in healthy humans. *Am. J. Clin. Nutr.* **2008**, *87*, 778–784. [CrossRef]
53. Brown, A.L.; Lane, J.; Coverly, J.; Stocks, J.; Jackson, S.; Stephen, A.; Bluck, L.; Coward, A.; Hendrickx, H. Effects of dietary supplementation with the green tea polyphenol epigallocatechin-3-gallate on insulin resistance and associated metabolic risk factors: Randomized controlled trial. *Br. J. Nutr.* **2009**, *101*, 886–894. [CrossRef]
54. Wang, Y.J.; Zhu, W.F.; Wang, X.K. Study on the effect of Qinggan Jiangtang tablet in improving the insulin resistance in patients with multiple metabolic syndrome. *Zhongguo Zhong Xi Yi Jie He Za Zhi* **2005**, *25*, 412–415. [PubMed]
55. Mohammad, A.; Shahnaz, T.; Sorayya, K. Effect of 8 weeks' supplementation grape seed extract on insulin resistance in Iranian adolescents with metabolic syndrome: A randomized controlled trial. *Diabetes Metab. Syndr.* **2021**, *15*, 197–203. [CrossRef] [PubMed]
56. Hirano, T. Pathophysiology of diabetic dyslipidemia. *J. Atherosclerosis Thromb.* **2018**, *25*, 771–782. [CrossRef] [PubMed]
57. Lin, C.-F.; Chang, Y.-H.; Chien, S.-C.; Lin, Y.-H.; Yeh, H.-Y. Epidemiology of dyslipidemia in the Asia pacific region. *Int. J. Gerontol.* **2018**, *12*, 2–6. [CrossRef]
58. Mbikay, M. Therapeutic potential of Moringa oleifera leaves in chronic hyperglycemia and dyslipidemia: A review. *Front. Pharmacol.* **2012**, *3*, 24. [CrossRef] [PubMed]
59. Haimeur, A.; Ulmann, L.; Mimouni, V.; Guéno, F.; Pineau-Vincent, F.; Meskini, N.; Tremblin, G. The role of *Odontella aurita*, a marine diatom rich in EPA, as a dietary supplement in dyslipidemia, platelet function and oxidative stress in high-fat fed rats. *Lipids Health Dis.* **2012**, *11*, 147. [CrossRef] [PubMed]
60. Vormund, K.; Braun, J.; Rohrmann, S.; Bopp, M.; Ballmer, P.; Faeh, D. Mediterranean diet and mortality in Switzerland: An alpine paradox? *Eur. J. Nutr.* **2015**, *54*, 139–148. [CrossRef] [PubMed]
61. Alam, F.; Saqib, Q.N.U.; Ashraf, M. *Zanthoxylum armatum* DC extracts from fruit, bark and leaf induce hypolipidemic and hypoglycemic effects in mice-in vivo and in vitro study. *BMC Complement. Altern. Med.* **2018**, *18*, 68. [CrossRef]

62. Wat, E.; Wang, Y.; Chan, K.; Law, H.W.; Koon, C.M.; Lau, K.M.; Leung, P.C.; Yan, C.; San Lau, C.B. An in vitro and in vivo study of a 4-herb formula on the management of diet-induced metabolic syndrome. *Phytomedicine* **2018**, *42*, 112–125. [CrossRef]
63. Manasa, V.; Tumaney, A.W. Evaluation of the anti-dyslipidemic effect of spice fixed oils in the in vitro assays and the high fat diet-induced dyslipidemic mice. *Food Biosci.* **2022**, *46*, 101574. [CrossRef]
64. Sandoval-Gallegos, E.M.; Ramírez-Moreno, E.; Lucio, J.G.D.; Arias-Rico, J.; Cruz-Cansino, N.; Ortiz, M.I.; Cariño-Cortés, R. In vitro bioaccessibility and effect of *Mangifera indica* (Ataulfo) leaf extract on induced dyslipidemia. *J. Med. Food* **2018**, *21*, 47–56. [CrossRef]
65. Venturini, D.; Simão, A.N.C.; Urbano, M.R.; Dichi, I. Effects of extra virgin olive oil and fish oil on lipid profile and oxidative stress in patients with metabolic syndrome. *Nutrition* **2015**, *31*, 834–840. [CrossRef] [PubMed]
66. De Lellis, L.F.; Morone, M.V.; Buccato, D.G.; Cordara, M.; Larsen, D.S.; Ullah, H.; Piccinocchi, R.; Piccinocchi, G.; Balaji, P.; Baldi, A.; et al. Efficacy of food supplement based on monacolins, γ-oryzanol, and γ-aminobutyric acid in mild dyslipidemia: A randomized, double-blind, parallel-armed, placebo-controlled clinical trial. *Nutrients* **2024**, *16*, 2983. [CrossRef] [PubMed]
67. Tinker, L.F.; Schneeman, B.O.; Davis, P.A.; Gallaher, D.D.; Waggoner, C.R. Consumption of prunes as a source of dietary fiber in men with mild hypercholesterolemia. *Am. J. Clin. Nutr.* **1991**, *53*, 1259–1265. [CrossRef] [PubMed]
68. Moghadam, M.H.; Ghasemi, Z.; Sepahi, S.; Rahbarian, R.; Mozaffari, H.M.; Mohajeri, S.A. Hypolipidemic effect of *Lactuca sativa* seed extract, an adjunctive treatment, in patients with hyperlipidemia: A randomized double-blind placebo-controlled pilot trial. *J. Herb. Med.* **2020**, *23*, 100373. [CrossRef]
69. Cicero, A.F.G.; Fogacci, F.; Bove, M.; Giovannini, M.; Borghi, C. Three-arm, placebo-controlled, randomized clinical trial evaluating the metabolic effect of a combined nutraceutical containing a bergamot standardized flavonoid extract in dyslipidemic overweight subjects. *Phytother. Res.* **2019**, *33*, 2094–2101. [CrossRef]
70. Kinoshita, H.; Ogata, Y. Effect of bitter melon extracts on lipid levels in Japanese subjects: A randomized controlled study. *Evid. Based Complement. Alternat. Med.* **2018**, *2018*, 4915784. [CrossRef] [PubMed]
71. De Bock, M.; Derraik, J.G.; Brennan, C.M.; Biggs, J.B.; Smith, G.C.; Cameron-Smith, D.; Wall, C.R.; Cutfield, W.S. Psyllium supplementation in adolescents improves fat distribution & lipid profile: A randomized, participant-blinded, placebo-controlled, crossover trial. *PLoS ONE* **2012**, *7*, e41735.
72. Morse, S.A.; Zhang, R.; Thakur, V.; Reisin, E. Hypertension and the metabolic syndrome. *Am. J. Med. Sci.* **2005**, *330*, 303–310. [CrossRef]
73. Conn, V.S.; Ruppar, T.M.; Chase, J.-A.D. Blood pressure outcomes of medication adherence interventions: Systematic review and meta-analysis. *J. Behav. Med.* **2016**, *39*, 1065–1075. [CrossRef]
74. McCormack, T.; Krause, T.; O'Flynn, N. Management of hypertension in adults in primary care: NICE guideline. *Br. J. Gen. Pract.* **2012**, *62*, 163–164. [CrossRef]
75. Schwingshackl, L.; Schwedhelm, C.; Hoffmann, G.; Knüppel, S.; Iqbal, K.; Andriolo, V.; Bechthold, A.; Schlesinger, S.; Boeing, H. Food groups and risk of hypertension: A systematic review and doseresponse meta-analysis of prospective studies. *Adv. Nutr.* **2017**, *8*, 793–803. [CrossRef]
76. Tziomalos, K.; Athyros, V.G.; Karagiannis, A.; Mikhailidis, D.P. Endothelial dysfunction in metabolic syndrome: Prevalence, pathogenesis and management. *Nutr. Metabol. Cardiovasc. Dis.* **2010**, *20*, 140–146. [CrossRef] [PubMed]
77. Luna-Vázquez, F.J.; Ibarra-Alvarado, C.; Rojas-Molina, A.; Rojas-Molina, J.I.; Yahia, E.M.; Rivera-Pastrana, D.M.; Rojas-Molina, A.; Zavala-Sánchez, M.Á. Nutraceutical value of black cherry *Prunus serotina* Ehrh. fruits: Antioxidant and antihypertensive properties. *Molecules* **2013**, *18*, 14597–14612. [CrossRef]
78. Liman, A.A.; Salihu, A.; Onyike, E. Effect of methanol extract of baobab (*Adansonia digitata* L.) fruit pulp on NG-Nitro-L-arginine methyl ester (L-NAME) induced hypertension in rats. *High Blood Press. Cardiovasc. Prev.* **2021**, *28*, 291–300. [CrossRef]
79. Kim, B.; Kim, K.W.; Lee, S.; Jo, C.; Lee, K.; Ham, I.; Choi, H.Y. Endothelium-dependent vasorelaxant effect of *Prunus persica* branch on isolated rat thoracic aorta. *Nutrients* **2019**, *11*, 1816. [CrossRef] [PubMed]
80. Connolly, E.L.; Liu, A.H.; Radavelli-Bagatini, S.; Shafaei, A.; Boyce, M.C.; Wood, L.G.; McCahon, L.; Koch, H.; Sim, M.; Hill, C.R.; et al. Cruciferous vegetables lower blood pressure in adults with mildly elevated blood pressure in a randomized, controlled, crossover trial: The VEgetableS for vaScular hEaLth (VESSEL) study. *BMC Med.* **2024**, *22*, 353. [CrossRef] [PubMed]
81. Dehkordi, F.R.; Kamkhah, A.F. Antihypertensive effect of Nigella sativa seed extract in patients with mild hypertension. *Fundam. Clin. Pharmacol.* **2008**, *22*, 447–452. [CrossRef]
82. Sleiman, C.; Daou, R.M.; Al Hazzouri, A.; Hamdan, Z.; Ghadieh, H.E.; Harbieh, B.; Romani, M. Garlic and Hypertension: Efficacy, Mechanism of Action, and Clinical Implications. *Nutrients* **2024**, *16*, 2895. [CrossRef]
83. Ried, K.; Frank, O.R.; Stocks, N.P. Aged garlic extract lowers blood pressure in patients with treated but uncontrolled hypertension: A randomised controlled trial. *Maturitas* **2010**, *67*, 144–150. [CrossRef]
84. Santhakumar, A.B.; Kundur, A.R.; Fanning, K.; Netzel, M.; Stanley, R.; Singh, I. Consumption of anthocyanin-rich Queen Garnet plum juice reduces platelet activation related thrombogenesis in healthy volunteers. *J. Funct. Foods* **2015**, *12*, 11–22. [CrossRef]

85. Santhakumar, A.B.; Kundur, A.R.; Sabapathy, S.; Stanley, R.; Singh, I. The potential of anthocyanin-rich Queen Garnet plum juice supplementation in alleviating thrombotic risk under induced oxidative stress conditions. *J. Funct. Foods* **2015**, *14*, 747–757. [CrossRef]
86. Burns Kraft, T.F.; Dey, M.; Rogers, R.B.; Ribnicky, D.M.; Gipp, D.M.; Cefalu, W.T.; Raskin, I.; Lila, M.A. Phytochemical composition and metabolic performance-enhancing activity of dietary berries traditionally used by native North Americans. *J. Agric. Food Chem.* **2008**, *56*, 654–660. [CrossRef]
87. Akindele, A.J.; Adeneye, A.A.; Salau, O.S.; Sofidiya, M.O.; Benebo, A.S. Dose and time-dependent sub-chronic toxicity study of hydroethanolic leaf extract of *Flabellaria paniculata* Cav.(Malpighiaceae) in rodents. *Front. Pharmacol.* **2014**, *5*, 78. [CrossRef] [PubMed]
88. Adewunmi, C.O.; Ojewole, J.A.O. Safety of traditional medicines, complementary and alternative medicines in Africa. *Afr. J. Tradit. Complement. Altern. Med.* **2004**, *1*, 1–3. [CrossRef]
89. Likhitsup, A.; Chen, V.L.; Fontana, R.J. Estimated exposure to 6 potentially hepatotoxic botanicals in US adults. *JAMA Netw. Open* **2024**, *7*, e2425822. [CrossRef] [PubMed]
90. de Sousa Lima, C.M.; Fujishima, M.A.T.; de Paula Lima, B.; Mastroianni, P.C.; de Sousa, F.F.O.; da Silva, J.O. Microbial contamination in herbal medicines: A serious health hazard to elderly consumers. *BMC Complement. Med. Ther.* **2020**, *20*, 17. [CrossRef]
91. Luo, L.; Wang, B.; Jiang, J.; Fitzgerald, M.; Huang, Q.; Yu, Z.; Li, H.; Zhang, J.; Wei, J.; Yang, C.h.; et al. Heavy metal contaminations in herbal medicines: Determination, comprehensive risk assessments, and solutions. *Front. Pharmacol.* **2021**, *11*, 1–13. [CrossRef]
92. Campbell-Tofte, J.I.A.; Mølgaard, P.; Winther, K. Harnessing the potential clinical use of medicinal plants as anti-diabetic agents. *Botanics Targets Ther.* **2012**, *2*, 7–19. [CrossRef]
93. Hellión-lbarrola, M.C.; Montalbetti, Y.; Heinichen, O.; Alvarenga, N.; Figueredo, A.; Ferro, E.A. Isolation of hypotensive compounds from *Solanum sisymbriifolium*. *J. Ethnopharmacol.* **2000**, *70*, 301–307. [CrossRef]
94. Ahmed, M.; Khan, M.A.; Arshad, M.; Zafar, M. Ethnophytotherapical approaches for the treatment of diabetes by the local inhabitants of district Attock (Pakistan). *Ethnobotanical Leafl.* **2006**, *10*, 41–48.
95. Perera, L.M.S.; Escobar, A.; Souccar, C.; Remigio, M.A.; Mancebo, B. Pharmacological and toxicological evaluation of Rhizophora mangle L., as a potential antiulcerogenic drug: Chemical composition of active extract. *J. Pharmacognosy Phytother.* **2010**, *2*, 56–63.
96. Afolabi, S.O.; Akindele, A.J.; Awodele, O.; Anunobi, C.C.; Adeyemi, O.O. A 90 day chronic toxicity study of Nigerian herbal preparation DAS77 in rats. *BMC Complement. Altern. Med.* **2012**, *12*, 79. [CrossRef]
97. Verpoorte, R.; Choi, Y.H.; Kim, H.K. Ethnopharmacology and systems biology: A perfect holistic match. *J. Ethnopharmacol.* **2005**, *100*, 53–56. [CrossRef] [PubMed]
98. Ijinu, T.P.; Rani, M.P.; Sasidharan, S.P.; Shanmugarama, S.; Govindarajan, R.; George, V.; Pushpangadan, P. Clinical significance of herb–drug interactions. In *Nutraceuticals: A Holistic Approach to Disease Prevention*; Ullah, H., Rauf, A., Daglia, M., Eds.; De Gruyter: Berlin, Germany, 2024; p. 103.
99. Seden, K.; Dickinson, L.; Khoo, S.; Back, D. Grapefruit-drug interactions. *Drugs* **2010**, *70*, 2373–2407. [CrossRef]
100. Yuan, C.S.; Wei, G.A.N.G.; Dey, L. American ginseng reduces warfarin's effect in healthy patients: A randomized, controlled trial. *ACC Curr. J. Rev.* **2004**, *13*, 9–10. [CrossRef]
101. Mohammed Abdul, M.I.; Jiang, X.; Williams, K.M.; Day, R.O.; Roufogalis, B.D.; Liauw, W.S.; Xu, H.; McLachlan, A.J. Pharmacodynamic interaction of warfarin with cranberry but not with garlic in healthy subjects. *Br. J. Pharmacol.* **2008**, *154*, 1691–1700. [CrossRef]
102. Thakkar, S.; Anklam, E.; Xu, A.; Ulberth, F.; Li, J.; Li, B.; Hugas, M.; Sarma, N.; Crerar, S.; Swift, S.; et al. Regulatory landscape of dietary supplements and herbal medicines from a global perspective. *Regul. Toxicol. Pharmacol.* **2020**, *114*, 104647. [CrossRef] [PubMed]
103. Hosseinpour-Niazi, S.; Malmir, H.; Mirmiran, P.; Shabani, M.; Hasheminia, M.; Azizi, F. Fruit and vegetable intake modifies the association between ultra-processed food and metabolic syndrome. *Nutr. Metab.* **2024**, *21*, 58. [CrossRef]
104. Joana Gil-Chávez, G.; Villa, J.A.; Fernando Ayala-Zavala, J.; Basilio Heredia, J.; Sepulveda, D.; Yahia, E.M.; González-Aguilar, G.A. Technologies for extraction and production of bioactive compounds to be used as nutraceuticals and food ingredients: An overview. *Compr. Rev. Food Sci. Food Saf.* **2013**, *12*, 5–23. [CrossRef]
105. Mohammad Azmin, S.N.H.; Abdul Manan, Z.; Wan Alwi, S.R.; Chua, L.S.; Mustaffa, A.A.; Yunus, N.A. Herbal processing and extraction technologies. *Sep. Purif. Rev.* **2016**, *45*, 305–320. [CrossRef]
106. Jha, A.K.; Sit, N. Extraction of bioactive compounds from plant materials using combination of various novel methods: A review. *Trends Food Sci. Technol.* **2021**, *119*, 579–591. [CrossRef]
107. Wells, M.J. Principles of extraction and the extraction of semivolatile organics from liquids. In *Sample Preparation Techniques in Analytical Chemistry*; Mitra, S., Ed.; Wiley & Sons, Inc.: Hoboken, NJ, USA, 2003; pp. 37–138.

108. Murakami, H.; Omiya, M.; Miki, Y.; Umemura, T.; Esaka, Y.; Inoue, Y.; Teshima, N. Evaluation of the adsorption properties of nucleobase-modified sorbents for a solid-phase extraction of watersoluble compounds. *Talanta* **2020**, *217*, 121052. [CrossRef] [PubMed]
109. Merkle, S.; Kleeberg, K.K.; Fritsche, J. Recent developments and applications of solid phase microextraction (SPME) in food and environmental analysis—A review. *Chromatography* **2015**, *2*, 293–381. [CrossRef]
110. Chemat, F.; Tomao, V.; Virot, M. Ultrasound-assisted extraction in food analysis. In *Handbook of Food Analysis Instruments*; Otles, S., Ed.; CRC Press: Boca Raton, FL, USA, 2008; pp. 85–103.
111. Jambrak, A.R.; Mason, T.J.; Lelas, V.; Herceg, Z.; Herceg, I.L. Effect of ultrasound treatment on solubility and foaming properties of whey protein suspensions. *J. Food Eng.* **2008**, *86*, 281–287. [CrossRef]
112. Nadar, S.S.; Rao, P.; Rathod, V.K. Enzyme assisted extraction of biomolecules as an approach to novel extraction technology: A review. *Food Res. Int.* **2018**, *108*, 309–330. [CrossRef]
113. Yahya, N.A.; Attan, N.; Wahab, R.A. An overview of cosmeceutically relevant plant extracts and strategies for extraction of plant-based bioactive compounds. *Food Bioprod. Process.* **2018**, *112*, 69–85. [CrossRef]
114. Pasrija, D.; Anandharamakrishnan, C. Techniques for extraction of green tea polyphenols: A review. *Food Bioprod. Process.* **2015**, *8*, 935–950. [CrossRef]
115. Brunner, G. Supercritical fluids: Technology and application to food processing. *J. Food Eng.* **2005**, *67*, 21–33. [CrossRef]
116. Gupta, A.; Naraniwal, M.; Kothari, V. Modern extraction methods for preparation of bioactive plant extracts. *Int. J. Appl. Nat. Sci.* **2012**, *1*, 8–26.
117. Jadhav, D.; Rekha, B.N.; Gogate, P.R.; Rathod, V.K. Extraction of vanillin from vanilla pods: A comparison study of conventional Soxhlet and ultrasound assisted extraction. *J. Food Eng.* **2009**, *93*, 421–426. [CrossRef]
118. Cho, Y.J.; Hong, J.Y.; Chun, H.S.; Lee, S.K.; Min, H.Y. Ultrasonication assisted extraction of resveratrol from grapes. *J. Food Eng.* **2006**, *77*, 725–730. [CrossRef]
119. Sun, Y.; Liu, Z.; Wang, J. Ultrasound-assisted extraction of five isoflavones from Iris tectorum Maxim. *Sep. Purif. Technol.* **2011**, *78*, 49–54. [CrossRef]
120. Pan, X.; Niu, G.; Lio, H. Comparision of microwave assisted extraction and conventional extraction techniques for the extraction of tanshinones from *Saliva miltiorrhiza* bunge. *Biochem. Eng. J.* **2002**, *12*, 71–77. [CrossRef]
121. Huie, C.W. A review of modern sample-preparation techniques for the extraction and analysis of medicinal plants. *Anal. Bioanal. Chem.* **2002**, *373*, 23–30. [CrossRef] [PubMed]
122. Thomas, R.; Tripathi, R.; Kamat, S.D.; Kamat, D.V. Comparative study of phenolics and antioxidant activity of phytochemicals of T. chebula extracted using microwave and ultrasonication. *Int. J. Pharm. Sci. Res.* **2012**, *3*, 194–197.
123. Reverchon, E.; Marco, I. Supercritical fluid extraction and fractionation of natural matter. *J. Supercrit Fluids.* **2006**, *38*, 146–166. [CrossRef]
124. Aleksovski, S.; Sovova, H.; Urapova, B.; Poposka, F. Supercritical CO_2 extraction and Soxhlet extraction of grape seeds oil. *Bull. Chem. Technol. Macedonia* **1998**, *17*, 129–134.
125. Kothari, V.; Gupta, A.; Naraniwal, M. Comparative study of various methods for extraction of antioxidant and antibacterial compounds from plant seeds. *J. Nat. Remedies* **2012**, *12*, 162–173.
126. Moelants, K.R.; Lemmens, L.; Vandebroeck, M.; Van Buggenhout, S.; Van Loey, A.M.; Hendrickx, M.E. Relation between particle size and carotenoid bioaccessibility in carrot-and tomato-derived suspensions. *J. Agric. Food Chem.* **2012**, *60*, 11995–12003. [CrossRef]
127. Porter, C.J.; Trevaskis, N.L.; Charman, W.N. Lipids and lipidbased formulations: Optimizing the oral delivery of lipophilic drugs. *Nat. Rev. Drug Discov.* **2007**, *6*, 231–248. [CrossRef]
128. Pouton, C.W.; Porter, C.J. Formulation of lipid-based delivery systems for oral administration: Materials, methods and strategies. *Adv. Drug Deliv. Rev.* **2008**, *60*, 625–637. [CrossRef]
129. Martinez, M.N.; Amidon, G.L. A mechanistic approach to understanding the factors affecting drug absorption: A review of fundamentals. *J. Clin. Pharmacol.* **2002**, *42*, 620–643. [CrossRef]
130. Actis-Goretta, L.; Leveques, A.; Rein, M.; Teml, A.; Schäfer, C.; Hofmann, U.; Li, H.; Schwab, M.; Eichelbaum, M.; Williamson, G. Intestinal absorption, metabolism, and excretion of (−)-epicatechin in healthy humans assessed by using an intestinal perfusion technique. *Am. J. Clin. Nutr.* **2013**, *98*, 924–933. [CrossRef] [PubMed]
131. Ozkan, G.; Ceyhan, T.; Çatalkaya, G.; Rajan, L.; Ullah, H.; Daglia, M.; Capanoglu, E. Encapsulated phenolic compounds: Clinical efficacy of a novel delivery method. *Phytochem. Rev.* **2024**, *23*, 781–819. [CrossRef]
132. Khan, H.; Ullah, H.; Martorell, M.; Valdes, S.E.; Belwal, T.; Tejada, S.; Sureda, A.; Kamal, M.A. Flavonoids nanoparticles in cancer: Treatment, prevention and clinical prospects. *Semin. Cancer Biol.* **2021**, *69*, 200–211. [CrossRef]
133. Dias, D.R.; Botrel, D.A.; Fernandes, R.V.D.B.; Borges, S.V. Encapsulation as a tool for bioprocessing of functional foods. *Curr. Opin. Food Sci.* **2017**, *13*, 31–37. [CrossRef]

134. Naczk, M.; Shahidi, F. Phenolics in cereals, fruits and vegetables: Occurrence, extraction and analysis. *J. Pharm. Biomed. Anal.* **2006**, *41*, 1523–1542. [CrossRef] [PubMed]
135. Del Rio, D.; Rodriguez-Mateos, A.; Spencer, J.P.; Tognolini, M.; Borges, G.; Crozier, A. Dietary (poly) phenolics in human health: Structures, bioavailability, and evidence of protective effects against chronic diseases. *Antioxid. Redox. Signal.* **2013**, *18*, 1818–1892. [CrossRef]
136. Ezhilarasi, P.N.; Karthik, P.; Chhanwal, N.; Anandharamakrishnan, C. Nanoencapsulation techniques for food bioactive components: A review. *Food Bioproc. Tech.* **2013**, *6*, 628–647. [CrossRef]
137. Fang, Z.; Bhandari, B. Encapsulation of polyphenols–a review. *Trends Food Sci. Technol.* **2010**, *21*, 510–523. [CrossRef]
138. Munin, A.; Edwards-Le'vy, F. Encapsulation of natural polyphenolic compounds; a review. *Pharmaceutics* **2011**, *3*, 793–829. [CrossRef]
139. Mishra, M. Materials of natural origin for encapsulation. In *Handbook of Encapsulation and Controlled Release*; Mishra, M., Ed.; CRC Press: Boca Raton, FL, USA, 2015; pp. 517–540.
140. Fernandes, A.; Sousa, A.; Azevedo, J.; Mateus, N.; de Freitas, V. Effect of cyclodextrins on the thermodynamic and kinetic properties of cyanidin-3-O-glucoside. *Food Res. Int.* **2013**, *51*, 748–755. [CrossRef]
141. Ezzat, H.M.; Elnaggar, Y.S.R.; Abdallah, O.Y. Improved oral bioavailability of the anticancer drug catechin using chitosomes: Design, in-vitro appraisal and in-vivo studies. *Int. J. Pharm.* **2019**, *565*, 488–498. [CrossRef] [PubMed]
142. Peng, Y.; Meng, Q.; Zhou, J.; Chen, B.; Xi, J.; Long, P.; Zhang, L.; Hou, R. Nanoemulsion delivery system of tea polyphenols enhanced the bioavailability of catechins in rats. *Food Chem.* **2018**, *242*, 527–532. [CrossRef] [PubMed]
143. Kadari, A.; Gudem, S.; Kulhari, H.; Bhandi, M.M.; Borkar, R.M.; Kolapalli, V.R.M.; Sistla, R. Enhanced oral bioavailability and anticancer efficacy of fisetin by encapsulating as inclusion complex with HPbCD in polymeric nanoparticles. *Drug Deliv.* **2017**, *26*, 224–232. [CrossRef]
144. Salem, M.A.; Aborehab, N.M.; Abdelhafez, M.M.; Ismail, S.H.; Maurice, N.W.; Azzam, M.A.; Alseekh, S.; Fernie, A.R.; Salama, M.M.; Ezzat, S.M. Anti-obesity effect of a tea mixture nano-formulation on rats occurs via the upregulation of AMP-activated protein kinase/sirtuin-1/glucose transporter type 4 and peroxisome proliferator-activated receptor gamma pathways. *Metabolites* **2023**, *13*, 871. [CrossRef]
145. Wattanathorn, J.; Kawvised, S.; Thukham-mee, W. Encapsulated mulberry fruit extract alleviates changes in an animal model of menopause with metabolic syndrome. *Oxidative Med. Cell Longev.* **2019**, *2019*, 1–23. [CrossRef] [PubMed]
146. Colorado, D.; Fernandez, M.; Orozco, J.; Lopera, Y.; Muñoz, D.L.; Acín, S.; Balcazar, N. Metabolic activity of anthocyanin extracts loaded into non-ionic niosomes in diet-induced obese mice. *Pharm. Res.* **2020**, *37*, 152. [CrossRef]
147. Sreerekha, P.R.; Dara, P.K.; Vijayan, D.K.; Chatterjee, N.S.; Raghavankutty, M.; Mathew, S.; Ravishankar, C.N.; Anandan, R. Dietary supplementation of encapsulated anthocyanin loaded-chitosan nanoparticles attenuates hyperlipidemic aberrations in male Wistar rats. *Carbohydr. Polym. Technol. Appl.* **2021**, *2*, 100051. [CrossRef]
148. Christman, L.M.; Dean, L.L.; Allen, J.C.; Godinez, S.F.; Toomer, O.T. Peanut skin phenolic extract attenuates hyperglycemic responses in vivo and in vitro. *PLoS ONE* **2019**, *14*, e0214591. [CrossRef]
149. Faria, W.C.S.; da Silva, A.A.; Veggi, N.; Kawashita, N.H.; de França Lemes, S.A.; de Barros, W.M.; da Conceiçao Cardoso, E.; Converti, A.; de Melo Moura, W.; Bragagnolo, N. Acute and subacute oral toxicity assessment of dry encapsulated and nonencapsulated green coffee fruit extracts. *J. Food Drug Anal.* **2020**, *28*, 337. [PubMed]
150. Hussain, S.A.; Hameed, A.; Nazir, Y.; Naz, T.; Wu, Y.; Suleria, H.A.R.; Song, Y. Microencapsulation and the characterization of polyherbal formulation (PHF) rich in natural polyphenolic compounds. *Nutrients* **2018**, *10*, 843. [CrossRef] [PubMed]
151. Wanjiru, J.; Gathirwa, J.; Sauli, E.; Swai, H.S. Formulation, optimization, and evaluation of Moringa oleifera leaf polyphenol-loaded phytosome delivery system against breast cancer cell lines. *Molecules* **2022**, *27*, 4430. [CrossRef] [PubMed]
152. Vitaglione, P.; Lumaga, R.B.; Ferracane, R.; Sellitto, S.; Morelló, J.R.; Miranda, J.R.; Shimoni, E.; Fogliano, V. Human bioavailability of flavanols and phenolic acids from cocoa-nut creams enriched with free or microencapsulated cocoa polyphenols. *Br. J. Nutr.* **2013**, *109*, 1832–1843. [CrossRef]
153. Garrido, I.; Urpi-Sarda, M.; Monagas, M.; Gómez-Cordovés, C.; Martín-Álvarez, P.J.; Llorach, R.; Bartolomé, B.; Andrés-Lacueva, C. Targeted analysis of conjugated and microbial-derived phenolic metabolites in human urine after consumption of an almond skin phenolic extract. *J. Nutr.* **2010**, *140*, 1799–1807. [CrossRef] [PubMed]
154. Shahbaz, M.U.; Arshad, M.; Mukhtar, K.; Nabi, B.G.; Goksen, G.; Starowicz, M.; Nawaz, A.; Ahmad, I.; Walayat, N.; Manzoor, M.F.; et al. Natural plant extracts: An update about novel spraying as an alternative of chemical pesticides to extend the postharvest shelf life of fruits and vegetables. *Molecules* **2022**, *27*, 5152. [CrossRef] [PubMed]
155. Zabot, G.L.; Schaefer Rodrigues, F.; Polano Ody, L.; Vinícius Tres, M.; Herrera, E.; Palacin, H.; Córdova-Ramos, J.S.; Best, I.; Olivera-Montenegro, L. Encapsulation of bioactive compounds for food and agricultural applications. *Polymers* **2022**, *14*, 4194. [CrossRef] [PubMed]
156. Gouin, S. Microencapsulation: Industrial appraisal of existing technologies and trends. *Trends Food Sci. Technol.* **2004**, *15*, 330–347. [CrossRef]

157. Tonon, R.V.; Brabet, C.; Hubinger, M.D. Influence of process conditions on the physicochemical properties of açai (Euterpe oleraceae Mart.) powder produced by spray drying. *J. Food Eng.* **2008**, *88*, 411–418. [CrossRef]
158. Kuck, L.S.; Noreña, C.P.Z. Microencapsulation of grape (Vitis labrusca var. Bordo) skin phenolic extract using gum Arabic, polydextrose, and partially hydrolyzed guar gum as encapsulating agents. *Food Chem.* **2016**, *194*, 569–576. [CrossRef]
159. Rashidinejad, A. The road ahead for functional foods: Promising opportunities amidst industry challenges. *Future Postharvest Food* **2024**, *1*, 266–273. [CrossRef]
160. Kandemir, K.; Piskin, E.; Xiao, J.; Tomas, M.; Capanoglu, E. Fruit juice industry wastes as a source of bioactives. *J. Agric. Food Chem.* **2022**, *70*, 6805–6832. [CrossRef] [PubMed]
161. Galanakis, C.M. Functionality of food components and emerging technologies. *Foods* **2021**, *10*, 128. [CrossRef] [PubMed]
162. Alu'datt, M.H.; Alrosan, M.; Gammoh, S.; Tranchant, C.C.; Alhamad, M.N.; Rababah, T.; Alzoubi, H.; Ghatasheh, S.; Ghozlan, K.; Tan, T.C. Encapsulation-based technologies for bioactive compounds and their application in the food industry: A roadmap for food-derived functional and health-promoting ingredients. *Food Biosci.* **2022**, *50*, 101971. [CrossRef]
163. Zhang, R.; Zhang, Z.; McClements, D.J. Nanoemulsions: An emerging platform for increasing the efficacy of nutraceuticals in foods. *Colloids Surf. B Biointerfaces* **2020**, *194*, 111202. [CrossRef] [PubMed]

Disclaimer/Publisher's Note: The statements, opinions and data contained in all publications are solely those of the individual author(s) and contributor(s) and not of MDPI and/or the editor(s). MDPI and/or the editor(s) disclaim responsibility for any injury to people or property resulting from any ideas, methods, instructions or products referred to in the content.

nutrients

MDPI

Review

The Potential of Nutraceutical Supplementation in Counteracting Cancer Development and Progression: A Pathophysiological Perspective

Carmen Altomare [1], Roberta Macrì [1,*], Maria Serra [1,*], Sara Ussia [1], Giovanna Ritorto [1], Jessica Maiuolo [2], Carolina Muscoli [1], Enzo Perri [3] and Vincenzo Mollace [1]

[1] Pharmacology Laboratory, Institute of Research for Food Safety and Health IRC-FSH, Department of Health Sciences, University Magna Graecia of Catanzaro, 88100 Catanzaro, Italy; carmen.altomare@studenti.unicz.it (C.A.); saraussia1598@gmail.com (S.U.); giovanna.ritorto@studenti.unicz.it (G.R.); muscoli@unicz.it (C.M.); mollace@libero.it (V.M.)

[2] Laboratory of Pharmaceutical Biology, IRC-FSH Department of Health Sciences, University "Magna Græcia" of Catanzaro, 88100 Catanzaro, Italy; maiuolo@unicz.it

[3] Research Centre for Olive, Fruit and Citrus Crops, Council for Agricultural Research and Economics, 87036 Rende, Italy; enzo.perri@crea.gov.it

* Correspondence: roberta.macri@unicz.it (R.M.); maria.serra@studenti.unicz.it (M.S.)

Abstract

Cancer is a major cause of morbidity and mortality across the globe, with a substantial increase in cases anticipated over the next few decades. Given the constraints and adverse effects associated with standard cancer therapies, the contribution of diet and nutraceuticals to cancer prevention and treatment is receiving increased scrutiny. A diet rich in plant-based foods, extra virgin olive oil (EVOO), and bioactive compounds, including the Mediterranean Diet, has been associated with reduced cancer risk and improved treatment outcomes. This review aims to explore the complex mechanisms of the MedDiet and nutraceuticals (polyphenols, flavonoids, terpenoids) in cancer prevention, to determine their potential as cancer treatment adjuvants. Promising results show that key compounds such as bergamot polyphenolic fraction (BPF), cynaropicrin, oleuropein, quercetin, resveratrol, and serotonin can modulate oxidative stress, inflammation, the tumor microenvironment, the cell cycle, and drug resistance. A significant observation is that many of these substances demonstrate dual dose-dependent activity; they function as antioxidants in healthy cells but induce pro-oxidant and pro-apoptotic effects in cancerous cells. Their ability to boost chemotherapy's effectiveness and safety while lessening side effects and offering combined advantages is also explored. To summarize, this review suggests that the Mediterranean Diet and nutraceutical supplements may help prevent and manage cancer, but more research is needed to confirm their benefits.

Keywords: Mediterranean Diet; nutraceuticals; dietary polyphenols; antioxidant compounds; oxidative stress; inflammation; cancer prevention; health-promoting phytochemicals

1. Introduction

Cancer is the second leading cause of death globally, trailing only heart disease. According to the International Agency for Research on Cancer (IARC), there were about 20 million new cancer diagnoses and 9.7 million deaths globally. By 2050, annual cases could hit 35 million, assuming current incidence levels persist [1]. Several factors, including lifestyle, daily routines, and diet, contribute to the rising cancer rates [2]. Epidemiological

and clinical research shows a link between nutrition and the development or progression of various cancers (colon, breast, and prostate), classifying them as diet related [3]. The beneficial effects of a healthy lifestyle, and its correlation with the Mediterranean Diet's (MedDiet) wide range of health benefits, are supported by several studies [4], including reduced risk of cancer and cardiovascular disease (CVD), reduced metabolic risk of diabetes mellitus (DM), obesity, and metabolic syndrome (MS), increased longevity, and improved cognitive function. Furthermore, the MedDiet is linked to a healthy gut microbiome, impacting cancer development and treatment.

The hallmark of cancer is the conversion of some normal cells into malignant neoplastic cells [5].

Therefore, uncontrolled proliferation, evasion of growth suppressors and the immune system, angiogenesis, metastasis, and metabolic reprogramming are the main characteristics [6]. Cellular and subcellular microenvironments and genetic instabilities are key to this multistep process. Malfunction of the core cell cycle leads to unstable deoxyribonucleic acid (DNA) and mutations, furthering tumorigenesis [7]. The high number of cancer cases urgently requires new treatment approaches to address the weaknesses of traditional methods like surgery, hormone replacement therapy (HRT), chemotherapy, and radiation, which often cause drug resistance and harmful side effects [8]. Because they boost tumor response to treatments and decrease systemic toxicity, the wide array of natural compounds in the MedDiet are a potential cancer-fighting strategy [9]. This review aims to highlight the effects of natural compounds, as nutraceuticals, in the management of cancer therapy. Due to their proven antioxidant and inflammatory properties, as well as their ability to modulate the cell cycle, natural compounds—in particular extracts from a selection of foods characteristic of the MedDiet, such as *Citrus bergamia* Risso & Poiteau, *Cynara cardunculus* L., *Olea Europaea* L., foods rich in quercetin, resveratrol (RV), as well as Mediterranean plants such as *Ferula communis* L.—may be relevant for synergism with chemotherapeutic drugs while reducing their related toxic effects.

1.1. Complexities of Cancer Pathogenesis

Cancer development is a complex process influenced by various factors, leading to diverse clinical presentations, and various factors contribute to its pathogenesis, each a potential therapeutic target (e.g., chemicals, viruses, genetic, and non-genetic factors).

Several studies have shown that carcinogenesis is related to somatic mutations of stem cells, which generate a subpopulation of cancer stem cells (CSCs) with self-renewal capabilities, producing daughter cells with highly tumorigenic and invasive potential, originating primary tumors [10]. Evidence suggests that epigenetic mutations can provide tumor cells with a reproductive advantage over normal cells, leading to impaired tumor suppression and uncontrolled tumor growth [11]. However, the inherent adaptability of healthy cells, allowing epigenetic and phenotypic shifts leading to CSC formation, is pivotal in cancer development [12]. Oncogene and tumor suppressor alterations in this scenario accelerate cell growth and may cause a more aggressive metastatic phenotype.

The occurrence of Rat sarcoma virus (RAS) and its family genes, Kirsten rat sarcoma viral oncogene homolog (KRAS) (*KRAS4A* and *KRAS4B*), Neuroblastoma RAS viral oncogene homolog (NRAS), or Harvey Rat sarcoma virus (HRAS) [13] are among the most dysregulated protooncogenes and best characterized. Oncogenic activation of RAS results in ligand-independent hyperstimulation of downstream signaling cascades, including the extracellular signal-regulated kinase 1/2 (ERK1/2) [14] and phosphatidylinositol 3-kinase (PI3K) promoting cell growth, cell cycle entry, cell survival, and cell adhesion. Moreover, mutations in KRAS lead to chemoresistance mechanisms [15]. The function of tumor protein p53 (p53), a tumor suppressor, is widely understood. p53 gene mutations disrupt the

normal response to DNA damage, blocking apoptosis and cell cycle arrest, thus causing abnormal cell division. The development of cancer is linked to the epithelial–mesenchymal transition (EMT) and a metabolic shift from glycolysis to oxidative phosphorylation [16]. Epithelial cells undergoing EMT lose apical-basal polarity and cell–cell junctions, gaining mesenchymal characteristics, such as invasion and migration. In addition, cells develop stem cell characteristics and become resistant to chemotherapy [17]. Signaling pathways to activate and maintain EMT include notch signaling pathway (NOTCH), wingless-related integration site (Wnt), glycogen synthase kinase 3 beta (GSK-3β), and transforming growth factor beta (TGF-β) [18]. These pathways lead to loss of cell–cell adhesion and increased migratory cell ability by activating transcription factors including Slug, Twist, Snail, or Zinc finger E-box binding homeobox 1 and Zinc finger E-box binding homeobox 2 (ZEB1/2) [19], which in turn repress epithelial markers such as E-cadherin. Cancer cells metabolism shift from production energy by glycolysis to oxidative phosphorylation, mediated by pathways such as PI3K/Akt/mTOR and AMP-activated protein kinase (AMPK) [20,21]. This network encompasses cancerous and non-cancerous host cells, alongside the modified extracellular matrix (ECM) and vascularization. Tumor cell invasion is fueled by the tumor microenvironment (TME), a key factor in tumor development and resistance to treatment. Its inflammatory, hypoxic nature drives adaptive pathways, enzyme overexpression, high adenosine triphosphate (ATP), and low pH, resulting in acidity [22]. The TME includes immune cells from both innate and adaptative systems, endothelial cells (ECs), cancer-associated fibroblasts (CAFs), pericytes, adipocytes, and other cell types that vary by tissue. In the TME, there are also myeloid-derived suppressor cells (MDSCs), tumor-associated macrophages (TAMs), and regulatory T-cells (Tregs), which secrete immunosuppressive molecules such as transforming growth factor beta (TGF-β) or modulating immune checkpoint [23]. Furthermore, the tumor tissue's commensal microbiome is a key TME component, affecting tumor development and growth. The distinct intratumoral and intracellular microbial composition of different tumor types allows for the correlation of microbial metabolic pathways and drug treatment characteristics. Moreover, dysbiosis can trigger a persistent inflammatory immune response, via the microbial activation of nuclear factor kappa-light-chain-enhancer of activated B cells (NF-κβ), a cancer-linked inflammation regulator, thus promoting tumor growth [24].

1.2. Nutrition and Nutraceutical Compounds in Cancer Risk Modulation

Diet, nutrition, and lifestyle are correlated with cancer incidence, progression, and treatment response in some epidemiological studies. Age-related cardiovascular and metabolic diseases are also linked, according to scientific evidence. Human and animal studies demonstrate a link between diet, epigenetic changes, and cancer risk. It is possible to assert that lifestyle and diet, and particularly the MedDiet model, play a key role as a modulator of cancer risk. It represents not only a diet but also a lifestyle model in the Mediterranean area, where the incidence of several types of cancer is lower than in other areas [25]. Such incidence is associated with a potential protective role of the MedDiet on human health [26]. The plan emphasizes plenty of vegetables, fruits, legumes, whole grains, and nuts. The diet features extra virgin olive oil (EVOO) as its main fat, plus regular fish, moderate animal protein, and red wine.

The MedDiet has a high intake of B vitamins (vitamins B1, B2, niacin, B6, folate or B12), antioxidant vitamins (vitamins E and C), minerals (iron, selenium, phosphorus, and potassium), and fiber. A variety of nutraceuticals included in the MedDiet have shown an inverse association with CVD, metabolic disease, neurodegenerative disease, and various types of cancer, both directly and through epigenetic mechanisms [27]. Strict adherence to the MedDiet is associated with a lower risk of multiple diseases thanks to phytochemicals

("non-nutrient" components) present in its constituent foods, such as polyphenols, phytosterols, carotenoids, monounsaturated fatty acids (MUFAs) and polyunsaturated fatty acids (PUFAs) [28]. Specifically, polyphenols, water-soluble phenylpropanoids, contain at least one aromatic ring and a benzene ring with hydroxyl substituents. Plants synthesize these secondary metabolites to cope with stress like pathogen attacks, ultraviolet radiation (UV) radiation, or harsh weather. They are classified as: (i) flavonoids, characterized by the formula C6-C3-C6, among which there are flavonols, flavanols, flavones, flavanones, isoflavones, and anthocyanins; (ii) non-flavonoids, characterized by only one phenolic ring, including phenolic acids (hydroxybenzoic acids such as vanillic acid and gallic acid) and cinnamic acids (ferulic and caffeic acids), lignans, tannins, and stilbenes, including RV [29]. Foods contain various polyphenols such as flavan-3-ols, isoflavones, flavonols, flavanones, flavones, anthocyanins, and stilbenes, impacting color, taste, smell, bitterness, astringency, and resistance to oxidation. The range of polyphenol levels is widely conditioned by environmental conditions and soil type [30]. Studies demonstrate the relationship between the structural chemical conformation of polyphenols and their biological actions, affecting bioavailability and absorption [31]. In fact, the complex nature of polyphenols results in poor small intestinal absorption. Following absorption, liver enzymes (glucuronidation, sulfonation, methylation) modify phenolic substances before systemic circulation and tissue distribution. The inability of complex phenols to be absorbed leads to their biotransformation by the gut microbiota into smaller, bioavailable derivatives [32]. Epidemiological studies suggest that sufficient polyphenol intake, from food or supplements, may reduce oxidative stress, chronic inflammation, and cancer risk [33]. Moreover, increased polyphenol intake enhances cardiometabolic health via anti-inflammatory, antioxidant, vasodilatory, high-density lipoprotein (HDL)-raising actions, and by inhibiting low density lipoprotein (LDL) oxidation [34]. Polyphenols have been shown to reduce blood glucose levels by mechanisms including the inhibition of glucose uptake in the gut and other tissues [35]. Indeed, epidemiological studies also demonstrate that polyphenols protect against Metabolic Syndrome, a combination of hypertension, dyslipidemia, insulin resistance, and central obesity that contributes to cardiovascular and metabolic diseases [36]. Polyphenols can restore redox balance [37], impacting arachidonic acid metabolism through the inhibition of various enzymes, such as phospholipase A2 (PLA2), lipoxygenase (LOX), and cyclooxygenases (COX-1 and COX-2); consequently, there is a reduction in the release of prostaglandins, thromboxanes, leukotrienes, and other mediators of inflammation [38]. Metal ion chelation mechanisms enable these molecules to exert their chemoprotective effects, including cell cycle arrest induction, pro-apoptotic process induction, and immune system regulation [39]. Polyphenols have both estrogenic and antiestrogenic effects, impacting how anticancer drugs are processed in the body, thus reducing their toxicity [40]. In addition, some polyphenols have been shown to be able to disrupt the elongation of telomeric ends, which could have an important impact on cancer cell replication, and they are effective as anti-aging compounds [41]. In fact, the level of antioxidants in plasma depends on the consumption of antioxidant-rich foods and supplements, such as those containing polyphenols. Natural compounds, by modulating specific proteins, can regulate drug resistance, which occurs through several mechanisms, including enhanced DNA damage repair, invasiveness, altered drug efflux and metabolism, modification of drug targets and TME [42]. The important role of nutraceuticals in oncology has led to them being called onconutraceuticals [43]. In cancer treatment, their application focuses on discovering synergistic effects with anticancer drugs to improve treatment success, decrease side effects (e.g., cardiotoxicity, hepatotoxicity), and overcome drug resistance. Table 1 generated from the literature data, presents the principal biological

properties of the key nutraceuticals of the MedDiet and Figure 1 shows the molecular diagrams of the main natural compounds discussed in this review.

Table 1. The Mediterranean Diet, nutraceuticals, and their biological properties.

Nutraceuticals	Bioactive Compounds	Main Sources	Biological Effects	References
Citrus bergamia Risso & Poiteau extract	Naringin, neohesperidin, neoeriocitrin, C-glucoside, flavanone O-glycosides, rhoifolin, 40-O-glucoside, neodiosmin, rhoifolin, poncirin limonene, linalool, linalyl acetate	Bergamot juice (BJ), bergamot essential oil (BEO)	Hypolipemic, hypoglycaemic anti-inflammatory, antioxidant, anticancer	[44–47]
Cynara cardunculus L. extract	Cynaropicrin (cyn), chlorogenic acid, dicaffeoylquinic acids, luteolin, inulin	Leaves, flowers, roots, by-products	Hepatoprotective, antioxidant, antimicrobial, antiobesity, chemopreventive	[48,49]
Olea Europaea L. extract	Hydroxytyrosol, oleuropein, tyrosol, oleic acid, omega-3, omega-6	Olive oil (OO), olive leaves, Olive mill wastewater (OMWW)	Antioxidant, cardioprotective, antitumoral, anti-inflammatory, anti-aging, antibacterial, prevention of metabolic disorders and chronic diseases	[50–53]
Quercetin	Flavonol (free and glycosylated forms)	Onions, apples, berries, broccoli, tea, cherries, tomatoes, asparagus, peas, grapes, coriander seeds	Antioxidant, anti-inflammatory, antiproliferative, antiviral, cardioprotective, antiaging, prevention of metabolic disorders, chronic diseases, platelet aggregation, lipid peroxidation, and capillary permeability, modulating the composition of the gut microbiota	[54,55]
Resveratrol	Trans-RV	Grapes skin, red wines, blueberry, cranberry, peanuts, bilberry	Antioxidant, anti-inflammatory, pro-apoptotic, antitumor, telomerase inhibition, improves gut barrier	[30,56–58]
Ferula Communis L. extract	Ferutinin, sesquiterpenes, ferulenol, ferulone A and B, flavonoids	Roots, rhizomes, latex	Selective estrogen receptor modulator (SERM-like), antiproliferative, dose-dependent estrogenic effect; antioxidant effects, antidiabetic, antimicrobial, cytotoxic actions	[59,60]

BJ: bergamot juice; BEO: bergamot essential oil; Cyn: cynaropicrin; OO: olive oil; OMWW: olive mill wastewater; RV: resveratrol; SERM-like: selective estrogen receptor modulator.

1.2.1. Bioactive Compounds from *Citrus bergamia* Risso & Poiteau and *Cynara cardunculus* L.

Citrus bergamia Risso & Poiteau, commonly referred to as "Bergamot", is a Mediterranean citrus fruit, and is considered an endemic plant of the Calabria region. In fact, while its precise botanical and geographical origins are unknown, bergamot is cultivated

along the Calabrian Ionian coast, between Bianco and Reggio Calabria [44]. This plant belongs to the *Rutaceae* family, *Esperidea* subfamily. Three varieties of bergamot are known—"*Fantastico*", "*Femminello*", and "*Castagnaro*". The relevance of this plant stems from the biological role of herbal preparations, particularly BEO and BJ. BEO is a volatile oil obtained by scraping and cold pressing the fruit peel; it contains up to 93–96% volatile compounds (limonene, linalool, and linalyl acetate), while the remaining percentage is a variable fraction of non-volatile substances (pigments, waxes, coumarins, and psoralens) [45]. BJ is derived from the endocarp and pulp of bergamot fruits, featuring a distinctive composition of compounds also present in albedo, including flavonoids like naringin, neohesperidin, and neoeriocitrin, as well as C-glucoside, flavanone O-glycosides, and flavone O-glycosides such as rhoifolin 40-O-glucoside, neodiosmin, rhoifolin, and poncirin, along with furanocoumarins like bergapten and bergamottin. The major biologically active polyphenols from BJ were found in the bergamot polyphenolic fraction (BPF). High-dose toxic furanocoumarins are removed from the BJ through an alkalinization step in production [61]. The key attraction of bergamot is the diverse health benefits stemming from the pharmacological activity of its components. Furthermore, the recent circular economy approach has highlighted the value of bergamot waste, supporting its use in therapies and advancing scientific understanding [46,47].

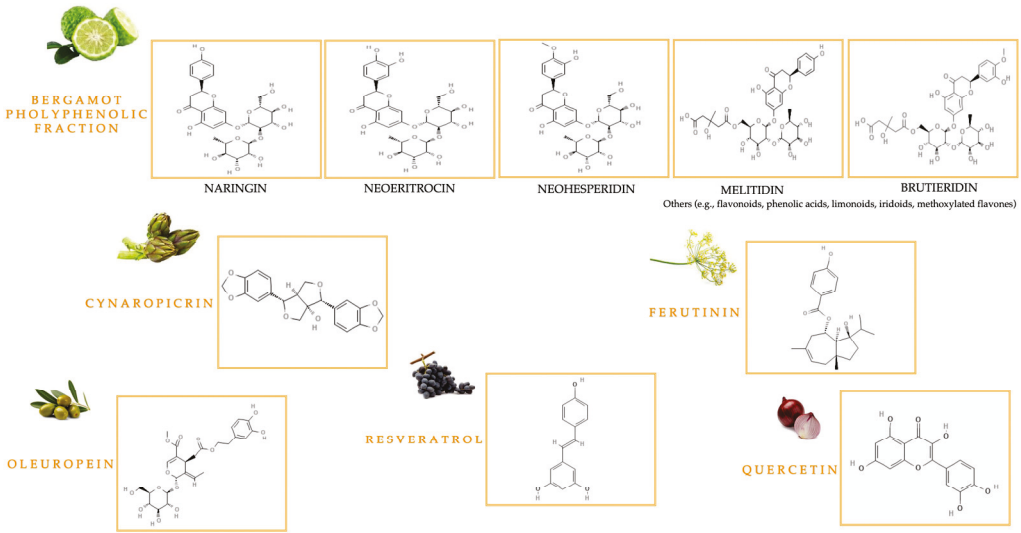

Figure 1. Diagrams of molecular structures.

Cynara cardunculus L., commonly referred to as "cardoon," represents a perennial Mediterranean plant belonging to the *Cardueae tribe Cass*. (*Cynarae Less*.), *Asteraceae* family, which includes three botanical taxa, the artichoke (*C. cardunculus* L. var. *scolymus* L. Flowers), the perennial wild thistle (*C. cardunculus* L. var. *sylvestris* (Lamk) Flowers), and the domestic thistle (*C. cardunculus* L. var. *altilis* DC.). This Mediterranean plant thrives despite harsh conditions, including extreme temperature swings and poor soil [62]. The immature flower structure of the artichoke, encompassing the leaves (bracts) and upper receptacle, is what is edible. Due to its nutritional profile—high in minerals, vitamins, amino acids, proteins, and low in lipids—cardoon qualifies as a functional food. The roots and rhizomes are rich in inulin, a crucial carbohydrate contributing to its high nutritional value and supporting gut microbiota [49], while cardoon leaves are a source of antioxidants such as dicaffeoylquinic acids and luteolin. Inedible plant matter accounts for 80–85% of plant biomass, resulting in wasted bioactive substances. Thus, the byproduct use of non-food parts yields useful pharmacologically active molecules such as polyphenols and flavonoids. Chlorogenic acid (5-O-caffeoylquinic acid) and cynaropicrin, a sesquiterpene

lactone, are responsible for cardoon's bioactivity, including hepatoprotective, antioxidant, chemopreventive, antiobesity, and antimicrobial properties [48].

1.2.2. Bioactive Polyphenolic Compounds in Olive Oil

Olive Oil (OO) represents the most important product obtained from the evergreen tree in the Mediterranean basin *Olea Europaea* L., a key component of the MedDiet. The process uses only water and room temperature to crush the olives during malaxation, creating the product without chemical solvents. The biological activity of Olive Oil is largely due to its rich phytochemical composition, most notably the lipophilic fraction (95–97%) of MUFAs (e.g., oleic acid) and PUFAs (e.g., omega-3 and omega-6). The other fraction consists of tocopherols, phytosterols, squalene, and phenols including oleuropein, tyrosol, and hydroxytyrosol [63,64]. The European Food Safety Authority (EFSA) has determined that "phenols in Extra Virgin Olive Oil (EVOO) contribute to the protection of blood lipids from oxidative stress," and this claim can be added to a product label when it contains at least 5 mg of hydroxytyrosol and its derivatives (e.g., oleuropein) per 20 g. Preclinical data indicates that oleuropein and hydroxytyrosol offer cardioprotection via mechanisms, including oxidative stress reduction, anti-inflammation, and homocysteine/cholesterol level modulation [50]. EVOO's unique phenolic profile, shaped by factors like cultivar and processing, is vital to its role in preventing a range of diseases, from Metabolic Syndrome to cancer [51,52]. Furthermore, Olive Mill Wastewater (OMWW) a byproduct from industrial EVOO processing, contains a high concentration of bioactive polyphenolic compounds (e.g., oleuropein) [53].

1.2.3. The Key Bioactive Role of Quercetin and Resveratrol

Quercetin and resveratrol, bioavailable polyphenols with antioxidant, anti-inflammatory, antiviral, and antiproliferative properties, are commonly found in foods characteristic of the MedDiet. Specifically, the flavonol quercetin (2-(3,4-dihydroxyphenyl)-3,5,7-trihydroxychromen-4-one) is prevalent in nature; key dietary sources include fruits and vegetables such as apples, berries, and onions [65]. Plants contain quercetin as glycosides (with attached sugars) or aglycones (without attached sugars), but the most common type, quercetin-3-O-glucoside, is hydrophilic and thus poorly absorbed. Consequently, quercetin demonstrates very low oral bioavailability. Extensive research focuses on this plant compound due to its effects on metabolic disorders, eye diseases, arthritis, and CVD [54,55].

Resveratrol is a stilbene and is produced by UV irradiation or fungal infection. However, antitumor, antioxidant, and anti-inflammatory activities are due to the trans-form of this bioactive compound [56], whereas there is currently only limited evidence for the cis-isomer [66]. RV is found in various nutritious foods, including grape skins and seeds, and is frequently detected in red wine, blueberries, cranberries, peanuts, and bilberries. The glycosylation of RV in food enhances its stability and bioavailability by preventing enzymatic oxidation [67]. The nutraceutical potential of quercetin and RV is being actively researched due to their effects on inflammation, gut microbiota, oxidative stress, and cancer [57,58].

1.2.4. Bioactive Compounds from *Ferula communis* L.

The genus *Ferula communis* L. subsp. *communis* (Giant fennel) belongs to the *Apiaceae* family and is an herbaceous perennial plant containing latex. Central and South-West Asia, North Africa, and the Mediterranean region are home to approximately 180 species. Two distinct chemotypes have been identified, exhibiting different biological effects: a poisonous type with prenylated coumarins, and a non-poisonous type with sesquiterpene daucane esters. In addition, in plants of the genus *Ferula*, oleo-gum-resins are also found [68]. They are defined by many natural bioactive compounds, primarily from roots, leaves, and

rhizomes, including sesquiterpenes, sesquiterpene lactones, flavonoids, coumarins (like ferulenol), coumarin esters (like ferulone A, B), and phytoestrogens (like ferutinin) [69]. The non-toxic chemotype's phytoestrogens make it estrogenic—high extract concentrations can thus create a doubled ferutinin dose–response; unlike the other chemotype, which is toxic and causes severe hemorrhagic intoxication from the ingestion of its aerial parts leading to potentially lethal "ferulosis" [70]. The toxicity is due to the prenylated coumarin ferulenol; removing it makes the extracts non-toxic since the remaining prenylated coumarins are not toxic at their concentrations. Several *in vivo* and *in vitro* studies reported its pharmacological properties, including antidiabetic, antimicrobial, antiproliferative, and cytotoxic actions [59,60]. *In vitro* studies and preclinical models have shown that ferutinin can be considered a selective estrogen receptor modulator (SERM), but its mechanism of action is not totally clear compared with classical SERMs. Its action on estrogen receptors depends on cell type and concentration; it is an estrogen receptor alpha (ERα) agonist and may act as an estrogen receptor beta (ERβ) agonist or antagonist. Therefore, the effects of ferutinin on gene expression and cell signaling pathways within estrogen-sensitive cancers (e.g., ER-positive breast cancer (BC) and endometrial cancer (EC)) are dose-dependent [71]. Further studies of this typical Mediterranean plant need to explore the underlying mechanisms and potential pharmaceutical applications.

2. Biological Functions and Pathological Implications of Reactive Oxygen and Nitrogen Species

Reactive oxygen/nitrogen species (ROS and RNS) are unstable, thus highly reactive and partially reduced, oxygen- and nitrogen-derived molecules that include superoxide anion (O_2^-), hypochlorous acid (HOCl), hydroxyl radical, peroxyl radicals, nitric oxide, and peroxynitrite. The presence of a free electron on the oxygen atom allows oxygenated free radicals to react with sugars, proteins, and lipids; among free radicals, the superoxide anion is the most prevalent: oxidative phosphorylation in mitochondria, along with activated phagocytes, produces it via electron leakage from the electron transport chain to molecular oxygen [72].

Primarily, superoxide (O_2^-) will dismutate into oxygen and hydrogen peroxide (H_2O_2). Although superoxide is unreactive with DNA, H_2O_2, in the presence of iron or copper, can become highly reactive hydroxyl radicals (•OH) through the Fenton reaction. The generation of ROS, including this process and superoxide-derived ROS, is linked to various diseases, including cancer, cardiovascular diseases, and neurodegenerative disorders [73,74]. In hepatocytes and macrophages, ROS are produced during processes like aerobic respiration and inflammation. ROS signaling, regulated by molecules and post-translational modifications (PTMs), triggers specific cellular responses based on ROS generation's nature and duration [75]. Cell differentiation and apoptosis, induced by ROS, contribute to physiological aging. RNS include nitric oxide and peroxynitrite: these molecules readily oxidize, thus damaging DNA and other biomolecules. Oxidative stress biomarkers are ROS-production enzymes such as nicotinamide adenine dinucleotide phosphate (NADPH) oxidase, myeloperoxidase, xanthine oxidase (XO), and endothelial nitric oxide synthase (eNOS). Well known biomarkers of ROS-induced chemical modifications are the advanced glycation end products (AGEs), the oxidized low-density lipoprotein (OxLDL), and malondialdehyde (MDA) [76]. Therefore, a crucial factor is keeping the body's oxidative state balanced by generating and eliminating free radicals properly [77].

Indeed, high cellular ROS levels damage intracellular components like DNA, causing mutations and cell transformation [78]. Current findings suggest a link between ROS production and both internal and external influences. The electron transport chain within mitochondria is the primary endogenous source of ROS. High ROS levels cause DNA

damage, oncogene activation, and tumor growth, whereas moderate levels induce cell death or senescence, thus suppressing tumor development [79].

Exogenous sources of ROS involve an unbalanced diet, anticancer therapy, radiation, smoking, drugs, and alcohol [80]. Chemotherapy drugs, including anthracyclines (doxorubicin (Dox), daunorubicin (Daun)), and camptothecins can cause various complications in the CV system due to ROS [81]. This is related to an increased lipid peroxidation and reduced levels of antioxidant molecules such as glutathione (GSH) [82]. It represents a non-enzymatic antioxidant, along with vitamins A, C, and E, and flavonoids. Enzymatic antioxidants include glutathione peroxidase (GPX), glutathione reductase (GRX), catalase (CAT), superoxide dismutase (SOD), superoxide reductase, thyroxine (TRX), and peroxiredoxin (PRX). The GSH system involves GSH, GR, glutathione transferase (GST), and GPX. Its deficiency or an altered GSH/GSSH ratio can lead to inflammation and tumor progression due to the occurrence of oxidative stress [83]. Dietary antioxidants are crucial, as evidenced by research on the diverse array of antioxidant systems [84,85]. By modulating oxidative stress, natural compounds can boost the effectiveness of therapies: the Mediterranean region, in this context, boasts an abundance of antioxidant-rich natural compounds [48,86].

2.1. Oxidative Stress in Cancer Development: The Role of Scavenger Enzymes

Increasing ROS release is observed during tumor development, activating mechanisms that drive tumor progression. This causes DNA damage and genetic instability, thus increasing cancer cell survival and resistance to cell death; consequently, cancer cells develop a more aggressive nature and capacity for metastasis. Additionally, high ROS levels trigger resistance mechanisms in tumor cells, which concurrently maintain protumorigenic signaling. Furthermore, oxidative stress contributes to resistance against chemotherapy [87]. Therefore, altering the oxidized/reduced state ratio may offer an oncological treatment, linked to the antioxidant effects of various natural compounds [88]. Unbalanced oxidative stress levels lead to the activation of oncogenes and reduction in the activity of tumor suppressors. High ROS production in cancer can result in the inactivation of H_2O_2 scavenger enzymes like glutathione peroxidase (GPX), glutathione reductase (GRX), catalase (CAT), superoxide dismutase (SOD), superoxide reductase, thyroxine (TRX), and peroxiredoxin (PRX) and the tumor suppressor gene phosphatase and tensin homolog (PTEN), a negative regulator of the PI3K/AKT signaling pathway, as well as the oxidation and inactivation of many other protein tyrosine phosphatases (PTPs) such as tyrosine-protein phosphatase non-receptor type 1 (PTP1B) [89]. PTEN oxidation and inactivation results in cell survival through the activation of PI3K and protein kinase B (Akt) pathways [90]. Akt is involved in cell survival through phosphorylation and the inactivation of its target proteins, including the pro-apoptotic transcription factors: forkhead box transcription factors (FOXO), BCL2 associated agonist of cell death (BAD), BCL2 associated X apoptosis regulator (BAX), and B-cell lymphoma 2 (Bcl-2)-like protein 11 (BCL2L11) [91]. Additionally, several cancers, including esophageal squamous cell carcinomas, stomach adenocarcinomas, and colorectal carcinomas (CRCs), show increased expression of genes that code for SOD proteins [92]. Tumor pathogenesis is associated with mutations in transcription factors, such as nuclear erythroid 2-related factor (Nrf2), and tumor suppressor genes, such as p53 [93]. In fact, under physiological conditions, the expression and activity of the transcription factor Nrf2 are strictly degraded by Kelch-like ECH-associated protein 1 (KEAP1), an adaptor of Cullin 3-based E3 ubiquitin ligase [94]. Cytosolic KEAP1 binding to Nrf2 triggers Nrf2 ubiquitination and proteasomal degradation; consequently, Nrf2 levels remain low under normal conditions. Oxidative stress causes the oxidation of thiol groups within KEAP1 (e.g., S-S cross-links) and this conformational

change causes the release of Nrf2 in the cytosol, with its subsequent translocation to the nucleus, where Nrf2 activates antioxidant response element (ARE), which regulates antioxidant enzymes such as NAD(P)H quinone oxidoreductase (NQO1), glutathione S-transferases (GSTs), thioredoxin reductase-1 (TXNRD1), thioredoxin, ferritin, glutamate-cysteine ligase, and heme oxygenase-1 (HO-1), depending upon the binding site present in the promoter region. Nrf2 has been reported to be active and overexpressed in cancer, promoting tumor progression and cancer cell survival [95]. Its activation can also be mediated by other signal transduction pathways such as AMPK, extracellular signal-regulated kinase (ERK), c-Jun amino-terminal kinase (JNK), and PI3K/AKT [96].

2.2. Pathways Involved in Oxidative Stress-Induced Tumorigenesis

Tumorigenesis frequently involves the constitutive activation of the Nrf2 pathway, as shown in various studies. This activation arises from mechanisms including oncogene (KRAS, B-Raf proto-oncogene serine/threonine kinase (BRAF), cellular myelocytomatosis oncogene (c-myc) driven transcription, KEAP1 epigenetic suppression, or KEAP1 somatic mutations disrupting Nrf2 binding [97]. In addition, growth factors and KRAS-stimulated pathways have been shown to activate MAPK/ERK 1/2 in cancer, a protein kinase that is a member of the mitogen-activated protein kinase (MAPK) family resulting in increased cell proliferation [98]. Estrogen metabolism generates H_2O_2, which triggers the ERK1/2 signaling pathway in various cancers, such as BC; cancer cell motility and anchorage-independent growth are also impacted by the latter. Mitochondrial dysfunction-induced ROS production increase promotes NF-κB upregulation [99] which induces the up-regulation of epidermal growth factor receptor (EGFR) and its ligands through polycystin 1, transient receptor potential channel interacting (PKD1)-mediated signaling. PKD-family serine/threonine kinases act downstream of protein kinase C (PKC) and other signaling pathways, including those of Src and Abl, play a key role in detoxification from ROS and the transcription of anti-apoptotic genes [100]. The promotion of tumor progression by PKD1 involves supporting mechanisms for cancer cell survival. This includes activating ERK1/2 and regulating the JNK pathway, with effects varying based on the cellular environment [101]. Low H_2O_2 levels can trigger NF-κB, an oxidative stress detector; this can trigger the production of anti-apoptotic genes and pro-cancer cytokines like interleukin-6 (IL-6) and tumor necrosis factor alpha (TNF-α) and may activate or suppress MAPK phosphorylation. Moreover, blocking NF-κB may overcome drug resistance, a key factor in the development of chemo-resistance [102]. Reduced ROS activates hypoxia-inducible factor 1-alpha (HIF1-α), leading to the expression of genes essential for cancer growth, such as the vascular endothelial growth factor (VEGF) and its receptors; high ROS levels can directly cause oxidative DNA damage [103] and interfere with the function of epigenetic modifiers, such as DNA methyltransferases (DNMTs) and histone deacetylases (HDACs), resulting in both the hypomethylation and hypermethylation of DNA. Oxidative DNA damage causes alterations such as base pair deletions, insertions, mutations, and double-strand breaks (DSBs), forming mutagenic 8-oxo-2′-deoxyguanosine (8-oxodG), which can accumulate and cause cancer. Furthermore, telomere 8-oxo-G accumulation affects length and impairs end-capping maintenance [104]. ROS have a direct impact on the ability of transcription factors (TFs) to bind DNA: increased localization of Fos/Jun DNA-binding redox factor-1 (Ref-1) protein and ataxia-telangiectasia mutated (ATM) serine/threonine kinase—key to DNA repair—occurs in the nucleus. High ROS levels promote cancer metastasis by suppressing natural killer (NK) cell activity [105] and can regulate macrophages recruitment and cancer cell invasion. In fact, ROS contribute to the acquisition of metastatic potential by cancer cells through EMT and the expression of TF Snail, which downregulates the expression of epithelial cadherin (E-cadherin) and promotes the expression of neural

cadherin (N-cadherin) and vimentin. Excessive levels of ROS can lead to the activation of intrinsic and extrinsic apoptosis; in particular, mitochondrial excess ROS levels play a key role in initiating intrinsic apoptosis. High ROS levels lead to the release of cytochrome C (cyt C) into the cytosol, where it engages the apoptotic protease-activating factor 1 (APAF1), followed by the formation of the apoptosome and the activation of caspase-9 [106]. ROS can activate the extrinsic apoptotic pathway by modulating death receptors at the transmembrane level, including Fas (CD95), tumor necrosis factor receptor 1 (TNFR-1/TNF-α receptor) and tumor necrosis factor-related apoptosis-inducing ligand receptors (TRAIL-R1/2). Activated receptors, in the cytosol, recruit adaptor proteins (e.g., Fas-Associated Death Domain Protein (FADD)) and procaspases-8/10, forming death-inducing signaling complexes (DISCs) that activate caspases-8 and -10. Direct activation of effector caspases -3, -6, and -7 is possible via the latter; however, in some cases, they cleave Bid into tBid, which in turn stimulates mitochondrial outer membrane permeabilization (MOMP), blocking the anti-apoptotic activity of Bcl-2 and Bcl-XL, and leading to the release of cyt C, thereby activating the intrinsic pathway [107]. Oxidative stress and DNA damage, byproducts of chemo and radiotherapy, can cause tumor cells to develop drug resistance.

The Dual Action of Nutraceutical Compounds and Their Therapeutic Role

In vitro and *in vivo* studies support the idea that eating antioxidant-rich foods is a good way to reduce cancer risk. Some natural compounds have demonstrated dual action: they act as antioxidants to protect healthy cells from treatment-related oxidative stress, and as pro-oxidants in cancer cells, activating pro-apoptotic pathways. The antioxidant properties of bergamot polyphenolic fraction (BPF) are shown by its ability to reduce oxidative stress biomarkers and intracellular ROS levels [108]. Studies show that BPF can reduce MDA levels in rats fed a hyperlipidemic diet (HLD) [109] and in rats fed a high-fat diet (HFD) [110]. Bergamot's lipid-lowering effects, alongside reductions in MDA, Lectin-like oxidized low-density lipoprotein receptor-1 (LOX-1), and protein-kinase B (PKB), indicate improved potential, especially for those on statins [111]. BPF also improves the activity of endogenous antioxidant enzymes, including GPX and SOD. By reducing peroxynitrite, it improves antioxidant defense mechanisms, thus preventing oxidative stress-induced tissue damage. High-fat Western diet-fed (WD SW) mice treated with BPF showed reduced 3-nitrotyrosine (3-NT) in their livers compared to controls; 3-NT is a biomarker of peroxynitrite oxidative damage [112]. The protective effect of BPF on dox-induced ROS accumulation in cardiomyocytes *in vivo*, leading to a reduction in Dox-induced cardiomyopathy by enhancing the resident c-kit^{+} CD45^{neg} CD31^{neg} endogenous cardiac stem cells (eCSCs) and preventing 8-hydroxy-2′-deoxyguanosine (8-OHdG) nuclear accumulation has been demonstrated [113]. Phenolic compounds found in *Cynara cardunculus* extract, including caffeic acid and chlorogenic acid are effective antioxidants [114] acting as free radical scavengers and modulating the expression of genes coding for antioxidant enzymes such as SOD, GPX, and CAT [115]. Moreover, the sesquiterpene cynaropicrin has antioxidant properties [116] and pro-oxidant action in cancer cells [117]. In fact, inhibiting thioredoxin reductase (TxR), a key enzyme in cellular redox homeostasis, causes intracellular ROS increase and triggers apoptosis in cancer cells [118]. Cynaropicrin treatment increased nuclear Nrf2 in A375 human melanoma cells, as demonstrated by *in vitro* antioxidant assays. This is linked to a time-dependent rise in the transcription of genes that code for antioxidant enzymes like glutamate-cysteine ligase (GCL) and heme oxygenase (HMOX-1) [119]. *In vivo* studies reveal the effect of cynaropicrin on the antioxidant enzymes (SOD, CAT, Glutathione Peroxidase (GSH-PX)), and on 8-OHdg in the control and cerebral ischemia–reperfusion (I/R) injury in rats, highlighting that it supports the antioxidants defense system against oxidative-stress [120]. Specifically, bergamot extract formulations with

Cynara cardunculus show synergistic effects, potentially expanding treatment options for various diseases, including cancer, thanks to their antioxidant properties [121]. An *in vivo* study has shown the increasing level serum of GPX and SOD after 16 weeks of treatment with BPF and *Cynara cardunculus* phytocomplex, named Bergacyn®, accompanied by a reduction in serum MDA levels [122].

It has been shown that oleuropein is able to increase the activity of antioxidant enzymes (i.e., SOD, GPX, GRX, CAT) and non-enzymatic antioxidant systems such as GSH [123]. It is established that oleuropein's antioxidant activity is dependent on factors such as cell type, concentration, exposure time, and oxidative stress levels [53]. In fact, its pro-oxidant action has been shown in several *in vitro* cancer cell lines, for example, MCF-7 BC cells [124], HepG2 hepatocellular carcinoma (HCC) cells [125], and HEY human epithelial ovarian cancer cell line [126], thus contributing to cell death by promoting cell damage and leading to apoptosis. Recent studies also demonstrate that oleuropein, BPF, and *Cynara cardunculus* extract lessen Dox's cardiotoxic effects within an *in vitro* rat embryonic cardiac myoblast (H9c2) model [113,127,128]. Moreover, their contribution to upholding the integrity of cellular plasma membranes' phospholipid bilayer could be pivotal via lipid content regulation. These natural compounds reportedly prevent endoplasmic reticulum (ER) dysfunction and promote apoptosis by modulating intracellular calcium [129]. Nevertheless, more research is necessary to verify the effectiveness and safety of these compounds for human use.

The preventative and therapeutic effects of quercetin and RV on various cancers are well-documented and dose-related [130]. At low doses, these agents exhibit antioxidant properties (ROS neutralization), but at higher doses, they stimulate ROS production, leading to apoptosis via the intrinsic pathway (cyt C release, caspase activation) and extrinsic pathway (death receptor activation) [131]. Low doses of quercetin and RV stimulate GSH synthesis and modulate antioxidant enzymes (SOD, CAT, GPX), offering protection. KEAP1 residue oxidation and subsequent inhibition leads to Nrf2 accumulation in the cytoplasm, followed by nuclear translocation and ARE activation [132]. Through AMPK and silent mating type information regulation 2 homolog 1 (SIRT1) activation, RV inhibits the mammalian target of rapamycin (mTOR) and deacetylates/activates forehead transcription factor O subfamily member 3a (FOXO3a), boosting antioxidant enzyme gene expression [133]. While at high doses, they interfere with mitochondrial function, generating dissipation of membrane potential, with the release of cyt C [134]. By suppressing intracellular ROS accumulation, RV protected H9c2 cardiac cells form Dox-caused toxicity [135]. Because of its strong antioxidant properties, quercetin enhances Dox's antitumor activity by inhibiting topoisomerase II (Topo II) and intercalating with DNA [136].

Several studies highlighted the biphasic effect of ferutinin [137]: low doses, in fact, show antioxidant and protective effects on healthy cells, decreasing oxidative damage. Ferutinin pretreatment at a low dose significantly reduced Dox-induced cardiotoxicity in H9c2 cells, according to Macrì et al. [138]. In addition, ferutinin at low concentrations demonstrated hyperproliferative effects with phytoestrogenic action in MCF-7 BC cells. At higher concentrations, ferutinin can increase oxidative stress in cancer cells with antiproliferative effect [139], showing a lower toxicity in healthy cells with respect to cancer cells. Bax upregulation and cyt C release, hallmarks of mitochondrial apoptosis, are dose-dependently increased by ferutinin [140]. It shows selective toxicity toward cancer cells over healthy cells, with effects varying by dose and cell type. Specifically, high ferutinin levels suppressed the growth of MCF-7 (estrogen-dependent) and MDA-MB-231 (estrogen-independent) BC cells [141]. Furthermore, ferutinin pretreatment decreased ROS and MDA buildup in lipopolysaccharide-stimulated (LPS) neurons and shielded human oligodendrocytes (MO3.13) and neurons (SH-SY5Y) from LPS-caused oxidative stress [142]. Therefore, further *in vitro* and *in vivo* research is needed to clarify the dose-dependent

mechanisms of nutraceuticals' dual effects on cancer cells (Table 2) and their potential as cancer therapy adjuvants.

Table 2. Dose-dependent Action of Nutraceuticals.

Nutraceutical	Low Dose Effect (Protective/Antioxidant)	High Dose Effect (Pro-Oxidant/Anticancer)	Mechanism	References
Bergamot polyphenolic fraction	↓ MDA/ROS; ↑ SOD/GPX; ↓ 3-NT/LOX-1; ↑ protective effect.	Synergistic support in redox balance, not directly cytotoxic.	↓ peroxynitrite; ↑ antioxidant enzymes (cardiomyocytes, liver).	[108–111,113,128,143]
Cynaropicrin	↑ Nrf2/SOD/CAT/GSH-PX; antioxidant in A375, brain, liver tissues.	Inhibits TxR → ↑ ROS → apoptosis in cancer cells.	Activates antioxidant genes (GCL, HMOX-1), pro-apoptotic in melanoma, neural, liver cells.	[117–119]
Oleuropein	↑ SOD/GPX/GRX/CAT; ↓ ROS; protects membrane and ER integrity.	↑ ROS, mitochondrial dysfunction, cyt C release; apoptotic in MCF-7, HepG2, HEY cancer cells.	Dose- and cell-type specific redox modulation.	[124,125]
Quercetin	Activates Nrf2; ↑ GSH/SOD/GPX; inhibits Topo II; protection from Dox cardiotoxicity.	↑ ROS; DNA damage; cyt C release; apoptosis via intrinsic/extrinsic pathways.	Caspase cascade, KEAP1 oxidation, ARE activation, Topo II inhibition.	[132]
Resveratrol	↑ SIRT1/AMPK/FOXO3a, antioxidant genes; prevents Dox toxicity.	↑ ROS; mitochondrial permeability transition pore (mPTP) opening; apoptosis through caspase activation.	Mitochondrial depolarization; dual effect depending on dose and exposure time.	[133–135]
Ferutinin	Antioxidant, phytoestrogenic; ↓ ROS/MDA; protects H9c2 and neural cells.	↑ ROS, ↑ Bax, cyt C; apoptosis in MCF-7, MDA-MB-231 BC cells.	SERM-like; mitochondrial apoptosis; cell-selective effects.	[138–142]

The arrows indicate decrease (↓) and increase (↑), and progression (→), respectively; MDA: malondialdehyde; ROS: reactive oxygen species; SOD: superoxide dismutase; GPX: glutathione peroxidase; 3-NT: 3-nitrotyrosine; LOX-1: lectin-like oxidized low-density lipoprotein receptor-1; Nrf2: nuclear erythroid 2-related factor; CAT: catalase; GSH-PX: glutathione peroxidase; TxR: thioredoxin reductase; GCL: glutamate-cysteine ligase; HMOX-1: heme oxygenase; GRX: glutathione reductase; Cyt C: cytochrome C; GSH: glutathione; Topo II: topoisomerase II; Dox: doxorubicin; DNA: deoxyribonucleic acid; KEAP1: kelch-like ECH-associated protein 1; ARE: antioxidant response element; SIRT1: silent mating type information regulation 2 homolog 1; AMPK: AMP-activated protein kinase; FOXO3a: forkhead transcription factor O subfamily member 3a; mPTP: mitochondrial permeability transition pore; BC: breast cancer; SERM-like: selective estrogen receptor modulator-like.

3. Highlights of the Inflammatory Process

Inflammation plays a crucial role in cancer development and metastasis, thus a key focus for cancer therapies. The growth of blood vessels, stimulated by cytokine production, aids carcinogenesis, while the resulting ROS leads to DNA damage. Moreover, the promotion of resistance mechanisms in cancer cells by inflammation can lead to chemoresistance.

This occurs both through increased DNA damage due to inflammation, with activation of oncogenic bypass signaling pathways (e.g., mesenchymal–epithelial transition factor (C-MET), PI3K/AKT, MAPK), and through the action of some mediators of inflammation, including IL-6 and interleukin-1 alpha and interleukin-1 beta (IL-1α/β), which modulate apoptotic and autophagic processes [144]. Tissue damage triggers inflammation—the body's complex response involving a cascade of pro- and anti-inflammatory mediators (e.g., cytokines, prostaglandins) to various insults (ischemia, trauma, infection, toxins).

The inflammatory process recruits microcirculation ECs and white blood cells, a process driven by molecular signals and balanced levels of pro- and anti-inflammatory mediators which are essential to maintain homeostasis [145]. A persistent inflammatory trigger or a failed initial response can shift an acute inflammatory to a chronic process. Aggressive cancer phenotypes, marked by increased survival, proliferation, invasion, angiogenesis, and metastasis, are often facilitated by the pro-cancer microenvironment generated from chronic inflammation.

The inflammatory response, characterized by toll-like receptor (TLR) activation, is linked to and modified by dysbiosis [146], NOD-like receptors (NLRs), C-type lectin receptors (CLRs), and retinoic acid-inducible gene (RIG)-I-like receptors (RLRs) by neutrophils/macrophages in response to pathogen-associated molecular patterns (PAMPs) [147].

Leukocyte recruitment and infiltration are mediated by chemokines like interleukin-8 (IL-8) and macrophage-inflammatory protein 2 (MIP-2) alongside inflammatory mediators including complement C5a complement fragments, platelet-activating factor (PAF), and leukotriene B4 (LTB4) [148] from the venous system to sites of tissue damage, and there is their attachment to the ECM. Activated ECs express adhesion molecules, such as the intercellular adhesion molecule 1 (ICAM-1) and intercellular adhesion molecule 2 (ICAM-2), facilitating leukocyte adhesion and diapedesis. This process involves adhesion molecules (i.e., L-P- and E-selectin) and chemokines/cytokines (i.e., TNF-α, TGF-β, IL-1β, IL-6) secreted by activated macrophages, which regulate inflammatory cascade. The pro-inflammatory phenotypes in ECs and fibroblasts are mainly triggered by TNF-α, IL-6, and IL-1β, which activate TNFR, interleukin-6 receptor (IL-6R), and interleukin-1 receptor (IL-1R), resulting in the activation of NF-κB, MAPK, and Janus kinase/signal transducer and activator of transcription (JAK-STAT) signaling pathways [149].

3.1. Hallmarks of Cancer Inflammation

The research focuses on understanding the mechanisms through which inflammation impacts cancer, aiming to identify more selective therapeutic targets within specific pathways [144]. Findings from basic and clinical research demonstrate the importance of inflammatory molecules in the initiation and advancement of multiple cancer types, including breast, lung, and liver cancers [150]: these molecules could impact every phase of tumor growth, from malignant change to metastasis [151]. Conversely, acute inflammation may inhibit cancer progression: indeed, it can stimulate the immune system to help remove tumor cells. The onset of chronic inflammation increases the risk of developing highly invasive cancers. In particular, an inverse correlation between MedDiet and chronic inflammation, with lower levels of inflammatory biomarkers (i.e., CRP and IL-6) and lower risk of several cancers, has been reported [152]. Inflammation can promote tumor initiation, due to infections (e.g., Human Papillomavirus (HPV), *Helicobacter pylori* (*H. pylori*), Hepatitis B Virus (HBV), Hepatitis C virus (HCV) or carcinogens (e.g., cigarette smoke, toxic substances, ionizing radiation) [153]. Conditions such as diabetes, hyperlipidemia, and CVD are associated with low-grade inflammation that may predispose to the risk of developing cancer (e.g., BC, HCC, pancreatic cancer (PC)) [154]. The activation of Signal

Transducer and Activator of Transcription proteins (STAT), especially Signal Transducer and Activator of Transcription 3 (STAT3), a transcription factor regulating genes related to cell growth, survival, and immunity, is heavily involved in cancer development across many tissues and inflammatory responses in cancers of the stomach, liver, lung, colon, and pancreas. ROS and RNS, substances produced by leukocytes and other phagocytic cells, can cause irreversible DNA damage (oncogenic mutations like RAS and myc, and the inactivation of p53 and retinoblastoma protein 1 (RB1)), increasing cancer risk. The cytokine MIF, released from macrophages, T lymphocytes, and tumor cells, can aggravate DNA damage and the accumulation of oncogenic mutations [155]. By suppressing p53's transcriptional activity, MIF interacts with it and promotes the survival of damaged cells. By suppressing pro-apoptotic gene activation and stimulating cell proliferation through PI3K/AKT and NF-κB signaling, this mechanism contributes to tumor development. The release of pro-inflammatory cytokines (TNF-α, IL-1, IL-6, IL-8, and interleukin-23 (IL-23)) from macrophages and T-lymphocytes indirectly leads to genetic instability via epithelial cell ROS production [151]. NF-κB signaling is activated via TNFR and IL-1 receptor engagement by TNF-α and IL-1 cytokines, thereby promoting a pro-inflammatory phenotype in ECs and fibroblasts. The JAK/STAT3 pathway is mainly activated by IL-6 and IL-23, contributing to the development of inflammatory tumors. In addition, the binding of IL-22 to its receptor (Interleukin-22 Receptor Subunit 1(IL-22R1)/Interleukin-10 Receptor Subunit 2 (IL-10R2)) triggers the janus kinase 1 and tyrosine kinase 2 (JAK1/TYK2) pathway, causing STAT3 phosphorylation and subsequent nuclear translocation to activate target genes involved in epithelial cell survival and regeneration. The roles of NF-κB and STAT3 pathways in tumor formation are widespread across many tissue types and strongly associated with inflammation in cancers of the stomach, colon, liver, lung, and pancreas, influencing cell proliferation, survival, angiogenesis, and immune evasion [156]. The TME comprises cancer cells, stroma, blood vessels, CAFs, ECs, pericytes, dendritic cells (DCs), and activated macrophages; these components are crucial for both antigen-specific immunity and immune tolerance, bridging innate and adaptive immunity. The TME significantly involves TAMs, which are derived from circulating monocytic precursors and are directed toward the tumor and are induced by interferon-gamma (IFN-γ)-mediated classical activation or alternatively by the helper T 2 cells (Th2) and cytokines like interleukin-4 (IL-4) and interleukin-13 (IL-13). TAMs can stimulate tumor cell proliferation, promote angiogenesis, and promote invasion and metastasis. Inflammatory-TME also includes polymorphonuclear leukocytes, and various inflammatory cells such as T lymphocytes (sometimes B cells) [157,158]. Consequently, the link between oxidative stress, chronic inflammation, and cancer development is clear. Recent findings indicate a link between the aberrant activation of Wntβ/catenin signaling and the progression of tumors and chronic inflammatory diseases. Research into Wnt/β-catenin signaling reveals opposing roles for peroxisome proliferator-activated receptor-gamma (PPARγ), which is downregulated in chronic inflammation and cancer [159,160]. PPARγ's role is context and tissue-specific, with evidence suggesting it can function as an oncosuppressor in certain situations, causing cell cycle arrest and apoptosis while lowering cell invasion, migration, and inflammation [161]. Deregulation in pro-inflammatory or hyperlipidic conditions promotes oncogenesis [162]. Conversely, the NF-κB pathway upregulates pro-inflammatory cytokines (interleukin-6 (IL-6), VEGF, (IL-8)), Inducible nitric oxide synthase (iNOs), TGF-β, indirectly boosts WNT/β-catenin, thus fueling inflammation and tumor growth. Survival and prognosis may be indicated by the grade of tumor infiltration, which varies by tumor type.

3.2. Modulation of Inflammatory Pathways by Nutraceutical Compounds from the Mediterranean Diet

The effect of diet on acute and chronic inflammation is associated with the development of cancer. [163]. The anti-inflammatory properties of numerous natural compounds suggest their potential use as supplemental components within alternative anti-inflammatory treatment systems (Figure 2).

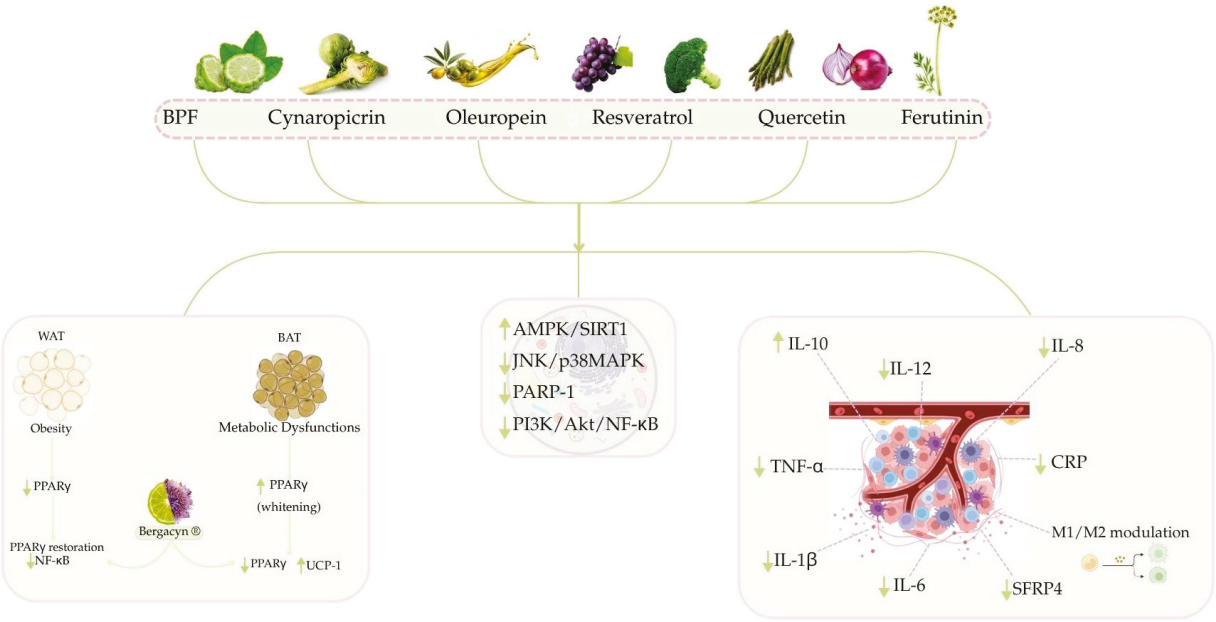

Figure 2. BPF, cyn, oleuropein, RV, quercetin, and ferutinin are able to modulate inflammatory pathways including AMPK/SIRT1, JNK/p38MAPK, PARP-1, and PI3K/Akt/NF-κB; modulate the secretome of tumor cells by reducing the secretion of pro-inflammatory cytokines (IL-12, IL-8, CRP, SFRP4, IL-6, IL-1β, TNF- α) and increasing the secretion of anti-inflammatory cytokines (IL-10), and modulate the activation state of macrophages. Bergacyn® restored PPARγ levels and prevented NF-κB overexpression in obese WAT, where PPARγ is significantly reduced. Whereas, in BAT, despite the increased expression of PPARγ, during metabolic dysfunction and "whitening," Bergacyn® reduced PPARγ. Restoration of adipose tissue homeostasis and regulation of PPARγ by Bergacyn® could reduce inflammation and metabolic signals involved in some cancers. The arrows indicate decrease (↓) and increase (↑), respectively. Bergamot polyphenolic fraction (BPF); cynaropicrin (cyn); resveratrol (RV); AMP-activated protein kinase/silent mating type information regulation 2 homolog 1 (AMPK/SIRT1); c-Jun amino-terminal kinase/p38 mitogen-activated protein kinase (JNK/p38MAPK); poly (ADP-ribose) polymerase-1(PARP-1); phosphatidylinositol 3-kinase/protein kinase B/Nuclear factor kappa-light-chain-enhancer of activated B cells (PI3K/Akt/NF-κB); interleukin-12, -8, -6, -1β, -10 (IL-12, -8, -6, -1β, -10); C reactive protein (CRP); secreted frizzled-related protein 4 (SFRP4); tumor necrosis factor alpha (TNF- α); peroxisome proliferator-activated receptor-gamma (PPARγ); brown adipose tissue (BAT); white adipose tissue (WAT).

3.2.1. Anti-Inflammatory Activity of Citrus Bergamia

Citrus bergamia derivatives have demonstrated anti-inflammatory activity, linked to AMPK/SIRT1 axis activation [164]. The activation of AMPK, a key regulator of energy and senescence, is linked to changes in inflammatory factors such as IL-6 and TNF-α [133]. Importantly, BPF might reduce levels of serum glucose, transaminases, gamma-glutamyl transferase (GGT), and inflammatory biomarkers such as TNF-α and CRP [165]: this prevents worsening liver inflammation and fibrosis [112]. Reduced hepatic inflammation, via IL-6 reduction and Interleukin-10 (IL-10) mRNA upregulation, has been linked to BPF supplementation [166]. By lowering phospho-JNK and phospho-p38 MAPK, it can control the release of pro-inflammatory cytokines such as IL-1β. The reduction in inflammation and

hepatocellular ballooning, key to cancer initiation, also supports this effect [112,150]. This effect may also be due to BPF's antioxidant activity, which lowers excessive poly (ADP-ribose) polymerase-1 (PARP-1) activity. In disease states, the second choice has been observed to decrease the levels of the MAPK inhibitor mitogen-activated protein kinase phosphatase 1 (MKP-1), leading to elevated inflammation. Consequently, BPF's anti-inflammatory effect stems from the decreased PARP-1 repression of MKP-1, leading to JNK/p38 MAPK inhibition [167]. Findings from a randomized, double-blind, placebo-controlled study in type 2 diabetes mellitus/non-alcoholic fatty liver disease (T2DM/NAFLD) patients show that Bergacyn® improves NAFLD and liver fibrosis markers by modulating inflammatory biomarkers [122].

3.2.2. The Beneficial Effects of Cynaropicrin and Bergacyn® to Counteract Inflammation

Recently, *in vivo* studies evaluated Bergacyn®'s potential for tissue-specific PPARγ modulation. In obese white adipose tissue (WAT), where PPARγ is significantly reduced, Bergacyn® restored PPARγ levels and prevented NF-κB overexpression. Despite increased PPARγ expression in brown adipose tissue (BAT) during metabolic dysfunction and "whitening," Bergacyn® downregulates PPARγ, thus promoting a thermogenic and metabolically active state [121]. PPARγ's involvement in colorectal, lung, breast, prostate, and pancreatic cancer (proliferation, differentiation, and inflammation) makes the tissue-specific Bergacyn® modulation data highly impactful [168,169]. Moreover, the inflammatory microenvironment, a consequence of obesity-linked adipose tissue dysfunction, can promote tumor progression. Therefore, the restoration of adipose tissue homeostasis and PPARγ regulation by Bergacyn® could lessen inflammation and metabolic signals involved in certain cancers [121] (Figure 2). Several studies highlight cynaropicrin's involvement in the inhibition of the NF-κB transcriptional activation pathway [170]. *In vitro* studies on the murine macrophage cell line RAW264.7 show its ability to inhibit inflammatory cytokine secretion following the induction of inflammation with LPS [171]. In the A375 cell line treated with cynaropicrin, the p65/RelA protein, a member of the NF-κB family, was reduced [119]. *In vivo* studies report that dosage-based cynaropicrin treatment on rats with cerebral I/R injury-induced significantly reversed the increased level of the pro-inflammatory cytokines (TNF-α, IL-6, and IL-1β), and appreciably reduced the mRNA level of NF-κB [120].

3.2.3. Anti-Inflammatory Activity of Oleuropein

In vitro oleuropein has been shown to reduce the secretion of pro-inflammatory cytokines and inflammatory mediators [172,173]. In a RAW264.7 macrophage line activated with LPS (M1 phenotype), oleuropein treatment reduced Interleukin-12 (IL-12) and TNF-α levels in the cell culture supernatant and the oleuropein action on readjusting the M1/M2 macrophage polarization towards the anti-inflammatory M2 phenotype has been reported [174]. RAW264.7 cells were used to assess oleuropein's ability to reduce LPS-induced inflammation by reducing levels of IL-1β, IL-6, and TNF-α [175,176]. Oleuropein pretreatment in LPS-activated Human Umbilical Vein Endothelial Cells (HUVECs) has been shown to potentially lower mRNA levels of pro-inflammatory cytokines like IL-1β, IL-6, TNF-α, and IL-8 [172]. Several *in vivo* studies demonstrated oleuropein's anti-inflammatory action via reduced pro-inflammatory cytokine levels [177,178]. In addition, oleuropein treatment effectively mitigated the adverse effects of inflammation in obese mice. Specifically, the treatment led to higher PPARγ levels in fat and the liver, and lower JNK-1 levels in the liver [179].

3.2.4. The Beneficial Role of Resveratrol and Quercetin to Counteract Inflammation

Recent research indicates RV and quercetin, at varying doses, decrease inflammation by impacting SFRP4, a protein involved in obesity, diabetes, and pancreatic inflammation,

thus highlighting a connection between obesity-driven inflammation and dysfunctional insulin response. Resveratrol and quercetin's potent antioxidant and anti-inflammatory effects suggest their potential as pancreatic oxidative stress drug candidates [180].

Extensive research supports the growing potential of natural compounds like resveratrol and quercetin to treat inflammation; these compounds reduced weight gain, dyslipidemia, and inflammation in a study of obese rats. Reduced body weight gain, adipocyte size, and adipose tissue mass, as well as improved serum dyslipidemia, are linked to the anti-obesity effects of quercetin and resveratrol. A quercetin and resveratrol blend's obesity-reducing effects are linked to its anti-inflammatory properties; it decreases adipokine secretion, activates AMPKα1/SIRT1 signaling, and thus may reduce HFD-induced obesity and inflammation [181].

Further evidence supports quercetin's neuroprotective effects, potentially by promoting microglia/macrophage M2 polarization via the PI3K/Akt/NF-κB pathway. These results suggest quercetin may be a useful treatment for ischemic stroke [182].

Cardiac hypertrophy in mice was induced by implanting Ang II osmotic pumps. Researchers investigated primary neonatal rat cardiomyocytes and heart tissues to understand resveratrol's mechanism in preventing Ang II-induced cardiac hypertrophy. This research reveals important new mechanisms by which resveratrol protects against Ang II-induced cardiac hypertrophy, specifically by blocking NF-κB signaling and pro-inflammatory cytokines. The findings add to the evidence that REV may be a promising drug for treating cardiac hypertrophy and heart failure [183].

3.2.5. Preliminary Evidence of Anti-Inflammatory Activity of Ferutinin

Antioxidant, anti-inflammatory, and anticancer effects of bioactive compounds from plants and herbs were demonstrated *in vitro* and *in vivo*.

Reducing oxidative stress lowers the risk of developing various diseases, including cancer and chronic inflammatory diseases. The antioxidant activity of flavonoids, phenolic acids, stilbenes, tannins, and lignans (phenolic plants) is demonstrated *in vivo* and *in vitro*: the presence of hydroxyl groups on their aromatic rings is responsible for reducing oxidative stress, with antioxidant capacity increasing with the number of these groups. Specifically, bergamot flavonoids have demonstrated pleiotropic effects, reducing oxidative stress and inflammation at the cellular and tissue levels. Moreover, *in vitro* data suggests antioxidant activity in monoterpenes, sesquiterpenes, and diterpenes, bioactive compounds extracted from various plants and fruits. In fact, sesquiterpenes show significant anticancer, anti-inflammatory, and bactericidal effects, suggesting an important role in human diseases. Different experiments suggest that sesquiterpenes offer protection in low doses, while high doses cause severe toxicity; the bipolar effect is a dose-dependent increase in the permeability of lipid bilayers and mitochondrial membranes to cations—particularly divalent cations like calcium—caused by sesquiterpenes, which are important in various pathophysiological processes [137]. Furthermore, ferutinin demonstrates anti-inflammatory effects by reducing oxidative stress. The anti-inflammatory effects of ferutinin were evaluated using an edema model. Specifically, the reduction in inflammation during the early stages was significant, likely due to histamine and serotonin. Notably, at this stage, ferutinin demonstrated a significantly more potent anti-inflammatory effect compared to the aspirin control dose. This study implies ferutinin's anti-inflammatory action likely results from blocking histamine and/or serotonin activity [184]; however, further studies are needed to better explain the pathway under these mechanisms.

4. Cell Cycle Regulation: Key Mechanisms and Links to Tumorigenesis

A misregulation in cell cycle regulation can promote the development of diseases, including cancer. The cell cycle is controlled by molecular mechanisms involving distinct CDK-cyclin complexes, arising from the interplay between cyclin-dependent kinases (CDKs) and cyclins [185], and through three checkpoints: (i) G1 checkpoint, (ii) G2 checkpoint, and (iii) M checkpoint, also known as spindle assembly checkpoint (SAC). The G1 checkpoint's activity is determined by growth factors, capable of both promoting and suppressing cell growth, thus monitoring the transition between the G1 phase and the S phase. The regulation of the G1 checkpoint hinges on the crucial roles played by CDKs and tumor suppressor proteins, notably p53 and pRb. If a cell identifies damage or irregularities, it activates DNA repair; if this fails, apoptosis is triggered.

The tumor suppressor p53 controls cell metabolism, redox balance, and DNA repair, inducing cell cycle arrest and cell death. Cell cycle arrest results from p53 binding to upstream promoter regions of the p21 gene, leading to its transcriptional activation; in particular, p21 protein inhibits cyclin E/Cdk2 and cyclin D/Cdk4/6 complexes, resulting in cell cycle arrest in the G1 phase [186]. Findings suggest that zinc finger protein 57 (ZFP57), a key regulator of BRCA1 expression in ovarian cancer, might impact the G1 cell cycle checkpoint [187]. The silencing of CEP192, a novel gene involved in the development of NAFLD and HCC, has been recently shown to cause cell cycle arrest in the G0/G1 phase of cancer cells, thereby decreasing their proliferation and self-renewal. These results reveal the onco-immunological involvement of CEP192 in the establishment of a TME [188]. The cell uses the G2 checkpoint to confirm successful DNA replication before beginning mitosis. Its regulation involves a complex network including CDKs and checkpoint kinases (Chk1 and Chk2), along with other proteins and signaling pathways. Overexpression of polo-like kinase 1 (PLK1), a crucial mitotic checkpoint protein for cell cycle progression, is associated with unfavorable prognoses in some cancers (e.g., pancreatic adenocarcinoma) [189]. The M checkpoint monitors kinetochore–microtubule binding during mitosis; its regulation involves Mad, Bub proteins, CDKs, and other signaling pathways [190]. The regulation of all cell cycle phases, including G1/S and G2/M transitions, by the PTEN oncosuppressor gene is crucial for cell proliferation and survival. Furthermore, it plays a role in preserving chromosome structure, safeguarding the genome against structural and numerical chromosomal instability (CIN). CDKs, specifically A, B, D, and E, are key to the molecular mechanisms governing cell cycle control. Cyclins, each produced and degraded at specific cell cycle stages, bind to particular CDKs, forming active complexes essential for each phase and their activity is positively modulated by cyclins and inhibited by CDK inhibitors (CKIs). Transcriptional and post-translational modifications, along with the ubiquitin-proteasome system's rapid degradation of cyclins and CKIs, control the activation state. Dysregulation of cyclin expression and activity, and mutations or changes in the genes that regulate checkpoints, can lead to uncontrolled cell division and contribute to cancer development [191].

4.1. Mechanistic Insights into Cell Cycle Alterations in Cancer Development

Cell cycle dysregulation arises from multiple pathways: checkpoint failures, spindle checkpoint defects, CDK/cyclin mutations, abnormal cyclin D and E levels, and telomerase-driven immortality. The initial step in tumor formation is cell immortalization, or the evasion of senescence; the immortalization is related to the activity of enzyme telomerase, which increases telomere length at the ends of chromosomes [192]. Common alterations in the cell cycle include elevated levels of CDK4/6 and CDK2, both vital kinases in the G1 to S phase progression. Phosphorylated Rb underlies these alterations, leading to E2F release and activation of genes essential for cell cycle's S phase initiation. Overactive complexes

correlate with boosted cancer cell growth, aging, migration, and blood vessel formation, alongside apoptosis resistance and therapy resistance (like against CDK inhibitors) in cancers such as breast and ovarian cancers [193]. Genes regulating cell cycle checkpoints, including p53 and FRP1, also show mutations or deletions in cancer cells. The lack of p53 crucially affects cell cycle checkpoint regulators, leading to the increased expression of genes such as p21 (a growth inhibitor) and pro-apoptotic genes, mainly after DNA damage halts the cell cycle at G1 [186]. Uncontrolled cell cycle progression may result from the loss of oncosuppressor genes, including Rb1, p16INK4A, p15INK4B, and p14ARF. Furthermore, mutations in p16, Rb loss, or increased CDK2 activity can lessen the effectiveness of CDK4/6 inhibitors (e.g., palbociclib, ribociclib, abemaciclib). This has prompted the development of combination, or second-generation, strategies to overcome therapeutic resistance [193]. The link between checkpoint failure and cancerous phenotypes in normal cells is established; however, the specific genetic alterations responsible are still unknown. Furthermore, the direct causal link between checkpoint malfunction and cell transformation, versus the involvement of other regulatory genes after immortalization, requires further investigation. In cancer treatment, genes involved in checkpoints may be useful as diagnostic tools and as targets for new drugs [194].

4.2. Nutraceutical-Induced Cell Cycle Modulation in Cancer and Chemotherapy—Induced Cytotoxicity

The effects of natural compounds on inhibiting tumor cell proliferation by modulating specific cell cycle checkpoints and interfering with mitotic progression have been shown; their effects on cell cycle regulation are reported in Table 3. This suggests both their potential use as coadjuvants in the treatment of some types of cancer, and as a treatment to reduce the toxic effects induced by chemotherapeutic drugs in non-cancerous cells [195] (Figure 3).

Table 3. Effects of Natural Compounds on Cell Cycle Regulation.

Natural Compound/Plant	Cell Cycle Phase	Molecular Mechanism	Cell Type	References
Citrus bergamia	G1/S	Silent mating type information regulation 2 homolog 2 (SIRT2)/Akt/p53 ↑ apoptosis	THP-1, SH-SY5Y	[196–198]
Cynaropicrin	G2/M	↓ Pyruvate kinase M2 (PKM2)/PARP	CAL-62, 8505C, SW1736, A549	[199,200]
Oleuropein	G1/S	↑ p21, p53, CKIs	MCF-7, MDA-MB-231, MDA-MB-468	[201–203]
Resveratrol	S	↑ p53/p21/p27/Bax/p53 upregulated modulator of apoptosis (PUMA) ↓ cyclins D/E ↓ cyclin-dependent kinase 2, 4, 6 (CDK2/4/6)	C-3, LNCaP, A431, T47D	[204–208]
Quercetin	G1/G2/M	↑ p21/p27 ↓ CDK2/6, cyclins A/E/D ↓ Rb phosphorylation	HOS, OSCC, T47D, A375, p39, YD10B, YD38, OSCC, KON	[209–212]
Ferutinin	↓ G1 and restoring cell cycle	↑ apoptosis ↑ protective effect	H9c2	[138,140,213]

The arrows indicate decrease (↓) and increase (↑), respectively. SIRT2: silent mating type information regulation 2 homolog 2; PKM2: pyruvate kinase M2; PARP: poly-ADP-ribose-polymerase; p53: tumor protein p53; CKIs: CDK inhibitors; Bax: BCL2 associated X, apoptosis regulator; PUMA: p53 upregulated modulator of apoptosis; CDK: cyclin-dependent kinase; Rb: retinoblastoma protein.

The anti-proliferative effects of *Citrus bergamia* natural derivatives on different cancer cell types were evaluated through cell cycle arrest in multiple *in vitro* studies [143]. Human leukemia THP-1 cells treated with Flavonoid-Rich Extract (FRE) of BJ showed cell cycle arrest in the S phase, leading to apoptosis through the SIRT2/AKT/p53 pathway [196];

in addition, *Citrus bergamia* juice decreased human neuroblastoma SH-SY5Y cell growth *in vitro* via G1 cell cycle arrest and reduced cell adhesion [197]. Animal studies showed that FRE of BJ decreased levels of baculoviral inhibitor of apoptosis repeat-containing 5 (Birc5) and the cell cycle regulator p21, potentially increasing tumor cell death [198].

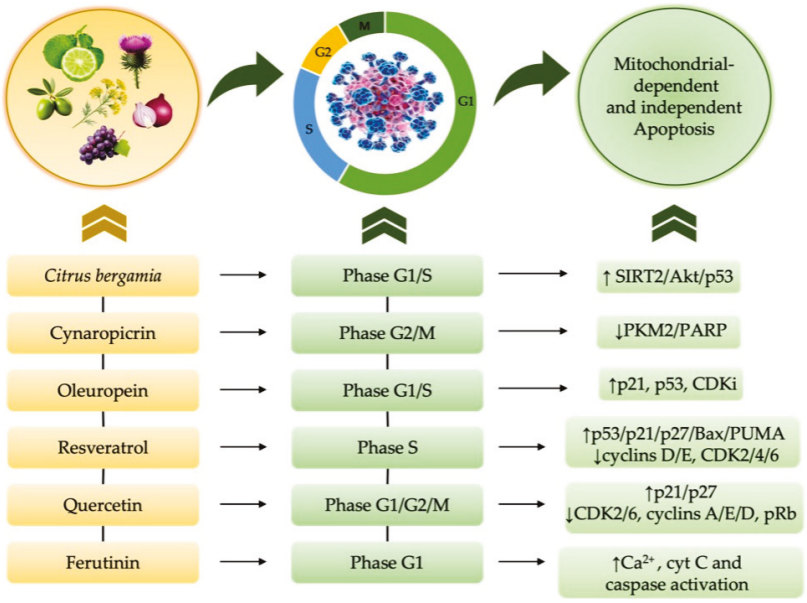

Figure 3. The anti-proliferative effects of natural extract derivatives on different cancer cell types were evaluated through cell cycle arrest in multiple *in vitro* studies. *Citrus bergamia* has been shown to possess an antiproliferative effect by arresting the cell cycle in the G1/S phase through the modulation of the SIRT2/Akt/p53 pathway. Cynaropicrin arrested the cell cycle in the G2/M phase by modulating the PKM2/PARP pathway. Oleuropein exerts an antiproliferative effect by arresting the cell cycle in the G1/S phase by increasing p21/p53/CDKi. RV treatment arrested the cell cycle in the S phase by modulating p53/p21/p27/Bax/PUMA and the reduction in cyclins D/E and CDK 2/4/6. Treatment with quercetin causes cell cycle arrest in G1/G2/M phases with the modulation of p21/p27 and reduction in CDK 2/6 and cyclins A/E/D and phosphorylation of Rb. Ferutinin treatment has been shown to exsert an antiproliferative effect leading to cell cycle arrest in the G1 phase by increasing intracytoplasmic Ca 2+ concentration, inducing cyt C release and caspases activation. The arrows indicate decrease (↓) and increase (↑), respectively. Silent mating type information regulation 2 homolog 2 (SIRT2); protein kinase B (Akt); tumor protein p53 (p53); Cynaropicrin (Cyn); Pyruvate kinase M2 (PKM2); poly-ADP-ribose-polymerase (PARP); tumor protein p21/p53; Cyclin-dependent kinase inhibitor (CDKi); Resveratrol (RV); p53/p21/p27; BCL2 associated X, apoptosis regulator (Bax); p53 upregulated modulator of apoptosis (PUMA); Cyclin-dependent kinases (CDK 2/4/6); Cytochrome C (Cyt C).

Other evidence highlighted that cynaropicrin could inhibit cellular growth by cell cycle arrest, mainly in the G2/M phase, in thyroid cancer cell lines CAL-62, 8505C, and SW1736 cells, by a dose- and time-dependent way [199]. This also demonstrates PKM2 inhibition in A549 cells, causing increased p53, decreased DNA repair enzyme PARP, with a subsequent cell cycle arrest [200].

Oleuropein significantly modulates the cell cycle, notably by upregulating CDK inhibitor levels, thus causing cell cycle arrest, and by increasing p53 and p21 levels, which then affects gene expression to activate both intrinsic and extrinsic apoptosis pathways [201]. *In vitro* investigations using MCF-7 and MDA-MB-231 BC cells revealed that oleuropein treatment induced cell cycle arrest at the G1 and S phases [202]; its effects on MDA-MB-231 and MDA-MB-468 BC cell lines include cell proliferation inhibition, apoptosis induction through S-phase arrest, and caspase-1, -4, and -14 expression [203].

Several *in vitro* studies [209] indicate quercetin's role in modulating the cell cycle. Myeloid cell line p39 and osteosarcoma cells HOS showed increased G1 cell cycle arrest after treatment, accompanied by decreased CDK-2, -6, cyclins A, D, E, Rb phosphorylation, and increased p21 and p27 expression [210]. Furthermore, quercetin triggered G1 cell cycle arrest in oral squamous cell carcinoma cell lines YD10B and YD38 OSCC [211].

It has been suggested that quercetin treatment leads to G2/M cell cycle arrest in T47D and KON BC cells and A375 melanoma cells [212].

Moreover, RV's *in vitro* effects included enhanced G1 to S phase transition, S phase cell cycle arrest, and reduced cancer cell proliferation and viability. Prostate cancer cells (LNCaP and PC-3) treated with RV showed reduced expression of cyclins D1 and E, CDK4, and cyclin D1/CDK4 kinase activity [204]. RV's ability to decrease A431 and colon cancer cell proliferation has been linked to lower levels of cyclins D1/D2/E2, CDK2/4/6, and higher levels of p21 and p27 [205]. RV was found to activate p53 along with its target genes p21, p27, Bax, PUMA, MDM2, and cyclin G [206]. Therefore, RV may stimulate the G1-to-S phase transition in BC cells, subsequently halting their progression through the S phase, thus diminishing their proliferation and viability [207]. In addition, it has been reported that RV reduces *Versican* (VCAN) secretion by CAFs, presumably by modulating the cell cycle [208].

Exposure to ferutinin leads to a decreased G1 phase and increased cell death, modifying the cell cycle profile [140]. In addition, it was shown that ferutinin, thanks to its cell-type dependent activity, restores the cell cycle in H9c2 myoblasts incubated with Dox [138], suggesting its protective role in cell cycle progression, highlighting its potential as a therapeutic agent in cancer treatment and in mitigating chemotherapy-induced cardiac damage (CIC) (Figure 4) [213].

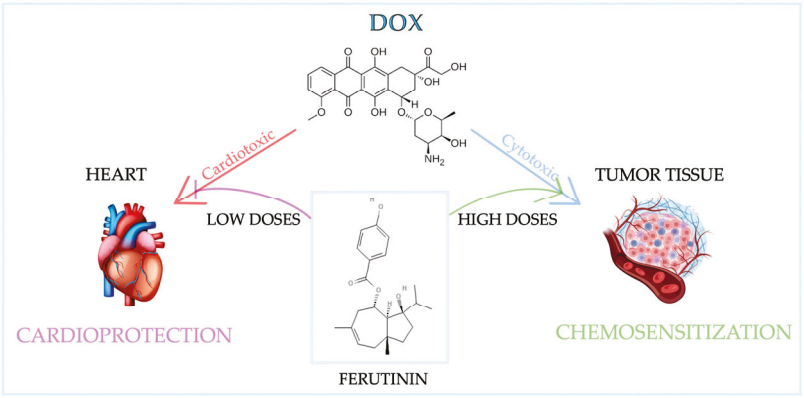

Figure 4. The tissue-dependent and dose-dependent effect of ferutinin. At low doses, ferutinin ca counteract the cardiotoxic effect of Dox. At high doses, ferutinin can enhance Dox chemosensitization in tumor tissues. Doxorubicin (Dox).

5. The Human Microbial Landscape in Cancer Development

The human microbiota comprises approximately 300 bacterial, fungal, and viral species, totaling almost 40 trillion microorganisms [214,215]. Over 97% of the human microbiota is located in the gastrointestinal tract, mainly the colon, and is known as the gut microbiota. In addition, current findings demonstrate a diverse microbiome within previously considered sterile tumor tissues (lung, breast, liver), which is closely associated with oncogenesis [216,217]. Consequently, the intratumoral microbiota (ITM) concept emerged and ITM's anti- and pro-tumorigenic effects have been demonstrated through mechanistic studies [218]. Tumor-inhibiting metabolites are produced by T and NK cells activated by the ITM. These may raise oxidative stress, causing genomic instability and mutations, affecting epigenetics, weakening immunity, and stimulating inflammation, thus, leading to

tumor initiation and progression [219], representing an integral part of TME [218]. Tumors in mucosal organs, including the colon, cervix, esophagus, and lung, are colonized by the ITM [220].

Non-mucosal organs such as the pancreas, liver, breast, and prostate also contained ITM, which suggests the existence of both adjacent tissue invasion and hematogenous spread during colonization [218]. This supports the hypothesis that TME colonization by the ITM may result from malformed blood vessels [217]. Tumor subtype differences in intratumoral microbial composition have been demonstrated [221]. Tumors can arise from viral infections and persistent bacterial inflammation, such as that caused by *H. pylori* and gastritis.

Evidence on the colon cancer microbiota has shown the presence of bacteria *Bacteroides fragilis*, *Escherichia coli* (*E. coli*), and *Fusobacterium nucleatum*—frequently detected in malignant pancreatic and BC—and fungal species such as *Candida albicans* [219]. The species of *Blastomyces* are prevalent in lung cancers, while the species of *Malassezia* are abundant within BC [216]. TME regulation originates from both the tumor and gut microbiota, impacting immune responses and cancer cell metabolism; consequently, this crosstalk between intratumoral and gut microbiota might elicit specific immune reactions [222]. Metagenomics, using next-generation sequencing (NGS) and computational analysis of 16S rRNA amplicons, has enabled the characterization of gut microbiota diversity and abundance [223,224]. *Firmicutes* and *Bacteroidetes* are the most prevalent phyla among the roughly 1000 bacterial species in the gut microbiota. The gut's microbiome plays a critical role in numerous physiological processes, including vitamin production, the metabolism of food components, protection from pathogens, and the shaping of the host's immune system [225]. The pharmacomicrobiomic concept has established the gut microbiota's role in influencing drug effects, such as chemotherapy. In fact, the gut's microbes can alter drug metabolism, impacting their absorption, effectiveness, or safety [226]. Dysbiosis, an imbalance of gut microbiota, is linked to cardiovascular, metabolic, and neurodegenerative diseases, as well as cancer [227]. Studies of the gut microbiome via metabolomics and metagenomics show its dual impact on cancer prevention, onset, and therapy, having both suppressing and oncogenic activity [228]. Several studies indicate that communication between colorectal cells and gut bacteria is vital for the body's overall health and immune response, especially in metabolism. The influence of gut microbiota on cancer initiation, progression, and metastasis, as well as its potential in cancer treatment, is a promising area in precision medicine [229].

Emerging Connections and Therapeutic Perspectives of Gut Microbiota and Nutraceuticals in Cancer

An interplay between the gut microbiota, diet-induced inflammation, and cancer pathogenesis has been found. In fact, an altered microbiota associated with chronic inflammation in colon, pancreatic, breast, gastric, liver, and prostate cancer, has been identified. Consequently, investigations on nutraceutical compounds potentially able to modulate the microbiota, with implications on cancer pathogenesis, are crucial. A correlation between diet and healthy gut microbiota has been demonstrated, highlighting the implication of dietary natural compounds in affecting cancer through the gut microbiota [230]; thus, this relationship between diet and cancer through the gut microbiota may provide new insights for cancer treatment [231] (Figure 5). Specifically, metabolic changes like obesity are linked to persistent low-level inflammation, a connection between obesity and cancer supported by many studies. The increasing prevalence of excessive fat dietary intake is linked to the adoption of HFD in many countries, with a lack of fiber intake [232]. In comparison to traditional rural populations, HFD populations showed reduced bacterial diversity [233]. HFDs impact gut microbiota to produce more leucine, subsequently activating the mam-

malian target of rapamycin complex 1 (mTORC1) in bone marrow, leading to increased polymorphonuclear myeloid-derived suppressor cells (PMN-MDSC) differentiation and faster BC growth through the gut–bone marrow–tumor axis.

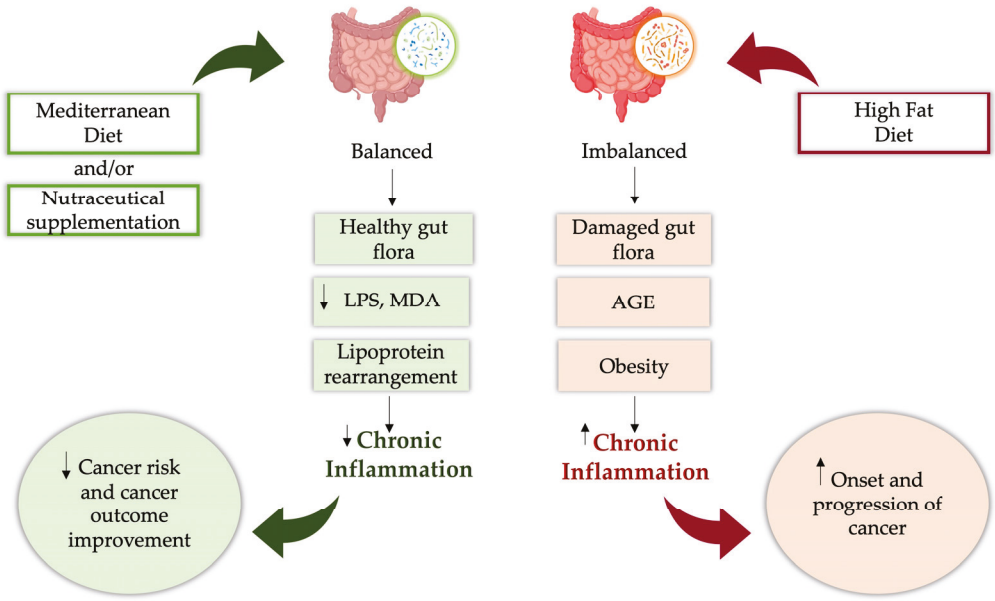

Figure 5. Mediterranean-style dietary model and/or nutraceutical supplementation are directly related to health gut microbiota. The MedDiet, rich in fiber and natural compounds such as polyphenols, supports a balanced microbiota, reduces inflammation, LPS and MDA levels, promotes lipoprotein rearrangement, and contributes to reduction in cancer risk and cancer outcome improvement. Controversially an HFD alters the composition of the microbiota, promoting AGEs production, with increased chronic inflammatory state—associated with obesity, and activating the gut–bone marrow–tumor axis, resulting in increased onset and progression of cancer. The arrows indicate decrease (↓) and increase (↑), respectively. Mediterranean Diet (MedDiet); lipopolysaccharide (LPS); malondialdehyde (MDA); high fat diet (HFD); advanced glycation end product (AGE).

Evidence indicates a positive correlation between good adherence to the MedDiet and the health of the gut microbiota and could potentially represent an important pattern in reducing the incidence of a range of diseases, including cancer [234]. Several natural compounds hold promise as gut microbiota modifiers and cancer prevention/treatment aids. Notably, many dietary polyphenols can beneficially alter the gut microbiota and directly act as antioxidants, synergistically enhancing probiotic effects [235]. Polyphenols such as RV and quercetin boost intestinal health by modulating Nrf2 and NF-κB, thus improving barrier function, repairing the gut lining, reducing inflammation, and regulating immunity. RV and quercetin modulate intestinal tight junction protein expression and distribution, thus raising trans-epithelial electrical resistance (TEER), according to reports. Therefore, they beneficially impact the gut barrier, helping to manage numerous diseases stemming from gut barrier dysfunction [236]. In diet-induced obese mice, oleuropein's protection of metabolism and vasculature is linked to its immunomodulatory effects and improved gut barrier function by reducing dysbiosis [179]. A recent *in vivo* study highlighted that a bergamot polyphenol extract (BPE) with micronized albedo and pulp fibers (BMF) helps maintain gut microbiota health in animals fed an HFD. A four-week trial using a 50/50% BPE/BMF mixture in rats fed a HFD resulted in significantly better metabolic profiles and lower gut LPS levels, which are vital in cancer development [237,238], reducing MDA levels and leading lipoprotein size re-arrangement. This effect is related to improvements in gut microbiota composition, particularly through the modulation of the Gram-negative bacteria *Proteobacteria* and the dominant phyla *Firmicutes* and *Bacteroidetes* [110]. The find-

ings suggest that the interaction between nutraceuticals, microbiota, and cancer is a highly promising field of research, and could offer new strategies for prevention and therapeutic support in oncology. Indeed, a complex interplay of various cell types with diverse metabolic states and shared metabolites creates the TME. The complex cellular structure produces a profile of available nutrients and reactive metabolites, including advanced glycation end-products. The literature analysis reveals that the receptor for advanced glycation end products (RAGE) and its ligands link energy metabolism (often disrupted by mitochondrial dysfunction) to immune responses (shaped by local microbiota), impacting tumor development. Investigating metabolic processes in cancer and immune cells reveals novel therapeutic strategies, potentially broadening immunotherapy's reach and effectiveness. Targeting the RAGE and its ligands in immunotherapy shows promise for treating CRC, according to the literature review [239].

6. Limitations of Nutraceutical Supplementation: Current Challenges and Emerging Evidence-Based Strategies

Although nutraceuticals offer proven benefits, their widespread use in clinical practice is hindered by considerable limitations. Factors such as the poor bioavailability of active compounds, inconsistent dose-response, and insufficient clinical trial data hinder progress [240]. In addition, responses vary considerably between individuals due to genetic, gut microbiome, dietary, age-related, and health factors, complicating the determination of ideal dosages [241–243]. While exhibiting significant *in vitro* potential, the bioavailability of polyphenols (frequently researched for nutraceutical purposes) is low due to digestive breakdown and limited absorption in the upper gut. Primarily, only a small percentage of low molecular weight polyphenols (like glycosylated flavonoids) are absorbed in the upper small intestine, mainly the duodenum and jejunum. Most complex polyphenols bypass absorption until reaching the colon, undergoing microbial biotransformation into absorbable simpler metabolites (e.g., phenolic acids) [244]. In addition, a recent study demonstrated that innovative natural formulations significantly increased plasma metabolite levels in treated animals, overcoming the poor bioavailability of polyphenols and maximizing their beneficial effects [46]. Nutraceutical safety and efficacy, and their contribution to health, will improve if "bed-to-bench" issues are addressed.

7. Conclusions

This review summarizes results and evidence showing that Mediterranean nutraceuticals hold promise in cancer prevention and treatment. The antioxidant, anti-inflammatory, and pro-apoptotic properties of Mediterranean nutraceuticals, such as polyphenols and phytochemicals from *Citrus bergamia* Risso & Poiteau, *Cynara cardunculus*, *Olea europea* L., quercetin, resveratrol, and *Ferula communis* L., are promising as complementary treatments against cancer, providing a solid basis for considering them as effective adjuvants in conventional cancer therapies. Crucially, many nutraceuticals demonstrate dual dose-dependent effects; low concentrations act as antioxidants, and high concentrations induce selective cancer cell death via oxidative stress. This two-stage process holds significant promise for preventing and enhancing the effectiveness of cancer treatment: better outcomes and reduced side effects, particularly cardiotoxicity, may result from using them with standard cancer treatments. Furthermore, the interaction of natural compounds with the main molecular pathways involved in chronic inflammation (e.g., NF-κB, STAT3, PI3K/Akt) and oxidative stress (e.g., Nrf2/KEAP1, AMPK/SIRT1) highlights their potential in remodeling the TME. The active control of metastasis and chronic inflammation is suggested by the ability to adjust macrophage polarization, cytokine production, and the innate immune response. Developing validated anticancer therapies critically depends on integrating

nutraceuticals, oncology, and pharmacology to optimize drug mechanisms, combinations, nutraceutical dosages (BPF, cynaropicrin, quercetin, RV, and ferutinin), and therapeutic translation. Despite this, natural compounds are not intended to replace conventional cancer treatments like chemotherapy, but rather to enhance them in a personalized approach for each patient. Low bioavailability, lack of extensive clinical trials, and inconsistent patient responses are delaying the clinical translation of these results. The efficacy of nutraceuticals in oncology requires confirmation through rigorous randomized controlled trials to implement positive preclinical results into proven therapeutic applications. Further *in vitro* and *in vivo* studies are needed to optimize bioavailability (e.g., formulation with nanocarriers), characterize pharmacokinetics, determine optimal dosages, and evaluate long-term safety. In closing, the emerging concept of onconutraceuticals represents an integrated paradigm that combines prevention, therapeutic support, and personalized medicine. In this context, the "Mediterranean" approach could offer a sustainable and evidence-based dietary-pharmacological model, useful not only for the management of neoplastic disease but also for the promotion of global health.

Author Contributions: Conceptualization, V.M., R.M. and C.A.; writing—original draft, C.A., R.M. and M.S.; writing—review and editing, G.R., S.U., C.A. and J.M.; Tables and graphs, G.R., S.U. and C.A.; supervision, V.M., C.M. and E.P.; funding acquisition, V.M. and C.M. All authors have read and agreed to the published version of the manuscript.

Funding: This work was supported by PON-MIUR 03PE000_78_1, PON-MIUR 03PE000_78_2, and PRIR Calabria Asse 1/Azione 1.5.1/FESR (Progetto AgrInfra Calabria), SAP01-2023-000077—Bando A Cascata Rome Technopole Spoke 1 e Spoke 6-PRODIGI (CUP B83C22002820006).

Conflicts of Interest: The authors declare that the research was conducted in the absence of any commercial or financial relationships that could be construed as potential conflicts of interest.

Abbreviations

8-oxodG	8-oxo-2′-deoxyguanosine
8-OHdG	8-hydroxy-2′-deoxyguanosine
3-NT	3-nitrotyrosine
AGEs	advanced glycation end products
Akt	protein kinase B
AMPK	AMP-activated protein kinase
APAF1	apoptotic protease-activating factor 1
ARE	antioxidant response element
ATM	ataxia-telangiectasia mutated
ATP	Adenosine Triphosphate
BAD	BCL2 associated agonist of cell death
BAT	brown adipose tissue
Bax	BCL2 Associated X, Apoptosis Regulator
BC	breast cancer
BCL2L11	B-cell lymphoma 2 (Bcl-2)-like protein 11
BEO	bergamot essential oil
Birc5	Baculoviral Inhibitor of Apoptosis Repeat-containing 5
BMF	albedo and pulp-derived micronized fibers
BJ	bergamot juice
BPE	bergamot polyphenol extract
BPF	bergamot polyphenolic fraction
BRAF	B-Raf proto-oncogene serine/threonine kinase
c-Met	mesenchymal–epithelial transition factor
c-myc	cellular myelocytomatosis oncogene

CAFs	cancer-associated fibroblasts
CAT	catalase
CDK	cyclin-dependent kinase
CDKs	cyclin-dependent kinases
Chk1	checkpoint kinases 1
Chk2	checkpoint kinases 2
CIC	chemotherapy-induced cardiac damage
CIN	chromosomal instability
CKIs	CDK inhibitors
CLRs	C-type lectin receptors
COX-1	cyclooxygenases 1
COX-2	cyclooxygenases 2
CRC	colorectal carcinoma
CRP	C reactive protein
CSCs	cancer stem cells
CVD	cardiovascular disease
Cyn	cynaropicrin
Cyt C	cytochrome C
Daun	daunorubicin
DCs	dendritic cells
DISCs	death-inducing signaling complexes
DM	diabetes mellitus
DNA	DeoxyriboNucleic Acid
DNMTs	DNA methyltransferases
DSBs	double-strand breaks
Dox	doxorubicin
E. coli	Escherichia coli
EC	endometrial cancer
ECM	extracellular matrix
ECs	endothelial cells
eCSCs	endogenous cardiac stem cells
EFSA	The European Food Safety Authority
EGFR	epidermal growth factor receptor
EMT	Epithelial–Mesenchymal Transition
eNOS	endothelial nitric oxide synthase
ER	endoplasmic reticulum
ERK	extracellular signal-regulated kinase
ERK1/2	extracellular signal-regulated kinase ½
ERα	Estrogen receptor alpha
ERβ	Estrogen receptor beta
EVOO	extra virgin olive oil
FADD	Fas-Associated Death Domain Protein
FOXO	Forkhead box transcription factors
FOXO3a	Forkhead Transcription Factor O Subfamily Member 3a
FRE	Flavonoid-Rich Extract
GCL	glutamate-cysteine ligase
GGT	gamma-glutamyl transferase
GPX	glutathione peroxidase
GRX	glutathione reductase
GSH-PX	Glutathione Peroxidase
GSH	glutathione
GSK-3β	glycogen synthase kinase 3 beta
GST	glutathione transferase
GSTs	glutathione S-transferases

H. pylori	Helicobacter pylori
H_2O_2	Hydrogen Peroxide
H9c2	rat embryonic cardiac myoblast
HBV	Hepatitis B Virus
HCC	hepatocellular carcinoma
HCV	Hepatitis C virus
HDACs	histone deacetylases
HDL	high density lipoprotein
HFD	high-fat diets
HIF1-α	hypoxia-inducible factor 1-alpha
HLD	hyperlipidemic diet
HMOX-1	heme oxygenase
HO-1	heme oxygenase-1
HOCl	hypochlorous acid
HPV	Human Papillomavirus
HRAS	Harvey Rat sarcoma virus
HRT	hormone therapy
HUVECs	Human Umbilical Vein Endothelial Cells
I/R	ischemia–reperfusion
IARC	International Agency for Research on Cancer
ICAM-1	intercellular adhesion molecule 1
ICAM-2	intercellular adhesion molecule 2
IFN-γ	interferon-gamma
IL-10	Interleukin-10
IL-10R2	Interleukin-10 Receptor Subunit 2
IL-12	Interleukin-12
IL-13	interleukin-13
IL-1R	interleukin-1 receptor
IL-1α	Interleukin-1 alpha
IL-1β	Interleukin-1 beta
IL-22R1	Interleukin-22 Receptor Subunit 1
IL-23	interleukin-23
IL-4	interleukin-4
IL-6	interleukin-6
IL-6R	interleukin-6 receptor
IL-8	interleukin-8
iNOs	Inducible nitric oxide synthase
ITM	intratumoral microbiota
JAK-STAT	Janus kinase (JAK)/signal transducer and activator of transcription (STAT)
JAK1/TYK2	Janus kinase 1 and Tyrosine kinase 2
JNK-1	c-Jun N-terminal kinase 1
JNK	c-Jun amino-terminal kinase
KEAP1	Kelch-like ECH-associated protein 1
KRAS	Kirsten rat sarcoma viral oncogene homolog
LDL	low density lipoprotein
LOX-1	Lectin-like oxidized low-density lipoprotein receptor-1
LOX	lipoxygenase
LPS	lipopolysaccharide
LTB4	leukotriene B4
MAPK	Mitogen-Activated Protein Kinase
MDA	Malondialdehyde
MDSCs	myeloid-derived suppressor cells
MedDiet	Mediterranean Diet
MIP-2	Macrophage-inflammatory protein 2

MKP-1	Mitogen-activated protein kinase phosphatase 1
MOMP	mitochondrial outer membrane permeabilization
MS	metabolic syndrome
mTOR	mammalian target of rapamycin
mTORC1	mammalian target of rapamycin complex 1
MUFAs	monounsaturated fatty acids
NADPH	nicotinamide adenine dinucleotide phosphate
NAFLD	Non-alcoholic fatty liver disease
NF-κβ	Nuclear factor kappa-light-chain-enhancer of activated B cells
NGS	next-generation sequencing
NK	natural killer
NLRs	NOD-like receptors
NOTCH	Notch signaling pathway
NQO1	NAD(P)H quinone oxidoreductase 1
NRAS	Neuroblastoma RAS viral oncogene homolog
Nrf2	nuclear erythroid 2-related factor
O_2^-	superoxide anion
O_2	dioxygen
OMWW	Olive Mill Wastewater
OxLDL	oxidized low-density lipoprotein
P53	tumor protein p53
PAF	platelet-activating factor
PAMPs	pathogen-associated molecular patterns
PARP-1	poly (ADP-ribose) polymerase-1.
PARP	poly-ADP-ribose-polymerase
PC	pancreatic cancer
PI3K	phosphatidylinositol 3-kinase
PKB	protein-kinase B
PKC	protein kinase C
PKD1	Polycystin 1, Transient Receptor Potential Channel Interacting
PKM2	Pyruvate kinase M2
PLA2	phospholipase A2
PLK1	polo-like kinase 1
PMN-MDSC	polymorphonuclear myeloid-derived suppressor cells
PPARγ	peroxisome proliferator-activated receptor-gamma
PRX	peroxiredoxin
PTEN	Phosphatase and tensin homolog
PTMs	post-translational modifications
PTP1B	Tyrosine-protein phosphatase non-receptor type 1
PTPs	Protein Tyrosine Phosphatases
PUFAs	polyunsaturated fatty acids
PUMA	p53 upregulated modulator of apoptosis
RAGE	Receptor for advanced glycation end products
RAS	Rat sarcoma virus
Rb	Retinoblastoma protein
Ref-1	Redox Effector Factor-1
RLRs	RIG-I-like receptors
RNS	Reactive nitrogen species
ROS	Reactive oxygen species
RV	Resveratrol
SAC	spindle assembly checkpoint
SERM	selective estrogen receptor modulator
SIRT1	silent mating type information regulation 2 homolog 1
SIRT2	Silent mating type information regulation 2 homolog 2

SFRP4	secreted frizzled-related protein 4
SOD	superoxide dismutase
STAT	Signal Transducer and Activator of Transcription
STAT3	Signal Transducer and Activator of Transcription 3
T2DM	type 2 diabetes mellitus
TAMs	tumor-associated macrophages
TEER	trans-epithelial electrical resistance
TFs	transcription factors
TGF-β	Transforming growth factor beta
Th2	helper T 2 cells
TLR	Toll-like receptor
TME	tumor microenvironment
TNF-α	Tumor Necrosis Factor Alpha
TNFR-1	tumor necrosis factor receptor 1
Topo II	topoisomerase II
TRAIL-R1/2	tumor necrosis factor-related apoptosis-inducing ligand receptors
Tregs	regulatory T-cells
TRX	thyroxine
TXNRD1	thioredoxin reductase-1
TxR	thioredoxin reductase
UV	Ultraviolet radiation
VEGF	Vascular Endothelial Growth Factor
VOO	virgin olive oil
WAT	white adipose tissue
WD SW	High-fat Western diet-fed
Wnt	Wingless-related integration site
XO	xanthine oxidase
ZEB1/2	Zinc finger E-box binding homeobox 1 and Zinc finger E-box binding homeobox 2
ZFP57	zinc finger protein 57

References

1. WHO. *Cancer*; World Health Organization: Geneva, Switzerland, 2024. Available online: https://www.who.int/news-room/fact-sheets/detail/cancer (accessed on 13 June 2025).
2. Hausman, D.M. What Is Cancer? *Perspect. Biol. Med.* **2019**, *62*, 778–784. [CrossRef] [PubMed]
3. Mumtaz, S.; Akhtar, N.; Ahmed, A.; Qazi, A.S. Dietary Pattern and Cancer. *Cancer Treat. Res.* **2024**, *191*, 191–216. [CrossRef] [PubMed]
4. Guasch-Ferré, M.; Willett, W.C. The Mediterranean diet and health: A comprehensive overview. *J. Intern. Med.* **2021**, *290*, 549–566. [CrossRef] [PubMed]
5. Barber, T.M.; Kabisch, S.; Pfeiffer, A.F.H.; Weickert, M.O. The Effects of the Mediterranean Diet on Health and Gut Microbiota. *Nutrients* **2023**, *15*, 2150. [CrossRef] [PubMed]
6. Hanahan, D. Hallmarks of Cancer: New Dimensions. *Cancer Discov.* **2022**, *12*, 31–46. [CrossRef] [PubMed]
7. Levatić, J.; Salvadores, M.; Fuster-Tormo, F.; Supek, F. Mutational signatures are markers of drug sensitivity of cancer cells. *Nat. Commun.* **2022**, *25*, 2926. [CrossRef] [PubMed]
8. Liu, Y.P.; Zheng, C.C.; Huang, Y.N.; He, M.L.; Xu, W.W.; Li, B. Molecular mechanisms of chemo- and radiotherapy resistance and the potential implications for cancer treatment. *MedComm* **2021**, *10*, 315–340. [CrossRef] [PubMed]
9. Cháirez-Ramírez, M.H.; de la Cruz-López, K.G.; García-Carrancá, A. Polyphenols as Antitumor Agents Targeting Key Players in Cancer-Driving Signaling Pathways. *Front. Pharmacol.* **2021**, *20*, 710304. [CrossRef] [PubMed]
10. Luo, H.; Xia, X.; Huang, L.B.; An, H.; Cao, M.; Kim, G.D.; Chen, H.N.; Zhang, W.H.; Shu, Y.; Kong, X.; et al. Pan-cancer single-cell analysis reveals the heterogeneity and plasticity of cancer-associated fibroblasts in the tumor microenvironment. *Nat. Commun.* **2022**, *4*, 6619. [CrossRef] [PubMed]
11. Musella, M.; Guarracino, A.; Manduca, N.; Galassi, C.; Ruggiero, E.; Potenza, A.; Maccafeo, E.; Manic, G.; Mattiello, L.; Soliman Abdel Rehim, S. Type I IFNs promote cancer cell stemness by triggering the epigenetic regulator KDM1B. *Nat. Immunol.* **2022**, *23*, 1379–1392. [CrossRef] [PubMed]

12. Fanelli, G.N.; Naccarato, A.G.; Scatena, C. Recent Advances in Cancer Plasticity: Cellular Mechanisms, Surveillance Strategies, and Therapeutic Optimization. *Front. Oncol.* **2020**, *22*, 569. [CrossRef] [PubMed]
13. Nyga, A.; Ganguli, S.; Matthews, H.K.; Baum, B. The role of RAS oncogenes in controlling epithelial mechanics. *Trends Cell Biol.* **2023**, *33*, 60–69. [CrossRef] [PubMed]
14. Lavoie, H.; Gagnon, J.; Therrien, M. ERK signalling: A master regulator of cell behaviour, life and fate. *Nat. Rev. Mol. Cell Biol.* **2020**, *21*, 607–632. [CrossRef] [PubMed]
15. Bahar, M.E.; Kim, H.J.; Kim, D.R. Targeting the RAS/RAF/MAPK pathway for cancer therapy: From mechanism to clinical studies. *Signal Transduct. Target. Ther.* **2023**, *18*, 455. [CrossRef] [PubMed]
16. Cordani, M.; Dando, I.; Ambrosini, G.; González-Menéndez, P. Signaling, cancer cell plasticity, and intratumor heterogeneity. *Cell Commun. Signal.* **2024**, *3*, 255. [CrossRef] [PubMed]
17. Jolly, M.K.; Somarelli, J.A.; Sheth, M.; Biddle, A.; Tripathi, S.C.; Armstrong, A.J.; Hanash, S.M.; Bapat, S.A.; Rangarajan, A.; Levine, H. Hybrid epithelial/mesenchymal phenotypes promote metastasis and therapy resistance across carcinomas. *Pharmacol. Ther.* **2019**, *194*, 161–184. [CrossRef] [PubMed]
18. Kang, A.R.; Kim, J.L.; Kim, Y.; Kang, S.; Oh, S.C.; Park, J.K. A novel RIP1-mediated canonical WNT signaling pathway that promotes colorectal cancer metastasis via β -catenin stabilization-induced EMT. *Cancer Gene Ther.* **2023**, *30*, 1403–1413. [CrossRef] [PubMed]
19. Vasaikar, S.V.; Deshmukh, A.P.; den Hollander, P.; Addanki, S.; Kuburich, N.A.; Kudaravalli, S.; Joseph, R.; Chang, J.T.; Soundararajan, R.; Mani, S.A. EMTome: A resource for pan-cancer analysis of epithelial-mesenchymal transition genes and signatures. *Br. J. Cancer* **2021**, *124*, 259–269. [CrossRef] [PubMed]
20. Hoxhaj, G.; Manning, B.D. The PI3K-AKT network at the interface of oncogenic signalling and cancer metabolism. *Nat. Rev. Cancer* **2020**, *20*, 74–88. [CrossRef] [PubMed]
21. Tan, Y.; Li, J.; Zhao, G.; Huang, K.C.; Cardenas, H.; Wang, Y.; Matei, D.; Cheng, J.X. Metabolic reprogramming from glycolysis to fatty acid uptake and beta-oxidation in platinum-resistant cancer cells. *Nat. Commun.* **2022**, *5*, 4554. [CrossRef] [PubMed]
22. Shah, D.D.; Chorawala, M.R.; Raghani, N.R.; Patel, R.; Fareed, M.; Kashid, V.A.; Prajapati, B.G. Tumor microenvironment: Recent advances in understanding and its role in modulating cancer therapies. *Med. Oncol.* **2025**, *42*, 117. [CrossRef] [PubMed]
23. Bejarano, L.; Jordão, M.J.C.; Joyce, J.A. Therapeutic Targeting of the Tumor Microenvironment. *Cancer Discov.* **2021**, *11*, 933–959. [CrossRef] [PubMed]
24. Elinav, E.; Nowarski, R.; Thaiss, C.A.; Hu, B.; Jin, C.; Flavell, R.A. Inflammation-induced cancer: Crosstalk between tumours, immune cells and microorganisms. *Nat. Rev. Cancer* **2013**, *13*, 759–771. [CrossRef] [PubMed]
25. Karimi, M.; Asbaghi, O.; Hooshmand, F.; Aghayan, A.H.; Shariati, A.A.; Kazemi, K.; Amirpour, M.; Davoodi, S.H.; Larijani, B. Adherence to Mediterranean Diet and Breast Cancer Risk: A Meta-Analysis of Prospective Observational Studies. *Health Sci. Rep.* **2025**, *8*, 70736. [CrossRef] [PubMed]
26. Giordano, G.; Mastrantoni, L.; Terranova, R.; Colloca, G.F.; Zuccalà, G.; Landi, F. The role of Mediterranean diet in cancer incidence and mortality in the older adults. *NPJ Aging* **2024**, *10*, 61. [CrossRef] [PubMed]
27. Pan, B.; Wu, Y.; Yang, Q.; Ge, L.; Gao, C.; Xun, Y.; Tian, J.; Ding, G. The impact of major dietary patterns on glycemic control, cardiovascular risk factors, and weight loss in patients with type 2 diabetes: A network meta-analysis. *J. Evid. Based Med.* **2019**, *12*, 29–39. [CrossRef] [PubMed]
28. Oppedisano, F.; Mollace, R.; Tavernese, A.; Gliozzi, M.; Musolino, V.; Macrì, R.; Carresi, C.; Maiuolo, J.; Serra, M.; Cardamone, A.; et al. PUFA Supplementation and Heart Failure: Effects on Fibrosis and Cardiac Remodeling. *Nutrients* **2021**, *13*, 2965. [CrossRef] [PubMed]
29. Tufarelli, V.; Casalino, E.; D'Alessandro, A.G.; Laudadio, V. Dietary Phenolic Compounds: Biochemistry, Metabolism and Significance in Animal and Human Health. *Curr. Drug Metab.* **2017**, *18*, 905–913. [CrossRef] [PubMed]
30. Rana, A.; Samtiya, M.; Dhewa, T.; Mishra, V.; Aluko, R.E. Health benefits of polyphenols: A concise review. *J. Food Biochem.* **2022**, *46*, 14264. [CrossRef] [PubMed]
31. Williamson, G. Bioavailability of Food Polyphenols: Current State of Knowledge. *Annu. Rev. Food Sci. Technol.* **2025**, *16*, 315–332. [CrossRef] [PubMed]
32. Di Lorenzo, C.; Colombo, F.; Biella, S.; Stockley, C.; Restani, P. Polyphenols and Human Health: The Role of Bioavailability. *Nutrients* **2021**, *13*, 273. [CrossRef] [PubMed]
33. Bobrysheva, T.N.; Anisimov, G.S.; Zolotoreva, M.S.; Bobryshev, D.V.; Budkevich, R.O.; Moskalev, A.A. [Polyphenols as promising bioactive compounds]. *Vopr. Pitan.* **2023**, *92*, 92–107. [CrossRef] [PubMed]
34. Wan, S.; Luo, J.; Zhu, Y.; An, P.; Luo, Y.; Xing, Q. The Effect of Antioxidant Polyphenol Supplementation on Cardiometabolic Risk Factors: A Systematic Review and Meta-Analysis. *Nutrients* **2024**, *16*, 4206. [CrossRef] [PubMed]
35. Cao, H.; Ou, J.; Chen, L.; Zhang, Y.; Szkudelski, T.; Delmas, D.; Daglia, M.; Xiao, J. Dietary polyphenols and type 2 diabetes: Human Study and Clinical Trial. *Crit. Rev. Food Sci. Nutr.* **2019**, *59*, 3371–3379. [CrossRef] [PubMed]

36. Wang, S.; Du, Q.; Meng, X.; Zhang, Y. Natural polyphenols: A potential prevention and treatment strategy for metabolic syndrome. *Food Funct.* **2022**, *13*, 9734–9753. [CrossRef] [PubMed]
37. Jomova, K.; Alomar, S.Y.; Valko, R.; Liska, J.; Nepovimova, E.; Kuca, K.; Valko, M. Flavonoids and their role in oxidative stress, inflammation, and human diseases. *Chem. Biol. Interact.* **2025**, *25*, 111489. [CrossRef] [PubMed]
38. González Mosquera, D.M.; Hernández Ortega, Y.; Fernández, P.L.; González, Y.; Doens, D.; Vander Heyden, Y.; Foubert, K.; Pieters, L. Flavonoids from Boldoa purpurascens inhibit proinflammatory cytokines (TNF-α and IL-6) and the expression of COX-2. *Phytother. Res.* **2018**, *32*, 1750–1754. [CrossRef] [PubMed]
39. Singaravelan, N.; Tollefsbol, T.O. Polyphenol-Based Prevention and Treatment of Cancer Through Epigenetic and Combinatorial Mechanisms. *Nutrients* **2025**, *17*, 616. [CrossRef] [PubMed]
40. Benvenuto, M.; Albonici, L.; Focaccetti, C.; Ciuffa, S.; Fazi, S.; Cifaldi, L.; Miele, M.T.; De Maio, F.; Tresoldi, I.; Manzari, V.; et al. Polyphenol-Mediated Autophagy in Cancer: Evidence of In Vitro and in vivo Studies. *Int. J. Mol. Sci.* **2020**, *21*, 6635. [CrossRef] [PubMed]
41. Martemucci, G.; Khalil, M.; Di Luca, A.; Abdallah, H.; D'Alessandro, A.G. Comprehensive Strategies for Metabolic Syndrome: How Nutrition, Dietary Polyphenols, Physical Activity, and Lifestyle Modifications Address Diabesity, Cardiovascular Diseases, and Neurodegenerative Conditions. *Metabolites* **2024**, *14*, 327. [CrossRef] [PubMed]
42. Roszkowska, M. Multilevel Mechanisms of Cancer Drug Resistance. *Int. J. Mol. Sci.* **2024**, *25*, 12402. [CrossRef] [PubMed]
43. Auti, A.; Tathode, M.; Marino, M.M.; Vitiello, A.; Ballini, A.; Miele, F.; Mazzone, V.; Ambrosino, A.; Boccellino, M. Nature's weapons: Bioactive compounds as anti-cancer agents. *AIMS Public Health* **2024**, *11*, 747–772. [CrossRef] [PubMed]
44. Pierdomenico, M.; Cicero, A.F.G.; Veronesi, M.; Fogacci, F.; Riccioni, C.; Benassi, B. Effect of Citrus bergamia extract on lipid profile: A combined in vitro and human study. *Phytother. Res.* **2023**, *37*, 4185–4195. [CrossRef] [PubMed]
45. Cordeiro, K.C.; Scaffo, J.; Flexa, B.N.; Gama, C.C.A.; Ferreira, M.A.; Cruz, R.A.S.; Aguiar-Alves, F.; Rocha, L.; Machado, F.P.; Fernandes, C.P. Characterization of bergamot essential oil: Chemical, microbiological and colloidal aspects. *Braz. J. Biol.* **2024**, *26*, 275622. [CrossRef] [PubMed]
46. Mollace, V.; Scicchitano, M.; Paone, S.; Casale, F.; Calandruccio, C.; Gliozzi, M.; Musolino, V.; Carresi, C.; Maiuolo, J.; Nucera, S.; et al. Hypoglycemic and Hypolipemic Effects of a New Lecithin Formulation of Bergamot Polyphenolic Fraction: A Double Blind, Randomized, Placebo- Controlled Study. *Endocr. Metab. Immune Disord.-Drug Targets* **2019**, *19*, 136–143. [CrossRef] [PubMed]
47. Mollace, V.; Sacco, I.; Janda, E.; Malara, C.; Ventrice, D.; Colica, C.; Visalli, V.; Muscoli, S.; Ragusa, S.; Muscoli, C.; et al. Hypolipemic and hypoglycaemic activity of bergamot polyphenols: From animal models to human studies. *Fitoterapia* **2011**, *82*, 309–316. [CrossRef] [PubMed]
48. Bavaro, A.R.; Tarantini, A.; Bruno, A.; Logrieco, A.F.; Gallo, A.; Mita, G.; Valerio, F.; Bleve, G.; Cardinali, A. Functional foods in Mediterranean diet: Exploring the functional features of vegetable case-studies obtained also by biotechnological approaches. *Aging Clin. Exp. Res.* **2024**, *36*, 208. [CrossRef] [PubMed]
49. Ding, X.; Chen, Y.; Du, L.; Li, J.; Meng, X.; Lv, H.; Tong, B.; Niu, G.; Jian, T.; Chen, J. Benefits of inulin and fructo-oligosaccharides on high fat diet-induced type 2 diabetes mellitus by regulating the gut microbiota in mice. *J. Nutr. Biochem.* **2025**, *141*, 109908. [CrossRef] [PubMed]
50. Tsimihodimos, V.; Psoma, O. Extra Virgin Olive Oil and Metabolic Diseases. *Int. J. Mol. Sci.* **2024**, *25*, 8117. [CrossRef] [PubMed]
51. Maruca, A.; Catalano, R.; Bagetta, D.; Mesiti, F.; Ambrosio, F.A.; Romeo, I.; Moraca, F.; Rocca, R.; Ortuso, F.; Artese, A.; et al. The Mediterranean Diet as source of bioactive compounds with multi-targeting anti-cancer profile. *Eur. J. Med. Chem.* **2019**, *181*, 111579. [CrossRef] [PubMed]
52. Lammi, C.; Bellumori, M.; Cecchi, L.; Bartolomei, M.; Bollati, C.; Clodoveo, M.L.; Corbo, F.; Arnoldi, A.; Mulinacci, N. Extra Virgin Olive Oil Phenol Extracts Exert Hypocholesterolemic Effects through the Modulation of the LDLR Pathway: In Vitro and Cellular Mechanism of Action Elucidation. *Nutrients* **2020**, *12*, 1723. [CrossRef] [PubMed]
53. Rishmawi, S.; Haddad, F.; Dokmak, G.; Karaman, R. A Comprehensive Review on the Anti-Cancer Effects of Oleuropein. *Life* **2022**, *12*, 1140. [CrossRef] [PubMed]
54. Alizadeh, S.R.; Ebrahimzadeh, M.A. Quercetin derivatives: Drug design, development, and biological activities, a review. *Eur. J. Med. Chem.* **2022**, *229*, 114068. [CrossRef] [PubMed]
55. Ileriturk, M.; Kandemir, O.; Kandemir, F.M. Evaluation of protective effects of quercetin against cypermethrin-induced lung toxicity in rats via oxidative stress, inflammation, apoptosis, autophagy, and endoplasmic reticulum stress pathway. *Environ. Toxicol.* **2022**, *37*, 2639–2650. [CrossRef] [PubMed]
56. Wu, S.X.; Xiong, R.G.; Huang, S.Y.; Zhou, D.D.; Saimaiti, A.; Zhao, C.N.; Shang, A.; Zhang, Y.J.; Gan, R.Y.; Li, H.B. Effects and mechanisms of resveratrol for prevention and management of cancers: An updated review. *Crit. Rev. Food Sci. Nutr.* **2023**, *63*, 12422–12440. [CrossRef] [PubMed]
57. Nani, A.; Murtaza, B.; Sayed Khan, A.; Khan, N.A.; Hichami, A. Antioxidant and Anti-Inflammatory Potential of Polyphenols Contained in Mediterranean Diet in Obesity: Molecular Mechanisms. *Molecules* **2021**, *26*, 985. [CrossRef] [PubMed]

58. Cheng, H.; Zhang, D.; Wu, J.; Liu, J.; Zhou, Y.; Tan, Y.; Feng, W.; Peng, C. Interactions between gut microbiota and polyphenols: A mechanistic and metabolomic review. *Phytomedicine* **2023**, *119*, 154979. [CrossRef] [PubMed]
59. Ed-Dahmani, I.; El Fadili, M.; Nouioura, G.; Kandsi, F.; Atki, Y.E.; Abuelizz, H.A.; Conte, R.; Zahra Lafdil, F.; Taleb, A.; Abdellaoui, A.; et al. *Ferula communis* leaf extract: Antioxidant capacity, UHPLC-MS/MS analysis, and in vivo and In Silico toxicity investigations. *Front. Chem.* **2025**, *12*, 1485463. [CrossRef] [PubMed]
60. Macrì, R.; Maiuolo, J.; Scarano, F.; Musolino, V.; Fregola, A.; Gliozzi, M.; Carresi, C.; Nucera, S.; Serra, M.; Caminiti, R.; et al. Evaluation of the Potential Beneficial Effects of *Ferula communis* L. Extract Supplementation in Postmenopausal Discomfort. *Nutrients* **2024**, *16*, 2651. [CrossRef] [PubMed]
61. Salerno, R.; Casale, F.; Calandruccio, C.; Procopio, A. Characterization of flavonoids in Citrus bergamia (Bergamot) polyphenolic fraction by liquid chromatography–high resolution mass spectrometry (LC/HRMS). *PharmaNutrition* **2016**, *4*, 2213–4344. [CrossRef]
62. Buzzanca, C.; Di Stefano, V.; D'Amico, A.; Gallina, A.; Melilli, M.G. A systematic review on *Cynara cardunculus* L.: Bioactive compounds, nutritional properties and food-industry applications of a sustainable food. *Nat. Prod. Res.* **2024**, *3*, 20. [CrossRef] [PubMed]
63. Li, X.; Muñoz-Díez, C.; Miho, H.; Zhang, L.; Li, P.; Priego, F.; Oulbi, S.; Uyanik, E.B.; Koubouris, G.; Perri, E.; et al. Evaluation of phenolics in the analysis of virgin olive oil using near infrared spectroscopy. *Spectrochim. Acta A Mol. Biomol. Spectrosc.* **2025**, *326*, 125262. [CrossRef] [PubMed]
64. Ussia, S.; Ritorto, G.; Mollace, R.; Serra, M.; Tavernese, A.; Altomare, C.; Muscoli, C.; Fini, M.; Barillà, F.; Indolfi, C.; et al. Exploring the Benefits of Extra Virgin Olive Oil on Cardiovascular Health Enhancement and Disease Prevention: A Systematic Review. *Nutrients* **2025**, *17*, 1843. [CrossRef] [PubMed]
65. Sun, W.; Shahrajabian, M.H. Therapeutic Potential of Phenolic Compounds in Medicinal Plants-Natural Health Products for Human Health. *Molecules* **2023**, *28*, 1845. [CrossRef] [PubMed]
66. Leischner, C.; Burkard, M.; Michel, A.; Berchtold, S.; Niessner, H.; Marongiu, L.; Busch, C.; Frank, J.; Lauer, U.M.; Venturelli, S. Comparative Analysis of the Antitumor Activity of Cis- and Trans-Resveratrol in Human Cancer Cells with Different p53 Status. *Molecules* **2021**, *26*, 5586. [CrossRef] [PubMed]
67. Tian, B.; Liu, J. Resveratrol: A review of plant sources, synthesis, stability, modification and food application. *J. Sci. Food Agric.* **2020**, *100*, 1392–1404. [CrossRef] [PubMed]
68. Nouioura, G.; El Fadili, M.; El Barnossi, A.; Loukili, E.H.; Laaroussi, H.; Bouhrim, M.; Giesy, J.P.; Aboul-Soud, M.A.M.; Al-Sheikh, Y.A.; Lyoussi, B.; et al. Comprehensive analysis of different solvent extracts of Ferula communis L. fruit reveals phenolic compounds and their biological properties via in vitro and in silico assays. *Sci. Rep.* **2024**, *14*, 8325. [CrossRef] [PubMed]
69. Sonigra, P.; Meena, M. Metabolic Profile, Bioactivities, and Variations in the Chemical Constituents of Essential Oils of the *Ferula* Genus (Apiaceae). *Front. Pharmacol.* **2021**, *11*, 608649. [CrossRef] [PubMed]
70. Louvet, M.S.; Gault, G.; Lefebvre, S.; Popowycz, F.; Boulven, M.; Besse, S.; Benoit, E.; Lattard, V.; Grancher, D. Comparative inhibitory effect of prenylated coumarins, ferulenol and ferprenin, contained in the 'poisonous chemotype' of Ferula communis on mammal liver microsomal VKORC1 activity. *Phytochemistry* **2015**, *118*, 124–130. [CrossRef] [PubMed]
71. Naji Reyhani Garmroudi, S.; Karimi, E.; Oskoueian, E.; Homayouni-Tabrizi, M.; Iranshahi, M. Ferutinin: A phytoestrogen from ferula and its anticancer, antioxidant, and toxicity properties. *J. Biochem. Mol. Toxicol.* **2021**, *35*, 22713. [CrossRef] [PubMed]
72. Nolfi-Donegan, D.; Braganza, A.; Shiva, S. Mitochondrial electron transport chain: Oxidative phosphorylation, oxidant production, and methods of measurement. *Redox Biol.* **2020**, *37*, 101674. [CrossRef] [PubMed]
73. Jelic, M.D.; Mandic, A.D.; Maricic, S.M.; Srdjenovic, B.U. Oxidative stress and its role in cancer. *J. Cancer Res. Ther.* **2021**, *17*, 22–28. [CrossRef] [PubMed]
74. Wu, Q.; Yao, J.; Xiao, M.; Zhang, X.; Zhang, M.; Xi, X. Targeting Nrf2 signaling pathway: New therapeutic strategy for cardiovascular diseases. *J. Drug Target.* **2024**, *32*, 874–883. [CrossRef] [PubMed]
75. Sciaccotta, R.; Gangemi, S.; Penna, G.; Giordano, L.; Pioggia, G.; Allegra, A. Potential New Therapies "ROS-Based" in CLL: An Innovative Paradigm in the Induction of Tumor Cell Apoptosis. *Antioxidants* **2024**, *13*, 475. [CrossRef] [PubMed]
76. Altomare, A.; Baron, G.; Gianazza, E.; Banfi, C.; Carini, M.; Aldini, G. Lipid peroxidation derived reactive carbonyl species in free and conjugated forms as an index of lipid peroxidation: Limits and perspectives. *Redox Biol.* **2021**, *42*, 101899. [CrossRef] [PubMed]
77. Jomova, K.; Raptova, R.; Alomar, S.Y.; Alwasel, S.H.; Nepovimova, E.; Kuca, K.; Valko, M. Reactive oxygen species, toxicity, oxidative stress, and antioxidants: Chronic diseases and aging. *Arch. Toxicol.* **2023**, *97*, 2499–2574. [CrossRef] [PubMed]
78. Guo, H.; Yang, Y.; Lou, Y.; Zuo, Z.; Cui, H.; Deng, H.; Zhu, Y.; Fang, J. Apoptosis and DNA damage mediated by ROS involved in male reproductive toxicity in mice induced by Nickel. *Ecotoxicol. Environ. Saf.* **2023**, *268*, 115679. [CrossRef] [PubMed]
79. Chen, B.; Lu, M.; Chen, Q.; Zou, E.; Bo, Z.; Li, J.; Zhao, R.; Zhao, J.; Yu, Z.; Chen, G.; et al. Systematic profiling of mitochondria-related transcriptome in tumorigenesis, prognosis, and tumor immune microenvironment of intrahepatic cholangiocarcinoma: A multi-center cohort study. *Front. Genet.* **2024**, *15*, 1430885. [CrossRef] [PubMed]

80. Ávila-Escalante, M.L.; Coop-Gamas, F.; Cervantes-Rodríguez, M.; Méndez-Iturbide, D.; Aranda-González, I.I. The effect of diet on oxidative stress and metabolic diseases-Clinically controlled trials. *J. Food Biochem.* **2020**, *44*, 13191. [CrossRef] [PubMed]
81. Kong, C.Y.; Guo, Z.; Song, P.; Zhang, X.; Yuan, Y.P.; Teng, T.; Yan, L.; Tang, Q.Z. Underlying the Mechanisms of Doxorubicin-Induced Acute Cardiotoxicity: Oxidative Stress and Cell Death. *Int. J. Biol. Sci.* **2022**, *18*, 760–770. [CrossRef] [PubMed]
82. de Almeida, A.J.P.O.; de Oliveira, J.C.P.L.; da Silva Pontes, L.V.; de Souza Júnior, J.F.; Gonçalves, T.A.F.; Dantas, S.H.; de Almeida Feitosa, M.S.; Silva, A.O.; de Medeiros, I.A. ROS: Basic Concepts, Sources, Cellular Signaling, and its Implications in Aging Pathways. *Oxid. Med. Cell Longev.* **2022**, *19*, 1225578. [CrossRef] [PubMed]
83. Vašková, J.; Kočan, L.; Vaško, L.; Perjési, P. Glutathione-Related Enzymes and Proteins: A Review. *Molecules* **2023**, *28*, 1447. [CrossRef] [PubMed]
84. Bianchi, E.; Erbasan, H.; Riso, P.; Perna, S. Impact of the Mediterranean Diet on Athletic Performance, Muscle Strength, Body Composition, and Antioxidant Markers in Both Athletes and Non-Professional Athletes: A Systematic Review of Intervention Trials. *Nutrients* **2024**, *16*, 3454. [CrossRef] [PubMed]
85. Zhu, R.; Fogelholm, M.; Poppitt, S.D.; Silvestre, M.P.; Møller, G.; Huttunen-Lenz, M.; Stratton, G.; Sundvall, J.; Råman, L.; Jalo, E.; et al. Adherence to a Plant-Based Diet and Consumption of Specific Plant Foods-Associations with 3-Year Weight-Loss Maintenance and Cardiometabolic Risk Factors: A Secondary Analysis of the PREVIEW Intervention Study. *Nutrients* **2021**, *13*, 3916. [CrossRef] [PubMed]
86. La Scala, S.; Naselli, F.; Quatrini, P.; Gallo, G.; Caradonna, F. Drought-Adapted Mediterranean Diet Plants: A Source of Bioactive Molecules Able to Give Nutrigenomic Effects per sè or to Obtain Functional Foods. *Int. J. Mol. Sci.* **2024**, *25*, 2235. [CrossRef] [PubMed]
87. Nazari, A.; Osati, P.; Seifollahy Fakhr, S.; Faghihkhorasani, F.; Ghanaatian, M.; Faghihkhorasani, F.; Rezaei-Tazangi, F.; Pazhouhesh Far, N.; Shourideh, A.; Ebrahimi, N.; et al. New Emerging Therapeutic Strategies Based on Manipulation of the Redox Regulation Against Therapy Resistance in Cancer. *Antioxid. Redox Signal.* **2024**. [CrossRef] [PubMed]
88. Yuan, M.; Zhang, G.; Bai, W.; Han, X.; Li, C.; Bian, S. The Role of Bioactive Compounds in Natural Products Extracted from Plants in Cancer Treatment and Their Mechanisms Related to Anticancer Effects. *Oxid. Med. Cell Longev.* **2022**, *15*, 1429869. [CrossRef] [PubMed]
89. Trinh, V.H.; Nguyen Huu, T.; Sah, D.K.; Choi, J.M.; Yoon, H.J.; Park, S.C.; Jung, Y.S.; Lee, S.R. Redox Regulation of PTEN by Reactive Oxygen Species: Its Role in Physiological Processes. *Antioxidants* **2024**, *13*, 199. [CrossRef] [PubMed]
90. Ghofrani-Shahpar, M.; Pakravan, K.; Razmara, E.; Amooie, F.; Mahmoudian, M.; Heshmati, M.; Babashah, S. Cancer-associated fibroblasts drive colorectal cancer cell progression through exosomal miR-20a-5p-mediated targeting of PTEN and stimulating interleukin-6 production. *BMC Cancer* **2024**, *24*, 400. [CrossRef] [PubMed]
91. Glaviano, A.; Foo, A.S.C.; Lam, H.Y.; Yap, K.C.H.; Jacot, W.; Jones, R.H.; Eng, H.; Nair, M.G.; Makvandi, P.; Geoerger, B.; et al. PI3K/AKT/mTOR signaling transduction pathway and targeted therapies in cancer. *Mol. Cancer.* **2023**, *22*, 138. [CrossRef] [PubMed]
92. Mohideen, K.; Chandrasekaran, K.; Kareema, M.; Jeyanthikumari, T.; Dhungel, S.; Ghosh, S. Assessment of Antioxidant Enzyme Superoxide Dismutase (SOD) in Oral Cancer: Systematic Review and Meta-Analysis. *Dis. Markers* **2024**, *16*, 2264251. [CrossRef] [PubMed]
93. Liu, Y.; Su, Z.; Tavana, O.; Gu, W. Understanding the complexity of p53 in a new era of tumor suppression. *Cancer Cell.* **2024**, *42*, 946–967. [CrossRef] [PubMed]
94. Suzuki, T.; Takahashi, J.; Yamamoto, M. Molecular Basis of the KEAP1-NRF2 Signaling Pathway. *Mol. Cells.* **2023**, *46*, 133–141. [CrossRef] [PubMed]
95. Tülüce, Y.; Keleş, A.Y.; Köstekci, S. Assessment of redox homeostasis via genotoxicity, cytotoxicity, apoptosis and NRF-2 in colorectal cancer cell lines after treatment with *Ganoderma lucidum* extract. *Drug Chem. Toxicol.* **2024**, *47*, 693–709. [CrossRef] [PubMed]
96. Averill-Bates, D. Reactive oxygen species and cell signaling. Review. *Biochim. Biophys. Acta Mol. Cell Res.* **2024**, *1871*, 119573. [CrossRef] [PubMed]
97. Adinolfi, S.; Patinen, T.; Jawahar Deen, A.; Pitkänen, S.; Härkönen, J.; Kansanen, E.; Küblbeck, J.; Levonen, A.L. The KEAP1-NRF2 pathway: Targets for therapy and role in cancer. *Redox Biol.* **2023**, *63*, 102726. [CrossRef] [PubMed]
98. Moon, H.; Ro, S.W. MAPK/ERK Signaling Pathway in Hepatocellular Carcinoma. *Cancers* **2021**, *13*, 3026. [CrossRef] [PubMed]
99. Chen, J.Y.; Yang, Y.J.; Meng, X.Y.; Lin, R.H.; Tian, X.Y.; Zhang, Y.; Lai, W.F.; Yang, C.; Ma, X.Q.; Huang, M.Q. Oxysophoridine inhibits oxidative stress and inflammation in hepatic fibrosis via regulating Nrf2 and NF-κB pathways. *Phytomedicine* **2024**, *132*, 155585. [CrossRef] [PubMed]
100. Zhou, X.; An, B.; Lin, Y.; Ni, Y.; Zhao, X.; Liang, X. Molecular mechanisms of ROS-modulated cancer chemoresistance and therapeutic strategies. *Biomed. Pharmacother.* **2023**, *165*, 115036. [CrossRef] [PubMed]
101. Fleming Martinez, A.K.; Storz, P. Protein kinase D1—A targetable mediator of pancreatic cancer development. *Biochim. Biophys. Acta Mol. Cell Res.* **2024**, *1871*, 119646. [CrossRef] [PubMed]

102. Li, Y.; Zhao, B.; Peng, J.; Tang, H.; Wang, S.; Peng, S.; Ye, F.; Wang, J.; Ouyang, K.; Li, J.; et al. Inhibition of NF-κB signaling unveils novel strategies to overcome drug resistance in cancers. *Drug Resist. Updat.* **2024**, *73*, 101042. [CrossRef] [PubMed]
103. Iqbal, M.J.; Kabeer, A.; Abbas, Z.; Siddiqui, H.A.; Calina, D.; Sharifi-Rad, J.; Cho, W.C. Interplay of oxidative stress, cellular communication and signaling pathways in cancer. *Cell Commun. Signal.* **2024**, *22*, 7. [CrossRef] [PubMed]
104. De Rosa, M.; Johnson, S.A.; Opresko, P.L. Roles for the 8-Oxoguanine DNA Repair System in Protecting Telomeres From Oxidative Stress. *Front. Cell Dev. Biol.* **2021**, *9*, 758402. [CrossRef] [PubMed]
105. Verma, P.; Rishi, B.; George, N.G.; Kushwaha, N.; Dhandha, H.; Kaur, M.; Jain, A.; Jain, A.; Chaudhry, S.; Singh, A.; et al. Recent advances and future directions in etiopathogenesis and mechanisms of reactive oxygen species in cancer treatment. *Pathol. Oncol. Res.* **2023**, *29*, 1611415. [CrossRef] [PubMed]
106. Morse, P.T.; Arroum, T.; Wan, J.; Pham, L.; Vaishnav, A.; Bell, J.; Pavelich, L.; Malek, M.H.; Sanderson, T.H.; Edwards, B.F.P.; et al. Phosphorylations and Acetylations of Cytochrome *c* Control Mitochondrial Respiration, Mitochondrial Membrane Potential, Energy, ROS, and Apoptosis. *Cells* **2024**, *13*, 493. [CrossRef] [PubMed]
107. Mustafa, M.; Ahmad, R.; Tantry, I.Q.; Ahmad, W.; Siddiqui, S.; Alam, M.; Abbas, K.; Moinuddin; Hassan, M.I.; Habib, S.; et al. Apoptosis: A Comprehensive Overview of Signaling Pathways, Morphological Changes, and Physiological Significance and Therapeutic Implications. *Cells* **2024**, *13*, 1838. [CrossRef] [PubMed]
108. Algieri, C.; Bernardini, C.; Oppedisano, F.; La Mantia, D.; Trombetti, F.; Palma, E.; Forni, M.; Mollace, V.; Romeo, G.; Nesci, S. Mitochondria Bioenergetic Functions and Cell Metabolism Are Modulated by the Bergamot Polyphenolic Fraction. *Cells* **2022**, *11*, 1401. [CrossRef] [PubMed]
109. Mollace, R.; Macrì, R.; Tavernese, A.; Gliozzi, M.; Musolino, V.; Carresi, C.; Maiuolo, J.; Fini, M.; Volterrani, M.; Mollace, V. Comparative Effect of Bergamot Polyphenolic Fraction and Red Yeast Rice Extract in Rats Fed a Hyperlipidemic Diet: Role of Antioxidant Properties and PCSK9 Expression. *Nutrients* **2022**, *14*, 477. [CrossRef] [PubMed]
110. Mollace, R.; Macrì, R.; Nicita, M.; Musolino, V.; Gliozzi, M.; Carresi, C.; Bava, I.; Maiuolo, J.; Tavernese, A.; Cardamone, A.; et al. Bergamot Polyphenolic Extract Combined with Albedo and Pulp Fibres Counteracts Changes in Gut Microbiota Associated with High-Fat Diet: Implications for Lipoprotein Size Re-Arrangement. *Int. J. Mol. Sci.* **2023**, *24*, 12967. [CrossRef] [PubMed]
111. Gliozzi, M.; Walker, R.; Muscoli, S.; Vitale, C.; Gratteri, S.; Carresi, C.; Musolino, V.; Russo, V.; Janda, E.; Ragusa, S.; et al. Bergamot polyphenolic fraction enhances rosuvastatin-induced effect on LDL-cholesterol, LOX-1 expression and protein kinase B phosphorylation in patients with hyperlipidemia. *Int. J. Cardiol.* **2013**, *170*, 140–145. [CrossRef] [PubMed]
112. Musolino, V.; Gliozzi, M.; Scarano, F.; Bosco, F.; Scicchitano, M.; Nucera, S.; Carresi, C.; Ruga, S.; Zito, M.C.; Maiuolo, J.; et al. Bergamot Polyphenols Improve Dyslipidemia and Pathophysiological Features in a Mouse Model of Non-Alcoholic Fatty Liver Disease. *Sci. Rep.* **2020**, *10*, 2565. [CrossRef] [PubMed]
113. Carresi, C.; Musolino, V.; Gliozzi, M.; Maiuolo, J.; Mollace, R.; Nucera, S.; Maretta, A.; Sergi, D.; Muscoli, S.; Gratteri, S.; et al. Anti-oxidant effect of bergamot polyphenolic fraction counteracts doxorubicin-induced cardiomyopathy: Role of autophagy and c-kit^{pos}CD45^{neg}CD31^{neg} cardiac stem cell activation. *J. Mol. Cell Cardiol.* **2018**, *119*, 10–18. [CrossRef] [PubMed]
114. Masala, V.; Jokić, S.; Aladić, K.; Molnar, M.; Casula, M.; Tuberoso, C.I.G. Chemical Profiling and Evaluation of Antioxidant Activity of Artichoke (*Cynara cardunculus* var. *scolymus*) Leaf By-Products' Extracts Obtained with Green Extraction Techniques. *Molecules* **2024**, *29*, 4816. [CrossRef]
115. Acquaviva, R.; Malfa, G.A.; Santangelo, R.; Bianchi, S.; Pappalardo, F.; Taviano, M.F.; Miceli, N.; Di Giacomo, C.; Tomasello, B. Wild Artichoke (*Cynara cardunculus* subsp. *sylvestris*, Asteraceae) Leaf Extract: Phenolic Profile and Oxidative Stress Inhibitory Effects on HepG2 Cells. *Molecules* **2023**, *28*, 2475. [CrossRef]
116. D'Antuono, I.; Garbetta, A.; Linsalata, V.; Minervini, F.; Cardinali, A. Polyphenols from artichoke heads (Cynara cardunculus (L.) subsp. scolymus Hayek): In vitro bio-accessibility, intestinal uptake and bioavailability. *Food Funct.* **2015**, *6*, 1268-77. [CrossRef] [PubMed]
117. Cho, J.Y.; Kim, A.R.; Jung, J.H.; Chun, T.; Rhee, M.H.; Yoo, E.S. Cytotoxic and pro-apoptotic activities of cynaropicrin, a sesquiterpene lactone, on the viability of leukocyte cancer cell lines. *Eur. J. Pharmacol.* **2004**, *492*, 85–94. [CrossRef] [PubMed]
118. Liu, T.; Zhang, J.; Han, X.; Xu, J.; Wu, Y.; Fang, J. Promotion of HeLa cells apoptosis by cynaropicrin involving inhibition of thioredoxin reductase and induction of oxidative stress. *Free Radic. Biol. Med.* **2019**, *135*, 216–226. [CrossRef] [PubMed]
119. De Cicco, P.; Busà, R.; Ercolano, G.; Formisano, C.; Allegra, M.; Taglialatela-Scafati, O.; Ianaro, A. Inhibitory effects of cynaropicrin on human melanoma progression by targeting MAPK, NF-κB, and Nrf-2 signaling pathways in vitro. *Phytother. Res.* **2021**, *35*, 1432–1442. [CrossRef] [PubMed]
120. Jin, T.; Leng, B. Cynaropicrin Averts the Oxidative Stress and Neuroinflammation in Ischemic/Reperfusion Injury Through the Modulation of NF-kB. *Appl. Biochem. Biotechnol.* **2023**, *195*, 5424–5438. [CrossRef] [PubMed]
121. Nucera, S.; Scarano, F.; Macrì, R.; Mollace, R.; Gliozzi, M.; Carresi, C.; Ruga, S.; Serra, M.; Tavernese, A.; Caminiti, R.; et al. The Effect of an Innovative Combination of Bergamot Polyphenolic Fraction and *Cynara cardunculus* L. Extract on Weight Gain Reduction and Fat Browning in Obese Mice. *Int. J. Mol. Sci.* **2024**, *25*, 191. [CrossRef] [PubMed]

122. Musolino, V.; Gliozzi, M.; Bombardelli, E.; Nucera, S.; Carresi, C.; Maiuolo, J.; Mollace, R.; Paone, S.; Bosco, F.; Scarano, F.; et al. The synergistic effect of *Citrus bergamia* and *Cynara cardunculus* extracts on vascular inflammation and oxidative stress in non-alcoholic fatty liver disease. *J. Tradit. Complement. Med.* **2020**, *10*, 268–274. [CrossRef] [PubMed]
123. Bulotta, S.; Corradino, R.; Celano, M.; D'Agostino, M.; Maiuolo, J.; Oliverio, M.; Procopio, A.; Iannone, M.; Rotiroti, D.; Russo, D. Antiproliferative and antioxidant effects on breast cancer cells of oleuropein and its semisynthetic peracetylated derivatives. *Food Chem.* **2011**, *127*, 0308–8146. [CrossRef]
124. Liman, R.; Çoban, F.K.; Ciğerci, I.H.; İbrahim, B.; Bozkurt, S. Antiangiogenic and Apoptotic Effects of Oleuropein on Breast Cancer Cells. *J. Pharm. Res.* **2017**, *16*, 1–10. [CrossRef]
125. Yan, C.M.; Chai, E.Q.; Cai, H.Y.; Miao, G.Y.; Ma, W. Oleuropein induces apoptosis via activation of caspases and suppression of phosphatidylinositol 3-kinase/protein kinase B pathway in HepG2 human hepatoma cell line. *Mol. Med. Rep.* **2015**, *11*, 4617–4624. [CrossRef] [PubMed]
126. Scicchitano, S.; Vecchio, E.; Battaglia, A.M.; Oliverio, M.; Nardi, M.; Procopio, A.; Costanzo, F.; Biamonte, F.; Faniello, M.C. The Double-Edged Sword of Oleuropein in Ovarian Cancer Cells: From Antioxidant Functions to Cytotoxic Effects. *Int. J. Mol. Sci.* **2023**, *24*, 842. [CrossRef]
127. Maiuolo, J.; Bava, I.; Carresi, C.; Gliozzi, M.; Musolino, V.; Scarano, F.; Nucera, S.; Scicchitano, M.; Bosco, F.; Ruga, S.; et al. The Effects of Bergamot Polyphenolic Fraction, *Cynara cardunculus* and *Olea europea* L. Extract on Doxorubicin-Induced Cardiotoxicity. *Nutrients* **2021**, *13*, 2158. [CrossRef] [PubMed]
128. Algieri, C.; Bernardini, C.; Oppedisano, F.; La Mantia, D.; Trombetti, F.; Palma, E.; Forni, M.; Mollace, V.; Romeo, G.; Troisio, I.; et al. The Impairment of Cell Metabolism by Cardiovascular Toxicity of Doxorubicin Is Reversed by Bergamot Polyphenolic Fraction Treatment in Endothelial Cells. *Int. J. Mol. Sci.* **2022**, *23*, 8977. [CrossRef] [PubMed]
129. Maiuolo, J.; Carresi, C.; Gliozzi, M.; Musolino, V.; Scarano, F.; Coppoletta, A.R.; Guarnieri, L.; Nucera, S.; Scicchitano, M.; Bosco, F.; et al. Effects of Bergamot Polyphenols on Mitochondrial Dysfunction and Sarcoplasmic Reticulum Stress in Diabetic Cardiomyopathy. *Nutrients* **2021**, *13*, 2476. [CrossRef] [PubMed]
130. Tuerxun, H.; Zhao, Y.; Li, Y.; Liu, X.; Wen, S.; Zhao, Y. Resveratrol alleviates testicular toxicity induced by anti-PD-1 through regulating the NRF2-SLC7A11-GPX4 pathway. *Front. Immunol.* **2025**, *16*, 1529991. [CrossRef] [PubMed]
131. Biswas, P.; Dey, D.; Biswas, P.K.; Rahaman, T.I.; Saha, S.; Parvez, A.; Khan, D.A.; Lily, N.J.; Saha, K.; Sohel, M.; et al. A Comprehensive Analysis and Anti-Cancer Activities of Quercetin in ROS-Mediated Cancer and Cancer Stem Cells. *Int. J. Mol. Sci.* **2022**, *23*, 11746. [CrossRef] [PubMed]
132. Dewanjee, S.; Bhattacharya, H.; Bhattacharyya, C.; Chakraborty, P.; Fleishman, J.; Alexiou, A.; Papadakis, M.; Jha, S.K. Nrf2/Keap1/ARE regulation by plant secondary metabolites: A new horizon in brain tumor management. *Cell Commun. Signal.* **2024**, *15*, 497. [CrossRef] [PubMed]
133. Guan, G.; Chen, Y.; Dong, Y. Unraveling the AMPK-SIRT1-FOXO Pathway: The In-Depth Analysis and Breakthrough Prospects of Oxidative Stress-Induced Diseases. *Antioxidants* **2025**, *14*, 70. [CrossRef] [PubMed]
134. Rajesh, R.U.; Sangeetha, D. Therapeutic potentials and targeting strategies of quercetin on cancer cells: Challenges and future prospects. *Phytomedicine* **2024**, *133*, 155902. [CrossRef] [PubMed]
135. Khattar, S.; Khan, S.A.; Zaidi, S.A.A.; Darvishikolour, M.; Farooq, U.; Naseef, P.P.; Kurunian, M.S.; Khan, M.Z.; Shamim, A.; Khan, M.M.U.; et al. Resveratrol from Dietary Supplement to a Drug Candidate: An Assessment of Potential. *Pharmaceuticals* **2022**, *15*, 957. [CrossRef] [PubMed]
136. Sitarek, P.; Merecz-Sadowska, A.; Sikora, J.; Dudzic, M.; Wiertek-Płoszaj, N.; Picot, L.; Śliwiński, T.; Kowalczyk, T. Flavonoids and their derivatives as DNA topoisomerase inhibitors with anti-cancer activity in various cell models: Exploring a novel mode of action. *Pharmacol. Res.* **2024**, *209*, 107457. [CrossRef] [PubMed]
137. Macrì, R.; Musolino, V.; Gliozzi, M.; Carresi, C.; Maiuolo, J.; Nucera, S.; Scicchitano, M.; Bosco, F.; Scarano, F.; Ruga, S.; et al. *Ferula* L. Plant Extracts and Dose-Dependent Activity of Natural Sesquiterpene Ferutinin: From Antioxidant Potential to Cytotoxic Effects. *Molecules* **2020**, *25*, 5768. [CrossRef] [PubMed]
138. Macrì, R.; Bava, I.; Scarano, F.; Mollace, R.; Musolino, V.; Gliozzi, M.; Greco, M.; Foti, D.; Tucci, L.; Maiuolo, J.; et al. In Vitro Evaluation of Ferutinin Rich-*Ferula communis* L., ssp. *glauca*, Root Extract on Doxorubicin-Induced Cardiotoxicity: Antioxidant Properties and Cell Cycle Modulation. *Int. J. Mol. Sci.* **2023**, *24*, 12735. [CrossRef]
139. Maiuolo, J.; Musolino, V.; Guarnieri, L.; Macrì, R.; Coppoletta, A.R.; Cardamone, A.; Serra, M.; Gliozzi, M.; Bava, I.; Lupia, C.; et al. *Ferula communis* L. (*Apiaceae*) Root Acetone-Water Extract: Phytochemical Analysis, Cytotoxicity and In Vitro Evaluation of Estrogenic Properties. *Plants* **2022**, *11*, 1905. [CrossRef] [PubMed]
140. Maiuolo, J.; Miceli, N.; Davì, F.; Bava, I.; Tucci, L.; Ragusa, S.; Taviano, M.F.; Musolino, V.; Gliozzi, M.; Carresi, C.; et al. *Ferula communis* Root Extract: In Vitro Evaluation of the Potential Additive Effect with Chemotherapy Tamoxifen in Breast Cancer (MCF-7) Cells Part II. *Plants* **2023**, *12*, 1194. [CrossRef] [PubMed]
141. Safi, R.; Hamade, A.; Bteich, N.; El Saghir, J.; Assaf, M.D.; El-Sabban, M.; Najjar, F. A ferutinin analogue with enhanced potency and selectivity against ER-positive breast cancer cells in vitro. *Biomed. Pharmacother.* **2018**, *105*, 267–273. [CrossRef] [PubMed]

142. Maiuolo, J.; Bava, I.; Carresi, C.; Gliozzi, M.; Musolino, V.; Scicchitano, M.; Macri, R.; Oppedisano, F.; Scarano, F.; Caterina Zito, M.; et al. The Effect of *Ferula communis* Extract in *Escherichia coli* Lipopolysaccharide-Induced Neuroinflammation in Cultured Neurons and Oligodendrocytes. *Int. J. Mol. Sci.* **2021**, *22*, 7910. [CrossRef] [PubMed]
143. Adorisio, S.; Muscari, I.; Fierabracci, A.; Thi Thuy, T.; Marchetti, M.C.; Ayroldi, E.; Delfino, D.V. Biological effects of bergamot and its potential therapeutic use as an anti-inflammatory, antioxidant, and anticancer agent. *Pharm. Biol.* **2023**, *61*, 639–646. [CrossRef] [PubMed]
144. Tripathi, S.; Sharma, Y.; Kumar, D. Unveiling the link between chronic inflammation and cancer. *Metabol. Open.* **2025**, *25*, 100347. [CrossRef] [PubMed]
145. Xie, Y.; Liu, F.; Wu, Y.; Zhu, Y.; Jiang, Y.; Wu, Q.; Dong, Z.; Liu, K. Inflammation in cancer: Therapeutic opportunities from new insights. *Mol. Cancer* **2025**, *24*, 51. [CrossRef] [PubMed]
146. Wang, M.; Zhang, L.; Chang, W.; Zhang, Y. The crosstalk between the gut microbiota and tumor immunity: Implications for cancer progression and treatment outcomes. *Front. Immunol.* **2023**, *13*, 1096551. [CrossRef] [PubMed]
147. Chen, L.; Deng, H.; Cui, H.; Fang, J.; Zuo, Z.; Deng, J.; Li, Y.; Wang, X.; Zhao, L. Inflammatory responses and inflammation-associated diseases in organs. *Oncotarget* **2017**, *9*, 7204–7218. [CrossRef] [PubMed]
148. Zhao, H.; Wu, L.; Yan, G.; Chen, Y.; Zhou, M.; Wu, Y.; Li, Y. Inflammation and tumor progression: Signaling pathways and targeted intervention. *Signal Transduct. Target. Ther.* **2021**, *6*, 263. [CrossRef] [PubMed]
149. Zhu, A.S.; Mustafa, T.; Connell, J.P.; Grande-Allen, K.J. Tumor necrosis factor alpha and interleukin 1 beta suppress myofibroblast activation via nuclear factor kappa B signaling in 3D-cultured mitral valve interstitial cells. *Acta Biomater.* **2021**, *127*, 159–168. [CrossRef] [PubMed]
150. Ait-Ahmed, Y.; Lafdil, F. Novel insights into the impact of liver inflammatory responses on primary liver cancer development. *Liver Res.* **2023**, *7*, 26–34. [CrossRef] [PubMed]
151. Nishida, A.; Andoh, A. The Role of Inflammation in Cancer: Mechanisms of Tumor Initiation, Progression, and Metastasis. *Cells* **2025**, *14*, 488. [CrossRef] [PubMed]
152. Tristan Asensi, M.; Napoletano, A.; Sofi, F.; Dinu, M. Low-Grade Inflammation and Ultra-Processed Foods Consumption: A Review. *Nutrients* **2023**, *15*, 1546. [CrossRef] [PubMed]
153. Minarovits, J. Human tumor viruses: Induction of three-dimensional alterations in the host genome structure. *Front. Microbiol.* **2023**, *14*, 1280210. [CrossRef] [PubMed]
154. Sun, M.; Zhu, S.; Wang, Y.; Zhao, Y.; Yan, K.; Li, X.; Wang, X.; He, C.; Ding, C.; Chen, Y.; et al. Effect of inflammation on association between cancer and coronary artery disease. *BMC Cardiovasc. Disord.* **2024**, *24*, 72. [CrossRef] [PubMed]
155. Mora Barthelmess, R.; Stijlemans, B.; Van Ginderachter, J.A. Hallmarks of Cancer Affected by the MIF Cytokine Family. *Cancers* **2023**, *15*, 395. [CrossRef] [PubMed]
156. Gao, S.P.; Mark, K.G.; Leslie, K.; Pao, W.; Motoi, N.; Gerald, W.L.; Travis, W.D.; Bornmann, W.; Veach, D.; Clarkson, B.; et al. Mutations in the EGFR kinase domain mediate STAT3 activation via IL-6 production in human lung adenocarcinomas. *J. Clin. Investig.* **2007**, *117*, 3846–3856. [CrossRef] [PubMed]
157. Leone, P.; Malerba, E.; Susca, N.; Favoino, E.; Perosa, F.; Brunori, G.; Prete, M.; Racanelli, V. Endothelial cells in tumor microenvironment: Insights and perspectives. *Front. Immunol.* **2024**, *15*, 1367875. [CrossRef] [PubMed]
158. Xiao, Y.; Yu, D. Tumor microenvironment as a therapeutic target in cancer. *Pharmacol. Ther.* **2021**, *221*, 107753. [CrossRef] [PubMed]
159. Vallée, A.; Lecarpentier, Y. Crosstalk Between Peroxisome Proliferator-Activated Receptor Gamma and the Canonical WNT/β-Catenin Pathway in Chronic Inflammation and Oxidative Stress During Carcinogenesis. *Front. Immunol.* **2018**, *9*, 745. [CrossRef] [PubMed]
160. Sabatino, L.; Pancione, M.; Votino, C.; Colangelo, T.; Lupo, A.; Novellino, E.; Lavecchia, A.; Colantuoni, V. Emerging role of the β-catenin-PPARγ axis in the pathogenesis of colorectal cancer. *World J. Gastroenterol.* **2014**, *20*, 7137–7151. [CrossRef] [PubMed]
161. Chi, T.; Wang, M.; Wang, X.; Yang, K.; Xie, F.; Liao, Z.; Wei, P. PPAR-γ Modulators as Current and Potential Cancer Treatments. *Front. Oncol.* **2021**, *11*, 737776. [CrossRef] [PubMed]
162. Hernandez-Quiles, M.; Broekema, M.F.; Kalkhoven, E. PPARgamma in Metabolism, Immunity, and Cancer: Unified and Diverse Mechanisms of Action. *Front. Endocrinol.* **2021**, *12*, 624112. [CrossRef] [PubMed]
163. Kurowska, A.; Ziemichód, W.; Herbet, M.; Piątkowska-Chmiel, I. The Role of Diet as a Modulator of the Inflammatory Process in the Neurological Diseases. *Nutrients* **2023**, *15*, 1436. [CrossRef] [PubMed]
164. Russo, C.; Lombardo, G.E.; Bruschetta, G.; Rapisarda, A.; Maugeri, A.; Navarra, M. Bergamot Byproducts: A Sustainable Source to Counteract Inflammation. *Nutrients* **2024**, *16*, 259. [CrossRef] [PubMed]
165. Carresi, C.; Mollace, R.; Macrì, R.; Scicchitano, M.; Bosco, F.; Scarano, F.; Coppoletta, A.R.; Guarnieri, L.; Ruga, S.; Zito, M.C.; et al. Oxidative Stress Triggers Defective Autophagy in Endothelial Cells: Role in Atherothrombosis Development. *Antioxidants* **2021**, *10*, 387. [CrossRef] [PubMed]

166. Parafati, M.; Lascala, A.; La Russa, D.; Mignogna, C.; Trimboli, F.; Morittu, V.M.; Riillo, C.; Macirella, R.; Mollace, V.; Brunelli, E.; et al. Bergamot Polyphenols Boost Therapeutic Effects of the Diet on Non-Alcoholic Steatohepatitis (NASH) Induced by "Junk Food": Evidence for Anti-Inflammatory Activity. *Nutrients* **2018**, *10*, 1604. [CrossRef] [PubMed]
167. Gallyas, F., Jr.; Sumegi, B. Mitochondrial Protection by PARP Inhibition. *Int. J. Mol. Sci.* **2020**, *21*, 2767. [CrossRef] [PubMed]
168. Sun, J.; Yu, L.; Qu, X.; Huang, T. The role of peroxisome proliferator-activated receptors in the tumor microenvironment, tumor cell metabolism, and anticancer therapy. *Front. Pharmacol.* **2023**, *14*, 1184794. [CrossRef] [PubMed]
169. Chen, S.; Liu, Z.; Wu, H.; Wang, B.; Ouyang, Y.; Liu, J.; Zheng, X.; Zhang, H.; Li, X.; Feng, X.; et al. Adipocyte-rich microenvironment promotes chemoresistance via upregulation of peroxisome proliferator-activated receptor gamma/ABCG2 in epithelial ovarian cancer. *Int. J. Mol. Med.* **2024**, *53*, 37. [CrossRef] [PubMed]
170. Nakamura, T.; Pitna, D.B.; Kimura, K.; Yoshimoto, Y.; Uchiyama, T.; Mori, T.; Kondo, R.; Hara, S.; Egoshi, Y.; Yamaguchi, S.; et al. Total synthesis of cynaropicrin. *Org. Biomol. Chem.* **2021**, *19*, 6038–6044. [CrossRef] [PubMed]
171. Chen, J.; Liu, X. Cynaropicrin attenuates inflammatory cytokines in LPS-induced RAW264.7 cells and ovalbumin-induced asthmatic mice. *J. Biochem. Mol. Toxicol.* **2024**, *38*, e23836. [CrossRef] [PubMed]
172. Silvestrini, A.; Giordani, C.; Bonacci, S.; Giuliani, A.; Ramini, D.; Matacchione, G.; Sabbatinelli, J.; Di Valerio, S.; Pacetti, D.; Procopio, A.D.; et al. Anti-Inflammatory Effects of Olive Leaf Extract and Its Bioactive Compounds Oleacin and Oleuropein-Aglycone on Senescent Endothelial and Small Airway Epithelial Cells. *Antioxidants* **2023**, *12*, 1509. [CrossRef] [PubMed]
173. Tamburini, B.; Di Liberto, D.; Pratelli, G.; Rizzo, C.; Barbera, L.; Lauricella, M.; Carlisi, D.; Maggio, A.; Palumbo Piccionello, A.; D'Anneo, A.; et al. Extra Virgin Olive Oil Polyphenol-Enriched Extracts Exert Antioxidant and Anti-Inflammatory Effects on Peripheral Blood Mononuclear Cells from Rheumatoid Arthritis Patients. *Antioxidants* **2025**, *14*, 171. [CrossRef] [PubMed]
174. Mirsanei, Z.; Heidari, N.; Hazrati, A.; Asemani, Y.; Niknam, B.; Yousefi, Z.; Jafari, R. Oleuropein reduces LPS-induced inflammation via stimulating M2 macrophage polarization. *Biomed. Pharmacother.* **2023**, *163*, 114857. [CrossRef] [PubMed]
175. Ruzzolini, J.; Chioccioli, S.; Monaco, N.; Peppicelli, S.; Andreucci, E.; Urciuoli, S.; Romani, A.; Luceri, C.; Tortora, K.; Calorini, L.; et al. Oleuropein-Rich Leaf Extract as a Broad Inhibitor of Tumour and Macrophage iNOS in an Apc Mutant Rat Model. *Antioxidants* **2021**, *10*, 1577. [CrossRef] [PubMed]
176. Bigagli, E.; Cinci, L.; Paccosi, S.; Parenti, A.; D'Ambrosio, M.; Luceri, C. Nutritionally relevant concentrations of resveratrol and hydroxytyrosol mitigate oxidative burst of human granulocytes and monocytes and the production of pro-inflammatory mediators in LPS-stimulated RAW 264.7 macrophages. *Int. Immunopharmacol.* **2017**, *43*, 147–155. [CrossRef] [PubMed]
177. Jin, H.X.; Zhang, Y.H.; Guo, R.N.; Zhao, S.N. Inhibition of MEK/ERK/STAT3 signaling in oleuropein treatment inhibits myocardial ischemia/reperfusion. *Int. J. Mol. Med.* **2018**, *42*, 1034–1043. [CrossRef] [PubMed]
178. Karakoç, M.D.; Sekkin, S. Effects of Oleuropein on Epirubicin and Cyclophosphamide Combination Treatment in Rats. *Turk. J. Pharm. Sci.* **2021**, *18*, 420–429. [CrossRef] [PubMed]
179. Vezza, T.; Rodríguez-Nogales, A.; Algieri, F.; Garrido-Mesa, J.; Romero, M.; Sánchez, M.; Toral, M.; Martín-García, B.; Gómez-Caravaca, A.M.; Arráez-Román, D.; et al. The metabolic and vascular protective effects of olive (*Olea europaea* L.) leaf extract in diet-induced obesity in mice are related to the amelioration of gut microbiota dysbiosis and to its immunomodulatory properties. *Pharmacol. Res.* **2019**, *150*, 104487. [CrossRef] [PubMed]
180. Rehman, A.; Bukhari, S.A.; Chauhdary, Z.; Akhter, N.; Noreen, R. Effect of resveratrol and quercetin on SFRP4 as a biomarker of diabesity: In silico and in vivo studies. *Biochem. Biophys. Res. Commun.* **2025**, *761*, 151748. [CrossRef] [PubMed]
181. Zhao, L.; Cen, F.; Tian, F.; Li, M.J.; Zhang, Q.; Shen, H.Y.; Shen, X.C.; Zhou, M.M.; Du, J. Combination treatment with quercetin and resveratrol attenuates high fat diet-induced obesity and associated inflammation in rats via the AMPKα1/SIRT1 signaling pathway. *Exp. Ther. Med.* **2017**, *14*, 5942–5948. [CrossRef] [PubMed]
182. Li, L.; Jiang, W.; Yu, B.; Liang, H.; Mao, S.; Hu, X.; Feng, Y.; Xu, J.; Chu, L. Quercetin improves cerebral ischemia/reperfusion injury by promoting microglia/macrophages M2 polarization via regulating PI3K/Akt/NF-κB signaling pathway. *Biomed. Pharmacother.* **2023**, *168*, 115653. [CrossRef] [PubMed]
183. Ma, E.; Wu, C.; Chen, J.; Wo, D.; Ren, D.N.; Yan, H.; Peng, L.; Zhu, W. Resveratrol prevents Ang II-induced cardiac hypertrophy by inhibition of NF-κB signaling. *Biomed. Pharmacother.* **2023**, *165*, 115275. [CrossRef] [PubMed]
184. Geroushi, A.; Auzi, A.A.; Elhwuegi, A.S.; Elzawam, F.; Elsherif, A.; Nahar, L.; Sarker, S.D. Antiinflammatory sesquiterpenes from the root oil of Ferula hermonis. *Phytother. Res.* **2011**, *25*, 774–777. [CrossRef] [PubMed]
185. Zhang, M.; Zhang, L.; Hei, R.; Li, X.; Cai, H.; Wu, X.; Zheng, Q.; Cai, C. CDK inhibitors in cancer therapy, an overview of recent development. *Am. J. Cancer Res.* **2021**, *11*, 1913–1935. [PubMed]
186. Ozaki, T.; Nakagawara, A. Role of p53 in Cell Death and Human Cancers. *Cancers* **2011**, *3*, 994–1013. [CrossRef] [PubMed]
187. Fan, W.; Xiong, R.; Zhou, Z.; Zhang, C.; Han, Y.; Shi, T.; Qiu, J.; Zhang, R. ZFP57 promotes ovarian cancer progression by transcriptionally regulating BRCA1 and managing G1 checkpoint. *J. Cancer* **2023**, *14*, 2039–2050. [CrossRef] [PubMed]
188. Liu, Y.; Liang, W.; Chang, Y.; He, Z.; Wu, M.; Zheng, H.; Ke, X.; Lv, M.; Liu, Q.; Liu, Q.; et al. CEP192 is a novel prognostic marker and correlates with the immune microenvironment in hepatocellular carcinoma. *Front. Immunol.* **2022**, *13*, 950884. [CrossRef] [PubMed]

189. Gheghiani, L.; Wang, L.; Zhang, Y.; Moore, X.T.R.; Zhang, J.; Smith, S.C.; Tian, Y.; Wang, L.; Turner, K.; Jackson-Cook, C.K.; et al. PLK1 Induces Chromosomal Instability and Overrides Cell-Cycle Checkpoints to Drive Tumorigenesis. *Cancer Res.* **2021**, *81*, 1293–1307. [CrossRef] [PubMed]
190. Corno, A.; Cordeiro, M.H.; Allan, L.A.; Lim, Q.W.; Harrington, E.; Smith, R.J.; Saurin, A.T. A bifunctional kinase-phosphatase module balances mitotic checkpoint strength and kinetochore-microtubule attachment stability. *EMBO J.* **2023**, *42*, 112630. [CrossRef] [PubMed]
191. Łukasik, P.; Załuski, M.; Gutowska, I. Cyclin-Dependent Kinases (CDK) and Their Role in Diseases Development-Review. *Int. J. Mol. Sci.* **2021**, *22*, 2935. [CrossRef] [PubMed]
192. Boccardi, V.; Marano, L. Aging, Cancer, and Inflammation: The Telomerase Connection. *Int. J. Mol. Sci.* **2024**, *25*, 8542. [CrossRef] [PubMed]
193. Dietrich, C.; Trub, A.; Ahn, A.; Taylor, M.; Ambani, K.; Chan, K.T.; Lu, K.H.; Mahendra, C.A.; Blyth, C.; Coulson, R.; et al. INX-315, a Selective CDK2 Inhibitor, Induces Cell Cycle Arrest and Senescence in Solid Tumors. *Cancer Discov.* **2024**, *14*, 446–467. [CrossRef] [PubMed]
194. Singh, S.R.; Bhaskar, R.; Ghosh, S.; Yarlagadda, B.; Singh, K.K.; Verma, P.; Sengupta, S.; Mladenov, M.; Hadzi-Petrushev, N.; Stojchevski, R.; et al. Exploring the Genetic Orchestra of Cancer: The Interplay Between Oncogenes and Tumor-Suppressor Genes. *Cancers* **2025**, *17*, 1082. [CrossRef] [PubMed]
195. Garcia-Oliveira, P.; Otero, P.; Pereira, A.G.; Chamorro, F.; Carpena, M.; Echave, J.; Fraga-Corral, M.; Simal-Gandara, J.; Prieto, M.A. Status and Challenges of Plant-Anticancer Compounds in Cancer Treatment. *Pharmaceuticals* **2021**, *14*, 157. [CrossRef] [PubMed]
196. Maugeri, A.; Russo, C.; Musumeci, L.; Lombardo, G.E.; De Sarro, G.; Barreca, D.; Cirmi, S.; Navarra, M. The Anticancer Effect of a Flavonoid-Rich Extract of Bergamot Juice in THP-1 Cells Engages the SIRT2/AKT/p53 Pathway. *Pharmaceutics* **2022**, *14*, 2168. [CrossRef]
197. Delle Monache, S.; Sanità, P.; Trapasso, E.; Ursino, M.R.; Dugo, P.; Russo, M.; Ferlazzo, N.; Calapai, G.; Angelucci, A.; Navarra, M. Mechanisms underlying the anti-tumoral effects of Citrus Bergamia juice. *PLoS ONE* **2013**, *8*, 61484. [CrossRef] [PubMed]
198. Navarra, M.; Femia, A.P.; Romagnoli, A.; Tortora, K.; Luceri, C.; Cirmi, S.; Ferlazzo, N.; Caderni, G. A flavonoid-rich extract from bergamot juice prevents carcinogenesis in a genetic model of colorectal cancer, the Pirc rat (F344/NTac-Apc^{am1137}). *Eur. J. Nutr.* **2020**, *59*, 885–894. [CrossRef] [PubMed]
199. Lepore, S.M.; Maggisano, V.; Lombardo, G.E.; Maiuolo, J.; Mollace, V.; Bulotta, S.; Russo, D.; Celano, M. Antiproliferative Effects of Cynaropicrin on Anaplastic Thyroid Cancer Cells. *Endocr. Metab. Immune Disord. Drug Targets* **2019**, *19*, 59–66. [CrossRef] [PubMed]
200. Ding, Z.; Xi, J.; Zhong, M.; Chen, F.; Zhao, H.; Zhang, B.; Fang, J. Cynaropicrin Induces Cell Cycle Arrest and Apoptosis by Inhibiting PKM2 to Cause DNA Damage and Mitochondrial Fission in A549 Cells. *J. Agric. Food Chem.* **2021**, *69*, 13557–13567. [CrossRef] [PubMed]
201. Pessoa, H.R.; Zago, L.; Difonzo, G.; Pasqualone, A.; Caponio, F.; Ferraz da Costa, D.C. Olive Leaves as a Source of Anticancer Compounds: In Vitro Evidence and Mechanisms. *Molecules* **2024**, *29*, 4249. [CrossRef] [PubMed]
202. Han, S.; Hou, H.; Zhang, Y.; Fang, Z.; Li, Y.; Zhang, L.; Wang, Y.; Zhang, S.; Zhang, H.; Jin, Q.; et al. Oleuropein and its hydrolysate from extra virgin olive oil inhibit breast cancer cells proliferation interfering with the PI3K-AKT signal pathway. *J. Funct. Foods* **2023**, *110*, 1756–4646. [CrossRef]
203. Messeha, S.S.; Zarmouh, N.O.; Asiri, A.; Soliman, K.F.A. Gene Expression Alterations Associated with Oleuropein-Induced Antiproliferative Effects and S-Phase Cell Cycle Arrest in Triple-Negative Breast Cancer Cells. *Nutrients* **2020**, *12*, 3755. [CrossRef] [PubMed]
204. Benitez, D.A.; Pozo-Guisado, E.; Alvarez-Barrientos, A.; Fernandez-Salguero, P.M.; Castellón, E.A. Mechanisms involved in resveratrol-induced apoptosis and cell cycle arrest in prostate cancer-derived cell lines. *J. Androl.* **2007**, *28*, 282–293. [CrossRef] [PubMed]
205. Ahmad, N.; Adhami, V.M.; Afaq, F.; Feyes, D.K.; Mukhtar, H. Resveratrol causes WAF-1/p21-mediated G(1)-phase arrest of cell cycle and induction of apoptosis in human epidermoid carcinoma A431 cells. *Clin. Cancer Res.* **2001**, *7*, 1466–1473. [PubMed]
206. Bailon-Moscoso, N.; Cevallos-Solorzano, G.; Romero-Benavides, J.C.; Orellana, M.I. Natural Compounds as Modulators of Cell Cycle Arrest: Application for Anticancer Chemotherapies. *Curr. Genom.* **2017**, *18*, 106–131. [CrossRef] [PubMed]
207. Wu, H.; Chen, L.; Zhu, F.; Han, X.; Sun, L.; Chen, K. The Cytotoxicity Effect of Resveratrol: Cell Cycle Arrest and Induced Apoptosis of Breast Cancer 4T1 Cells. *Toxins* **2019**, *11*, 731. [CrossRef] [PubMed]
208. Shi, Y.; Cai, G.; Zhang, C.; Li, H.; Nie, Y.; Yu, S.; Zhang, B.; Wu, M.; Luo, W.; Liu, J.; et al. Resveratrol suppresses growth and VCAN expression in a Cancer-associated fibroblast-breast Cancer hybrid organoid. *Int. Immunopharmacol.* **2025**, *153*, 114451. [CrossRef] [PubMed]
209. Catanzaro, D.; Ragazzi, E.; Vianello, C.; Caparrotta, L.; Montopoli, M. Effect of Quercetin on Cell Cycle and Cyclin Expression in Ovarian Carcinoma and Osteosarcoma Cell Lines. *Nat. Prod. Commun.* **2015**, *10*, 1365–1368. [CrossRef] [PubMed]

210. Suh, D.K.; Lee, E.J.; Kim, H.C.; Kim, J.H. Induction of G(1)/S phase arrest and apoptosis by quercetin in human osteosarcoma cells. *Arch. Pharm. Res.* **2010**, *33*, 781–785. [CrossRef] [PubMed]
211. Son, H.K.; Kim, D. Quercetin Induces Cell Cycle Arrest and Apoptosis in YD10B and YD38 Oral Squamous Cell Carcinoma Cells. *Asian Pac. J. Cancer Prev.* **2023**, *24*, 283–289. [CrossRef] [PubMed]
212. Hussein, S.A.; Ababneh, N.A.; Tarawneh, N.; Ismail, M.A.; Awidi, A.; Abdalla, S. Antitumor Effects of Quercetin and Luteolin in A375 Cutaneous Melanoma Cell Line Are Mediated by Upregulation of P-ERK, c-Myc, and the Upstream GPER. *Life* **2025**, *15*, 417. [CrossRef] [PubMed]
213. Keshmirshekan, F.; Mohamadi-Zarch, S.M.; Bagheri, S.M. A Review of Anticancer Potential of Conferone, Diversin and Ferutinin; Which One is Stronger for Cancer Therapy? *Anti-Cancer Agents Med. Chem.* **2025**, *25*, 378–387. [CrossRef] [PubMed]
214. Sasso, J.M.; Ammar, R.M.; Tenchov, R.; Lemmel, S.; Kelber, O.; Grieswelle, M.; Zhou, Q.A. Gut Microbiome-Brain Alliance: A Landscape View into Mental and Gastrointestinal Health and Disorders. *ACS Chem. Neurosci.* **2023**, *14*, 1717–1763. [CrossRef] [PubMed]
215. Zhai, B.; Ola, M.; Rolling, T.; Tosini, N.L.; Joshowitz, S.; Littmann, E.R.; Amoretti, L.A.; Fontana, E.; Wright, R.J.; Miranda, E.; et al. High-resolution mycobiota analysis reveals dynamic intestinal translocation preceding invasive candidiasis. *Nat. Med.* **2020**, *26*, 59–64. [CrossRef] [PubMed]
216. Dohlman, A.B.; Klug, J.; Mesko, M.; Gao, I.H.; Lipkin, S.M.; Shen, X.; Iliev, I.D. A pan-cancer mycobiome analysis reveals fungal involvement in gastrointestinal and lung tumors. *Cell* **2022**, *185*, 3807–3822.e12. [CrossRef] [PubMed]
217. Galeano Niño, J.L.; Wu, H.; LaCourse, K.D.; Kempchinsky, A.G.; Baryiames, A.; Barber, B.; Futran, N.; Houlton, J.; Sather, C.; Sicinska, E.; et al. Effect of the intratumoral microbiota on spatial and cellular heterogeneity in cancer. *Nature* **2022**, *611*, 810–817. [CrossRef] [PubMed]
218. Cao, Y.; Xia, H.; Tan, X.; Shi, C.; Ma, Y.; Meng, D.; Zhou, M.; Lv, Z.; Wang, S.; Jin, Y. Intratumoural microbiota: A new frontier in cancer development and therapy. *Signal Transduct. Target. Ther.* **2024**, *9*, 15. [CrossRef] [PubMed]
219. Liu, G.; Liu, K.; Ji, L.; Li, Y. Intratumoral microbiota, fatty acid metabolism, and tumor microenvironment constitute an unresolved trinity in colon adenocarcinoma. *Sci. Rep.* **2025**, *15*, 2568. [CrossRef] [PubMed]
220. Ruiz-Malagón, A.J.; Rodríguez-Sojo, M.J.; Redondo, E.; Rodríguez-Cabezas, M.E.; Gálvez, J.; Rodríguez-Nogales, A. Systematic review: The gut microbiota as a link between colorectal cancer and obesity. *Obes. Rev.* **2025**, *26*, 13872. [CrossRef] [PubMed]
221. Xu, J.; Cheng, M.; Liu, J.; Cui, M.; Yin, B.; Liang, J. Research progress on the impact of intratumoral microbiota on the immune microenvironment of malignant tumors and its role in immunotherapy. *Front. Immunol.* **2024**, *15*, 1389446. [CrossRef] [PubMed]
222. Hu, Z.J.; Zhu, H.R.; Jin, Y.J.; Liu, P.; Yu, X.W.; Zhang, Y.R. Correlation between gut microbiota and tumor immune microenvironment: A bibliometric and visualized study. *World J. Clin. Oncol.* **2025**, *16*, 101611. [CrossRef] [PubMed]
223. Jovel, J.; Patterson, J.; Wang, W.; Hotte, N.; O'Keefe, S.; Mitchel, T.; Perry, T.; Kao, D.; Mason, A.L.; Madsen, K.L.; et al. Characterization of the Gut Microbiome Using 16S or Shotgun Metagenomics. *Front. Microbiol.* **2016**, *7*, 459. [CrossRef] [PubMed]
224. Wensel, C.R.; Pluznick, J.L.; Salzberg, S.L.; Sears, C.L. Next-generation sequencing: Insights to advance clinical investigations of the microbiome. *J. Clin. Investig.* **2022**, *132*, 154944. [CrossRef] [PubMed]
225. Zhang, Y.J.; Li, S.; Gan, R.Y.; Zhou, T.; Xu, D.P.; Li, H.B. Impacts of gut bacteria on human health and diseases. *Int. J. Mol. Sci.* **2015**, *16*, 7493–7519. [CrossRef] [PubMed]
226. Weersma, R.K.; Zhernakova, A.; Fu, J. Interaction between drugs and the gut microbiome. *Gut* **2020**, *69*, 1510–1519. [CrossRef] [PubMed]
227. Riehl, L.; Fürst, J.; Kress, M.; Rykalo, N. The importance of the gut microbiome and its signals for a healthy nervous system and the multifaceted mechanisms of neuropsychiatric disorders. *Front. Neurosci.* **2024**, *17*, 1302957. [CrossRef] [PubMed]
228. Sun, J.; Chen, F.; Wu, G. Potential effects of gut microbiota on host cancers: Focus on immunity, DNA damage, cellular pathways, and anticancer therapy. *ISME J.* **2023**, *17*, 1535–1551. [CrossRef] [PubMed]
229. He, R.; Qi, P.; Shu, L.; Ding, Y.; Zeng, P.; Wen, G.; Xiong, Y.; Deng, H. Dysbiosis and extraintestinal cancers. *J. Exp. Clin. Cancer Res.* **2025**, *44*, 44. [CrossRef] [PubMed]
230. Zhang, P. Influence of Foods and Nutrition on the Gut Microbiome and Implications for Intestinal Health. *Int. J. Mol. Sci.* **2022**, *23*, 9588. [CrossRef] [PubMed]
231. Tang, Y.; Cai, Q.; Tian, Z.; Chen, W.; Tang, H. Crosstalk between Gut Microbiota and Cancer Immunotherapy: Present Investigations and Future Perspective. *Research* **2025**, *8*, 0600. [CrossRef] [PubMed]
232. McGill, C.R.; Fulgoni, V.L., 3rd; Devareddy, L. Ten-year trends in fiber and whole grain intakes and food sources for the United States population: National Health and Nutrition Examination Survey 2001–2010. *Nutrients* **2015**, *7*, 1119–1130. [CrossRef] [PubMed]
233. Schnorr, S.L.; Candela, M.; Rampelli, S.; Centanni, M.; Consolandi, C.; Basaglia, G.; Turroni, S.; Biagi, E.; Peano, C.; Severgnini, M.; et al. Gut microbiome of the Hadza hunter-gatherers. *Nat. Commun.* **2014**, *5*, 3654. [CrossRef] [PubMed]

234. Wang, D.D.; Qi, Q.; Wang, Z.; Usyk, M.; Sotres-Alvarez, D.; Mattei, J.; Tamez, M.; Gellman, M.D.; Daviglus, M.; Hu, F.B.; et al. The Gut Microbiome Modifies the Association Between a Mediterranean Diet and Diabetes in USA Hispanic/Latino Population. *J. Clin. Endocrinol. Metab.* **2022**, *107*, e924–e934. [CrossRef] [PubMed]
235. Zeb, F.; Naqeeb, H.; Osaili, T.; Faris, M.E.; Ismail, L.C.; Obaid, R.S.; Naja, F.; Radwan, H.; Hasan, H.; Hashim, M.; et al. Molecular crosstalk between polyphenols and gut microbiota in cancer prevention. *Nutr. Res.* **2024**, *124*, 21–42. [CrossRef] [PubMed]
236. Li, C.; Xu, Y.; Zhang, J.; Zhang, Y.; He, W.; Ju, J.; Wu, Y.; Wang, Y. The effect of resveratrol, curcumin and quercetin combination on immuno-suppression of tumor microenvironment for breast tumor-bearing mice. *Sci. Rep.* **2023**, *13*, 13278. [CrossRef] [PubMed]
237. Mandle, H.B.; Jenab, M.; Gunter, M.J.; Tjønneland, A.; Olsen, A.; Dahm, C.C.; Zhang, J.; Sugier, P.E.; Rothwell, J.; Severi, G.; et al. Inflammation and gut barrier function-related genes and colorectal cancer risk in western European populations. *Mutagenesis* **2025**, *40*, 48–60. [CrossRef] [PubMed]
238. Ke, J.; Zhang, C.J.; Wang, L.Z.; Xie, F.S.; Wu, H.Y.; Li, T.; Bian, C.W.; Wu, R.L. Lipopolysaccharide promotes cancer cell migration and invasion through METTL3/PI3K/AKT signaling in human cholangiocarcinoma. *Heliyon* **2024**, *10*, 29683. [CrossRef] [PubMed]
239. Mollace, A.; Coluccio, M.L.; Donato, G.; Mollace, V.; Malara, N. Cross-talks in colon cancer between RAGE/AGEs axis and inflammation/immunotherapy. *Oncotarget* **2021**, *12*, 1281–1295. [CrossRef] [PubMed]
240. Ramamoorthy Rajalakshmi, R.; Melians, M.A.; Pon, F.F.; Cosio, D.S.; Buvarahamurthy, V.; Jayakumar, A.R.; Paidas, M.J. *Advantages and Disadvantages of Nutraceuticals*; Springer Nature: Singapore, 2023; pp. 245–286. [CrossRef]
241. Shaman, J.A. The Future of Pharmacogenomics: Integrating Epigenetics, Nutrigenomics, and Beyond. *J. Pers. Med.* **2024**, *14*, 1121. [CrossRef] [PubMed]
242. Zhang, B.; Zhang, Y.; Xing, X.; Wang, S. Health benefits of dietary polyphenols: Insight into interindividual variability in absorption and metabolism. *Curr. Opin. Food Sci.* **2022**, *48*, 2214–7993. [CrossRef]
243. Favari, C.; Rinaldi de Alvarenga, J.F.; Sánchez-Martínez, L.; Tosi, N.; Mignogna, C.; Cremonini, E.; Manach, C.; Bresciani, L.; Del Rio, D.; Mena, P. Factors driving the inter-individual variability in the metabolism and bioavailability of (poly)phenolic metabolites: A systematic review of human studies. *Redox Biol.* **2024**, *71*, 103095. [CrossRef] [PubMed]
244. Sahraeian, S.; Rashidinejad, A.; Golmakani, M.-T. Recent advances in the conjugation approaches for enhancing the bioavailability of polyphenols. *Food Hydrocoll.* **2024**, *146*, 109221. [CrossRef]

Disclaimer/Publisher's Note: The statements, opinions and data contained in all publications are solely those of the individual author(s) and contributor(s) and not of MDPI and/or the editor(s). MDPI and/or the editor(s) disclaim responsibility for any injury to people or property resulting from any ideas, methods, instructions or products referred to in the content.

nutrients

MDPI

Article

The Antioxidant and Chemopreventive Activity of a Nutraceutical Derived from *Brassicaceae* Seed Extracts for Colorectal Cancer

Ana Guzmán-Carrasco [1,2], Cristina Mesas [1,3], Kevin Doello [1,3,4,5], Jesús M. Porres [2], Alejandro García-Beltrán [2], Rosario Martínez [2], Francisco Bermúdez [6], Mercedes Peña [1,3], Consolación Melguizo [1,3,5,*] and Jose Prados [1,3,5]

[1] Instituto de Investigación Biosanitaria de Granada, ibs.GRANADA, 18012 Granada, Spain; anaguzman@correo.ugr.es (A.G.-C.); cristinam@ugr.es (C.M.); mpenacontreras@ugr.es (M.P.); jcprados@ugr.es (J.P.)
[2] Department of Physiology, Institute of Nutrition and Food Technology (INyTA), Biomedical Research Center (CIBM), Sport and Health University Research Institute (IMUDS), Universidad de Granada, 18016 Granada, Spain; jmporres@ugr.es (J.M.P.); alejandrogb@ugr.es (A.G.-B.); rosariomz@ugr.es (R.M.)
[3] Institute of Biopathology and Regenerative Medicine (IBIMER), Center of Biomedical Research (CIBM), University of Granada, 18100 Granada, Spain
[4] Medical Oncology Service, Virgen de las Nieves Hospital, 18016 Granada, Spain
[5] Department of Anatomy and Embryology, Faculty of Medicine, University of Granada, 18071 Granada, Spain
[6] Seed for Innovation S.L., Scientific Headquarters of the Almería Technology Park, Universidad de Almería, 04128 Almería, Spain; francisco.bermudez@beyond-seeds.com
* Correspondence: melguizo@ugr.es; Tel.: +34-958-243-535

Abstract

Background. Worldwide, colorectal cancer is the third most commonly diagnosed cancer. It is the second leading cause of cancer-related mortality. Recent studies establish a relationship between natural compounds from plants with the prevention and treatment of cancer. Specifically, glucosinolates with antitumoral capacity and polyphenols with the ability to scavenge free radicals that can cause cell damage have been identified in the *Brassicaceae* family. **Objectives**. Based on the previously mentioned factors, this study aimed to develop a nutraceutical made with extracts from different *Brassicaceae* seeds and study its antioxidant and antiproliferative action in vitro and in vivo using the AOM/DSS model in CC57BL6J mice. **Results**. Extract from the seeds of *Eruca sativa* and *Sinapis alba* showed the highest antioxidant capacity among the different species studied and were selected for nutraceutical formulation, which was potentially absorbable (73%) after an in vitro digestion process. In total, thirty compounds were identified in the nutraceutical that could be responsible for its antioxidant and tumoral prevention capacity. The intake of nutraceutical was a successful intervention to prevent the development of polyps by 31.6% and their size by 53.9%. When the nutritional intervention was used in combination with a physical exercise protocol, these parameters dropped to 52.3% and 62.6%, respectively. **Conclusions**. These findings suggest that the consumption of a diet rich in bioactive compounds from *Brassica* species, in combination with physical activity, is a valuable prevention strategy for colorectal cancer. However, more research is required to evaluate the efficacy and safety of these interventions in clinical settings.

Keywords: *Brassicaceae*; nutraceutical; *Eruca sativa*; *Sinapis alba*; colorectal cancer; cancer prevention

1. Introduction

Colorectal cancer (CRC), defined as the abnormal and excessive proliferation of cells in the colon and rectum [1], is the third most common cancer worldwide. According to the World Health Organization (WHO), 1.93 million new cases of CRC were reported in 2020, affecting 1.07 million men and 865,630 women. It is also the second cause of cancer-related deaths, with 916,000 fatalities reported in 2022 (515,639 men and 419,536 women) [2]. The study published by Santucci et al. [3] evaluates cancer mortality data in the European Union from 1970–1974 to 2015–2019, showing a stronger decline from the year 2000 onwards. According to the prediction of these investigators, this trend is expected to continue. The predicted CRC mortality rate for 2024 (compared with data from 2015 to 2019) showed a decrease of 6.9% and 11.8% for men and women, respectively, considering all age groups. However, an increase in CRC-associated mortality is estimated in the 25–49 age group. Specifically, in Spain, an increase of 5.5% is expected in men, while in Italy, both sexes are affected. The sharpest increases for the predicted CRC mortality rate have been detected in the UK, with 26.1% in men and 38.6% in women. By 2040, the global mortality burden of CRC is expected to rise to 1.6 million deaths.

Risk factors for the development of CRC include (i) age, as it is diagnosed more frequently in individuals over 50 years old; (ii) predisposing diseases, especially the presence of intestinal polyps or inflammatory bowel disease; (iii) a history of CRC, since individuals with a previous CRC diagnosis are at higher risk of recurrence and metachronous intestinal tumors; (iv) genetic and familial factors, with approximately 25% of cases presenting a family history of CRC and 10% involving a hereditary component; (v) lifestyle factors, particularly physical inactivity; and (vi) dietary factors, which play an essential role and are under continuous research. In fact, this pathology has been associated with excessive alcohol intake, overweight and obesity, and certain types of food (e.g., processed meat) [2].

A consistent inverse association has been observed between the intake of legumes, vegetables, and fruits and the risk of cancer development. Thus, a higher consumption of vegetables is linked to a reduced cancer risk [2,4]. Recommended vegetables include carrots, green leafy vegetables, and vegetables of the genus Allium and the *Brassicaceae* family, among others. The recommendation of *Brassicaceae* consumption for CRC prevention is based on the content of molecules naturally present in this family known as glucosinolates, which are converted into bioactive products known as isothiocyanates (ITCs) through the action of the enzyme myrosinase and the intestinal microbiota. In addition, their high polyphenol content contributes to chemoprevention by scavenging free radicals that can cause cellular damage and enhancing the activity of detoxifying enzymes that inhibit the early stages of CRC development [5,6]. There are many factors that negatively affect the population's direct intake of *Brassicacea* such as its characteristic bitter taste and smell [7]. This effect is mainly due to the presence of glucosinolates with a thiourea fraction which can negatively influence the preference in individuals more sensitive to this taste, an effect that is genetically determined [8,9]. In addition, these compounds can be altered and lose their functionality during cooking techniques involving high temperatures [10]. Specifically, between 20 and 40% of these compounds are lost during boiling [11].

However, despite their promising chemopreventive effects, the direct ingestion of *Brassicaceae* vegetables for further absorption and conversion into ITCs may not be sufficient to achieve therapeutic activity [12]. In this context, the use of nutraceuticals becomes an effective strategy in the prevention of CRC. Nutraceuticals are defined as food-derived products containing bioactive components that contribute to disease prevention and treatment. In oncology, these compounds have demonstrated significant efficacy in the prevention of tumor development by modulating the proliferation, differentiation, apoptosis, inflammation, angiogenesis, and metastasis of cancer cells. Moreover, their antioxidant properties may

protect cells from free radicals that could cause DNA alterations [13,14]. Glucosinolates and phenolic compounds present in *Brassica* exert numerous health benefits, including antioxidant, anticancerogenic, antiaggregant, and detoxifying enzyme-inducing activities [15,16].

Based on the above-mentioned information, we hypothesize that a diet rich in bioactive compounds from *Brassica* species, combined with a structured physical exercise protocol, represents an effective therapeutic approach for CRC prevention. Additionally, dietary supplementation with a nutraceutical derived from *Brassica* seed extracts with high antioxidant capacity may help reduce oxidative stress and modulate gut microbiota. Therefore, this study aimed to (i) design a nutraceutical with high antioxidant and detoxifying enzyme-inducing capacity using different *Brassica* seed extracts, (ii) develop an animal experimental model of in situ CRC in mice, and (iii) assess the positive effects of a dietary intervention with the designed nutraceuticals and a mixed exercise program on oxidative stress, inflammation, and intestinal dysbiosis, aiming to expand our understanding of the molecular mechanisms underlying our experimental findings.

2. Materials and Methods

All procedures were carried out collaboratively between the Biomedical Research Center (CIBM) and the Sport and Health University Research Institute (IMUDS) of the University of Granada, Spain.

2.1. Plant Material

All the seeds that were analyzed in this study were supplied by the company Beyond Seeds S.L. (Almería, Spain). A total of six different plants from the *Brassicaceae* family were studied, including three different species, namely *Brassica oleracea*, *Eruca sativa* (*rocket*), and *Sinapis alba* (*mustard*), and three varieties of *Brassica oleracea*, *Brassica oleracea* var. *sabellica* (*Kale*), *Brassica oleracea* var. *italica* (*broccoli*), and *Brassica oleracea var. botrytis* (*cauliflower*).

2.2. Functional Extracts and Nutraceutical Formulation

Two distinct methods were employed to extract bioactive compounds from the plant material: (i) ethanolic extraction for the enhanced extraction of phenolic compounds and glucosinolates and (ii) the hydrolysis of proteins to produce bioactive peptides.

Ethanolic extraction: Seeds or freeze-dried plants were mixed with a hydroalcoholic solution (ethanol:water:HCl, 50:50:0.2 *v*/*v*/*v*) and extracted sequentially for 30 min under continuous stirring at 4 °C and at a pH of 2. This was followed by centrifugation (3500 rpm, 10 min), and the resulting pellet was reused for a new extraction procedure. All supernatants were pooled to form the final ethanolic extract, which was stored at –20 °C. To prevent oxidation, nitrogen (N_2) was used following the method described by Kapravelou et al. [17].

Protein extraction and hydrolysis: Samples were mixed with distilled water (1:4) and extracted for 30 min under the following conditions: pH 8.8, T = 33 °C, and continuous stirred, as described by Kapravelou et al. [18]. After centrifugation (3500 rpm, 5 min), the pellet was subjected to a new extraction process, and combined supernatants were heated to 47 °C for 15 min, followed by the addition of 0.1 M $CaCl_2$ and $MgSO_4$ (1:100 *v*/*v*). Protein hydrolysis was conducted through the sequential addition of proteases from *Bacillus licheniformis* (0.3 AU/g protein) and *Aspergillus oryzae* (100 AU/g protein), each for 30 min at a pH of 8.8 and 47 °C.

Nutraceutical formulation: The nutraceutical was formulated by combining extracts to maximize their synergistic effects on oxidative stress, inflammation, detoxifying enzymes, and intestinal microbiome. The final selection was based on total polyphenol content, which was indicative of the antioxidant capacity. Because of differences in the freeze-drying behavior between ethanolic extracts and protein hydrolysates, the final formulation

consisted of 10% ethanolic extract from *Eruca sativa* seeds, 10% from *Sinapis alba* seeds, 40% protein hydrolysate from *Eruca sativa*, and 40% from *Sinapis alba*.

The volumes of each extract were determined based on the yields after lyophilization (Cryodos-50, TELSTAR, Madrid, Spain). Prior to freezing, ethanol was removed from ethanolic extracts via vacuum evaporation (ThermoSci, Waltham, MA, USA).

2.3. In Vitro Digestion

The designed nutraceutical was subjected to an in vitro digestion process following the methodology described by Porres et al. [19], with slight modifications [20]. The process consisted of three phases: (i) gastric digestion for 2 h, (ii) pH equilibration for 30 min, and (iii) digestion and intestinal absorption through a 2 h equilibrium dialysis process (12,000–14,000 Da, Medicell Membranes Ltd., London, UK). To carry out the in vitro digestion process, 5 g of the sample was mixed with 100 mL of 0.01 N HCl, and the solution was adjusted to a pH of 2 using 1 N HCl. For gastric digestion, 20 mL of the digestion aliquot was mixed with 1 mL of the pepsin solution (0.16 g/mL in 0.1 N HCl). Following the initial preparation steps, dialysis membranes were introduced into the digestion vessels prior to pH adjustment using 0.1 N sodium bicarbonate ($NaHCO_3$). Subsequently, 5 mL of 0.1 N $NaHCO_3$ with bile salts (25 mg/mL) and pancreatin (4 mg/mL) was added to simulate intestinal digestion conditions. Upon completion of the digestion process, the contents inside the dialysis membranes, representing the dialyzed and potentially absorbable fraction, and those remaining outside, representing non-absorbed components potentially reaching the colon, were separately collected and stored at –20 °C for further analyses. Negative control assays were conducted using an equivalent volume of 0.01 N HCl. All procedures were carried out at 37 °C under constant agitation to mimic physiological conditions.

2.4. Antioxidant Activity

The quantification of total polyphenolic content was carried out via a modified Folin–Ciocalteu method according to Martínez et al. [21]. A gallic acid standard curve (0–600 μg/L) was constructed, and absorbance was measured at 760 nm using a Multiskan FC Microplate Photometer (Thermo Fisher Scientific, Waltham, MA, USA). The results were expressed as micrograms of gallic acid equivalents per milligram of extract (μg GAE/mg). A radical cation decolorization assay, ABTS [2,2′-azino-bis(3-ethylbenzothiazoline-6-sulfonic acid)], was assessed using the protocol established by Miller et al. [22]. Briefly, 6 μL of the extract or gallic acid standard solution (0–600 μg/L) was combined with 294 μL of the ABTS solution and incubated for 1–5 min. Absorbance was recorded at 620 nm, and the antioxidant capacity was expressed as μg GAE/mg of extract.

The Fe^{2+} chelating activity of the extracts was determined spectrophotometrically according to the method by Dinis et al. [23], while the reducing power (Fe^{3+} to Fe^{2+}) was determined based on the procedures described by Oyaizu [24] and Duh et al. [25].

2.5. Chromatographic Studies via UPLC-QTOF Analysis

High-resolution mass spectrometric analysis of bioactive compounds in the nutraceutical formulation was performed using ultra-performance liquid chromatography coupled with quadrupole time-of-flight mass spectrometry (UPLC-QTOF; ACQUITY H CLASS and SYNAP G2, Waters, Milford, MA, USA). Prior to analysis, samples were filtered through 0.22 μm nylon syringe filters (Millipore, Burlington, MA, USA), and 10 μL aliquots were injected into the chromatographic system.

Phenolic compounds were separated using an ACQUITY HSS T3 analytical column (100 mm × 2.1 mm, 1.8 μm particle size), in accordance with the method detailed by Martínez et al. [26]. Mass spectrometry was performed under negative electrospray ionization (ESI^-) mode by using high-purity nitrogen as both the desolvation gas (600 L/h)

and the cone gas (30 L/h). Spectra were acquired across a mass-to-charge (m/z) range of 50–1200. Compound identification was tentatively performed based on retention times and characteristic mass fragmentation patterns using the MassLynx software v4.1 (Waters Corp., Milford, MA, USA).

2.6. In Vivo Experimental Design

2.6.1. Animals

For the in vivo assay, 55 male C57BL/6J mice (body weight 15.3 ± 1.1 g at 4 weeks of age) were acquired from Charles River Laboratories (Barcelona, Spain). The mice were randomly assigned to four experimental groups and housed in groups of five per cage in a properly aerated and temperature-regulated space (21 ± 2 °C) (Animal Experimental Unit, CIC, University of Granada). The experiment lasted for 17 weeks, with the first week dedicated to allowing the animals to acclimate to their diet, housing, and training conditions. All animal procedures were conducted in accordance with the ethical guidelines for the care and use of laboratory animals and were approved by the Animal Experimentation Ethics Committee of the University of Granada, Spain (5/10/2021/148). The number of animals used (n = 15 for experimental group and 10 for CT−) was calculated following the principles of the 3Rs to ensure ethical research conduct [27]. It is worth noting that no mouse was excluded during the experimentation.

2.6.2. Experimental Design

The experimental period lasted 17 weeks. Mice were randomly allocated to the following groups: CT−, the healthy control group that received a normocaloric standard diet (TD110675; 3.6 kcal/g, Teklad); CT+, which received a normocaloric standard diet and was subjected to CRC induction.; NT, which received a standard diet supplemented with 0.6% of the formulated nutraceutical following CRC induction; and NT + Ex, which received the same nutraceutical-supplemented diet as the NT group and underwent a structured training protocol during the whole experimental period. Animals were maintained under a reversed light/dark cycle (12:12 h), with ad libitum access to filtered water (type 2) and their respective diets. Daily food consumption was recorded, and body weight was measured weekly at a consistent time point. To ensure blinding, one of the authors was responsible for randomly assigning the experimental groups and providing the diet. At the conclusion of the experimental period, mice were anesthetized via intraperitoneal (IP) injection of ketamine (75 mg/kg) and xylazine (10 mg/kg). Organs were harvested, weighed, and examined for macroscopic abnormalities and immediately immersed in formaldehyde for histological processing. For colon tissue, the Swiss roll technique was used to facilitate the visualization of the intestinal epithelial morphology [28]. Additionally, a section of the colon was preserved in RNAlater (Ambion) and stored at –80 °C for subsequent RNA extraction.

2.6.3. Tumor Induction in the Colon

Tumor induction was performed following the protocol described by Mesas et al. [29], with minor modifications. The development of a tumor was induced by an intraperitoneal injection of azoxymethane (Ref. A5486, Sigma-Aldrich, Madrid, Spain) at a dose of 12 mg/kg and three doses of 2% DSS (Ref. 42867-100MG, Sigma-Aldrich, Madrid, Spain) in drinking water.

2.6.4. Exercise Protocol

To assess maximal aerobic capacity, an incremental treadmill running test was conducted to determine the maximal oxygen consumption (VO_2 max) of the animals, following the protocol by Yang et al. [30], with minor modifications. Testing was conducted using a single-lane treadmill (Panlab LE8708) connected to an LE405 gas analyzer (Panlab, Harvard

Apparatus, Barcelona, Spain). The initial treadmill speed of 20 cm/s was progressively increased by 3 cm/s every minute until a maximum speed of 100 cm/s was reached or until the animal reached exhaustion. For the exercise intervention, animals in the NT + Ex group were trained using a motorized rodent treadmill (Panlab LE8710RTS). During the first week, mice underwent an adaptation period consisting of 10 min of treadmill running per day at 12 cm/s on a 0° incline. This was followed by a structured training program developed by our research group (see Table 1). The protocol consisted of moderate-to-high intensity aerobic exercise performed 5 days per week during the animals' dark cycle, with each session lasting 25 min. In brief, the protocol included a 5 min warm-up at 20% VO_2 max, followed by a first moderate-intensity cycle that consisted of 1.5 min of a progressive speed increase from 30 to 45% VO_2 max and 1 min at 45% VO_2 max. This was followed by four moderate-intensity sets in which the speed of 45% VO_2 max was maintained for 2 min, with additional intervals at 30% VO_2 max for 1 min and 1.5 min rest.

Table 1. Training protocol.

Phase	Time	% VO_2 Max
Warm-up	5′	20
Exercise program		
1×	1′30″ 1′	20 → 45 45
4×	2′ 1′ 1′30″	45 30 Rest

2.6.5. Morphological and Histological Analysis

The colons of the mice were excised, opened, and photographed using the ImageJ software v1.54d for polyp counting and measurement. The fixation of both organs and Swiss roll sections was performed in paraformaldehyde (24 h) and embedded in paraffin blocks. Subsequently, 5 µm sections were cut on a rotary microtome (Leica, Wetzlar, Germany). Finally, the sections were deparaffinized, hydrated, and stained with hematoxylin and eosin (H&E).

2.6.6. Gene Expression Assays

After homogenizing the colon aliquots, total RNA was extracted using 1 mL of Tri-Reagent (Sigma-Aldrich), solubilized in RNase-free water, and treated with DNase (Applied Biosystems, Waltham, MA, USA) to eliminate any DNA. Reverse transcription of RNA (100–250 ng) was then performed in a Lifepro thermal cycler (Bioer Serves Life, Hangzhou, China) according to standard protocols. Quantitative RT-PCR was performed with the Quantum Studio 12 K Flex Real-Time PCR System using primers (Applied Biosystems) for genes involved in oxidative metabolism, detoxification pathways, inflammatory processes, or in tumor development (Table 2). For the PCR reaction, the master mix consisted of the first-strand cDNA template, primers, 2X TaqMan Fast Universal PCR Master Mix, and No AmpErase UNG (Applied Biosystems). *ß-actin* was used as an internal control. Data analysis was performed using the 2 ΔΔCt method with the control group as the reference.

2.6.7. Metagenomic Analysis

Cecal contents were collected for the isolation of genomic DNA (gDNA). Extraction was performed using the QIAamp® (Venlo, The Netherlands) PowerFecal® (Woodcliff Lake, NJ, USA) DNA kit according to the manufacturer's protocol for process automation using the QIAcube robot. The concentration of gDNA was determined using fluorometry

(qubit). The V4 region (233 bp) of 16S ribosomal RNA (rRNA) genes was sequenced by the MiSeq system (Illumina, San Diego, CA, USA) for the analysis of gDNA samples. The Institute of Parasitology and Biomedicine López-Neyra (IPBLN) of the Spanish National Research Council (CSIC, Granada, Spain) performed the library preparation, pooling, and miniSeq sequencing.

Table 2. Reference of primers for genes analyzed in the study.

Function	Genes	Primers
Oxidative metabolism	*cat*	Mm00437992
	gpx2	Mm01286848
	sod1	Mm01344233_g1
Detoxification pathways	*nqo1*	Mm00500822_g1
	gsta1	Mm03019257_g1
Inflammatory process	*IL-1b*	Mm00434228_m1
	IL-6	Mm00446190_m1
Tumor development	*cadm1*	Mm00457551_m1
	cdc42	Mm01194005_g1
	pik3cd	Mm00435674_m1
	slc20	Mm00489378_m1

2.7. Statistical Analysis

Descriptive statistical methods were employed, like absolute frequency statistics which are expressed as the mean and standard deviation and relative frequency ones which are expressed as percentages. Significant differences were analyzed using one-way analysis of variance (ANOVA), and Tukey's test was used to distinguish differences between means. Results are reported as the mean plus standard deviation (SD) of three replicates for in vitro experiments and of ten (the CT− group) and fifteen (CT+, NT, and NT + Ex groups) replicates for the in vivo study. Eight animals were included in the gene expression analysis. For in vitro digestion results, student's *t*-tests were applied to analyze significant differences. Statistical Package for Social Sciences (IBM SPSS for Windows®, version 22.0, Armonk, NY, USA) was used for all the analyses, and the significance level was set at $p < 0.05$.

3. Results

3.1. Antioxidant Capacity of Brassicaceae Extracts

The extraction yield and antioxidant capacity of the different functional extracts obtained from *Brassicaceae* seeds, as well as the nutraceutical formulated, are shown in Table 3. Regarding the ethanolic extracts, *Sinapis alba* seeds showed a higher extraction yield (120.8 ± 1.3 mg of extract per gram of flour), as well as a significantly higher concentration of total polyphenols (60.5 ± 1.0 μg gallic acid equivalent per mg of extract). The ethanolic extract of *Eruca sativa* seeds demonstrated the highest antioxidant capacity in the rest of the tests. Specifically, in the ABTS test and iron-reducing capacity assay, it achieved values of 15.0 ± 0.0 and 43.5 ± 1.4 μg gallic acid equivalent per mg of extract, respectively, while its iron-chelating activity was 3.99 ± 0.06 chelating activity units per mg of extract (CAU/mg).

A similar trend of results was obtained from the protein hydrosylates. The protein hydrolysate from *Eruca sativa* seeds exhibited significantly higher values than the other species tested in their ability to scavenge ABTS free radicals (17.0 ± 0.4 μg gallic acid/mg hydrolysate) and their iron-chelating activity (1.34 ± 0.02 CAU/mg HP), whereas the protein hydrolysate from *Sinapis alba* seeds yielded the highest extraction efficiency (31.9 ± 1.1%). In this case, the highest concentration of total polyphenols was observed in the hydrolysates

of both seeds, with 33.6 ± 0.4, and 31.7 ± 0.4 µg gallic acid/mg hydrolysate for *Eruca sativa* and *Sinapis alba*, respectively. Based on these findings, a nutraceutical was developed using these two plant species, which maintained the antioxidant capacity in all chemical assays (Table 3).

Table 3. Antioxidant capacity of the different *Brassicaceae* seed extracts and the nutraceutical.

	Yield (mg/g)	TPC (µg GA)	ABTS (µg GA)	ICC (CAU)	IRC (µg GA)
			EtOH		
BO var. *sabellica*	115.4 ± 2.9 ^{b}	30.9 ± 0.5 ^{b}	11.6 ± 0.4 ^{bc}	1.56 ± 0.11 ^{b}	25.9 ± 1.4 ^{b}
BO var. *italica*	115.3 ± 9.7 ^{b}	31.4 ± 0.9 ^{b}	12.8 ± 0.1 ^{c}	1.29 ± 0.09 ^{b}	27.7 ± 0.3 ^{b}
BO var. *botrytis*	132.1 ± 4.6 ^{b}	27.9 ± 0.4 ^{a}	10.2 ± 0.7 ^{b}	0.87 ± 0.01 ^{a}	20.1 ± 0.6 ^{a}
Eruca sativa	86.9 ± 1.9 ^{a}	43.5 ± 0.4 ^{c}	15.0 ± 0.0 ^{d}	3.99 ± 0.06 ^{c}	43.5 ± 1.4 ^{c}
Sinapis alba	120.8 ± 1.3 ^{b}	60.5 ± 1.0 ^{d}	7.4 ± 0.1 ^{a}	0.98 ± 0.05 ^{a}	18.8 ± 1.2 ^{a}
			HP		
BO var. *sabellica*	24.4 ± 0.2 ^{b}	28.5 ± 0.3 ^{b}	12.2 ± 0.7 ^{a}	1.00 ± 0.03 ^{a}	13.1 ± 0.3 ^{b}
BO var. *italica*	27.3 ± 0.3 ^{c}	26.2 ± 0.3 ^{ab}	10.2 ± 0.3 ^{a}	1.10 ± 0.02 ^{ab}	12.9 ± 0.2 ^{b}
BO var. *botrytis*	29.3 ± 0.6 ^{cd}	25.1 ± 1.1 ^{a}	11.5 ± 0.7 ^{a}	1.19 ± 0.07 ^{b}	13.0 ± 0.2 ^{b}
Eruca sativa	20.3 ± 0.4 ^{a}	33.6 ± 0.4 ^{c}	17.0 ± 0.4 ^{b}	1.34 ± 0.02 ^{c}	12.8 ± 0.1 ^{b}
Sinapis alba	31.9 ± 1.1 ^{d}	31.7 ± 0.4 ^{c}	11.1 ± 0.4 ^{a}	0.98 ± 0.02 ^{a}	8.0 ± 0.1 ^{a}
NT		32.5 (0.3)	7.8 (0.1)	0.93 (0.04)	9.1 (0.1)

BO, *Brassica oleracea*. CAU, chelating activity unit. EtOH, ethanolic extract. GA, gallic acid. HP, protein hydrolysate. ABTS, 2,2′-azino-bis3-ethylbenzothiazoline-6-sulfonic acid. ICC, iron-chelating capacity. IRC, iron-reducing capacity. NT, nutraceutical. TPC, total polyphenol content. Results are the means plus the SD (in parenthesis) of four replicates expressed per milligram of extract. Means with different letters (a, b, c and d) indicate significant differences (ANOVA $p < 0.05$).

3.2. In Vitro Digestion

The results of the in vitro digestion tests are summarized in Table 4. After the digestion process, 73.1% of the formulated nutraceutical was found to be potentially absorbable. Additionally, in vitro digestion did not affect the antioxidant capacity of either the bioavailable (dialyzed) fraction or the non-absorbable components (retained) that reach the colon. In both cases, the antioxidant capacity remained significantly higher than that of the blank.

Table 4. Dializability and antioxidant activity of NT after an in vitro digestion.

	Dialyzed		Retained	
	Blank	NT	Blank	NT
Dializability (%)		73.1 ± 2.3		
TPC (µg GA)	7.21 ± 0.23	54.5 ± 1.1 *	8.24 ± 0.4	56.8 ± 1.2 *
ABTS (µg GA)	8.96 ± 0.23	16.0 ± 0.4 *	7.05 ± 0.27	15.7 ± 0.4 *
ICC (CAU)	0.59 ± 0.03	1.44 ± 0.01 *	0.41 ± 0.02	2.48 ± 0.03 *
IRC (µg GA)	0.80 ± 0.11	11.1 ± 0.55 *	1.53 ± 0.16	8.9 ± 0.3 *

CAU, chelating activity unit. GA, gallic acid. ICC, iron-chelating capacity. IRC, iron-reducing capacity. NT, nutraceutical. TPC, total polyphenol content. Results are the means plus the SD (in parenthesis) of four replicates expressed per milligram of sample. (*) Statistical significance compared to the blank according to Student's *t*-test ($p < 0.01$).

3.3. Mass Spectrometry Identification of Bioactive Compounds

The chromatographic profile and the main compounds tentatively identified in the nutraceutical formulation are presented in Figure 1 and Table 5, respectively. A total of 30 biocompounds were identified, with flavonoids being the most representative class including 10 compounds (cucumerin B, dichamanetin, epigallocatechin, eucalyptin, gallocatechin,

moracenin D, nobiletin, pectolinarigenin, prenylnaringenin, and quercetin), followed by terpenoids with 6 compounds (chamissonolide, hydrangenoside A, kirenol, ligustrosidic acid, lucidumoside C, and pyrohyperforin). In addition, two compounds were identified within the phenolic acid class (curculigoside A and populin), as well as two phenilpropanoids (atharticin and nothoapiole) and two glucosids (marinoid D and prunioside A). Other identified compounds belonged to the following groups: alkaloid (nesodine), chromones (cimifugin), quinone (rubialatin A), isoflavans, furans (mumefural), isoflavones (glycitin), ether (crotepoxide), long-chain fatty alcohol (persealide), and lignans (diphyllin).

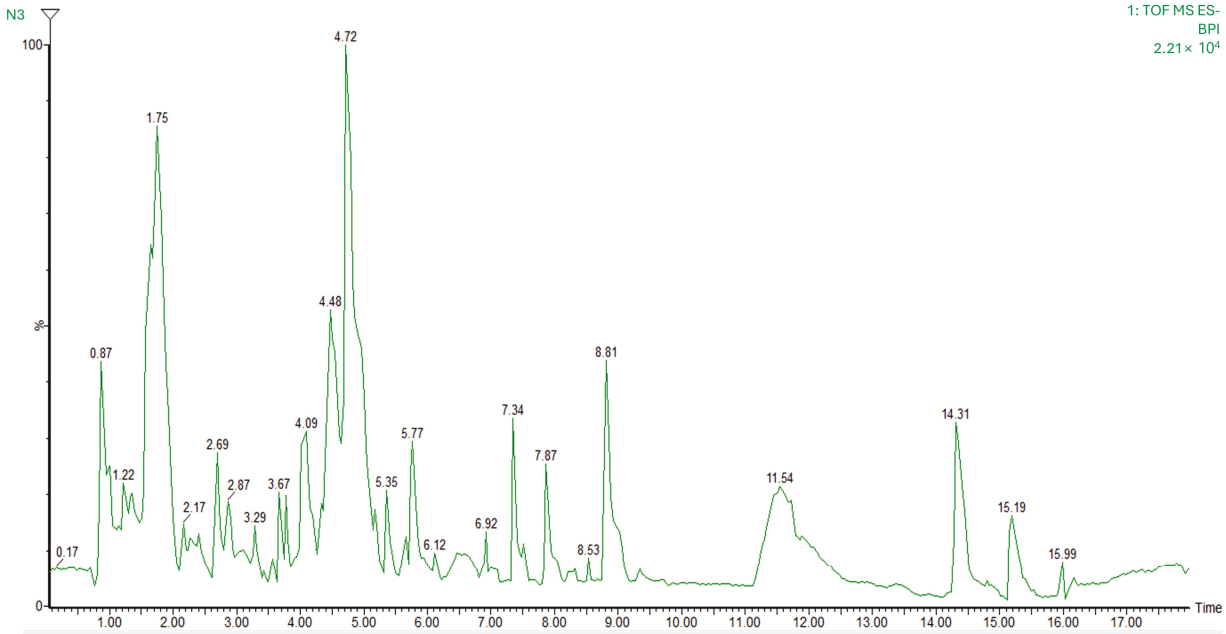

Figure 1. Chromatographic profile of bioactive compounds identified in the nutraceutical using high-performance liquid chromatography.

Table 5. Identification of bioactive compounds in the nutraceutical.

RT	MS	COMPOUND	MF [H$^-$]	% FIT	F1	F2	F3
0.95	313.0712	Pectolinarigenin	$C_{17}H_{13}O_6$	96.65	225.0631	180.0354	120.0542
1.22	299.0403	Mumefural	$C_{12}H_{11}O_9$	98.65	240.0316	225.069	220.0431
2.17	379.0818	Diphyllin	$C_{21}H_{15}O_7$	34.36	293.0519	280.1175	105.0269
2.41	471.0927	Epigallocatechin ([1])	$C_{23}H_{19}O_{11}$	99.45	331.0149	253.0714	209.0065
2.67	471.108	Rubialatin A	$C_{27}H_{19}O_8$	69.13	347.0891	293.041	267.1032
2.69	361.0923	Crotepoxide	$C_{18}H_{17}O_8$	99.94	220.0375	159.0295	119.0415
2.70	505.171	Prunioside A	$C_{25}H_{29}O_{11}$	93.83	347.0891	293.041	267.1032
3.57	305.066	(+)-Gallocatechin	$C_{15}H_{13}O_7$	99.1	267.0891	239.0623	221.0522
3.78	465.1397	Curculigoside A	$C_{22}H_{25}O_{11}$	99.5	347.0685	331.0488	253.0787
4.01	167.1553	Cimifugin ([2])	$C_{22}H_{27}O_{11}$	99.33	227.0043	220.0349	209.0298
4.16	583.2027	Lucidumoside C	$C_{27}H_{35}O_{14}$	89.84	301.1084	262.0572	220.0384
4.19	551.1553	Cucumerin B	$C_{29}H_{27}O_{11}$	2.85	315.1268	294.0228	262.0588
4.33	553.1557	Ligustrosidic acid	$C_{25}H_{29}O_{14}$	99.07	294.0379	267.0679	253.0775
4.35	553.1557	Marinoid D	$C_{25}H_{29}O_{14}$	99.07	317.038	267.0788	250.0633
4.65	445.1135	Glycitin	$C_{22}H_{21}O_{10}$	1.49	317.0562	267.0958	250.0111
4.68	771.1773	Quercetin ([3])	$C_{36}H_{35}O_{19}$	8.75	267.0869	253.084	227.0035
4.72	467.1495	Dichamanetin	$C_{29}H_{23}O_6$	10.39	253.0823	239.0681	195.0144
5.73	401.1236	Nobiletin	$C_{21}H_{21}O_8$	91.69	347.0704	253.0765	239.0632
6.12	709.2285	Moracenin D	$C_{40}H_{37}O_{12}$	38.63	668.2699	267.0976	239.0707
6.92	551.2856	Lokundjoside	$C_{29}H_{43}O_{10}$	84.27	287.1523	267.1325	165.0612

Table 5. *Cont.*

RT	MS	COMPOUND	MF [H⁻]	% FIT	F1	F2	F3
6.95	389.1236	Populin/Populoside	$C_{20}H_{21}O_8$	84.36	301.1513	220.0353	195.0285
7.34	323.1495	Chamissonolide	$C_{17}H_{23}O_6$	99.75	309.135	262.0421	221.0459
7.87	251.0919	Nothoapiole	$C_{13}H_{15}O_5$	n/a	220.036	207.0571	158.9771
8.32	753.2242	Catharticin	$C_{34}H_{41}O_{19}$	15.22	331.0123	253.071	239.0514
8.53	325.1076	Eucalyptin	$C_{19}H_{17}O_5$	94.85	299.1306	267.0681	220.025
8.81	619.2391	Hydrangenoside A	$C_{31}H_{39}O_{13}$	54.88	556.2574	262.052	220.054
9.86	339.1232	8-Prenylnaringenin	$C_{20}H_{19}O_5$	98.19	339.1318	239.0277	105.0285
11.36	533.3631	Pyrohyperforin	$C_{35}H_{49}O_4$	16.01	400.2627	301.1781	159.0122
12.91	433.2015	Nesodine	$C_{27}H_{29}O_5$	25.23	317.0427	267.1048	239.073
14.31	337.2379	Kirenol	$C_{20}H_{33}O_4$	n/a	323.22	136.0556	119.0428
15.19	339.2535	Persealide	$C_{20}H_{35}O_4$	n/a	325.2375	207.0567	159.0379

F1, F2, and F3: fragments. MF, molecular formula. MS, mass. RT, retention time. n/a, not applicable. ([1]) Epigallocatechin-O-(3-O-methyl) gallate. ([2]) Cimifugin ß-D-glucopyranoside. ([3]) Quercetin 3-O-a-6‴-caffeoylglucosyl-ß-1.2-rhamnoside.

3.4. In Vivo Experimental Model

3.4.1. Body Weight and Food/Water Intake

Figure 2 illustrates the effects of colon cancer induction and interventions on body weight and food/water intake in mice throughout the experimental period. The initial animal weight was 15 ± 1 g, and all animals reached 22 ± 2 g by the end of the study period (Figure 2A). A temporary weight loss was observed at weeks 5, 8, and 11 in the CT+, NT, and NT + Ex groups, corresponding to the administration of DSS in drinking water for tumor induction. Regarding food intake (Figure 2B), no significant differences were observed between groups, except at weeks 5, 8, and 10, when a decrease in intake was detected in the tumor-bearing groups (CT+, NT, and NT + Ex) due to DSS-induced discomfort. However, there were no significant differences in the intake of drinking water when the DSS was administered (Figure 2C).

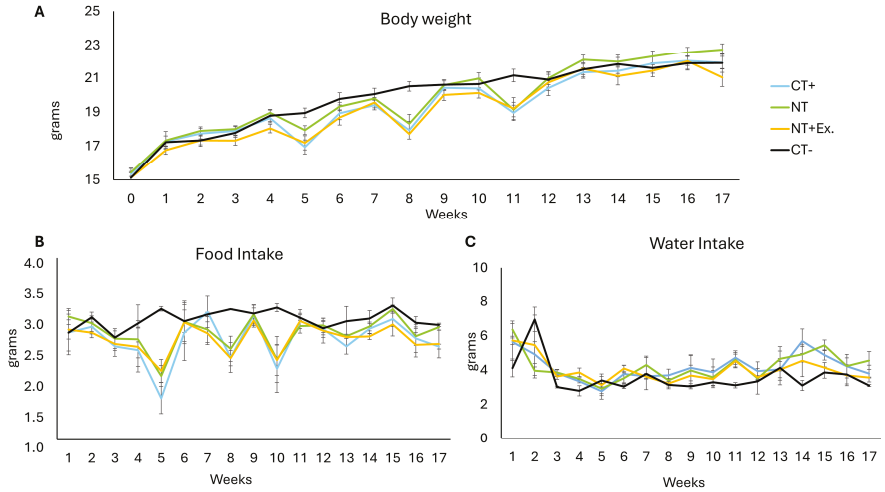

Figure 2. (**A**) Body weight, (**B**) food intake, and (**C**) water intake of mice fed different experimental diets. CT−, healthy animals fed the control diet. CT+, tumor-induced animals fed the control diet. NT, tumor-induced animals fed the control diet supplemented with the nutraceutical. NT + Ex, tumor-induced animals fed the control diet supplemented with the nutraceutical combined with the exercise protocol. Results are expressed as the means plus the SD (vertical bars) of 15 replicates.

3.4.2. Tissue and Organ Weights

The effects of tumor development and the different interventions performed on organ weight and colon length are presented in Table 6. Tumor development led to a significant

increase in the weight of the colon, spleen, and liver, although the increment in liver weight was not statistically significant. In addition, tumor development led to a shortening of the colon and the thickening of its wall. Only the nutritional intervention (NT group) significantly reduced colon weight (0.25 ± 0.02 g) and prevented colon shortening, with values comparable to the healthy control group (6.28 ± 0.15 cm vs. 6.88 ± 0.18 cm, respectively).

Table 6. Effect of tumor development and nutritional or physical exercise interventions on organ weights (g) and colon length (cm).

	CT−	CT+	NT	NT + Ex
Liver	0.798 ± 0.026 ^{a}	0.863 ± 0.026 ^{ab}	0.868 ± 0.014 ^{ab}	0.886 ± 0.017 ^{b}
Kidneys	0.108 ± 0.002 ^{a}	0.109 ± 0.002 ^{a}	0.113 ± 0.002 ^{a}	0.109 ± 0.002 ^{a}
Heart	0.113 ± 0.002 ^{a}	0.105 ± 0.002 ^{a}	0.109 ± 0.002 ^{a}	0.107 ± 0.003 ^{a}
Spleen	0.071 ± 0.001 ^{a}	0.165 ± 0.017 ^{b}	0.132 ± 0.009 ^{b}	0.150 ± 0.016 ^{b}
Plantaris	0.013 ± 0.000 ^{a}	0.012 ± 0.001 ^{a}	0.013 ± 0.000 ^{a}	0.013 ± 0.000 ^{a}
Cecum	0.096 ± 0.005 ^{a}	0.103 ± 0.004 ^{a}	0.099 ± 0.002 ^{a}	0.096 ± 0.004 ^{a}
Gastrocnemius	0.095 ± 0.003 ^{a}	0.095 ± 0.002 ^{a}	0.103 ± 0.002 ^{a}	0.105 ± 0.003 ^{a}
Colon	0.119 ± 0.015 ^{a}	0.338 ± 0.031 ^{c}	0.248 ± 0.022 ^{b}	0.262 ± 0.009 ^{bc}
Colon length	6.88 ± 0.18 ^{b}	5.99 ± 0.28 ^{a}	6.28 ± 0.15 ^{ab}	6.08 ± 0.13 ^{a}

CT−, healthy animals fed the control diet. CT+, tumor-induced animals fed the control diet. NT, tumor-induced animals fed the control diet supplemented with the nutraceutical. NT + Ex, tumor-induced animals fed the control diet supplemented with the nutraceutical combined with the exercise protocol. Results are expressed as the means plus the SD (parenthesis) of 15 replicates. Means values with different letters (a, b, and c) represent significant differences (ANOVA, $p < 0.05$).

3.4.3. Modulation of Polyp Size and Number

The effect of the nutritional intervention, alone or combined with the physical exercise protocol, on the number of polyps and the area occupied by these polyps is shown in Figure 3. Tumor induction resulted in polyp development in the positive control group (CT+) of 24.3 ± 2.9% of the total colon area. In the NT group, polyps were significantly smaller, occupying 11.2 ± 1.0% of the total colon area. Although not statistically significant, the area occupied by the tumor was further reduced to 9.1 ± 0.8% when the nutraceutical was combined with the exercise program (NT + Ex). Regarding the number of polyps, the CT+ group showed a mean of 5.45 ± 0.52 polyps, whereas the NT group significantly reduced this number to 3.73 ± 0.38 polyps. In the NT + Ex group, polyps were further reduced to 2.60 ± 0.31.

3.4.4. Histological Analysis

The histological analyses using H&E staining of samples from the Swiss Roll colon, liver, spleen, and kidney are shown in Figures 4 and 5. The positive control (CT+) exhibited disrupted colonic crypt architecture, the absence of goblet cells, and dysplastic polyps marked by colonic epithelial cells with abnormal nuclei. In contrast, the Swiss roll colon samples from treated mice (NT and NT + Ex) showed a significantly lower number of polyps, and those that developed polyps exhibited a lower degree of dysplasia compared to those in the untreated group (CT+). In the CT+ group, a disruption in the organization between the white pulp and the red pulp of the spleen was also observed. The groups that ingested the nutraceutical throughout the experimental period were able to reverse this effect, showing an organization very similar to that of the healthy control group.

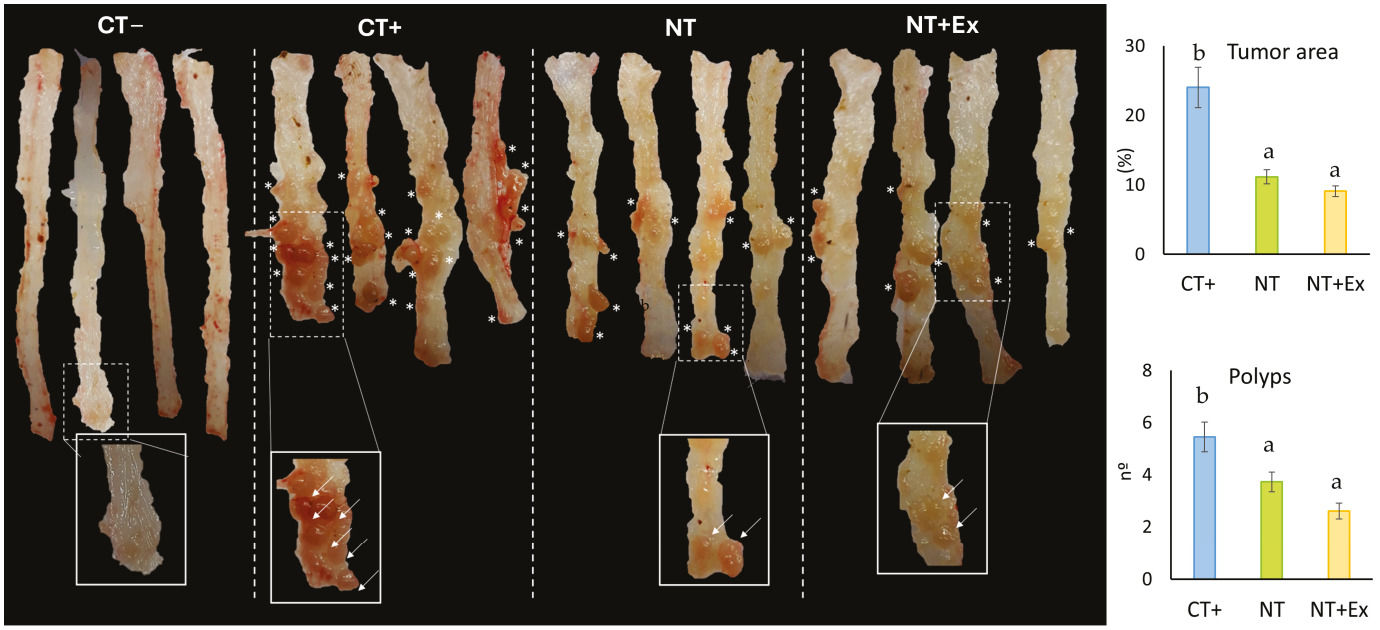

Figure 3. Effect of the nutritional intervention (NT), alone or in combination with physical exercise (NT + Ex), on the number of polyps and the area occupied by polyps. Asterisks (*) indicate each of the polyps identified in the colons of the animals. Arrows point to the polyps located in the enlarged segment of the colon. Results are expressed as the means plus the SD (parenthesis) of 15 replicates. Means values with different letters (a and b) represent significant differences (ANOVA, $p < 0.05$).

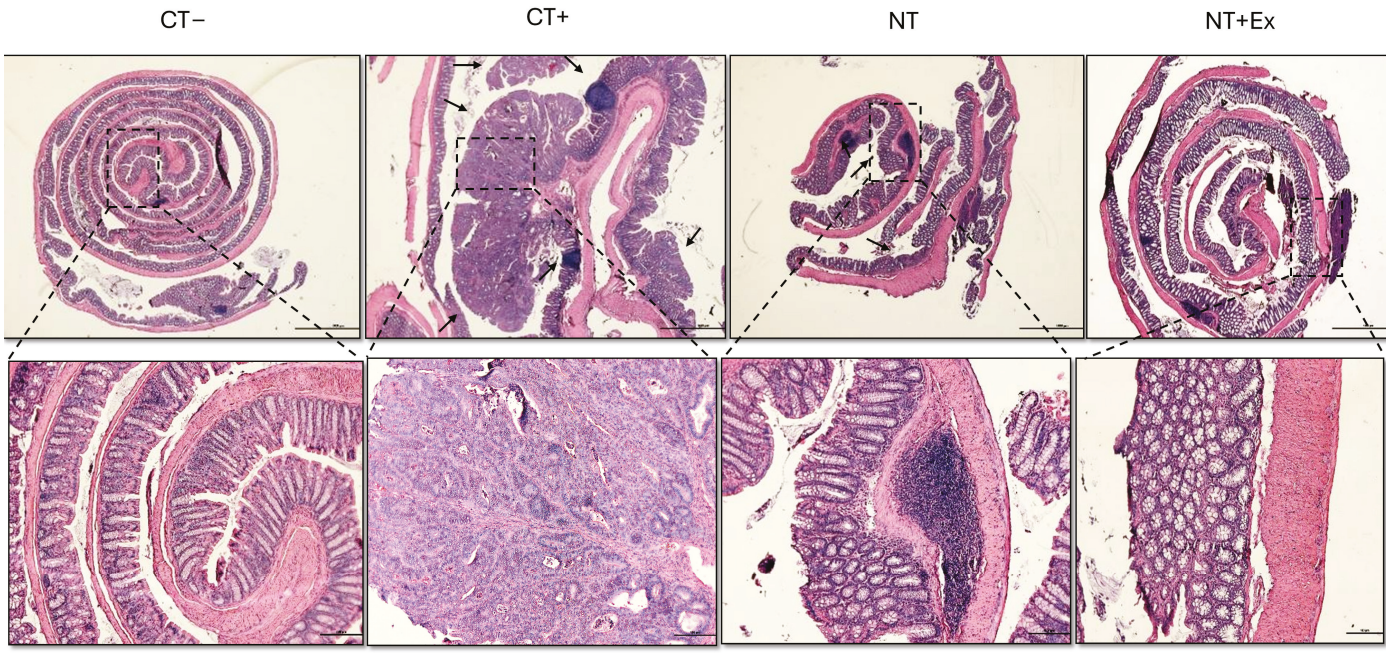

Figure 4. Representative H&E-stained histological images following tumor induction via AOM/DSS. The Swiss roll technique was used to analyze the colon (scale bar = 1000 μm [top row] and 100 μm [bottom row]). Arrows indicate polyps with dysplasia. CT−, healthy animals fed the control diet. CT+, tumor-induced animals fed the control diet. NT, tumor-induced animals fed the control diet supplemented with the nutraceutical. NT + Ex, tumor-induced animals fed the control diet supplemented with the nutraceutical combined with the exercise protocol.

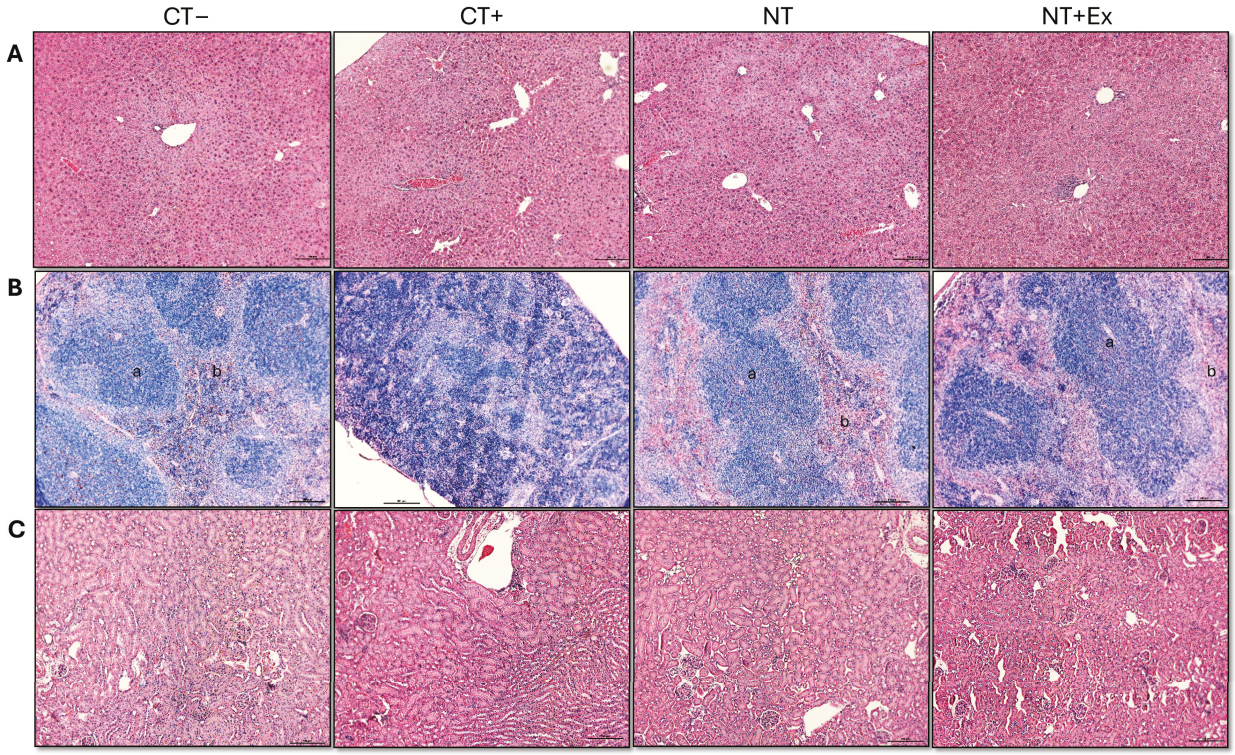

Figure 5. Representative images of the histological analysis of organs from different experimental groups. The H&E method was used to analyze the liver (**A**), spleen (**B**), and kidneys (**C**). In spleen samples, the white pulp and the red pulp are indicated by (a) and (b), respectively. Bars, 100 µm.

3.4.5. Gene Expression

Table 7 presents the gene expression levels in the colon of experimental animals. Tumor induction and development led to a significant increase in the expression of the *slc20*, *pik3cd*, and *IL-1b* genes, whereas the expression of *gpx2*, *sod1*, *gsta1*, and *IL-6* was reduced. The different interventions successfully restored the expression levels of *gpx2*, *sod1*, *pik3cd*, and *slc20* to normal values. Moreover, they significantly increased the expression of *noq1* and decreased the expression of cadm1, *cdc42*, and *IL-6*, even below the levels observed in the control group.

Table 7. Gene expression levels in the colon of mice at the end of the experimental period.

	CT−	CT+	NT	NT + Ex
cat	1.00 ± 0.18^{b}	0.77 ± 0.08^{ab}	0.93 ± 0.04^{ab}	0.75 ± 0.04^{a}
gpx2	1.00 ± 0.12^{b}	0.64 ± 0.08^{a}	1.21 ± 0.09^{b}	1.05 ± 0.04^{b}
sod1	1.00 ± 0.16^{c}	0.38 ± 0.05^{a}	0.86 ± 0.06^{bc}	0.72 ± 0.03^{b}
nqo1	1.00 ± 0.18^{a}	0.79 ± 0.14^{a}	2.36 ± 0.11^{b}	2.23 ± 0.11^{b}
gsta1	1.00 ± 0.14^{c}	0.65 ± 0.08^{b}	0.72 ± 0.08^{b}	0.27 ± 0.02^{a}
cadm1	1.00 ± 0.16^{b}	1.00 ± 0.14^{b}	0.75 ± 0.03^{a}	0.67 ± 0.03^{a}
cdc42	1.00 ± 0.15^{b}	1.23 ± 0.23^{b}	0.64 ± 0.04^{a}	0.55 ± 0.01^{a}
IL-1ß	1.00 ± 0.11^{a}	1.73 ± 0.17^{b}	1.56 ± 0.18^{b}	1.29 ± 0.09^{ab}
IL-6	1.00 ± 0.21^{c}	0.54 ± 0.09^{b}	0.39 ± 0.03^{ab}	0.18 ± 0.01^{a}
pik3cd	1.00 ± 0.09^{b}	2.64 ± 0.28^{c}	0.70 ± 0.07^{ab}	0.52 ± 0.04^{a}
slc20	1.00 ± 0.09^{a}	4.49 ± 0.40^{b}	0.97 ± 0.08^{a}	0.70 ± 0.03^{a}

CT−, healthy animals fed the control diet. CT+, tumor-induced animals fed the control diet. NT, tumor-induced animals fed the control diet supplemented with the nutraceutical. NT + Ex, tumor-induced animals fed the control diet supplemented with the nutraceutical combined with the exercise protocol. Results are expressed as means plus the SD (parenthesis) of 15 replicates. Mean values with different letters (a, b, and c) represent significant differences (ANOVA, $p < 0.05$).

3.4.6. Metagenomic Analysis

Figure 6 illustrates the effect of tumor development, nutritional interventions, and physical exercise on the relative abundance of bacteria in the cecum content of the experimental groups. Tumor development resulted in a significant increase in the phylum *Verrucomicrobia* that was not reversed with the different interventions applied. No additional significant differences related to tumor development were observed, but the presence of bacteria belonging to the phylum *Firmicutes* and *Actinobacteria* was reduced in the groups that had developed a tumor and had been fed the nutraceutical, while the presence of *Bacteroidetes* was increased in the group that also underwent the physical exercise protocol. Consequently, the ratio of Firmicutes/Bacteroidetes was significantly decreased by the nutritional intervention. The development of CRC significantly increased the presence of bacteria belonging to the *Verricomicrobiaceae* family and other unclassified families and decreased that of *Lachnospiraceae* and *Porphyromonadaceae*. These last two were reverted to the standard values of healthy mice when the nutraceutical was administered in the diet and the physical exercise protocol was performed.

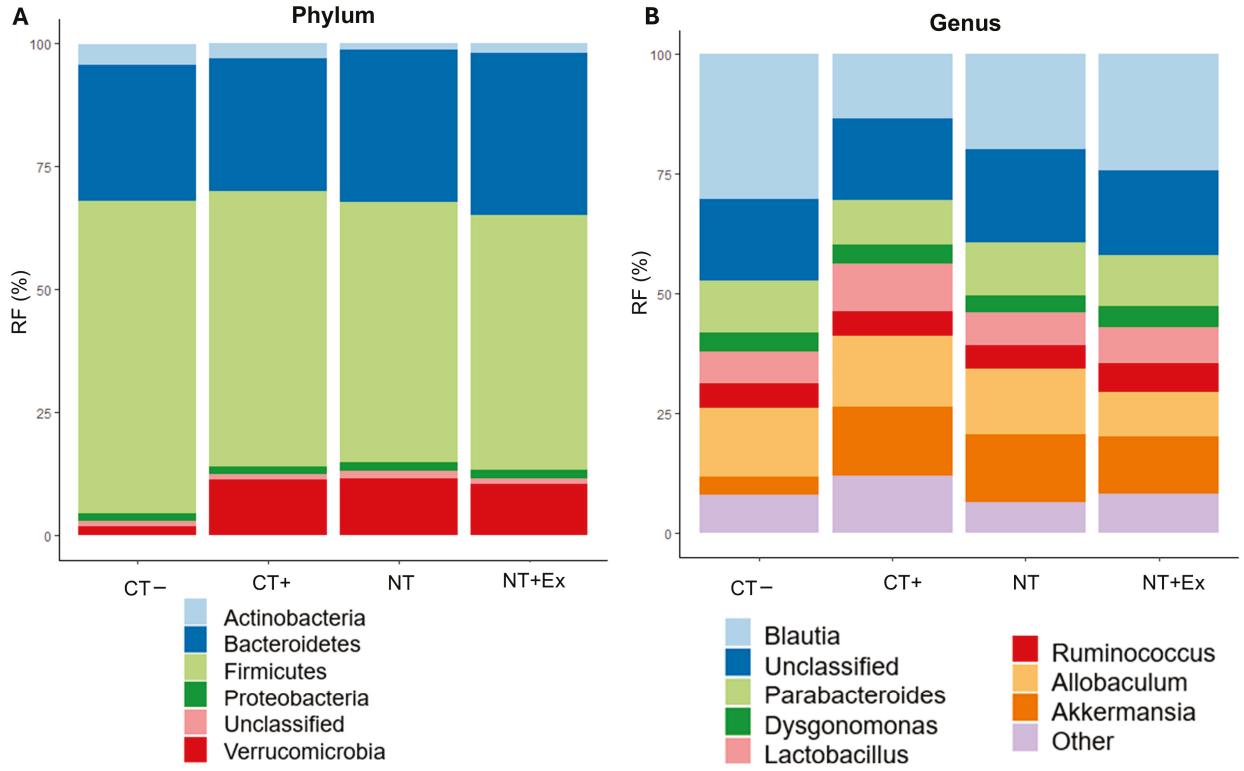

Figure 6. Metagenomic analysis of caecum content in the experimental groups, showing bacterial abundance at the level of phylum (**A**) and genus (**B**). CT−, healthy animals fed the control diet. CT+, tumor-induced animals fed the control diet. NT, tumor-induced animals fed the control diet supplemented with the nutraceutical. NT + Ex, tumor-induced animals fed the control diet supplemented with the nutraceutical combined with the exercise protocol. Results are the means of 8 replicates.

At the genus level, *Blautia* was significantly reduced due to tumor development. However, its concentration increased with the nutritional intervention treatment, reaching levels comparable to those of healthy mice (CT−) when combined with the physical exercise protocol (NT + Ex). The *Lactobacillus* genus significantly increased its concentration with tumor development and was influenced by the nutritional intervention, showing similar values to the control group, that is, those animals that had been fed the nutraceutical (NT). The presence of the genus *Akkermansia* showed a significant increase in all groups that had developed the tumor.

4. Discussion

Natural products are a promising tool for treating or preventing CRC. Nearly 50% of the currently available treatments for CRC have been developed directly or indirectly from natural compounds [31,32]. Among these, the *Brassicaceae* family has been identified as an excellent source of bioactive compounds with antitumor properties [33]. Of all the *Brassicaceae* extracts analyzed in this study, the highest extraction yield and the highest polyphenol content were obtained in the ethanolic extract of *Sinapis alba* seeds. For ABTS, lipid peroxidation inhibition, and iron-chelating or iron-reducing capacity tests, the best results were achieved with the *Eruca sativa* seed extract. These results are consistent with the findings by Khalil et al. [34], who reported that *Eruca sativa* seeds showed a significantly enhanced ability to scavenge 2,2-diphenyl-1-picrylhydrazyl (DPPH) free radicals in comparison to other *Brassicaceae* species.

To induce in situ CRC in C57BL-6J mice, an intraperitoneal administration of AOM and three administrations of DSS in the drinking water were employed. This CRC induction model has been successfully validated in previous studies from our research group [29] and is widely used in the study of CRC, as it accurately replicates the full process of colon carcinogenesis, from the initial crypt proliferation phase to the final development of carcinoma [35]. Specifically, as we demonstrate in histological studies, the induction by AOM and DSS induces dysplastic polyps that are the previous step to invasive carcinoma, as described by Robertis et al. [36] AOM/DSS-induced tumors have mutations of Kas and β-catenin but not p53 mutations.

The nutritional intervention, either on its own or combined with the training protocol, significantly reduced the number of polyps developed in the colon with respect to the untreated control group (CT+). This effect can be attributed to the bioactive compounds identified in the nutraceutical, as in vitro digestibility tests confirmed that dialysates and retained fractions from nutraceutical-enriched diets exhibited higher antioxidant activity than those from the control diet. These findings suggest that some of the antioxidant compounds in the nutraceutical were potentially absorbable, which facilitates the exertion of beneficial systemic effects [37,38]. Specifically, several bioactive molecules identified in the nutraceutical have been previously studied for their anticancer properties in CRC. The flavonoid pectolinarigenin has demonstrated anticancer effects both in vitro and in vivo by inhibiting the cell growth, migration, and invasion of colon cancer cells (HCT116 and CT26). Furthermore, it has been shown to reduce the size and number of tumor nodules in a subcutaneous cancer model of Balb/c mice induced with CT26 colon cancer cells [39], T24 bladder cancer cells [40], or ACS gastric cancer cells [41]. Other authors have reported that the flavonoid epigallocatechin is able to inhibit tumor cell growth via the PI3K pathway and can be used as a chemotherapeutic [42], a chemopreventive agent [43], or as combinatorial therapy with anti-CTLA4 [44] against CRC. Dichamentin has shown a cytotoxic effect against HCT-116 CRC cells while demonstrating no cytotoxic effects on the non-cancerous lung cell line MRC-5 [45]. Quercetin exerts chemopreventive effects by inducing a large number of transcription factors that regulate metabolic pathways such as cell cycle, cell adhesion, gene transcription, or the immune response [46]. Nobiletin is another flavonoid with preventive effects on CRC progression, which is mediated by modulating the Akt signaling pathway, suppressing angiogenesis, and inhibiting CRC progression [47].

The preventive effect of *Brassicaceae* consumption against tumor development has been demonstrated in several studies. For instance, Baenas et al. [48] reported that the administration of 100 mg/kg of an aqueous extract from broccoli sprouts 30 days before tumor induction significantly reduced brain tumor size and progression in an experimental rat model. Similarly, *Brassicaceae* consumption has been shown to reduce preneoplastic colon lesions as well as the expression of cancer stem cell markers in rats [49]. This

effect has been attributed to the set of phenolic compounds, isothiocyanates, vitamins, and nutrients present in these species, which act as an effective and favorable matrix in the stimulation of detoxifying enzymes and activators of the cellular antioxidant defense process [48]. Several population-based studies have examined the relationship between *Brassica* consumption and the decrease in the risk of developing CRC [50]. In the study by Mori et al. [51], no significant association was found between *Brassica* consumption and the risk of developing CRC in the Japanese population. However, these authors identified a positive association between plant-derived polyphenol consumption and CRC prevention, which is in agreement with our findings.

In the present study, no metabolic alterations or organ lesions derived from nutraceutical ingestion were found. In fact, the null toxicity of ethanolic extracts of *Eruca sativa* and *Sinapis alba* seeds has been reported by other authors. For instance, Xian et al. [52] demonstrated that the ingestion of up to 2500 mg/kg (maximum tested dose) of an ethanolic extract of *Sinapis alba* seeds proved to be innocuous in an experimental animal model of Balb/c mice, showing no signs of toxicity, deterioration, or death in the animals. Similarly, the nasogastric administration of up to 200 mg/kg of an ethanolic extract of *Eruca sativa* seeds also showed no signs of toxicity in an experimental Wistar rat model [53].

CRC is associated with oxidative stress and chronic inflammation [54,55]. In this experiment, tumor development led to a reduced expression of antioxidant enzymes (*gpx* and *sod1*) and the detoxification enzyme *gst*, along with an increased expression of transcription factors related to inflammatory activity such as *IL-1ß*. All these parameters were reversed in the groups that ingested the nutraceutical. Furthermore, the former intervention increased the transcript expression of quinone reductase enzyme (*nqo1*), which is involved in cellular detoxification, and decreased the expression of *IL-6*. These effects are assignable to the high phenolic content of the nutraceutical, as phenolic compounds are potent antioxidants capable of neutralizing free radicals; preventing the oxidation of lipids, proteins, and nucleic acids; and reducing colonic mucosa inflammation [56]. Other authors have reported that the administration of 200 mg/kg of an ethanolic extract from *Sinapis alba* seeds reduced the mRNA expression of *TNFα*, *IL-1ß*, and *IL-6* in the colon of Balb/c mice [52]. Similarly, the ingestion of 200 mg/kg of an ethanolic extract from *Eruca sativa* seeds increased the activity of the antioxidant enzymes sod and gpx in the testes of Wistar rats exposed to acrylamide-induced oxidative stress [53]. Therefore, these compounds may reduce the risk of exposure and susceptibility to carcinogenesis [5]. In addition to their previously reported antiproliferative in vitro and in vivo effects, flavonoids play a pivotal role in tumor prevention by modulating oxidative stress and chronic inflammation. As discussed earlier, reactive oxygen species (ROS) can activate transcription factors involved in tumor generation and progression by increasing genomic instability, cell proliferation, and the risk of DNA damage or mutation. Furthermore, the tumor microenvironment is highly oxidative, which inhibits the activity of endogenous antioxidant enzymes such as glutathione peroxidase. Therefore, the antioxidant capacity conferred by these molecules is essential for counteracting these tumor-promoting factors [14,57].

As described by Mesas et al. [29], the effect in the prevention of new dysplastic polyps in colonic mucosa could be related to the anti-inflammatory effect of the extract that could reduce ROS production and the mutagenesis related to polyp formation.

Tumor development increased *pik3cd* and *slc20a1* expression with respect to the healthy control group. The overexpression of *pik3cd* correlates with increased *β-catenin* levels, which translates to increased signaling of the Wnt/β-catenin pathway, which is involved in CRC initiation and progression [58]. Although *Slc20a1* is not a specific CRC marker, its overexpression has been related with a poor prognosis of prostate cancer [59] and breast cancer [60]. Moreover, *Slc20a1* is involved in Wnt/β-catenin signaling pathway activation [61]. The

expression of these markers was reversed following the different interventions implemented, with the effect being more pronounced in the group combining both interventions (NT + Ex). *Cdc42* is crucial in tumor generation, invasion, and metastasis because of its role in essential physiological processes, including cytoskeleton and microtubule regulation, transcription, cell cycle progression, and apoptosis [62]. Therefore, its overexpression is strongly associated with CRC development [63]. However, in our study, *cdc42* expression did not show significant differences with tumor development, although its expression was reduced in animals that receive the nutritional intervention, either alone or combined with physical exercise. Similar results were reported in a study by Guo et al. [13], where tumor development in AOM/DSS-induced CRC in C57BL/6 mice led to an increase in *pik3cd* and *cdc42* expression, whereas it was reduced in the group of mice that ingested 2% curcumin for 12 weeks.

The significant impact of nutraceutical administration on the microbiome under our experimental conditions can be clarified by the large percentage of ingested flavonoids that are not absorbed in the small intestine and reach the colon directly, where they interact with the microbiota, stimulating the production of short-chain fatty acids and the proliferation of beneficial bacteria [64]. The composition of the microbiome in animals that have developed CRC revealed an increased concentration of the phylum Verrucomicrobia, whereas the relative abundance of the phylum Firmicutes and Actinobacteria was significantly lower compared to the healthy control group (CT−). These findings are consistent with those reported by Hidalgo-García et al. and Song et al. [65,66]. However, while these authors also observed an increase in the phylum Bacteroidetes, such a shift was not detected in our study. These abnormal changes in microbiome composition may involve the destruction of the intestinal barrier by increasing the inflammatory response and damage to the gut mucosa [65,67]. The observed decrease in Firmicutes abundance could be due to the pro-inflammatory state associated with tumor induction, as this CRC model is characterized by inflammation-driven tumorigenesis [66,68].

The Firmicutes/Bacteroidetes (F/B) ratio is typically reduced in CRC development and tends to increase following dietary or therapeutic interventions [65,69,70]. This effect may be linked to an increase in Firmicutes, which are associated with butyrate production, a short-chain fatty acid that has been shown to induce apoptosis in colon cancer cells, reduce inflammation, and preserve intestinal mucosal integrity [71]. Under our experimental conditions, the F/B ratio was reduced following CRC induction and further decreased after the nutraceutical and exercise interventions. However, it is important to note that while the F/B ratio is often used as a biomarker for gut dysbiosis, its interpretation remains controversial, as its significance may vary across different pathological conditions [66,72].

As previously mentioned, none of the interventions carried out were able to reverse these alterations. Conversely, an increase in the abundance of Bateroidetes, a phylum associated with CRC susceptibility and promotion [71], was observed. However, since Bacteroidetes was not represented at the genus level, it is unlikely that there was an increased presence of harmful species such as Bacteroides fragilis, a key contributor to CRC development due to its ability to induce inflammation and alter gut ecology, thereby facilitating the colonization of pathogenic bacteria such as *E. coli* and *Fusobacterium nucleatum* [73]. In fact, under our experimental conditions, the presence of *Blautia* (phylum *Bacillota*, family *Lachnospiraceae*) was increased compared to CT+. *Blautia* has been reported to inhibit CRC progression by enhancing CD8+ immune cell activity [74]. Similarly, we detected an increase in *Akkermansia* (phylum *Verrucomicrobia*, family *Verrucomicrobiaceae*), specifically *Akkermansia muciniphila*, which has been shown to protect against CRC development in murine models by inhibiting the *AhR/β*-catenin signaling pathway [75], in addition to promoting the release of extracellular vesicles that have a multitude of regulatory ef-

fects on health, including improved mucosal integrity, reduced intestinal permeability, and an increase in beneficial bacteria [76]. Consequently, this genus is associated with a healthy microbiome that can protect against CRC development [65]. However, to establish a definitive link between microbiome modulation and CRC prevention, further studies are needed to identify the abundance and composition of microbial populations in precancerous tissues [73].

The gut microbiome can exert a direct influence on the organism's oxidative and inflammatory status. Specifically, microorganisms can activate the host's antioxidant defense mechanisms or exert their effects by activating their own antioxidant enzymes, including superoxide dismutase (SOD) and catalase. Additionally, they produce metabolites such as short-chain fatty acids (SCFAs), which can regulate the organism's oxidative status. Specifically, SCFAs (acetate, propionate, and butyrate) induce the activity of the transcription factor nuclear factor erythroid 2-related factor 2 (Nrf2) in epithelial cells, which regulates the expression of antioxidant and detoxifying enzymes, thereby enhancing antioxidant activity [77]. Any disruption of the microbiome may lead to the proliferation of pro-oxidant bacteria such as Listeria and Clostridium, which can impair epithelial cell metabolic function by producing hydrogen sulfide (H_2S) through the degradation of sulfur-containing amino acids. This metabolite inhibits the mitochondrial electron transport chain in epithelial cells, thereby promoting oxidative stress.

It is well-established that an imbalance in oxidative status triggers the expression of pro-inflammatory cytokines. These changes increase membrane permeability, facilitating the translocation of bacteria into the lamina propria and further amplifying ROS production and the inflammatory response. Sustained disruption of this balance over time contributes to the development of colitis and colorectal cancer [77].

The limitations of this study are that the AOM/DSS model for polyp development will be affected by the type of mouse strain used, since the mouse strains used present different sensitivity to the treatment. Another limitation is the impossibility to control the daily intake of DSS consumed by each mouse. Therefore, we propose to experimenters who intend to reproduce the study in the future to evaluate the dose of AOM/DSS to be used in their study in a previous trial to minimize environmental variations in their trial and to place an automatic water system, if possible. Another factor to consider is that animals during treatment with AOM/DSS can lose a significant amount of weight, so we recommend weighing the animals daily (during DSS intake and one week after), and in case of marked weight loss and weakness, administer 1mL of saline solution via IP.

5. Conclusions

The outcomes of this study reveal the beneficial effects of *Brassicaceae* extracts on health and support their potential use as dietary supplements for the prevention of pathological conditions in which oxidative stress plays a key role. Bioactive compounds derived from this family could be a key element in reducing the risk and incidence of CRC by scavenging unstable molecules such as reactive oxygen species (ROS), which can initiate the process of carcinogenesis. The intake of a *Brassica* seed-based nutraceutical proved to be an effective intervention, reducing polyp development by 31.6% and polyp size by 53.9%, this effect was increased to 52.3% and 62.6%, respectively, when the nutritional intervention was combined with a physical exercise protocol. Despite the promising results of this study, further trials are needed to define whether similar results can be achieved in other animal models and to transfer their potential applicability to CRC prevention in humans.

Author Contributions: Conceptualization, F.B., J.M.P., C.M. (Consolación Melguizo) and J.P.; methodology, A.G.-C., C.M. (Cristina Mesas), K.D., J.M.P. and R.M.; software, A.G.-C., A.G.-B. and M.P.; validation, K.D.; formal analysis, A.G.-C., C.M. (Cristina Mesas), A.G.-B. and M.P.; investigation,

A.G.-C., C.M. (Cristina Mesas), K.D., J.M.P. and R.M.; resources, F.B.; writing—original draft preparation, A.G.-C. and C.M. (Cristina Mesas); writing—review and editing, C.M. (Consolación Melguizo) and J.P.; visualization, J.P.; supervision, J.M.P., R.M. and J.P.; funding acquisition, F.B. and C.M. (Consolación Melguizo). All authors have read and agreed to the published version of the manuscript.

Funding: This research was funded by the University of Granada, Junta de Andalucía, Spanish Ministry of Science, Innovation, and Universities as well as the European Union through project RTC2019-006870-1 and the FEDER program. In addition, this work was supported by funds from research groups CTS107 and AGR145 (Andalusian Government).

Institutional Review Board Statement: All animal procedures were conducted in accordance with the ethical guidelines for the care and use of laboratory animals and were approved by the Animal Experimentation Ethics Committee of the University of Granada, Spain (5 October 2021; number 148).

Informed Consent Statement: Not applicable.

Data Availability Statement: Data are available upon request due to time limitations.

Acknowledgments: We want to thank Susana Ibáñez from the analytical unit (CIC, UGR) for her dedicated and skillful assistance.

Conflicts of Interest: The authors declare no conflicts of interest. F.B. was employed by Seed for Innovation S.L. The remaining authors declare that the research was conducted in the absence of any commercial or financial relationships that could be construed as a potential conflict of interest.

References

1. Gómez-España, M.A.; Montes, A.F.; Garcia-Carbonero, R.; Mercadé, T.M.; Maurel, J.; Martín, A.M.; Pazo-Cid, R.; Vera, R.; Carrato, A.; Feliu, J. SEOM Clinical Guidelines for Pancreatic and Biliary Tract Cancer (2020). *Clin. Transl. Oncol.* **2021**, *23*, 988–1000. [CrossRef]
2. WHO. Colorectal Cancer. Available online: https://www.who.int/news-room/fact-sheets/detail/colorectal-cancer (accessed on 5 February 2025).
3. Santucci, C.; Mignozzi, S.; Malvezzi, M.; Boffetta, P.; Collatuzzo, G.; Levi, F.; Vecchia, C.L.; Negri, E. European Cancer Mortality Predictions for the Year 2024 with Focus on Colorectal Cancer. *Ann. Oncol.* **2024**, *35*, 308–316. [CrossRef]
4. Hardt, L.; Mahamat-Saleh, Y.; Aune, D.; Schlesinger, S. Plant-Based Diets and Cancer Prognosis: A Review of Recent Research. *Curr. Nutr. Rep.* **2022**, *11*, 695–716. [CrossRef]
5. Macharia, J.M.; Mwangi, R.W.; Rozmann, N.; Zsolt, K.; Varjas, T.; Uchechukwu, P.O.; Wagara, I.N.; Raposa, B.L. Medicinal Plants with Anti-Colorectal Cancer Bioactive Compounds: Potential Game-Changers in Colorectal Cancer Management. *Biomed. Pharmacother.* **2022**, *153*, 113383. [CrossRef]
6. Sanchez-Guzman, X.; Alvarez-Domínguez, L.; Ramírez-Torres, M.F.; Montes-Alvarado, J.B.; Garcia-Ibañez, P.; Moreno, D.A.; Domínguez, F.; Maycotte, P. Cruciferous Plant Extracts, Their Isothyocianate or Indol Derivatives, and Their Effect on Cellular Viability of Breast Cancer Cell Lines. *J. Med. Food* **2024**, *27*, 1183–1192. [CrossRef]
7. Favela-González, K.M.; Hernández-Almanza, A.Y.; De la Fuente-Salcido, N.M. The Value of Bioactive Compounds of Cruciferous Vegetables (Brassica) as Antimicrobials and Antioxidants: A Review. *J. Food Biochem.* **2020**, *44*, e13414. [CrossRef]
8. Yang, W.Y.; Lim, K.Y.; Yen, P.L.; Ong, S.H.; Naumovski, N.; Jani, R. The Association between Consumption of Bitter-Taste Vegetables in Asian Culture and Metabolic Syndrome Risk Factors in Children: A Narrative Review. *Explor. Res. Hypothesis Med.* **2024**, *9*, 47–54. [CrossRef]
9. Mohd Nor, N.D.; Houston-Price, C.; Harvey, K.; Methven, L. The Effects of Taste Sensitivity and Repeated Taste Exposure on Children's Intake and Liking of Turnip (*Brassica* Rapa Subsp. Rapa); a Bitter *Brassica* Vegetable. *Appetite* **2021**, *157*, 104991. [CrossRef]
10. Nowak, K.; Rohn, S.; Halagarda, M. Impact of Cooking Techniques on the Dietary Fiber Profile in Selected Cruciferous Vegetables. *Molecules* **2025**, *30*, 590. [CrossRef]
11. Baenas, N.; Marhuenda, J.; García-Viguera, C.; Zafrilla, P.; Moreno, D.A. Influence of Cooking Methods on Glucosinolates and Isothiocyanates Content in Novel Cruciferous Foods. *Foods* **2019**, *8*, 257. [CrossRef]
12. Pereira, S.S.; Guimarães, M.; Monteiro, M.P. Towards Precision Medicine in Bariatric Surgery Prescription. *Rev. Endocr. Metab. Disord.* **2023**, *24*, 961–977. [CrossRef] [PubMed]

13. Guo, Y.; Wu, R.; Gaspar, J.M.; Sargsyan, D.; Su, Z.-Y.; Zhang, C.; Gao, L.; Cheng, D.; Li, W.; Wang, C.; et al. DNA Methylome and Transcriptome Alterations and Cancer Prevention by Curcumin in Colitis-Accelerated Colon Cancer in Mice. *Carcinogenesis* **2018**, *39*, 669–680. [CrossRef]
14. Marino, P.; Pepe, G.; Basilicata, M.G.; Vestuto, V.; Marzocco, S.; Autore, G.; Procino, A.; Gomez-Monterrey, I.M.; Manfra, M.; Campiglia, P. Potential Role of Natural Antioxidant Products in Oncological Diseases. *Antioxidants* **2023**, *12*, 704. [CrossRef] [PubMed]
15. Lučić, D.; Pavlović, I.; Brkljačić, L.; Bogdanović, S.; Farkaš, V.; Cedilak, A.; Nanić, L.; Rubelj, I.; Salopek-Sondi, B. Antioxidant and Antiproliferative Activities of Kale (*Brassica oleracea* L. Var. Acephala DC.) and Wild Cabbage (*Brassica incana* Ten.) Polyphenolic Extracts. *Molecules* **2023**, *28*, 1840. [CrossRef]
16. Zhang, Y.; Lv, X.; Wang, D.; Zheng, C.; Chen, H.; Yuan, Y.; Wei, F. Metabolomics Combined with Biochemical Analyses Revealed Phenolic Profiles and Antioxidant Properties of Rapeseeds. *Food Chem.* **2025**, *466*, 142250. [CrossRef]
17. Kapravelou, G.; Martínez, R.; Andrade, A.M.; Chaves, C.L.; López-Jurado, M.; Aranda, P.; Arrebola, F.; Cañizares, F.J.; Galisteo, M.; Porres, J.M. Improvement of the Antioxidant and Hypolipidaemic Effects of Cowpea Flours (Vigna Unguiculata) by Fermentation: Results of in Vitro and in Vivo Experiments. *J. Sci. Food Agric.* **2015**, *95*, 1207–1216. [CrossRef] [PubMed]
18. Kapravelou, G.; Martínez, R.; Andrade, A.M.; Sánchez, C.; Chaves, C.L.; López-Jurado, M.; Aranda, P.; Cantarero, S.; Arrebola, F.; Fernández-Segura, E.; et al. Health Promoting Effects of Lupin (*Lupinus albus* var. *multolupa*) Protein Hydrolyzate and Insoluble Fiber in a Diet-Induced Animal Experimental Model of Hypercholesterolemia. *Food Res. Int.* **2013**, *54*, 1471–1481. [CrossRef]
19. Porres, J.M.; Aranda, P.; López-Jurado, M.; Urbano, G. Nutritional Evaluation of Protein, Phosphorus, Calcium and Magnesium Bioavailability from Lupin (*Lupinus albus* var. *multolupa*)-Based Diets in Growing Rats: Effect of α-Galactoside Oligosaccharide Extraction and Phytase Supplementation. *Br. J. Nutr.* **2006**, *95*, 1102–1111. [CrossRef]
20. Martínez, R.; Mesas, C.; Guzmán, A.; Galisteo, M.; López-Jurado, M.; Prados, J.; Melguizo, C.; Bermúdez, F.; Porres, J.M. Bioavailability and Biotransformation of Linolenic Acid from Basil Seed Oil as a Novel Source of Omega-3 Fatty Acids Tested on a Rat Experimental Model. *Food Funct.* **2022**, *13*, 7614–7628. [CrossRef]
21. Martínez, R.; Kapravelou, G.; Donaire, A.; Lopez-Chaves, C.; Arrebola, F.; Galisteo, M.; Cantarero, S.; Aranda, P.; Porres, J.M.; López-Jurado, M. Effects of a Combined Intervention with a Lentil Protein Hydrolysate and a Mixed Training Protocol on the Lipid Metabolism and Hepatic Markers of NAFLD in Zucker Rats. *Food Funct.* **2018**, *9*, 830–850. [CrossRef]
22. Miller, N.J.; Rice-Evans, C.; Davies, M.J.; Gopinathan, V.; Milner, A. A Novel Method for Measuring Antioxidant Capacity and Its Application to Monitoring the Antioxidant Status in Premature Neonates. *Clin. Sci.* **1993**, *84*, 407–412. [CrossRef]
23. Dinis, T.C.; Maderia, V.M.; Almeida, L.M. Action of Phenolic Derivatives (Acetaminophen, Salicylate, and 5-Aminosalicylate) as Inhibitors of Membrane Lipid Peroxidation and as Peroxyl Radical Scavengers. *Arch. Biochem. Biophys.* **1994**, *315*, 161–169. [CrossRef] [PubMed]
24. Oyaizu, M. Studies on Products of Browning Reaction. Antioxidative Activities of Products of Browning Reaction Prepared from Glucosamine. *Jpn. J. Nutr. Diet.* **1986**, *44*, 307–315. [CrossRef]
25. Duh, P.-D.; Tu, Y.-Y.; Yen, G.-C. Antioxidant Activity of Water Extract of Harng Jyur (Chrysanthemum Morifolium Ramat). *LWT-Food Sci. Technol.* **1999**, *32*, 269–277. [CrossRef]
26. Martínez, R.; Kapravelou, G.; Porres, J.M.; Melesio, A.M.; Heras, L.; Cantarero, S.; Gribble, F.M.; Parker, H.; Aranda, P.; López-Jurado, M. *Medicago sativa* L., a Functional Food to Relieve Hypertension and Metabolic Disorders in a Spontaneously Hypertensive Rat Model. *J. Funct. Foods* **2016**, *26*, 470–484. [CrossRef]
27. Hubrecht, R.C.; Carter, E. The 3Rs and Humane Experimental Technique: Implementing Change. *Animals* **2019**, *9*, 754. [CrossRef]
28. Bialkowska, A.B.; Ghaleb, A.M.; Nandan, M.O.; Yang, V.W. Improved Swiss-Rolling Technique for Intestinal Tissue Preparation for Immunohistochemical and Immunofluorescent Analyses. *J. Vis. Exp.* **2016**, *113*, e54161. [CrossRef]
29. Mesas, C.; Martínez, R.; Doello, K.; Ortiz, R.; López-Jurado, M.; Bermúdez, F.; Quiñonero, F.; Prados, J.; Porres, J.M.; Melguizo, C. In Vivo Antitumor Activity of Euphorbia Lathyris Ethanol Extract in Colon Cancer Models. *Biomed. Pharmacother.* **2022**, *149*, 112883. [CrossRef]
30. Yang, W.; Liu, Y.; Yang, G.; Meng, B.; Yi, Z.; Yang, G.; Chen, M.; Hou, P.; Wang, H.; Xu, X. Moderate-Intensity Physical Exercise Affects the Exercise Performance and Gut Microbiota of Mice. *Front. Cell Infect. Microbiol.* **2021**, *11*, 712381. [CrossRef]
31. Hossain, M.S.; Karuniawati, H.; Jairoun, A.A.; Urbi, Z.; Ooi, D.J.; John, A.; Lim, Y.C.; Kibria, K.M.K.; Mohiuddin, A.K.M.; Ming, L.C.; et al. Colorectal Cancer: A Review of Carcinogenesis, Global Epidemiology, Current Challenges, Risk Factors, Preventive and Treatment Strategies. *Cancers* **2022**, *14*, 1732. [CrossRef]
32. Huang, X.-M.; Yang, Z.-J.; Xie, Q.; Zhang, Z.-K.; Zhang, H.; Ma, J.-Y. Natural Products for Treating Colorectal Cancer: A Mechanistic Review. *Biomed. Pharmacother.* **2019**, *117*, 109142. [CrossRef]
33. Peña, M.; Guzmán, A.; Martínez, R.; Mesas, C.; Prados, J.; Porres, J.M.; Melguizo, C. Preventive Effects of Brassicaceae Family for Colon Cancer Prevention: A Focus on in Vitro Studies. *Biomed. Pharmacother.* **2022**, *151*, 113145. [CrossRef] [PubMed]

34. Khalil, N.; Gad, H.A.; Al Musayeib, N.M.; Bishr, M.; Ashour, M.L. Correlation of Glucosinolates and Volatile Constituents of Six Brassicaceae Seeds with Their Antioxidant Activities Based on Partial Least Squares Regression. *Plants* **2022**, *11*, 1116. [CrossRef] [PubMed]
35. Dzhalilova, D.; Zolotova, N.; Fokichev, N.; Makarova, O. Murine Models of Colorectal Cancer: The Azoxymethane (AOM)/Dextran Sulfate Sodium (DSS) Model of Colitis-Associated Cancer. *PeerJ* **2023**, *11*, e16159. [CrossRef]
36. Robertis, M.D.; Massi, E.; Poeta, M.L.; Carotti, S.; Morini, S.; Cecchetelli, L.; Signori, E.; Fazio, V.M. The AOM/DSS Murine Model for the Study of Colon Carcinogenesis: From Pathways to Diagnosis and Therapy Studies. *J. Carcinog.* **2011**, *10*, 9. [CrossRef] [PubMed]
37. Di Lorenzo, C.; Colombo, F.; Biella, S.; Stockley, C.; Restani, P. Polyphenols and Human Health: The Role of Bioavailability. *Nutrients* **2021**, *13*, 273. [CrossRef]
38. Qin, W.; Ketnawa, S. Exploring the Bioaccessibility of Roasted Japanese Green Tea: Impact of Simulated Gastrointestinal Digestion. *Foods* **2025**, *14*, 311. [CrossRef] [PubMed]
39. Gan, C.; Li, Y.; Yu, Y.; Yu, X.; Liu, H.; Zhang, Q.; Yin, W.; Yu, L.; Ye, T. Natural Product Pectolinarigenin Exhibits Potent Anti-Metastatic Activity in Colorectal Carcinoma Cells in Vitro and in Vivo. *Bioorg. Med. Chem.* **2019**, *27*, 115089. [CrossRef]
40. Deng, Z.; Shen, D.; Yu, M.; Zhou, F.; Shan, D.; Fang, Y.; Jin, W.; Qian, K.; Li, S.; Wang, G.; et al. Pectolinarigenin Inhibits Bladder Urothelial Carcinoma Cell Proliferation by Regulating DNA Damage/Autophagy Pathways. *Cell Death Discov.* **2023**, *9*, 214. [CrossRef]
41. Lee, H.J.; Kwon, Y.S.; Lee, J.H.; Moon, Y.G.; Choi, J.; Hyun, M.; Tak, T.K.; Kim, J.-H.; Heo, J.D. Pectolinarigenin Regulates the Tumor-Associated Proteins in AGS-Xenograft BALB/c Nude Mice. *Mol. Biol. Rep.* **2024**, *51*, 305. [CrossRef]
42. Ding, F.; Yang, S. Epigallocatechin-3-Gallate Inhibits Proliferation and Triggers Apoptosis in Colon Cancer via the Hedgehog/Phosphoinositide 3-Kinase Pathways. *Can. J. Physiol. Pharmacol.* **2021**, *99*, 910–920. [CrossRef]
43. Wubetu, G.Y.; Shimada, M.; Morine, Y.; Ikemoto, T.; Ishikawa, D.; Iwahashi, S.; Yamada, S.; Saito, Y.; Arakawa, Y.; Imura, S. Epigallocatechin Gallate Hinders Human Hepatoma and Colon Cancer Sphere Formation. *J. Gastroenterol. Hepatol.* **2016**, *31*, 256–264. [CrossRef]
44. Lei, J.; Chen, J.; Chen, J.; Fang, J.; Zhou, Z.; Xu, A. Epigallocatechin-3-Gallate Induces Immunogenic Cell Death and Enhances Cancer Immunotherapy in Colorectal Cancer. *Biochem. Biophys. Res. Commun.* **2024**, *736*, 150907. [CrossRef]
45. Costa, E.V.; Soares, L.d.N.; Chaar, J.d.S.; Silva, V.R.; Santos, L.d.S.; Koolen, H.H.F.; da Silva, F.M.A.; Tavares, J.F.; Zengin, G.; Soares, M.B.P.; et al. Benzylated Dihydroflavones and Isoquinoline-Derived Alkaloids from the Bark of Diclinanona Calycina (Annonaceae) and Their Cytotoxicities. *Molecules* **2021**, *26*, 3714. [CrossRef]
46. Huminiecki, L. Evidence for Multilevel Chemopreventive Activities of Natural Phenols from Functional Genomic Studies of Curcumin, Resveratrol, Genistein, Quercetin, and Luteolin. *Int. J. Mol. Sci.* **2022**, *23*, 14957. [CrossRef] [PubMed]
47. Kisacam, M.A. Nobiletin Is Capable of Regulating Certain Anti-Cancer Pathways in a Colon Cancer Cell Line. *Naunyn-Schmiedeberg's Arch. Pharmacol.* **2023**, *396*, 547–555. [CrossRef] [PubMed]
48. Baenas, N.; Vega-García, A.; Manjarrez-Marmolejo, J.; Moreno, D.A.; Feria-Romero, I.A. The Preventive Effects of Broccoli Bioactives against Cancer: Evidence from a Validated Rat Glioma Model. *Biomed. Pharmacother.* **2023**, *168*, 115720. [CrossRef] [PubMed]
49. Kim, S.; Trudo, S.P.; Gallaher, D.D. Apiaceous and Cruciferous Vegetables Fed During the Post-Initiation Stage Reduce Colon Cancer Risk Markers in Rats. *J. Nutr.* **2019**, *149*, 249–257. [CrossRef]
50. Tse, G.; Eslick, G.D. Cruciferous Vegetables and Risk of Colorectal Neoplasms: A Systematic Review and Meta-Analysis. *Nutr. Cancer* **2014**, *66*, 128–139. [CrossRef]
51. Mori, N.; Murphy, N.; Sawada, N.; Achaintre, D.; Yamaji, T.; Scalbert, A.; Iwasaki, M.; Inoue, M.; Gunter, M.J.; Tsugane, S. Prediagnostic Plasma Polyphenol Concentrations and Colon Cancer Risk: The JPHC Nested Case–Control Study. *Clin. Nutr.* **2022**, *41*, 1950–1960. [CrossRef]
52. Xian, Y.-F.; Hu, Z.; Ip, S.-P.; Chen, J.-N.; Su, Z.-R.; Lai, X.-P.; Lin, Z.-X. Comparison of the Anti-Inflammatory Effects of Sinapis Alba and Brassica Juncea in Mouse Models of Inflammation. *Phytomedicine* **2018**, *50*, 196–204. [CrossRef] [PubMed]
53. Abd-Elsalam, R.M.; El Badawy, S.A.; Ogaly, H.A.; Ibrahim, F.M.; Farag, O.M.; Ahmed, K.A. Eruca Sativa Seed Extract Modulates Oxidative Stress and Apoptosis and Up-Regulates the Expression of Bcl-2 and Bax Genes in Acrylamide-Induced Testicular Dysfunction in Rats. *Environ. Sci. Pollut. Res. Int.* **2021**, *28*, 53249–53266. [CrossRef]
54. Fan, Q.; Wang, J.; Tian, M.; Sawut, A.; Xiao, D.; Yi, Z.; Chen, L. Circulating Inflammatory Cytokines and Colorectal Cancer: New Insights from Mendelian Randomization. *Medicine* **2025**, *104*, e41331. [CrossRef]
55. Nelson, V.K.; Nuli, M.V.; Mastanaiah, J.; Saleem, T.S.M.; Birudala, G.; Jamous, Y.F.; Alshargi, O.; Kotha, K.K.; Sudhan, H.H.; Mani, R.R.; et al. Reactive Oxygen Species Mediated Apoptotic Death of Colon Cancer Cells: Therapeutic Potential of Plant Derived Alkaloids. *Front. Endocrinol.* **2023**, *14*, 1201198. [CrossRef]
56. Zhang, H.; Tang, J.; Cao, H.; Wang, C.; Shen, C.; Liu, J. Effect and Mechanism of *Magnolia Officinalis* in Colorectal Cancer: Multi-Component-Multi-Target Approach. *J. Ethnopharmacol.* **2025**, *338*, 119007. [CrossRef] [PubMed]

57. Cid-Gallegos, M.S.; Sánchez-Chino, X.M.; Álvarez-González, I.; Madrigal-Bujaidar, E.; Vásquez-Garzón, V.R.; Baltiérrez-Hoyos, R.; Villa-Treviño, S.; Dávila-Ortíz, G.; Jiménez-Martínez, C. Modification of In Vitro and In Vivo Antioxidant Activity by Consumption of Cooked Chickpea in a Colon Cancer Model. *Nutrients* **2020**, *12*, 2572. [CrossRef]
58. Chen, J.-S.; Huang, J.-Q.; Luo, B.; Dong, S.-H.; Wang, R.-C.; Jiang, Z.-K.; Xie, Y.-K.; Yi, W.; Wen, G.-M.; Zhong, J.-F. PIK3CD Induces Cell Growth and Invasion by Activating AKT/GSK-3β/β-Catenin Signaling in Colorectal Cancer. *Cancer Sci.* **2019**, *110*, 997–1011. [CrossRef]
59. Okamoto, T.; Onaga, C.; Matsuoka, I.; Ozaki, A.; Matsuda, C.; Kasai, T.; Xiong, Y.; Harada, Y.; Sato, T.; Nakano, Y.; et al. High SLC20A1 Expression Indicates Poor Prognosis in Prostate Cancer. *Cancer Diagn. Progn.* **2023**, *3*, 439–448. [CrossRef] [PubMed]
60. Onaga, C.; Tamori, S.; Matsuoka, I.; Ozaki, A.; Motomura, H.; Nagashima, Y.; Sato, T.; Sato, K.; Tahata, K.; Xiong, Y.; et al. High SLC20A1 Expression Is Associated With Poor Prognosis for Radiotherapy of Estrogen Receptor-Positive Breast Cancer. *Cancer Diagn. Progn.* **2022**, *2*, 429–442. [CrossRef]
61. Li, J.; Dong, W.; Li, Z.; Wang, H.; Gao, H.; Zhang, Y. Impact of SLC20A1 on the Wnt/B-catenin Signaling Pathway in Somatotroph Adenomas. *Mol. Med. Rep.* **2019**, *20*, 3276–3284. [CrossRef]
62. Murphy, N.P.; Binti Ahmad Mokhtar, A.M.; Mott, H.R.; Owen, D. Molecular Subversion of Cdc42 Signalling in Cancer. *Biochem. Soc. Trans.* **2021**, *49*, 1425–1442. [CrossRef]
63. Cai, J.-W.; Huang, X.-M.; Li, X.-L.; Qin, S.; Rong, Y.-M.; Chen, X.; Weng, J.-R.; Zou, Y.-F.; Lin, X.-T. An 11-Gene Signature for the Prediction of Systemic Recurrences in Colon Adenocarcinoma. *Gastroenterol. Rep.* **2021**, *9*, 451–460. [CrossRef]
64. Wang, L.; Li, M.; Gu, Y.; Shi, J.; Yan, J.; Wang, X.; Li, B.; Wang, B.; Zhong, W.; Cao, H. Dietary Flavonoids-Microbiota Crosstalk in Intestinal Inflammation and Carcinogenesis. *J. Nutr. Biochem.* **2024**, *125*, 109494. [CrossRef] [PubMed]
65. Hidalgo-García, L.; Ruiz-Malagon, A.J.; Huertas, F.; Rodríguez-Sojo, M.J.; Molina-Tijeras, J.A.; Diez-Echave, P.; Becerra, P.; Mirón, B.; Morón, R.; Rodríguez-Nogales, A.; et al. Administration of Intestinal Mesenchymal Stromal Cells Reduces Colitis-Associated Cancer in C57BL/6J Mice Modulating the Immune Response and Gut Dysbiosis. *Pharmacol. Res.* **2023**, *195*, 106891. [CrossRef]
66. Song, C.-H.; Kim, N.; Nam, R.H.; Choi, S.I.; Jang, J.Y.; Lee, H.-N. Changes in Gut Microbiome upon Orchiectomy and Testosterone Administration in AOM/DSS-Induced Colon Cancer Mouse Model. *Cancer Res. Treat.* **2023**, *55*, 196–218. [CrossRef] [PubMed]
67. Zhang, M.-M.; Yin, D.-K.; Rui, X.-L.; Shao, F.-P.; Li, J.-C.; Xu, L.; Yang, Y. Protective Effect of Pai-Nong-San against AOM/DSS-Induced CAC in Mice through Inhibiting the Wnt Signaling Pathway. *Chin. J. Nat. Med.* **2021**, *19*, 912–920. [CrossRef] [PubMed]
68. Parang, B.; Barret, C.W.; Williams, C.S. AOM/DSS Model of Colitis-Associated Cancer. *Methods Mol. Biol.* **2016**, *1422*, 297–307. [CrossRef]
69. Deng, Y.; Huang, X.; Chen, X.; Wang, M.; Tian, L.; Zhou, H.; Yang, W.; He, F.; Yin, W. Chemopreventive Effects of Polysaccharides and Flavonoids from Okra Flowers in Azomethane/Dextran Sulfate Sodium-Induced Murine Colitis-Associated Cancer. *Nutrients* **2023**, *15*, 4820. [CrossRef]
70. Zhu, J.; Liu, W.; Bian, Z.; Ma, Y.; Kang, Z.; Jin, J.; Li, X.; Ge, S.; Hao, Y.; Zhang, H.; et al. Lactobacillus Plantarum Zhang-LL Inhibits Colitis-Related Tumorigenesis by Regulating Arachidonic Acid Metabolism and CD22-Mediated B-Cell Receptor Regulation. *Nutrients* **2023**, *15*, 4512. [CrossRef]
71. Pal, P.; Shastry, R.P. Exploring the Complex Role of Gut Microbiome in the Development of Precision Medicine Strategies for Targeting Microbial Imbalance-Induced Colon Cancer. *Folia Microbiol.* **2023**, *68*, 691–701. [CrossRef]
72. Yin, Y.; Yang, T.; Tian, Z.; Shi, C.; Yan, C.; Li, H.; Du, Y.; Li, G. Progress in the Investigation of the Firmicutes/Bacteroidetes Ratio as a Potential Pathogenic Factor in Ulcerative Colitis. *J. Med. Microbiol.* **2025**, *74*, 001966. [CrossRef] [PubMed]
73. Gong, D.; Adomako-Bonsu, A.G.; Wang, M.; Li, J. Three Specific Gut Bacteria in the Occurrence and Development of Colorectal Cancer: A Concerted Effort. *PeerJ* **2023**, *11*, e15777. [CrossRef] [PubMed]
74. Zhang, X.; Yu, D.; Wu, D.; Gao, X.; Shao, F.; Zhao, M.; Wang, J.; Ma, J.; Wang, W.; Qin, X.; et al. Tissue-Resident Lachnospiraceae Family Bacteria Protect against Colorectal Carcinogenesis by Promoting Tumor Immune Surveillance. *Cell Host Microbe* **2023**, *31*, 418–432.e8. [CrossRef]
75. Zhang, L.; Ji, Q.; Chen, Q.; Wei, Z.; Liu, S.; Zhang, L.; Zhang, Y.; Li, Z.; Liu, H.; Sui, H. Akkermansia Muciniphila Inhibits Tryptophan Metabolism via the AhR/β-Catenin Signaling Pathway to Counter the Progression of Colorectal Cancer. *Int. J. Biol. Sci.* **2023**, *19*, 4393–4410. [CrossRef] [PubMed]
76. Zheng, T.; Hao, H.; Liu, Q.; Li, J.; Yao, Y.; Liu, Y.; Zhang, T.; Zhang, Z.; Yi, H. Effect of Extracelluar Vesicles Derived from Akkermansia Muciniphila on Intestinal Barrier in Colitis Mice. *Nutrients* **2023**, *15*, 4722. [CrossRef]
77. Kunst, C.; Schmid, S.; Michalski, M.; Tümen, D.; Buttenschön, J.; Müller, M.; Gülow, K. The Influence of Gut Microbiota on Oxidative Stress and the Immune System. *Biomedicines* **2023**, *11*, 1388. [CrossRef]

Disclaimer/Publisher's Note: The statements, opinions and data contained in all publications are solely those of the individual author(s) and contributor(s) and not of MDPI and/or the editor(s). MDPI and/or the editor(s) disclaim responsibility for any injury to people or property resulting from any ideas, methods, instructions or products referred to in the content.

nutrients

MDPI

Article

Effects of Polyphenols from Oat and Oat Bran on Anti-Inflammatory Activity and Intestinal Barrier Function in Raw264.7 and Caco-2 Models

Wen Duan [1], Bisheng Zheng [1,2], Tong Li [3] and Rui Hai Liu [3,*]

[1] School of Food Sciences and Engineering, South China University of Technology, Guangzhou 510641, China; 15754367187@163.com (W.D.); febzheng@scut.edu.cn (B.Z.)
[2] Overseas Expertise Introduction Center for Discipline Innovation of Food Nutrition and Human Health, School of Food Sciences and Engineering, South China University of Technology, Guangzhou 510641, China
[3] Department of Food Science, Cornell University, Ithaca, NY 14853, USA; tl24@cornell.edu
* Correspondence: rl23@cornell.edu; Tel.: +1-607-255-6235

Abstract

Background/Objectives: Oats and oat bran are rich in dietary fiber, polyphenols and other phytochemicals. Methods: In this study, we evaluated the phytochemical content and established LPS-induced RAW264.7 macrophage inflammation and DSS-induced Caco-2 cell inflammation models to investigate the anti-inflammatory activities of oat and oat bran polyphenols and their molecular mechanisms. Results: The results showed that oat and oat bran polyphenols (free and bound polyphenols) enhanced phagocytosis, decreased the expression of nitric oxide synthase (iNOS) and cyclooxygenase-2 (COX-2), reduced the production of NO and ROS, increased the mitochondrial membrane potential, and reduced the inflammatory cytokines (TNF-α, IL-1β, and IL-6) at the gene level in the RAW264.7 macrophage inflammation model induced by LPS expression, thus demonstrating strong anti-inflammatory activity. In Caco-2 cells, oat and oat bran polyphenols pretreatment attenuated the DSS-induced decrease in trans-epithelial electron resistance value, increased tight junction protein expression, and reduced cell permeability in Caco-2 cell monolayers, which in turn reduced inflammatory damage in the organism. Conclusions: In summary, the present study not only reveals the mechanism by which oat and oat bran polyphenols inhibit macrophage inflammation and impairment of intestinal barrier function at defined concentration in vitro, but also highlights potential for oat bran as a functional food.

Keywords: oats; bran; polyphenols; inflammation; intestinal barrier

1. Introduction

Inflammation is a complex protective physiological response to the immune defense mechanism that occurs when the body is exposed to external stimuli or injury [1]. The inflammatory response is a fundamental immune reaction that maintains tissue homeostasis. However, abnormalities in this process can lead to various diseases, such as irritable bowel syndrome and Parkinson's disease [2]. Prolonged metabolic chronic low-grade inflammation can lead to various metabolic disorders. Currently, several drugs are used clinically to treat inflammation and can exhibit anti-inflammatory effects to some extent. However, long-term use of these drugs can lead to side effects and other issues [3]. While functional foods are not a replacement for clinical drug therapy, they can serve as a nutritional intervention to help mitigate chronic inflammatory responses. Therefore, the research

and development of new, safe, and non-toxic anti-inflammatory health foods or drugs derived from natural plants have become major focal points in the field of life sciences.

The health of the human gut is of paramount importance. The gut is not only a major organ for digestion, absorption, and metabolism, but it also serves as a crucial physical, chemical, immune, and microbial barrier [4]. The intestinal barrier is the body's first line of defense against luminal microorganisms and food antigens. Structural damage to this barrier can allow harmful substances, such as toxins and pathogenic bacteria, to enter the circulatory system, initiating an immune response that can result in localized inflammation or systemic disease [5]. Abnormalities in the barrier function of the intestinal mucosa are significant causes of inflammatory bowel disease [6], intestinal stress syndrome, and intestinal tumorigenesis. The structure of the intestinal epithelium, composed of intestinal epithelial cells and intercellular junctions, is crucial for preventing the invasion of pathogenic microorganisms and bacterial translocation. Therefore, improving the function of the intestinal epithelium and maintaining the integrity of the intercellular tight junctions will help mitigate the inflammatory response [7].

A growing body of research suggests that the disruption of gut barrier may lead to disease onset or accelerated disease progression. Loss of barrier integrity can increase the translocation of bacterial antigens, stimulate intestinal mucosal inflammation, and trigger the onset of intestinal disease [8]. Studies have shown that some functional components in cereals can inhibit or alleviate inflammation in the body without toxic side effects [9,10]. Additionally, the abundant polyphenolic compounds in cereals can scavenge a large number of reactive oxygen species in the body due to their excellent antioxidant activity, thus preventing the occurrence of diseases [11,12].

Oats are a traditional cereal food that can regulate the human gut microbiota, thus positively affecting health [13]. Oat bran, the main by-product of oat processing, has high nutritional value and is rich in dietary fiber. However, a large amount of oat bran is currently used as feed, leading to low utilization and economic benefits. It is well known that oats and oat bran are rich in β-glucans and phenolic acids, which have antioxidant, anti-inflammatory, and gut health-regulating effects [14–16].

It has been reported that about 60–85% of polyphenols in wheat bran exist in bound polyphenols, and bound polyphenols in grains exhibit high biological activities such as antioxidant and antihyperglycemic properties [17,18]. The experimental results of Chen et al. (2019) [19] demonstrated that the in vitro digestion process significantly reduced the concentration of polyphenols in oats. The degradation of polyphenols primarily occurs in the intestinal tract, where they undergo absorption and transit during the digestive process [19]. Li et al. (2022) found that highland barley attenuates inflammation and intestinal dysbiosis induced by a high-fat diet by inhibiting inflammatory factors and reestablishing the gut microbiome and lipid metabolism [20]. Hong et al. (2020) used LPS-induced RAW264.7 cells to establish inflammation model to evaluate the anti-inflammatory activity of sorghum polyphenols and showed that sorghum polyphenol extracts significantly reduced NO and ROS levels in cells [21]. Numerous studies have demonstrated the efficacy of polyphenolic substances in natural products in modulating intestinal inflammation [22].

Plant flavonoids can protect barrier integrity by acting on intestinal tight junction structures and maintaining mucosal homeostasis. Human colon cancer Caco-2 cells are a classic cell line used to study the secretion of intestinal mucosal epithelial cells and the function of intestinal barrier damage in vitro [23]. Kim et al. used a lipopolysaccharide-stimulated Caco-2/RAW264.7 co-culture model to determine the effects of acai berries on intestinal inflammation. The results showed that the addition of acai berries restored the epithelial resistive value, inhibited IL-8 and IL-6 mRNA expression in Caco-2 cells, and restored cell barrier function, thereby improving intestinal health [24]. In conclusion, the

exact mechanism by which oat and bran polyphenols modulate macrophage inflammation and the intestinal cell barrier is still unknown.

Therefore, in this study, we established an LPS-induced inflammation model of RAW264.7 cells and a DSS-induced inflammation model of Caco-2 cells in vitro. We explored the protective effects of polyphenols from oats and bran on macrophage inflammation and barrier damage in Caco-2 cells by determining the expression of inflammatory factors and the level of tight junction proteins. Our aim was to elucidate the mechanism of the anti-inflammatory efficacy of oats and oat bran and provide theoretical references for the development and utilization of oats and bran as precision nutritional foods.

2. Materials and Methods

2.1. Materials and Reagents

Fluorescein sodium salt, dichlorofluorescin diacetate (DCFH-DA) and lipopolysaccharide (LPS) (*Escherichia coli*, serotype 0111:04) were purchased from Sigma-Aldrich Chemical Co. (St. Louis, MO, USA). The NO assay kit, neutral red, high-efficiency RIPA cell lysis solution was purchased from Beijing Solepol Technology Co. (Beijing, China). The oat and oat bran samples were provided by Yangufang Group (Inner Mongolia, Wuchuan, China).

2.2. Sample Preparation

Polyphenol was obtained according to the method of Adom [11] (Adom & Liu, 2002). Free polyphenol: An amount of 20 g of oat flour was mixed with 80% chilled acetone (1:10, w/v), homogenized using Virtis High Speed Homogenizer in 12,000$\times$ g for 5 min, and centrifuged at 4 °C, 10,000 r/min for 10 min to collected the supernatant. Repeat 3 times. All supernatants were combined and evaporated to dryness by vacuum rotary concentration at 45 °C and further reconstituted with 20 mL of 80% methanol for standby. Bound polyphenol: Add 2 M NaOH to the residue after extraction, shake for 1 h, and then adjust the pH of the reaction to 2 with concentrated HCl. The lipids were removed by 2 times extraction with n-hexane, followed by adding ethyl acetate to collected bound polyphenol. The extraction was repeated 6 times. The organic solution was combined, concentrated by vacuum rotation, and then volumetized to 20 mL by 80% methanol and stored at -40 °C for subsequent experiments.

2.3. Phytochemical Profiles Analysis by HPLC

Phytochemical profiles of oats was obtained using the method of He et al. (2022) [25] with modifications. The HPLC system (Waters Corporation, Milford, MA, USA) was used to analyze standard products. The determination conditions were based on the method of He et al. (2022) [25].

2.4. Cell Culture and Viability

Human colon cancer Caco-2 cells and RAW264.7 cells were obtained from ATCC Co. (Manassas, VA, USA). The cell generations were in the range of 10–20, and the medium was changed every two days.

RAW264.7 cells were spread in 96-well plates (1×10^4 cells/well) and incubated for 24 h. Subsequently, 1 μg/mL LPS and different concentrations of polyphenol samples were added to the cells for 24 h. After the incubation was completed, the cell viability of each group was determined using the MTT assay. Caco-2 cells were spread in 96-well plates (3×10^4 cells/well), pretreated with polyphenols for 24 h, and then stimulated with 1.5% DSS for 24 h. The cell viability of each group was determined using the MTT assay [26].

2.5. NO Assay

The determination of NO was carried out according to the Biyuntian NO detection kit [26]. During the pre-experimental stage, we first evaluated the NO inhibition efficiency at a concentration of 100 μg/mL using 96-well plates (see Figure A1). Based on the experimental results, a concentration range of 200–750 μg/mL was selected as the gradient for the formal experiments. RAW264.7 cells were spread in 12-well plates (1×10^5 cells/well) and incubated in an incubator for 24 h. Then, different concentrations of polyphenol samples were incubated for 6 h and treated with 1 μg/mL LPS for 24 h. The supernatant was collected, and the absorbance was measured.

2.6. Phagocytosis Assay

The method of Xiong et al. (2018) [27] was referred to and slightly modified. RAW264.7 cells were cultured, and the inflammatory response was stimulated as described in Section 2.2, followed by incubation for 24 h. The cells were divided into 14 groups: blank control group, LPS-treated group, oat free phenol low-, medium-, and high-dose groups, oat bound polyphenol low-, medium-, and high-dose groups, bran free phenol low-, medium-, and high-dose groups, and bran bound polyphenol low-, medium-, and high-dose groups. After incubation for 24 h, the supernatant was discarded, 100 μL of 0.05% neutral red solution was added for staining, and the staining solution was aspirated after 1 h. After washing with PBS three times, 150 μL of cell lysate was added and then measured at a wavelength of 550 nm after 15 min of oscillation.

2.7. ROS Assay

The determination of ROS was carried out from our established protocol with slight modifications [28]. RAW264.7 cells (1.0×10^4 cells/well) were inoculated in 96-well black plates for 24 h. Following 6 h polyphenol pretreatment, LPS (1 μg/mL) was added and incubated for 24 h. The medium without samples was used as a control. Then, the fluorescence intensity was detected immediately after adding DCFH-DA solution (50 μmol) to the 96-well plate. The assay conditions were as follows: 37 °C, detection wavelength: 485 nm, emission wavelength: 538 nm, and the fluorescence intensity was measured every 5 min for 2 h. The fluorescence intensity was measured at the same time.

2.8. Mitochondrial Membrane Potential Assay

Referring to the method of Kapoor et al. (2023) [29] with appropriate modifications, RAW264.7 cells were inoculated at a density of 4 × 105 cells and incubated for 24 h. The cells were treated with polyphenols for 6 h, and then LPS (1 μg/mL) was added and incubated for 24 h. After aspirating the supernatant, 1 mL of JC-1 staining working solution was added and mixed thoroughly. After the cells were incubated at a constant temperature of 37 °C for 20 min, the culture supernatant was discarded and washed three times using JC-1 staining buffer. The processed cells were subsequently resuspended in 2 mL of fresh culture solution for fluorescence microscopic observation.

2.9. Establishment of the Caco-2 Monolayer Model

The monolayer membrane model of Caco-2 cells was established with reference to the method of Yang et al. (2022) [30]. Cells were inoculated in the upper chamber of Transwell plates with 1.5 mL of complete medium in the lower chamber, and the blank group was given complete medium (0.5 and 1.5 mL) in both the upper and lower chambers. The culture medium was changed every two days for the first week and then every day until the culture reached 21 d. The monolayer formation of Caco-2 cells was assessed using the following three methods.

(1) The transmembrane electrical resistance (TEER) of cell membranes was measured using a resistivity meter to assess the integrity and tightness of the monolayers. The TEER of the cell membranes was measured every two days, and Caco-2 monolayers with a TEER value exceeding 500 $\Omega \cdot cm^2$ were used for subsequent experiments. The formula is as follows:

$$TEER = (R1 - R2) \times A\ (\Omega \cdot cm^2)$$

R1 (Ω) is the resistance measurement of the Caco-2 cell compartment, R2 (Ω) is the resistance measurement of the blank control group, and A (cm^2) represents the membrane area of the compartment.

(2) The polarity of the Caco-2 cell monolayer membrane can be assessed by measuring the ratio of alkaline phosphatase (ALP) activity between the upper and lower compartments of Transwell plates. The monolayer polarity of the Caco-2 cell model was tested by aspirating the culture fluid from the upper (AP) and lower (BL) chambers of the Transwell plate every two days, determining their ALP activities, and calculating the ratio of AP side to BL side.

(3) Caco-2 cell monolayer integrity was detected by measuring the passive diffusion of sodium fluorescein. Standard solutions of sodium fluorescein at concentrations of 0.5, 1, 2, 4, 6, 8, and 10 μg/mL were prepared with HBSS buffer, and the fluorescence intensity was measured using a multifunctional enzyme marker to generate a standard curve. When Caco-2 cells were cultured on Transwell plates for 21 d, the AP side and BL side of the chambers were washed three times using HBSS buffer; HBSS buffer was added, and after equilibrating in the incubator for 30 min, 0.5 mL of sodium fluorescein solution was added to the AP side, while 1.5 mL of HBSS buffer was added to the BL side. The chambers were cultured in CO_2 incubator, and 100 μL of BL buffer was taken from the chambers at 60, 120, and 180 min. A total of 100 μL of BL side transporter solution was taken, the fluorescence intensity was measured by molecular ID3, and the concentration of sodium fluorescein was calculated according to the standard curve. The formula for calculating the transmittance of sodium fluorescein is as follows:

$$\text{transmission rate (\%)} = (\text{Mass of sodium fluorescein on the BL side})/(\text{Mass of sodium fluorescein on the initial AP side}) \times 100$$

2.10. Cytokine Assays

The levels of IL-6, IL-10, and TNF-α in the supernatant were determined using an ELISA kit (Multi Sciences Biotech Co., Ltd., Hangzhou, Zhejiang, China). Caco-2 cells were pretreated with different concentrations of polyphenols for 24 h and then stimulated with 1.5% DSS for 24 h. The measurement of IL-6 and IL-8 in the supernatants was conducted.

2.11. Real-Time PCR

The relative transcription levels of inflammatory mediators were determined by the qPCR analysis according to our reported method [31]. RAW 264.5 cells were inoculated at 4×10^5 cells/mL. After 24 h, the cells were pretreated with oat and bran polyphenols for 6 h, followed by stimulation with LPS (1 μg/mL) for 24 h. Cell grouping refer to 2.4. At the end of culture, cells were rinsed twice with PBS after medium removal. Total RNA extraction was then performed through direct lysis using 500 μL TRIzol reagent per well, followed by reverse transcription to generate cDNA templates for subsequent qPCR amplification. The primers used were as follows: GAPDH, (F:CTCGTCCCGTAGACAAAATGGT,R:GAGGTCAATGAAGGGGTCGTT); iNOS, (F:CCTTACGAGGCGAAGAAGGACAG,R:CAGTTTGAGAGAGGAGGCTCCG); COX2, (F:GAGAGATGTATCCTCCCACAGTCA,R:GACCAGGCACCAGACCAAAG); TNF-α, (F:CAGGCG

GTGCCTATGTCTC,R:CGATCACCCCGAAGTTCAGTAG); IL-6, (F:CTGCAAGAGACTTC CATCCAG, R:AGTGGTATAGACAGGTCTGTTGG); Trl4, (F:CAACATCATCCAGGAAGGC, R:GAAGGCGATACAATTCCACC). Caco-2 cells Sample processing for the Caco-2 cells model was referred to the steps described in Section 2.10, and at the end of the intervention, RNA was extracted separately. The primer sequences are as follows: GAPDH (F: TCCACTGGCGTCTTCACCACCAT, R: GGAGGCATTGCTGATGATCTTGAGG); Occludin (F: ATGAGACAGACTACACAACTGG, R: TTGTATTCATCAGCAGCAGCAGC). The relative expression of target genes was calculated using the $2^{-\Delta\Delta CT}$ method.

2.12. Statistical Analysis

Method analysis and Tukey's test were used to evaluate the correlation between the data (SPSS version 19), significance analysis $p < 0.05$. All tests were repeated 3 times, and the test data were expressed as mean ± standard deviation.

3. Results

3.1. Phenolic Profiles

The content of phenolic acids in oat varieties and products is shown in Table A1. Eight phenolic compounds were detected in oat, namely gallic acid, protocatechuic acid, p-Hydroxybenzoic acid, vanillic acid, caffeic acid, p-Coumaric acid, ferulic acid and avenanthramides C. The ferulic acid content of the oat and bran ranged from 5.26 to 335.15 μg/g DW. Compared with oats, the content of ferulic acid (335.15 ± 1.64 μg/g DW) in bound polyphenol and Avenanthramides C (8.82 ± 4.04 μg/g DW) in free form in oat bran is higher. Ferulic acid is the most abundant phenolic substance and exists both as free and bound polyphenol, primarily in the bound form.

3.2. Effect of Oat and Oat Bran Polyphenols on Cell Viability

The effects of different concentrations of oat and oat bran polyphenols on RAW264.7 and Caco-2 cell viability after 24 h of intervention are shown in Figure 1. In Figure 1A, oat polyphenols and oat bran polyphenols showed no cytotoxic effects on cells across concentrations ranging from 0 to 5 mg/mL, respectively. In Figure 1B, compared with the blank group, none of the samples had cytotoxic effects at 1000 μg/mL concentration, except for the LPS-stimulated oat bran bound polyphenol (BB) (1000 μg/mL), which exhibited toxicity after 24 h of stimulation. Therefore, oat free polyphenol (OF) (200, 500, 750 μg/mL), oat bound polyphenol (OB) (200, 500, 750 μg/mL), oat bran free polyphenol (BF) (200, 500, 750 μg/mL), and oat bran bound polyphenol (BB) (200, 500, 750 μg/mL) were selected as the concentration gradients for subsequent tests. In Figure 1C, we evaluated the toxicity of oat and oat bran polyphenols on Caco-2 cells. After treatment with oat and bran polyphenols for 24 h, oat polyphenols did not show toxic effects up to a concentration of 5 mg/mL, whereas oat bran polyphenols inhibited the growth of Caco-2 cells at a concentration of 5 mg/mL, producing toxic effects. Following treatment with 1.5% DSS, both polyphenols did not produce toxicity at a concentration of 1 mg/mL. Therefore, the maximum dose examined (1 mg/mL) was selected to treat Caco-2 cells in subsequent experiments.

3.3. Effect of Oat and Oat Bran Polyphenols on Phagocytosis of RAW264.7 Cells

In Figure 2, LPS stimulation significantly stimulated macrophages phagocytosis of neutral red after 24 h of stimulation, increasing phagocytosis compared to the blank group. However, after pretreatment with 200, 500, and 750 μg/mL oat and oat bran polyphenols, LPS-induced phagocytosis of mouse macrophages was significantly inhibited, with the highest inhibition observed at high doses.

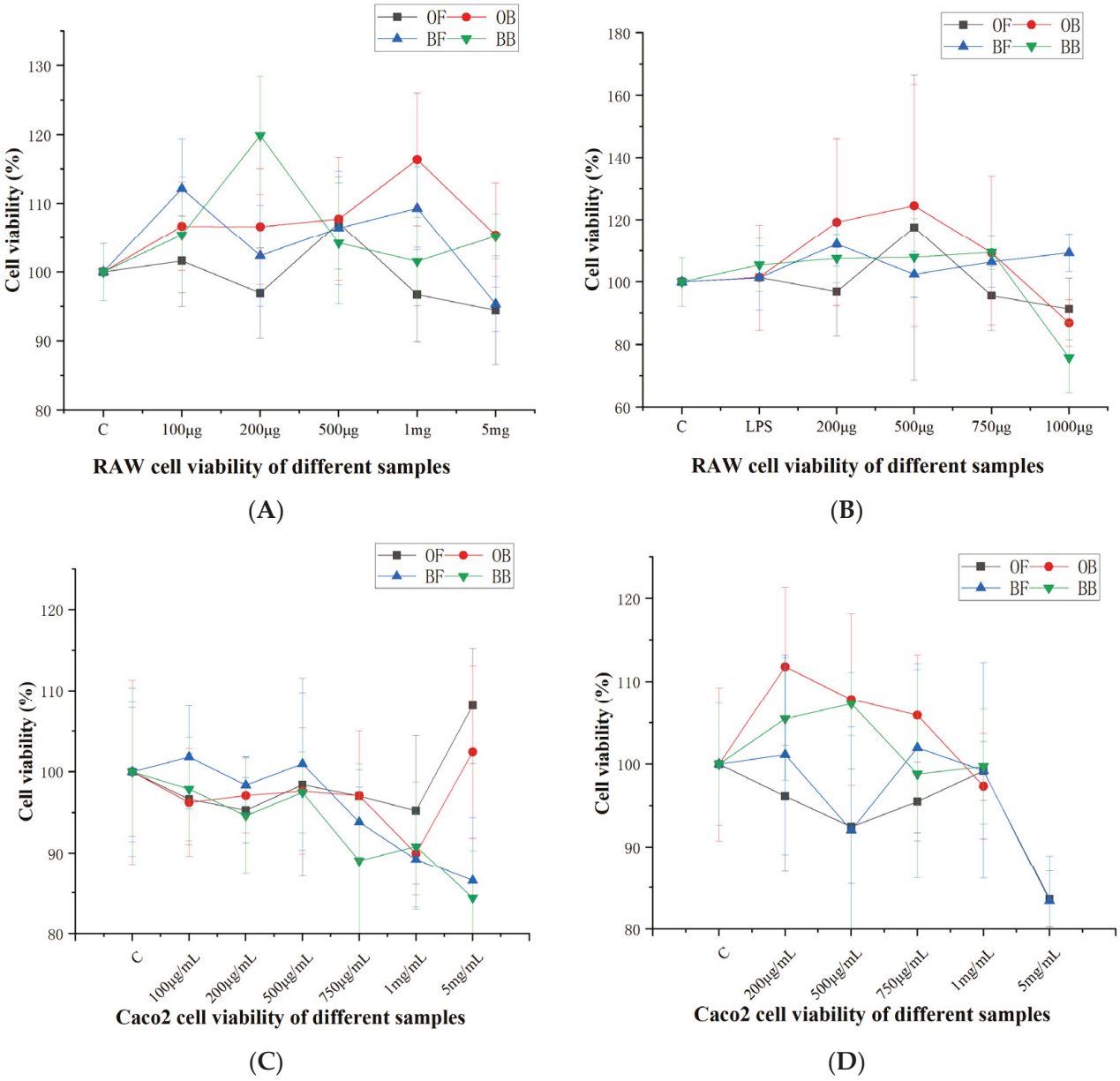

Figure 1. Effects of oat and bran polyphenol on Raw264.7 cell viability (**A**), in LPS-induced Raw264.7 cell viability (**B**), on Caco-2 cell viability (**C**), in DSS-induced Caco-2 cell viability (**D**). OF (oat free polyphenol); BF (bran free polyphenol); OB (oat bound polyphenol); BB (oat bran bound polyphenol).

3.4. NO and ROS Production

As shown in Figure 3A, after 24 h of LPS stimulation, the secretion of NO from RAW264.7 cells in the control group was low, while NO and ROS release in the model group were significantly higher than those in the blank group, indicating successful establishment of the inflammatory cell model. All concentrations of oat polyphenols and oat bran polyphenols significantly reduced NO release compared to the model group. The inhibition of NO secretion was most pronounced at concentrations of 750 μg/mL for oat free phenol, oat bound polyphenol, and oat bran free phenol, reducing NO production rates by 37.57%, 45.63%, and 38.62%, respectively. In Figure 3B, the relative expression of ROS after pretreatment with different concentrations of oat polyphenols and oat bran polyphenols ranged from 113.25% to 198.73%. Intracellular ROS release was significantly lower than that in the LPS group, and the inhibitory effect of high concentrations of polyphenols on ROS release was the strongest.

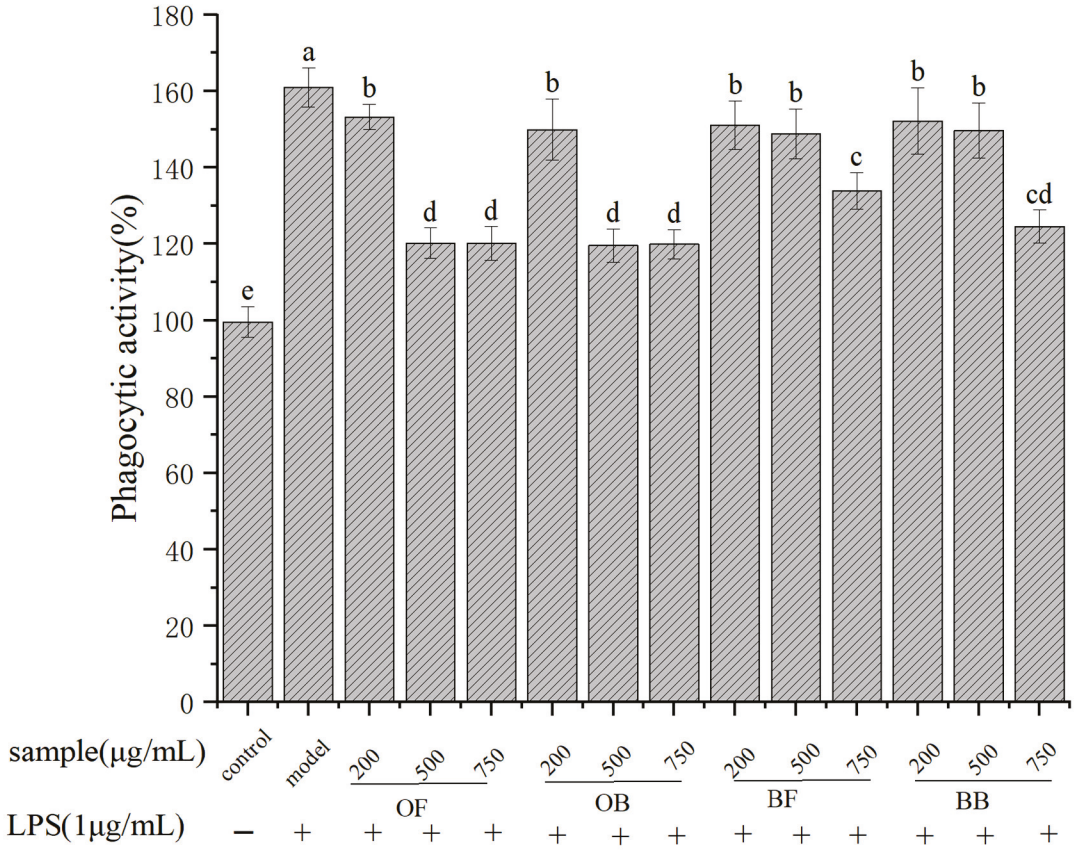

Figure 2. Effect of oat and bran polyphenols in LPS-induced phagocytosis of Raw264.7 macrophages cells. OF (oat free polyphenol); BF (bran free polyphenol); OB (oat bound polyphenol); BB (oat bran bound polyphenol). Different lowercase represent significant differences among groups.

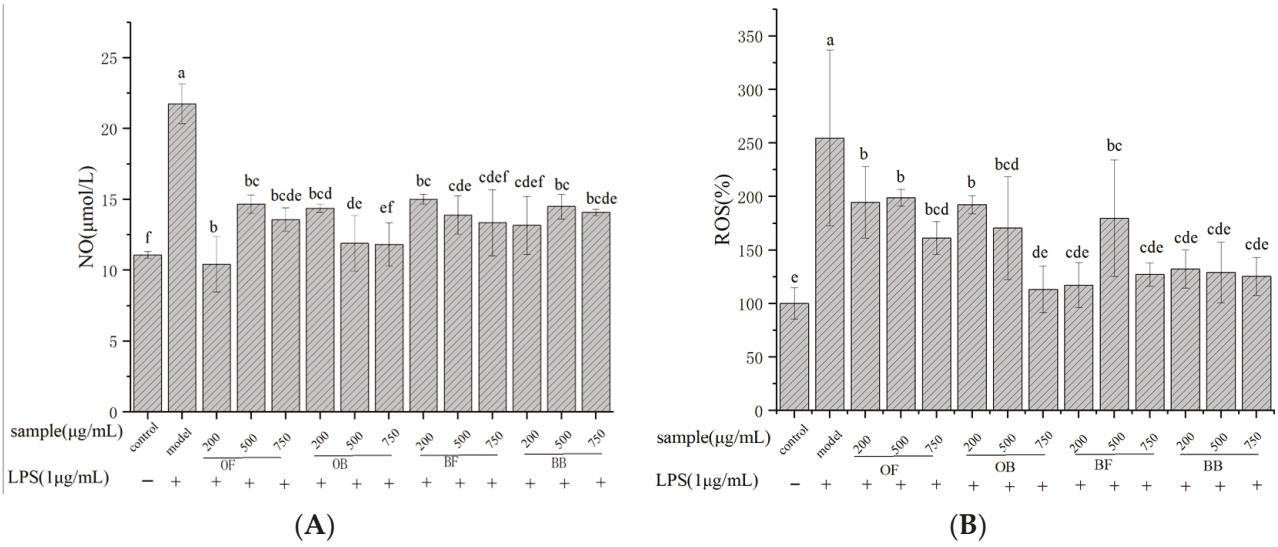

Figure 3. Effects of oat and bran polyphenol on NO (**A**) and ROS (**B**) in Raw 264.7 macrophages cell. OF (oat free polyphenol); BF (bran free polyphenol); OB (oat bound polyphenol); BB (oat bran bound polyphenol). Different lowercase represent significant differences among groups.

3.5. Inflammatory Cytokine Expression in Cells

We determined the inhibitory effects of oat and oat bran polyphenols on the secretion of IL-6, TNF-α, and IL-10. In Figure 4A–C, in the model group, RAW264.7 cells secreted significantly higher levels of pro-inflammatory factors IL-6 and TNF-α compared to the

blank group, indicating successful induction of an inflammatory response by LPS in RAW264.7 cells. Compared to the model group, the polyphenol-treated groups showed significant inhibition of pro-inflammatory factor secretion, with the level of secretion gradually decreasing with increasing treatment concentration. The secretion of the anti-inflammatory factor IL-10 exhibited a certain concentration dependence on increasing polyphenol treatment concentration, particularly showing significant enhancement at a concentration of 750 μg/mL. These findings further indicate that oat and bran polyphenols can alleviate the inflammatory response of macrophages induced by LPS and exhibit potent in vitro anti-inflammatory activity.

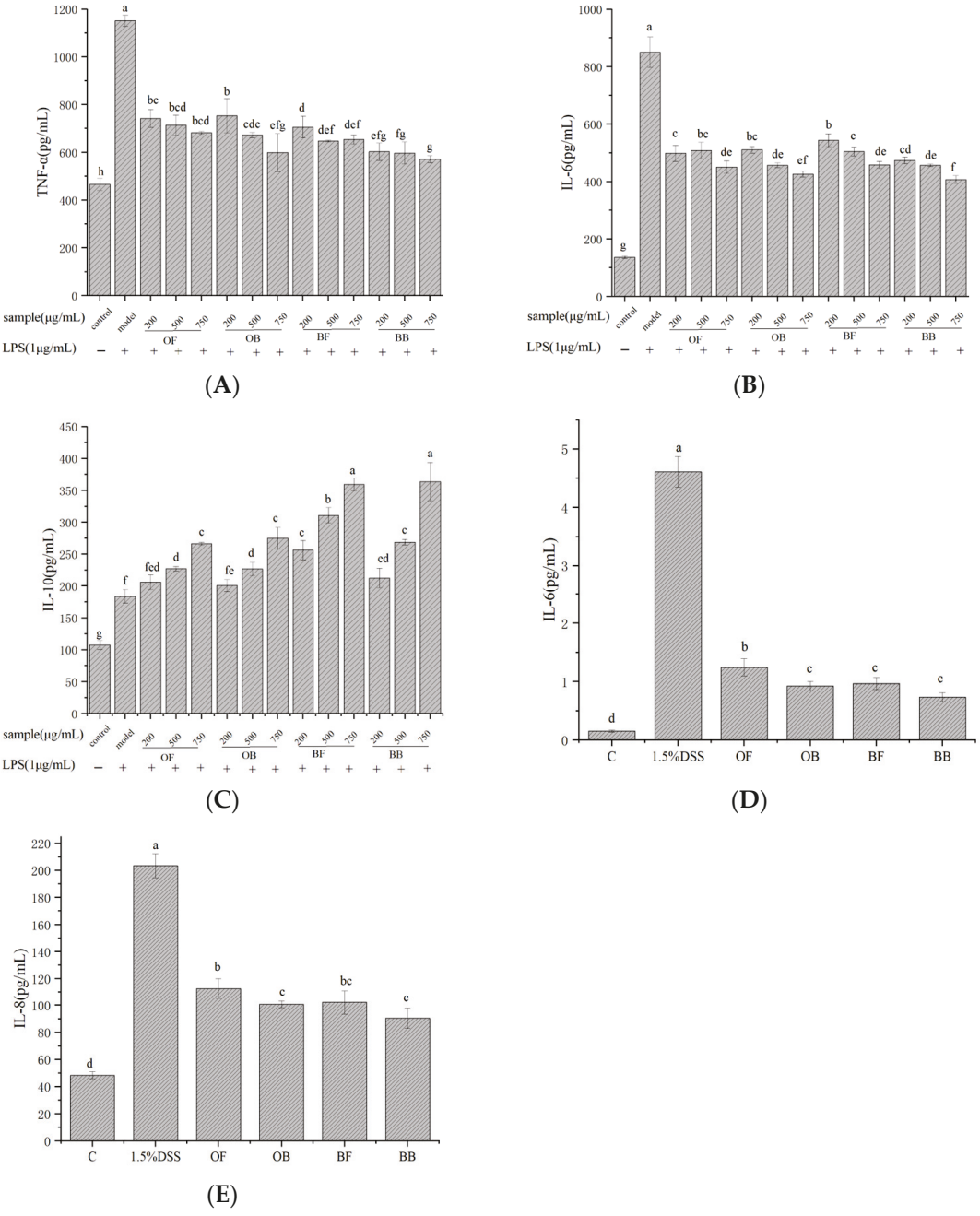

Figure 4. Effects of oat and bran polyphenol on the production of TNF-α (**A**), IL-6 (**B**), and IL-10 (**C**) in LPS-induced Raw264.7 macrophages and on the production of IL-6 (**D**) and IL-8 (**E**) in DSS-induced Caco-2 cell. OF (oat free polyphenol); BF (bran free polyphenol); OB (oat bound polyphenol); BB (oat bran bound polyphenol). Different lowercase represent significant differences among groups.

As shown in Figure 4D,E, compared to the blank group, DSS treatment significantly increased the levels of IL-6 and IL-8 to 4.60 pg/mL and 203.44 pg/mL, respectively. However, pretreatment with oat and oat bran polyphenols significantly inhibited the secretion of cytokines IL-6 and IL-8. The inhibitory effect of oat bran polyphenols was notably higher than that of oat polyphenols. Oat bound polyphenol and bran bound polyphenol reduced IL-6 levels by 73.07% and 84.04%, and IL-8 secretion levels by 50.56% and 55.53%, respectively, compared to DSS-induced model cells. While the inhibitory effect of bound polyphenol was higher than that of free phenols, the difference was not significant. This suggests that oat and bran polyphenols can protect the intestinal barrier from DSS and alleviate the inflammatory response induced by DSS.

3.6. Mitochondrial Membrane Potential

As shown in Figure 5, compared to the blank group, the fluorescence signals of JC-1 aggregates (red fluorescence) were significantly weakened, and the fluorescence signals of JC-1 monomers (green fluorescence) were significantly strengthened after 24 h of LPS stimulation. This indicates a significant decrease in cellular mitochondrial membrane potential. However, after treating the cells with oat and oat bran polyphenols, normal mitochondrial potential was restored.

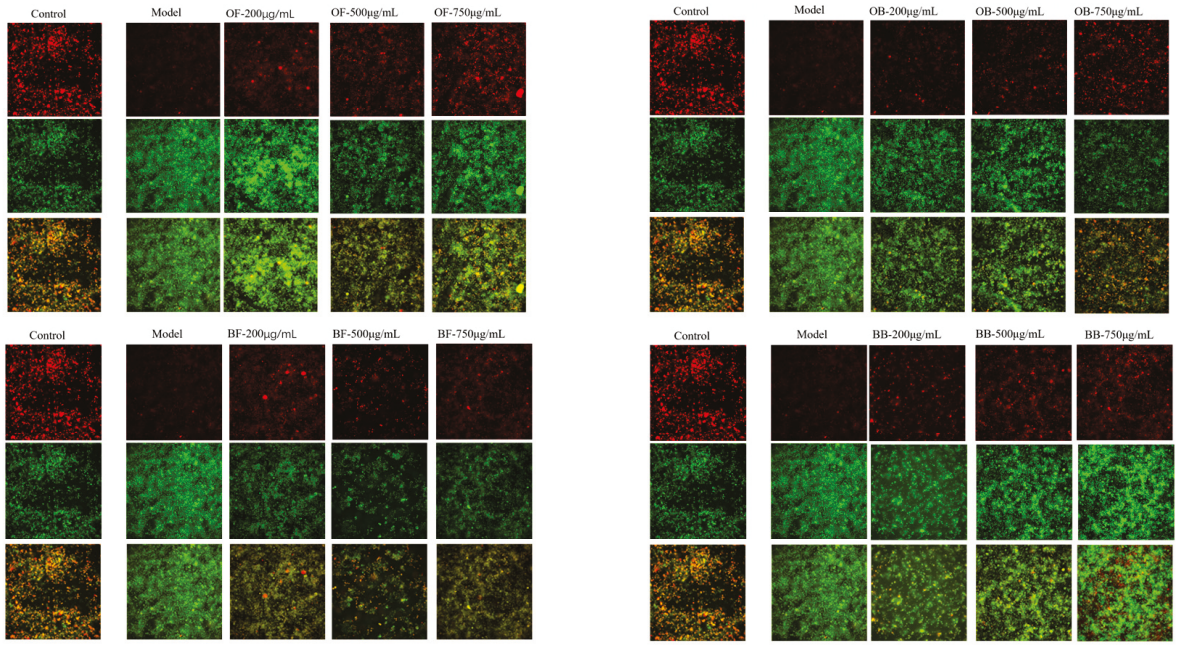

Figure 5. Effect of oat and bran polyphenols in LPS-induced mitochondrial membrane potential of Raw264.7 cells.

3.7. Effect of Oat and Bran Polyphenols on the mRNA Expression of Inflammatory Factors

After LPS stimulation, the mRNA expression levels of all inflammatory mediators significantly increased in the cells, showing highly significant differences compared to the blank group. Specifically, TNF-α expression in the model group increased 2.24-fold compared to the blank group, IL-6 increased by 11.44-fold, iNOS increased 7.27-fold, COX-2 increased 4.24-fold, TLR4 increased 2.13-fold, and IL-10 increased 2.80-fold.

The effects of oat and oat bran polyphenols on the relative expression of IL-6, TNF-α, and IL-10, inflammation-related enzymes COX-2 and iNOS, as well as the cell surface receptor TLR4, were measured by RT-qPCR. In Figure 6, after LPS stimulation, the mRNA expression levels of all inflammatory mediators significantly increased in the cells, showing highly significant differences compared to the blank group. Specifically, TNF-α expression

in the model group increased 2.24-fold compared to the blank group, IL-6 increased 11.44-fold, iNOS increased 7.27-fold, COX-2 increased 4.24-fold, TLR4 increased 2.13-fold, and IL-10 increased 2.80-fold. Compared to the model group, the relative gene expression of TNF-α and IL-6 was significantly decreased after cells were treated with oat and oat bran polyphenols. Oat and oat bran polyphenols significantly increased the relative expression of IL-10 genes after 24 h of LPS induction. After 24 h of LPS induction, high-dose oat and oat bran polyphenol (750 μg/mL) pretreatment had a significant inhibitory effect on the expression of COX-2, iNOS and TLR4 genes, but bran free phenol (500 μg/mL) pretreatment prompted a significant increase in the relative expression of iNOS and TLR4 genes compared with that of the high-dose (750 μg/mL) group.

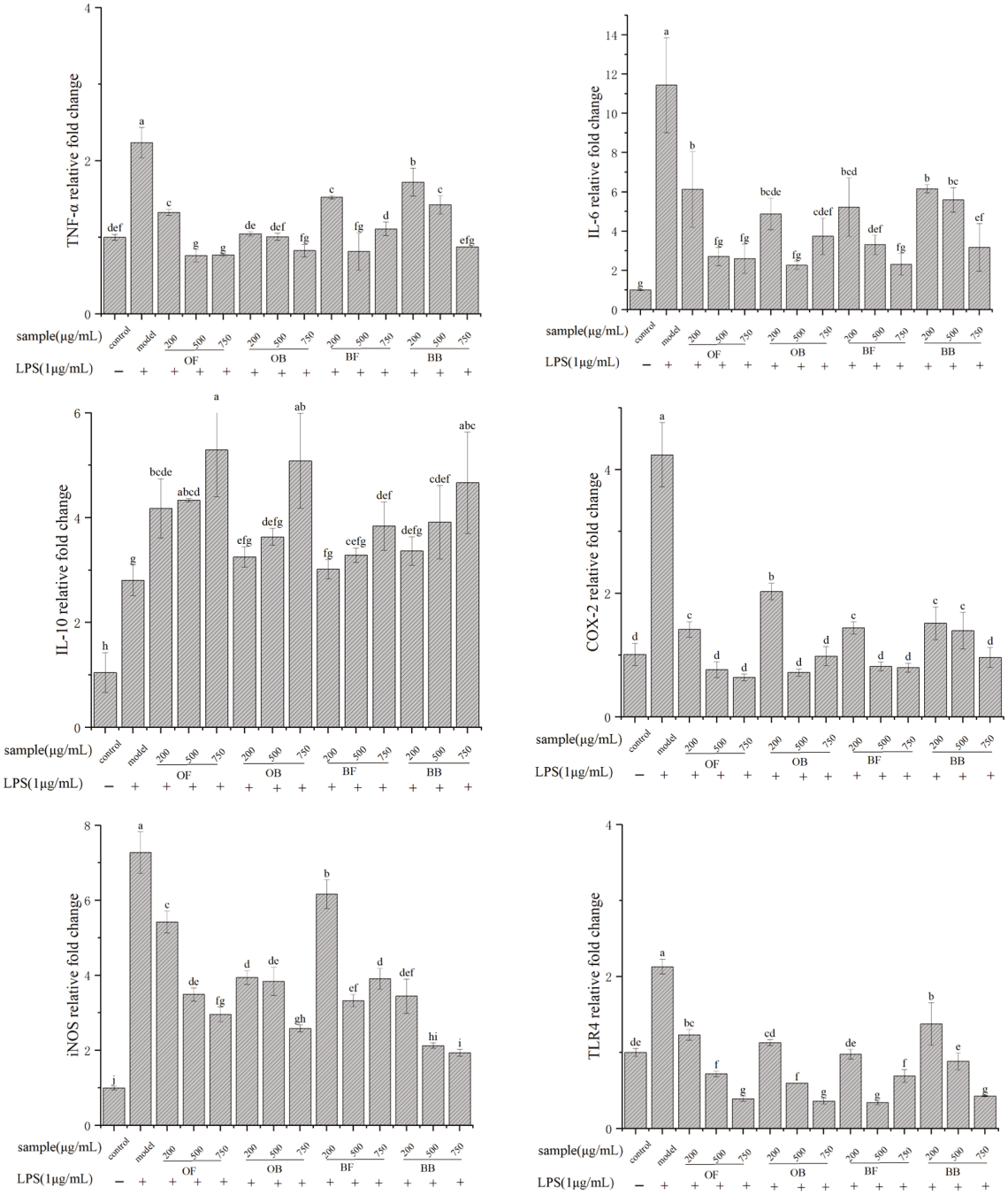

Figure 6. Effects of oat and bran polyphenol on the mRNA expression of TNF- α, IL-6, IL-10, COX-2, iNOS, and TLR4in Raw264.7 cells. Different lowercase represent significant differences among groups.

3.8. Protection of the Intestinal Barrier by the Oat and Oat Bran Polyphenols

A Caco-2 cell monolayer model was used to mimic the intestinal epithelial cell barrier. To induce inflammation, differentiated Caco-2 cells were pretreated with oat and oat bran polyphenols for 24 h and then induced with 1.5% DSS for another 24 h to test their protective effect on the intestinal barrier. Figure 7A–C display the TEER values, ALP activity ratio (AP/BL), and sodium fluorescein transmission rate of the Caco-2 cells over 21 days during the establishment of the monolayer model. As the cells were incubated in the Transwell plate over time, the TEER value increased to 487.30 $\Omega \cdot cm^2$, and the ALP activity ratio (AP/BL) gradually rose to 5.74 by the 21st day. The TEER value of the Caco-2 cells increased more rapidly during the initial 12 days of culture, slowed between days 12 to 16, and remained nearly constant from days 16 to 22. The sodium fluorescein transmittance rate was rapid in the blank group, while it was only 2.39% in the control group over 180 min. This indicated that after 21 days of culture, the Caco-2 cells had formed a dense monolayer, demonstrating good integrity of the cellular monolayer barrier. Thus, the in vitro model of the intestinal barrier was successfully established for subsequent experiments.

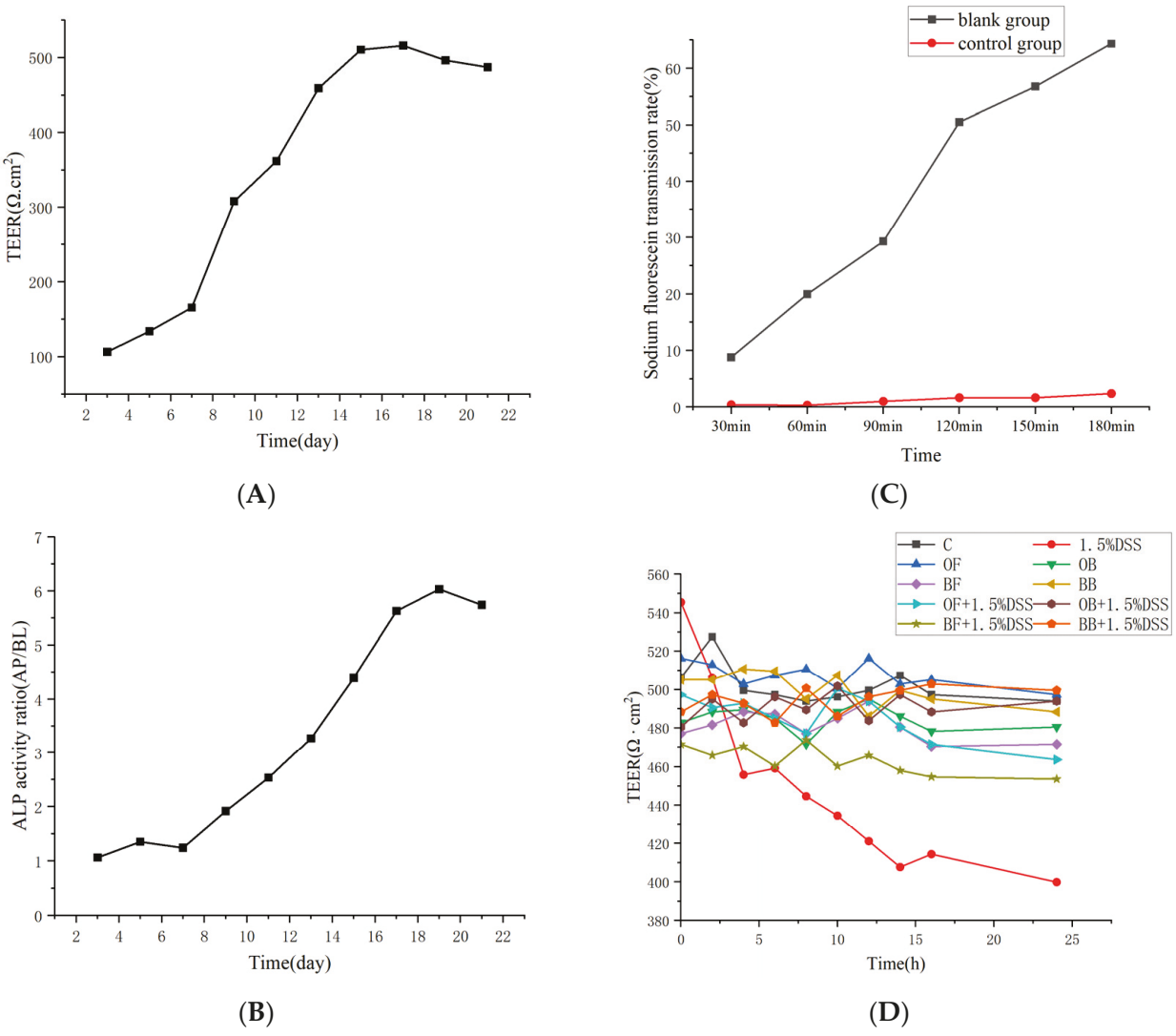

Figure 7. Change in TEER during the establishment of the Caco-2 monolayer (**A**), alkaline phosphatase activity (**B**), sodium fluorescein transmission rate (**C**), and TEER treated with 1.5% DSS and then with oat and bran polyphenols concentrations (1 mg/mL) to 24 h (**D**).

In Figure 7D, the resistance values of oat and bran polyphenols alone remained essentially unchanged after treating the cells for 24 h and did not affect the permeability of the cell membranes, and the addition of 1.5% DSS alone resulted in a drastic decrease in the TEER values from 0 to 12 h, and with the extension of the time, the resistance values eventually leveled off,, and the increase in intestinal permeability, indicating that the DSS disrupted the structure of the epithelial cellular barriers. Compared to the model group, administration of 1 mg/mL oat and bran polyphenols significantly attenuated the DSS-induced increase in cell barrier permeability, thereby protecting the cells from DSS-induced barrier damage. Bound polyphenol exhibited better protective effects in this regard.

3.9. Effect of Oat and Oat Bran Polyphenols on Intestinal Epithelial Barrier Genes

To further investigate the molecular mechanisms by which oat and bran polyphenols protect epithelial barrier function, we examined the mRNA expression levels of tight junction proteins (Occludin and Claudin-1) in Caco-2 monolayer cells. In Figure 8, the gene expression levels of Occludin and Claudin-1 were significantly reduced after 1.5% DSS stimulation compared to the normal group, indicating that DSS disrupted the integrity of the intestinal epithelial barrier by decreasing Occludin and Claudin-1 gene expression. Compared to the model group, Claudin-1 expression was increased 1.63-fold by oat bound polyphenol, and 1.88-fold and 1.91-fold by bran free phenol and bound polyphenol, respectively. Additionally, the gene expression level in the bound-polyphenol group was higher than in the free-polyphenol group. In contrast, compared to the model group, oat bound phenol, oat bran free polyphenol, and oat bran bound polyphenol treatment groups showed significantly higher Occludin gene expression levels. Oat free phenol and bound polyphenol increased Occludin gene expression 1.39-fold and 1.26-fold, respectively, while bran free phenol and bound polyphenol increased Occludin gene expression 1.59-fold and 1.77-fold, respectively. This suggests that oat and bran polyphenols can promote Occludin and Claudin-1 gene expression in cells, thereby protecting the intestinal epithelial barrier function.

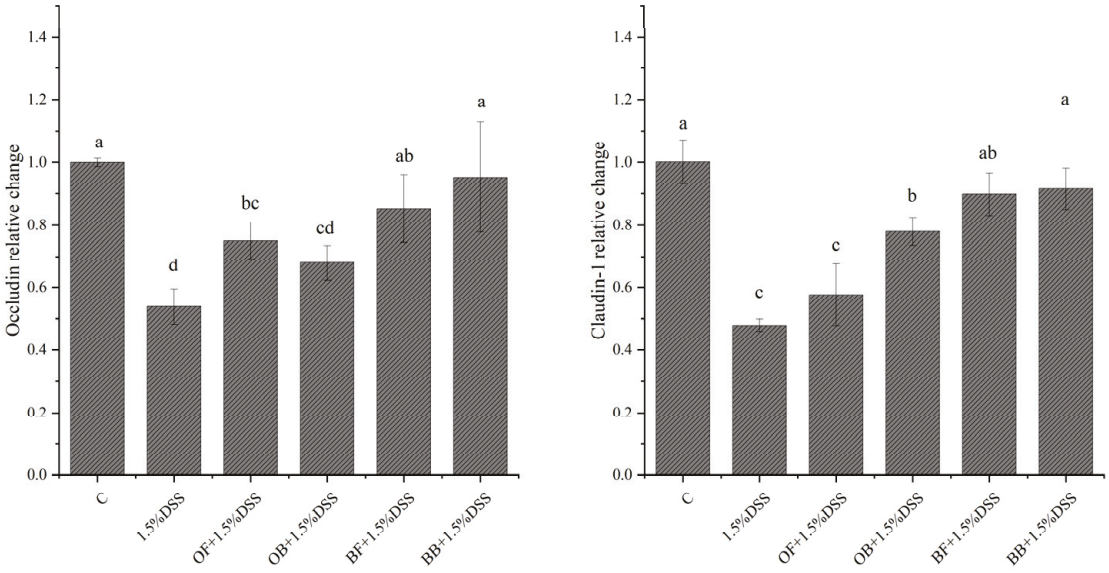

Figure 8. Effects of oat and bran polyphenol on the expression of Occludin and Claudin-1gene in DSS-induced Caco-2 cells. Different lowercase represent significant differences among groups.

4. Discussion

Phenolic acids of most cereals are concentrated in bran and germ, which are divided into free and bound states, and mainly in the bound state. The bound phenolic acids are connected with the main components of cell wall, such as protein and cellulose, in the form of ester bonds. Gong et al. (2019) [32] showed that the content of free phenols and free flavonoids in cereals is lower than that of bound polyphenol and bound flavonoids, which is consistent with the experimental results. Ferulic acid is mainly distributed in conjugated phenols. Gong et al. [32] reported that ferulic acid is also the main phenolic substance in oats, and this consistent with our study. Adom et al. (2002) [11] similarly found that 98% of ferulic acid in cereals was present in the bound polyphenol. Of course, because oat alkaloids are easy to degrade under strong alkaline conditions, we only measured free polyphenols. Hu et al. (2020) [33] showed that the total alkaloid content of six commercial sprouted oats was from 7.85 to 133.3 μg/g. Through comparative analysis, the content of alkaloid C in oats grown in European and American countries is generally higher than that in oats tested in this experiment (1.33–8.82 μg/g DW), which may be related to the growth environment, geographical location and extraction method of oats. Consistent with our experimental results, Hitayezu et al. (2015) [34] showed that the content of alkaloids in oats gradually decreased from outer bran to aleurone layer and then to endosperm, the content of avenanthramides C in bran was significantly higher than oats.

Macrophages are the first line of defense of the body's immune response, with the functions of recognizing, phagocytosing, and removing bacteria and foreign objects. However, when macrophages are abnormally activated, they can secrete large amounts of pro-inflammatory cytokines, playing an important role in immune system homeostasis, and regulating excessive inflammation is essential for recovery of body functions [35,36]. The tight junction of intestinal epithelial cells is closely related to the development of various intestinal-related diseases such as impaired intestinal mucosal barrier function [7]. Therefore, the establishment of in vitro models of inflammation in macrophages and intestinal epithelial cells is necessary for studying the anti-inflammatory effects of drugs.

In our study, we assessed the potential of oat and oat bran polyphenols to alleviate cellular damage induced by LPS-stimulated RAW264.7 macrophages and DSS-stimulated Caco-2 cells. Macrophage phagocytosis plays a crucial role in the body's defense against pathogen infections. In addition, the effects of oat and bran polyphenols on phagocytic activity of RAW264.7 cells were determined by neutral red assay. The results revealed that LPS stimulation significantly enhanced the phagocytosis of RAW264.7 cells. However, pretreatment with oat and bran polyphenols inhibited LPS-induced phagocytosis, indicating that oat and bran polyphenols enhance the cells' anti-inflammatory capacity by modulating their phagocytic function and thereby protect the organism against antigenic infections.

It has been shown that macrophages stimulated by LPS release large amounts of inflammatory mediators such as NO and ROS. NO is a cytokine that maintains immunity and participates in various physiological processes within the organism. Excessive NO secretion during inflammation can lead to cell death [37–39]. ROS, as the primary mediator of cellular oxidative stress responses, can damage mitochondria and exacerbate cellular damage and inflammatory responses by reducing mitochondrial membrane potential [40]. Studies have demonstrated that the bioavailability of active compounds in physiological systems is often significantly lower than under in vitro conditions, primarily due to limited aqueous solubility, poor in vivo absorption, and inadequate metabolic stability. This discrepancy poses challenges in translating concentrations effective in cellular or animal models to clinically relevant dosages. Moreover, conventional in vitro experimental paradigms tend to emphasize acute cellular interactions, often overlooking the effects of prolonged exposure and the role of post-metabolic mechanisms of action [41]. The concentration of 100 μg/mL

did not significantly inhibit NO production, which may be due to insufficient concentration, resulting in an intracellular concentration below the threshold needed for effective action. Moreover, the anti-inflammatory effects of polyphenolic substances showed high variability depending on the source and extraction methods. Therefore, in this experiment, oat and bran polyphenols at concentrations ranging from 200 to 750 μg/mL significantly inhibited NO and ROS production in a concentration-dependent manner. The inhibitory effect on NO and ROS production was particularly pronounced at higher doses. Furthermore, the present study demonstrated that pretreatment with oat and oat bran polyphenols restored mitochondrial membrane potential.

In addition, activated inflammatory cells secrete inflammatory factors, such as TNF-α and IL-6, which further exacerbate the systemic inflammatory response. TNF-α plays a crucial role in the onset and progression of inflammation, promoting the synthesis and release of other inflammatory cytokines [42]. IL-6 is produced by a wide range of immune cells and is involved in regulating the majority of inflammation-induced acute phase proteins [43]. The results of this study showed that pretreatment with polyphenols from oats and oat bran significantly reduced the production of TNF-α and IL-6, while markedly increasing the level of IL-10, thereby further alleviating the inflammatory response exhibited by macrophages.

Existing studies have shown that the mechanism of LPS-induced inflammatory response in RAW264.7 cells is mainly attributed to LPS binding to the cell surface receptor TLR4 and activating intracellular pathways related to inflammation, thereby promoting the secretion of large amounts of inflammatory factors by cells. Cell injury further activates key enzymes such as iNOS and COX-2, triggering an inflammatory response [44]. iNOS and COX-2 are key enzymes upstream of NO and PGE2 synthesis. Previous findings have shown that RAW264.7 cells stimulated by LPS express significant quantities of COX-2 and iNOS mRNA, leading to the production of substantial amounts of NO and PGE2 [45]. In this study, gene expression was measured, revealing that the expression level of the TLR4 in the model group was significantly higher than that in the blank group, suggesting that TLR4 activation promotes downstream inflammatory factor expression. The subsequent increase in IL-6 and TNF further activates the inflammatory pathway, exacerbating the inflammatory response. After pretreatment with oat and bran polyphenols, the expression of COX-2 and iNOS mRNA was significantly inhibited, reducing the synthesis and secretion of pro-inflammatory cytokines, and decreasing macrophage phagocytosis. This alleviated and inhibited the onset and progression of inflammation, indicating that oat and bran polyphenols exhibit pronounced anti-inflammatory effects [44].

The degree of change in cell membrane permeability can reflect the function of intercellular tight junctions and cell monolayer barrier. The intestinal epithelium is an important barrier that protects the body from external harmful substances [46]. TEER values accurately indicate the integrity and permeability of the epithelial barrier. Higher TEER values indicate better intestinal barrier integrity and lower permeability. In this study, to assess intestinal epithelial barrier function, we measured cell permeability by evaluating TEER values using sodium fluorescein and alkaline phosphatase activity. Treatment with DSS has been shown to damage intestinal cells and increase intestinal permeability, thereby impairing intestinal barrier function [47]. Abnormal expression of inflammatory cytokines such as IL-6 and IL-8 is a major cause of disrupted intercellular tight junctions in intestinal tissues and damage to the epithelial barrier. In this study, we observed that DSS-stimulated Caco-2 cells produced inflammatory factors IL-6 and IL-8, which led to decreased TEER values. Treatment with oat and bran polyphenols stabilized TEER values, mitigated hyperpermeability in the model group, and preserved the integrity of the cellular monolayer, thereby reducing inflammation in intestinal cells. Notably, the present study found that oat

bran polyphenols exhibited toxicity at a concentration of 5 mg/mL in the Caco-2 cell model, while showing cytoprotective effects at lower concentrations. This finding is consistent with previous studies, which indicate that dietary polyphenols have cytoprotective effects at low doses. However, at high doses, they may cause toxic side effects, leading to negative outcomes [48].

Occludin and Claudin-1 are structurally important proteins that constitute tight junctions (TJs) and are major protein molecules that maintain intestinal epithelial barrier function and determine intestinal permeability [49]. Our results indicate that DSS-induced damage to the epithelial barrier was reversed by both oat and oat bran polyphenols treatments, and the anti-inflammatory effects of oat and bran polyphenols in intestinal cells Caco-2 are mainly reflected in the alleviation of DSS-induced intestinal barrier disruption by decreasing pro-inflammatory cytokine release and increasing the expression of tight junctions proteins, thus enhancing the intestinal mucosal barrier function.

5. Limitations

It should be noted that this study did not model the potential effects of the digestion process on the structure and anti-inflammatory activity of polyphenols. Future research will incorporate in vitro digestion models, such as the INFOGEST protocol, to more accurately evaluate the bioavailability and biological activity of oat-derived polyphenols in vivo.

6. Conclusions

Based on an in vitro cellular inflammation model, we explored the anti-inflammatory activities of oat and bran polyphenols. The results demonstrated that the extract exhibited anti-inflammatory activity within the effective concentration range of 200–750 μg/mL. Oat and oat bran polyphenols effectively inhibited NO and ROS production, suppressed the secretion of IL-6 and TNF-α inflammatory factors, increased mitochondrial membrane potential, and down-regulated the expression of inflammation-related genes TNF-α and IL-6. These actions could reduce organismal damage and exert anti-inflammatory effects. In the Caco-2 intestinal cell barrier model stimulated with DSS, oat and bran polyphenol treatments increased the mRNA expression levels of Claudin-1 and Occludin proteins in Caco-2 cells, thereby exerting a protective effect on intestinal barrier function. The study initially explored the in vitro anti-inflammatory activity of oat and bran polyphenols. Although its efficacy in vivo remains to be further validated, this is particularly important given that many polyphenols may exhibit low absorption and bioavailability. Therefore, follow-up studies are needed to further validate these findings using Caco-2 cell transporter assays or dynamic digestion models. Based on the current experimental results, future research will include the evaluation of the pharmacokinetic profile in animal models and the validation of in vivo anti-inflammatory effects at doses approximating dietary intake, and relevant data will be published in subsequent work. Additionally, we plan to establish a Caco-2/RAW264.7 co-culture system in a follow-up study to dynamically analyze the trans-barrier transport of oat polyphenols and their modulation of macrophage inflammation. It is also important to determine whether a single component or a mixture of components is responsible for their observed effects. This study confirms that oat and bran polyphenol extracts exhibit anti-inflammatory effects; however, the potential influence of other phytochemicals on their bioavailability requires further in-depth investigation.

Author Contributions: W.D. methodology, original draft preparation; T.L. and B.Z. investigation; R.H.L. resources, project administration. All authors have read and agreed to the published version of the manuscript.

Funding: This study was partially supported by Cornell China Center, Food and Health Fund, and YanGuFang Research Laboratory (2022-8950).

Institutional Review Board Statement: Not applicable.

Informed Consent Statement: Not applicable.

Data Availability Statement: The raw data supporting the conclusions of this article will be made available by the authors on request.

Conflicts of Interest: The authors declare that they have no conflicts of interest.

Appendix A

Table A1. Contents of common phenolic components of oat and oat bran.

Samples	Part	Phytochemicals (μg/g DW)							
		Gallic Acid	Protocatechuic Acid	p-Hydroxy-benzoic Acid	Vanillic Acid	Caffeic Acid	p-Coumaric Acid	Ferulic Acid	Avenanthramides C
Oat	Free	2.72 ± 0.04	0.52 ± 0.01	0.92 ± 0.01	1.2 ± 0.12	6.86 ± 0.17	1.15 ± 0.14	5.26 ± 0.02	1.33 ± 0.19
	Bound	ND	5.73 ± 0.03	8.32 ± 0.03	1.47 ± 0.09	0.86 ± 0.05	0.75 ± 0.74	198.09 ± 0.76	ND
	Total	2.72 ± 0.04	6.24 ± 0.03	9.24 ± 0.03	2.67 ± 0.08	7.71 ± 0.14	1.91 ± 0.88	203.36 ± 0.74	1.33 ± 0.19
Oat Bran	Free	6.48 ± 0.02	1.13 ± 0.01	7.82 ± 0.03	0.93 ± 0.01	1.22 ± 0	2.91 ± 0.14	11.28 ± 0.02	8.82 ± 4.04
	Bound	ND	10.49 ± 0.05	8.03 ± 0.07	0.29 ± 0.04	1.76 ± 0.06	2.92 ± 0.11	335.15 ± 1.64	ND
	Total	6.48 ± 0.02	11.62 ± 0.04	15.85 ± 0.09	1.22 ± 0.04	2.98 ± 0.06	5.83 ± 0.19	346.43 ± 1.62	8.82 ± 4.04

Notes: ND: not detected.

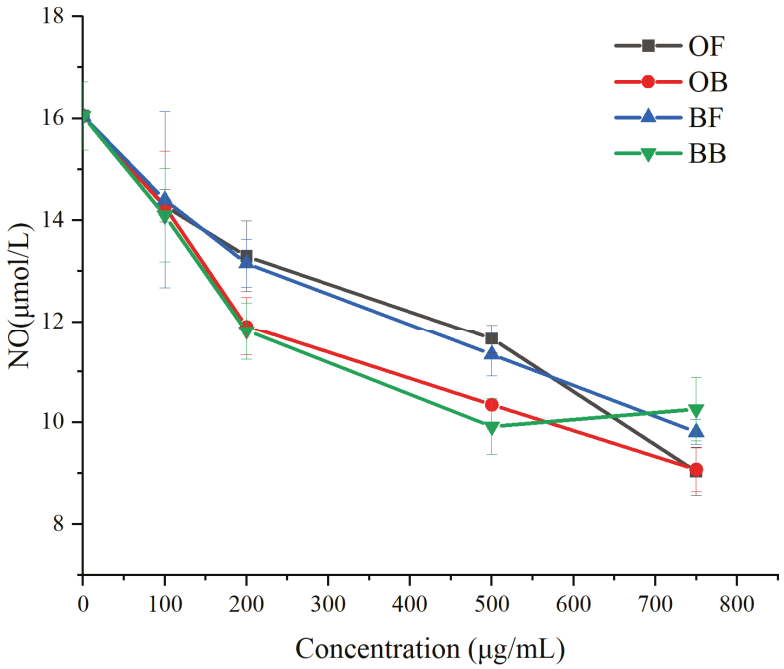

Figure A1. Effects of different concentrations of oat and oat bran polyphenols on NO formation in Raw 264.7 macrophages. OF (oat free polyphenol); BF (bran free polyphenol); OB (oat bound polyphenol) and BB (oat bran bound polyphenol).

References

1. Kellow, N.J.; Coughlan, M.T. Effect of diet-derived advanced glycation end products on inflammation. *Nutr. Rev.* **2015**, *73*, 737–759. [CrossRef] [PubMed]
2. Fredman, G. DELineating resolution of inflammation. *Nat. Immunol.* **2019**, *20*, 2–3. [CrossRef] [PubMed]
3. Grant, W.B. Diet, Inflammation, and infectious diseases. *Nutrients* **2023**, *15*, 2891. [CrossRef] [PubMed]
4. Zhang, Z.; Tanaka, I.; Pan, Z.; Ernst, P.B.; Kiyono, H.; Kurashima, Y. Intestinal homeostasis and inflammation: Gut microbiota at the crossroads of pancreas–intestinal barrier axis. *Eur. J. Immunol.* **2022**, *52*, 1035–1046. [CrossRef]

5. Martins-Gomes, C.; Nunes, F.M.; Silva, A.M. Natural products as dietary agents for the prevention and mitigation of oxidative damage and inflammation in the intestinal barrier. *Antioxidants* **2024**, *13*, 65. [CrossRef]
6. Kaplan, G.G.; Ng, S.C. Understanding and preventing the global increase of inflammatory bowel disease. *Gastroenterology* **2017**, *152*, 313–321.e2. [CrossRef]
7. Davis, E.M.; Kaufmann, Y.; Goyne, H.; Wang, Y.X.; Chen, T.; Theus, S.; Liu, J.J. Pyroptosis of intestinal epithelial cells is crucial to the development of mucosal barrier dysfunction and intestinal inflammation. *Gastroenterology* **2017**, *152*, S967. [CrossRef]
8. Song, X.; Zhang, X.; Ma, C.; Hu, X.; Chen, F. Rediscovering the nutrition of whole foods: The emerging role of gut microbiota. *Curr. Opin. Food Sci.* **2022**, *48*, 100908. [CrossRef]
9. Fang, W.; Peng, W.; Qi, W.; Zhang, J.; Song, G.; Pang, S.; Wang, Y. Ferulic acid combined with different dietary fibers improve glucose metabolism and intestinal barrier function by regulating gut microbiota in high-fat diet-fed mice. *J. Funct. Foods* **2024**, *112*, 105919. [CrossRef]
10. Roager, H.M.; Vogt, J.K.; Kristensen, M.; Hansen, L.B.S.; Ibrügger, S.; Mærkedahl, R.B.; Licht, T.R. Whole grain-rich diet reduces body weight and systemic low-grade inflammation without inducing major changes of the gut microbiome: A randomised cross-over trial. *Gut* **2019**, *68*, 83. [CrossRef]
11. Adom, K.K.; Liu, R.H. Antioxidant activity of grains. *J. Agric. Food Chem.* **2002**, *50*, 6182–6187. [CrossRef] [PubMed]
12. Awika, J.M.; Rose, D.J.; Simsek, S. Complementary effects of cereal and pulse polyphenols and dietary fiber on chronic inflammation and gut health. *Food Funct.* **2018**, *9*, 1389–1409. [CrossRef] [PubMed]
13. Gao, H.; Song, R.J.; Jiang, H.; Zhang, W.; Han, S.F. Oat fiber supplementation alleviates intestinal inflammation and ameliorates intestinal mucosal barrier via acting on gut microbiota-derived metabolites in $LDLR^{-/-}$ mice. *Nutrition* **2022**, *95*, 111558. [CrossRef] [PubMed]
14. Dong, L.; Qin, C.; Li, Y.; Wu, Z.; Liu, L. Oat phenolic compounds regulate metabolic syndrome in high fat diet-fed mice via gut microbiota. *Food Biosci.* **2022**, *50*, 101946. [CrossRef]
15. Ma, L.; Luo, Z.; Huang, Y.; Li, Y.; Guan, J.; Zhou, T.; Cao, S. Modulating gut microbiota and metabolites with dietary fiber oat β-glucan interventions to improve growth performance and intestinal function in weaned rabbits. *Front. Microbiol.* **2022**, *13*, 1074036. [CrossRef]
16. Soycan, G.; Schär, M.Y.; Kristek, A.; Boberska, J.; Alsharif, S.N.S.; Corona, G.; Spencer, J.P.E. Composition and content of phenolic acids and avenanthramides in commercial oat products: Are oats an important polyphenol source for consumers? *Food Chem. X* **2019**, *3*, 100047. [CrossRef]
17. Zhang, L.; Wu, T.; Zhang, Y.; Chen, Y.; Ge, X.; Sui, W.; Zhang, M. Release of bound polyphenols from wheat bran soluble dietary fiber during simulated gastrointestinal digestion and colonic fermentation in vitro. *Food Chem.* **2023**, *402*, 134111. [CrossRef]
18. Li, J.; Zhang, H.; Yang, X.; Zhu, L.; Wu, G.; Qi, X.; Zhang, H. Trapping of reactive carbonyl species by fiber-bound polyphenols from whole grains under simulated physiological conditions. *Food Res. Int.* **2022**, *156*, 111142. [CrossRef]
19. Chen, C.; Wang, L.; Chen, Z.X.; Luo, X.H.; Li, Y.F.; Wang, R.; Li, J.; Li, Y.A.; Wang, T.; Wu, J. Effects of milk proteins on the bioaccessibility and antioxidant activity of oat phenolics during in vitro digestion. *J. Food Sci.* **2019**, *84*, 895–903. [CrossRef]
20. Li, X.; Du, Y.; Zhang, C.; Tu, Z.; Wang, L. Modified highland barley regulates lipid metabolism, liver inflammation and gut microbiota in high-fat/cholesterol diet mice as revealed by LC-MS based metabonomics. *Food Funct.* **2022**, *13*, 9119–9142. [CrossRef]
21. Hong, S.; Pangloli, P.; Perumal, R.; Cox, S.; Noronha, L.E.; Dia, V.P.; Smolensky, D. A comparative study on phenolic content, antioxidant activity and anti-inflammatory capacity of aqueous and ethanolic extracts of sorghum in lipopolysaccharide-induced RAW264.7 macrophages. *Antioxidants* **2020**, *9*, 1297. [CrossRef] [PubMed]
22. Yang, R.; Shan, S.; Zhang, C.; Shi, J.; Li, H.; Li, Z. Inhibitory effects of bound polyphenol from foxtail millet bran on colitis-associated carcinogenesis by the restoration of gut microbiota in a mice model. *J. Agric. Food Chem.* **2020**, *68*, 3506–3517. [CrossRef] [PubMed]
23. Chen, S.W.; Zhu, J.; Zuo, S.; Zhang, J.; Chen, Z.Y.; Chen, G.W.; Wang, P. Protective effect of hydrogen sulfide on TNF-α and IFN-γ-induced injury of intestinal epithelial barrier function in Caco-2 monolayers. *Inflamm. Res.* **2015**, *64*, 789–797. [CrossRef] [PubMed]
24. Kim, K.J.; Kim, Y.; Jin, S.G.; Kim, J.Y. Acai berry extract as a regulator of intestinal inflammation pathways in a Caco-2 and RAW264.7 co-culture model. *J. Food Biochem.* **2021**, *45*, e13848. [CrossRef]
25. He, Z.Q.; Deng, N.; Zheng, B.S.; Li, T.; Liu, R.H.; Yuan, L.; Li, W.Z. Changes in polyphenol fractions and bacterial composition after in vitrofermentation of apple peel polyphenol by gut microbiota. *Int. J. Food Sci. Technol.* **2022**, *57*, 4268–4276. [CrossRef]
26. Ji, K.-Y.; Kim, K.M.; Kim, Y.H.; Im, A.R.; Lee, J.Y.; Park, B.; Chae, S. The enhancing immune response and anti-inflammatory effects of Anemarrhena asphodeloides extract in RAW264.7 cells. *Phytomedicine* **2019**, *59*, 152789. [CrossRef]
27. Xiong, L.; Ouyang, K.H.; Jiang, Y.; Yang, Z.W.; Hu, W.-B.; Chen, H.; Wang, W.J. Chemical composition of Cyclocarya paliurus polysaccharide and inflammatory effects in lipopolysaccharide-stimulated RAW264.7 macrophage. *Int. J. Biol. Macromol.* **2018**, *107*, 1898–1907. [CrossRef]

28. Wang, H.; Guo, X.; Liu, J.; Li, T.; Fu, X.; Liu, R.H. Comparative suppression of NLRP3 inflammasome activation with LPS-induced inflammation by blueberry extracts (*Vaccinium* spp.). *RSC Adv.* **2017**, *7*, 28931–28939. [CrossRef]
29. Kapoor, S.; Padwad, Y.S. Phloretin suppresses intestinal inflammation and maintained epithelial tight junction integrity by modulating cytokines secretion in model of gut inflammation. *Cell. Immunol.* **2023**, *391-392*, 104754. [CrossRef]
30. Yang, Y.; Ren, R.R.; Chen, Q.Q.; Zhang, Q.Q.; Wu, J.J.; Yin, D.K. Coptis chinensis polysaccharides dynamically influence the paracellular absorption pathway in the small intestine by modulating the intestinal mucosal immunity microenvironment. *Phytomedicine* **2022**, *104*, 154322. [CrossRef]
31. Guo, T.Y.; Lin, Q.L.; Li, X.H.; Nie, Y.; Wang, L.; Shi, L.M.; Luo, F.J. Octacosanol attenuates inflammation in both RAW264.7 macrophages and a mouse model of colitis. *J. Agric. Food Chem.* **2017**, *65*, 3647–3658. [CrossRef] [PubMed]
32. Gong, E.S.; Gao, N.X.; Li, T.; Chen, H.Y.; Wan, Y.H.; Si, X.; Liu, R.H. Effect of in vitro digestion on phytochemical profiles and cellular antioxidant activity of whole grains. *J. Agric. Food Chem.* **2019**, *67*, 7016–7024. [CrossRef] [PubMed]
33. Hu, C.L.; Tang, Y.; Zhao, Y.T.; Sang, S.M. Quantitative analysis and anti-inflammatory activity evaluation of the a-type avenanthramides in commercial sprouted oat products. *J. Agric. Food Chem.* **2020**, *68*, 13068–13075. [CrossRef]
34. Hitayezu, R.; Baakdah, M.M.; Kinnin, J.; Henderson, K.; Tsopmo, A. Antioxidant activity, avenanthramide and phenolic acid contents of oat milling fractions. *J. Cereal Sci.* **2015**, *63*, 35–40. [CrossRef]
35. Schultze, J.L.; Rosenstiel, P.; Consortium, S. Systems medicine in chronic inflammatory diseases. *Immunity* **2018**, *48*, 608–613. [CrossRef]
36. Van den Bossche, J.; Baardman, J.; Otto, N.A.; van der Velden, S.; Neele, A.E.; van den Berg, S.M.; de Winther, M.P.J. Mitochondrial dysfunction prevents repolarization of inflammatory macrophages. *Cell Rep.* **2016**, *17*, 684–696. [CrossRef]
37. Guo, C.; Yang, L.; Luo, J.; Zhang, C.; Xia, Y.Z.; Ma, T.; Kong, L.Y. Sophoraflavanone G from inhibits lipopolysaccharide-induced inflammation in RAW264.7 cells by targeting PI3K/Akt, JAK/STAT and Nrf2/HO-1 pathways. *Int. Immunopharmacol.* **2016**, *38*, 349–356. [CrossRef]
38. Hsieh, S.C.; Hsieh, W.J.; Chiang, A.N.; Su, N.W.; Yeh, Y.T.; Liao, Y.C. The methanol-ethyl acetate partitioned fraction from Chinese olive fruits inhibits cancer cell proliferation and tumor growth by promoting apoptosis through the suppression of the NF-κB signaling pathway. *Food Funct.* **2016**, *7*, 4797–4803. [CrossRef]
39. Nathan, C.; Xie, Q.W. Nitric oxide synthases: Roles, tolls, and controls. *Cell* **1994**, *78*, 915–918. [CrossRef]
40. Ishii, M.; Nakahara, T.; Araho, D.; Murakami, J.; Nishimura, M. Glycolipids from spinach suppress LPS-induced vascular inflammation through eNOS and NK-κB signaling. *Biomed. Pharmacother.* **2017**, *91*, 111–120. [CrossRef]
41. Yang, B.Y.; Dong, Y.X.; Wang, F.; Zhang, Y. Nanoformulations to enhance the bioavailability and physiological functions of polyphenols. *Molecules* **2020**, *25*, 4613. [CrossRef] [PubMed]
42. Wang, S.Y.; Shi, X.J.; Li, J.; Huang, Q.P.; Ji, Q.; Yao, Y.; Yang, G. A small molecule selected from a DNA-Encoded library of natural products that binds to TNF-α and attenuates inflammation in vivo. *Adv. Sci.* **2022**, *9*, 2201258. [CrossRef] [PubMed]
43. Ye, M.; Joosse, M.E.; Liu, L.; Sun, Y.; Dong, Y.; Cai, C.C.; Li, X.H. Deletion of IL-6 exacerbates colitis and induces systemic inflammation in IL-10-deficient mice. *J. Crohn's Colitis* **2020**, *14*, 831–840. [CrossRef] [PubMed]
44. He, J.; Han, S.; Li, X.X.; Wang, Q.Q.; Cui, Y.; Chen, Y.; Yang, S. Diethyl blechnic exhibits anti-Inflammatory and antioxidative activity via the TLR4/MyD88 signaling pathway in LPS-stimulated RAW264.7 cells. *Molecules* **2019**, *24*, 4502. [CrossRef]
45. George, G.; Shyni, G.L.; Abraham, B.; Nisha, P.; Raghu, K.G. Downregulation of TLR4/MyD88/p38MAPK and JAK/STAT pathway in RAW264.7 cells by Alpinia galanga reveals its beneficial effects in inflammation. *J. Ethnopharmacol.* **2021**, *275*, 114132. [CrossRef]
46. Jutanom, M.; Kato, S.; Yamashita, S.; Toda, M.; Kinoshita, M.; Nakagawa, K. Analysis of oxidized glucosylceramide and its effects on altering gene expressions of inflammation induced by LPS in intestinal tract cell models. *Sci. Rep.* **2023**, *13*, 22537. [CrossRef]
47. Chen, Y.H.; Shin, J.Y.; Wei, H.M.; Lin, C.C.; Yu, L.C.H.; Liao, W.T.; Chu, C.L. Prevention of dextran sulfate sodium-induced mouse colitis by the fungal protein Ling Zhi-8 promoting the barrier function of intestinal epithelial cells. *Food Funct.* **2021**, *12*, 1639–1650. [CrossRef]
48. Calabrese, V.; Cornelius, C.; Trovato-Salinaro, A.; Cambria, M.T.; Locascio, M.S.; Di Rienzo, L.; Condorelli, D.F.; Mancuso, C.; De Lorenzo, A.; Calabrese, E.J. The hormetic role of dietary antioxidants in free radical-related diseases. *Curr. Pharm. Des.* **2010**, *16*, 877–883. [CrossRef]
49. Bein, A.; Zilbershtein, A.; Golosovsky, M.; Davidov, D.; Schwartz, B. LPS induces hyper-permeability of intestinal epithelial cells. *J. Cell. Physiol.* **2017**, *232*, 381–390. [CrossRef]

Disclaimer/Publisher's Note: The statements, opinions and data contained in all publications are solely those of the individual author(s) and contributor(s) and not of MDPI and/or the editor(s). MDPI and/or the editor(s) disclaim responsibility for any injury to people or property resulting from any ideas, methods, instructions or products referred to in the content.

nutrients

MDPI

Article

Assessing the Role of Dark Sweet Cherry (*Prunus avium* L.) Consumption on Cognitive Function, Neuropeptides, and Circadian Rhythm in Obesity: Results from a Randomized Controlled Trial

Shirley Arbizu [1], Susanne U. Mertens-Talcott [1], Stephen Talcott [1], Aaron Riviere [2], Steven E. Riechman [2,3] and Giuliana D. Noratto [1,*]

[1] Department of Food Science and Technology, Texas A&M University, College Station, TX 77843, USA
[2] Department of Health and Kinesiology, Texas A&M University, College Station, TX 77843, USA
[3] Department of Nutrition, Texas A&M University, College Station, TX 77843, USA
* Correspondence: gnoratto@tamu.edu

Abstract

Background/Objectives: Obesity is linked to a higher risk of cognitive impairment. The objective of this single blind randomized trial was to evaluate the impact of dark sweet cherry (DSC) intake on cognitive function in obese adults. **Methods:** Participants (body mass index (BMI): 30–40 kg/m^2, >18 years, without chronic diseases and/or antibiotic use) consumed 200 mL of DSC drink with 3 g of cherry powder (n = 19) or an isocaloric placebo drink (n = 21) twice daily for 30 days. Cognitive function was assessed at Day 1 (D1) and Day 30 (D30) using standardized cognitive tests and the NeuroTracker (NT) 3D training program. Blood biomarkers related to cognitive health (neurotensin, substance p, and oxytocin) and circadian rhythm (melatonin and cortisol) were assessed at D1 and D30 using a Luminex multiplex bead-based immunoassay. **Results:** DSC supplementation significantly improved working memory and concentration, as indicated by higher scores in the digit span forward (DSF, p = 0.006) and backward (DSB, p = 0.01) tests. However, processing speed, sustained attention, and visual spatial skills, assessed through the trail making (TMT) and digit symbol substitution (DSST) tests, as well as visual cognitive performance (VCP) evaluated by the NT program, showed no significant differences between groups. Neurotensin, associated with cognitive deficits, increased in both cherry and placebo groups but was significant only in the placebo group (p = 0.007). Similarly, melatonin increased in both groups, reaching significance only in the placebo group (p = 0.02), and it correlated positively with IFNγ, suggesting a compensatory response to inflammation. **Conclusions:** These findings suggest DSC supplementation may enhance specific cognitive functions in obese adults. Further clinical trials are needed to confirm these results.

Keywords: dark sweet cherries; cognition; obesity; human clinical study; neuropeptides; circadian rhythm

1. Introduction

The prevalence of obesity has steadily increased in the U.S. since 1999, and it is expected to affect nearly 50% of the adult population by 2030 [1]. Obesity is a significant public health issue as it is a major risk factor for various illnesses and is associated with poorer outcomes for chronic diseases [1]. Additionally, obesity has been associated with

impaired cognitive performance, cognitive decline, and neurodegenerative disorders [2]. Research conducted previously revealed that obese patients exhibited poorer performance in tasks assessing overall cognitive function, particularly in attention and memory [3]. Similarly, deficits in executive function (attention, processing speed, decision making, working memory, concept formation, and problem solving) have been reported in obese subjects [2,3].

Although the mechanisms underlying the relationship between obesity and cognitive dysfunction remain unclear, evidence indicates that inflammation caused by obesity might play a significant role in the development of cognitive impairment [4]. More specifically, the development of low-chronic inflammation in obese individuals may eventually spread into the central nervous system, leading to negative cognitive outcomes [4,5].

Obesity-induced inflammatory processes might contribute to cognitive and behavioral decline by altering genes related to learning and memory, such as neuropeptides [5]. These small proteinaceous peptides are implicated in the dysregulation underlying obesity-associated cognitive dysfunction [6]. Thus, targeting neuropeptides such as neurotensin, substance p and oxytocin might be a beneficial strategy to address cognitive deficits associated under obesity conditions [7]. Neurotensin modulates a range of diverse biological activities including learning and memory processes [6], and it has been positively correlated with perceived stress, anxiety, depression and eating disorders in female obese patients [8]. Substance P is a neuropeptide that influences many physiological processes, such as inflammation, intestinal motility, mucosal secretion and epithelial ion transmission [9]. Moreover, it acts as both a neurotransmitter and neuromodulator in the central nervous system, regulating a variety of behavioral functions, including general and motor activity, pain, food and water intake, anxiety, and memory consolidation [10]. Oxytocin is another neuropeptide that affects cognitive, emotional, and behavioral processes, including food intake and eating disorders [11], and its serum levels have been found to be reduced in type 2 diabetes and obese subjects [12].

Obesity has also been linked to the dysregulation of circadian rhythm. As such, clinical studies have reported the disturbance of hormones that regulate the circadian rhythm such as melatonin [13] and cortisol [14] in obese subjects. Circadian rhythms are internally driven cycles that influence complex cognitive tasks such as selective attention and executive function [15]. In addition, circadian rhythm disruption is considered a risk factor for obesity development.

Polyphenol-rich foods have received particular attention as numerous studies have investigated whether their consumption is associated with cognitive-enhancing effects and neuroprotective benefits [16]. Cherries contain polyphenols such as phenolic acids (i.e., hydroxycinnamic acids) and flavonoids (i.e., anthocyanins), showing high antioxidant and anti-inflammatory potential [17]. These compounds exert neuroprotective effects via multiple mechanisms, including antioxidant activity, anti-inflammatory properties, and the modulation of neuronal signaling pathways. Anthocyanins (ACNs) have been shown to enhance cognitive function by increasing cerebral blood flow, reducing oxidative stress, and inhibiting neuroinflammation [18,19]. ACNs also promote synaptic plasticity and modulate signaling pathways, such as the cAMP response element-binding protein (CREB) pathway, which is critical for memory formation and learning [18,19]. ACNs might also improve cognitive performance by crossing the blood–brain barrier (BBB) and acting as antioxidants to neutralize reactive oxygen species (ROS) [18,19]. Phenolic acids also play a role in neuroprotection by reducing neuroinflammation and oxidative damage [20]. Moreover, phenolic acids may prevent the aggregation of proteins linked to the development of various neurodegenerative diseases associated with cognitive decline, such as Alzheimer's disease, Parkinson's disease, and multiple system atrophy [20].

Even though sweet and tart cherries are good sources of polyphenols, tart cherries are rarely eaten as fresh fruit due to their sour taste. In contrast to sweet cherries, tart cherries are commonly processed into products involving heat, which can degrade polyphenols. Still, tart cherries have been credited with the potential to enhance cognitive function and exert neuroprotective effects. For example, the daily supplementation of a diet containing 2% freeze-dried tart cherry powder improved working memory in Fischer 344 aged rats [21]. Likewise, visual sustained attention and subjective memory were significantly improved in older adults after 12-week consumption of 480 mL of tart cherry juice [22]. Previous *in vitro* studies using neuronal cell models have highlighted the potential of sweet cherries in supporting cognitive function and neuroprotection. For example, Matias et al. [23] reported that a phenolic-rich extract from Portuguese Saco sweet cherry culls exhibited strong antioxidant activity in SK-N-MC neuronal cells exposed to oxidative stress. Similarly, Antognoni et al. [24] demonstrated the neuroprotective potential of new sweet cherry cultivars in neuron-like SH-SY5Y cells as these cultivars protected against oxidative stress and upregulated brain-derived neurotrophic factors (BDNF), reinforcing their potential role in preventing neurodegeneration. These findings suggest that sweet cherries might mitigate oxidative stress-related disorders and exert a neuroprotective effect, potentially supporting cognitive function. To our knowledge, only one study investigated the daily consumption of sweet Bing cherry juice (200 mL) over 12 weeks in participants with aging-associated cognitive decline [25]. In this study, the cherry juice intake improved verbal fluency, short-term memory, and long-term memory in older adults with mild-to moderate dementia [25]. Therefore, the influence of dark sweet cherries (DSCs) in obesity-related cognitive dysfunction remains to be investigated. Furthermore, considering that obesity-induced inflammation can disrupt circadian regulation and neuropeptide signaling, leading to impairments in cognitive function, the objective of this study was to evaluate the influence of daily DSC drink consumption for 30 days on cognitive performance, neuropeptides, and circadian rhythm biomarkers in obese adults.

2. Materials and Methods

2.1. Study Design and Participant Eligibility

The study design and participant eligibility were reported in detail previously [26]. This 30-day single-blind randomized controlled trial was conducted at Texas A&M University (College Station, TX). The decision to conduct a 30-day intervention was based on the study's complexity with participant compliance and potential dropout rates being critical considerations. Participants were exclusively recruited from the A&M campus, allowing for controlled enrollment and enhanced monitoring, which ensured better compliance with the intervention. Adults aged 18 years and older were recruited between January 2020 and August 2021 based on the following inclusion criteria: body mass index (BMI) $\geq$30 and $\leq$40 and no history of chronic diseases or intestinal disorders [26,27]. Participants were excluded if they had any of the following conditions within the previous 6 months: acute cardiac event, stroke, cancer, hepatitis (B or C), HIV, liver or renal dysfunction, macular degeneration, glaucoma, retinitis pigmentosa, optic neuropathy, retinal vascular occlusions, strabismus, autoimmune disorders related to visual health, history of dizziness/fainting during and after blood draws, gluten sensitivity or celiac disease. Antibiotic use, excessive alcohol consumption, smoking, berry allergies or sensitivities, pregnancy or lactation were also considered exclusion criteria [26,27]. After completing a 2-week run-in period, during which participants were instructed to avoid polyphenol-rich foods, an adaptive randomization method was implemented to balance key prognostic factors (BMI, gender, and age) across treatment groups and ensure sample representativeness, minimizing selection bias. After the 2-week run-in period, participants were scheduled for study visits: Day 1

(D1), Day 15 during the intervention (D15), and Day 30 at the end of the study (D30). A schematic representation of the study schedule is presented in Figure 1. This study was approved by the Institutional Review Board (IRB2019-0597F) on 13 November 2019 at Texas A&M University and registered at clinicaltrials.gov as NCT05586386 on 19 October 2022.

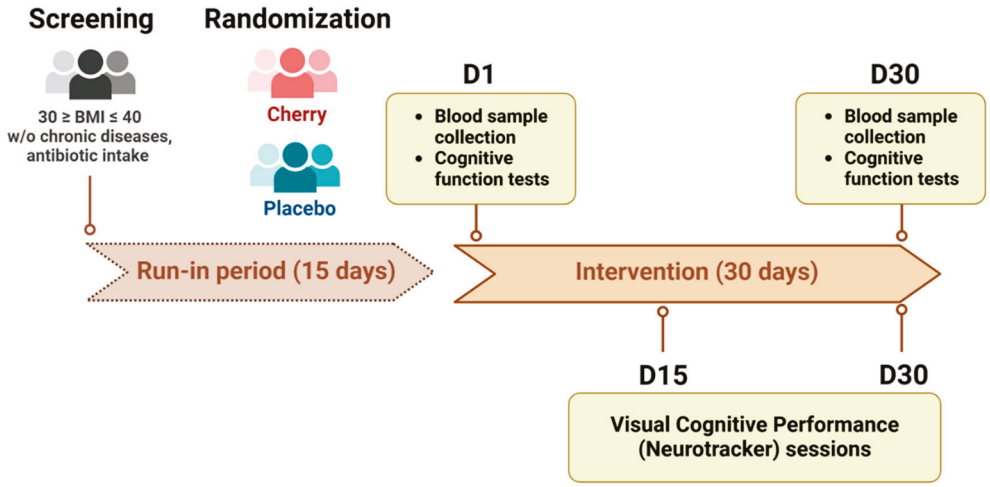

Figure 1. Schematic representation of study protocol. D1: Day 1, D15: Day 15 and D30: Day 30.

2.2. DSC Supplementation and Dietary Assessment

On D1, participants received 50 mL of DSC concentrated juice which was kindly provided by FruitSmart® (Grandview, WA, USA) and supplemented with 3 g of DSC powder kindly provided by Anderson Advance Ingredients (Irvine, CA, USA) with instructions to reconstitute with water up to 200 mL (~8 oz). The placebo concentrated drink was prepared by study personnel according to good manufacturing practices in the Department of Food Science and Technology at Texas A&M University. The nutritional and physicochemical characteristics of the DSC concentrated juice, DSC powder, reconstituted DSC drink, and placebo concentrated drink formulation have been previously detailed and can be accessed at https://www.mdpi.com/article/10.3390/nu15030681/s1 (accessed on 29 January 2023). The reconstituted DSC drink contained bioactive compounds from both DSC juice and DSC powder, providing 0.11 g of fiber, 439.6 mg of total phenolics (as gallic acid equivalents), and 70.21 mg of cyanidin 3-glucoside anthocyanins [26,27]. Participants were instructed to drink the reconstituted DSC or placebo beverage twice a day for 30 days and to maintain their usual physical activity and diet. Additionally, participants were provided with both verbal and written instructions to limit their consumption of foods high in polyphenols and to avoid berry intake during the study. Participants were instructed to track their daily food and beverage intake over 15 days during the 30-day intervention using MyFitnessPal (https://www.myfitnesspal.com) to evaluate the impact of their nutritional habits on the study outcomes [26]. Nutritional intake, including calories, carbohydrates, fat, protein, fiber, and cholesterol, was used to estimate Healthy Eating Index (HEI) scores, which reflect how closely a diet aligns with the key recommendations of the Dietary Guidelines for Americans. A detailed description of the data collection and analysis methods has been previously published [26].

2.3. Cognitive Performance

Cognitive performance was assessed through the evaluation of executive function skills and visual cognitive performance.

(a) Executive Function Skills: The trail making test (TMT), digit span (DS) and digit symbol substitution test (DSST) were used to evaluate executive function skills at D1 and D30.

- TMT: Executive attention and visual–spatial functions (visual search, scanning and mental flexibility) were assessed by trail making tests A (TMT-A) and B (TMT-B) [28]. In TMT-A, participants were asked to draw lines to connect numbered circles (1–25) in ascending order. In TMT-B, participants were asked to draw lines to connect circles in an ascending pattern but with the added task of alternating between the numbers (1–13) and letters (A–L). Participants were instructed to complete TMT-A and -B as fast as possible without lifting their pen/pencil from the paper, and the time in which each test was completed was recorded [28]. The results for both TMT-A and TMT-B were expressed as the time in seconds taken to complete the task; thus, higher scores indicated greater cognitive impairment.
- DS: Working memory, cognitive flexibility and concentration skills were evaluated by the digit span forward (DSF) and backward (DSB) tests [29]. In the DSF test, participants were asked to repeat a set of numbers in the same order as read by the study coordinator, while the DSB test required participants to repeat numbers in the reverse order of that given. Scores were given according to the set of numbers that were repeated correctly. For both DSF and DSB, a higher score indicates better ability to manage and process information in short-term and working memory tasks.
- DSST: Processing speed, sustained attention, and visual perceptual functions (scanning and basic manual dexterity) were evaluated with DSST [30]. In this test, participants were tasked to associate a collection of symbols with numerical digits within a 90-second timeframe, and their score was determined by the quantity of accurately matched symbols completed within this time limit. In this test, a higher score indicates that an individual processes information quickly and accurately.

(b) Visual Cognitive Performance (VCP): VCP refers to the ability of the brain to interpret and process visual information to perform cognitive tasks effectively [31]. VCP was evaluated during the last 15 days (D15–D30) of the intervention using the NeuroTracker™ CORE program (NT) (CogniSens Athletic Inc., Montreal, QC, Canada). The NT is a computerized 3-dimensional multiple object tracking training (3D-MOT) that evaluates cognitive tasks such as attention, short-term memory, working memory, problem solving, decision making, and information processing speed [32,33]. Participants visited our facility 10× over the last 15 days of the intervention and alternated between 1 or 2 NT training sessions at each visit to complete a total of 15 sessions. During each session, participants were instructed to track the spatial location of 4 target spheres among 4 spheres identical in shape and color. The spheres moved within a 3D virtual space, colliding with one another or the edges of the screen and changing direction, as well as passing in front of or behind one another. The sessions were based on a staircase procedure in which an algorithm shifts the speed of the target spheres in response to the participant's performance [33]. When participants could identify the target spheres after 6 s of movement, the speed increased by 0.05 log; otherwise, with each incorrect response, the speed decreased by 0.05 log [33]. Participants performed 20 trials within a single NT training session obtaining a speed threshold, which is the level at which participants correctly tracked and selected the correct spheres 50% of the time. Each NT training session was performed in a quiet and dark room. Software was run on a customized Dell computer with NVIDIA GeForce GTX video graphics driver output to a 50″ Sony 3D TV synchronized with active 3D glasses. Each of the 10 visits involved data collection on factors that could affect cognitive performance such as sleep patterns (measured by the Stanford Sleepiness Scale) oxygen saturation (measured with pulseox), hydration levels (evaluated by a validated urine color scale),

body weight and composition, blood pressure as well as the timing of exercise and recent fluid consumption [31]. The VCP speed scores were determined throughout the 15 sessions over 10 visits to our facility.

2.4. Blood Sample Collection

Participants were instructed to fast for 12 h prior to each study appointment and to consume plenty of water to facilitate blood collection. Blood samples were collected on D1 and D30 in Vacutainer ® SST™ (BD, Franklin Lakes, NJ, USA) to obtain the serum. Blood samples were inverted ~5× to facilitate the clotting process and sited at an ambient temperature for 30 min after collection. Serum was obtained from whole blood left undisturbed at room temperature for 30 min followed by centrifugation at 2000 rpm for 10 min. Serum fractions were aliquoted and stored at −80 °C for analysis of biomarkers related to cognitive dysfunction (neuropeptides) and circadian regulation (cortisol and melatonin).

(a) Analysis of neuropeptides

Serum samples collected on D1 and D30 were used to assess neuropeptide levels using the Milliplex ® MAP Human Neuropeptide Magnetic Bead Panel (EMD Millipore; Billerica, MA, USA) according to the manufacturer's protocol. Analytes included neurotensin, substance p and oxytocin. Data were analyzed using the Luminex xPonent 3.1 software.

(b) Analysis of circadian biomarkers

Circadian rhythm biomarkers, cortisol and melatonin were quantified in serum samples collected on D1 and D30 using the Human Circadian/Stress Magnetic Bead Panel (EMD Millipore; Billerica, MA, USA) following the manufacturer's instructions. Analytes included cortisol and melatonin. Data were analyzed using the Luminex xPonent 3.1 software.

2.5. Statistical Analysis

Statistical analyses were performed using Graphpad Prism Software (Version 9.3.1, La Jolla, CA, USA). Descriptive statistics were calculated and data are presented as mean with 95% confidence interval (95% CI) unless otherwise indicated. Normality was assessed using the Shapiro–Wilk test, and data not following a normal distribution were log-transformed and noted accordingly. The differences in D1 values between the cherry and placebo groups were assessed using parametric unpaired t-tests. Age, gender, BMI, physical activity, and HEI scores were considered as covariates, but their impact on the dependent variables was found to be non-significant ($p > 0.05$) [26,27].

Data on executive function skills, neuropeptides and circadian rhythm were analyzed by the repeated measures (RM) two-way ANOVA test followed by Sidak's multiple comparisons. The effect of treatment, day and their interaction were evaluated. In addition, the mean change (Δ) D30-D1 was computed for each treatment and used to examine treatment differences by the unpaired-t test. Data statistically significant due to treatment or day effect were stratified by BMI (low: 30–34, high: 35–40) and gender (male, female).

A mixed-effect analysis compared the effect of DSC intake on VCP which was assessed using the 15-day NT speed threshold. In addition, the speed threshold analysis included (a) evaluating mean performance and (b) comparing the baseline NT sessions (sessions 1–3 or baseline 3) to the final NT sessions (sessions 13–15 or final 3) and (c) comparing Δ (final baseline) values. For all analyses, a p-value < 0.05 was considered statistically significant.

Spearman correlation analyses were performed in GraphPad Prism to examine associations between significant changes in cognitive performance, obesity-related biomarkers and gut microbiota composition previously evaluated and published following DSC supplementation [26,27]. Correlations with r > 0.40 and $p < 0.05$ were considered indicative of a moderate association between the variables examined [34].

3. Results

3.1. Participant Characteristics and Nutritional Assessment

As previously reported, 40 participants successfully completed the study (19 in the cherry group: 11 females and 8 males; and 21 in the placebo group: 14 females and 7 males) [26,27]. Comprehensive data on anthropometric and physiological measurements, nutrient intake, and HEI results have been documented and are available at https://www.mdpi.com/2072-6643/15/3/681 (accessed on 29 January 2023). Briefly, there were no significant differences in anthropometric measurements (body weight, BMI, body fat, and waist circumference) or physiological measurements (heart rate and oxygen saturation) between the cherry and placebo groups after the 30-day intervention [26]. However, DSC supplementation resulted in a reduction in systolic blood pressure (SBP) (p = 0.05) and diastolic blood pressure (DBP) (p = 0.04) at D30 compared to the placebo group [26]. Analysis of 15-day dietary records revealed no significant differences between the study groups in mean nutrient intake and HEI scores [26].

3.2. Cognitive Performance

3.2.1. Executive Function Skills

At D1, the scores for TMT-A and TMT-B were similar between cherry and placebo groups. However, at D30, participants in the cherry and placebo groups showed significantly lower TMT-A scores compared to D1 (Table 1), implying similar improvement in executive attention and visual–spatial function in both groups. Moreover, Δ TMT-A and Δ TMT-B analyses showed no significant differences between groups (Supplementary Table S1). Both TMT-A and TMT-B results for participants in the cherry and placebo groups were within the average range (29 s for TMT-A and 75 s for TMT-B) [35], suggesting that participants did not show impairments in these cognition markers.

Table 1. Cognitive function tasks scores before and after intervention in cherry and placebo groups.

Test	Day	Treatment		2-Way ANOVA p Values			Sliced by Treatment and/or Day
		Cherry (n = 19)	Placebo (n = 21)	Treatment	Day	Interaction	
TMT-A	D1	29.2 (24.4, 34.2) ^{X}	27.9 (24.8, 31.1) ^{X}	*0.75*	*0.0004*	*0.99*	Placebo (p = 0.01) ↓ D30 Cherry (p = 0.02) ↓ D30
	D30	24.6 (21.2, 28.0) ^{Y}	24.3 (20.8, 27.9) ^{Y}				
TMT-B	D1	61.2 (50.5, 72.0)	56.5 (48.9, 64.2) n = 20	0.44	0.03	0.78	ns
	D30	53.1 (44.1, 62.0)	50.1 (41.7, 58.5) n = 20				
DSF	D1	10.2 (8.9, 11.5) ^{X}	10.5 (9.4, 11.6)	*0.88*	*0.007*	*0.09*	Cherry (p = 0.006) ↑ D30
	D30	11.6 (10.2, 12.9) ^{Y}	10.9 (9.6, 12.2)				
DSB	D1	6.9 (5.8, 7.9) ^{X}	7.5 (6.7, 8.4)	0.91	0.04	0.06	Cherry (p = 0.01) ↑ D30
	D30	8.1 (6.9, 9.1) ^{Y}	7.6 (6.5, 8.6)				
DSST	D1	63.5 (58.8, 68.2)	61.5 (55.8, 67.1)	0.63	0.008	0.92	ns
	D30	67.3 (60.2, 74.3)	65.5 (58.7, 72.1)				

Values are mean (95% CI). The impact of treatment, day and the interaction (treatment and day) was assessed by repeated measures 2-way ANOVA, which was followed by Šidák multiple comparison. Statistically significant results ($p < 0.05$) are represented by the letters X and Y (indicating significant differences within treatment). TMT-A: trail making test A, TMT-B: trail making test B, DSF: digit span forward, DSB: digit span backward, DSST: digit symbol substitution test. Italicized p values are for log transformed data; untransformed data are presented. ns: not significant. ↑: increase, ↓: decrease. ns: not significant.

Working memory and attention skills, assessed by the DSF and DSB tests, revealed that participants in both the cherry and placebo groups had scores that did not suggest

cognitive impairment [36]. However, significant changes were detected only in the cherry group, as evidenced by significantly higher DSF ($p = 0.006$) and DSB ($p = 0.01$) scores at D30 vs. D1, while no significant changes were detected in the placebo group (Table 1, Figure 2A,B). Furthermore, Δ DSB in the cherry group was higher than in the placebo group but did not reach significance ($p = 0.06$) due to the high variability among participants (Figure 2C and Supplementary Table S1). Stratification analyses revealed that the statistical differences in Δ DSB were significant for participants with high BMI ($p = 0.01$) and females ($p = 0.04$) (Figure 2D,E, Supplementary Table S2).

Participants in the cherry and placebo groups showed improvements in processing speed, sustained attention, and visual perceptual functions as evidenced by higher DSST scores at D30 vs. D1 at similar extent (Table 1).

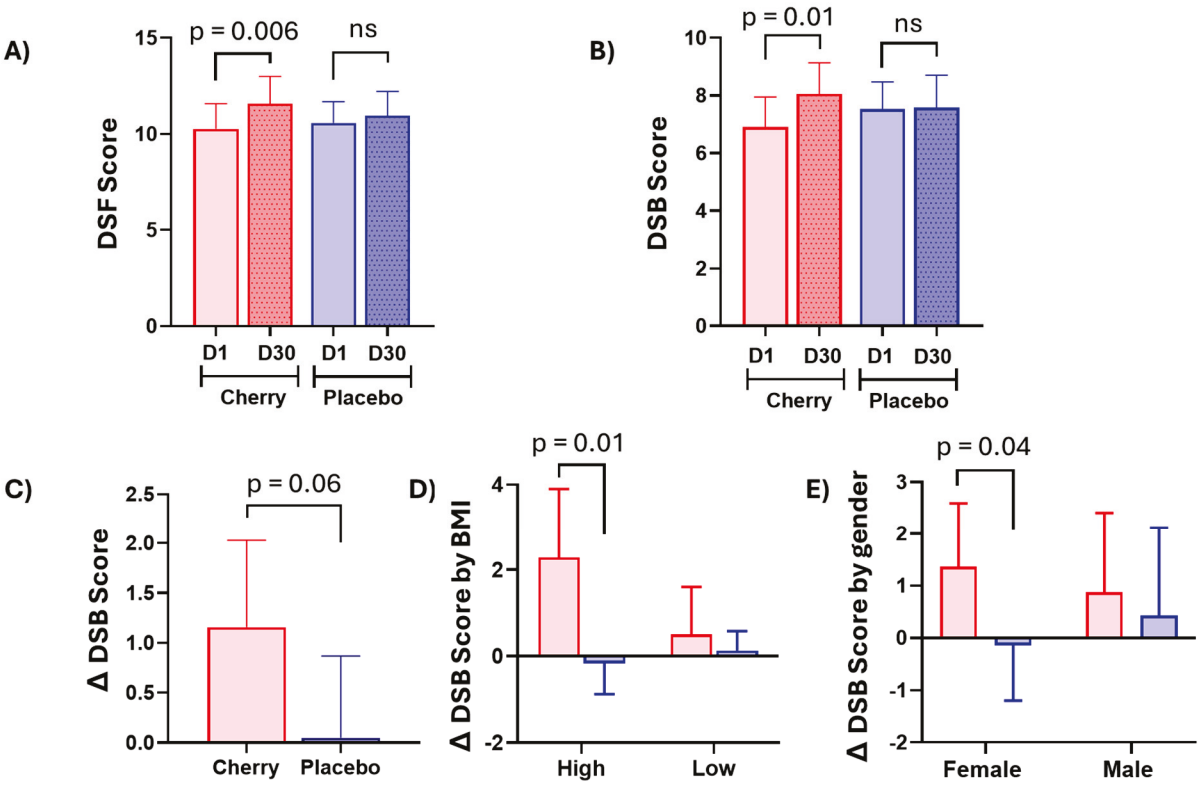

Figure 2. DSC supplementation improved working memory in adults with obesity. (**A**) DSF and (**B**) DBS scores at D1 and 30 in cherry and placebo groups. Values are mean, 95% CI. The difference between treatments was assessed by Sidak's multiple comparison test (**C**) Δ DSB in cherry and placebo groups. (**D**) Δ DSB scores stratified by BMI and (**E**) gender in cherry and placebo groups. Values are mean, 95% CI. The difference between treatments was assessed by unpaired *t*-tests. Δ = D30-D1. DSF: digit span forward, DSB: digit span backward, ns: not significant.

3.2.2. Visual Cognitive Performance (VCP)

The mixed effect analysis showed that VCP speed scores, assessed by the NT training system, improved significantly in the cherry and placebo groups (Supplementary Figure S1A). The final VCP scores improved significantly in the cherry ($p < 0.0001$) and placebo ($p = 0.0001$) groups compared to their respective baseline values, while no significant differences were detected between treatments (Table 2). Similarly, Δ VCP in the cherry group and Δ VCP in the placebo group showed no significant differences between treatments (Table 2). Stratification analyses showed that high BMI and female participants in the cherry group had slightly higher VCP scores (1.54 and 1.47, respectively) compared to those in the placebo group (1.06 and 1.41, respectively) at D30, but the differences among treatments were not significant (Supplementary Figure S1B,C and Supplementary Table S3).

The mean values of variables assessed before each NT session showed significant differences in hydration status, as indicated by urine color, between the cherry and placebo groups. A similar outcome was detected for SBP and DBP, which were measured before each NT session (Supplementary Table S4). These variables were used as covariates to analyze the differences between Δ VCP scores in the cherry and placebo groups; however, these differences were deemed non-significant (Table 2).

Table 2. Visual cognitive performance (VCP) speed scores in cherry and placebo groups.

	Cherry (n = 19)	Placebo (n = 20)	p Value
Mean of 15	1.35 (1.18, 1.52)	1.37 (1.16, 1.58)	0.89
Baseline (3)	1.23 (1.04, 1.41)	1.20 (0.97, 1.42)	0.81
Final (3)	1.50 (1.34, 1.65) *	1.44 (1.20, 1.68) *	0.69
Mean change (Δ)	0.26 (0.15, 0.37) #	0.25 (0.14, 0.36) #	0.94

Values are mean, 95% CI. Baseline values are from the first 3 NT sessions, and final values are from the last 3 NT sessions. Mean change in VCP (Δ): Final (3) - baseline (3). (*) Indicates significant difference between baseline and final values, $p \leq 0.0001$ for cherry and $p = 0.0001$ for placebo. (#) Δ values were adjusted for significant urine, SBP and DBP values.

3.3. Neuropeptides and Circadian Rhythm Biomarkers

Serum levels of neuropeptides and circadian rhythm biomarkers are presented in Table 3. Neurotensin, a neuropeptide with a multifaceted role in cognitive processes [6], increased significantly in the placebo group at D30 ($p = 0.007$) compared to D1 values (Table 3, Figure 3), while in the cherry group, there was a trend to increase at D30 vs. D1 without reaching significance. However, Δ neurotensin did not differ significantly between treatment groups (Supplementary Table S5). Similarly, substance p and oxytocin showed a trend of increase in both cherry and placebo groups (Table 3), though neither Δ substance p nor Δ oxytocin reached statistical significance between treatments (Supplementary Table S5).

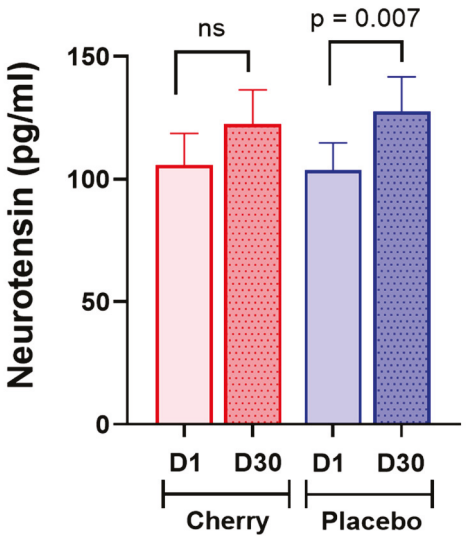

Figure 3. Neurotensin increased significantly in the placebo group. The difference between treatment was assessed by Sidak's multiple comparison test. Values are mean, 95% CI. Ns: non-significant.

The levels of cortisol decreased in the cherry group, whereas levels in the placebo group showed an opposite trend at D30 vs. D1 values without reaching significance (Table 3). Serum melatonin increased in the cherry and placebo groups; however, only significant changes were detected in the placebo group ($p = 0.02$) (Table 3). Similarly, Δ cortisol and Δ melatonin did not show significant differences between the cherry and placebo groups (Supplementary Table S5).

Table 3. Blood levels of neuropeptides and circadian biomarkers before and after intervention in cherry and placebo groups.

Variable	Day	Treatment		*p* Values			Sliced by Treatment and/or Day
		Cherry (*n* = 19)	Placebo (*n* = 21)	Treatment	Day	Interaction	
Neuropeptides							
Neurotensin (pg/mL)	D1	105.81 (92.95, 118.67) *n* = 18	103.70 (92.65, 114.75) ^{X}	*0.89*	*0.001*	*0.52*	Placebo (p = 0.007) ↑ D30
	D30	122.41 (108.5, 136.6) *n* = 18	127.57 (113.48, 141.67) ^{Y}				
Substance p (pg/mL)	D1	21.94 (18.26, 25.61) *n* = 18	21.40 (18.13, 24.67)	*0.63*	*0.09*	*0.59*	ns
	D30	28.65 (19.55, 37.76) *n* = 18	27.59 (24.11, 31.07)				
Oxytocin (pg/mL)	D1	96.75 (68.36, 125.15) *n* = 18	97.95 (69.39, 126.51)	0.94	0.06	0.86	ns
	D30	126.11 (95.19, 157.03) *n* = 18	122.64 (95.24, 150.04)				
Circadian Rhythm							
Cortisol (ng/mL)	D1	170.6 (86.4, 254.9) *n* = 18	215.4 (131.299.3)	*0.40*	*0.70*	*0.71*	ns
	D30	167. 4 (74.7, 260.1) *n* = 18	276.2 (113.9, 404.8)				
Melatonin (pg/mL)	D1	3.36 (2.43, 4.29) *n* = 18	3.37 (2.30, 4.45) ^{X} *n* = 17	*0.34*	*0.008*	*0.29*	Placebo (p = 0.02) ↑ D30
	D30	4.97 (3.05, 6.89) *n* = 18	14.41 (4.01, 24.80) ^{Y} *n* = 17				

Values are mean (95% CI). The impact of treatment, day and the interaction (treatment and day) was assessed by repeated measures 2-way ANOVA, which was followed by Šidák multiple comparison. Statistically significant results ($p < 0.05$) are represented by the letters X and Y (indicating significant differences within treatment). Italicized *p* values are for log transformed data; untransformed data are presented. ↑: increase.

3.4. Correlation Analyses of Significant Cognitive Function Biomarkers Assessed During Intervention

Previously, it was reported that DSC juice supplementation lowered obesity-related biomarkers such as SBP and DBP as well as decreased pro-inflammatory interferon gamma (IFNγ) in obese adults [26]. Similarly, we also reported that DSC intake decreased the abundance of bacteria associated with inflammation such as *Alistipes shahii* and *Bilophila* and prevented the decrease in *Bifidobacterium* genus, which has been suggested to play a role in reducing symptoms of anxiety and depression [27]. Interestingly, results from the Spearman correlation analysis in the placebo group showed that Δ neurotensin was positively correlated with Δ *A. hadrus* (r = 0.43, p = 0.04), whereas Δ melatonin showed a significant positive correlation with Δ IFNγ (r = 0.54, p = 0.02) (Supplementary Table S6). Such correlations were not found in the cherry group.

4. Discussion

To our knowledge, this is the first study investigating the role of DSC supplementation in cognitive function, neuropeptides, and circadian rhythm biomarkers in obese adults. Obesity is associated with cognitive decline and elevated risk of neurodegenerative diseases [2,3]. As such, obese individuals show deficits in learning, memory, and executive function compared to normal-weight subjects [2,3]. The results from this study suggest that DSC supplementation may improve specific cognitive abilities in adults with obesity

such as working memory and concentration skills as assessed by the DSF and DSB tests. Interestingly, improvements in the DSB tasks were more apparent in females and high BMI participants. Given the increased risk of cognitive impairments and neurological disorders in individuals with obesity, these findings support the potential of DSC as a promising dietary intervention to improve cognitive health. Moreover, DSC supplementation showed a trend toward improved executive attention and visual–spatial functions evaluated by the TMT-A, but the high variability between subjects prevented it from reaching significance. The findings from our study are in line with a clinical study that reported improvements in verbal fluency as well as short and long-term memory in older adults with mild-to moderate dementia after 12-weeks of sweet Bing cherry juice supplementation (200 mL) [25]. However, our study was conducted over 30 days (~4 weeks) in adults with obesity, and our results suggest that cognitive improvements may occur over a shorter duration in this population. This has important implications for dietary and clinical interventions, as it indicates that the regular consumption of polyphenol-rich foods like DSCs may exert acute effects on cognitive function in individuals at risk of cognitive impairment within a shorter duration.

The dietary intake of polyphenol-rich foods, such as blueberries, blackcurrants, grapes, and strawberries, is associated with enhanced cognitive function and a reduced risk of neurodegenerative diseases in young and older adults [37–40]. This suggests that polyphenol compounds contribute to preventing cognitive decline across different age groups. DSC is a rich source of polyphenols, including a variety of flavonoids and phenolic acids which contribute to their strong antioxidant properties. The DSC juice used on this study had anthocyanins (ACNs) and flavan-3-ols as the most prevalent (approximately 22% and 29%, respectively) polyphenols, and lower amounts of flavonols and phenolic acids (approximately 8% and 12%, respectively) [41]. These compounds have been associated with cognitive enhancement properties and might play a role in improving working memory and concentration skills in obese adults. For example, ACNs might cross the BBB, allowing them to exert direct effects within the central nervous system. Once in the brain, they neutralize ROS, thereby reducing oxidative stress, which is a key factor in cognitive decline [18,19,42,43]. In addition, ACNs might also inhibit the activation of pro-inflammatory signaling pathways, such as nuclear factor-kappa B (NF-κB), and reduce the production of pro-inflammatory cytokines. This anti-inflammatory action is thought to contribute to the neuroprotective effects of ACNs, such as improved memory, learning, cognitive, and motor functions [44]. Similarly, flavan-3-ols and other classes of flavonoids play a crucial role in supporting cognitive function by mitigating oxidative stress and neuroinflammation [45]. Phenolic acids contribute to cognitive function through multiple neuroprotective mechanisms. They help reduce oxidative stress by lowering pro-oxidant levels, enhancing antioxidant activity, and increasing the production of anti-inflammatory mediators [20], supporting cognitive processes such as learning and memory [20]. However, these beneficial effects appear to be selective on certain cognitive domains. As such, verbal memory is consistently reported as a cognitive domain showing the greatest sensitivity to polyphenols supplementation [16]. This evidence might support the results of this study, as DSC supplementation significantly improved working memory and concentration skills assessed by the DSF and DSB tasks, while other executive function domains (executive attention, processing speed and visual spatial skills) assessed by TMT-A and -B and DSST were partially or not improved. Consequently, the extent to which DSC may provide protective effects on cognitive domains altered during obesity deserves further investigation.

Overall, the mechanism of action behind polyphenols' cognitive enhancement properties is thought to be exerted by their capacity to mitigate inflammatory markers, resulting in blood pressure-lowering effects [25]. For example, Chai et al. [46] reported lower SBP

and C-reactive protein (CRP) levels in older adults after the intake of tart cherry juice for 12 weeks. Interestingly, these results were accompanied by improved visual sustained attention and spatial working memory [22]. Similarly, Kent et al. [25] demonstrated a significant improvement in cognitive abilities and decreased SBP levels in older adults with mild-to moderate dementia after a 12-week intake of sweet cherry juice (200 mL). We previously reported that DSC intake significantly decreased SBP and DBP, which were positively correlated with lower levels of pro-inflammatory IFNγ [26]. However, no direct correlation was found between IFNγ, blood pressure levels and cognitive tests assessed in this study. This suggests that while the anti-inflammatory and blood pressure-lowering effects of DSC might contribute to the observed cognitive benefits, these factors alone do not fully explain the improvements. Other mechanisms, potentially beyond inflammation and blood pressure regulation, may be involved in enhancing cognitive function and should be further investigated.

The lack of effect observed in the TMT-A and -B, DSST and VCP could be attributed to the duration of DSC intervention. Based on previous findings, the cognitive improvement effects of tart and sweet cherries were reached through a minimum of 12 weeks supplementation [22,25], as it has been suggested that polyphenols may take several weeks to accumulate in brain tissues [22]. Thus, it cannot be excluded that interventions longer than 30 days might be required to elicit enhanced cognitive abilities in obese adults.

In addition to polyphenols, DSCs are also a source of dietary fiber (DF), which might also contribute to their cognitive health benefits. DF is fermented in the lower gastrointestinal tract and may enhance cognitive function by promoting a greater microbial diversity to produce a variety of health-promoting metabolites [47]. For example, better performance on memory tasks was reported in healthy older adults after the daily intake of a berry beverage high in ACNs (~795 mg) and fiber (11 gr) for 5 weeks [40]. In this study, the ACN and fiber content were lower (~70 mg/200 mL and 0.11 gr, respectively) [26] and the study duration was shorter (30 days or ~4 weeks), which might explain why executive attention, processing speed and visual spatial skills were not improved.

Research on neurotensin suggests it plays a role in both obesity and cognitive function, often intersecting with neuroinflammatory pathways that can contribute to cognitive deficits [48]. Serum neurotensin increased significantly in the placebo group, while levels in the cherry group tended to increase without attaining significance, suggesting the protective effects of DSC supplementation against cognitive deficits in obese subjects. Interestingly, a positive relationship between Δ neurotensin and Δ *A. hadrus* was detected only in the placebo group. *A. hadrus* is a butyrate-producing bacterium that promotes anti-inflammatory responses and supports gut barrier integrity; however, its presence might exacerbate inflammation under dysbiosis or in combination with other pro-inflammatory factors [27]. We previously reported an unchanged abundance of Δ *A. hadrus* in the placebo group [27], suggesting that increased neurotensin levels might correlate with an unchanged abundance of *A. hadrus*, potentially contributing to cognitive deficits.

Currently, no previous studies have investigated the potential of DSC in the modulation of neurotensin; thus, the comparability of results from this study is limited. However, it was previously suggested that some flavonoids may have the potential to modulate neuropeptides involved in food intake and satiety (e.g., neuropeptide Y) due to their capacity to cross the BBB where they can exert antioxidant and anti-inflammatory effects [49] and promote cognitive health. In this study, the lack of effect observed on substance p and oxytocin could be attributed to the relatively short DSC intervention.

Circadian rhythms are internally driven cycles that influence complex cognitive tasks such as attention, working memory and executive function [15]. The disruption of the circadian system is considered a risk factor for obesity, type 2 diabetes, and metabolic

syndrome development. Cortisol, commonly known as the "stress hormone", plays an essential role in metabolic and immune processes, the diurnal sleep–wake cycle, stress response, and blood pressure regulation [50]. In addition, increased cortisol levels are strongly related to abdominal obesity and to specific mental disorders [51]. In this study, cortisol levels tended to decrease following the DSC intervention, whereas an opposite trend was observed in the placebo group. Stratification analysis further indicated that this trend was more pronounced among women in the cherry group compared to those in the placebo group. However, the difference did not reach significance ($p = 0.08$) due to the high variability among participants. These findings warrant further investigation, as increased levels of cortisol might interfere with cognitive processes and further aggravate mental disorders (stress, anxiety, and depression) associated with obesity [51,52].

Cherries are considered an important source of melatonin, and their daily consumption might increase the endogenous production of melatonin, enhancing antioxidant and anti-inflammatory effects as well as improving sleep quality in adults with metabolic disorders [53,54]. Unexpectedly, melatonin levels increased significantly in the placebo group by D30, while levels in the cherry group remained unchanged. These results may seem controversial because cherries are presented as a good source of exogenous melatonin and as a protective dietary strategy against obesity-associated metabolic disturbances. However, elevated levels of melatonin in placebo participants may be a compensatory mechanism to counteract the higher inflammatory status. Melatonin can inhibit the translocation of NF-κB to the nucleus, preventing the upregulation of inflammatory cytokines, which helps reduce inflammation [55]. Therefore, the upregulation of melatonin observed in the placebo might be due to the endogenous melatonin synthesis to counteract obesity-associated inflammation as evidenced by the strong correlation between Δ melatonin and Δ IFNγ found only in the placebo group ($r = 0.54$, $p = 0.02$).

Results from this study should be considered exploratory and interpreted with caution because the measurement of melatonin was performed on serum samples collected after ~12 h fasting, and this might represent a limitation in terms of evaluating melatonin status. Melatonin levels should be measured in samples collected around sleep time because melatonin is predominantly secreted at night. However, fasting blood samples were necessary for assessing additional biomarkers, including inflammatory markers, lipid profile, glucose, and lipopolysaccharide-binding protein, as part of our study's broader objectives, and published previously [26,27]. Given that these measurements required a standardized fasting state, the collection time could not be adjusted specifically for circadian rhythm assessment. The evaluation of urine 6-sulphatoxymelatonin (6-SMT) in urine, which is a metabolite of melatonin, should be performed in further studies, since it is considered an accurate and reliable method to explore the impact of dietary interventions in melatonin profile [56].

The strengths of this study include that participants in the cherry group did not report serious adverse effects, and compliance was 90%, suggesting DSC drink as a safe and healthier alternative to artificially sweetened beverages, since no significant changes in BMI, body weight, fat and blood glucose were detected after the 30-day intervention [26]. Limitations of this study include the timing and scope of physical activity monitoring. We controlled physical activity halfway through the intervention (cherry: $n = 8$, placebo: $n = 11$) and assessed whether it was a significant covariate. Our analysis indicated that physical activity did not significantly impact the results. However, we acknowledge that monitoring halfway through the study does not account for variations in activity levels before or after the monitoring period, which could still influence cognitive outcomes.

A longer DSC intervention lasting up to 12 weeks may be necessary to observe meaningful improvements in various aspects of cognitive function, as indicated by studies

involving sweet and tart cherries. Moreover, longer interventions may reveal benefits in more complex cognitive domains, such as executive function, processing speed, and working memory, which may require sustained exposure to bioactive compounds to show measurable improvements.

A longer intervention period could also help reduce practice effects associated with cognitive tasks, which might mask a decline in cognitive performance or overestimate the effects of the intervention [22,25,57]. The exposure to cognitive tests might have increased familiarity with the tasks, leading to learning or memory effects that improved participants' performance over time. To better account for these practice effects in future studies, it would be useful to include alternative versions of the tasks or introduce longer intervals between assessments. Additionally, counterbalancing the order of task administration could help reduce the impact of repeated testing.

Participants in both the cherry and placebo groups showed no apparent cognitive deficiencies, as their TMT-A TMT-B, DSF and DSB scores within normal ranges [35,58]. This raises the question of whether DSC supplementation could be beneficial for individuals without cognitive impairment. While previous studies have shown that sweet and/or tart cherries can slow or reverse age-related cognitive decline, this is the first to assess cognitive performance in obese adults in response to DSC consumption. Results from this study are promising and provide a platform for future research investigating the role of DSC interventions on populations showing cognitive dysfunction associated with obesity.

5. Conclusions

This study showed that daily DSC drink intake might enhance working memory and concentration skills in obese adults. Although DSC consumption did not decrease neurotensin levels, it helped prevent a significant increase observed in the placebo group, suggesting the protective effects of DSC drink intake against cognitive deficits related to learning and memory processes in obese subjects. Increased melatonin levels were significantly correlated with IFNγ in the placebo group, implying a mechanism to counteract inflammation. Further clinical studies with larger sample sizes and longer durations are necessary to confirm these effects and explore the long-term clinical application of DSC supplementation. Finally, this study highlights DSC drink as a potential dietary strategy aimed at promoting cognitive health in obese adults who are under greater risk to develop cognitive impairments and neurological disorders.

Supplementary Materials: The following supporting information can be downloaded at https://www.mdpi.com/article/10.3390/nu17050784/s1, Figure S1. Participants in the cherry group showed a trend for higher Visual cognitive performance (VCP) speed scores. VCP scores in (A) cherry and placebo groups, (B) VCP scores in cherry and placebo groups stratified by high BMI (35–40), and (C) gender: female participants. VCP was assessed by the Neurotracker 3D training system. Values are mean ± SEM. Table S1. Analysis of Δ TMT-A, Δ TMT-B, Δ DSF, Δ DSB and Δ DSST between cherry and placebo groups. Table S2. Variation of Δ DSB scores according to BMI and gender in cherry and placebo groups. Table S3. Stratification analysis of VCP scores by BMI and gender: female between cherry and placebo groups. Table S4. Variables assessed before visual cognitive performance using the Neurotracker training system in cherry and placebo groups. Table S5. Analysis of Δ Neuropeptides and Δ Circadian rhythm biomarkers in cherry and placebo groups. Table S6. Spearman correlation analysis in cherry and placebo groups.

Author Contributions: Study conception and design: G.D.N.; funding acquisition: G.D.N.; data acquisition: S.A., G.D.N., A.R. and S.E.R.; study supervision: G.D.N.; analysis and data interpretation: S.A. and G.D.N.; writing—original draft preparation, S.A.; writing—review and editing S.A., G.D.N. and A.R.; resources: G.D.N., S.U.M.-T. and S.E.R.; critical review: G.D.N., S.U.M.-T., A.R., S.E.R. and S.T. All authors have read and agreed to the published version of the manuscript.

Funding: This study was funded by the Northwest Cherry Growers, Washington State Fruit Commission Award # M1902546.

Institutional Review Board Statement: This study was approved by the Institutional Review Board (IRB2019-0597F) on 13 November 2019 at Texas A&M University and conducted in accordance with the Declaration of Helsinki.

Informed Consent Statement: All participants in the study provided informed consent.

Data Availability Statement: The original contributions presented in the study are included in the article/Supplementary Materials, further inquiries can be directed to the corresponding authors.

Acknowledgments: The authors acknowledge participants for their time and effort in contributing to this study.

Conflicts of Interest: The authors declare no conflicts of interest.

References

1. Wang, Y.; Beydoun, M.A.; Min, J.; Xue, H.; Kaminsky, L.A.; Cheskin, L.J. Has the prevalence of overweight, obesity and central obesity levelled off in the United States? Trends, patterns, disparities, and future projections for the obesity epidemic. *Int. J. Epidemiol.* **2020**, *49*, 810–823. [CrossRef]
2. Dye, L.; Boyle, N.B.; Champ, C.; Lawton, C. The relationship between obesity and cognitive health and decline. *Proc. Nutr. Soc.* **2017**, *76*, 443–454. [CrossRef] [PubMed]
3. Fulton, S.; Décarie-Spain, L.; Fioramonti, X.; Guiard, B.; Nakajima, S. The menace of obesity to depression and anxiety prevalence. *Trends Endocrinol. Metab.* **2022**, *33*, 18–35. [CrossRef]
4. Solas, M.; Milagro, F.I.; Ramírez, M.J.; Martínez, J.A. Inflammation and gut-brain axis link obesity to cognitive dysfunction: Plausible pharmacological interventions. *Curr. Opin. Pharmacol.* **2017**, *37*, 87–92. [CrossRef]
5. Spyridaki, E.C.; Avgoustinaki, P.D.; Margioris, A.N. Obesity, inflammation and cognition. *Curr. Opin. Behav. Sci.* **2016**, *9*, 169–175. [CrossRef]
6. Saiyasit, N.; Sripetchwandee, J.; Chattipakorn, N.; Chattipakorn, S.C. Potential roles of neurotensin on cognition in conditions of obese-insulin resistance. *Neuropeptides* **2018**, *72*, 12–22. [CrossRef] [PubMed]
7. Yeo, X.Y.; Cunliffe, G.; Ho, R.C.; Lee, S.S.; Jung, S. Potentials of Neuropeptides as Therapeutic Agents for Neurological Diseases. *Biomedicines* **2022**, *10*, 343. [CrossRef] [PubMed]
8. Wölk, E.; Stengel, A.; Schaper, S.J.; Rose, M.; Hofmann, T. Neurotensin and Xenin Show Positive Correlations With Perceived Stress, Anxiety, Depressiveness and Eating Disorder Symptoms in Female Obese Patients. *Front. Behav. Neurosci.* **2021**, *15*, 18. [CrossRef]
9. Atas, U.; Erin, N.; Tazegul, G.; Elpek, G.O.; Yildirim, B. Changes in ghrelin, substance P and vasoactive intestinal peptide levels in the gastroduodenal mucosa of patients with morbid obesity. *Neuropeptides* **2021**, *89*, 102164. [CrossRef] [PubMed]
10. Lénárd, L.; László, K.; Kertes, E.; Ollmann, T.; Péczely, L.; Kovács, A.; Kállai, V.; Zagorácz, O.; Gálosi, R.; Karádi, Z. Substance P and neurotensin in the limbic system: Their roles in reinforcement and memory consolidation. *Neurosci. Biobehav. Rev.* **2018**, *85*, 1–20. [CrossRef] [PubMed]
11. Plessow, F.; Eddy, K.T.; Lawson, E.A. The Neuropeptide Hormone Oxytocin in Eating Disorders. *Curr. Psychiatry Rep.* **2018**, *20*, 91. [CrossRef] [PubMed]
12. Qian, W.; Zhu, T.; Tang, B.; Yu, S.; Hu, H.; Sun, W.; Pan, R.; Wang, J.; Wang, D.; Yang, L.; et al. Decreased circulating levels of oxytocin in obesity and newly diagnosed type 2 diabetic patients. *J. Clin. Endocrinol. Metab.* **2014**, *99*, 4683–4689. [CrossRef]
13. Gombert, M.; Martin-Carbonell, V.; Pin-Arboledas, G.; Carrasco-Luna, J.; Carrasco-García, Á.; Codoñer-Franch, P. Melatonin levels in children with obesity are associated with metabolic risk and inflammatory parameters. *Nutrients* **2021**, *13*, 3629. [CrossRef] [PubMed]
14. Herhaus, B.; Petrowski, K. Cortisol stress reactivity to the trier social stress test in obese adults. *Obes. Facts* **2018**, *11*, 491–500. [CrossRef] [PubMed]
15. Valdez, P. Focus: Attention Science: Circadian Rhythms in Attention. *Yale J. Biol. Med.* **2019**, *92*, 81.
16. Lamport, D.J.; Williams, C.M. Polyphenols and cognition in humans: An overview of current evidence from recent systematic reviews and meta-analyses. *Brain Plast.* **2020**, *6*, 139–153. [CrossRef] [PubMed]
17. Kelley, D.S.; Adkins, Y.; Laugero, K.D. A review of the health benefits of cherries. *Nutrients* **2018**, *10*, 368. [CrossRef] [PubMed]
18. Zhong, H.; Xu, J.; Yang, M.; Hussain, M.; Liu, X.; Feng, F.; Guan, R. Protective effect of anthocyanins against neurodegenerative diseases through the microbial-intestinal-brain axis: A critical review. *Nutrients* **2023**, *15*, 496. [CrossRef] [PubMed]

19. Banji, O.J.; Banji, D.; Makeen, H.A.; Alqahtani, S.S.; Alshahrani, S. Neuroinflammation: The role of anthocyanins as neuroprotectants. *Curr. Neuropharmacol.* **2022**, *20*, 2156. [CrossRef] [PubMed]
20. Caruso, G.; Godos, J.; Privitera, A.; Lanza, G.; Castellano, S.; Chillemi, A.; Bruni, O.; Ferri, R.; Caraci, F.; Grosso, G. Phenolic acids and prevention of cognitive decline: Polyphenols with a neuroprotective role in cognitive disorders and Alzheimer's disease. *Nutrients* **2022**, *14*, 819. [CrossRef] [PubMed]
21. Thangthaeng, N.; Poulose, S.M.; Gomes, S.M.; Miller, M.G.; Bielinski, D.F.; Shukitt-Hale, B. Tart cherry supplementation improves working memory, hippocampal inflammation, and autophagy in aged rats. *Age* **2016**, *38*, 393–404. [CrossRef] [PubMed]
22. Chai, S.C.; Jerusik, J.; Davis, K.; Wright, R.S.; Zhang, Z. Effect of Montmorency tart cherry juice on cognitive performance in older adults: A randomized controlled trial. *Food Funct.* **2019**, *10*, 4423–4431. [CrossRef] [PubMed]
23. Matias, A.A.; Rosado-Ramos, R.; Nunes, S.L.; Figueira, I.; Serra, A.T.; Bronze, M.R.; Santos, C.N.; Duarte, C.M.M. Protective Effect of a (Poly)phenol-Rich Extract Derived from Sweet Cherries Culls against Oxidative Cell Damage. *Molecules* **2016**, *21*, 406. [CrossRef] [PubMed]
24. Antognoni, F.; Potente, G.; Mandrioli, R.; Angeloni, C.; Freschi, M.; Malaguti, M.; Hrelia, S.; Lugli, S.; Gennari, F.; Muzzi, E.; et al. Fruit Quality Characterization of New Sweet Cherry Cultivars as a Good Source of Bioactive Phenolic Compounds with Antioxidant and Neuroprotective Potential. *Antioxidants* **2020**, *9*, 677. [CrossRef]
25. Kent, K.; Charlton, K.; Roodenrys, S.; Batterham, M.; Potter, J.; Traynor, V.; Gilbert, H.; Morgan, O.; Richards, R. Consumption of anthocyanin-rich cherry juice for 12 weeks improves memory and cognition in older adults with mild-to-moderate dementia. *Eur. J. Nutr.* **2017**, *56*, 333–341. [CrossRef]
26. Arbizu, S.; Mertens-Talcott, S.U.; Talcott, S.; Noratto, G.D. Dark Sweet Cherry (*Prunus avium*) Supplementation Reduced Blood Pressure and Pro-Inflammatory Interferon Gamma (IFNγ) in Obese Adults without Affecting Lipid Profile, Glucose Levels and Liver Enzymes. *Nutrients* **2023**, *15*, 681. [CrossRef] [PubMed]
27. Arbizu, S.; Mertens-Talcott, S.U.; Talcott, S.; Noratto, G.D. Effect of dark sweet cherry (*Prunus avium*) supplementation on the fecal microbiota, metabolic endotoxemia, and intestinal permeability in obese subjects: A single-blind randomized trial. *Food Funct.* **2024**, *15*, 9563–9578. [CrossRef] [PubMed]
28. Park, S.-Y.; Schott, N. The trail-making-test: Comparison between paper-and-pencil and computerized versions in young and healthy older adults. *Appl. Neuropsychol. Adult* **2022**, *29*, 1208–1220. [CrossRef] [PubMed]
29. Gignac, G.E.; Kovacs, K.; Reynolds, M.R. Backward and forward serial recall across modalities: An individual differences perspective. *Personal. Individ. Differ.* **2018**, *121*, 147–151. [CrossRef]
30. Jaeger, J. Digit Symbol Substitution Test: The Case for Sensitivity over Specificity in Neuropsychological Testing. *J. Clin. Psychopharmacol.* **2018**, *38*, 513–519. [CrossRef] [PubMed]
31. Beathard, K.M.; Georghiades, N.; Goulart, J.B.; Riviere, A.J.; Sullivan, C.; Mascarro, M.; Riechman, S.E. The impact of nutrition on visual cognitive performance in the nutrition, vision, and cognition in sport study. *Front. Nutr.* **2023**, *10*, 1208890. [CrossRef] [PubMed]
32. Vater, C.; Gray, R.; Holcombe, A.O. A critical systematic review of the Neurotracker perceptual-cognitive training tool. *Psychon. Bull. Rev.* **2021**, *28*, 1458–1483. [CrossRef]
33. Spaner, C.; Musteata, S.; Kenny, R.; Gawryluk, J.; Hofer, S.; Christie, B. 3-Dimensional multiple object tracking training can enhance selective attention, psychomotor speed, and cognitive flexibility in healthy older adults. *Ageing Sci. Ment. Health Stud.* **2019**, *3*, 1–12.
34. Akoglu, H. User's guide to correlation coefficients. *Turk. J. Emerg. Med.* **2018**, *18*, 91–93. [CrossRef]
35. Ciolek, C.H.; Lee, S.Y. Cognitive issues in the older adult. In *Guccione's Geriatric Physical Therapy E-Book*; Elsevier Health Sciences: St. Louis, MO, USA, 2019; p. 425.
36. Monaco, M.; Costa, A.; Caltagirone, C.; Carlesimo, G.A. Forward and backward span for verbal and visuo-spatial data: Standardization and normative data from an Italian adult population. *Neurol. Sci.* **2013**, *34*, 749–754. [CrossRef]
37. Watson, A.W.; Haskell-Ramsay, C.F.; Kennedy, D.O.; Cooney, J.M.; Trower, T.; Scheepens, A. Acute supplementation with blackcurrant extracts modulates cognitive functioning and inhibits monoamine oxidase-B in healthy young adults. *J. Funct. Foods* **2015**, *17*, 524–539. [CrossRef]
38. Calapai, G.; Bonina, F.; Bonina, A.; Rizza, L.; Mannucci, C.; Arcoraci, V.; Laganà, G.; Alibrandi, A.; Pollicino, C.; Inferrera, S. A Randomized, double-blinded, clinical trial on effects of a Vitis vinifera extract on cognitive function in healthy older adults. *Front. Pharmacol.* **2017**, *8*, 776. [CrossRef]
39. Boespflug, E.L.; Eliassen, J.C.; Dudley, J.A.; Shidler, M.D.; Kalt, W.; Summer, S.S.; Stein, A.L.; Stover, A.N.; Krikorian, R. Enhanced neural activation with blueberry supplementation in mild cognitive impairment. *Nutr. Neurosci.* **2018**, *21*, 297–305. [CrossRef] [PubMed]
40. Nilsson, A.; Salo, I.; Plaza, M.; Björck, I. Effects of a mixed berry beverage on cognitive functions and cardiometabolic risk markers; A randomized cross-over study in healthy older adults. *PLoS ONE* **2017**, *12*, e0188173. [CrossRef]

41. Lage, N.N.; Layosa, M.A.A.; Arbizu, S.; Chew, B.P.; Pedrosa, M.L.; Mertens-Talcott, S.; Talcott, S.; Noratto, G.D. Dark sweet cherry (*Prunus avium*) phenolics enriched in anthocyanins exhibit enhanced activity against the most aggressive breast cancer subtypes without toxicity to normal breast cells. *J. Funct. Foods* **2020**, *64*, 103710. [CrossRef]
42. Salehi, B.; Sharifi-Rad, J.; Cappellini, F.; Reiner, Ž.; Zorzan, D.; Imran, M.; Sener, B.; Kilic, M.; El-Shazly, M.; Fahmy, N.M.; et al. The Therapeutic Potential of Anthocyanins: Current Approaches Based on Their Molecular Mechanism of Action. *Front. Pharmacol.* **2020**, *11*, 1300. [CrossRef] [PubMed]
43. Winter, A.N.; Bickford, P.C. Anthocyanins and Their Metabolites as Therapeutic Agents for Neurodegenerative Disease. *Antioxidants* **2019**, *8*, 333. [CrossRef]
44. Kent, K.; Charlton, K.E.; Netzel, M.; Fanning, K. Food-based anthocyanin intake and cognitive outcomes in human intervention trials: A systematic review. *J. Hum. Nutr. Diet.* **2017**, *30*, 260–274. [CrossRef]
45. Godos, J.; Micek, A.; Mena, P.; Del Rio, D.; Galvano, F.; Castellano, S.; Grosso, G. Dietary (Poly) phenols and Cognitive Decline: A Systematic Review and Meta-Analysis of Observational Studies. *Mol. Nutr. Food Res.* **2024**, *68*, 2300472. [CrossRef] [PubMed]
46. Chai, S.C.; Davis, K.; Wright, R.S.; Kuczmarski, M.F.; Zhang, Z. Impact of tart cherry juice on systolic blood pressure and low-density lipoprotein cholesterol in older adults: A randomized controlled trial. *Food Funct.* **2018**, *9*, 3185–3194. [CrossRef]
47. Berding, K.; Carbia, C.; Cryan, J.F. Going with the grain: Fiber, cognition, and the microbiota-gut-brain-axis. *Exp. Biol. Med.* **2021**, *246*, 796–811. [CrossRef]
48. Li, J.; Song, J.; Zaytseva, Y.Y.; Liu, Y.; Rychahou, P.; Jiang, K.; Starr, M.E.; Kim, J.T.; Harris, J.W.; Yiannikouris, F.B. An obligatory role for neurotensin in high-fat-diet-induced obesity. *Nature* **2016**, *533*, 411–415. [CrossRef]
49. Panickar, K.S. Effects of dietary polyphenols on neuroregulatory factors and pathways that mediate food intake and energy regulation in obesity. *Mol. Nutr. Food Res.* **2013**, *57*, 34–47. [CrossRef] [PubMed]
50. Baudrand, R.; Vaidya, A. Cortisol dysregulation in obesity-related metabolic disorders. *Curr. Opin. Endocrinol. Diabetes Obes.* **2015**, *22*, 143. [CrossRef]
51. Van der Valk, E.S.; Savas, M.; van Rossum, E.F. Stress and obesity: Are there more susceptible individuals? *Curr. Obes. Rep.* **2018**, *7*, 193–203. [CrossRef]
52. Dziurkowska, E.; Wesolowski, M. Cortisol as a Biomarker of Mental Disorder Severity. *J. Clin. Med.* **2021**, *10*, 5204. [CrossRef]
53. Genario, R.; Cipolla-Neto, J.; Bueno, A.A.; Santos, H.O. Melatonin supplementation in the management of obesity and obesity-associated disorders: A review of physiological mechanisms and clinical applications. *Pharmacol. Res.* **2021**, *163*, 105254. [CrossRef] [PubMed]
54. Pivonello, C.; Negri, M.; Patalano, R.; Amatrudo, F.; Montò, T.; Liccardi, A.; Graziadio, C.; Muscogiuri, G.; Pivonello, R.; Colao, A. The role of melatonin in the molecular mechanisms underlying metaflammation and infections in obesity: A narrative review. *Obes. Rev.* **2021**, *23*, e13390. [CrossRef] [PubMed]
55. Cho, J.H.; Bhutani, S.; Kim, C.H.; Irwin, M.R. Anti-inflammatory effects of melatonin: A systematic review and meta-analysis of clinical trials. *Brain Behav. Immun.* **2021**, *93*, 245–253. [CrossRef]
56. Howatson, G.; Bell, P.G.; Tallent, J.; Middleton, B.; McHugh, M.P.; Ellis, J. Effect of tart cherry juice (*Prunus cerasus*) on melatonin levels and enhanced sleep quality. *Eur. J. Nutr.* **2012**, *51*, 909–916. [CrossRef]
57. Kimble, R.; Keane, K.M.; Lodge, J.K.; Cheung, W.; Haskell-Ramsay, C.F.; Howatson, G. Polyphenol-rich tart cherries (*Prunus cerasus*, cv Montmorency) improve sustained attention, feelings of alertness and mental fatigue and influence the plasma metabolome in middle-aged adults: A randomised, placebo-controlled trial. *Br. J. Nutr.* **2022**, *128*, 2409–2420. [CrossRef]
58. Cullum, C.M. 4.11—Neuropsychological Assessment of Adults. In *Comprehensive Clinical Psychology*; Bellack, A.S., Hersen, M., Eds.; Pergamon: Oxford, UK, 1998; pp. 303–347.

Disclaimer/Publisher's Note: The statements, opinions and data contained in all publications are solely those of the individual author(s) and contributor(s) and not of MDPI and/or the editor(s). MDPI and/or the editor(s) disclaim responsibility for any injury to people or property resulting from any ideas, methods, instructions or products referred to in the content.

nutrients

MDPI

Article

Effect of Peanut Shell Extract and Luteolin on Gut Microbiota and High-Fat Diet-Induced Sequelae of the Inflammatory Continuum in a Metabolic Syndrome-like Murine Model

Hemalata Deshmukh [1,2,†], Roberto Mendóza [1,†], Julianna M. Santos [1,3], Sathish Sivaprakasam [4], Moamen M. Elmassry [5], Jonathan M. Miranda [4], Patrick Q. Pham [1], Zarek Driver [1], Matthew Bender [1], Jannette M. Dufour [4,6,7,8] and Chwan-Li Shen [1,6,7,8,9,*]

[1] Department of Pathology, Texas Tech University Health Sciences Center, Lubbock, TX 79430, USA; hemalata.deshmukh@ttu.edu (H.D.); robert.mendoza@ttuhsc.edu (R.M.); julianna.santos@ttuhsc.edu (J.M.S.); patrick.q.pham@ttu.edu (P.Q.P.); zarek.driver@ttuhsc.edu (Z.D.); matthew.bender@ttuhsc.edu (M.B.)
[2] Department of Biological Sciences, Texas Tech University, Lubbock, TX 79409, USA
[3] Woody L. Hunt School of Dental Medicine, Texas Tech University Health Sciences Center, El Paso, TX 79905, USA
[4] Department of Cell Biology and Biochemistry, Texas Tech University Health Sciences Center, Lubbock, TX 79430, USA; sathish.sivaprakasam@ttuhsc.edu (S.S.); jonathan.m.miranda@ttuhsc.edu (J.M.M.); jannette.dufour@ttuhsc.edu (J.M.D.)
[5] Department of Molecular Biology, Princeton University, Princeton, NJ 08544, USA; elmassry@princeton.edu
[6] Department of Medical Education, Texas Tech University Health Sciences Center, Lubbock, TX 79430, USA
[7] Center of Excellence for Integrative Health, Texas Tech University Health Sciences Center, Lubbock, TX 79430, USA
[8] Obesity Research Institute, Texas Tech University, Lubbock, TX 79430, USA
[9] Center of Excellence for Translational Neuroscience and Therapeutics, Texas Tech University Health Sciences Center, Lubbock, TX 79430, USA
* Correspondence: leslie.shen@ttuhsc.edu; Tel.: +1-(806)-743-2815; Fax: +1-(806)-743-2117
† These authors contributed equally to this work.

Abstract

Background: Metabolic syndrome (MetS) is characterized by chronic inflammation, oxidative stress, and mitochondrial dysfunction. MetS is associated with increased intestinal permeability and dysbiosis. The objective of this study was to investigate the effects of peanut shell extract (PSE) and luteolin (LUT) on the kidneys, colon, and ileum in a MetS-like murine model. **Methods:** Thirty-six male Slc6a14$^{y/-}$ mice were divided into four groups: low-fat diet (LFD), high-fat diet (HFD), HFD + 200 mg PSE/kg BW (PSE, p.o.), and HFD + 100 mg LUT/kg BW (LUT, p.o.) for 4 months. Outcome measures included glucose homeostasis, intestinal permeability, gut microbiome composition, and mRNA gene expression of mitochondrial homeostasis and inflammation/oxidative stress in the kidneys, colon, and ileum. **Results:** HFD resulted in glucose dysregulation with hyperglycemia and insulin resistance. PSE and LUT improved insulin tolerance and beta-cell function. PSE and LUT mitigated HFD-increased serum lipopolysaccharide-binding protein concentration. Perturbations in the gut microbiome were associated with HFD, and PSE or LUT reversed some of these changes. Specifically, *Phocaeicola vulgatus* was depleted by HFD and reverted by PSE or LUT. Relative to the LFD group, the HFD group (1) upregulated mitochondrial fusion (MFN1, MFN2, OPA1), mitophagy (TLR4, PINK1, LC3B), and inflammation (NFκB, TNFα, IL6), and (2) downregulated mitochondrial fission (FIS1, DRP1), biosynthesis (PGC1α, NRF1, NRF2, TFAM), electron transport chain (complex I), and antioxidant enzyme (SOD1) in the kidneys, colon, and ileum. **Conclusions:** PSE and LUT reversed such HFD-induced changes in the aforementioned gene expression levels.

Keywords: bioactive compounds; luteolin; mitochondria; microbiome; colon; kidney; ileum; tissues; diabetes; mice

1. Introduction

The growing incidence of diseases within the inflammatory continuum, such as metabolic syndrome (MetS), often concomitant type 2 diabetes mellitus (T2DM), and their chronic associated sequelae, is a major public health concern with global reach [1]. The World Health Organization estimates that 60% of all global deaths are attributable to chronic inflammatory diseases, including MetS, diabetes mellitus, obesity, cancer, cardiovascular disease, and autoimmune disease [2]. It is estimated that a quarter of all adults worldwide are affected by MetS, with approximately 30–40% of adults in the USA being affected [3].

Metabolic syndrome is characterized by a collection of derangements, including insulin resistance, hypertension, dyslipidemia, and central obesity, which together elevate the risk of conditions like cardiovascular disease and T2DM [4]. Emerging studies have highlighted gut dysbiosis as playing an important role in MetS and glucose homeostasis, influencing insulin sensitivity, inflammation, and the development of related diseases like T2DM [5–7]. Gut dysbiosis is closely associated with chronic inflammation and metabolic disturbances of the normal gut microenvironment, including (1) reduction in symbionts, (2) overgrowth of harmful microbes, and (3) loss of microbial diversity itself [8,9]. As a major site of microbial activity with the highest concentration of gut microbiota ($\approx 10^{12}$ cells/mL), the colon is particularly vulnerable to such disturbances, especially considering factors such as antibiotics, poor diet, chronic stress, or illness [10]. Two other tissues, the ileum and kidneys, are also particularly exposed to these inflammatory signals relative to other organs, with the former playing a central role in immune sensing and nutrient absorption allowing for possibly greater antigen translocation, and the latter filtering circulating endotoxins and uremic toxins, activating proximal tubule epithelial cells to secrete cytokines and chemokines, where subsequent perpetuation of inflammatory cascades ensue [11,12].

Mitochondrial dysfunction, which acts as a potent inducer of inflammatory signaling in the gastrointestinal (GI) tissues, is a hallmark of MetS [13,14]. Such dysfunction can result in impaired adenosine triphosphate (ATP) production, accumulation of reactive oxygen species (ROS), activation of the NLRP3 inflammasome, and disruption of effector signaling pathways, contributing to the development of MetS [15,16]. Dysfunction of mitochondria can also compromise the integrity of the intestinal epithelial lining, particularly at tight junctions, leading to increased permeability and subsequent antigenemia-induced inflammation [17]. Furthermore, these aberrances have been implicated in damage to the renal and GI tissues, such as the colon and ileum, and disease progression in the context of MetS [16–18]. As the prevalence of MetS continues to rise, exploring novel therapeutic approaches is warranted to mitigate the impact of MetS on disrupted glucose homeostasis, gut dysbiosis, and mitochondrial dysfunction in GI tissues and overall health.

Peanut shell extract (PSE) is derived from the outer hull of peanuts and is rich in polyphenolic compounds which combat free radicals like ROS, leading to a reduction in general inflammation. Emerging evidence has substantiated the potent anti-inflammatory and antioxidant properties of PSE for its therapeutic role in obesity-induced diabetic animals [19,20]. Luteolin (LUT), a flavonoid antioxidant commonly found in fruits and vegetables [21] as well as in peanut shells [22], has been reported to mitigate inflammation-related diseases in animals with MetS [23–25] and diabetes [26,27] through its anti-inflammatory properties. Previous studies have demonstrated that PSE and LUT can lower blood glucose levels in diabetic mice, suggesting their potential in managing MetS [26,28,29]. For exam-

ple, LUT reduces glycemic levels in diabetic mice [26], induces adipocyte browning [26], and ameliorates insulin resistance [27]. However, no studies that we know of have yet evaluated the effects of PSE or PSE-extracted LUT on the kidney-GI-microbiome axis using a MetS-like murine model.

In this study, we selected the kidney and two GI organs (colon and ileum) because all three tissue types are notably affected by microbial activity. Microbial activity within the colon allows for production of useful metabolites, namely short-chain fatty acids (e.g., acetate, propionate, and butyrate), which serve as critical energy substrates and modulators of host immune responses [30]. Disruption of short-chain fatty acid production contributes to systemic inflammation and metabolic dysfunction [10]. The kidneys, through their roles in metabolic homeostasis and filtration, and the ileum, as a key site of nutrient absorption and immune surveillance, particularly vulnerable to the systemic inflammation and oxidative stress associated with MetS [11,31]. Gut dysbiosis-associated alterations have been implicated in MetS, contributing to the production of harmful metabolites that potentially exacerbate MetS-affected organ damage [32].

We used Slc6a14$^{y/-}$ gene knockout mice (analogous to the human SLC6A14 gene), which leads to disruption of the normal function of the solute carrier protein product that is involved in the transport of amino acids and other metabolites crucial for energy homeostasis. As a result, this genetic predisposition allows for a MetS-like state to develop, such as obesity, insulin resistance, dyslipidemia, and hypertension, where these gene knockout mice are prone to MetS symptomatology and associated T2DM development when the mice are placed on a HFD [33]. The chronic inflammation, oxidative stress, and mitochondrial dysfunction that characterize MetS are also well represented in Slc6a14$^{y/-}$ mice, making them a robust MetS-like model for evaluating potential therapeutic interventions, such as PSE and PSE-extracted LUT for eventual human benefit [33].

This study aims to investigate the effects of PSE and PSE-extracted LUT on glucose homeostasis and GI health (in terms of gut microbiome composition and mitochondrial homeostasis) in mice with a predisposition toward a MetS-like state. We hypothesized that PSE and PSE-extracted LUT administration would increase insulin tolerance and sensitivity, decrease intestinal permeability and dysbiosis, and improve mitochondrial homeostasis and dynamics of renal and GI tissues in MetS-like mice. By examining gene expression profiles of mitochondrial homeostasis and markers of proinflammatory cytokines and antioxidant enzyme in the kidneys, colon, and ileum, we uncovered the potential therapeutic benefits of PSE and LUT in improving renal and GI function of MetS-like mice. Understanding these biochemical and molecular mechanisms can pave the way for the development of novel adjuvant interventions to mitigate the progression of MetS.

2. Materials and Methods

2.1. Animals and Treatments

A total of thirty-six male Slc6a14$^{y/-}$ mice were utilized to investigate diet-induced obesity, hepatic steatosis, and a metabolic syndrome-like state, based on the model established in a previous study [33]. The mice were kindly provided by Dr. Vadivel Ganapathy, TTUHSC, Lubbock, TX, USA, and were housed under standard laboratory conditions. Mice were randomly divided into four experimental groups (n = 9 per group): (1) a low-fat diet (LFD) negative control group receiving diet D12450J (Research Diets, New Brunswick, NJ, USA); (2) a high-fat diet (HFD) positive control group fed diet D12492 containing 60% of calories from fat mainly from lard (Research Diets); (3) a treatment group receiving HFD along with PSE administered orally at 200 mg/kg BW per day; and (4) a second treatment group given HFD with LUT at a dose of 100 mg/kg BW per day by oral gavage. The intervention lasted for 4 months. PSE and LUT were administered at the aforementioned

daily doses for 4 months. These doses were selected based on prior preclinical studies demonstrating beneficial effects on metabolic dysfunction and inflammation in high-fat diet-fed rodents [21,34–36]. The selected doses fall within the safe and effective range for chronic administration in murine models. Both the PSE (final extract ratio: 100:1 to 110:1, standardized to contain 20% LUT, Catalog number 1503) and the LUT (extracted from PSE with 99.04% LUT purity based on the results of high-performance liquid chromatography) were gifts provided by Sabinsa Corporation (East Windsor, NJ, USA).

Animals were housed two per cage under controlled environmental conditions (temperature: 22 ± 2 °C; relative humidity: 55 ± 5%) with a light/dark cycle of 12 h. Food and water were available ad libitum throughout the study duration. Weekly measurements included body weight, dietary intake, water consumption, and fasting blood glucose levels.

Based on our prior statistical power calculations [33], a sample size of 6–8 mice per group was sufficient to detect significant differences in insulin levels at $\alpha = 0.05$ with 90% power. Thus, a group size of nine animals was selected to ensure adequate statistical robustness. All experimental procedures were approved by the Institutional Animal Care and Use Committee (IACUC) on 27 May 2022.

2.2. Sample Collection

Following the 4-month dietary intervention, mice were fasted for 4 h to assess blood glucose levels using a glucometer (Accu-Chek Aviva Glucose Meter, Roche Diabetes Care, Inc., Indianapolis, IN, USA). Animals were then anesthetized with isoflurane, and blood was collected via cardiac puncture. The mice were subsequently euthanized, and tissue samples—including kidneys, colon, ileum, and cecal feces—were harvested and immediately stored at −80 °C for future analyses [33]. Blood samples were centrifuged to separate the serum, which was also preserved at −80 °C for biochemical evaluations. Pancreatic tissue was fixed in Z-fix solution (AnaTech Ltd., Battle Creek, MI, USA) at room temperature for subsequent histological analysis of insulin and glucagon expression.

2.3. Glucose and Insulin Tolerance Tests

At baseline, and following the 4-month intervention period, all mice underwent glucose tolerance tests (GTT) and insulin tolerance tests (ITT) after a 4 h fasting period. For the GTT, glucose was administered intraperitoneally at a dose of 2 g/kg BW. For the ITT, insulin (Humulin; Abbott, Chicago, IL, USA) was delivered intraperitoneally at 1 U/kg BW. Blood glucose levels were measured from the tail vein at 0, 15, 30, 60, and 120 min post-injection using a glucometer (AmiStrip Plus, Germaine Laboratories, Inc., San Antonio, TX, USA) [20]. The area under the curve (AUC) for glucose levels during both tests was determined using the trapezoidal rule:

$$\mathrm{AUC} \approx \sum_{i=1}^{n} \frac{(t_i - t_{i-1})}{2} [G_i + G_{i-1}]$$

where t_i and t_{i-1} are time points, and G_i and G_{i-1} are corresponding glucose concentrations.

2.4. Serum Insulin and HOMA Assessment

Serum insulin concentrations were measured using a commercially available ELISA kit (EMD Millipore Co., Billerica, MA, USA). To evaluate insulin resistance, the HOMA-IR (Homeostatic Model Assessment for Insulin Resistance) index was calculated using the formula: HOMA-IR = [fasting glucose (mmol/L) × fasting insulin (pmol/L)] ÷ 22.5, where 22.5 is the normalization constant [20]. β-cell function was assessed by computing the HOMA-B (Homeostatic Model Assessment for Beta-Cell Function) index using the formula: HOMA-B = [20 × fasting insulin (pmol/L)] ÷ [fasting glucose (mmol/L) − 2.5], where 2.5 is the empirically derived physiological baseline for fasting glucose [20].

2.5. Histology on Pancreas Tissue

Pancreatic tissue sections were subjected to immunohistochemical staining to detect insulin and glucagon using guinea pig anti-insulin (1:1000 dilution; Dako Agilent Pathology Solutions, Santa Clara, CA, USA) and mouse anti-glucagon (1:5000 dilution; Millipore Sigma, Burlington, MA, USA) primary antibodies, respectively, following protocols described in our previous work [20]. Hematoxylin was used as a counterstain.

2.6. Measurement of Intestinal Permeability

Intestinal permeability was assessed by quantifying serum levels of lipopolysaccharide-binding protein (LBP) using a commercially available ELISA kit (LifeSpan Biosciences, Inc., Shirley, MA, USA).

2.7. Gene Profiling of Gut Microbiota and Data Analysis

Fecal microbial DNA was extracted using the PowerFecal DNA Isolation Kit (Qiagen Inc., Germantown, MD, USA). Sequencing of the V4 region of the 16S rRNA gene was carried out by MR DNA (Molecular Research LP, Shallowater, TX, USA), following protocols established in our previous publication [37]. Amplicons were purified with Ampure XP beads and subsequently used to construct DNA libraries for Illumina sequencing. The raw sequence data have been deposited in the NCBI BioProject database under accession number PRJNA1258714.

2.8. RNA Extraction and qRT-PCR

Total RNA was extracted from renal, colonic, and ileal tissues following procedures described in our previously published study [38]. Complementary DNA (cDNA) was synthesized from the isolated RNA and used for quantitative PCR amplification of target genes using specific primers listed in Supplement Table S1, in accordance with our earlier methodology [37]. Gene expression levels were normalized to β-actin as a housekeeping gene and calculated using the formula: $x = 2^{-(\Delta CT \times 1000)}$ as described by [39].

2.9. Statistical Analysis

All data are presented as mean ± standard error of the mean (SEM). Group comparisons were performed using one-way analysis of variance (ANOVA), followed by the Tukey post hoc test and the uncorrected Fisher least significant difference (LSD) test using version 9 of GraphPad Prism (GraphPad Software, San Diego, CA, USA). Statistical significance was denoted as follows: * $p < 0.05$, ** $p < 0.005$, *** $p < 0.0005$, **** $p < 0.00005$, and # for trends where $0.05 < p < 0.1$.

For the gut microbiota analysis, sequencing depth median was 796,231 (1st quartile: 720,060—3rd quartile: 842,909) and amplicon sequence variants (ASVs) frequency median was 458,985 (1st quartile: 406,360—3rd quartile: 524,197) after quality filtering and denoising. Finally, we discovered the number of ASVs (7013). For taxonomy classification of ASVs, we used the Greengenes2 database. QIIME2 v. 2023.7 was used in 16S rRNA amplicon data analysis. For relative abundance statistical significance testing, we used LOCOM analysis (followed by Benjamini–Hochberg Procedure $P_{adj} \leq 0.05$).

3. Results

3.1. PSE and LUT Improved Insulin Tolerance and Pancreatic Islet Function

The effects of PSE and LUT supplementation on glucose homeostasis (Figure 1) were assessed by GTT, ITT, serum insulin, HOMA-IR, HOMA-B, pancreatic insulin, and pancreatic glucagon. At the baseline, there were no differences in GTT, ITT, and respective GTT AUC and ITT AUC among the groups. At the end of the study, relative to the

LFD group, the HFD group exhibited hyperglycemia (Figure 1A) and glucose intolerance (Figure 1B). Supplementation of PSE and LUT did not improve glucose intolerance in the obese Slc6a14$^{y/-}$ mice, as shown by GTT AUC (Figure 1B).

Compared to the LFD group, the HFD group developed insulin resistance, as shown by increased glucose concentration (Figure 1C) along with AUC (Figure 1D) from ITT, as well as increased serum insulin levels (Figure 1E) and HOMA-IR (Figure 1F), indicative of diabetes. Supplementation of PSE and LUT to obese Slc6a14$^{y/-}$ mice significantly improved insulin tolerance as demonstrated by the lower levels of ITT AUC, serum insulin, and HOMA-IR, compared with those without PSE and LUT (Figure 1D–F). PSE and LUT supplementation also significantly reduced HFD-induced HOMA-B relative to that in the LFD group (Figure 1G). Immunohistochemical staining of pancreatic tissue sections for insulin (Figure 1H) and glucagon (Figure 1I) revealed normal pancreatic islets with typical distribution of islet beta- and alpha-cells regardless of the treatment group.

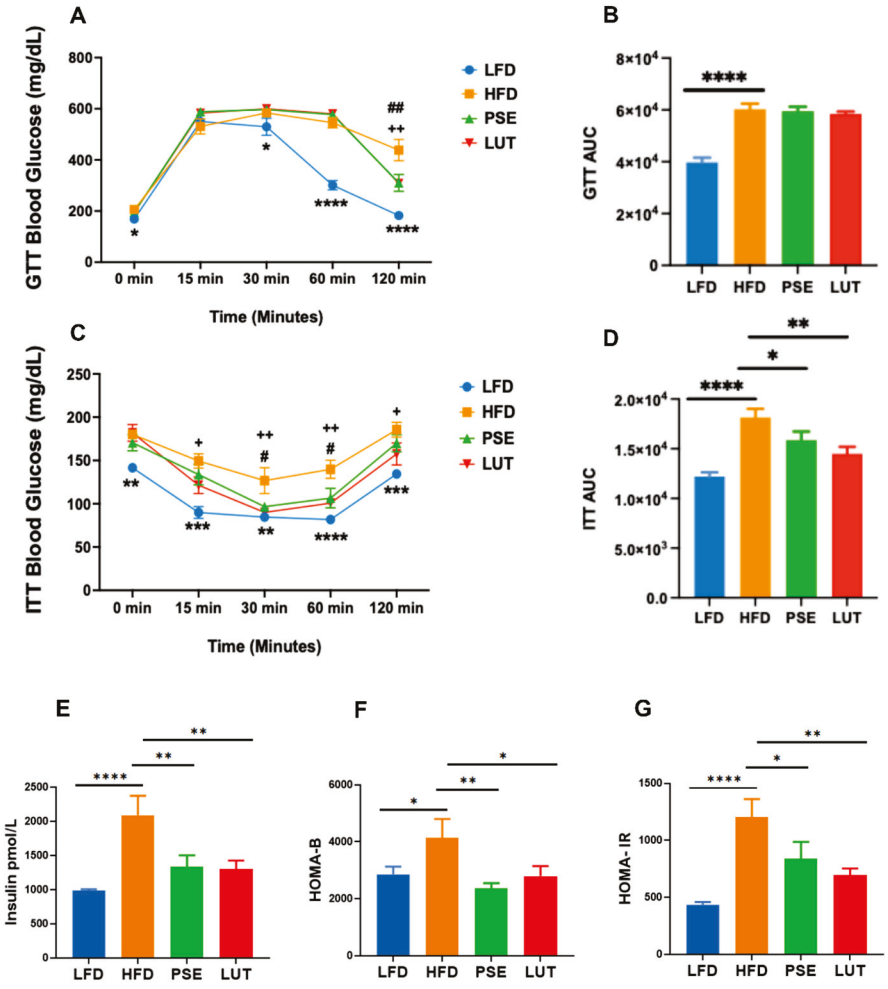

Figure 1. *Cont.*

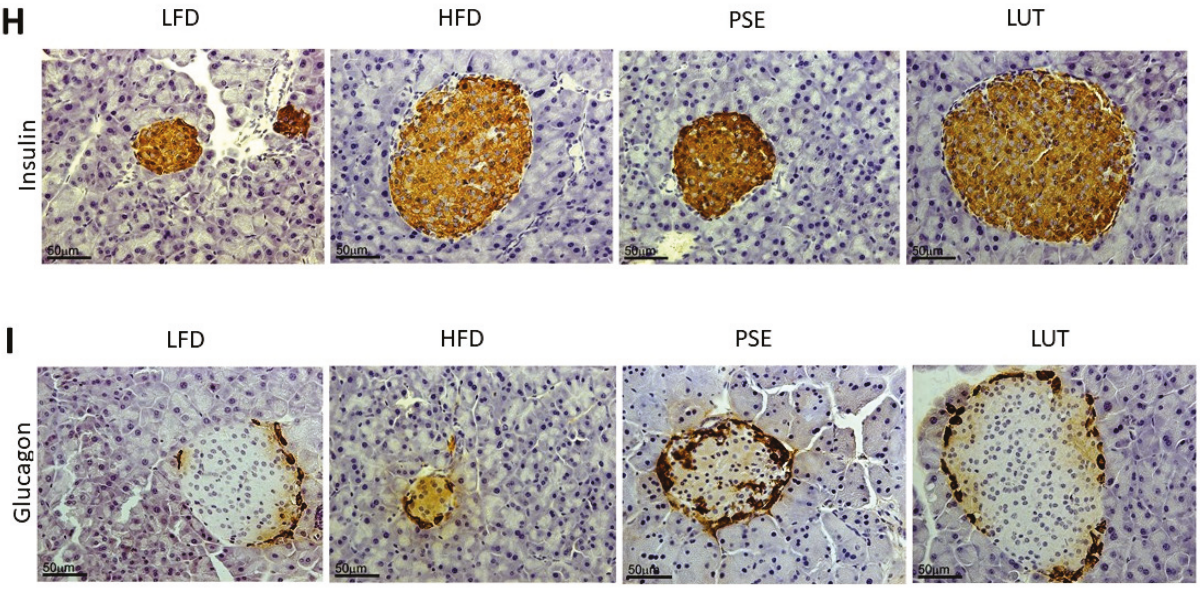

Figure 1. Effect of PSE and LUT on glucose homeostasis and pancreatic islet function: GTT (**A**), GTT AUC (**B**), ITT (**C**), ITT AUC (**D**), serum insulin (**E**), HOMA-IR (**F**), HOMA-B (**G**). n = 6–8 per group. The data are expressed as mean ± SEM and analyzed by one-way ANOVA followed by the Fisher LSD test. * HFD vs. LFD, # HFD vs. PSE, + HFD vs. LUT, * $p < 0.05$, ** $p < 0.005$, *** $p < 0.0005$, **** $p < 0.00005$. # $p < 0.05$, ## $p < 0.005$, + $p < 0.05$, ++ $p < 0.005$. Pancreatic tissue sections were immunostained for insulin ((**H**); marker of islet beta-cells) or glucagon ((**I**); marker of islet alpha-cells). Sections were counterstained with hematoxylin and images were 40× magnification.

3.2. PSE and LUT Decreased Intestinal Permeability

At the end of the study, we noted an increase in intestinal permability, as shown by increased LBP concentration in the plasma of the HFD group when compared to the LFD group. PSE and LUT supplementation significantly decreased plasma LBP concentration, suggesting decreased intestinal permeability (Figure 2).

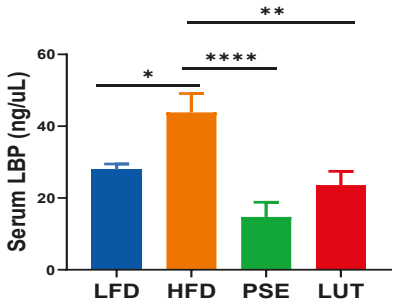

Figure 2. Effect of PSE and LUT on intestinal permeability in obese Slc6a14$^{y/-}$ mice. Data are expressed as mean ± SEM, n = 7–9 per group, and analyzed by one-way ANOVA followed by the Tukey test. * $p < 0.05$, ** $p < 0.005$, **** $p < 0.00005$.

3.3. Gut Microbiome Analysis

3.3.1. Microbiome Alpha Diversity

We first examined the microbiome alpha diversity between groups. The HFD group increased species evenness compared to the LFD group ($p \leq 0.05$, Kruskal–Wallis test followed by the Dunn test on Pielou evenness). Supplementation with PSE or LUT did not change the HFD-induced effect in animals ($p > 0.05$). Unlike evenness, species richness across all groups did not change ($p > 0.05$, Kruskal–Wallis test followed by the Dunn test on Faith phylogenetic diversity) (Figure 3).

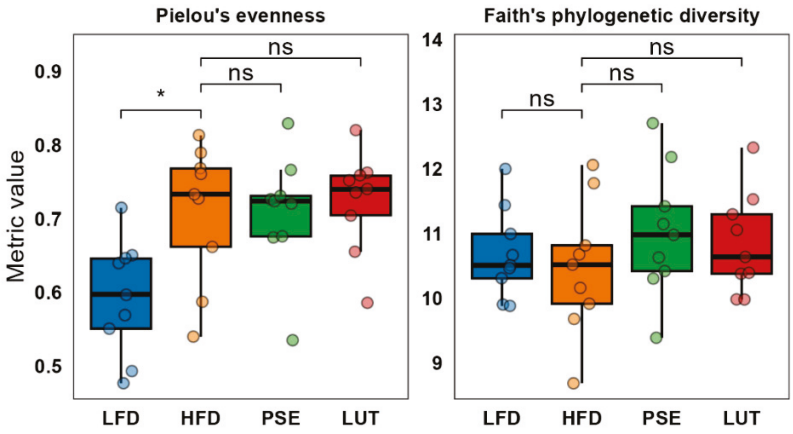

Figure 3. Alpha evenness and diversity metrics across different experimental groups. Kruskal–Wallis test followed by the Dunn test was used to determine statistical significance. * $p < 0.05$.

3.3.2. Microbiome Beta Diversity

We observed differences between the microbiome groups as indicated from weighted UniFrac distance measure ($p \leq 0.05$, PERMANOVA followed by pairwise comparison) (Figure 4). Specifically, LFD vs. HFD, PSE, or LUT exhibited a statistically significant difference ($p \leq 0.05$), as well as HFD vs. PSE or LUT ($p \leq 0.05$). This indicates that the microbiome composition of all groups is potentially different, which might be reflected on the relative abundance of specific taxa.

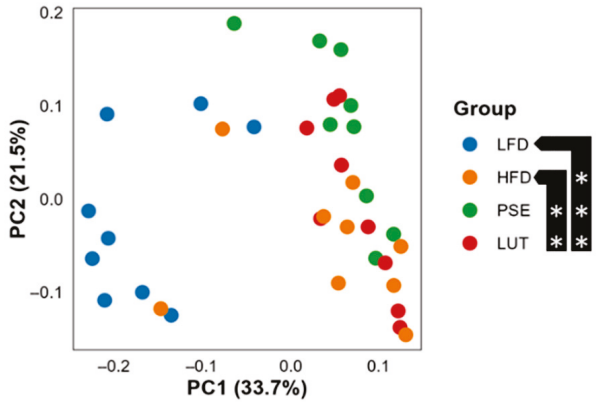

Figure 4. Beta diversity analysis of the gut microbiome across groups. PERMANOVA followed by pairwise comparison was used to determine statistical significance. ** $p < 0.005$, *** $p < 0.0005$.

3.3.3. Microbiome Composition Analysis

We first examined the effects of PSE and LUT on microbiome composition in cecal feces (Figure 5). The most dominant phyla in all groups were Firmicutes, followed by Bacteroidota, comprising more than 85% of the community. Relative to the LFD group, the HFD group exhibited increased relative abundance of Desulfobacterota and Patescibacteria and decreased relative abundance of Actinobacteriota and Proteobacteria. Compared to the HFD group, only the PSE group, not the LUT group, had significantly increased abundance of the Bacteroidota phylum.

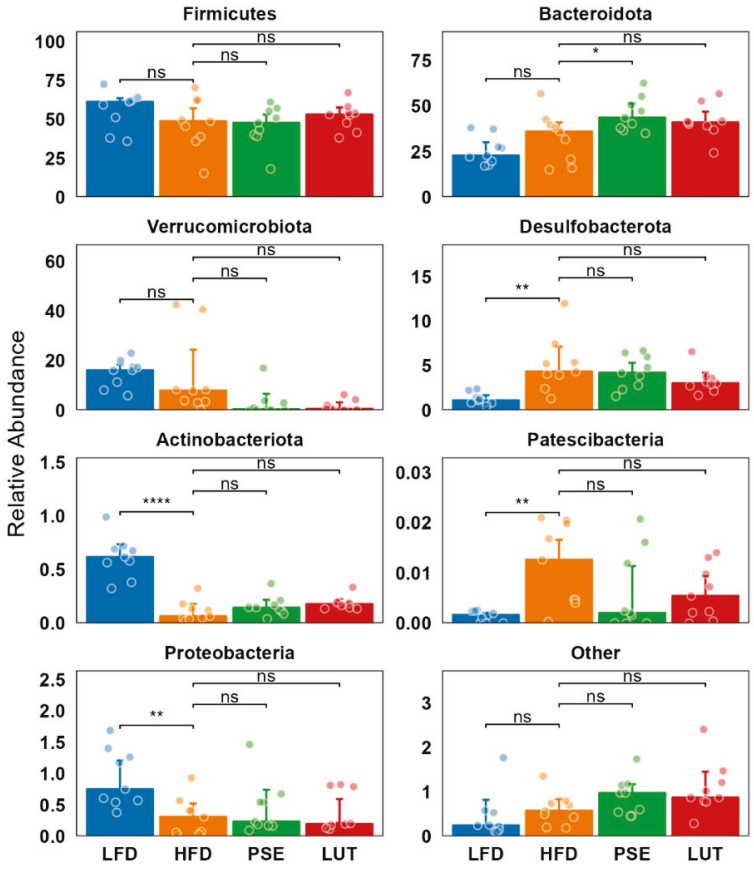

Figure 5. Effect of PSE and LUT on composition of the gut microbiome at the phylum level. * $p < 0.05$, ** $p < 0.005$, **** $p < 0.00005$.

Because we observed changes at this higher taxon level, we focused on the ASVs as they can be more informative. We observed changes in the relative abundance of ASVs in most phyla between HFD and LFD (Figure 6), including more than 50 ASVs that either increased or decreased in HFD. For instance, relative to the LFD group, the HFD group had greater abundance of two ASVs (*Staphylococcus* and *Choladousia* sp003612585), and lower abundance of nine ASVs (f_Eggerthellaceae, f_Muribaculaceae, f_Bacteroidaceae, f_Ruminococcaceae, f_Oscillospiraceae, f_CAG-74, and f_CAG-314). The addition of PSE or LUT reversed a few of the changes altered by HFD. Specifically, *Phocaeicola vulgatus* (previously known as *Bacteroides vulgatus*) was completely depleted by HFD ($P_{adj} \leq 0.01$), yet after PSE or LUT supplementation, the species recovered and increased in abundance ($P_{adj} \leq 0.05$).

Lastly, we focused on the changes in ASV abundance that were reverted by PSE or LUT supplementation (Figure 7). Among Bacteroidota phyla, both PSE and LUT supplementation significantly increased the abundance of HFD-depleted *Phocaeicola vulgatus*. LUT administration, not PSE, has shown to increase the abundance of two other HFD-depleted species (namely, *Phocaeicola barnesiae* and *Phocaeicola_A_858004*) in obese mice. On the other hand, PSE and LUT have differential effects on four species among *Firmicutes* phyla. For instance, relative to the HFD group, the PSE group had a decreased abundance of *Staphylococcus* and increased abundance of *WRMHO1*. Relative to the LFD group, LUT group showed decreased abundance of *CGA-41 sp001941225* and *Oribacterium*.

Figure 6. Effect of PSE and LUT on composition of the gut microbiome at ASVs level. LOCOM analysis was used to determine statistical significance, followed by FDR correction. * $p < 0.05$, ** $p < 0.005$.

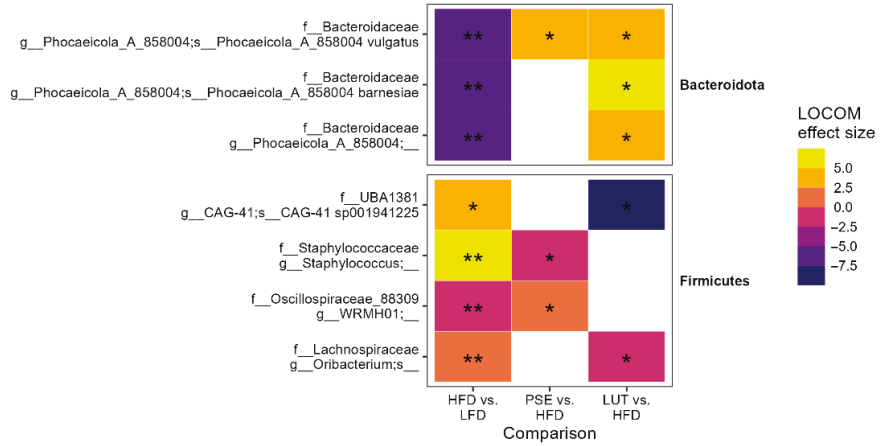

Figure 7. Gut microbiome ASVs reversed by PSE or LUT. LOCOM analysis was used to determine statistical significance, followed by FDR correction. Data in this figure are presented in Figure 6. * $p < 0.05$, ** $p < 0.005$.

3.4. Mitochondrial Fusion Markers: MFN1, MFN2, OPA1

Figure 8 shows the effects of PSE and LUT on mitochondrial fusion markers, namely MFN1 (Figure 8A), MFN2 (Figure 8B), and OPA1 (Figure 8C). The HFD mice had higher gene expression levels of MFN1 (kidney, colon), MFN2 (kidney, colon, and ileum) and OPA1 (colon and ileum) than those in the LFD mice. Administration of PSE and LUT to obese mice reverted such HFD-induced changes in MFN1, MFN2, and OPA1 gene expressions.

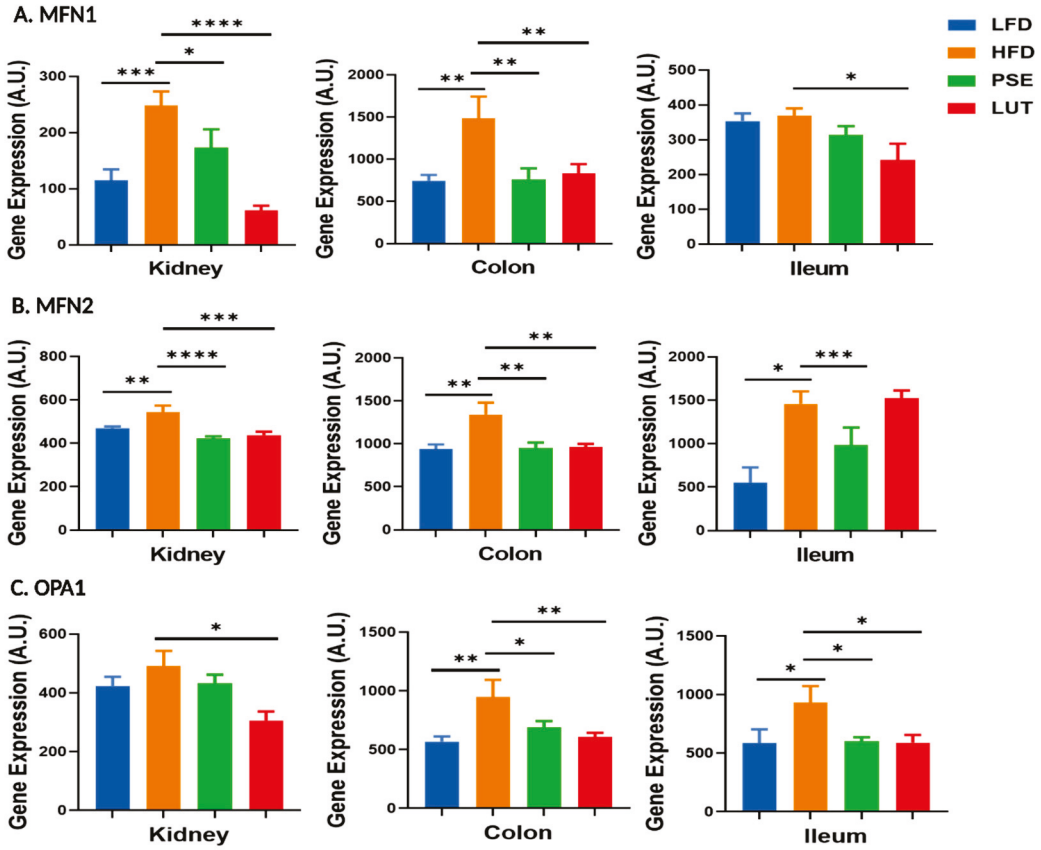

Figure 8. Effect of PSE and LUT on gene expression of MFN1 (**A**), MFN2 (**B**), and OPA1 (**C**) in the kidney, colon, and ileum. n = 6–8 per group. The data are expressed as mean ± SEM and analyzed by one-way ANOVA followed by the Fisher LSD test. * $p < 0.05$, ** $p < 0.005$, *** $p < 0.0005$, **** $p < 0.00005$.

3.5. Mitochondrial Fission Markers: FIS1, DRP1

Compared to the LFD mice, the HFD mice had decreased FIS1 and DRP1 gene expression levels across the kidneys, colon, and ileum (Figure 9). Supplementation of PSE and LUT significantly restored the levels of HFD-induced FIS1 and DRP1 gene expression in these tissues.

3.6. Mitochondrial Biosynthesis-Associated Markers: PGC1α, NRF1, NRF2, TFAM

We evaluated the impacts of PSE and LUT supplementation on the mitochondrial biosynthesis-associated markers, PGC1α (Figure 10A), NRF1 (Figure 10B), NRF2 (Figure 10C), and TFAM (Figure 10D) in the kidneys, colon, and ileum of mice. Relative to the LFD mice, the HFD mice had decreased mRNA expression levels of PGC1α (kidney, colon), NRF1 (all three tissues), NRF2 (all three tissues), and TFAM (kidney, ileum). PSE supplementation by oral gavage significantly restored these mRNA changes in the animals, as shown by increased gene expression levels of PGC1α (colon), NRF1 (colon, ileum), NRF2 (all three tissues), and TFAM (kidney, ileum). Similar to the PSE results, LUT administration

also increased mRNA expression levels of PGC1α (colon, ileum), NRF1 (all three tissues), NRF2 (all three tissues), and TFAM (kidney).

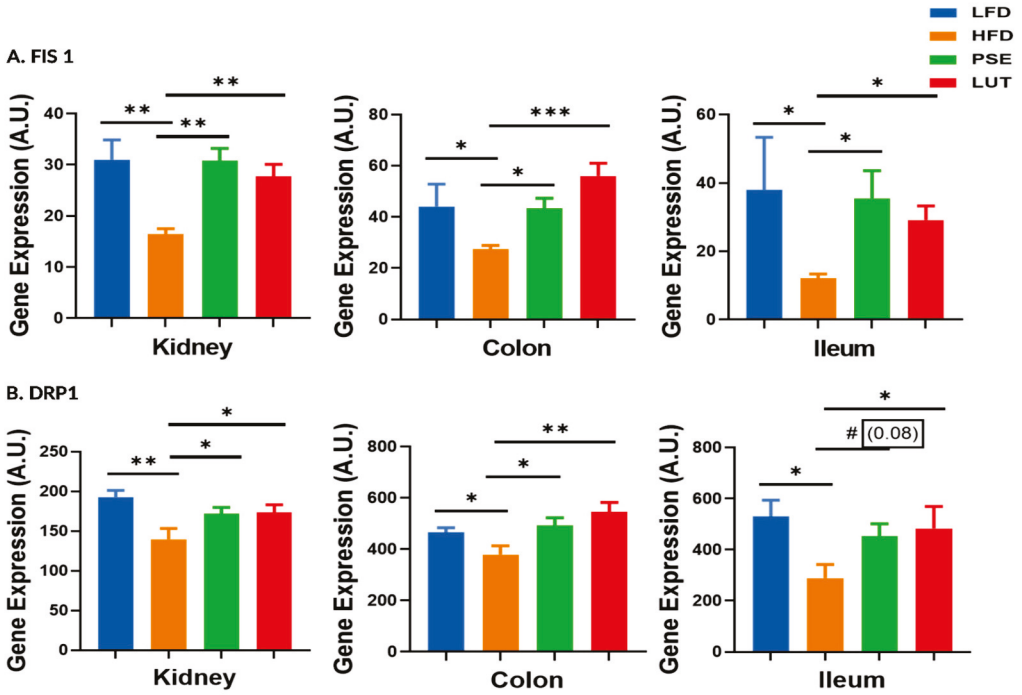

Figure 9. Effect of PSE and LUT on gene expression of FIS1 (**A**) and DRP1 (**B**) in the kidney, colon, and ileum. n = 6–8 per group. The data are expressed as mean ± SEM and analyzed by one-way ANOVA followed by the Fisher LSD test. * $p < 0.05$, ** $p < 0.005$, *** $p < 0.0005$, and # $0.05 < p < 0.1$.

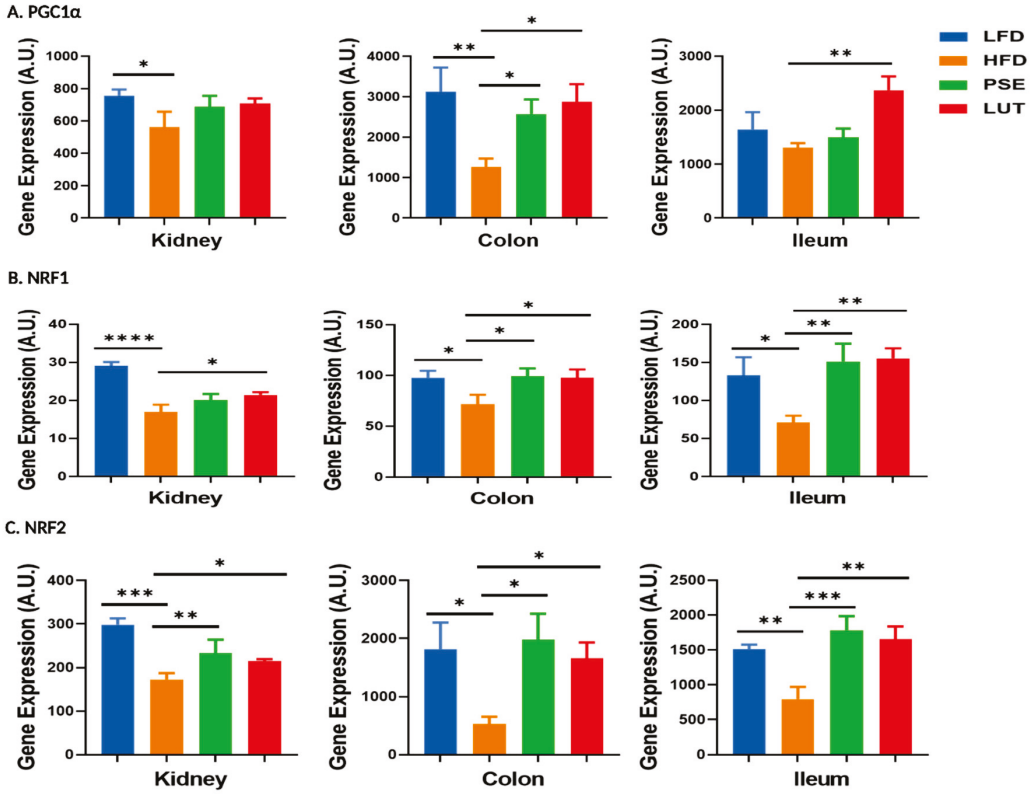

Figure 10. *Cont.*

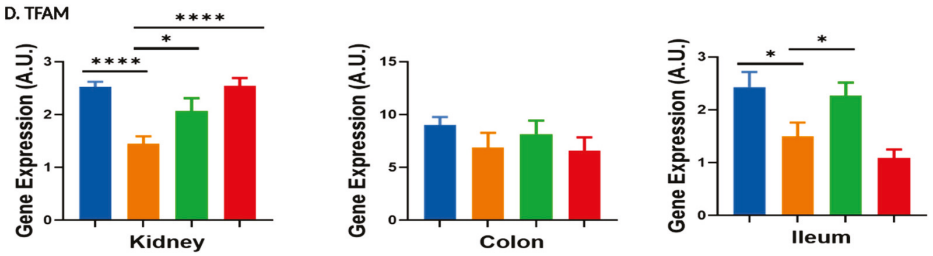

Figure 10. Effect of PSE and LUT on gene expression of PGC1α (**A**), NRF1 (**B**), NRF2 (**C**), and TFAM (**D**) in the kidney, colon, and ileum. n = 6–8 per group. The data are expressed as mean ± SEM and analyzed by one-way ANOVA followed by the Fisher LSD test. * $p < 0.05$, ** $p < 0.005$, *** $p < 0.0005$, and **** $p < 0.00005$.

3.7. Mitophagy-Associated Markers: TLR4, PINK1, LC3B

Figure 11 shows the effects of PSE and LUT supplementation on mitophagy-associated markers, TLR4 (A), PINK1 (B), and LC3B (C) in kidney, colon, and ileum. In general, the HFD group had higher TLR4, PINK1, and LC3B gene expression levels in collected tissues, when compared to the LFD group. Relative to the HFD group, both PSE and LUT groups had lower TLR4, PINK1, and LC3B in all three tissues, except for kidney with no effects on PINK1 gene expression.

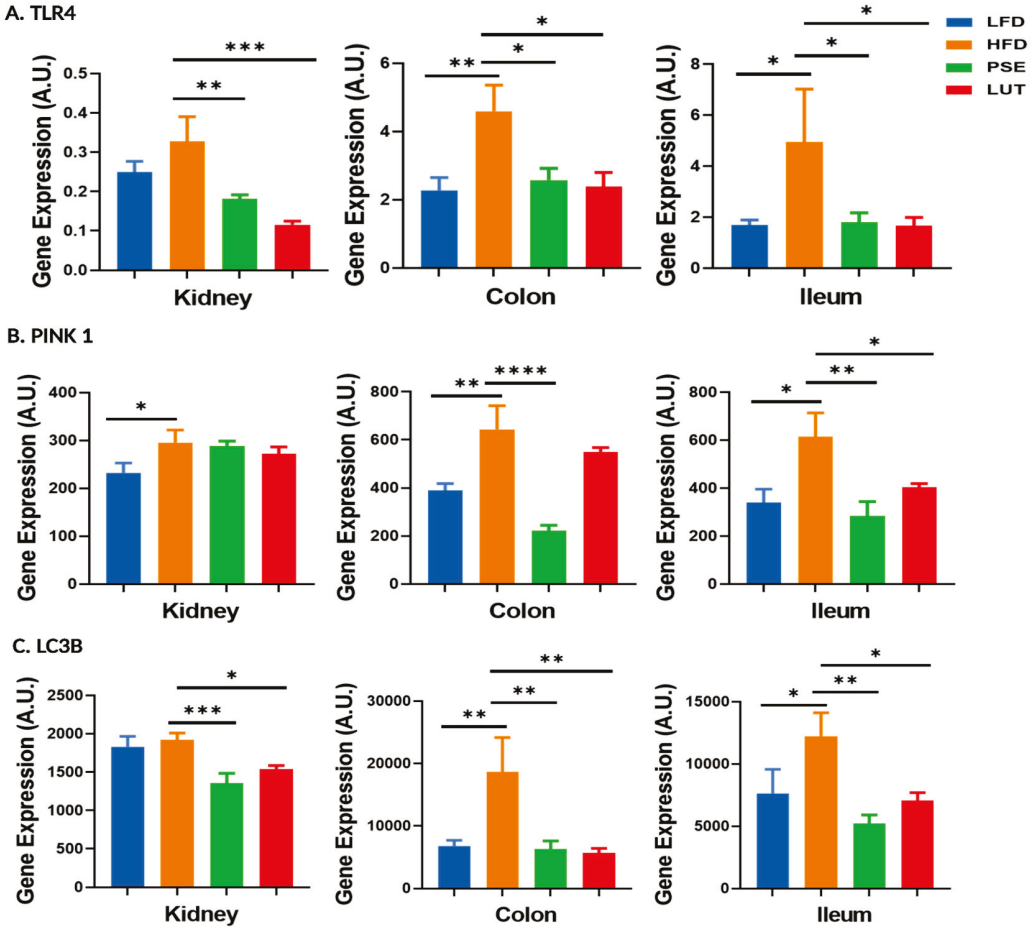

Figure 11. Effect of PSE and LUT on gene expression of TLR4 (**A**), PINK1 (**B**), and LC3B (**C**) in the kidney, colon, and ileum. n = 6–8 per group. The data are expressed as mean ± SEM and analyzed by one-way ANOVA followed by the Fisher LSD test. * $p < 0.05$, ** $p < 0.005$, *** $p < 0.0005$, and **** $p < 0.00005$.

3.8. Mitochondrial Electron Transport Chain (ETC) Markers: Complex I, Complex III

We assessed the effects of PSE and LUT on mitochondrial ETC markers complex I and complex III in the kidneys, colon, and ileum of obese mice (Figure 12). PSE and LUT administration increased both HFD-depleted complex I and complex III mRNA expression levels in these tissues.

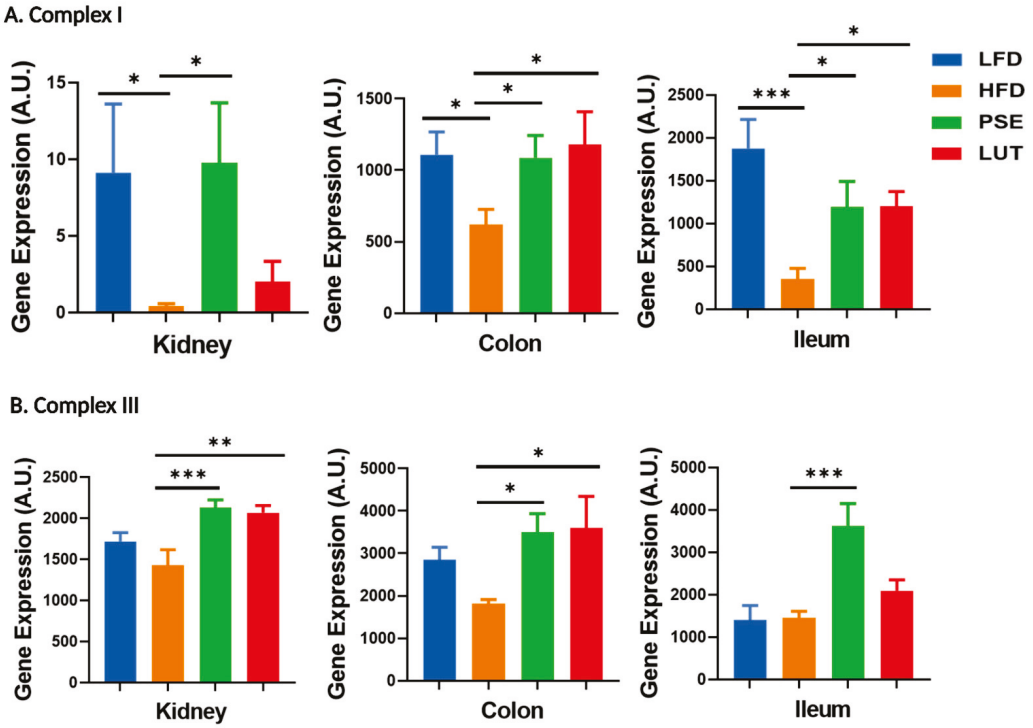

Figure 12. Effect of PSE and LUT on gene expression of complex I (**A**) and complex III (**B**) in the kidney, colon, and ileum. n = 6–8 per group. The data are expressed as mean ± SEM and analyzed by one-way ANOVA followed by the Fisher LSD test. * $p < 0.05$, ** $p < 0.005$, and *** $p < 0.0005$.

3.9. Proinflammatory Cytokines and Antioxidant Enzyme: NFκB, TNFα, IL6, SOD1

We evaluated the impacts of PSE and LUT supplementation on the pro-inflammation cytokine markers [NFκB (Figure 13A), TNFα (Figure 13B) and IL6 (Figure 13C)] and antioxidant enzyme marker [SOD1 (Figure 13D)] in the kidneys, colon, and ileum of MetS-like mice. Compared to the LFD negative control mice, the HFD positive control mice had (1) increased gene expression levels of NFκB, TNFα, and IL6 in all three tissues and (2) decreased gene expression level of SOD1 in kidney and ileum of mice. PSE administration decreased HFD-induced change in gene expression levels for NFκB, TNFα, IL6, and increased SOD1 in all studied tissues. LUT administration had (1) inhibitory effects on all NFκB, TNFα, and IL6 gene expression levels, except for NFκB in the kidneys, and (2) stimulatory effects on SOD1 gene expression levels in ileum only.

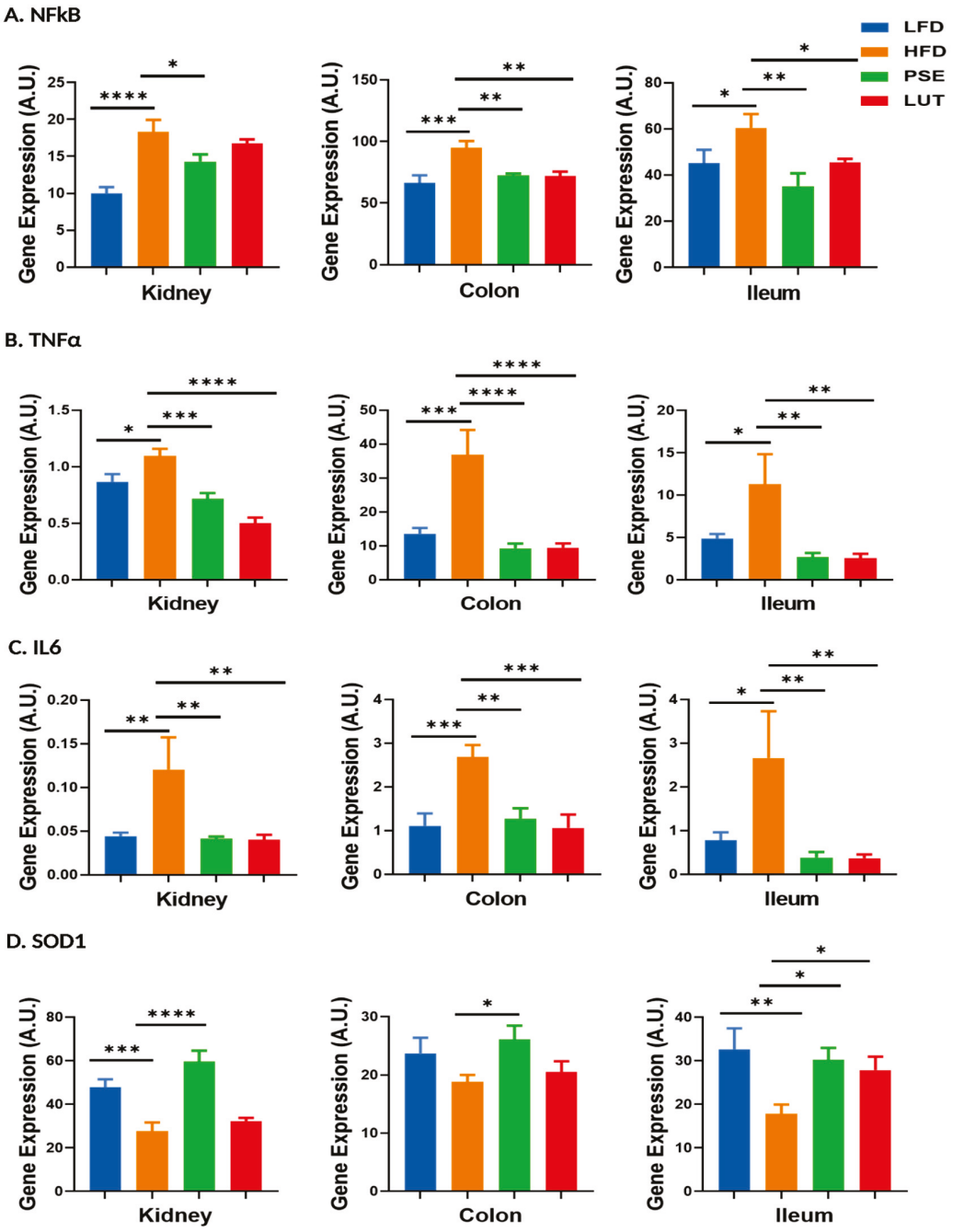

Figure 13. Effect of PSE and LUT on gene expression of NFκB (**A**), TNFα (**B**), IL6 (**C**), and SOD1 (**D**) in the kidney, colon, and ileum. n = 6–8 per group. The data are expressed as mean ± SEM and analyzed by one-way ANOVA followed by the Fisher LSD test. * $p < 0.05$, ** $p < 0.005$, *** $p < 0.0005$ and **** $p < 0.00005$.

4. Discussion

4.1. Glucose Homeostasis and Islet Cell Function in the Slc6a14$^{y/-}$ Mouse Model

Using the Slc6a14$^{y/-}$ mouse model, we successfully examined the effects of PSE and PSE-extracted LUT on glucose homeostasis, gut microbiota, and mitochondrial homeostasis in renal and GI tissues, namely the colon and ileum. Hyperglycemia and insulin resistance are key components of MetS. HOMA has been used to evaluate the interaction between glucose and insulin dynamics. HOMA-IR index is a measure of systemic insulin resistance, given the strong positive correlation between elevated HOMA-IR and the risk of developing MetS [40]. HOMA-B is a measure of beta-cell function in the pancreas; thus,

an elevated HOMA-B value indicates that beta-cells are working harder to compensate for insulin resistance [41]. In MetS, insulin resistance (elevated HOMA-IR) and beta-cell dysfunction (elevated HOMA-B) are often present together since the initial response of the body to insulin resistance is often a compensatory elevation in systemic insulin levels, resulting in initially elevated HOMA-B [42]. In this study, we reported that both PSE and PSE-extracted LUT improved glucose homeostasis (Figure 1A–D) and insulin sensitivity (Figure 1E–G) in the obese Slc6a14$^{y/-}$ mice, as shown in decreased AUC after ITT administration, serum insulin, HOMA-IR, and HOMA-B. Our findings of improved glucose homeostasis and insulin sensitivity by PSE are consistent with published studies on diabetic animals, including HFD/STZ rats [20,43,44], STZ rats [45], and Goto–Kakizaki rats [46]. Furthermore, our finding that PSE-extracted LUT alleviated MetS-like-induced insulin resistance in obese Slc6a14$^{y/-}$ mice is corroborated by published works testing LUT-enriched artichoke leaf [23] and LUT-enriched *Tecoma stans* (L.) Juss. Ex Kunth [47] in HFD-induced MetS mice.

In MetS, persistent hyperglycemia leads to beta-cell dysfunction in the islets of the pancreas, with eventual failure resulting from systemic insulin resistance. Insulin resistance and beta-cell dysfunction are inextricably linked and form a self-inducing cycle during the progression through the MetS inflammatory continuum [48]. Our pancreatic immunohistochemical results (Figure 1H,I) found normal islet structure with alpha- and beta-cells expressing glucagon and insulin, respectively. Normal islet histology after HFD treatment is consistent with the start of the development of insulin resistance as the beta-cells first appear normal but later have impaired function as measured by elevated insulin secretion and HOMA-B. Treatment with PSE and LUT did not alter the normal islet histology but did return serum insulin and beta-cell function (HOMA-B) to normal. Such findings that PSE or LUT had no effects on glucagon and insulin in islet histology were not consistent with the study by Sun et al. [43]. Sun et al. reported that PSE improved the cellular structural and pathological changes in pancreatic islets of the HFD/STZ rats [43].

4.2. Gut Microbiome, Intestinal Barrier Function, and Metabolic Syndrome

The gut microbiome has been strongly associated with obesity and related metabolic disease states, including MetS, though the mechanisms involved have remained unclear. A permeable intestinal epithelium (increased intestinal permeability or disrupted intestinal barrier) can allow bacteria and bacterial components like lipopolysaccharides from the gut to enter the bloodstream (i.e., endotoxemia), triggering chronic low-grade inflammation, potential insulin resistance, and obesity, all of which are key factors in MetS progression [49]. The present study is the first to demonstrate the direct impact of PSE and LUT on reducing intestinal permeability in MetS-like mice with insulin resistance, as shown by decreased plasma LBP (an intestinal permeability marker, Figure 2). Such a finding agrees with the study by Sun et al. that LUT supplementation restores the damaged intestinal mucosal barrier and reduces intestinal permeability in rats with non-alcoholic fatty liver disease via the gut–liver axis [50].

The gut microbiome, a complex ecosystem of trillions of microorganisms residing predominantly in the colon, has emerged as having a crucial role in regulating metabolic inflammatory processes, notably in the pathogenesis of MetS within its inflammatory continuum [7,51]. Gut dysbiosis is an imbalanced gut microbiota composition that can disrupt the epithelial barrier, leading to increased intestinal permeability and chronic low-grade inflammation. This imbalance manifests itself through a shift in the microbial populations favoring pathogenic or opportunistic species over beneficial commensals, which facilitates the translocation of microbial-derived antigens such as lipopolysaccharides into systemic circulation [5,52]. Intriguingly, this study shows that PSE and LUT groups

demonstrated a significant shift in gut microbiota beta diversity profiles compared to those in HFD groups (Figure 3), suggesting PSE and LUT administration significantly influenced microbiota composition of cecal feces in MetS-like mice. Such findings agree with published studies using LUT in a variety of disease models [53–55]. For instance, LUT has been shown to positively modulate gut microbiota beta diversity and mitigate gut microbiota dysbiosis in rodent models of inflammatory bowel disease [53], cadmium-induced liver and intestinal damage [54], and non-alcoholic fatty liver disease (now called metabolic dysfunction-associated steatotic liver disease or MASLD in humans) [55], potentially enhancing gut health and mitigating disease progression.

In general, mice and humans share two similar major phyla within their gut microbiota, namely Bacteroidetes and Firmicutes [56]. The development of MetS has been shown to be associated with decreased Bacteroidetes phylum, increased Firmicutes/Bacteroidetes ratio, and increased Proteobacteria phylum in the GI tract [57]. This study is the first study (Figure 7) to demonstrate both PSE and LUT administration exhibiting differential impacts on increasing the *Bacteroidota* genus (*P. vulgatus* in both PSE and LUT groups; *s. Phocaeicola_A_858005 barnesiae* in LUT group) in MetS-like mice. *P. vulgatus* has shown to be crucial for maintaining host health, including metabolic homeostasis, immunity, and gut–brain function [58]. The findings (Figure 7) that PSE and LUT supplementation reduced the abundance of *Firmicutes* genera or species (*f_Staphylococcaceae_g Staphylococcus* and *f_Oscillospiraceae_g_WRMHO1* in PSE group; *f_UBA1381_s_CAG-41 sp001941225* and *f_Lacnospiraceae_g_Oribacterium* in LUT group) agrees with the study by Gao et al., where it was reported that LUT attenuates *Staphylococcus aureus*-induced endometritis through inhibiting ferroptosis and inflammation via activating the NRF2 signaling pathway [59]. In addition, we also noted that the Firmicutes/Bacteroidetes ratio was also decreased in both PSE- and LUT-treated animals, providing evidence of their beneficial effects on the MetS-like state progression.

4.3. Mitochondrial Function, Biogenesis, and Inflammatory Modulation by PSE and LUT

Mitochondria are endosymbiotic cytoplasmic organelles that house the ETC on their inner mitochondrial membrane (IMM), which produces most adenosine triphosphate (ATP) molecules via oxidative phosphorylation, mediated by multiprotein complexes that shuttle electrons from nicotinamide adenine dinucleotide with hydrogen (NADH) and flavine adenine dinucleotide ($FADH_2$) to molecular oxygen, the last electron acceptor in the series that ultimately forms physiologic water. This is achieved by the proton motive force (Δp) including both a proton gradient (ΔpH) and an electron gradient known as the mitochondrial membrane potential ($\Delta\Psi mt$), where the ΔpH potential energy builds in the intermembrane space and the $\Delta\Psi mt$ is shuttled down the IMM, to produce a synergistic Δp at complex V (ATP synthase) for ATP gamma bond formation [33,60]. A compromised integrity or function of this structure and process increases uncontrolled ROS that serve as damaging catalysts for inflammatory cascades. It is important to note, however, ROS can serve as a signaling molecule in certain pathways when controlled [61]. When a single electron is transferred to molecular oxygen, it generates a highly reactive superoxide ($O_2^{-\bullet}$), which, at physiological pH, is rapidly dismutated into hydrogen peroxide (H_2O_2) by superoxide dismutase—SOD1 in the cytoplasm and SOD2 in the mitochondrial matrix [60]. While there are at least 11 mitochondrial sites known to produce $O_2^{-\bullet}$, complex I is the primary site in vivo, while complex III acts as an electron leak at the Qo site, especially as an underlying cause of non-communicable chronic disease, and is therefore part of the rationale behind this study [62].

As previously mentioned, mitochondrial dynamics are primarily a function of metabolic adaptation and quality control, with fusion increasing oxidative capacity and

fission facilitating degradation of damaged organelles and their replacement [63]. Mitochondrial fusion is mediated through dynamin-related GTPases mitofusin 1 (MFN1) and optic atrophy type 1 (OPA1), which mediate outer and inner mitochondrial membrane fusion, respectively [18]. Meanwhile, mitochondrial fission is regulated by dynamin-related protein 1 (DRP1) through translocation to, and binding of, outer mitochondrial membrane (OMM) protein adaptors such as fission 1 (FIS1), which facilitate contact with the endoplasmic reticulum, so that constriction and isolation of the mitochondrion can ensue [64]. Such processes allow for an anomalous mitochondrion to be averaged out among the presumably more numerous healthy mitochondria so that, in the presence of a stressor, nuclear communication through the mitochondrial unfolded protein response can activate signaling pathways that induce transcription of nuclear genes associated with mitochondrial quality control and survival [65]. Alternatively, mitophagy of impaired mitochondria can be triggered through direct association pathways or via parkin-mediated polyubiquitination of OMM proteins, a process initiated by PTEN-induced kinase 1 (PINK1) [66,67]. In this context, toll-like receptor 4 (TLR4) plays a dual role: it not only contributes to innate immune signaling but also promotes mitochondrial quality control by initiating mitophagy under inflammatory stress [66]. One of the key downstream effectors is LC3B, a microtubule-associated protein that is lipidated and recruited to autophagosomal membranes to facilitate mitochondrial clearance [66,67]. Furthermore, biogenesis and maintenance of mitochondrial mass are coordinated primarily by PGC1α through the transcription of mtDNA and nuclear-encoded mitochondrial proteins [68]. This pathway also involves NRF2 and TFAM, which together contribute to mitochondrial DNA replication, transcription, and antioxidant defense [68]. First described as a thermogenic factor in adipose tissue, PGC1α was soon after shown to induce expression of ETC proteins, driving Δp and mitochondrial dynamics [69]. Impairment of these dynamics, involving fission, fusion, mitophagy, and biogenesis, are crucial in the development of MetS. In the present study, both PSE and LUT supplementation decreased mitochondrial fusion markers (MFN1, MFN2, and OPA1), increased mitochondrial fission markers (FIS1 and DRP1), and decreased mitophagy markers (TLR4, PINK1, and LC3B) in the kidneys, colon, or ileum. Our current findings in the renal and GI tissues of MetS-like mice treated with PSE and LUT are consistent with previous studies in brain, liver, and adipose tissue of diabetic mice [19] and in brown fat development in in vitro 3T3-L1 adipocytes [26]. In addition, LUT has shown to reduce the initiation of excessive mitophagy in neuronal cell death via regulating autophagy and mitochondrial dynamics [70]. Such observations support our hypothesis that PSE and LUT improve mitochondrial dynamics in MetS-like mice.

Potential therapeutic means to mitigate mitochondrial dysfunction in MetS progression include enhancing mitochondrial biogenesis and ATP synthesis-associated enzymes [71]. In this study, both PSE and LUT administration have demonstrated (1) enhancing the mRNA levels of mitochondrial biogenesis markers (PGC1α, NRF1, NRF2, and TFAM) (Figure 10), (2) enhancing the mRNA levels of complex I and III (Figure 12), (3) enhancing the mRNA levels of antioxidant enzyme markers (SOD1) (Figure 13), and (4) decreasing the mRNA levels of inflammation markers (NFκB, TNFα, IL6) (Figure 13) in the kidneys, colon, and ileum. Our findings of mitochondrial biogenesis in the studied tissues are supported by previous studies in a variety of animal tissues [19,26]. For instance, PSE has been reported to increase the expression levels of genes like NRF1, NRF2, and TFAM in liver, brain, and white adipose tissue of db/db mice [19]. Liu et al. reported that both PSE and LUT treatments increased the gene expression levels of brown adipocyte-specific markers, like UCP1, PGC1α, and SIRT1, potentially contributing to mitochondrial biogenesis of brown tissues [26]. In this study, our findings that LUT mitigates inflammation markers in MetS-like mice corroborate previous studies that LUT (1) protects against

diabetic cardiomyopathy by inhibiting NFκB-mediated inflammation and activating the NRF2-mediated antioxidant responses in STZ-induced diabetic mice [72] and (2) reverses MetS-induced biochemical dysfunction and related cardiac injury via the suppression of apoptosis, inflammation, and stress in rats with MetS-associated cardiac injury [24].

5. Conclusions

Chronic inflammation and oxidative stress are central contributors to insulin resistance, beta-cell dysfunction, and tissue injury in MetS development. PSE and LUT administration to MetS-like mice improved glucose homeostasis, insulin sensitivity, and mitochondrial function in the kidney, colon, and ileum organs. Recovery in mitochondrial integrity could be, at least in part, linked to restoration of intestinal barrier integrity and a shift in the gut microbiome.

While this study provides mechanistic insights into the role gut dysbiosis plays in mitochondrial dysfunction and subsequent inflammatory sequelae, several limitations must be acknowledged. First, the findings are based exclusively on preclinical data from Slc6a14$^{y/-}$ male mice, limiting extrapolation to human physiology; moreover, future studies should either incorporate female cohorts with homozygous and/or heterozygous females to account for sex-specific or genotype-specific effects. Second, the oral doses of PSE (200 mg/kg of BW) and LUT (100 mg/kg of BW) used in this study do not yet reflect clinically equivalent or bioavailable concentrations for humans. Third, all MetS criteria were met in this murine model with the exception of direct measurement of lipid profiles for dyslipidemia, a characteristic feature of MetS, which is an important caveat and is why we term this model "MetS-like"; however, the model was presumed to exhibit dyslipidemia based on the prior study consistently demonstrating hepatic steatosis and increased NAS and fat accumulation scores in Slc6a14$^{y/-}$ mice fed a HFD [33]. Lastly, it is unclear whether the observed anti-inflammatory and antioxidant effects of PSE and LUT are mediated by direct cellular actions or indirectly via bioactive metabolites produced through microbial biotransformation, particularly in the gut. This uncertainty is especially relevant for LUT, which is known to exhibit poor oral bioavailability due to rapid metabolism and limited absorption [73], though this factor supports the observed positive shift in microbial composition. This may necessitate the future development of enhanced delivery systems (e.g., nanoemulsions, liposomal formulations, or co-administrations with bio-enhancers) for human application [74].

In terms of future research, this work establishes a strong foundation for investigating PSE and LUT as gut–microbiome–mitochondria ameliorating agents in metabolic disease. Future clinical trials are warranted to validate the glucose-lowering, anti-inflammatory, and microbiota-modulating effects of PSE and/or LUT from animal findings to the individuals with MetS or sequalae within the inflammatory continuum.

Supplementary Materials: The following supporting information can be downloaded at: https://www.mdpi.com/article/10.3390/nu17142290/s1, Table S1: List of primers for mRNA.

Author Contributions: H.D., R.M., J.M.S., S.S., J.M.D., M.M.E., M.B. and C.-L.S. participated in the study conceptualization. H.D., J.M.S., S.S., J.M.D., M.B. and C.-L.S. conducted sample collection. S.S. bred and provided Slc6a14$^{y/-}$ mice for the study. J.M.M. and J.M.D. performed glucose homeostasis and pancreas analysis. J.M.S. conducted plasma LBP measurement and performed data analysis. R.M., P.Q.P. and Z.D. conducted the gene expression experiments and analysis. M.M.E. conducted gut microbiome analysis and data interpretation. H.D., R.M., M.M.E., J.M.D. and C.-L.S. contributed to data interpretation and preparing the preliminary draft of the manuscript. C.-L.S. finished the first draft of the manuscript prior to submission. All authors have read and agreed to the published version of the manuscript.

Funding: The laboratory research received support from Texas Tech University Health Sciences Center (CLS, RM), The CH Foundation (JMD), Robert A. Welch Foundation (B1-0028, JMD), and TrUE Scholars Program at Texas Tech University (ZD).

Institutional Review Board Statement: All procedures outlined in this study received approval from the Institutional Animal Care and Use Committee (IACUC) at Texas Tech University Health Science Center (TTUHSC) in Lubbock, Texas, U.S.A. IACUC protocol number: 22017, approved 27 May 2022.

Informed Consent Statement: Not applicable.

Data Availability Statement: The raw sequencing data (BioProject access number PRJNA1258714) of 16S rRNA amplicon sequencing was deposited in the National Center for Biotechnology Information BioProject database. The original contributions presented in this study are included in the article. Further inquiries can be directed to the corresponding authors.

Acknowledgments: Real-time polymerase chain reaction data were generated in the "Molecular Biology Core Facility", which is supported in part by TTUHSC. Authors thanked for Jordan Beal for editing the manuscript.

Conflicts of Interest: The authors declare no conflicts of interest.

Abbreviations

BW: body weight; NLRP3: NOD-, LRR-, and pyrin domain-containing protein 3; PTEN: phosphatase and tensin homolog; UCP1: uncoupling protein 1; SIRT1: silent information regulator type 1; NAS: non-alcoholic fatty liver disease score.

References

1. WHO. Global Report on Diabetes 2023. Available online: https://www.who.int/health-topics/diabetes# (accessed on 1 April 2025).
2. Noubiap, J.J.; Nansseu, J.R.; Lontchi-Yimagou, E.; Nkeck, J.R.; Nyaga, U.F.; Ngouo, A.T.; Tounouga, D.N.; Tianyi, F.-L.; Foka, A.J.; Ndoadoumgue, A.L.; et al. Geographic distribution of metabolic syndrome and its components in the general adult population: A meta-analysis of global data from 28 million individuals. *Diabetes Res. Clin. Pract.* **2022**, *188*, 109924. [CrossRef] [PubMed]
3. Liang, X.; Or, B.; Tsoi, M.F.; Cheung, C.L.; Cheung, B.M.Y. Prevalence of metabolic syndrome in the United States National Health and Nutrition Examination Survey 2011–18. *Postgrad. Med. J.* **2023**, *99*, 985–992. [CrossRef] [PubMed]
4. Hayden, M.R. Overview and New Insights into the Metabolic Syndrome: Risk Factors and Emerging Variables in the Development of Type 2 Diabetes and Cerebrocardiovascular Disease. *Medicine* **2023**, *59*, 561. [CrossRef] [PubMed]
5. Crudele, L.; Gadaleta, R.M.; Cariello, M.; Moschetta, A. Gut microbiota in the pathogenesis and therapeutic approaches of diabetes. *eBiomedicine* **2023**, *97*, 104821. [CrossRef]
6. Chong, L.L.T.; Chong, C.K.; Jensen, S.L.; Lau, K.M. Gut microbiota in type 2 diabetes mellitus: A systematic review of compositional and functional alterations. *Front. Endocrinol.* **2024**, *15*, 104821. [CrossRef]
7. Craciun, C.-I.; Neag, M.-A.; Catinean, A.; Mitre, A.-O.; Rusu, A.; Bala, C.; Roman, G.; Buzoianu, A.-D.; Muntean, D.-M.; Craciun, A.-E. The Relationships between Gut Microbiota and Diabetes Mellitus, and Treatments for Diabetes Mellitus. *Biomedicines* **2022**, *1*, 308. [CrossRef] [PubMed]
8. Patloka, O.; Komprda, T.; Franke, G. Review of the Relationships Between Human Gut Microbiome, Diet, and Obesity. *Nutrients* **2024**, *16*, 3996. [CrossRef] [PubMed] [PubMed Central]
9. Boicean, A.; Ichim, C.; Sasu, S.M.; Todor, S.B. Key Insights into Gut Alterations in Metabolic Syndrome. *J. Clin. Med.* **2025**, *14*, 2678. [CrossRef] [PubMed] [PubMed Central]
10. de Vos, W.M.; Tilg, H.; Van Hul, M.; Cani, P.D. Gut microbiome and health: Mechanistic insights. *Gut* **2022**, *71*, 1020–1032. [CrossRef]
11. Li, X.J.; Shan, Q.Y.; Wu, X.; Miao, H.; Zhao, Y.Y. Gut microbiota regulates oxidative stress and inflammation: A double-edged sword in renal fibrosis. *Cell Mol Life Sci.* **2024**, *81*, 480. [CrossRef]
12. Daryabor, G.; Atashzar, M.R.; Kabelitz, D.; Meri, S.; Kalantar, K. The Effects of Type 2 Diabetes Mellitus on Organ Metabolism and the Immune System. *Front. Immunol.* **2020**, *1*, 1582. [CrossRef] [PubMed]
13. Masenga, S.K.; Kabwe, L.S.; Chakulya, M.; Kirabo, A. Mechanisms of Oxidative Stress in Metabolic Syndrome. *Int. J. Mol. Sci.* **2023**, *24*, 7898. [CrossRef]

14. Ezenabor, E.H.; Adeyemi, A.A.; Adeyemi, O.S. Gut Microbiota and Metabolic Syndrome: Relationships and Mechanisms. *Int. J. Endocrinol.* **2024**. [CrossRef]
15. Cojocaru, K.-A.L.I.; Goriuc, A.; Antoci, L.-M.; Ciobanu, C.-G.; Popescu, R.; Vlad, C.-E.; Blaj, M.; Foia, L.G. Mitochondrial dysfunction, oxidative stress, and therapeutic strategies in diabetes, obesity, and cardiovascular disease. *Antioxidants* **2023**, *12*, 658. [CrossRef]
16. Todosenko, N.; Khaziakhmatova, O.; Malashchenko, V.; Yurova, K.; Bograya, M.; Beletskaya, M.; Vulf, M.; Gazatova, N.; Litvinova, L. Mitochondrial Dysfunction Associated with mtDNA in Metabolic Syndrome and Obesity. *Int. J. Mol. Sci.* **2023**, *24*, 12012. [CrossRef] [PubMed] [PubMed Central]
17. Smith, S.A.; Ogawa, S.A.; Chau, L.; Whelan, K.A.; Hamilton, K.E.; Chen, J.; Tan, L.; Chen, E.Z.; Keilbaugh, S.; Fogt, F.; et al. Mitochondrial dysfunction in inflammatory bowel disease alters intestinal epithelial metabolism of hepatic acylcarnitines. *J. Clin. Investig.* **2021**, *131*, e133371. [CrossRef]
18. Kabootari, M.; Habibi Tirtashi, R.; Amouzegar, A.; Masoumi, S.; Azizi, F.; Amouzegar, A. Changes in metabolic syndrome status and risk of chronic kidney disease over a decade of follow-up in the Iranian population. *Sci. Rep.* **2025**, *15*, 19041. [CrossRef] [PubMed] [PubMed Central]
19. Deshmukh, H.; Santos, J.M.; Bender, M.; Dufour, J.M.; Lovett, J.; Shen, C.L. Peanut Shell Extract Improves Mitochondrial Function in db/db Mice via Suppression of Oxidative Stress and Inflammation. *Nutrients* **2024**, *16*, 1977. [CrossRef] [PubMed]
20. Bender, M.; Santos, J.M.; Dufour, J.M.; Deshmukh, H.; Trasti, S.; Elmassry, M.M.; Shen, C.-L. Peanut Shell Extract Improves Markers of Glucose Homeostasis in Diabetic Mice by Modulating Gut Dysbiosis and Suppressing Inflammatory Immune Response. *Nutrients* **2024**, *16*, 4158. [CrossRef] [PubMed] [PubMed Central]
21. Zhu, M.; Sun, Y.; Su, Y.; Guan, W.; Wang, Y.; Han, J.; Wang, S.; Yang, B.; Wang, Q.; Kuang, H. Luteolin: A promising multifunctional natural flavonoid for human diseases. *Phytother. Res.* **2024**, *38*, 3417–3443. [CrossRef] [PubMed]
22. Peng, M.M.; Chen, Z.S.; Deng, Q.P.; Zhu, S.J.; Wang, G. The roles of luteolin in peanut shell extract—Mediated protection of erythrocytes against hypoxanthine-xanthine oxidase-induced toxicity. *Food Biosci.* **2021**, *39*, 100826. [CrossRef]
23. Kwon, E.Y.; Kim, S.Y.; Choi, M.S. Luteolin-Enriched Artichoke Leaf Extract Alleviates the Metabolic Syndrome in Mice with High-Fat Diet-Induced Obesity. *Nutrients* **2018**, *10*, 979. [CrossRef] [PubMed]
24. Dai, X.Y.; Liang, B.; Sun, Y.L. Luteolin ameliorates rat model of metabolic syndrome-induced cardiac injury by apoptosis suppression and autophagy promotion via NR4A2/p53 regulation. *BMC Complement. Med. Ther.* **2025**, *25*, 14. [CrossRef]
25. Fikry, H.; Saleh, L.A.; Sadek, D.R.; Alkhalek, H.A.A. The possible protective effect of luteolin on cardiovascular and hepatic changes in metabolic syndrome rat model. *Cell Tissue Res.* **2025**, *399*, 27–60. [CrossRef] [PubMed]
26. Liu, W.R.; Wang, L.H.; Zhang, J. Peanut Shell Extract and Luteolin Regulate Lipid Metabolism and Induce Browning in 3T3-L1 Adipocytes. *Foods* **2022**, *11*, 2696. [CrossRef]
27. Xu, N.; Zhang, L.; Dong, J.; Zhang, X.; Chen, Y.-G.; Bao, B.; Liu, J. Low-dose diet supplement of a natural flavonoid, luteolin, ameliorates diet-induced obesity and insulin resistance in mice. *Mol. Nutr. Food Res.* **2014**, *58*, 1258–1268. [CrossRef] [PubMed]
28. Kahksha; Alam, O.; Al-Keridis, L.A.; Khan, J.; Naaz, S.; Alam, A.; Ashraf, S.A.; Alshammari, N.; Adnan, M.; Beg, A. Evaluation of Antidiabetic Effect of Luteolin in STZ Induced Diabetic Rats: Molecular Docking, Molecular Dynamics, In Vitro and In Vivo Studies. *J. Funct. Biomater.* **2023**, *14*, 126. [CrossRef] [PubMed] [PubMed Central]
29. Sangeetha, R. Luteolin in the management of type 2 diabetes mellitus. *Curr. Res. Nutr. Food Sci. J.* **2019**, *7*, 393–398. [CrossRef]
30. Thaiss, C.A.; Zeevi, D.; Levy, M.; Zilberman-Schapira, G.; Suez, J.; Tengeler, A.C.; Abramson, L.; Katz, M.N.; Korem, T.; Zmora, N.; et al. Transkingdom Control of Microbiota Diurnal Oscillations Promotes Metabolic Homeostasis. *Cell* **2014**, *159*, 514–529. [CrossRef]
31. Li, H.; Zou, L.; Long, Z.; Zhan, J. Immunometabolic alterations in type 2 diabetes mellitus revealed by single-cell RNA sequencing: Insights into subtypes and therapeutic targets. *Front. Immunol.* **2025**, *15*, 1537909. [CrossRef] [PubMed] [PubMed Central]
32. Wahlström, A.; Sayin, S.I.; Marschall, H.U.; Bäckhed, F. Intestinal Crosstalk between Bile Acids and Microbiota and Its Impact on Host Metabolism. *Cell Metab.* **2016**, *24*, 41–50. [CrossRef] [PubMed]
33. Sivaprakasam, S.; Sikder, M.O.; Ramalingam, L.; Kaur, G.; Dufour, J.M.; Moustaid-Moussa, N.; Wachtel, M.S.; Ganapathy, V. SLC6A14 deficiency is linked to obesity, fatty liver, and metabolic syndrome but only under conditions of a high-fat diet. *BBA-Mol. Basis Dis.* **2021**, *1867*, 166087. [CrossRef] [PubMed]
34. Taweesap, P.; Potue, P.; Khamseekaew, J.; Iampanichakul, M.; Jan-O, B.; Pakdeechote, P.; Maneesai, P. Luteolin Relieves Metabolic Dysfunction-Associated Fatty Liver Disease Caused by a High-Fat Diet in Rats Through Modulating the AdipoR1/AMPK/PPARgamma Signaling Pathway. *Int. J. Mol. Sci.* **2025**, *26*, 3804. [CrossRef] [PubMed] [PubMed Central]
35. Tan, X.; Yang, Y.; Xu, J.; Zhang, P.; Deng, R.; Mao, Y.; He, J.; Chen, Y.; Zhang, Y.; Ding, J.; et al. Luteolin Exerts Neuroprotection via Modulation of the p62/Keap1/Nrf2 Pathway in Intracerebral Hemorrhage. *Front. Pharmacol.* **2019**, *10*, 1551. [CrossRef] [PubMed] [PubMed Central]

36. Gao, A.X.; Xia, T.C.-X.; Peng, Z.-T.; Wu, Q.-Y.; Zhu, Y.; Dong, T.T.-X.; Tsim, K.W.-K. The ethanolic extract of peanut shell attenuates the depressive-like behaviors of mice through modulation of inflammation and gut microbiota. *Food Res. Int.* **2023**, *168*, 112765. [CrossRef] [PubMed]
37. Shen, C.-L.; Wang, R.; Santos, J.M.; Elmassry, M.M.; Stephens, E.; Kim, N.; Neugebauer, V. Ginger alleviates mechanical hypersensitivity and anxio-depressive behavior in rats with diabetic neuropathy through beneficial actions on gut microbiome composition, mitochondria, and neuroimmune cells of colon and spinal cord. *Nutr. Res.* **2024**, *124*, 73–84. [CrossRef] [PubMed]
38. Santos, J.M.; Deshmukh, H.; Elmassry, M.M.; Yakhnitsa, V.; Ji, G.; Kiritoshi, T.; Presto, P.; Antenucci, N.; Liu, X.; Neugebauer, V.; et al. Beneficial Effects of Ginger Root Extract on Pain Behaviors, Inflammation, and Mitochondrial Function in the Colon and Different Brain Regions of Male and Female Neuropathic Rats: A Gut-Brain Axis Study. *Nutrients* **2024**, *16*, 3563. [CrossRef] [PubMed] [PubMed Central]
39. Rao, X.; Huang, X.; Zhou, Z.; Lin, X. An improvement of the 2ˆ(-delta delta CT) method for quantitative real-time polymerase chain reaction data analysis. *Biostat. Bioinforma Biomath.* **2013**, *3*, 71–85. [PubMed] [PubMed Central]
40. Yoon, H.; Jeong, D.K.; Lee, K.S.; Kim, H.S.; Moon, A.E.; Park, J. Relationship between metabolic syndrome and metabolic syndrome score and beta cell function by gender in Korean populations with obesity. *Endocr. J.* **2016**, *63*, 785–793. [CrossRef]
41. Wallace, T.M.; Levy, J.C.; Matthews, D.R. Use and abuse of HOMA modeling. *Diabetes Care* **2004**, *27*, 1487–1495. [CrossRef]
42. Thomas, D.D.; Corkey, B.E.; Istfan, N.W.; Apovian, C.M. Hyperinsulinemia: An Early Indicator of Metabolic Dysfunction. *J. Endocr. Soc.* **2019**, *3*, 1727–1747. [CrossRef] [PubMed] [PubMed Central]
43. Sun, X.-M.; Ye, H.-Q.; Liu, J.-B.; Wu, L.; Lin, D.-B.; Yu, Y.-L.; Gao, F. Assessment of anti-diabetic activity of peanut shell polyphenol extracts. *J. Zhejiang Univ. B* **2018**, *19*, 764–775. [CrossRef] [PubMed]
44. Shehnaz, S.I.; Roy, A.; Vijayaraghavan, R.; Sivanesan, S. Luteolin Mitigates Diabetic Dyslipidemia in Rats by Modulating ACAT-2, PPARalpha, SREBP-2 Proteins, and Oxidative Stress. *Appl. Biochem. Biotechnol.* **2023**, *195*, 4893–4914. [CrossRef] [PubMed]
45. Xiao, C.; Chen, M.Y.; Han, Y.P.; Liu, L.J.; Yan, J.L.; Qian, L.B. The protection of luteolin against diabetic cardiomyopathy in rats is related to reversing JNK-suppressed autophagy. *Food Funct.* **2023**, *14*, 2740–2749. [CrossRef] [PubMed]
46. Queiroz, M.; Leandro, A.; Azul, L.; Figueirinha, A.; Seiça, R.; Sena, C.M. Luteolin Improves Perivascular Adipose Tissue Profile and Vascular Dysfunction in Goto-Kakizaki Rats. *Int. J. Mol. Sci.* **2021**, *22*, 13671. [CrossRef]
47. Morales-Ferra, D.L.; Zavala-Sanchez, M.A.; Jimenez-Ferrer, E.; Gonzalez-Cortazar, M.; Zamilpa, A. Effect of Tecoma stans (L.) Juss. ex Kunth in a Murine Model of Metabolic Syndrome. *Plants* **2022**, *11*, 1794. [CrossRef] [PubMed] [PubMed Central]
48. Hudish, L.I.; Reusch, J.E.B.; Sussel, L. β Cell dysfunction during progression of metabolic syndrome to type 2 diabetes. *J. Clin. Investig.* **2019**, *129*, 4001–4008. [CrossRef]
49. Fändriks, L. Roles of the gut in the metabolic syndrome: An overview. *J. Intern. Med.* **2017**, *281*, 319–336. [CrossRef]
50. Sun, W.-L.; Yang, J.-W.; Dou, H.-Y.; Li, G.-Q.; Li, X.-Y.; Shen, L.; Ji, H.-F. Anti-inflammatory effect of luteolin is related to the changes in the gut microbiota and contributes to preventing the progression from simple steatosis to nonalcoholic steatohepatitis. *Bioorg. Chem.* **2021**, *112*, 104966. [CrossRef]
51. Sinha, A.K.; Laursen, M.F.; Brinck, J.E.; Rybtke, M.L.; Hjørne, A.P.; Procházková, N.; Pedersen, M.; Roager, H.M.; Licht, T.R. Dietary fibre directs microbial tryptophan metabolism via metabolic interactions in the gut microbiota. *Nat. Microbiol.* **2024**, *9*, 1964–1978. [CrossRef] [PubMed] [PubMed Central]
52. Wang, P.X.; Deng, X.R.; Zhang, C.H.; Yuan, H.J. Gut microbiota and metabolic syndrome. *Chin. Med. J.* **2020**, *133*, 808–816. [CrossRef]
53. Yang, S.; Duan, H.; Yan, Z.; Xue, C.; Niu, T.; Cheng, W.; Zhang, Y.; Zhao, X.; Hu, J.; Zhang, L. Luteolin Alleviates Ulcerative Colitis in Mice by Modulating Gut Microbiota and Plasma Metabolism. *Nutrients* **2025**, *17*, 203. [CrossRef] [PubMed] [PubMed Central]
54. Zou, H.; Ali, W.; Deng, K.; Chen, Y.; Sun, J.; Wang, T.; Ma, Y.; Liu, Z. The protective effect of luteolin on cadmium induced liver intestinal toxicity in chicken by Gut-liver axis regulation. *Poult. Sci.* **2024**, *103*, 104242. [CrossRef] [PubMed]
55. Liu, X.; Sun, R.; Li, Z.; Xiao, R.; Lv, P.; Sun, X.; Olson, M.A.; Gong, Y. Luteolin alleviates non-alcoholic fatty liver disease in rats via restoration of intestinal mucosal barrier damage and microbiota imbalance involving in gut-liver axis. *Arch. Biochem. Biophys.* **2021**, *711*, 109019. [CrossRef] [PubMed]
56. Nguyen, T.L.A.; Vieira-Silva, S.; Liston, A.; Raes, J. How informative is the mouse for human gut microbiota research? *Dis. Model. Mech.* **2015**, *8*, 1–16. [CrossRef]
57. Festi, D.; Schiumerini, R.; Eusebi, L.H.; Marasco, G.; Taddia, M.; Colecchia, A. Gut microbiota and metabolic syndrome. *World J. Gastroenterol.* **2014**, *20*, 16079–16094. [CrossRef] [PubMed]
58. Jin, S.; Chen, P.; Yang, J.; Li, D.; Liu, X.; Zhang, Y.; Xia, Q.; Li, Y.; Chen, G.; Li, Y.; et al. alleviates diet-induced metabolic dysfunction-associated steatotic liver disease progression by downregulating histone acetylation level via 3-HPAA. *Gut Microbes* **2024**, *16*, 2309683. [CrossRef]
59. Gao, S.Y.; Gao, Y.J.; Cai, L.F.; Qin, R. Luteolin attenuates Staphylococcus aureus-induced endometritis through inhibiting ferroptosis and inflammation via activating the Nrf2/GPX4 signaling pathway. *Microbiol. Spectr.* **2024**, *12*, e0327923. [CrossRef]

60. Park, J.W.; Voss, P.G.; Grabski, S.; Wang, J.L.; Patterson, R.J. Association of galectin-1 and galectin-3 with Gemin4 in complexes containing the SMN protein. *Nucleic Acids Res.* **2008**, *29*, 3595–3602. [CrossRef] [PubMed] [PubMed Central]
61. Rigoulet, M.; Yoboue, E.D.; Devin, A. Mitochondrial ROS generation and its regulation: Mechanisms involved in H(2)O(2) signaling. *Antioxid. Redox Signal.* **2011**, *14*, 459–468. [CrossRef] [PubMed]
62. Wong, H.S.; Dighe, P.A.; Mezera, V.; Monternier, P.A.; Brand, M.D. Production of superoxide and hydrogen peroxide from specific mitochondrial sites under different bioenergetic conditions. *J. Biol. Chem.* **2017**, *292*, 16804–16809. [CrossRef] [PubMed] [PubMed Central]
63. Chen, W.; Zhao, H.; Li, Y. Mitochondrial dynamics in health and disease: Mechanisms and potential targets. *Signal Transduct. Target. Ther.* **2023**, *8*, 333. [CrossRef] [PubMed] [PubMed Central]
64. Losón, O.C.; Song, Z.Y.; Chen, H.C.; Chan, D.C. Fis1, Mff, MiD49, and MiD51 mediate Drp1 recruitment in mitochondrial fission. *Mol. Biol. Cell.* **2013**, *24*, 659–667. [CrossRef]
65. Shpilka, T.; Haynes, C.M. The mitochondrial UPR: Mechanisms, physiological functions and implications in ageing. *Nat. Rev. Mol. Cell Biol.* **2018**, *19*, 109–120. [CrossRef] [PubMed]
66. Nguyen, T.N.; Padman, B.S.; Lazarou, M. Deciphering the Molecular Signals of PINK1/Parkin Mitophagy. *Trends Cell Biol.* **2016**, *26*, 733–744. [CrossRef] [PubMed]
67. Koyano, F.; Yamano, K.; Kosako, H.; Kimura, Y.; Kimura, M.; Fujiki, Y.; Tanaka, K.; Matsuda, N. Parkin-mediated ubiquitylation redistributes MITOL/March5 from mitochondria to peroxisomes. *Embo Rep.* **2019**, *20*, e47728. [CrossRef]
68. Scarpulla, R.C.; Vega, R.B.; Kelly, D.P. Transcriptional integration of mitochondrial biogenesis. *Trends Endocrinol. Metab.* **2012**, *23*, 459–466. [CrossRef] [PubMed] [PubMed Central]
69. Puigserver, P.; Wu, Z.; Park, C.W.; Graves, R.; Wright, M.; Spiegelman, B.M. A cold-inducible coactivator of nuclear receptors linked to adaptive thermogenesis. *Cell* **1998**, *92*, 829–839. [CrossRef] [PubMed]
70. Vongthip, W.; Nilkhet, S.; Boonruang, K.; Sukprasansap, M.; Tencomnao, T.; Baek, S.J. Neuroprotective mechanisms of luteolin in glutamate-induced oxidative stress and autophagy-mediated neuronal cell death. *Sci. Rep.* **2024**, *14*, 7707. [CrossRef] [PubMed] [PubMed Central]
71. Prasun, P. Mitochondrial dysfunction in metabolic syndrome. *Biochim. Biophys. Acta Mol. Basis Dis.* **2020**, *1866*, 165838. [CrossRef] [PubMed]
72. Li, L.; Luo, W.; Qian, Y.; Zhu, W.; Qian, J.; Li, J.; Jin, Y.; Xu, X.; Liang, G. Luteolin protects against diabetic cardiomyopathy by inhibiting NF-κB-mediated inflammation and activating the Nrf2-mediated antioxidant responses. *Phytomedicine* **2019**, *59*, 152774. [CrossRef] [PubMed]
73. Dabeek, W.M.; Marra, M.V. Dietary Quercetin and Kaempferol: Bioavailability and Potential Cardiovascular-Related Bioactivity in Humans. *Nutrients* **2019**, *11*, 2288. [CrossRef] [PubMed] [PubMed Central]
74. Ezike, T.C.; Okpala, U.S.; Onoja, U.L.; Nwike, C.P.; Ezeako, E.C.; Okpara, O.J.; Okoroafor, C.C.; Eze, S.C.; Kalu, O.L.; Odoh, E.C.; et al. Advances in drug delivery systems, challenges and future directions. *Heliyon* **2023**, *9*, e17488. [CrossRef] [PubMed] [PubMed Central]

Disclaimer/Publisher's Note: The statements, opinions and data contained in all publications are solely those of the individual author(s) and contributor(s) and not of MDPI and/or the editor(s). MDPI and/or the editor(s) disclaim responsibility for any injury to people or property resulting from any ideas, methods, instructions or products referred to in the content.

nutrients

MDPI

Article

Efficacy and Satisfaction of a Chemically Characterized *Malva sylvestris* L. Extract-Based Food Supplement for Functional Constipation in Healthy Consumers: Preliminary Results of a Questionnaire-Based Survey

Lorenza Francesca De Lellis [1,†], Hammad Ullah [1,†], Maria Vittoria Morone [2,†], Daniele Giuseppe Buccato [1], Alessandra Baldi [1], Alessandro Di Minno [1,3], Danaé S. Larsen [4,*], Roberto Sacchi [5] and Maria Daglia [1,6,*]

[1] Department of Pharmacy, University of Napoli Federico II, Via D. Montesano 49, 80131 Naples, Italy; lo.delellis2@gmail.com (L.F.D.L.); hammadrph@gmail.com (H.U.); d.buccato@gmail.com (D.G.B.); alessandra.baldi.alimenti@gmail.com (A.B.); alessandro.diminno@unina.it (A.D.M.)
[2] Department of Experimental Medicine, Section of Microbiology and Clinical Microbiology, University of Campania "L. Vanvitelli", 80138 Naples, Italy; mariavittoria.morone@unicampania.it
[3] CEINGE-Biotecnologie Avanzate, Via Gaetano Salvatore 486, 80145 Naples, Italy
[4] School of Chemical Sciences, The University of Auckland, Auckland 1010, New Zealand
[5] Applied Statistic Unit, Department of Earth and Environmental Sciences, University of Pavia, Viale Taramelli 24, 27100 Pavia, Italy; roberto.sacchi@unipv.it
[6] International Research Center for Food Nutrition and Safety, Jiangsu University, Zhenjiang 212013, China
* Correspondence: d.larsen@auckland.ac.nz (D.S.L.); maria.daglia@unina.it (M.D.)
† These authors contributed equally to this work.

Abstract

Background/Objectives: *Malva sylvestris* L. is rich in mucilage and is traditionally used for the management of numerous ailments including gastrointestinal disorders. Functional constipation (FC) is a gastrointestinal condition characterized by defecation anomalies such as infrequent stools, difficulty in stool passage, or both in the absence of pathological abnormalities. FC can be reduced through lifestyle factors and dietary intervention. This consumer-based survey aimed to assess the efficacy of a *M. sylvestris* extract-based food supplement on the improvement of FC. Methods: Healthy participants (n = 56), enrolled in a consumer-based survey, took a food supplement containing a chemically characterized *M. sylvestris* extract at a dose of 20 mL/day (containing 750 mg of *M. sylvestris* extract rich in food fiber and polyphenols) for 20 days on the advice of their pharmacist. The study evaluated bowel movement frequency (intestinal diary), stool consistency (Bristol Stool Form Scale, BSFS), and abdominal pain (Visual Analogue Scale, VAS), at baseline (T0), after 10 days (T1), and after 20 days (T2). Results: A significant increase in bowel movement frequency and stool consistency ($p < 0.001$) with a significant decrease in abdominal pain ($p < 0.001$) was observed. Additionally, this food supplement was well-tolerated as no adverse effects were reported by the enrolled subjects. Conclusion: *M. sylvestris*-based food supplement showed promising effectiveness and satisfaction in improving FC in healthy subjects, however, randomized clinical studies are needed to confirm these preliminary results.

Keywords: *Malva sylvestris* L.; food supplement; functional constipation; consumer questionnaire-based survey

1. Introduction

Constipation refers to a group of gastrointestinal symptoms that include abdominal pain, firm stools, difficult or infrequent bowel movements/deviation from normal frequency, and/or the feeling of incomplete evacuation of stool. Functional constipation (FC) lacks anatomical abnormalities or systemic etiology. It is influenced by environmental factors, stress, and diet [1]. Constipation is primarily self-diagnosed via the self-reporting of symptoms or a symptom-based questionnaire in cross-sectional surveys [2]. Suares and Ford [3] conducted a comprehensive meta-analysis to evaluate the risk factors and prevalence of chronic idiopathic constipation in the community. The global prevalence of chronic idiopathic constipation is 14% under the Rome IV criteria but drops to 6.8% with the Rome III criteria. FC is inversely related to the quality of life of the affected subjects, and is also associated with increased frailty, particularly in elder subjects [4].

Increased dietary fiber and lifestyle changes are first-line treatments, followed by laxatives if necessary [5]. Dietary fiber is not digested in the small intestine; some are fermented by bacteria or can induce bulk formation in the colon, drawing water into the colon [6]. However, the results of systematic reviews indicate that soluble fiber rather than insoluble fiber alleviates symptoms related to constipation [7]. The soluble fiber psyllium has been demonstrated to lessen defecation discomfort and improve stool weight, frequency, and consistency [8]. Research has shown that a low dietary fiber intake (7 g/day) could be associated with a decrease in the frequency of stools, and it is generally advised to gradually increase fiber consumption, up to 30 g per day. In addition, despite the availability of over-the-counter laxatives and dietary modifications, many individuals with FC experience incomplete relief, adverse effects, or poor adherence. For instance, increased fiber consumption could also lead to adverse effects like gas, bloating, and distension [2]. This underscores the need for alternative therapies that are both effective and well-tolerated. Plant-based supplements offer a promising avenue for addressing these challenges by combining natural bioactive compounds with dietary fiber [9].

Malva sylvestris L. (Malvaceae) is notable for its many applications and has been consumed since 3000 BC [10]. Also known as common mallow, it is indigenous to Europe, North Africa, and Asia, and has a long history of use in the Mediterranean region as food, and because of its potential therapeutic uses [11]. The leaves, in particular, have antioxidant, anti-inflammatory, and skin tissue integrity properties [11]. Furthermore, recent studies have established anti-ulcerogenic effects, showing the aqueous extract of *Malva sylvestris* L. to be more efficacious than cimetidine, a peptic ulcer and heartburn drug [12]. In addition, it has hepatoprotective properties and a mild laxative effect, suggesting its use for gastrointestinal ailments [11]. *M. sylvestris* is rich in mucilage [13], with the leaves (6–7.2%), flowers (3.8–7.3%), and roots (7.5%) often containing the highest percentages of crude mucilage [14–16]. The main components of the mucilage include glucuronic acid, galacturonic acid, rhamnose, galactose, fructose, glucose, sucrose, and trehalose; however, additional components have been identified, including uronic acid, arabinose, mannose, xylose, fucose, raffinose, and 2″-*O*-α-(4-*O*-methyl-α-D-glucuronosyl)-xylotriose [14,15,17,18]. These compounds are believed to improve stool consistency, enhance water retention in the gut, and modulate the gut microbiota, making it a potential therapeutic agent for managing gastrointestinal disorders.

Thus, *M. sylvestris* has been identified as a potential therapy to improve FC via a nutritional intervention of increased dietary fiber intake and accelerated stool intestinal transit. The current study aimed to collect data via a survey of food supplement consumers to assess whether a *M. sylvestris* extract-based food supplement can help with FC. The questionnaire also assessed the frequency of gastrointestinal movements, stool consistency, and a possible improvement to the quality of life through a reduction in abdominal pain, as

well as consumers' acceptance of the food supplement. Moreover, the chemical composition of *M. sylvestris* extract was determined to understand the contribution of dietary fiber and other bioactive compounds present in *M. sylvestris* extract.

2. Materials and Methods

2.1. Food Supplement

The commercial food supplement Laxamov® (notification number: 171854) (Labomar S.p.A, Istriana, TV, Italy) was utilized in this study. The Italian Ministry of Health was notified of its distribution based on *M. sylvestris* extract (750 mg per 20 mL). The supplement also contains sorbitol (Labomar S.p.A, Istriana, TV, Italy) (10 g per 20 mL) as a food additive (E 420) at a dose lower than that considered responsible for laxative effects (50 g/day) [19,20]. According to the manufacturer's specifications, this food supplement complies with European specifications for contaminants and microbiological limits.

2.2. Total Dietary Fiber Determination

The total dietary fiber (TDF) content of *M. sylvestris* extract (mixed with maltodextrin (1:4) as a carrier) was determined in triplicate in accordance with the manufacturer's protocol using the TDF Assay Kit (Neogen, Lansing, MI, USA) [21], which represents a simplified version of the official AOAC 985.29 method. The total soluble and insoluble fiber content of *M. sylvestris* extract was determined using a gravimetric method. This involved eliminating starch and proteins through treatments with heat stable enzymes i.e., α-amylase (~55 U/mg), amyloglucosidase (~3260 U/mL), and protease (~6 U/mg of protein). Following these treatments, a precipitate was observed, indicating the presence of insoluble fiber. High-molecular-weight soluble fiber was precipitated using 78% ethanol (Merck Life Science S.r.l., Milano, Italy) and measured using the gravimetric method.

The carrier maltodextrin was also analyzed for dietary fiber content to ensure correction in the calculation of *M. sylvestris* extract fiber content. No dietary fiber was detected in maltodextrin, confirming that the soluble and insoluble fiber was determined to have originated from *M. sylvestris*. Five aliquots of *M. sylvestris* extract (1.000 ± 0.005 g) were incubated at 100 °C in 50 µL heat-stable α-amylase solution to allow starch gelatinization, hydrolysis, and depolymerization. The samples were then incubated at 60 °C with 100 µL protease solution (to solubilize and depolymerize the proteins) and 200 µL amyloglucosidase solution (to hydrolyze the starch fragments into glucose). After incubation, the samples were filtered to separate the insoluble fiber. The supernatant was treated with approximately four volumes of ethanol to precipitate soluble fibers and remove the depolymerized proteins and glucose (from starch). The samples were freeze-dried, and the residue analyzed for proteins using the Kjeldahl method [22], while ash content was determined by incineration at 525 °C. The TDF was calculated using the following formula:

$$\text{TDF} = (\text{Insolublefiber} + \text{Solublefiber}) - (\text{Protein} + \text{Ash})$$

2.3. UHPLC-HRMS Analysis of M. sylvestris Extract

2.3.1. Sample Preparation

The dry extract of *M. sylvestris* with maltodextrin used as a carrier was loaded on to a C18 solid-phase extraction (SPE) column previously conditioned with 5 mL methanol (MeOH; Merck Life Science S.r.l., MI, Italy) and 5 mL H_2O. After loading, the column was washed with 10 mL H_2O. The sample was eluted with a 2.5 mL mixture of MeOH:H_2O (95:5, *v*/*v*) and 1 mL of this solution was transferred to an autosampler vial for ultra-high-performance liquid chromatography–high-resolution mass spectrometry (UHPLC-HRMS) analysis.

2.3.2. UHPLC-HRMS Analysis

UHPLC-HRMS/MS analysis was performed on a Thermo Scientific™ Vanquish™ UHPLC system, equipped with a VF-P10-A binary solvent delivery system, a VC-D11-A photodiode array detector, a VH-C10-A column compartment, and VF-A10-A autosampler. The UHPLC system was coupled online to a Orbitrap Exploris 120 mass spectrometer (Thermo Fisher Scientific, Bremen, Germany) equipped with a heated electrospray ionization probe (HESI II) operating in negative and positive mode. The sample was weighed and solubilized in methanol at a concentration of 100 mg/mL, the sample was vortexed at RT for 30 min and centrifuged at 4 °C for 10 min, and the supernatant was collected and directly injected in UHPLC-HRMS.

Chromatographic separation was performed on a Kinetex® 2.6 µm EVO C18 100 Å, LC Column 150 × 2.1 mm (Phenomenex, Bologna, Italy). The column temperature and the flow rate were set at 40 °C and 0.4 mL/min, respectively. The mobile phases were as follows: H_2O (A) and ACN (B) both acidified with 0.1% HCOOH (*v*/*v*) with the following gradient: 0.01–2.00 min, isocratic to 2% B; 2.01–22.00 min, 2–95% B; 22.01–24.00 min, isocratic to 95% B; 24.01–25.00 min, 95–2% B; then, column re-equilibration was performed for five minutes.

MS was calibrated by Thermo Pierce™ FlexMix™ (Thermo Fischer Scientific, Waltham, MA, USA) calibration solutions in both polarities. Full MS (100–1500 *m*/*z*) and data-dependent MS/MS were performed at a resolution of 60,000 and 15,000 FWHM, respectively. A Normalized Collision Energy (NCE) value of 30 was used. Source parameters were as follows: sheath gas pressure, 40 arbitrary units; auxiliary gas flow, 15 arbitrary units; spray voltage, +3.0 kV, −2.0 kV; capillary temperature, 320 °C; and auxiliary gas heater temperature, 300 °C. The identification of investigated analytes was carried out by comparing their retention times and MS/MS data with those present in the literature. Data analysis and processing were performed using FreeStyle™ 1.8 SP2 and the commercial software Compound Discoverer v. 3.3.1.111 SP1 (Thermo Fisher Scientific, Bremen, Germany).

2.4. Evaluation of Efficacy and Tolerability

2.4.1. Survey Design

A questionnaire-based survey aimed at food supplement consumers was undertaken to evaluate the efficacy and satisfaction of a food supplement based on *M. sylvestris* extract in healthy subjects. The survey was in the form of a questionnaire encompassing an intestinal diary and validated questionnaires including the Bristol Stool Form Scale (BSFS) and a Visual Analogue Scale (VAS). The assessment of the tolerability of the food supplement was performed through evaluation of adverse reactions (ARs) using a form based on that used by the Italian Phytovigilance System (IPS) to report possible ARs after the ingestion of food supplements.

Enrollment was based on subjects who communicated symptoms related to FC to a pharmacist. These subjects were directed to a separate room, where they received an exhaustive explanation of the survey by a pharmacist. The participants underwent three interviews: at recruitment (i.e., at the baseline, t0), after 10 days (t1), and after 20 days (t2). At recruitment, the inclusion of the subjects in the survey was also evaluated by a physician, who validated their eligibility and health prior to participation. After they gave written consent, in addition to the self-completion of questionnaires administered by the physician, each subject was given the form to report possible ARs after the ingestion of food supplements. These forms were collected at the end of the survey (t2). All subjects were suggested to consume the *M. sylvestris* extract-based food supplement (20 mL/day), for 20 days. Any data gathered within this survey were treated in strict accordance with the European Data Protection Regulation (GDPR) and used for research purposes only.

Overall, the survey involved a cohort of 56 subjects with self-reporting FC, who had asked their pharmacist for a food supplement to treat FC and where the commercial *M. sylvestris*-based food supplement was suggested for them. The questionnaire-based survey of subjects was conducted between October 2023 to March 2024. Rome IV Criteria were used to classify subjects with FC and to enroll the subjects in this survey. Individuals who have had symptoms of chronic constipation for at least 3 months (with onset at least 6 months before) and no organic gastrointestinal pathology were classified according to the Rome IV Criteria as having irritable bowel syndrome with constipation (IBS-C), FC, opioid-induced constipation, and functional defecation disorders. Subjects suffering from IBS-C were excluded from the survey, as the focus was on individuals with simple FC, a condition considered non-pathological and for which the use of food supplements represents a more appropriate remedy. The inclusion criteria were subjects of either sex, aged 18 to 75 years, subjects able to understand and sign the informed consent, and subjects with FC and a number of bowel movements less than 2 per week. Exclusion criteria were subjects with IBS-C (according to the Rome IV Criteria), pregnant or breastfeeding females, subjects who regularly take laxatives, subjects suffering from organic intestinal pathologies, subjects who had undergone surgery on the gastrointestinal tract, subjects with gastroesophageal reflux, subjects with Parkinson's and Alzheimer's disorders, and individuals who use opioid medications or other medications that have a significant impact on intestinal function (i.e., antidepressants or antacids containing aluminum). Data collected by the physician included the demographics and baseline clinical data of the enrolled subjects.

2.4.2. Primary and Secondary Objectives

The primary objective of this investigation was to evaluate the impact of supplementation with *M. sylvestris* in subjects with FC for the frequency of gastrointestinal movements (bowel movements/week). The number of bowel movements per week was determined via a self-assessment questionnaire, which was inserted into the "intestinal diary" that the subject filled out daily. For the objective to be satisfied, the increase in the number of bowel movements must be at least one per week.

Secondary objectives of this investigation included consistency of stool (which, together with the frequency of intestinal evacuation, has been indicated in the European Medicines Agency (EMA) and European Food Safety Authority (EFSA) guidelines as an indicator of FC) and frequency of characteristic symptoms of the constipated subject, i.e., abdominal pain. The BSFS was used to assess the stool consistency on a spectrum of seven types. Stool types 1 and 2 denote hard or lumpy stools, while stool types 6 and 7 are indicative of loose or watery stools, where subjects with stool consistency type 1 and 2 were characterized as suffering from constipation. The abdominal pain was assessed via a VAS.

Current food regulations permit the use of all the components in the food supplement under study. However, the food supplement consumers were closely observed by the physician and pharmacist and any suspected adverse reactions were reported via the VigiErbe online phytovigilance system, according to the provisions of the Italian Istituto Superiore di Sanità [23].

2.5. Statistical Analysis

The sample size calculation was made using a 1-β power value of 0.95 and a significance level $\alpha = 0.05$. The sample size was determined to be 56 participants.

The objective of the statistical analysis was to compare the score values for the weekly evacuations, BSFS and VAS scales, and the characteristics of the subjects recruited (sex and age). The most suitable statistical analysis for this type of study is a linear mixed model (LMM) with random intercept, in which the score values of the scales is the dependent

variable, while the measurements (T0, T1, and T2), sex (two-levels factor), and age (standardized to mean = 0 and SD = 1) of the recruited subjects constitute the independent variables. The interaction sex × measurement was inserted to account for differential responses to measurements between males and females. The identity of the subjects was entered into the model as a random effect to control any differences due to the specific conditions of the persons recruited in the survey. All analyses were carried out in R 4.2.1 [24] using the package lme4 [25].

3. Results

3.1. Chemical Composition of M. sylvestris Extract

3.1.1. TDF Content

The analysis confirmed that *M. sylvestris* extract contained 2.7 ± 1.1 g/100 g of insoluble fiber and 5.9 ± 0.2 g/100 g of high-molecular-weight soluble fiber, with no detectable dietary fiber in the maltodextrin carrier. The content of dietary fiber in maltodextrin was determined to correct the content of dietary fiber of *M. sylvestris* extract. Dietary fiber was not found in maltodextrin, suggesting that the determined soluble and insoluble fiber was from *M. sylvestris*.

3.1.2. RP-UHPLC-MS Analysis

M. sylvestris extract was chemically characterized by using a chromatographic method coupled with mass spectrometry [26]. Using negative ionization mode, 32 compounds were identified (Figure 1A and Table 1), including phenolic acids (malic acid, gallic acid, 4-methoxybenzoic acid, caffeic acid, rosmarinic acid, *p*-coumaric acid, 4-hydroxybenzoic acid, and protocatechuic acid), flavonoids (vicenin 2, myricetin-3-hexoside-glucuronide, quercitrin, apigenin-4′-*O*-β-glucopyranoside, gossypetin, myricetin-3-*O*-glucuronide, quercetin-3-*O*-glucuronide, rubone, kaempferol-3-*O*-glucuronide, chysin, fisetin, quercetin, luteolin, kaempferide-3-glucuronide, naringenin, hesperetin, apigenin/genistein, kaempferol, and rhamnetin), and lipids (azelaic acid, 9,12,13-trihydroxy-octadecadienoic acid, 9,12,13-trihydroxy-octadecenoic acid, 1-*O*-palmitoylglyceride, and 9-hydroxy-10(E),12(Z),15(Z)-octadecatrienoic acid). Similarly, under positive ionization mode, we identified 16 compounds (Figure 1B and Table 2), including flavonoids (vicenin 2, quercetin-3-*O*-β-glucuronide, and kaempferol-3-*O*-glucuronide), acetamide (*N*-(9-oxodecyl) acetamide), carotenoids (loliolide), lipids (dehydrophytosphingosine, phytosphingosine, stearidonic acid, lysophosphatidylcholine (LPC; 16:0), 1-*O*-linolenoyl glyceride, oleamide, and erucamide), and chlorophyll derivatives (pheophorbide A).

Table 1. Identified compounds in *M. sylvestris* extract in negative ionization mode.

Peak	Rt	Compound	[M-H]$^-$	MS/MS	Molecular Formula	Error (ppm)
1	0.78	Malic acid	133.05	115.0035; 71.0137	$C_4H_6O_5$	4.3
2	4.35	Gallic acid	169.0142	125.0244; 79	$C7H_6O_5$	5.8
3	4.81	Vanillin (4-methoxybenzoic acid)	151.0401	136.0163; 107.0501	$C_8H_8O_3$	6.06
4	5.33	Caffeic acid	179.0346	135.0449; 134.0375	$C_9H_8O_4$	4.2
5	5.53	Rosmarinic acid	359.0772	135.0452	$C_{18}H_{16}O_8$	0.67
6	6.2	Vicenin 2	593.1505	353.0660; 473.1084; 383.0766; 503.1191	$C_{27}H_{30}O_{15}$	0.7

Table 1. *Cont.*

Peak	Rt	Compound	[M-H]$^-$	MS/MS	Molecular Formula	Error (ppm)
7	6.26	*p*-Coumaric acid	163.0401	119.0502; 91.0555	$C_9H_8O_3$	0.8
8	6.36	Myricetin-3-hexoside-glucuronide	655.1152	479.0824; 316.0220	$C_{27}H_{28}O_{19}$	−1.02
9	6.7	Quercitrin	447.0933	327.0507; 357.0609	$C_{21}H_{20}O_{11}$	−0.67
10	7.07	Apigenin-4′-*O*-β-glucopyranoside	431.0984	269.0472; 311.0557; 341.0664	$C_{21}H_{20}O_{10}$	−0.81
11	7.11	4-hydroxybenzoic acid	137.0242	93.0344	$C_7H_6O_3$	2.3
12	7.53	Azelaic acid	187.0972	125.0970; 169.0869; 97.0657	$C_9H_{16}O_4$	0.8
13	7.85	Gossypetin	317.0303	299.0194; 271.0243; 194.9932	$C_{15}H_{10}O_8$	1.87
14	8.11	Myricetin-3-*O*-glucuronide	493.0616	317.0298	$C_{21}H_{18}O_{14}$	0.74
15	8.17	Protocatechuic acid	153.0193	109.0294	$C_7H_6O_4$	5.88
16	8.38	Quercetin-3-*O*-glucuronide	477.0675	301.035	$C_{21}H_{18}O_{13}$	0.98
17	8.47	Rubone	373.1293	343.1179; 340.0942; 311.0916; 355.1180	$C_{20}H_{22}O_7$	2.93
18	8.59	Kaempferol-3-O-glucuronide (orluteolin)	461.0725	285.0401	$C_{21}H_{18}O_{12}$	2.09
19	8.65	Chysin	253.0502	143.1028; 119.0815	$C_{15}H_{10}O_4$	1.69
20	8.65	Fisetin	285.0399	135.3614	$C_{15}H_{10}O_6$	1.94
21	8.89	Quercetin	301.0354	178.9985; 151.0033	$C_{15}H_{10}O_7$	2.31
22	9.19	Luteolin	285.0402	151	$C_{15}H_{10}O_6$	2.26
23	9.57	Kaempferide-3-glucuronide	475.0898	299.0558; 284.0320	$C_{22}H_{20}O_{12}$	5.77
24	9.59	Naringenin	270.95	151.0034; 119.0503; 107.0135	$C_{15}H_{12}O_5$	2.66
25	9.73	Hesperetin	301.0718	151.0036; 178.9983	$C_{16}H_{14}O_6$	2.81
26	9.99	Apigenin/Genistein	269.0455	149.0242; 117.0363	$C_{15}H_{10}O_5$	2.66
27	9.99	9,12,13-trihydroxy-octadecadienoic acid	327.2172	211.1336; 229.1442; 171.1025	$C_{18}H_{32}O_5$	1.91

Table 1. *Cont.*

Peak	Rt	Compound	[M-H]$^-$	MS/MS	Molecular Formula	Error (ppm)
28	10.07	Kaempferol	285.0401	257.0454; 217.2520; 151.0031	$C_{15}H_{10}O_6$	2.58
29	10.28	Rhamnetin	315.051	164.9829; 300.0273	$C_{16}H_{12}O_7$	2.41
30	10.52	9,12,13-trihydroxy-octadecenoic acid	329.233	229.1444; 211.1339; 171.1025	$C_{18}H_{34}O_5$	2.19
31	10.94	1-*O*-palmitoylglyceride	329.2697	229.1443; 211.1337; 171.1020	$C_{19}H_{38}O_4$	1.91
32	13.97	9-hydroxy-10(E),12(Z),15(Z)-octadecatrienoic acid	293.2118	275.2013; 183.1389; 171.1025	$C_{18}H_{30}O_3$	0.98

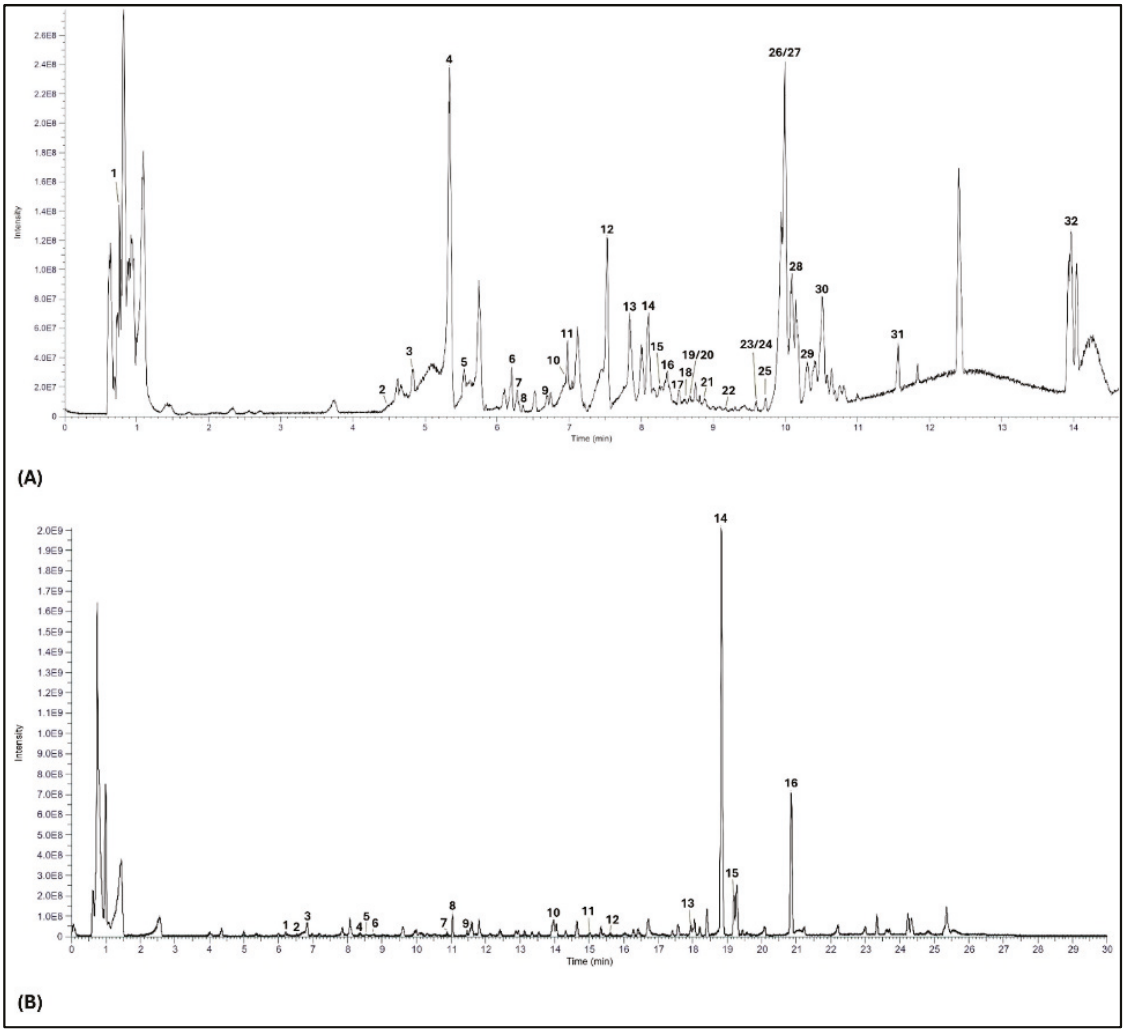

Figure 1. UHPLC chromatograms of *M. sylvestris* extract with UV detection, compounds identified both in negative ionization (**A**) and positive ionization (**B**) mode.

Table 2. Identified compounds in *M. sylvestris* extract in positive ionization mode.

Peak	Rt	Compound	$[M-H]^+$	MS/MS	Molecular Formula	Error (ppm)
1	6.2	Vicenin 2	595.1641	379.0807; 409.0908; 325.0702; 457.1110	$C_{27}H_{30}O_{15}$	−0.57
2	6.53	*N*-(9-oxodecyl) acetamide	214.1797	214.1798; 161.1321; 95.0853; 137.1322	$C_{12}H_{23}O_2N$	−1.47
3	6.83	Loliolide	197.1167	197.1169; 179.1063; 135.1165; 107.0853	$C_{11}H_{16}O_3$	−0.34
4	8.35	Quercetin-3-*O*-β-glucuronide (Miquelianin)	479.0808	303.0493; 141.8239; 53.2160	$C_{21}H_{18}O_{13}$	−0.73
5	8.53	Quercetin-3-*O*-β-glucuronide (Miquelianin)	479.0806	303.0493; 141.8239; 53.2160	$C_{21}H_{18}O_{13}$	−0.73
6	8.6	Kaempferol-3-*O*-glucuronide (orluteolin)	463.0858	287.0544; 152.0563; 72.5275	$C_{21}H_{18}O_{12}$	−0.8
7	10.89	Dehydrophytosphingosine	316.2839	60.0443; 280.2631; 316.2847	$C_{18}H_{37}O_3N$	−0.68
8	11.04	Dehydrophytosphingosine	316.2838	60.0443; 280.2631; 316.2847	$C_{18}H_{37}O_3N$	−0.81
9	11.46	Phytosphingosine	318.2994	60.0442; 282.2787; 318.2996	$C_{18}H_{39}O_3N$	−0.5
10	13.96	Stearidonic acid	277.2155	135.1166; 121.1010; 277.2161	$C_{19}H_{28}O_2$	−0.66
11	15.01	LPC (16:0)	496.3388	184.0730; 104.1068; 478.3288	$C_{24}H_{50}O_7NP$	−2.79
12	15.6	1-*O*-linolenoyl glyceride	353.2677	335.2576; 317.2469; 289.2525	$C_{21}H_{36}O_4$	0.35
13	17.94	Oleamide	282.2784	247.2416; 265.2520	$C_{18}H_{35}NO$	−0.73
14	18.83	Pheophorbide a	593.2738	533.2534	$C_{35}H_{36}O_5N_4$	−2.31
15	19.19	Pheophorbide a (isomer)	593.274	533.2535	$C_{35}H_{36}O_5N_4$	−2.31
16	20.85	Erucamide (13-cis-docosenamide)	338.3408	303.3041; 321.3145	$C_{22}H_{43}ON$	−2

3.2. Survey Among Consumers on the Evaluation of Efficacy and Satisfaction of the Food Supplement

The survey flow chart [27] is shown in Figure 2. The baseline characteristics of the subjects of each group are summarized in Table 3. In total, 56 subjects (12 males and 44 females) were enrolled in the survey, with the mean age for male subjects being

58.1 ± 18.3 years, and 52.2 ± 17.5 years for female subjects. As advised by the general physician, all the subjects were suggested to take the *M. sylvestris* supplement daily. The measurements were carried out in three-time intervals (T0, T1, and T2), and included the bowel movements per week, VAS, and Bristol index. Table 4 shows the descriptive data (mean ± SD, minimum and maximum values) for male and female subjects at the three-time measurements.

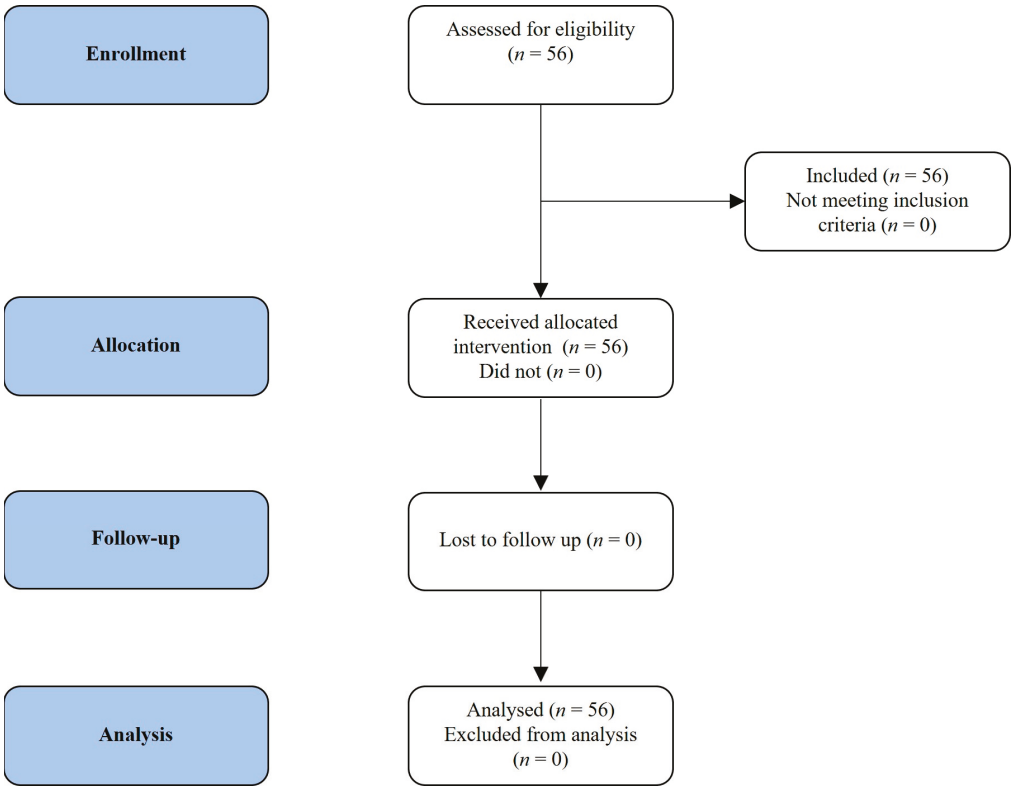

Figure 2. Survey flow chart diagram.

Table 3. Demographic characteristics of the population involved in the survey.

Characteristics	Values
Gender	
• Males	12
• Females	44
Age	
• Males	58.1 ± 18.3
• Females	52.2 ± 17.5
Ethnicity	Caucasian

Table 4. Descriptive statistics (mean, standard deviation, minimum, and maximum) for the three variables of response calculated for men and women across the three measurements.

Variable	Gender	T0	T1	T2
Bowel movements per week	Male (n = 12)	3.2 ± 1.9 (1–4)	5.5 ± 2.6 (1–10)	6 ± 2.5 (1–10)
	Female (n = 44)	2.6 ± 0.8 (1–4)	4.5 ± 1.7 (1–7)	5.2 ± 2.1 (1–11)
VAS	Male (n = 12)	4.2 ± 2.6 (0–8)	2.3 ± 2.2 (0–8)	2.3 ± 2.2 (0–8)
	Female (n = 44)	4.2 ± 2.7 (0–8)	2.8 ± 2.1 (0–8)	2.5 ± 1.9 (0–8)
Bristol	Male (n = 12)	2.2 ± 0.6 (1–3)	3.2 ± 0.8 (2–4)	3.2 ± 0.8 (2–4)
	Female (n = 44)	2.0 ± 1.1 (1–3)	3.2 ± 1.2 (1–7)	3.4 ± 1.2 (1–7)

3.2.1. Primary and Secondary Objectives

As reported in Table 5 and Figure 3, the LMM model for the number of bowel movements per week observed a significant effect for measurement ($p < 0.001$), but not by the age and sex of the subjects. In particular, the value of bowel movements per week increased significantly, both between T0 and T1 ($\beta = 1.9 \pm 0.2$, $t_{110} = 9.810$, $p < 0.001$) and between T1 and T2 ($\beta = 0.7 \pm 0.2$, t110 = 3.404, $p < 0.001$). Consequently, the difference between T0 and T2 is also statistically significant ($\beta = 2.6 \pm 0.2$, $t_{110} = 13.214$, $p < 0.001$).

Table 5. Results of LMM models.

Model		Gdl		F	*p*
EV/WK	Measurement	2	110	94.149	<0.001
	Sex	1	53	1.873	0.18
	Age	1	53	0.459	0.50
VAS	Measurement	2	110	43.743	<0.001
	Sex	1	53	0.001	0.98
	Age	1	53	4.402	0.04
Bristol	Measurement	2	110	68.958	<0.001
	Sex	1	53	0.026	0.87
	Age	1	53	2.311	0.13

The LMM model for the VAS (Table 5 and Figure 3) identified significant effects for the measurement ($p < 0.001$) and for age ($p = 0.04$), but not for the sex of the subjects. The VAS score decreased significantly between T0 and T1 ($\beta = 1.5 \pm 0.2$, $t_{110} = 7.453$, $p < 0.001$), but remained unchanged between T1 and T2 ($\beta = 0.2 \pm 0.2$, $t_{110} = 1.1167$, $p = 0.24$). The difference between T0 and T2 remained significant ($\beta = 1.7 \pm 0.2$, $t_{110} = 8.621$, $p < 0.001$). Regardless of the measurement, the VAS value decreased as the subject's age increased ($\beta = -0.035 \pm 0.017$, $t_{53} = 2.098$, $p = 0.041$).

The LMM model for the value of the Bristol scale (Table 5 and Figure 3) also identified a statistically significant effect for the measurement ($p < 0.001$), but not by the sex and age of the subjects. In particular, the value of the score increased significantly from T0 to T1 ($\beta = 1.2 \pm 0.1$, $t_{110} = 9.453$, $p < 0.001$) and remained unchanged between T1 and T2 ($\beta = 0.2 \pm 0.1$, $t_{110} = 1.309$, $p = 0.19$). Despite this, the difference between T0 and T2 was statistically significant ($\beta = 1.3 \pm 0.1$, $t_{110} = 10.761$, $p < 0.001$).

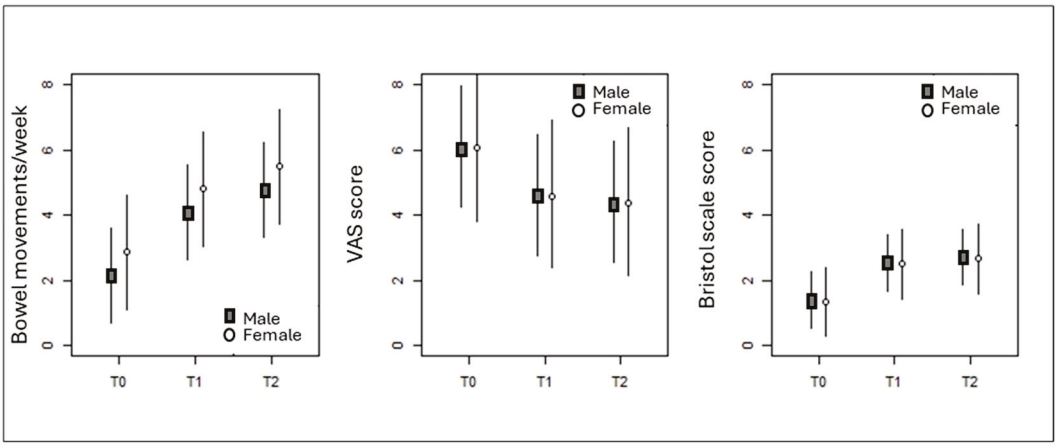

Figure 3. Trend of the three response variables in male and female subjects as a function of the three measurements as predicted (conditional effects) by the LMM models. The bars represent the 95% confidence intervals as predicted by a bootstrap (n = 10,000) on the variance–covariance matrix of the model coefficients for middle-aged individuals.

3.2.2. Tolerance and Satisfaction Assessment

To evaluate the tolerability of the *M. sylvestris* supplement, any adverse events were monitored throughout the period via spontaneous reporting by the participants to the general physician and pharmacist who performed the recruitment. During the 20-day period of taking the food supplement, no subject reported related adverse events, with the food supplement well-tolerated by the enrolled subjects.

4. Discussion

This study determined the effects of a food supplement based on a chemically characterized *M. sylvestris* extract for the management of FC by using self-assessment questionnaires on food supplement consumers, giving preliminary data regarding its efficacy and tolerability. The method used to perform this survey consisted of (i) a power analysis calculation, to determine the number of subjects involved in the survey; (ii) a definition of the inclusion and exclusion criteria; (iii) the use of validated questionnaires in the general population available in the Italian language to assess the frequency of bowel movements, stool consistency, and self-reported abdominal pain; and (iv) the use of inferential statistics to analyze the obtained results.

The results showed a significant improvement in bowel movements, with an average increase from 3.2 to 6.0 bowel movements per week in males and from 2.6 to 5.2 in females after using the supplement for 20 days. Stool consistency was improved as measured by the BSF scale, from hard and lumpy stools (type 1–2) to a 'normal' form (type 3–4). The VAS score indicated a marked reduction in the abdominal pain of participants. In addition, the supplement was well-tolerated and the participants' satisfaction was good. As far as the chemical characterization of the main ingredient of the food supplement is concerned, *M. sylvestris* extract included both soluble and insoluble dietary fiber and other bioactive compounds from different chemical classes. In particular, there were many polyphenols, which, being poorly absorbed, remain for the most part in the gut where they become available for fermentation by the gut microbiota and are known to positively modify the gut microbiota to facilitate the maintenance of gut health, for example, favoring *Bifidobacterium* and *Lactobacillus* while inhibiting the growth of potentially pathogenic bacteria [28]. Moreover, the food supplement also contained sorbitol (10 g per daily dose—20 mL), present at a non-laxative effect dose, which is not digested or absorbed in the small intestine and holds water in its molecules, leading to increased water in the gut lumen,

which could improve stool consistency. In addition, sorbitol is known to be fermented by the gut microbiota, increasing SCFA production [28].

Studies carried out over 50 years have revealed the presence of polysaccharides including mucilage in *M. sylvestris*, which possesses several biological properties and makes *M. sylvestris* extract a promising ingredient for food supplements and functional foods. The literature also indicates the presence of other phytochemicals in *M. sylvestris* extract such as amino acids (alanine, glycine, asparagine, glutamine, arginine, threonine, trigonelline, serine, and hydroxyproline), polyphenols (malvidin, malvin, delphidin, myricetin, apigenin, quercetin, kaempferol, genistein, phenolic acid derivatives, and coumarins), terpenoids (including carotenoids) [29,30]. The results of the current study confirmed the presence of polysaccharides in the *M. sylvestris* extract as indicated via the TDF content. Polysaccharides and mucilage are reported to increase the water content and weight of feces, enhance peristaltic movements, and speed up the gastric transit time. They may also restore hormones associated with the normal movements of the digestive tract [31,32]. Indirectly, mucilage possesses prebiotic actions while enhancing the growth of eubiotic bacteria strains and supporting overall health and wellbeing [33]. As revealed by the RP-UHPLC-MS analysis, *M. sylvestris* extract also contains phenolic acids, flavonoids, lipids, glycerides, amides, carotenoids, and chlorophyll derivatives (Tables 1 and 2), showing the diversity of bioactive compounds in the extract, which can contribute synergistically to potential benefits for gastrointestinal health. Phenolic compounds may support gastrointestinal health and improve constipation by increasing intestinal transit and colon water content, as well as by modulating the gut microbiota [28,34–36]. Observational studies showed a direct link between dietary carotenoid intake and the risk of constipation, as an increased intake of dietary carotenoids resulted in a decreased risk of chronic constipation in American adults [37,38]. Data from the National Health and Nutrition Examination Survey (NHANES) demonstrated a negative correlation between increased dietary antioxidant intake and the prevalence of constipation [39]. In addition, an inverse relation between dietary lipids and total fats with constipation has been established by Rollet et al. [40]. Dietary lipids may regulate bowel movements via the increased colonic myoelectric and motor activity [41]. Flaxseed, a rich dietary source of polyunsaturated fatty acids (mainly α-linoleic acid), was observed to improve constipation symptom scores in constipated patients in a randomized clinical trial [42]. Another study demonstrated the effectiveness of the daily consumption of olive oil and flaxseed oil in the reduction of constipation symptom scores and the improvement of bowel movements and stool consistency [43]. However, it is worth mentioning that gastrointestinal problems including constipation are often associated with a high-fat diet in general [44], which suggests the laxative effects may not be attributed to all lipids but only some 'healthy fats'.

The observed improvements in bowel movement frequency and stool consistency are consistent with earlier studies highlighting the role of mucilage and polyphenols in improving gastrointestinal transit. The ethnobotanical survey of *M. sylvestris* supports the effectiveness of its different components (leaves, flowers, aerial parts, roots, and whole plant) in managing abdominal pain and constipation, due to the presence of a high mucilage content [11]. Elsagh et al. [45] conducted a placebo-controlled trial to determine the efficacy of the aqueous extract obtained from *M. sylvestris* flowers on FC. Participants were randomized to receive either *M. sylvestris* flower extract (1 g/day) or a placebo for four weeks. The participants supplemented with *M. sylvestris* extract showed a significant increase in defecation frequency, improved stool consistency, and decreased overall constipation symptoms, suggesting *M. sylvestris* extract as a safe and effective preventive strategy in adults with FC. A study by Sleiman and Daher [12] demonstrated the anti-inflammatory and anti-ulcerogenic effects of *M. sylvestris* extract (500 mg/kg body weight)

in a murine model by offering protection against gastric ulcers, which may support the improvement of abdominal pain with *M. sylvestris* supplementation as observed in our study. Esteves et al. [46] reported promising anti-nociceptive effects of *M. sylvestris* extract against acetic acid-induced abdominal constrictions and a capsaicin-induced pain model in mice. Another study demonstrated the protective effects of *M. sylvestris* extract and its polysaccharides against experimental ulcerative colitis in rats, by reducing the signs of inflammation [47].

This survey has its strengths, as the method used to perform this survey consisted of (i) a power analysis calculation, (ii) well-defined inclusion and exclusion criteria for the recruited population, and (iii) validated questionnaires and a statistical analysis for data interpretation. However, the results of this survey are considered preliminary as it is not a clinical trial, which would use a placebo control, blinding, and randomized approach with a relatively longer study duration. The lack of a placebo and the small sample size could limit the ability to definitively attribute the observed effects of the food supplement while the lack of blinding and a randomized approach could increase bias and influence the objectives as participants knew they were taking an active ingredient. No control over other dietary or lifestyle factors could also increase the potential confounders, that could impact constipation. Moreover, the self-reporting of objectives could increase the likelihood of inaccuracies and bias in subjective symptoms.

5. Conclusions

This survey-based study demonstrated that a *M. sylvestris*-based food supplement can improve intestinal function in individuals with FC by increasing bowel movements, improving stool consistency, and reducing abdominal pain. These findings support the potential of *M. sylvestris* supplementation as an effective alternative therapy for managing FC, particularly in individuals seeking non-pharmaceutical interventions.

The practical applications of these findings extend to clinical settings where nutritional advice could include *M. sylvestris*-based supplements as part of personalized dietary recommendations. By addressing FC symptoms and improving overall gut health, such supplements may serve as a complementary approach to traditional laxative therapies, especially for patients with mild to moderate FC. Future research should focus on validating these findings through randomized, double-blind, placebo-controlled trials with larger sample sizes and longer durations. These studies should also compare the efficacy of *M. sylvestris* supplements with conventional laxatives and explore their role in broader gastrointestinal health management. Additionally, further investigation into the bioactive compounds of *M. sylvestris* and their pharmacological effects could provide insights into its potential therapeutic applications beyond FC. By expanding on the clinical implications and exploring new therapeutic avenues, *M. sylvestris* could become a key component in the development of innovative and natural approaches to gastrointestinal health.

Author Contributions: Conceptualization, M.D.; methodology, L.F.D.L., H.U. and D.G.B.; software, L.F.D.L., M.V.M. and A.D.M.; validation, D.G.B., A.B. and R.S.; formal analysis, H.U., M.V.M. and A.D.M.; investigation, A.B. and R.S.; resources, A.B. and A.D.M.; data curation, D.G.B. and D.S.L.; writing—original draft preparation, L.F.D.L., H.U., R.S. and M.D.; writing—review and editing, L.F.D.L., H.U., M.V.M., D.S.L. and M.D.; visualization, D.S.L.; supervision, M.D. All authors have read and agreed to the published version of the manuscript.

Funding: This research received no external funding.

Institutional Review Board Statement: The study was conducted in accordance with the Regulation (EU) 2016/679 OF THE EUROPEAN PARLIAMENT AND OF THE COUNCIL of 27 April 2016 on the protection of natural persons concerning the processing of personal data and on the free movement of

such data (internal protocol number: 021_2023, following art. 9, paragraph 2 letter a), and repealing Directive 95/46/EC (General Data Protection Regulation). At the end of the study, the data were collected and entered into a secure electronic system anonymously, and stored at the Department of Pharmacy for a period not exceeding that necessary for the purposes for which they were collected or subsequently processed as required by applicable regulations.

Informed Consent Statement: Informed consent was obtained from all subjects involved in the consumer survey.

Data Availability Statement: The data will be made available upon request.

Acknowledgments: The authors wish to extend their gratitude to Lobamar s.p.a. (Istriana, TV, Italy) for providing the food supplement tested in this consumer survey.

Conflicts of Interest: Author Alessandro Di Minno was employed by the non-profit consortium company CEINGE-Biotecnologie Avanzate, which counts among its members the University Hospital Federico II and the University of Naples Federico II. The remaining authors declare that the research was conducted in the absence of any commercial or financial relationships that could be construed as a potential conflict of interest.

References

1. Vriesman, M.H.; Koppen, I.J.; Camilleri, M.; Di Lorenzo, C.; Benninga, M.A. Management of functional constipation in children and adults. *Nat. Rev. Gastroenterol. Hepatol.* **2020**, *17*, 21–39. [CrossRef] [PubMed]
2. Pannemans, J.; Masuy, I.; Tack, J. Functional constipation: Individualising assessment and treatment. *Drugs* **2020**, *80*, 947–963. [CrossRef] [PubMed]
3. Suares, N.C.; Ford, A.C. Prevalence of, and risk factors for, chronic idiopathic constipation in the community: Systematic review and meta-analysis. *Am. J. Gastroenterol.* **2011**, *106*, 1582–1591. [CrossRef] [PubMed]
4. Arco, S.; Saldaña, E.; Serra-Prat, M.; Palomera, E.; Ribas, Y.; Font, S.; Clavé, P.; Mundet, L. Functional constipation in older adults: Prevalence, clinical symptoms and subtypes, association with frailty, and impact on quality of life. *Gerontology* **2022**, *68*, 397–406. [CrossRef]
5. Shin, J.E.; Park, K.S.; Nam, K. Chronic functional constipation. *Korean J. Gastroenterol.* **2019**, *73*, 92–98. [CrossRef] [PubMed]
6. Rao, S.S.C.; Yu, S.; Fedewa, A. Systematic review: Dietary fibre and FODMAP-restricted diet in the management of constipation and irritable bowel syndrome. *Aliment. Pharmacol. Ther.* **2015**, *41*, 1256–1270. [CrossRef] [PubMed]
7. Suares, N.C.; Ford, A.C. Systematic review: The effects of fibre in the management of chronic idiopathic constipation. *Aliment. Pharmacol. Ther.* **2011**, *33*, 895–901. [CrossRef]
8. Ashraf, W.; Park, F.; Lof, J.; Quigley, E.M.M. Effects of psyllium therapy on stool characteristics, colon transit and anorectal function in chronic idiopathic constipation. *Aliment. Pharmacol. Ther.* **1995**, *9*, 639–647. [CrossRef] [PubMed]
9. Liu, T.; Asif, I.M.; Bai, C.; Huang, Y.; Li, B.; Wang, L. The effectiveness and safety of natural food and food-derived extract supplements for treating functional gastrointestinal disorders—Current perspectives. *Nutr. Rev.* **2024**, nuae047, *online ahead of print*. [CrossRef] [PubMed]
10. Henry, A.G.; Piperno, D.R. Using plant microfossils from dental calculus to recover human diet: A case study from Tell al-Raqā'i, Syria. *J. Archaeol. Sci.* **2008**, *35*, 1943–1950. [CrossRef]
11. Gasparetto, J.C.; Martins, C.A.F.; Hayashi, S.S.; Otuky, M.F.; Pontarolo, R. Ethnobotanical and scientific aspects of *Malva sylvestris* L.: A millennial herbal medicine. *J. Pharm. Pharmacol.* **2012**, *64*, 172–189. [CrossRef] [PubMed]
12. Sleiman, N.H.; Daher, C.F. *Malva sylvestris* water extract: A potential anti-inflammatory and anti-ulcerogenic remedy. *Planta Med.* **2009**, *75*, PH10. [CrossRef]
13. Franova, S.; Nosalova, G.; Mokry, J. Phytotherapy of cough. *Adv. Phytomed.* **2006**, *2*, 111–131.
14. Karawya, M.S.; Balbaa, S.I.; Afifi, M.S.A. Investigation of the carbohydrate contents of certain mucilaginous plants. *Planta Med.* **1971**, *20*, 14–23. [CrossRef] [PubMed]
15. Classen, B.; Blaschek, W. High molecular weight acidic polysaccharides from *Malva sylvestris* and Alcea rosea. *Planta Med.* **1998**, *64*, 640–644. [CrossRef]
16. Hiçsönmez, Ü.; Ereeş, F.S.; Özdemir, C.; Özdemir, A.; Cam, S. Determination of major and minor elements in the *Malva sylvestris* L. from Turkey using ICP-OES techniques. *Biol. Trace Elem. Res.* **2009**, *128*, 248–257. [CrossRef] [PubMed]
17. Katapodis, P.; Kavarnou, A.; Kintzios, S.; Pistola, E.; Kekos, D.; Macris, B.J.; Christakopoulos, P. Production of acidic xylo-oligosaccharides by a family 10 endoxylanase from *Thermoascus aurantiacus* and use as plant growth regulators. *Biotechnol. Lett.* **2002**, *24*, 1413–1416. [CrossRef]

18. Barros, L.; Carvalho, A.M.; Ferreira, I.C. Leaves, flowers, immature fruits and leafy flowered stems of *Malva sylvestris*: A comparative study of the nutraceutical potential and composition. *Food Chem. Toxicol.* **2010**, *48*, 1466–1472. [CrossRef] [PubMed]
19. McRorie, J.; Zorich, N.; Riccardi, K.; Bishop, L.; Filloon, T.; Wason, S.; Giannella, R. Effects of olestra and sorbitol consumption on objective measures of diarrhea: Impact of stool viscosity on common gastrointestinal symptoms. *Regul. Toxicol. Pharmacol.* **2000**, *31*, 59–67. [CrossRef] [PubMed]
20. CFR—Code of Federal Regulations Title 21. Available online: https://www.accessdata.fda.gov/scripts/cdrh/cfdocs/cfcfr/CFRSearch.cfm?fr=184.1835&SearchTerm=sorbitol (accessed on 13 November 2024).
21. Megazyme Total Dietary Fiber. Available online: https://www.megazyme.com/total-dietary-fiber-assay-kit (accessed on 19 March 2024).
22. Bonjoch, N.P.; Tamayo, P.R. Protein content quantification by bradford method. In *Handbook of Plant Ecophysiology Techniques*; Roger, M.J.R., Ed.; Springer: Dordrecht, The Netherlands, 2001; pp. 283–295.
23. VigiErbe. Available online: www.vigierbe.it (accessed on 15 November 2024).
24. R Core Team, R. *A Language and Environment for Statistical Computing*; R Foundation for Statistical Computing: Vienna, Austria, 2020. Available online: http://www.r-project.org/index.html (accessed on 13 September 2024).
25. Bates, D.; Maechler, M.; Bolker, B.; Walker, S. Fitting linear mixed-effects models using lme4. *J. Stat. Softw.* **2015**, *67*, 1–48. [CrossRef]
26. Sumner, L.W.; Amberg, A.; Barrett, D.; Beale, M.H.; Beger, R.; Daykin, C.A.; Fan, T.W.M.; Fiehn, O.; Goodacre, R.; Griffin, J.L.; et al. Proposed minimum reporting standards for chemical analysis: Chemical analysis working group (CAWG) metabolomics standards initiative (MSI). *Metabolomics* **2007**, *3*, 211–221. [CrossRef]
27. Calvert, M.; Blazeby, J.; Altman, D.G.; Revicki, D.A.; Moher, D.; Brundage, M.D.; CONSORT PRO Group. Reporting of patient-reported outcomes in randomized trials: The CONSORT PRO extension. *JAMA* **2013**, *309*, 814–822. [CrossRef]
28. Katsirma, Z.; Dimidi, E.; Rodriguez-Mateos, A.; Whelan, K. Fruits and their impact on the gut microbiota, gut motility and constipation. *Food Funct.* **2021**, *12*, 8850–8866. [CrossRef] [PubMed]
29. Mousavi, S.M.; Hashemi, S.A.; Behbudi, G.; Mazraedoost, S.; Omidifar, N.; Gholami, A.; Chiang, W.H.; Babapoor, A.; Pynadathu Rumjit, N. A review on health benefits of *Malva sylvestris* L. nutritional compounds for metabolites, antioxidants, and anti-inflammatory, anticancer, and antimicrobial applications. *Evid.-Based Complement. Altern. Med.* **2021**, *2021*, 5548404. [CrossRef]
30. Sharifi-Rad, J.; Melgar-Lalanne, G.; Hernández-Álvarez, A.J.; Taheri, Y.; Shaheen, S.; Kregiel, D.; Antolak, H.; Pawlikowska, E.; Brdar-Jokanović, M.; Rajkovic, J.; et al. Malva species: Insights on its chemical composition towards pharmacological applications. *Phytother. Res.* **2020**, *34*, 546–567. [CrossRef] [PubMed]
31. Sari, Y.P.; Candraruna, D.B. The Potential of Polysaccharides from Various Plants as Constipation Treatment. *J. Appl. Food Technol.* **2023**, *10*, 48–57. [CrossRef]
32. Islambulchilar, M. Thirst-quenching and mucilage-containing herbs in Persian Medicine: New perspectives on old practice. *Adv. Integr. Med.* **2024**, *e-pub ahead of print*. [CrossRef]
33. Yang, Y.; Gupta, V.K.; Du, Y.; Aghbashlo, M.; Show, P.L.; Pan, J.; Tabatabaei, M.; Rajaei, A. Potential application of polysaccharide mucilages as a substitute for emulsifiers: A review. *Int. J. Biol. Macromol.* **2023**, *242*, 124800. [CrossRef] [PubMed]
34. Chen, Y.; Ding, Z.; Wu, Y.; Chen, Q.; Liu, M.; Yu, H.; Wang, D.; Zhang, Y.; Wang, T. Effects of Allium mongolicum Regel and its flavonoids on constipation. *Biomolecules* **2019**, *10*, 14. [CrossRef]
35. Zhou, P.; Wang, X.; Sun, M.; Yan, S. Effects of natural products on functional constipation: Analysis of active ingredient and mechanism. *Naunyn Schmiedebergs Arch. Pharmacol.* **2024**, *397*, 2083–2103. [CrossRef]
36. Kim, J.E.; Choi, Y.J.; Lee, S.J.; Gong, J.E.; Lee, Y.J.; Sung, J.E.; Jung, Y.S.; Lee, H.S.; Hong, J.T.; Hwang, D.Y. Antioxidant activity and laxative effects of tannin-enriched extract of Ecklonia cava in loperamide-induced constipation of SD rats. *PLoS ONE* **2021**, *16*, e0246363. [CrossRef] [PubMed]
37. Wang, J.; Kong, W.; Liu, M.; Wang, Y.; Zheng, Y.; Zhou, Y. Association between dietary carotenoids intake and chronic constipation in American men and women adults: A cross-sectional study. *BMC Public Health* **2023**, *23*, 1597. [CrossRef] [PubMed]
38. Sun, W.; Wang, Y.; Han, L.; Liu, Y.; Liu, H.; Tong, Y.; Jiang, Z.; Sun, D.; Xu, C. Association between different composite dietary antioxidant indexes and constipation in American male adults: A cross-sectional study. *Front. Nutr.* **2024**, *11*, 1404400.
39. Wei, S.; Yu, S.; Lan, Y.; Jia, Y. Association between the composite dietary antioxidant index and constipation: Evidence from NHANES 2005–2010. *PLoS ONE* **2024**, *19*, e0311168. [CrossRef] [PubMed]
40. Rollet, M.; Bohn, T.; Vahid, F.; ORISCAV Working Group. Association between dietary factors and constipation in adults living in Luxembourg and taking part in the ORISCAV-LUX 2 survey. *Nutrients* **2021**, *14*, 122. [CrossRef]
41. Renny, A.; Snape Jr, W.J.; Sun, E.A.; London, R.; Cohen, S. Role of cholecystokinin in the gastrocolonic response to a fat meal. *Gastroenterology* **1983**, *85*, 17–21. [CrossRef] [PubMed]
42. Soltanian, N.; Janghorbani, M. A randomized trial of the effects of flaxseed to manage constipation, weight, glycemia, and lipids in constipated patients with type 2 diabetes. *Nutr. Metab.* **2018**, *15*, 36. [CrossRef]

43. Ramos, C.I.; de Lima, A.F.A.; Grilli, D.G.; Cuppari, L. The short-term effects of olive oil and flaxseed oil for the treatment of constipation in hemodialysis patients. *J. Ren. Nutr.* **2015**, *25*, 50–56. [CrossRef]
44. Mukai, R. High-fat diet and constipation. *Free Radic. Biol. Med.* **2018**, *120*, S134–S135. [CrossRef]
45. Elsagh, M.; Fartookzadeh, M.R.; Kamalinejad, M.; Anushiravani, M.; Feizi, A.; Behbahani, F.A.; Rafiei, R.; Arjmandpour, A.; Adibi, P. Efficacy of the *Malva sylvestris* L. flowers aqueous extract for functional constipation: A placebo-controlled trial. *Complement. Ther. Clin. Pract.* **2015**, *21*, 105–111. [CrossRef] [PubMed]
46. Esteves, P.F.; Sato, A.; Esquibel, M.A.; de Campos-Buzzi, F.; Meira, A.V.; Cechinel-Filho, V. Antinociceptive activity of *Malva sylvestris* L. *Lat. Am. J. Pharm.* **2009**, *28*, 454–456.
47. Hamedi, A.; Rezaei, H.; Azarpira, N.; Jafarpour, M.; Ahmadi, F. Effects of *Malva sylvestris* and its isolated polysaccharide on experimental ulcerative colitis in rats. *J. Evid. Based Complement. Altern. Med.* **2016**, *21*, 14–22. [CrossRef]

Disclaimer/Publisher's Note: The statements, opinions and data contained in all publications are solely those of the individual author(s) and contributor(s) and not of MDPI and/or the editor(s). MDPI and/or the editor(s) disclaim responsibility for any injury to people or property resulting from any ideas, methods, instructions or products referred to in the content.

nutrients

MDPI

Article

Neuroprotective and Neurotrophic Potential of *Flammulina velutipes* Extracts in Primary Hippocampal Neuronal Culture

Sarmistha Mitra [1,*,†], Raju Dash [1,†], Md Abul Bashar [2], Kishor Mazumder [3] and Il Soo Moon [4,*]

[1] Department of New Biology, Daegu Gyeongbuk Institute of Science and Technology (DGIST), Daegu 42988, Republic of Korea; rajudash.bgctub@gmail.com
[2] Department of Pharmacy, Faculty of Biological Sciences, Islamic University, Kushtia 7003, Bangladesh; bashar.iu.ph@gmail.com
[3] Department of Pharmacy, Jashore University of Science and Technology, Jashore 7408, Bangladesh; kmazumder@just.edu.bd
[4] Department of Anatomy, Dongguk University College of Medicine, Gyeongju 38066, Republic of Korea
* Correspondence: sarmisthacu@gmail.com (S.M.); moonis2414@gmail.com (I.S.M.)
† These authors contributed equally to this work.

Abstract

Flammulina velutipes (enoki mushroom) is a functional edible mushroom rich in antioxidants, polysaccharides, mycosterols, fiber, and minerals. Accumulating evidence highlights its therapeutic potential across diverse pathological contexts, including boosting cognitive function. However, its role in neuromodulation has not been systematically explored. This study examined the effects of methanolic and ethanolic extracts of *F. velutipes* on primary hippocampal neurons. Neurons were treated with different extract concentrations, followed by assessments of cell viability, cytoarchitecture, neuritogenesis, maturation, and neuroprotection under oxidative stress. The extracts were further characterized by GC-MS to identify bioactive metabolites, and molecular docking combined with MM-GBSA binding energy analysis was employed to predict potential modulators. Our results demonstrated that the methanolic extract significantly enhanced neurite outgrowth, improved neuronal cytoarchitecture, and promoted survival under oxidative stress, whereas the ethanolic extract produced moderate effects. Mechanistic studies indicated that these neuroprotective and neurodevelopmental benefits were mediated through activation of the NTRK receptors, as validated by both in vitro assays and molecular docking studies. Collectively, these findings suggest that *F. velutipes* extracts, particularly methanolic fractions, may serve as promising neuromodulatory agents for promoting neuronal development and protecting neurons from oxidative stress.

Keywords: primary hippocampal neuron; neuritogenesis; neuroprotection; GC-MS; NTRK receptor pathway; flammulina velutipes metabolites

1. Introduction

Healthy functional foods with rich nutritional value are ideal for high-quality lifestyles and food habits. As people focus more on adopting healthier lifestyles and consuming nutritious organic foods, functional food is becoming increasingly popular, and awareness of it is being raised. Besides providing high nutrition, metabolites from functional foods can help in ailments of many diseases and health problems. Especially in the case of healthy aging, mushrooms work as an anti-aging super-food, which inhibits ROS accumulation with aging [1]. Mushrooms are a popular healthy choice of functional food because of their

low carbohydrate content, high protein, and fiber. Also, many healthy food metabolites with medicinal properties, like ergosterol, polyphenol, and tannin, are enriched in mushrooms [2]. According to the Department of Agriculture, the United States, mushrooms are categorized as "other vegetables" and are generally considered plant-sourced food [3,4]. Among the many health benefits of mushrooms, improving brain function and boosting memory are interesting factors that draw the attention of research studies and open a new window for drug design and therapeutic applications.

Flammulina velutipes, commonly known as "golden needle mushroom" or "enoki mushroom," is a common and widely consumed mushroom, especially in the Asian region [5]. Because of its high content of fiber, minerals, polysaccharides, and other healthy metabolites [6], this mushroom is a healthy choice. Apart from its traditional food value, it is also reported to have some medicinal properties. As it has a higher content of antioxidant agents, it protects neurons from damage and boosts brain function [7–9]. Recently, a neuroprotective peptide has been isolated from this mushroom, which can improve cognitive function [10]. Neurotropic natural compounds and brain-boosting agents have a very high therapeutic impact in the case of memory, as well as age-related neurodegenerative diseases. Memory loss, neurodegeneration, and cognitive dysfunction are some of the common phenomena in aging people [11–13] that degrade their quality of life and generate a significant burden on health care systems [14,15]. Different neurodegenerative diseases like Alzheimer's disease, Parkinson's disease, Amyotrophic lateral sclerosis, multiple sclerosis, and Huntington's disease are common examples among the aging population, affecting cognitive function and memory [16,17]. Besides medicine, functional foods and alternative natural therapies can help manage cognitive dysfunction and memory loss [18]. Previous research studies have shown that *F. velutipes* mushroom is a natural memory-boosting and cognition-enhancing agent [8–10,19]. It has been found that polysaccharides of *F. velutipes* show an acetylcholinesterase inhibitory effect, which is responsible for its memory and cognition improvement effect [8].

In the present study, we evaluated the direct impact of ethanolic (FVEE) and methanolic (FVME) extracts of this mushroom on cultured neuron cells (Figure 1a). Firstly, we performed GC-MS analysis of both extract types to characterize the metabolites or chemicals present in the extract. We analyzed the effects of both types of extract on neurons, estimated and compared their effects on neuronal growth, development, and survival, and unleashed the mechanisms of their neuromodulatory effect. Our in vitro experimental assay and in silico molecular docking study suggested the active compound of the extract regulates neuronal growth via NTRK receptors. Our analysis revealed that the metabolites of the mushroom extracts function as neurotropic agents and promote neuronal growth by upregulating the neurotrophin signaling pathway.

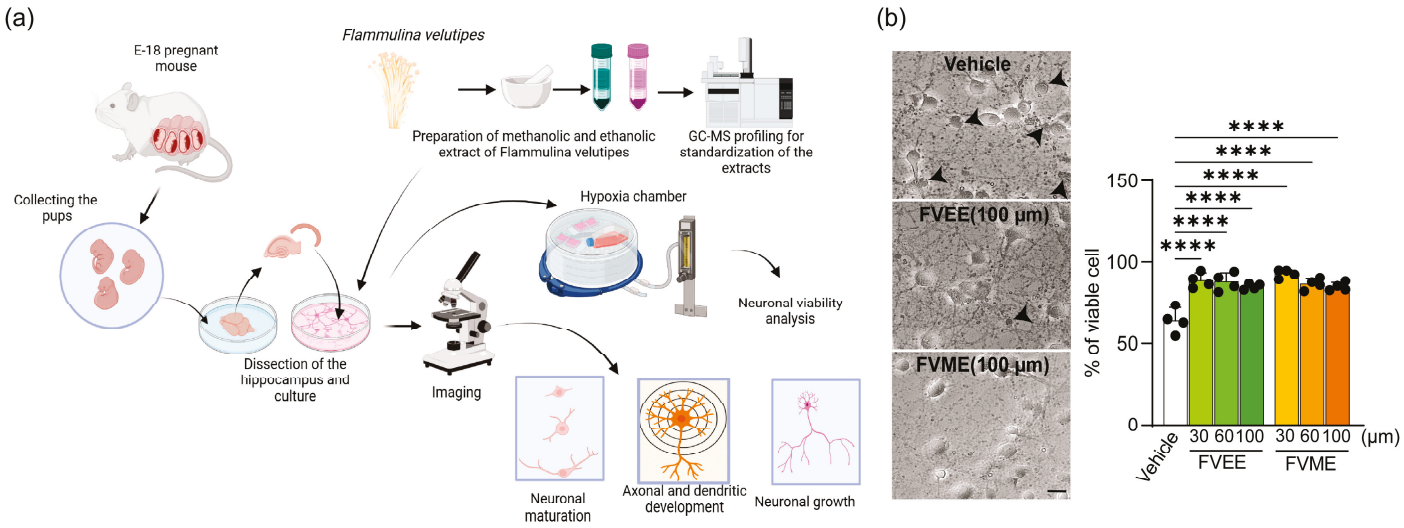

Figure 1. FVME and FVEE preserve the viability of neurons. (**a**) represents the overall experimental plan from primary neuronal culture to data analysis. (**b**) shows bright-field images of neurons grown until DIV8 and stained with trypan blue after being treated in the vehicle/FVEE/FVME condition. The dead neurons are marked with black arrows. Statistical analysis represents the viability of neurons with different doses of FVEE and FVME. Data are presented as mean ± SD from three independent biological replicates, with individual data points shown. Statistical significance was assessed by one-way ANOVA followed by Dunnett's multiple comparisons test versus vehicle (**** $p < 0.0001$). Scale bar: 20 µm. FVME, *Flammulina velutipes* methanolic extract; FVEE, *Flammulina velutipes* ethanolic extract.

2. Materials and Methods

2.1. Chemicals/Reagents

Media and all the supplements were bought from Invitrogen (Thermo Fisher Scientific, Waltham, MA, USA). Ethanol and methanol were bought from Sigma-Aldrich (Merck KGaA, St. Louis, MO, USA) for extract preparation. Linalool was purchased from MedChemExpress (Monmouth Junction, NJ, USA). and for use as a positive control in the experiments. Dil (1,1′-Dioctadecyl-3,3,3′,3′-Tetramethylindocarbocyanine Perchlorate) was purchased from Molecular Probes (Invitrogen, Eugene, OR, USA)

2.2. Preparation of Extract

Fresh fruiting bodies of *F. velutipes* were purchased from a local market in Gyeongju city/North Gyeongsang Province, South Korea. An author (Sarmistha Mitra) identified the species based on prior experience [20,21] with this species and examination of diagnostic macroscopic and microscopic characteristics, including cap morphology and color, gill attachment, stipe features, and spore size and shape. The species name was verified using MycoBank (https://www.mycobank.org, MycoBank No. 330940, accessed in 20 March 2021). A voucher specimen of *F. velutipes* has been deposited in the laboratory collection of the corresponding author and is available for future reference.

After cleaning and drying, the mushrooms were chopped and powdered using liquid nitrogen. The powdered mushroom material was soaked in separate containers in ethanol and methanol, and kept in a shaker for extract preparation. The powdered mushroom was filtered using filter paper. The dried concentrated extract was preserved at −20 °C, and a working extract of 8 mg/mL was prepared using dimethyl sulfoxide (DMSO) and further diluted with DMSO to reduce concentrations. The concentration–response curve was generated using the sum of all primary processes as a representative measure of mor-

phological effects. Data for all tested concentrations (7.5–100 μg/mL) were shown, with the most effective concentrations (30, 60, 100 μg/mL) highlighted for subsequent experiments.

2.3. Standardization of the Extracts

Both the extracts were characterized by using GC-MS (gas chromatography–mass spectroscopy) to identify and quantify the active components in the extracts. The dried extracts were dissolved in DMSO to dissolve the most polar and nonpolar metabolites. The Agilent Technologies (Santa Clara, CA, USA) 7890A capillary gas chromatographic equipment was used for GC-MS analysis. The mass spectrometer detector on the chromatograph was composed of 95% dimethylpolysiloxane and 5% phenyl. A silica capillary column (film: 0.25 μm) with the brand and model number HP-5MSI served as the chromatographic column. It had a 0.25 mm diameter and a length of 90 m. The extract was injected into the GC apparatus in a fused silica capillary column in a total volume of 6 μL. The carrier gas (99.999% helium) was set to flow at a 1 mL/min rate. The temperature of the injector was kept at 250 °C, and the iron source temperature was adjusted to 280 °C. Initially, an isothermal temperature of 110 °C was maintained for 2 min. The temperature then rose by 10 °C/min until it reached 200 °C. The temperature then rose at a rate of 5 °C/min until it reached 280 °C, which was maintained for 9 min. The mass spectrum was collected in the mass-to-charge ratio region of 50 to 550 m/z. The ionization source was kept at a temperature of 250 °C, while the mass spectrometer quadrupole (MS quad) was kept at 150 °C. The full GC-MS analysis procedure required 36 min to complete, including the time for data gathering and the numerous temperature ramps and holds. During the study, mass spectra of unexplained peaks were gathered. The acquired mass spectra were compared to the NIST (National Institute of Standards and Technology, Gaithersburg, MD, USA) databases to determine the chemicals in the extract.

2.4. Primary Hippocampal Neuronal Culture

Primary hippocampal culture was performed in time-pregnant Sprague-Dawley rats (19th day), which were accommodated according to the Principles of Laboratory Animal Care (NIH, Washington, DC, USA). The whole culture procedures followed the Principles of Laboratory Animal Care and were approved by the Institutional Animal Care and Use Committee of Dongguk University (approval certificate number IACUC-2023-07) on 4 May 2023. The fetal hippocampi were collected from the brain, and dissociated neuronal cultures were prepared. The dissociated cells were seeded onto 12 mm coverslips previously coated with poly-DL-lysine (Sigma-Aldrich, Merck KGaA, St. Louis, MO, USA) in 24-well culture plates at a 1.0 × 104 cells/cm^2 density. Media for neuronal cells were prepared using Neurobasal media supplemented with B27, glutamate, and β-mercaptoethanol, kept in the incubator at 37 °C, with 5% CO_2 and 95% air. Different extracts and/or vehicle concentrations were added to the culture plates before cell seeding. Also, linalool (50 nM) was used to compare the neuronal growth mediated by the extracts.

2.5. Hypoxia/Reoxygenation (H/R)-Induced Oxidative Stress

During culture, hippocampal cells were fed every 4 days by replacing 1/4 of the media with fresh prewarmed serum-free neurobasal media supplemented with B27, with or without sample extract. Hypoxia/reoxygenation (H/R) of rat hippocampal neurons was carried out, as described previously [22,23]. Briefly, after growing the cells for 10 days, the cells were transferred into a modular hypoxia chamber (Modular Incubator Chamber MIC-101; Billups-Rothenberg, Inc., Del Mar, CA, USA) in a 94% N2, 5% CO_2, and 1% O_2 atmosphere and incubated at 37 °C for 4 h. To reoxygenate hypoxic cells, culture plates were placed in a normal cell incubator (95% air, 5% CO_2) and reoxygenated for 3 days. Then, neuronal viability was measured using the trypan blue assay. Prior to H/R

treatment, cells received one of the following treatments: control, H/R stress without extracts (FVME/FVEE), or H/R stress with 30, 60, and 100 μg/mL concentrations of both FVME/FVEE for two hours.

2.6. Trypan Blue Exclusion Assay for Neuronal Viability

The trypan blue exclusion assay revealed the viability of neurons after treatment with different concentrations of extracts and after the H/R test. Cells were stained with 0.4% trypan blue solution for 30 min and washed with D-PBS solution before imaging. Phase-contrast images of all treatment groups were taken. The dead cells appeared dark blue; however, the viable cells appeared normal because they excluded the dye.

2.7. Immunocytochemistry

Immunocytochemistry was carried out in the same way as described in earlier works. After culturing the neurons on the coverslips for the indicated time, the neurons on the coverslips were washed briefly with D-PBS, fixed with a 4% paraformaldehyde and methanol fixation procedure, and blocked with 1% goat serum. Neurons were then incubated with primary antibodies overnight, followed by secondary antibody incubation for 2.5 h, and mounted on slides.

The following antibodies were used for immunostaining: primary antibodies of tubulin α-subunit (mouse monoclonal 12G10, 1:25; Developmental Studies Hybridoma Bank, University of Iowa, Iowa City, IA, USA), Ankyrin G (rabbit polyclonal H-215, 1:25; Santa Cruz Biotechnology Inc., Santa Cruz, CA, USA), MAP2 (mouse monoclonal clone HM-2; 1:250; Sigma, St. Louis, MO, USA), and Tau (rabbit polyclonal LF-PA0172; 1:100; AbFrontier, Seoul, Korea) and secondary antibodies (Alexa Fluor 488-conjugated goat anti-mouse IgG [1:500], Alexa Fluor 568-conjugated goat anti-rabbit IgG [1:1000], and Alexa Fluor 568-conjugated rabbit anti-goat IgG [1:1000], Molecular Probes, Eugene, OR, USA).

Neurones at the DIV3 were fixed and stained for 20 min at room temperature using Dil dye (20 μg/mL). The cells are rinsed three times with D-PBS after the incubation period.

2.8. Image Analysis and Quantification

Cells were fixed and processed for cytochemistry as described in Section 2.7. Imaging was performed using a Leica DM IRE2 research microscope (Leica Microsystems AG, Wetzlar, Germany) equipped with I3 S, N2.1S, and Y5 filter sets. Phase-contrast and epifluorescence images (1388 × 1039 pixels) were acquired with a high-resolution CoolSNAP™ CCD camera (Photometrics, Tucson, AZ, USA) under the control of Leica FW4000 software. Image acquisition parameters, including objective lens magnification, illumination settings, and exposure times, were constant across all experimental groups.

Morphometric analyses were conducted using ImageJ (v1.49) with the Simple Neurite Tracer plugin. Neurons were randomly selected, avoiding overlapping or truncated cells. Each cell was traced from the soma to the tips of all visible neurites, and the following features were quantified: axon length, the number of dendrites, dendritic length, axonal and dendritic branch number and length, and the number of branching points. Sholl analysis was performed using the Sholl analysis plugin (v1.0) with concentric circles spaced at 10 μm intervals from the soma center. Incomplete or overlapping neurites were excluded from the analysis.

For each experimental condition, 30 neurons from at least three independent cultures were analyzed. Digital measurements were exported and subjected to statistical analysis. Data normality was assessed using the Shapiro–Wilk test, and parametric and non-parametric tests were applied as appropriate. Results are presented as the mean ± SD. All acquisition, tracing, and analysis procedures were performed consistently to ensure reproducibility.

2.9. In Silico Identification of Potential Bioactive Compounds

2.9.1. Glide-Based Molecular Docking Analysis

To extract the chemical structures of the compounds found in the GC-MS results, we used the PubChem database. While we found a total of 21 and 22 compounds in ethanol and methanol extracts, respectively, we considered compounds for molecular docking, excluding duplicates and solvent compounds. Additionally, we retrieved two compounds considered as controls, 3β, 6β-dichloro-5-hydroxy-5α-cholestane and 7,8-dihydroxyflavone for NTRK1 (also called TrkA) and NTRK2 (also referred to as TrkB), respectively [24,25]. The LigPrep module of the Schrödinger suite 2023-2 was harnessed to construct three-dimensional (3D) representations of these structures. By adjusting the pH to 7.0 and employing the Epik 2.2 program, the ionization states of each ligand and control were predicted [25]. This study created a maximum of 32 probable conformers for each ligand and control, and from these, the conformer with the least energy was selected for additional analysis.

The 3D crystal structures of NTRK1 and NTRK2 bearing PDB IDs 1WWW (NTRK1) and 1HCF (NTRK2) were extracted from the RCSB protein databank. These structures were subsequently prepared utilizing the protein preparation module within the Schrödinger suite 2023-2 program, which involved assigning the appropriate charges, hydrogen, and bond orders to 3D structures. All hydrogen bonds (H-bonds) within the crystal structure were optimized at a neutral pH by removing irrelevant water molecules.

The procedure of minimization was carried out by utilizing the OPLS_4 force field, taking into consideration that the structural modification should not have exceeded 0.30 Å of its root mean square deviation. By constructing a grid box at the reference ligand binding site of the protein, the active site of the protein was set for docking simulation. The parameters of grid generation remained at their default settings, with a bounding box size of 15 Å × 15 Å × 15 Å, and post-minimization was carried out harnessing the OPLS_4 force field. The van der Waals scaling factor and charge cutoff were fixed at 1.00 and 0.25, respectively [26]. With the aid of Schrodinger-Maestro version 9.4 [27,28], glide docking via extra precision (XP) was executed, where all ligands and controls were regarded as flexible by considering the van der Waals factor (0.80) and the partial charge (0.15), and the OPLS_4 force field was employed to minimize the docked complex. Following docking, for each ligand and control, the docking pose with the lowest glide score was considered for further analysis [26].

2.9.2. Binding Energy (MM-GBSA) Analysis

Next, binding free energy (MM-GBSA) analyses were carried out harnessing the Prime MM-GBSA wizard of the Schrödinger suite 2023-2 program [29], in which an increased negative value indicates higher stability. The docking pose viewer file with the lowest glide score obtained following glide XP docking was subjected to analyses, in which the sampling minimization protocol was implemented with the OPLS2005 force field as Molecular Mechanics (MM) and Generalized Born Surface Accessible (GBSA) as the continuum model, maintaining the flexibility of the protein [30–33]. The dielectric solvent model, VSGB 2.0, was employed to rectify the empirical functions of π-stacking and H-bond interactions [34].

2.10. Statistical Analysis

The findings of this study were reported using the mean ± standard deviation (SD), which was obtained from at least three unique replicates of each test, except when specified differently. For neuritogenesis analysis, each data point in the graph represents the mean of ≤10 neurons per replicate, while for early neuronal differentiation, calculations were based

on 400–500 neurons per condition. With the assistance of GraphPad Prism, version 8.0.0 (San Diego, CA, USA), the normality of the datasets was assessed using the Shapiro–Wilk test. As all datasets passed the normality test ($p > 0.05$), parametric tests were applied. The statistical comparisons were carried out by employing either Student's *t*-test or one-way analysis of variance (ANOVA), which was subsequently accompanied by Dunnett's multiple-comparisons test. Results were considered statistically significant when the *p*-value was less than 0.05 (p-value < 0.05). Levels of significance are indicated as follows: * $p < 0.05$; ** $p < 0.01$; *** $p < 0.001$; **** $p < 0.0001$.

3. Results

3.1. Chemical Characterization of FVME and FVEE

From the GC-MS analysis of FVEE and FVME, we found 21 and 22 compounds, respectively (Supplementary Tables S1 and S2). Among all these compounds, linalool and dodecane, 1-fluoro- were common in both the extracts. GC-MS analysis of FVEE showed a peak area of 0.089% with a retention time of 9.17 min for linalool. On the other hand, linalool in FVME was represented by a peak area of 0.2335% with the same retention time.

3.2. Effects of FVME and FVEE on Cell Viability

By performing the trypan blue exclusion assay, the effect of different concentrations of FVME and FVEE on neuronal viability was tested. Here, the numbers of live cells and dead cells were counted. The bright-field images are presented in Figure 1b. The statistical analysis of the data showed that (Figure 1b) all concentrations of the extracts enhanced the viability of the neurons.

3.3. Dose-Dependent Effects of FVME and FVEE on Neuronal Development

3.3.1. FVME and FVEE Promote Neurite Outgrowth

From the morphological analysis performed on cultured hippocampal neuronal cells, we noticed a concentration-dependent growth effect of neurons due to treatment with FVME and FVEE. Cultured neurons were allowed to grow until the third day, with and/or without different concentrations of FVME and FVEE (Figures 2 and S1). On the third day, phase-contrast images were taken for performing analysis. We analyzed morphological parameters of neuronal growth, including the number of primary processes, the length of the longest process, and the total length of all processes, as shown in Figure 2b,c. According to all the parameters, the neurons showed significant growth in the extract-treated condition compared to the control (vehicle) condition. Fixed neurons (DIV3) were stained with Dil dye and are represented in Figure 2a. Based on the results, we used 30 μm FVME and 100 μm FVEE concentrations for further analysis (Figure S1).

However, the neuronal growth on FVME-treated neurons was more significant than that on FVEE-treated neurons. FVME treatment significantly improved all three growth parameters (Figure 2b). This implies that FVME has a more prominent effect on neuronal growth than FVEE. Based on this finding, we performed further neuro-architecture analysis by treating neurons with FVME.

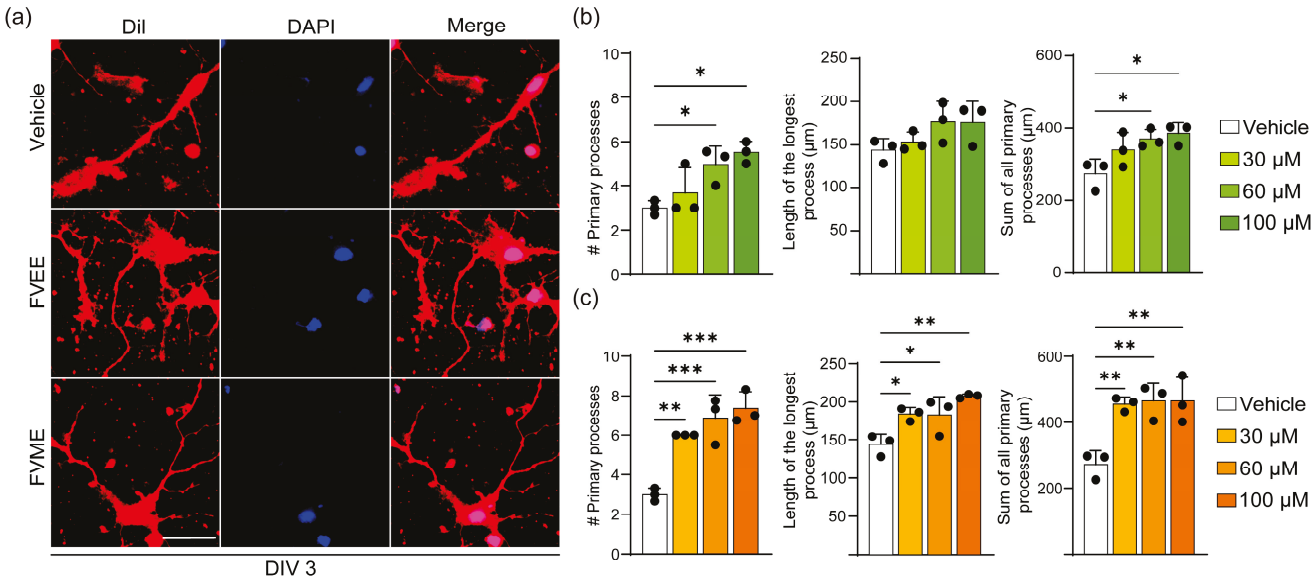

Figure 2. Neurons' morphological growth parameters significantly improved due to FVME and FVEE. Neuronal growth was observed on the third day of primary culture and stained with Dil dye (red), followed by counterstaining with DAPI (blue). (**a**) Representative fluorescent image of neurons grown with normal media/FVEE/FVME. Statistical analysis represents morphological parameters, the number of primary processes, the length of the longest process, and the sum of all the processes in neurons with different doses of FVEE (**b**) and FVME (**c**). Data are presented as mean ± SD from three independent biological replicates, with individual data points shown. Statistical significance was assessed by one-way ANOVA followed by Dunnett's multiple comparisons test versus vehicle. * $p < 0.05$; ** $p < 0.01$; *** $p < 0.001$; scale bar = 20 µm. FVEE, *Flammulina velutipes* ethanolic extract; FVME, *Flammulina velutipes* methanolic extract; Dil, 1,1′-Dioctadecyl-3,3,3′,3′-Tetramethylindocarbocyanine Perchlorate.

3.3.2. FVME and FVEE Promote Early Neuronal Development

After investigating the optimized concentrations of FVME and FVEE, we applied these concentrations to primary cultured neurons to investigate their impact on early development. Neuronal maturation or early development of neurons was analyzed by incubating the neurons with vehicles and the extracts at the mentioned concentrations until the first and second day of culture (Figure 3a,d). The developmental phases of neurons were divided into three categories: lamellipodia, minor processes, and axonal outgrowth (Figure 3b,e) [35]. Our statistical analysis (Figure 3c,f) showed that after treatment with FVME and FVEE, more neurons were transformed into the advanced developmental stage compared to those with the vehicle treatment. During the first 24 h, both the extracts showed significant advancement in developing the neurons into the minor process stage compared to the vehicles. At 48 h, the neuron' development into the axonal outgrowth stage was significantly promoted by both extracts. Neurons at 24 h and 48 h, with or without extract treatment, were immunostained with Tau and Map2 antibodies (Figure 3a,d), which are axonal and dendritic markers, respectively. Enlarged in-sets are represented in Figure 3b,e. In this experiment, 30 µM of FVME and 100 µM of FVEE were used.

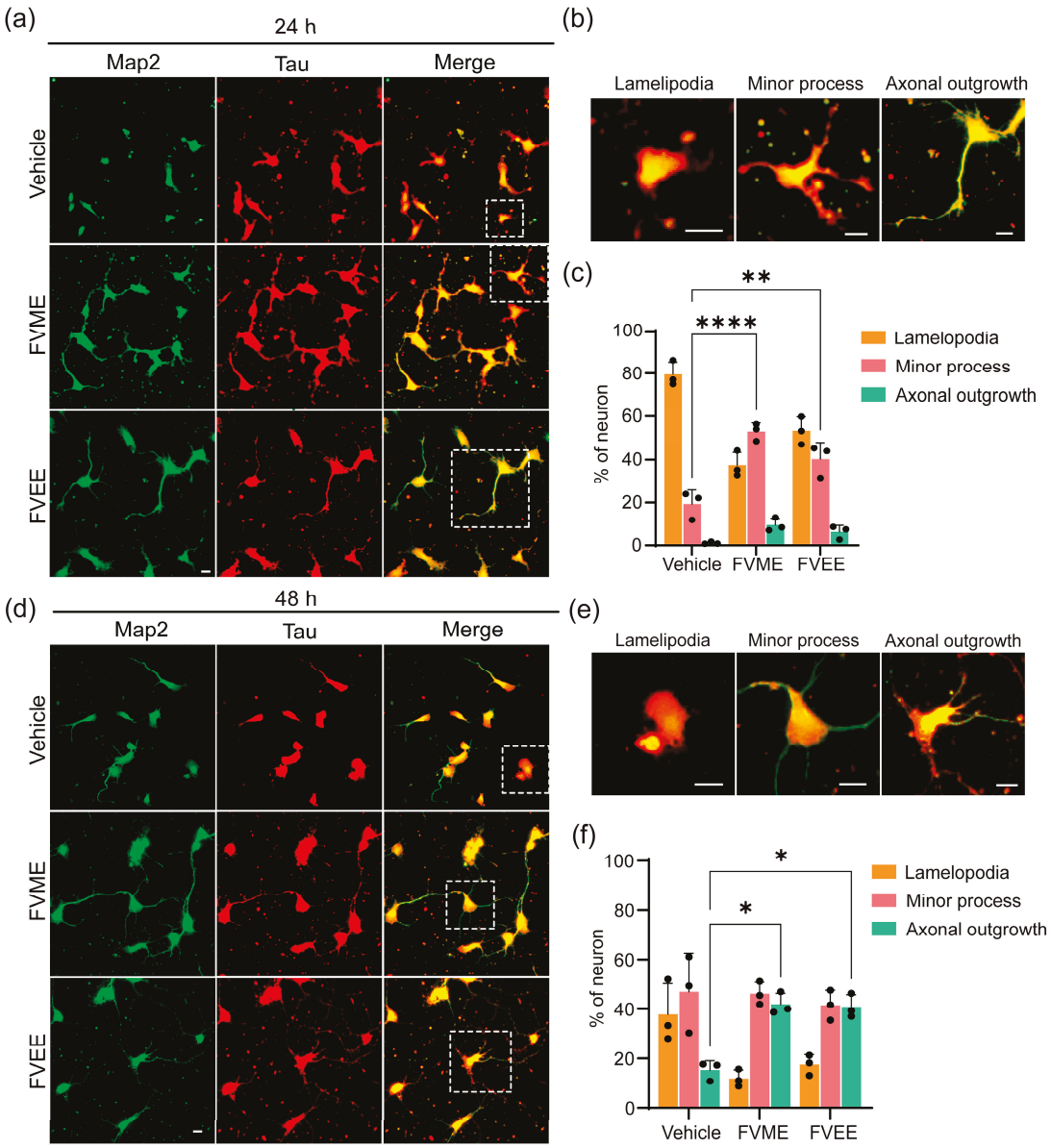

Figure 3. FVME and FVEE significantly promote neuronal maturation in the early stage of neuronal development. (**a**) Neuronal growth in the vehicle/FVME/FVEE-treated conditions at 24 h, immunostained with Map2 (neuronal marker, green) and Tau (dendritic marker, red). Representative images showing neuronal growth stages (lamellipodia, minor process, axonal outgrowth) at 24 h (**b**) and the corresponding statistical analysis (**c**). (**d**) Microscopic images showing the neuronal growth in the vehicle/FVME/FVEE-treated conditions at 48 h, immunostained with Map2 (green) and Tau (red). Representative images show neuronal growth stages (lamellipodia, minor process, axonal outgrowth) at 48 h (**e**) and the corresponding statistical analysis (**f**). Each statistical analysis presents data as mean ± SD from three independent biological replicates, with individual data points shown. Statistical significance was assessed by one-way ANOVA followed by Dunnett's multiple comparisons test versus vehicle (* $p < 0.05$; ** $p < 0.01$; **** $p < 0.0001$). Scale bar: 10 µm. FVME, *Flammulina velutipes* methanolic extract; FVEE, *Flammulina velutipes* ethanolic extract.

3.3.3. Axonal Development Due to FVME

Because the FVME showed a prominent neuronal development effect, we explored the effect of FVME (100 µg/mL concentration) on neuronal branching by "Sholl analysis". The morphological analysis showed that FVME significantly improved the axonal growth outcome in cells growing until the fifth day of the culture. The analysis showed FVME significantly improved axon length (Figure 4b) and branching of neurons (Figure 4c). As

represented by the statistical analysis (Figure 4c), FVME significantly increased the number and length of primary, secondary, and tertiary branches of axons. Neurons immunostained with the axonal marker Ankyrin G and microtubule marker α-Tubulin are represented in Figure 4a.

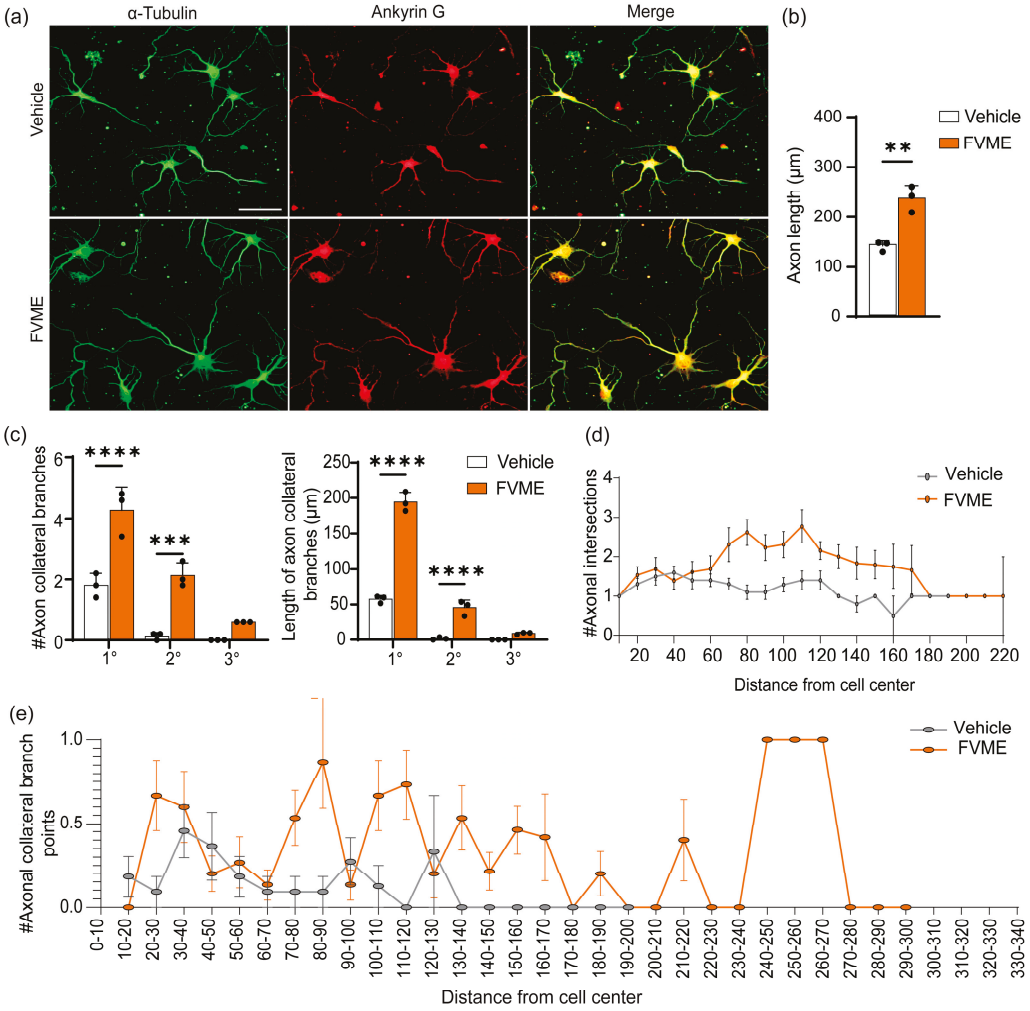

Figure 4. FVME promotes axonal growth significantly. (**a**) The primary cultured neurons were grown until DIV5. Neurons treated with the vehicle or FVME were immunostained with Ankyrin G (axonal marker, red) and α-Tubulin (microtubule marker, green). Morphological analysis showed that FVME significantly improved axonal length (**b**), axonal collateral branching (primary, secondary, and tertiary), and the length of axonal collateral branches (**c**). Sholl analysis of neurons revealed the number of axonal intersections (**d**) and axonal branching points (**e**). Data are presented as mean ± SD from three independent biological replicates, with individual data points shown. Statistical significance was determined using Student's *t*-test (** $p < 0.01$; *** $p < 0.001$; **** $p < 0.0001$). Scale bar: 50 µm. FVME, *Flammulina velutipes* methanolic extract.

For more detailed insight, we performed "Sholl analysis", which showed that FVME treatment increased axonal intersection and collateral branching, which eventually improved the cytoarchitecture of the neurons (Figure 4d,e).

Neurons treated with FVME had axonal intersections increase by 1.64-fold compared to vehicle-treated neurons (Figure 4d). Again, neurons treated with FVME showed axonal intersection up to the circle of 220 µm, while control neurons exhibited it only up to the 190 µm concentric Sholl circle. Furthermore, FVME increased the collateral branching points by 3.04-fold compared to the vehicle (Figure 4e), and thus, collateral branching

points for FVME-treated neurons could be observed up to the 270 µm Sholl circle, while there were none beyond 120 µm in the vehicle treatment.

3.3.4. Dendritogenic Arborization Due to FVME

Dendritic branching is a crucial factor for memory storage. So next, we analyzed the dendritic development after FVME treatment and incubation until DIV5 (Figure 5). The morphological analysis showed that FVME treatment promoted neurons to upregulate the number of dendrites and branches (Figure 5a,b). Firstly, the number and length of primary dendrites were significantly increased by FVME treatment (Figure 5c). Secondly, the number and length of branches (primary and secondary) of dendrites were elevated significantly (Figure 5d).

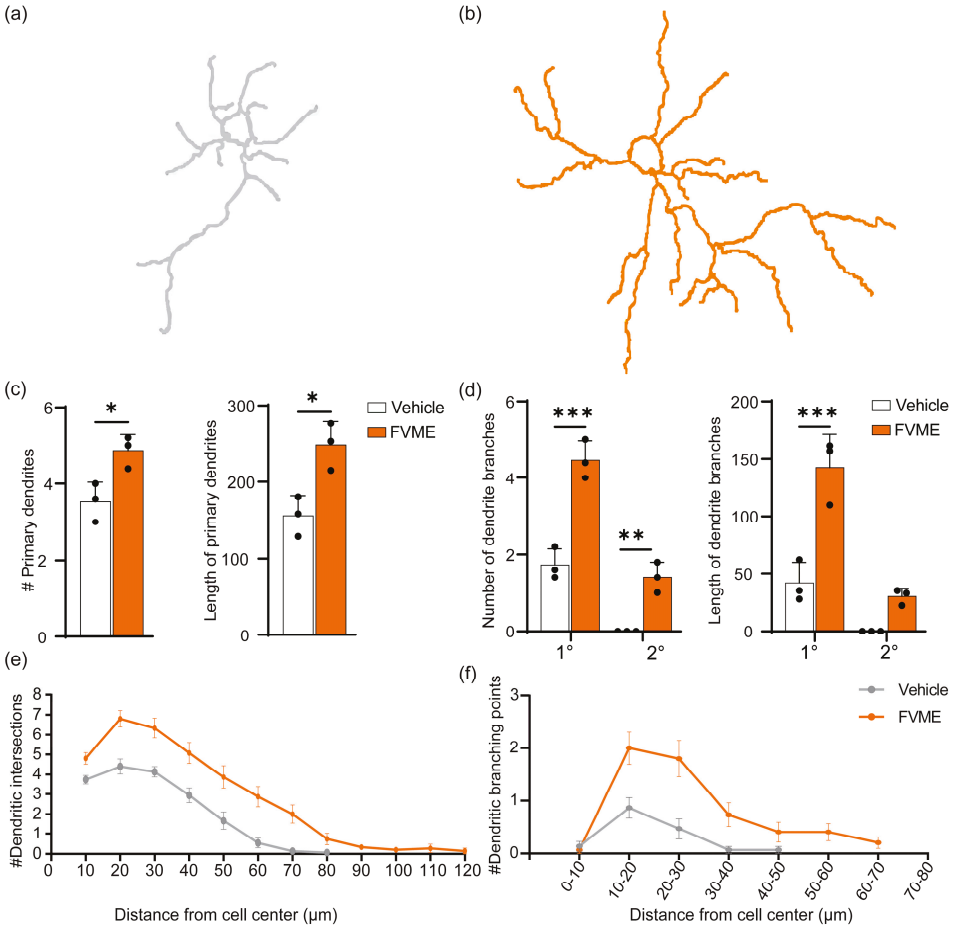

Figure 5. FVME upregulated dendritic arborization. Representative neurons traced for Sholl analysis are shown in (**a**,**b**), for the vehicle and FVME treatment, respectively. (**c**) Statistical analysis shows that FVME treatment significantly increased the number and length of primary dendrites. (**d**) Statistical analysis shows that FVME significantly increased the number and length of dendritic branches. Sholl analysis revealed numbers of dendritic intersections (**e**) and numbers of dendritic branching points (**f**), which were higher in the case of FVME treatment. Data are presented as mean ± SD from three independent biological replicates, with individual data points shown. Statistical significance was determined using Student's *t*-test (* $p < 0.05$; ** $p < 0.01$; *** $p < 0.001$). FVME, *Flammulina velutipes* methanolic extract.

Later, Sholl analysis also revealed an improvement in dendritic arborization. Treatment with FVME enhanced dendritic intersection 1.63-fold compared to the vehicle (Figure 5e). Also, dendritic branching points were increased 3.5-fold compared to those under the vehicle (Figure 5f). Altogether, this data suggests that FVME promotes dendritic development.

3.4. FVME and FVEE Protect Neurons Against H/R Injury

To evaluate the neuroprotective effect of FVME and FVEE, we induced hypoxia-mediated oxidative stress and cellular injury. Neurons are especially susceptible to hypoxia, as the absence of oxygen causes neuronal injury, initiates neuronal death, stops neuronal function, and restricts synaptic transmission [36]. Our experiment induced hypoxia for 4 h and analyzed the viability by trypan blue assay after 4 days of hypoxia.

Figure 6a,b shows that FVEE significantly increased neuronal viability compared to the vehicle treatment. FVEE at a 100 µM concentration significantly attenuated hypoxia-mediated neuronal death. In the case of FVME, all concentrations showed a significant neuroprotective effect compared to the vehicle (Figure 6c,d). However, the 60 µM concentration showed the best neuroprotective effect based on neuronal viability. These outcomes suggest that both FVME and FVEE can provide neuroprotection against hypoxia-induced brain injury and neuronal death.

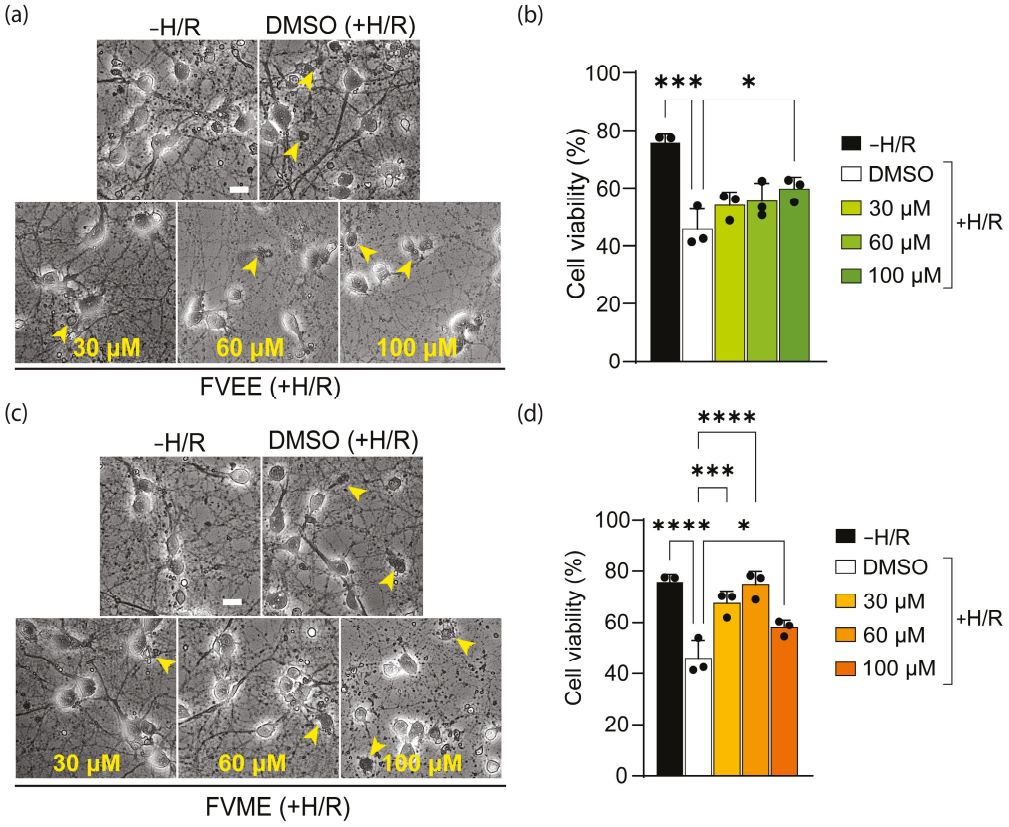

Figure 6. Neuroprotective effect of extracts (FVEE/FVME) on hypoxia-mediated neuronal death. (**a**) represents bright-field images of trypan blue-stained primary neurons grown until DIV13 in hypoxia/reoxygenation (H/R) conditions in the presence of the vehicle or various concentrations of FVEE. (**b**) The statistical analysis shows that various doses of FVEE improved neuronal viability; however, 100 µM significantly improved neuronal viability under H/R injury. (**c**) represents bright-field images of trypan blue-stained primary neurons grown until DIV13 in H/R conditions in the presence of the vehicle or various concentrations of FVME. (**d**) The statistical analysis shows that various doses of FVME (30, 60, 100 µM) improved neuronal viability significantly under H/R injury. The small arrow shows the dead cells in the culture. Data are presented as mean ± SD from three independent biological replicates, with individual data points shown. Statistical significance was by one-way ANOVA followed by Dunnett's multiple comparisons test versus DMSO (* $p < 0.05$; *** $p < 0.001$; **** $p < 0.0001$). Scale bar = 20 µm. FVME, *Flammulina velutipes* methanolic extract; FVEE, *Flammulina velutipes* ethanolic extract.

3.5. Mechanistic Analysis of the Neurogenic Effect of FVME and FVEE

Neuritogenesis is facilitated by neurotropic signaling pathways, wherein neurotrophins activate NTRK receptors and initiate downstream cascades that govern axonal and dendritic growth [37]. Furthermore, by activating NTRK receptors, this pathway is also implicated in neuroprotection by initiating neuronal survival pathways and inhibiting apoptosis [38–40]. Therefore, we explored whether the neurotropic signaling pathway is responsible for the neurotrogenic activity of FVME and FVEE. Using both NTRK1 and NTRK2 receptor inhibitors, we analyzed neuronal morphological growth and found neuronal growth inhibition in the presence of the inhibitors. We used GW441756 and Ana 12 as NTRK1 and NTRK2 inhibitors, respectively. Figure 7 shows neuronal growth restriction by inhibition of NTRK receptor subtypes. The representative images show neurons treated with the extract in the presence or absence of inhibitors (Figure 7a). The reduction in the morphological parameters (the sum of all the processes, number of primary processes, and length of the longest process) illustrates evidence that FVME and FVEE exert neurotropic action via the NTRK signaling pathway (Figure 7b–d). Statistical analysis showed that FVEE-mediated neuronal growth depends on NTRK1 and NTRK2 receptors, as both inhibitors downregulated the growth. Nevertheless, in the case of FVME, the growth parameters were mainly inhibited by Ana-12 (NTRK1 inhibitor), indicating NTRK1 receptor-mediated neurotropic action. We used 100 µM of FVEE and 60 µM of FVME.

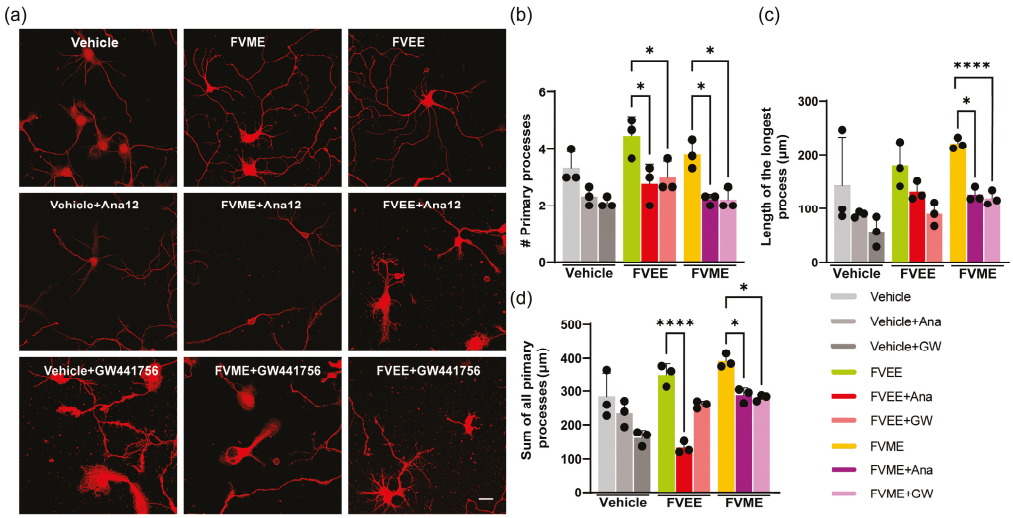

Figure 7. NTRK1 and NTRK2 receptors mediated neurodevelopment by FVME and FVEE. (**a**) represents neurons (DIV3) stained with tubulin in the absence or presence of the vehicle/FVME/FVEE with the NTRK1 inhibitor GW441756 and the NTRK2 inhibitor ANA12. Statistical analysis shows that neurodevelopmental parameters (the number of primary processes (**b**), length of the longest process (**c**), sum of all the processes (**d**) mediated by FVEE were inhibited by Ana12 and GW441756. FVME-mediated neuronal growth parameters were predominantly inhibited by Ana12. Scale bar = 20 µm. Data are presented as mean ± SD from three independent biological replicates, with individual data points shown. Statistical significance was determined by one-way ANOVA followed by Dunnett's multiple comparisons test versus vehicle (* $p < 0.05$; **** $p < 0.0001$). FVME, *Flammulina velutipes* methanolic extract; FVEE, *Flammulina velutipes* ethanolic extract; NTRK1, Neurotrophic tyrosine kinase receptor type 1; NTRK2, Neurotrophic tyrosine kinase receptor type 2.

3.6. In Silico-Based Identification of Potential NTRK Receptor Modulators

Next, we further assessed the binding efficiency of the compounds identified from methanol and ethanol extracts of *F. velutipes* by GC-MS, for two potential targets, NTRK1 and NTRK2, using molecular docking analysis and binding energy calculation. At first, we conducted molecular docking using an extra-precision algorithm, followed by MM-GBSA

binding energy calculation, which revealed that all compounds exhibited binding energy ranging from −9 kcal/mol to −38 kcal/mol with the NTRK1 receptor and from −10 to −43 kcal/mol with the NTRK2 receptor (Figures 8a and S2). Tricyclo [3.3.0.0(2,8)]octan-3-one, 4-[2-(m-anisyl)ethyl]-8-methyl- and benzenemethanol, .alpha.-(2-aminocyclopentyl)- identified in methanol extracts had the highest binding energy scores with NTRK1 and NTRK2 receptors, where the binding energies of tricyclo [3.3.0.0(2,8)]octan-3-one, 4-[2-(m-anisyl)ethyl]-8-methyl- with NTRK1 and NTRK2 were −36.9 kcal/mol and −30.3 kcal/mol, respectively, whereas the binding energies of benzenemethanol, .alpha.-(2-aminocyclopentyl)- were −36.2 kcal/mol and −32 kcal/mol, respectively (Figure S2). In contrast, in ethanolic extracts, hentriacontane and 5-acetoxymethyl-2,6,10-trimethyl-2,9-undecadien-6-ol had the highest binding energy scores, and Figure S2 demonstrates that the binding energies of hentriacontane with NTRK1 and NTRK2 were −38.2 kcal/mol and −43.7 kcal/mol, whereas the binding energies of 5-acetoxymethyl-2,6,10-trimethyl-2,9-undecadien-6-ol were −37.1 kcal/mol and −37.7 kcal/mol, respectively.

The controls, 3β, 6β-dichloro-5-hydroxy-5α-cholestane and 7,8-dihydroxyflavone, had binding energies of 34 kcal/mol and 30.9 kcal/mol against NTRK1 and NTRK2 receptors, respectively (Figure 8a). As shown in Figure 8b, the control, 3β, 6β-dichloro-5-hydroxy-5α-cholestane formed one H-bond with NTRK1 with the residue Gln350 and several hydrophobic interactions with Phe317, Leu322, Phe327, Thr352, Val354, and Asn355, whereas the other control, 7,8-dihydroxyflavone, formed double H-bonds with NTRK2 with the residue Asn350 and some hydrophobic interactions with Tyr319, Tyr329, and Ile330. Two compounds, linalool and dodecane, 1-fluoro-, were found common in both methanol and ethanol extracts, where linalool had binding energies of −23 kcal/mol and −23.2 kcal/mol with NTRK1 and NTRK2 receptors, respectively, whereas dodecane, 1-fluoro- showed binding energies of −20.3 kcal/mol and −25.5 kcal/mol, respectively. However, their binding energies with NTRK1 and NTRK2 were notably lower (Figure 8a). Since both compounds were found in both methanol and ethanol extracts, we analyzed their interaction profiles, which showed that both compounds formed interactions with several residues, including a few residues that formed bonds with controls (Figure 8b). As shown in Figure 8b, linalool formed a single hydrophobic interaction with Phe317 with NTRK1 receptors, whereas it formed multiple H-bonds with Val321 and Asn323. On the other hand, with NTRK2, linalool formed dual hydrophobic interactions with Tyr319 and Leu324 and double H-bonds with Ile323 and Ans325 (Figure 8b). Dodecane, 1-fluoro- formed several hydrophobic interactions with NTRK1 receptors with Phe327, Thr352, and Val354 residues. In contrast, dodecane, 1-fluoro- formed many hydrophobic interactions with NTRK2 receptors with Tyr319, Leu324, Tyr329, and Ile330 residues (Figure 8b).

We further tested the neuritogenic effect of linalool on primary culture hippocampal neurons in comparison to our experimental extracts, as linalool is a well-established compound that is involved in treating neurodegeneration [41–43] and has neuroprotective [42,44] and memory-boosting activity [45]. As shown in Figure S3, linalool significantly increased both the number and the total length of primary neurites compared to the control. In contrast, FVME significantly enhanced all measured parameters relative to the control and linalool.

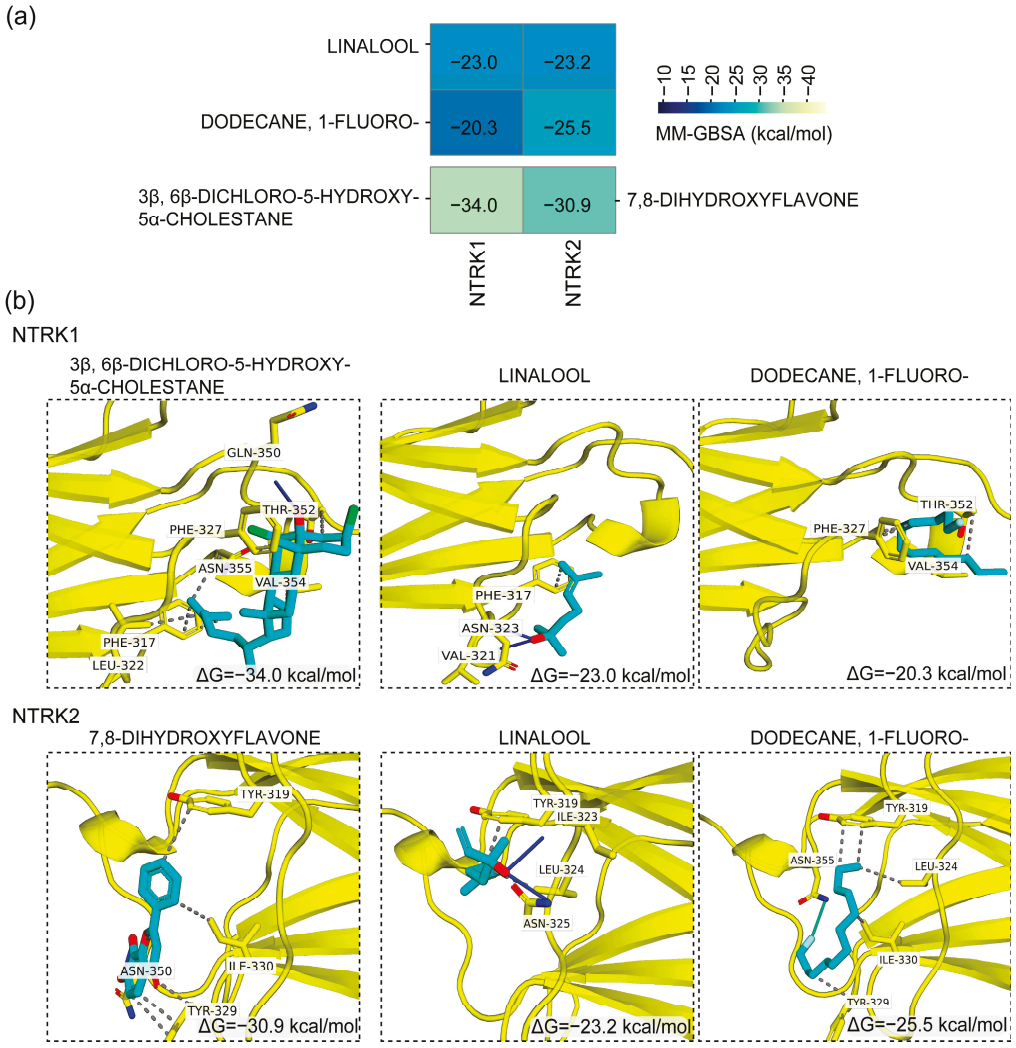

Figure 8. MM-GBSA binding energy-based screening and molecular interactions of compounds identified in methanol and ethanol extracts of *Flammulina velutipes*. (**a**) Heatmap of MM-GBSA binding energy of controls and compounds commonly found in methanol and ethanol extracts of *F. velutipes*. (**b**) Three-dimensional protein–ligand interaction profiling of controls and compounds from the methanol and ethanol extracts of *F. velutipes* with NTRK1 (top panel) and NTRK2 (bottom panel) receptors. The left panel displays 3D protein–ligand interactions of two controls, 3β, 6β-dichloro-5-hydroxy-5α-cholestane and 7,8-dihydroxyflavone, in the top and bottom panels, respectively, whereas the middle and right panels depict 3D protein–ligand interactions of compounds found in ethanolic and methanolic extracts of *F. velutipes*. In this case, the protein backbone and ligands are visualized using yellow and light blue colors, respectively, whereas the hydrophobic interactions and H-bonds are shown as dashed gray lines and solid blue lines, respectively. NTRK1, Neurotrophic tyrosine kinase receptor type 1; NTRK2, Neurotrophic tyrosine kinase receptor type 2.

4. Discussion

Neuroprotective and brain-boosting neurotrophic compounds found in natural sources can be used as future medicinal candidates for managing neurodegeneration. Loss of neurotrophic support is a hallmark of neurite degeneration leading to neurodegenerative disorders (NDs). Thus, pharmacological agents that promote neuritogenesis may offer therapeutic potential by reversing early pathological changes.

In this study, we demonstrated the efficacy of FVEE and FVME in promoting early development and differentiation of primary hippocampal neurons. From the initial viability, maturation, and neuro-morphological analysis, we found that FVME and FVEE initiate neuronal viability, neurite outgrowth, and network formation, indicating the presence of

neuro-developmental bioactive compounds with both neurotrophic and neuroprotective properties. However, neuromorphological analysis, early developmental analysis, and viability studies show that FVME has more neurodevelopmental potential than FVEE.

Across early stages (Stages I–II), both FVME and FVEE significantly promoted neurons from the early developmental phase (lamellipodia) to the mature phases (neurons with minor processes and axonal outgrowth). In both neuronal growth analysis and early development, FVME showed more prominent action than FVEE; therefore, we further analyzed the effect of FVME on mature neurodevelopmental stages. In the mature stage, axonal and dendritic extension and branching are key parameters for establishing robust neural networks. These morphological enhancements include improved synaptic plasticity and cognitive function [46,47]. According to our experimental findings, FVME significantly upregulated axonal and dendritic arborization and architecture (Figures 4 and 5). Upregulated axonal and dendritic arborization enhances neuronal connectivity by promoting synaptic architecture and network integration, thus implicating cognitive enhancement and memory function [48–50].

We further performed GC-MS analysis of ethanolic and methanolic extracts to characterize the key metabolites and the potential bioactive compounds promoting *F. velutipes*-mediated neuronal growth. GC-MS analysis identified 21 and 22 metabolites in FVEE and FVME, respectively, which were subsequently subjected to molecular docking against NTRK receptors. The docking results indicated multiple bioactive compounds from both extracts exhibiting high binding affinity toward NTRK receptors. Among the metabolites common to both extracts, linalool was selected for further validation in primary hippocampal culture. Linalool treatment elicited a significant neurotropic response, suggesting that the neurotropic activity of FVME and FVEE is partially attributable to linalool (Supplementary Figure S3). Furthermore, compared to FVME, the effect of linalool was less effective, which may be explained by synergistic interactions among multiple bioactive constituents of FVME, conferring a broader and stronger neuritogenesis effect than linalool alone.

GC-MS analysis identified linalool in both FVME and FVEE at a retention time of 9.17 min, consistent with previous findings [51,52], and this was reported to be detected by a similar thermal decomposition used in other studies [53–55]. The relative abundance was higher with FVME (0.2335% peak area) than with FVEE (0.089%). Linalool is a monoterpene volatile compound mostly available in aromatic plants [56], and many studies have established linalool as a potential phytochemical for treating neuronal diseases [42,57,58]. The binding analysis study with NTRK receptors suggested that linalool could bind effectively with NTRK receptors. Our molecular docking and binding energy calculation revealed that linalool effectively binds to both NTRK receptors. These interactions included residue Phe317 in NTRK1 and Tyr319 in NTRK2, which were also observed in controls (Figure 8b). The observed interaction between control and Phe317 in NTRK1 aligns with previous findings. Additionally, the control also formed further interactions within the NTRK1 at residues Leu322, Phe327, Gln350, Thr352, Val354, and Asn355 (Figure 8b), all of which have been documented in prior research [25].

Our findings highlight the NTRK signaling pathway-dependent neurodevelopmental mechanism through which FVME and FVEE promote neuronal growth, axonal and dendritic sprouting, and survival (Figure 9). While neurotrophin signaling appears to be a primary mediator, we do not exclude the possibility that the extracts modulate additional pathways through their diverse chemical constituents. A limitation of our study is that the experiments were conducted exclusively in vitro using crude extracts and linalool, which may not fully reflect the complexity of in vivo neuronal environments. Moreover, while GC-MS allowed us to identify several metabolites, thermal decomposition cannot be excluded, and other major bioactive compounds besides linalool remain to be investigated.

Finally, the lack of standardized positive controls limits the extent to which the neurotrophic potency of FVME and FVEE can be directly compared with known pharmacological agents. These results position *F. velutipes* extracts, particularly the methanolic fraction, as a promising natural source of neurotrophic compounds, as suggested by in silico molecular docking and binding energy calculations. Future in vitro and in vivo studies and detailed characterization of additional metabolites will be critical to translate these findings into potential therapeutic strategies for neurodegenerative disorders.

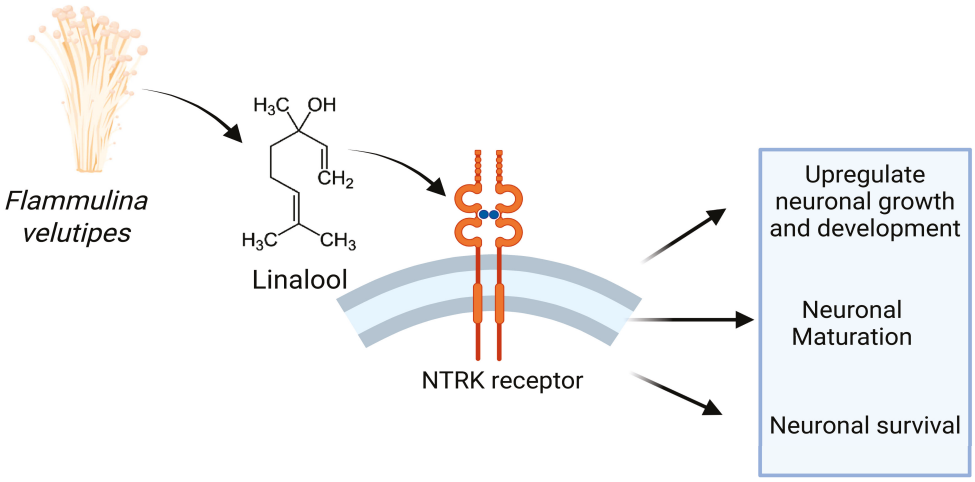

Figure 9. The pictorial representation shows that *Flammulina velutipes* modulates neuronal growth and viability in the NTRK-derived pathway. The NTRK receptors are activated by neurotrophic metabolites in the mushroom extracts and eventually promote neuronal maturation, morphological development, axonal and dendritic cytoarchitecture, and neuronal survival.

5. Conclusions

In this present work, we experimentally proved the role of methanolic and ethanolic extracts of *F. velutipes* mushroom as neurotrophic agents. Our in vitro analysis revealed that both extracts of *F. velutipes* mushroom have significant neuronal developmental and neuroprotective effects that can be useful in treating neurodegenerative and memory-related disorders. Altogether, this mushroom has the potential to be used as a medicinal agent for modulating the NTRK-dependent signaling pathway. Additional neuro-morphological and in silico molecular docking analysis also proved that bioactive metabolites of these extracts interact with NTRK receptors. These findings suggest that *F. velutipes* should be studied more and analyzed mechanistically for future drug design for neurodegenerative diseases and dementia.

Supplementary Materials: The following supporting information can be downloaded at https://www.mdpi.com/article/10.3390/nu17193107/s1. Figure S1: Dose-dependent effect of FVME and FVEE on neuritogenesis in primary hippocampal neurons. The line plot represents the average number of primary processes per neuron. Data are presented as mean ± SD from three independent biological replicates. FVME, *Flammulina velutipes* methanolic extract; FVEE, *Flammulina velutipes* ethanolic extract. Figure S2: Color-coded heatmap illustrating the MMGBSA binding energy of compounds found in methanol (left panel) and ethanol (right panel) extracts of *Flammulina velutipes*. Figure S3: Neuritogenic effect of linalool on primary neuronal culture. Morphological analysis showing the number of primary processes, the length of the longest process, and the total length of the primary processes. Data are presented as mean ± SD from three independent biological replicates. Statistical significance was assessed by one-way ANOVA followed by Dunnett's multiple comparisons test versus vehicle (* $p < 0.05$, ** $p < 0.01$, *** $p < 0.001$, **** $p < 0.0001$). Table S1: List of compounds identified from GC-MS analysis (ethanol extract, FVEE) along with their retention time,

peak area, and 2D structure. Table S2: List of compounds identified from GC-MS analysis (methanol extract, FVME) along with their retention time, peak area, and 2D structure.

Author Contributions: Conceptualization, S.M. and R.D.; methodology, S.M.; software, R.D. and M.A.B.; validation, S.M.; R.D. and M.A.B.; formal analysis, K.M.; investigation, S.M. and M.A.B.; resources, K.M. and I.S.M.; data curation, S.M. and R.D.; writing—original draft preparation, S.M.; writing—review and editing, R.D.; visualization, S.M.; supervision, R.D., I.S.M. and K.M.; project administration, S.M., R.D. and I.S.M.; funding acquisition, I.S.M. All authors have read and agreed to the published version of the manuscript.

Funding: The study was supported by the Basic Science Research Program through the National Research Foundation of Korea (NRF) (NRF-2021R1A2C1008564 to I.S.M.).

Institutional Review Board Statement: Animal handling was performed based on the guidelines provided by the Institutional Animal Care and Use Committee of Dongguk University, College of Medicine, Gyeongju, Republic of Korea, on 4 May 2023 (approval certificate number IACUC-2023-07).

Informed Consent Statement: Not applicable.

Data Availability Statement: Data presented in the manuscript will be available upon reasonable request.

Conflicts of Interest: The authors declare no conflicts of interest.

References

1. Luo, J.; Ganesan, K.; Xu, B. Unlocking the Power: New Insights into the Anti-Aging Properties of Mushrooms. *J. Fungi* **2024**, *10*, 215. [CrossRef]
2. Das, A.K.; Nanda, P.K.; Dandapat, P.; Bandyopadhyay, S.; Gullón, P.; Sivaraman, G.K.; McClements, D.J.; Gullón, B.; Lorenzo, J.M. Edible Mushrooms as Functional Ingredients for Development of Healthier and More Sustainable Muscle Foods: A Flexitarian Approach. *Molecules* **2021**, *26*, 2463. [CrossRef] [PubMed]
3. Agarwal, S.; Fulgoni Iii, V.L. Nutritional impact of adding a serving of mushrooms to USDA Food Patterns—A dietary modeling analysis. *Food Nutr. Res.* **2021**, *65*, 5618. [CrossRef] [PubMed]
4. You, S.W.; Hoskin, R.T.; Komarnytsky, S.; Moncada, M. Mushrooms as Functional and Nutritious Food Ingredients for Multiple Applications. *ACS Food Sci. Technol.* **2022**, *2*, 1184–1195. [CrossRef]
5. Tang, C.; Hoo, P.C.; Tan, L.T.; Pusparajah, P.; Khan, T.M.; Lee, L.H.; Goh, B.H.; Chan, K.G. Golden Needle Mushroom: A Culinary Medicine with Evidenced-Based Biological Activities and Health Promoting Properties. *Front. Pharmacol.* **2016**, *7*, 474. [CrossRef]
6. Ding, Y.; Chen, S.; Wang, H.; Li, S.; Ma, C.; Wang, J.; Cui, L. Identification of Secondary Metabolites in *Flammulina velutipes* by UPLC-Q-Exactive-Orbitrap MS. *J. Food Qual.* **2021**, *2021*, 4103952. [CrossRef]
7. Su, A.; Yang, W.; Zhao, L.; Pei, F.; Yuan, B.; Zhong, L.; Ma, G.; Hu, Q. *Flammulina velutipes* polysaccharides improve scopolamine-induced learning and memory impairment in mice by modulating gut microbiota composition. *Food Funct.* **2018**, *9*, 1424–1432. [CrossRef]
8. Yang, W.; Fang, Y.; Liang, J.; Hu, Q. Optimization of ultrasonic extraction of *Flammulina velutipes* polysaccharides and evaluation of its acetylcholinesterase inhibitory activity. *Food Res. Int.* **2011**, *44*, 1269–1275. [CrossRef]
9. Yang, W.; Yu, J.; Zhao, L.; Ma, N.; Fang, Y.; Pei, F.; Mariga, A.M.; Hu, Q. Polysaccharides from *Flammulina velutipes* improve scopolamine-induced impairment of learning and memory of rats. *J. Funct. Foods* **2015**, *18*, 411–422. [CrossRef]
10. Dong, Y.; Hu, Q.; Zhao, L.; Ma, G.; Ma, N.; Zhang, J.; Ji, Y.; Liu, L. A novel neuroprotective peptide YVYAETY identified and screened from *Flammulina velutipes* protein hydrolysates attenuates scopolamine-induced cognitive impairment in mice. *Food Funct.* **2024**, *15*, 6082–6094. [CrossRef]
11. Burns, A.; Zaudig, M. Mild cognitive impairment in older people. *Lancet* **2002**, *360*, 1963–1965. [CrossRef] [PubMed]
12. Small, G.W. What we need to know about age related memory loss. *BMJ* **2002**, *324*, 1502–1505. [CrossRef] [PubMed]
13. Watson, R. Research into ageing and older people. *J. Nurs. Manag.* **2008**, *16*, 99–104. [CrossRef] [PubMed]
14. Jing, W.; Willis, R.; Feng, Z. Factors influencing quality of life of elderly people with dementia and care implications: A systematic review. *Arch. Gerontol. Geriatr.* **2016**, *66*, 23–41. [CrossRef]
15. Holopainen, A.; Siltanen, H.; Pohjanvuori, A.; Mäkisalo-Ropponen, M.; Okkonen, E. Factors Associated with the Quality of Life of People with Dementia and with Quality of Life-Improving Interventions: Scoping Review. *Dementia* **2019**, *18*, 1507–1537. [CrossRef]

16. Orme, T.; Hernandez, D.; Ross, O.A.; Kun-Rodrigues, C.; Darwent, L.; Shepherd, C.E.; Parkkinen, L.; Ansorge, O.; Clark, L.; Honig, L.S.; et al. Analysis of neurodegenerative disease-causing genes in dementia with Lewy bodies. *Acta Neuropathol. Commun.* **2020**, *8*, 5. [CrossRef]
17. Birajdar, S.V.; Mulchandani, M.; Mazahir, F.; Yadav, A.K. Chapter 1—Dementia and neurodegenerative disorder: An introduction. In *Nanomedicine-Based Approaches for the Treatment of Dementia*; Gupta, U., Kesharwani, P., Eds.; Academic Press: Cambridge, MA, USA, 2023; pp. 1–36.
18. Nie, R.-Z.; Luo, H.-M.; Liu, Y.-P.; Wang, S.-S.; Hou, Y.-J.; Chen, C.; Wang, H.; Lv, H.-L.; Tao, X.-Y.; Jing, Z.-H.; et al. Food Functional Factors in Alzheimer's Disease Intervention: Current Research Progress. *Nutrients* **2024**, *16*, 3998. [CrossRef]
19. Zhang, Y.; Li, H.; Yang, X.; Jin, G.; Zhang, Y. Cognitive-enhancing effect of polysaccharides from *Flammulina velutipes* on Alzheimer's disease by compatibilizing with ginsenosides. *Int. J. Biol. Macromol.* **2018**, *112*, 788–795. [CrossRef]
20. Mitra, S.; Bhartiya, P.; Kaushik, N.; Nhat Nguyen, L.; Wahab, R.; Bekeschus, S.; Choi, E.H.; Kaushik, N.K. Plasma-Treated *Flammulina velutipes*-Derived Extract Showed Anticancer Potential in Human Breast Cancer Cells. *Appl. Sci.* **2020**, *10*, 8395. [CrossRef]
21. Mitra, S.; Veerana, M.; Choi, E.H.; Park, G. Effects of Pre-Treatment Using Plasma on the Antibacterial Activity of Mushroom Surfaces. *Foods* **2021**, *10*, 1888. [CrossRef]
22. Mohibbullah, M.; Hannan, M.A.; Choi, J.-Y.; Bhuiyan, M.M.H.; Hong, Y.-K.; Choi, J.-S.; Choi, I.S.; Moon, I.S. The Edible Marine Alga Gracilariopsis chorda Alleviates Hypoxia/Reoxygenation-Induced Oxidative Stress in Cultured Hippocampal Neurons. *J. Med. Food* **2015**, *18*, 960–971. [CrossRef]
23. Wu, Y.; Ding, A.-S.; Wu, L.-Y.; Ma, Z.-M.; Fan, M. Establishment of the model of oxygen-glucose deprivation in vitro rat hippocampal neurons. *Zhongguo Ying Yong Sheng Li Xue Za Zhi* **2003**, *19*, 197–200. [PubMed]
24. Chiu, Y.J.; Lin, T.H.; Chang, K.H.; Lin, W.; Hsieh-Li, H.M.; Su, M.T.; Chen, C.M.; Sun, Y.C.; Lee-Chen, G.J. Novel TRKB agonists activate TRKB and downstream ERK and AKT signaling to protect Aβ-GFP SH-SY5Y cells against Aβ toxicity. *Aging* **2022**, *14*, 7568–7586. [CrossRef] [PubMed]
25. Hannan, M.A.; Haque, M.N.; Dash, R.; Alam, M.; Moon, I.S. 3β, 6β-dichloro-5-hydroxy-5α-cholestane facilitates neuronal development through modulating TrkA signaling regulated proteins in primary hippocampal neuron. *Sci. Rep.* **2019**, *9*, 18919. [CrossRef] [PubMed]
26. Banerjee, K.; Gupta, U.; Gupta, S.; Wadhwa, G.; Gabrani, R.; Sharma, S.K.; Jain, C.K. Molecular docking of glucosamine-6-phosphate synthase in *Rhizopus oryzae*. *Bioinformation* **2011**, *7*, 285–290. [CrossRef]
27. Friesner, R.A.; Banks, J.L.; Murphy, R.B.; Halgren, T.A.; Klicic, J.J.; Mainz, D.T.; Repasky, M.P.; Knoll, E.H.; Shelley, M.; Perry, J.K.; et al. Glide: A New Approach for Rapid, Accurate Docking and Scoring. 1. Method and Assessment of Docking Accuracy. *J. Med. Chem.* **2004**, *47*, 1739–1749. [CrossRef]
28. Friesner, R.A.; Murphy, R.B.; Repasky, M.P.; Frye, L.L.; Greenwood, J.R.; Halgren, T.A.; Sanschagrin, P.C.; Mainz, D.T. Extra Precision Glide: Docking and Scoring Incorporating a Model of Hydrophobic Enclosure for Protein−Ligand Complexes. *J. Med. Chem.* **2006**, *49*, 6177–6196. [CrossRef]
29. Vijayakumar, B.; Umamaheswari, A.; Puratchikody, A.; Velmurugan, D. Selection of an improved HDAC8 inhibitor through structure-based drug design. *Bioinformation* **2011**, *7*, 134–141. [CrossRef]
30. Chen, X.; Zhang, F.; Liu, L.; Lei, B.-H.; Dong, X.; Yang, Z.; Li, H.; Pan, S. Li3AlSiO5: The first aluminosilicate as a potential deep-ultraviolet nonlinear optical crystal with the quaternary diamond-like structure. *Phys. Chem. Chem. Phys.* **2016**, *18*, 4362–4369. [CrossRef]
31. Hou, T.; Li, N.; Li, Y.; Wang, W. Characterization of domain-peptide interaction interface: Prediction of SH3 domain-mediated protein-protein interaction network in yeast by generic structure-based models. *J. Proteome Res.* **2012**, *11*, 2982–2995. [CrossRef]
32. Sun, H.; Li, Y.; Tian, S.; Xu, L.; Hou, T. Assessing the performance of MM/PBSA and MM/GBSA methods. 4. Accuracies of MM/PBSA and MM/GBSA methodologies evaluated by various simulation protocols using PDBbind data set. *Phys. Chem. Chem. Phys.* **2014**, *16*, 16719–16729. [CrossRef]
33. Sun, H.; Li, Y.; Shen, M.; Tian, S.; Xu, L.; Pan, P.; Guan, Y.; Hou, T. Assessing the performance of MM/PBSA and MM/GBSA methods. 5. Improved docking performance using high solute dielectric constant MM/GBSA and MM/PBSA rescoring. *Phys. Chem. Chem. Phys.* **2014**, *16*, 22035–22045. [CrossRef]
34. Li, J.; Abel, R.; Zhu, K.; Cao, Y.; Zhao, S.; Friesner, R.A. The VSGB 2.0 model: A next generation energy model for high resolution protein structure modeling. *Proteins* **2011**, *79*, 2794–2812. [CrossRef] [PubMed]
35. Mitra, S.; Munni, Y.A.; Dash, R.; Sultana, A.; Moon, I.S. Unveiling the effect of Withania somnifera on neuronal cytoarchitecture and synaptogenesis: A combined in vitro and network pharmacology approach. *Phytother. Res.* **2022**, *36*, 2524–2541. [CrossRef] [PubMed]
36. Nieber, K. Hypoxia and Neuronal Function Under In Vitro Conditions. *Pharmacol. Ther.* **1999**, *82*, 71–86. [CrossRef] [PubMed]
37. Chao, M.V. Neurotrophins and their receptors: A convergence point for many signalling pathways. *Nat. Rev. Neurosci.* **2003**, *4*, 299–309. [CrossRef]

38. Nguyen, T.L.; Kim, C.K.; Cho, J.H.; Lee, K.H.; Ahn, J.Y. Neuroprotection signaling pathway of nerve growth factor and brain-derived neurotrophic factor against staurosporine induced apoptosis in hippocampal H19-7/IGF-IR [corrected]. *Exp. Mol. Med.* **2010**, *42*, 583–595. [CrossRef]
39. Chen, A.; Xiong, L.J.; Tong, Y.; Mao, M. The neuroprotective roles of BDNF in hypoxic ischemic brain injury. *Biomed. Rep.* **2013**, *1*, 167–176. [CrossRef]
40. Saito, A.; Tominaga, T.; Chan, P.H. Neuroprotective role of neurotrophins: Relationship between nerve growth factor and apoptotic cell survival pathway after cerebral ischemia. *Curr. Atheroscler. Rep.* **2005**, *7*, 268–273. [CrossRef]
41. Sabogal-Guáqueta, A.M.; Osorio, E.; Cardona-Gómez, G.P. Linalool reverses neuropathological and behavioral impairments in old triple transgenic Alzheimer's mice. *Neuropharmacology* **2016**, *102*, 111–120. [CrossRef]
42. Chang, W.-H.; Hsu, H.-T.; Lin, C.-C.; An, L.-M.; Lee, C.-H.; Ko, H.-H.; Lin, C.-L.; Lo, Y.-C. Linalool, a Fragrance Compound in Plants, Protects Dopaminergic Neurons and Improves Motor Function and Skeletal Muscle Strength in Experimental Models of Parkinson's Disease. *Int. J. Mol. Sci.* **2024**, *25*, 2514. [CrossRef] [PubMed]
43. Yuan, C.; Shin, M.; Park, Y.; Choi, B.; Jang, S.; Lim, C.; Yun, H.S.; Lee, I.-S.; Won, S.-Y.; Cho, K.S. Linalool Alleviates Aβ42-Induced Neurodegeneration via Suppressing ROS Production and Inflammation in Fly and Rat Models of Alzheimer's Disease. *Oxidative Med. Cell. Longev.* **2021**, *2021*, 8887716. [CrossRef] [PubMed]
44. Pandur, E.; Major, B.; Rák, T.; Sipos, K.; Csutak, A.; Horváth, G. Linalool and Geraniol Defend Neurons from Oxidative Stress, Inflammation, and Iron Accumulation in In Vitro Parkinson's Models. *Antioxidants* **2024**, *13*, 917. [CrossRef] [PubMed]
45. Lee, B.K.; Jung, A.N.; Jung, Y.S. Linalool Ameliorates Memory Loss and Behavioral Impairment Induced by REM-Sleep Deprivation through the Serotonergic Pathway. *Biomol. Ther.* **2018**, *26*, 368–373. [CrossRef]
46. Lanoue, V.; Cooper, H.M. Branching mechanisms shaping dendrite architecture. *Dev. Biol.* **2019**, *451*, 16–24. [CrossRef]
47. Parekh, R.; Ascoli, G.A. Quantitative Investigations of Axonal and Dendritic Arbors:Development, Structure, Function, and Pathology. *Neuroscientist* **2015**, *21*, 241–254. [CrossRef]
48. Kirchner, J.H.; Euler, L.; Fritz, I.; Ferreira Castro, A.; Gjorgjieva, J. Dendritic growth and synaptic organization from activity-independent cues and local activity-dependent plasticity. *eLife* **2025**, *12*, RP87527. [CrossRef]
49. Ledda, F.; Paratcha, G. Mechanisms regulating dendritic arbor patterning. *Cell. Mol. Life Sci.* **2017**, *74*, 4511–4537. [CrossRef]
50. Peng, Y.R.; He, S.; Marie, H.; Zeng, S.Y.; Ma, J.; Tan, Z.J.; Lee, S.Y.; Malenka, R.C.; Yu, X. Coordinated changes in dendritic arborization and synaptic strength during neural circuit development. *Neuron* **2009**, *61*, 71–84. [CrossRef]
51. Jamann, N.; Jordan, M.; Engelhardt, M. Activity-Dependent Axonal Plasticity in Sensory Systems. *Neuroscience* **2018**, *368*, 268–282. [CrossRef]
52. Ginglinger, J.F.; Boachon, B.; Höfer, R.; Paetz, C.; Köllner, T.G.; Miesch, L.; Lugan, R.; Baltenweck, R.; Mutterer, J.; Ullmann, P.; et al. Gene coexpression analysis reveals complex metabolism of the monoterpene alcohol linalool in *Arabidopsis* flowers. *Plant Cell* **2013**, *25*, 4640–4657. [CrossRef] [PubMed]
53. Nie, C.-N.; Zhong, X.-X.; He, L.; Gao, Y.; Zhang, X.; Wang, C.-M.; Du, X. Comparison of different aroma-active compounds of Sichuan Dark brick tea (*Camellia sinensis*) and Sichuan Fuzhuan brick tea using gas chromatography–mass spectrometry (GC–MS) and aroma descriptive profile tests. *Eur. Food Res. Technol.* **2019**, *245*, 1963–1979. [CrossRef]
54. Xiao, M.; Zheng, F.; Xiao, M.; Qi, A.; Wang, H.; Dai, Q. Contribution of aroma-active compounds to the aroma of Lu'an Guapian tea. *Flavour Fragr. J.* **2022**, *37*, 83–95. [CrossRef]
55. Qu, F.-F.; Li, X.-H.; Wang, P.-Q.; Han, Y.-H.; Wu, Y.; Hu, J.-H.; Zhang, X.-F. Effect of thermal process on the key aroma components of green tea with chestnut-like aroma. *J. Sci. Food Agric.* **2023**, *103*, 657–665. [CrossRef] [PubMed]
56. Mączka, W.; Duda-Madej, A.; Grabarczyk, M.; Wińska, K. Natural Compounds in the Battle against Microorganisms-Linalool. *Molecules* **2022**, *27*, 6928. [CrossRef]
57. Satou, T.; Kamagata, M.; Nakashima, S.; Mori, K.; Yoshinari, M. Effects of Inhaled Linalool on the Autonomic Nervous System in Awake Mice. *Nat. Prod. Commun.* **2024**, *19*, 1934578X241232273. [CrossRef]
58. Chang, C.H.; Chang, S.T.; Liao, V.H. Potential anti-Parkinsonian's effect of S-(+)-linalool from *Cinnamomum osmophloeum* ct. linalool leaves are associated with mitochondrial regulation via *gas-1*, *nuo-1*, and *mev-1* in *Caenorhabditis elegans*. *Phytother. Res.* **2022**, *36*, 3325–3334. [CrossRef]

Disclaimer/Publisher's Note: The statements, opinions and data contained in all publications are solely those of the individual author(s) and contributor(s) and not of MDPI and/or the editor(s). MDPI and/or the editor(s) disclaim responsibility for any injury to people or property resulting from any ideas, methods, instructions or products referred to in the content.

nutrients

MDPI

Article

From Microbiota to Metabolomics: How *Corylus heterophylla* Fisch. Male Flower Extract Shields Mice from Cognitive Decline

Wei Lu [1,†], Yujie Li [1,†], Xinyuan Liao [1], Han Hu [2], Bolin Zhang [3], Lisong Liang [4] and Haina Gao [1,*]

[1] School of Food and Health, Beijing Technology and Business University, Beijing 100048, China; 19979779160@163.com (W.L.); liyujie_2001@163.com (Y.L.); liaoxy202410@163.com (X.L.)
[2] Bee Research Institute, Chinese Academy of Agricultural Sciences, Beijing 100093, China; wuhan_hh@126.com
[3] Beijing Key Laboratory of Forest Food Processing and Safety, Department of Food Science and Engineering, College of Biological Sciences and Technology, Beijing Forestry University, Beijing 100083, China; zhangbolin888@163.com
[4] Key Laboratory of Silviculture of State Forestry Administration, Research Institute of Forestry Chinese Academy of Forestry, Beijing 100091, China; lianglscaf@126.com
* Correspondence: gaohaina103@126.com
† These authors contributed equally to this work.

Abstract

Background/Objectives: Emerging evidence suggests that hippocampal neuroinflammation (HNF) drives cognitive decline via dysregulation of the microbiota-gut-brain axis. *Corylus heterophylla* Fisch. male flower extract (CFE), a flavonoid-rich by-product of hazelnut processing, presents a promising yet unexplored neuroprotective candidate. This study investigated the preventive effects and mechanisms of CFE against HNF-induced cognitive decline. **Methods:** In the present study, mice were pretreated with CFE (200 mg/kg) before the Lipopolysaccharide (LPS) administration. Cognitive function, inflammation, core pathology, neuroplasticity, gut microbiota and serum metabolites were assessed. The chemical composition of CFE was analyzed by UHPLC-MS and its direct immunomodulatory effects were investigated in BV2 cells. **Results:** Behavioral assessments demonstrated significant therapeutic efficacy. This was evidenced by the recovery from hippocampal damage, accompanied by reduced levels of core pathological markers (Aβ1–42, Tau, p-Tau (Ser404), GSK-3β), decreased expression of pro-inflammatory mediators including IL-33, elevated levels of neurotrophic factors (BDNF and MAP2), and attenuated abnormal activation of astrocytes and microglia. The 16S rRNA analysis confirmed that CFE ameliorated gut microbial dysbiosis. Notably, CFE significantly increased the relative abundance of *Muribaculaceae* and *Lachnospiraceae*, while significantly decreased *Staphylococcus* and *Helicobacter*. Metabolomics revealed enhanced levels of α-linolenic acid (ALA), serotonin (5-HT) and acetic acid, which correlated positively with *Muribaculaceae* and *Lachnospiraceae*. Phytochemical analysis identified luteolin and kaempferol as the predominant flavonoids in CFE. In BV2 cells, CFE, luteolin and kaempferol shifted microglial polarization from the M1 phenotype toward the M2 phenotype. **Conclusions:** CFE alleviated HNF-induced cognitive decline by regulating microbiota-gut-brain axis and microglial M1/M2 polarization.

Keywords: cognitive decline; hippocampal neuroinflammation; *Corylus heterophylla* Fisch. male flower extract; microbiota-gut-brain axis; flavonoids; microglial polarization

1. Introduction

Cognitive decline is increasingly observed in younger populations, a trend accelerated by the COVID-19 pandemic, with hippocampal neuroinflammation (HNF) recognized

as a pivotal driver in its pathogenesis [1,2]. Lipopolysaccharide (LPS)-induced HNF impairs neuronal synaptic plasticity and contributes to dysregulation across microbial, metabolic and microglial systems [3,4]. This inflammatory state facilitates the accumulation of amyloid-beta 1–42 (Aβ1–42) and promotes the aberrant phosphorylation of Tau protein [5,6]. A central kinase in this process, glycogen synthase kinase-3β (GSK-3β), drives the formation of phosphorylated Tau (P-Tau) and neurofibrillary tangles (NFTs) [7]. Concurrently, HNF triggers an upregulation of interleukin-33 (IL-33), leading to synaptic damage and a downregulation of brain-derived neurotrophic factor (BDNF) [8–10]. The resultant reduction in BDNF exacerbates neuronal vulnerability. Furthermore, inflammatory mediators compromise the integrity of microtubule-associated protein 2 (MAP2), disrupting neuronal structure and function, which culminates in dendritic damage and cognitive decline [11–13].

Peripheral inflammation can penetrate a compromised blood-brain barrier (BBB) to enter the central nervous system, thereby activating microglia [14]. Once aberrantly activated, microglia release pro-inflammatory factors (e.g., IL-1β, TNF-α, IL-33), generate reactive oxygen species (ROS), and further stimulate astrocytes, collectively amplifying HNF and driving cognitive decline [15]. The surface receptor cluster of differentiation 11b (CD11b), critical for microglial migration and phagocytosis, is significantly elevated during activation and serves as a biomarker for HNF severity [4]. As the primary immune effector cells in the brain, activated microglia polarize into pro-inflammatory (M1) and anti-inflammatory (M2) phenotypes. An imbalance in M1/M2 polarization is strongly implicated in the pathogenesis of HNF [16]. Notably, flavonoid compounds such as luteolin and kaempferol can promote a shift from the M1 to the M2 phenotype in microglial cells, characterized by the downregulation of M1 markers (iNOS, CD86, TNF-α) and upregulation of M2 markers (Arg-1, CD206, IL-10) [17,18].

The microbiota-gut-brain axis plays a significant role in modulating brain function [19]. LPS-induced gut microbial dysbiosis, marked by reduced diversity and abundance, exacerbates HNF [20]. Specifically, HNF correlates negatively with beneficial bacteria (e.g., *Muribaculaceae*, *Lachnospiraceae*) and positively with pathogenic genera (e.g., *Staphylococcus*, *Helicobacter*) [21–23]. Meanwhile, gut microbial metabolites, such as short-chain fatty acids (SCFAs), can cross the BBB and influence brain function, with evidence suggesting they ameliorate cognitive decline by elevating levels of BDNF and serotonin (5-HT) [24,25].

Accumulating evidence highlights the potential of floral extracts as natural neuroprotective agents against cognitive decline. For example, *Daphne genkwa* flower extract attenuated LPS-induced hippocampal neuronal loss and microglial activation by inhibiting TNF-α and IL-1β and enhancing BDNF expression [26]. *Abelmoschus Manihot Medicus* flower extract reversed cognitive decline in mice by elevating hippocampal levels of BDNF/TrkB/GluR1 [27]. *Hibiscus sabdariffa* extract improved cognitive decline by inhibiting cerebral P-Tau formation [28]. *Corylus heterophylla* Fisch., a wild hazelnut species of the family Betulaceae primarily distributed in Northeast China, notably in the Changbai Mountain region of Jilin Province, has been studied for its bioactive properties [29]. Preclinical studies indicate that the nut kernel possesses neuroprotective effects, including inhibition of Aβ generation and reduction in pro-inflammatory cytokines in the mouse hippocampus [30,31]. Pollen extracts from the male flowers of *Corylus heterophylla* Fisch. demonstrate potent antibacterial and antioxidant activities [32]. *Corylus heterophylla* Fisch. male flower extract (CFE), used traditionally for cirrhosis, demonstrates significant hepatoprotective activity against CCl4-induced liver injury in mice [33]. Furthermore, the total flavonoids from CFE protect against ischemic renal injury by mitigating oxidative stress, inhibiting profibrotic signaling, and reducing renal interstitial fibrosis [34]. However, the effects of CFE on HNF and associated cognitive decline remain unexplored. Therefore, we aimed to

investigate the protective effect of CFE against cognitive decline by examining its role in regulating microbiota-gut-brain axis and microglial polarization. This research seeks to elucidate the underlying mitigating mechanisms and provide novel therapeutic strategies for cognitive decline.

2. Materials and Methods

2.1. Preparation of Flower Extract

Corylus heterophylla Fisch. male flowers were collected in Yanqing, Beijing. Flower samples (0.5 g) were dried in an oven, pulverized using an electric blender, and sieved (80-mesh). Ultrasonic-assisted extraction was performed using four solvent systems: (A) Methanol-water (4:6, v/v), (B) Methanol-water (8:2, v/v), (C) Chloroform-methanol (6:4, v/v), and (D) Chloroform-methanol-water (6:3:1, $v/v/v$) (10 mL each) [35,36]. Subsequently, extracts were centrifuged (10 min, 8000 rpm, 4 °C), filtered through 0.22-μm membranes, and lyophilized. The dried extracts were stored at −20 °C until further use. Three independent extractions per solvent system were conducted under identical conditions.

2.2. Culture and Treatment of HT22 Cells

The mouse hippocampal neuronal cell line HT22 (iCell Bioscience Inc., Shanghai, China) was cultured in Dulbecco's Modified Eagle Medium (DMEM; cat. #11965092, Gibco, Grand Island, NY, USA) supplemented with 10% fetal bovine serum (FBS; cat. #SX1101, SORFA, Deqing, China) and 1% penicillin-streptomycin (P/S; cat. #15140122, Gibco, Grand Island, NY, USA), and maintained at 37 °C in a 5% CO_2 atmosphere. Cells were passaged using 0.25% trypsin-0.02% EDTA (cat. #C0201, Beyotime, Shanghai, China). For viability and ROS assays, cells were seeded in 96-well plates at a density of 5×10^4 cells/mL. Upon reaching 80% confluency, cells were serum-starved for 12 h and then assigned to the following groups (Figure 1A, N = 6 per group): Control: normal culture for 36 h; LPS: treated with 1 μg/mL LPS (cat. #L2880, Sigma, Kawasaki, Japan) for 24 h after 12 h of normal culture; CFE: pretreated with 200 μg/mL of solvent A/B/C/D extracts for 12 h, followed by 24 h LPS exposure. Cell viability was assessed using a CCK-8 kit (Meilunbio, Shanghai, China) by measuring the absorbance at 450 nm with an Infinite M200 microplate reader (TECAN, Männedorf, Switzerland). ROS levels were quantified with an assay kit (cat. #S0033S, Beyotime Institute of Biotechnology, Haimen, China). Briefly, cells were incubated with 10 μM 2′,7′-dichlorofluorescin diacetate (DCFH-DA) at 37 °C for 30 min. The suspensions were then centrifuged at 1000× g for 5 min and resuspended in fresh medium for fluorescence measurement [37].

2.3. The Chemical Composition of CFE Obtained with Solvent C Was Analyzed by UHPLC-MS

The chemical profile of CFE, the most effective extract obtained using solvent C, was characterized by UHPLC-MS. Chromatographic separation was carried out on a Hi Q Sil C18 column (250 mm × 4.6 mm, 5 μm) maintained at 40 °C. A gradient elution was applied over 35 min using 0.1% formic acid in water (mobile phase A) and acetonitrile (mobile phase B), at a flow rate of 0.3 mL/min. The injection volume was set to 4 μL. Mass spectrometry detection was performed in positive/negative polarity switching mode with the following parameters: sheath gas, 40 arb; auxiliary gas, 5 arb; spray voltage, 3500 V (positive) and 3000 V (negative); capillary temperature, 320 °C. Full-scan mass spectra were acquired across the m/z range of 80–1200 at a resolution of 70,000, with an AGC target of 3×10^6 and a maximum injection time of 200 ms. Quality control samples were analyzed periodically to ensure system stability. Quantification of the major flavonoid compounds was conducted using the external standard method.

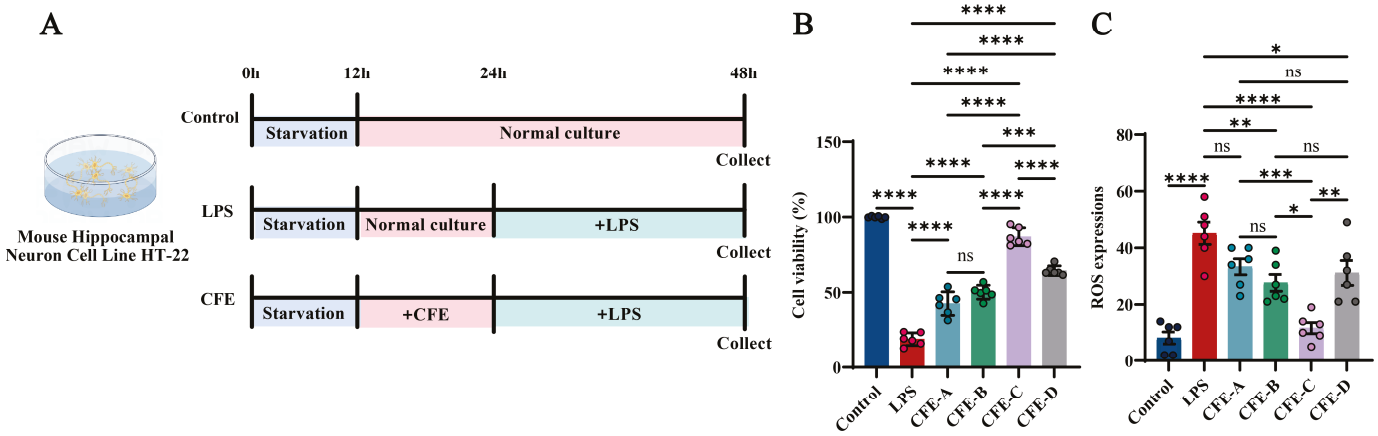

Figure 1. Effects of CFE on HT22 cells with lipopolysaccharide (LPS) administration. The colored dots represent data points from different sample groups. (**A**) Schematic of the experimental timeline for HT22 cell treatments. Cells were assigned to the Control, LPS and CFE groups. (**B**) Cell viability measured by CCK-8 assay. (**C**) Quantitative analysis of intracellular reactive oxygen species (ROS) levels. Data presented as means ± SEM (N = 6). Statistically significant differences were indicated: * $p < 0.05$, ** $p < 0.01$, *** $p < 0.001$, **** $p < 0.0001$, ns $p > 0.05$, compared to the LPS group.

2.4. Animal Treatment

All animal procedures were approved by the Animal Experimentation Ethics Committee of China Agricultural University (Protocol Aw71705202-6-04, 17 July 2025). As outlined in Figure 2A, a total of 30 male Balb/c mice (6 weeks old, 20–22 g; Beijing Sibeifu Biotechnology Co., Ltd., Beijing, China) were randomly assigned to three groups: Control, LPS and CFE. Following a 7-day acclimatization period, mice received daily intragastric gavage for 28 consecutive days. The Control and LPS groups were administered 0.2 mL of saline per day, whereas the CFE group received 0.2 mL of CFE (extracted with solvent C, 200 mg/kg) daily. The CFE dose was selected based on preliminary experiments and previous literature [38]. Upon completion of the 28-day gavage regimen, all mice except the Control group received a single intraperitoneal injection of LPS (1 mg/kg). Control mice were injected with an equal volume of saline. Body weight was recorded daily throughout the study.

2.5. Behavioral Assessments

2.5.1. Morris Water Maze (MWM)

Spatial learning and memory were assessed using the MWM test [37]. The apparatus consisted of a circular pool (120 cm in diameter) filled with water maintained at 25 °C. A submerged escape platform (10 cm in diameter, positioned 2 cm below the water surface) was placed in the center of quadrant III. During the training phase, mice that failed to locate the platform within 60 s were gently guided to it and allowed to remain there for 15 s. For the probe test, the platform was removed and each mouse was released into quadrant I. The following parameters were recorded over a 60 s period: the number of platform crossings, and the time spent and distance traveled in the target quadrant.

2.5.2. Novel Object Recognition Experiment (NOR)

In the NOR test, during the training phase, two identical rectangular objects (A and B) were placed in opposite corners of the arena. Mice were positioned facing away from the objects to avoid initial bias and allowed to explore freely for 5 min. In the subsequent test phase, object B was replaced with a novel cylindrical object (C). Mice were reintroduced into the arena, and their exploration was recorded for 5 min. The following parameters were quantified: movement trajectories, exploration time directed toward the familiar object A

(T_A), and exploration time directed toward the novel object C (T_C) [39]. The recognition index was calculated as follows: Recognition Index (%) = $[T_C/(T_A + T_C)] \times 100\%$.

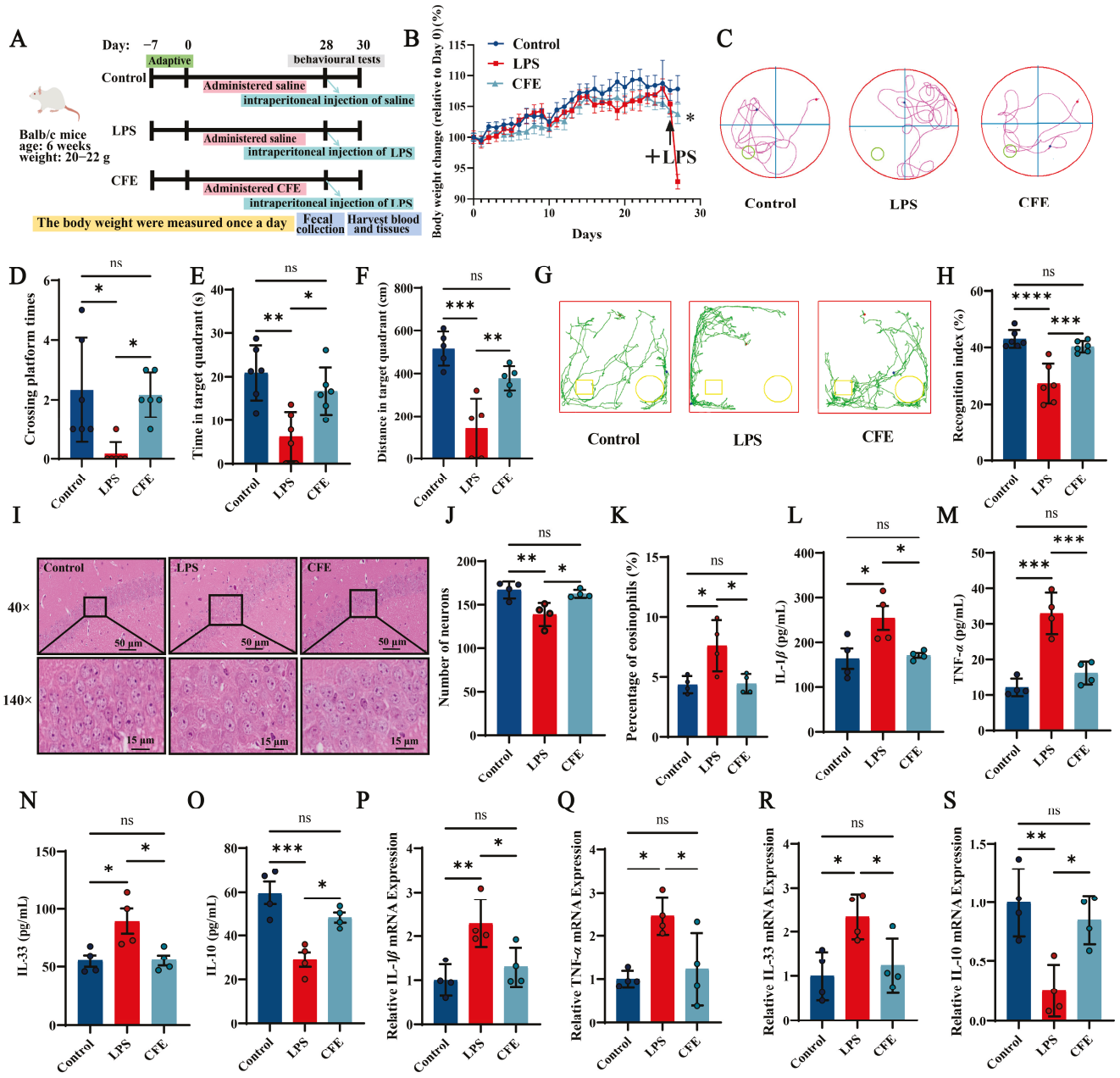

Figure 2. Pretreatment with *Corylus heterophylla* Fisch. male flower extract (CFE) ameliorated pathological outcomes in a mouse model of hippocampal neuroinflammation (HNF). The colored dots represent data points from different sample groups. (**A**) Schematic of the experimental timeline. (**B**) Rate of body weight change from Day 0 in mice. The arrows indicate intraperitoneal injection of LPS in mice on day 28. (**C**) Representative swimming trajectories from the Morris Water Maze test (N = 6). (**D**) Number of platform crossings within 60 s. (**E**) Time spent in the target quadrant within 60 s. (**F**) Distance traveled in the target quadrant within 60 s. (**G**) Representative exploration curves from the novel object recognition test (N = 6). (**H**) Recognition index for each group. (**I**) Representative hematoxylin and eosin (H&E)-stained sections of the hippocampus. (**J**) Quantification of neuronal density in the hippocampal cornu ammonis 1 (CA1) region. (**K**) Percentage of eosinophilic cells in the CA1 region. (**L**–**O**) Serum levels of IL-1β, TNF-α, IL-33, and IL-10 measured by ELISA. (**P**–**S**) Hippocampal mRNA expression of IL-1β, TNF-α, IL-33, and IL-10 assessed by RT-qPCR. Data are presented as mean ± SEM (N = 4). Statistically significant differences were indicated: * $p < 0.05$, ** $p < 0.01$, *** $p < 0.001$, **** $p < 0.0001$, ns $p > 0.05$, compared to the LPS group.

2.6. Hematoxylin and Eosin (H&E) Staining

Following behavioral testing, mice were transcardially perfused with saline followed by 4% paraformaldehyde. Brains were promptly dissected and further fixed by immersion in 4% PFA for 24 h at 4 °C. After graded ethanol dehydration, the tissues were paraffin embedded using a tissue embedding station. Subsequently, 4-μm-thick sections were cut and prepared for H&E staining. To evaluate neuronal damage in the hippocampal cornu ammonis 1 (CA1) region, we quantified the density of surviving neurons and the proportion of eosinophilic cells [40]. Analysis was conducted on four randomly selected 40× fields per section using ImageJ2x software (Rawak Software, Stuttgart, Germany).

2.7. Enzyme-Linked Immunosorbent Assay (ELISA)

Blood samples were collected from all mice (Control, LPS and CFE groups) via retro-orbital bleeding upon completion of behavioral testing, which was performed 2 days after the final LPS challenge and pretreatment administration. Samples were centrifuged at 3000× *g* for 15 min at 4 °C, and the serum was collected for analysis. Serum concentrations of IL-1β (Cat. #RX203063M, RUIXIN, Yueqing, China), TNF-α (Cat. #EK282, RUIXIN), IL-33 (Cat. #RX203053M, RUIXIN), IL-10 (Cat. #EK210, RUIXIN), 5-HT (Cat. #MM-0443M2, Jiangsu Meimian Industrial Co., Ltd., Yancheng, China), and ALA (Cat. #MM-926718O2, Jiangsu Meimian Industrial Co., Ltd.) were quantified using commercially available ELISA kits [41]. For hippocampal tissue analysis, 20 mg of tissue was homogenized in 1 mL of RIPA buffer (MA0151, Meilunbio) supplemented with protease inhibitors. The homogenate was centrifuged at 10,000× *g* for 5 min at 4 °C, and the resulting supernatant was collected. Hippocampal levels of 5-HT and ALA were measured using specific ELISA kits, with absorbance read on a microplate reader (model 3903 2010, Bio Rad, Hercules, CA, USA).

2.8. Quantitative Real-Time Polymerase Chain Reaction (qRT-PCR)

Total RNA was isolated from hippocampal tissue using TRIzol™ Reagent (Cat. #15596026, Invitrogen, Carlsbad, CA, USA). RNA quality and concentration were assessed using a NanoDrop 2000 spectrophotometer (Thermo Fisher Scientific, Shanghai, China). Complementary DNA (cDNA) was synthesized using the PrimeScript RT Reagent Kit (Cat. #DRR037A, TaKaRa, Osaka, Japan). qRT-PCR was then performed with TB Green Premix Ex Taq (Cat. #RR420A, Takara) on a real-time PCR system. Gene expression levels were calculated using the $2^{-\Delta\Delta Ct}$ method and normalized to the housekeeping gene GAPDH. The primer sequences used are listed in Supplementary Table S1.

2.9. Immunohistochemistry (IHC)

IHC staining of brain tissue sections was performed using primary antibodies against the following targets: Aβ1–42 (cat. #A9810, Sigma Aldrich, St. Louis, MO, USA), Tau (cat. #10274-1-AP, Proteintech, Rosemont, IL, USA), P-Tau (Ser404) (cat. #35834, Cell Signaling Technology, Danvers, MA, USA), BDNF (cat. #25699-1-AP, Proteintech), MAP2 (cat. #17490-1-AP, Proteintech) and CD11b (cat. #66519-1-IG, Proteintech). Antigen antibody complexes were detected using a horseradish peroxidase-conjugated secondary antibody followed by diaminobenzidine chromogenic development with a Vectastain ABC kit [42]. The average optical density (AOD) of immunopositive regions was quantified in four randomly selected fields within the hippocampal CA1 subregion using ImageJ2x software (Rawak Software, Germany).

2.10. Western Blot Analysis (WB)

Western blot analysis was performed following a previously described protocol with slight modifications [43]. Hippocampal tissues were homogenized on ice for 30 min in

RIPA lysis buffer supplemented with 1% PMSF and phosphatase inhibitors (Beyotime, Shanghai, China). After centrifugation at 12,000× *g* for 20 min at 4 °C, the supernatant was collected, and total protein concentration was determined using a bicinchoninic acid (BCA) assay kit (Beyotime, China). Protein samples were denatured by heating at 95 °C for 20 min, separated on 10% SDS-polyacrylamide gels, and transferred onto polyvinylidene fluoride (PVDF) membranes (cat. #IPVH00010, Millipore, Burlington, MA, USA). Membranes were blocked with 5% bovine serum albumin (BSA) in PBS for 1 h at room temperature and then incubated overnight at 4 °C with the following primary antibodies: Aβ1–42 (cat. #A9810, Sigma-Aldrich), Tau (cat. #10274-1-AP, Proteintech), P-Tau (Ser404) (cat. #35834, Cell Signaling Technology, Danvers, MA, USA), GSK-3β (cat. #22104-1-AP, Proteintech), BDNF (cat. #25699-1-AP, Proteintech), MAP2 (cat. #17490-1-AP, Proteintech), CD11b (cat. #ab184307, Abcam, Cambridge, UK), and GAPDH (cat. #10494-1-AP, Proteintech). After washing, membranes were incubated for 2 h at room temperature with an HRP-conjugated secondary antibody (cat. #SA00001 2, Proteintech). Protein bands were visualized using enhanced chemiluminescence (ECL) substrate on an Image Quant LAS4000 system (GE Healthcare, Chicago, IL, USA). Band intensities were quantified using ImageJ2x software (National Institutes of Health, Bethesda, MD, USA) and normalized to GAPDH.

2.11. Immunofluorescence (IF)

Brain tissues were fixed in 4% paraformaldehyde, embedded, and sectioned to a thickness of 40 μm using a cryostat. After three brief washes with PBS, sections were blocked with 5% BSA for 1 h at room temperature and then incubated overnight at 4 °C with the following primary antibodies: rabbit anti-Iba1 (1:500, ab178846, Abcam) and rabbit anti-GFAP (1:500, ab7260, Abcam). Following three PBS washes, sections were incubated with appropriate fluorescent dye conjugated secondary antibodies for 2 h at room temperature in the dark. After a final PBS wash, sections were mounted, air dried, and imaged using a laser scanning confocal microscope (Thermo Fisher Scientific, Waltham, MA, USA).

2.12. Metabolomic Profiling of Fecal Short-Chain Fatty Acids (SCFAs)

Quantitative analysis of fecal SCFAs (acetic, propionic and butyric acids) was performed by targeted metabolomics following an established methodology [44]. Fecal samples (25 mg) were subjected to acid extraction using 0.5% phosphoric acid (H_3PO_4), followed by cryogenic homogenization, sonication in an ice bath for 10 min, and centrifugation. The supernatant was derivatized with butanol containing 2-ethylbutyric acid as an internal standard, then vortexed, sonicated, and centrifuged. GC-MS analysis was carried out on an Agilent 8890B/5977B system equipped with an HP-FFAP column (30 m × 0.25 mm × 0.25 μm). The operating conditions were as follows: splitless injection at 260 °C; helium carrier gas at a constant flow of 1.0 mL/min; oven temperature programmed from 80 °C (held for 1 min) to 120 °C at 40 °C/min, then to 200 °C at 10 °C/min, and finally to 230 °C (held for 3 min). Detection was performed in selected ion monitoring (SIM) mode using electron ionization (70 eV). The ion source and transfer line temperatures were set to 230 °C, and the quadrupole temperature was 150 °C. Quantification was based on external calibration curves generated with MassHunter software (v10.0).

2.13. Sequencing of the Microbial 16S Ribosomal RNA (16S rRNA)

Fecal samples collected from the experimental mice were immediately frozen at −80 °C and processed within 3 h. DNA extraction and 16S rRNA gene sequencing were subsequently conducted by Majorbio Bio Pharm Technology Co., Ltd. (Shanghai, China). Briefly, the V3–V4 hypervariable regions of the bacterial 16S rRNA gene were amplified

and sequenced on an Illumina NextSeq 2000 platform. After DNA extraction and PCR amplification, the raw sequencing reads were subjected to quality filtering, paired end assembly, and clustering into operational taxonomic units (OTUs). Microbial diversity was analyzed with beta diversity assessed via principal coordinate analysis (PCoA) based on Bray-Curtis distances. Differentially abundant bacterial genera were identified using linear discriminant analysis effect size (LEfSe) with thresholds of LDA score > 3 and $p < 0.05$.

2.14. Serum Metabolomics Analysis

Untargeted metabolomic profiling of serum samples was conducted following an adapted protocol [45]. Briefly, serum proteins were precipitated using cold methanol acetonitrile (1:1, v/v). After centrifugation, the supernatant was collected, dried under nitrogen, reconstituted in an appropriate solvent, and analyzed on a UHPLC-MS/MS system (Thermo Scientific Q Exactive, Waltham, MA, USA). Chromatographic separation was performed on an HSS T3 column using a gradient of water and acetonitrile, each containing 0.1% formic acid. Mass spectrometry analysis was carried out in data dependent acquisition (DDA) mode with electrospray ionization in both positive and negative polarities at a resolution of 70,000.

2.15. Culture and Treatment of BV2 Cells

BV2 microglial cells were maintained in complete DMEM and seeded in 6 well plates at a density of 5×10^4 cells/mL. Upon reaching 80% confluency, cells were serum starved for 12 h. In a preliminary experiment, the optimal CFE concentration was determined using the following groups: Control (normal culture), LPS (1 μg/mL, 12 h normal culture + 24 h LPS) and CFE (200, 400, or 600 μg/mL; 12 h pretreatment with CFE + 24 h LPS). Based on cell viability results, 400 μg/mL CFE was selected for subsequent polarization studies. For M1 polarization, the experimental groups included: Control (normal culture), LPS (1 μg/mL, 12 h normal culture + 24 h LPS), CFE (400 μg/mL, 12 h pretreatment with CFE + 24 h LPS), luteolin (14 μM, CAS: 491-70-3, cat. #B20888, Shanghai Yuanye BioTechnology Co., Ltd., Shanghai, China, 12 h pretreatment with luteolin + 24 h LPS) and kaempferol (10 μM, CAS: 520-18-3, cat. #YZ-110861, Solarbio, Beijing, China, 12 h pretreatment with kaempferol + 24 h LPS). For M2 polarization, groups included: Control (normal culture), IL-4 (20 ng/mL, cat. #P00196, Solarbio, 12 h normal culture + 24 h IL-4), CFE (400 μg/mL, 12 h pretreatment with CFE+ 24 h IL-4), luteolin (14 μM, 12 h pretreatment with luteolin + 24 h IL-4) and kaempferol (10 μM, 12 h pretreatment with kaempferol + 24 h IL-4). Total RNA was extracted using TRIzol reagent, and cDNA was synthesized. mRNA expression levels of M1 markers (iNOS, CD86, TNF-α) and M2 markers (Arg1, CD206, IL-10) were analyzed by quantitative PCR using the $2^{-\Delta\Delta Ct}$ method (primer sequences are listed in Supplementary Table S1).

2.16. Data Processing

Data are presented as mean ± standard error of the mean (SEM). Statistical analyses were performed with Prism 9.5 (GraphPad Software, San Diego, CA, USA). Specifically, one-way analysis of variance (ANOVA) was applied, followed by Tukey's post hoc test for multiple comparisons. Differences were considered statistically significant at $p < 0.05$.

3. Results

3.1. CFE Enhanced Cell Viability and Attenuates ROS Production in HT22 Cells

We evaluated the effects of CFE on cell viability and ROS levels in HT22 cells using an LPS-induced model of HNF (Figure 1A–C). The CCK-8 assay revealed that LPS treatment significantly decreased HT22 cell viability compared to the Control group ($p < 0.0001$).

This decrease was significantly mitigated by pretreatment with CFE-A, CFE-B, CFE-C and CFE-D (200 μg/mL, all $p < 0.0001$). Furthermore, CFE exhibited antioxidant activity, as LPS-induced ROS overproduction ($p < 0.0001$) was significantly suppressed by CFE-B ($p < 0.001$), CFE-C ($p < 0.0001$) and CFE-D ($p < 0.05$), with the solvent C extract showing the most pronounced reduction. Based on the combined neuroprotective and antioxidant effects, CFE extracted with solvent C was selected for all subsequent experiments.

3.2. Metabolite Profiling of CFE Extracted with Solvent C

Metabolite analysis of the solvent C extract of CFE tentatively identified 274 compounds, which were categorized into the following chemical classes: 91 terpenoids, 75 flavonoids, 52 phenylpropanoids, 20 alkaloids, 9 polyketides, 9 shikimate/acetate-malonate pathway derived compounds, 7 fatty acid-related compounds, 7 amino acid-related compounds, and 4 others. The ten most abundant and biologically relevant compounds from each major class are listed in Table 1, along with their tentative identities, molecular formulas, retention times, and m/z values. Subsequently, targeted quantitative analysis of the ten principal flavonoids was performed by HPLC-MS/MS (Table 2). Among these, luteolin and kaempferol were the most abundant, with quantified concentrations of 10,796.37 ± 65.53 ng/mL and 3082.77 ± 110.12 ng/mL, respectively.

Table 1. Metabolites Identified in CFE.

ID.	Identified Compound	Formula	Rt (min)	M/Z
Terpenoids				
1	Valtrate	$C_{10}H_{12}O_5$	6.9529	211.06103219999
2	Loganic acid	$C_{16}H_{24}O_{10}$	7.1395	377.1417847
3	Geniposide	$C_{17}H_{24}O_{10}$	7.1689	387.1306856
4	Aucubin	$C_{15}H_{22}O_9$	7.6937	351.1048213
5	Geniposidic acid	$C_{16}H_{22}O_{10}$	7.1890	355.1044042
6	Verbenalin	$C_{17}H_{24}O_{10}$	7.8022	387.1307178
7	Asperuloside	$C_{18}H_{22}O_{11}$	11.5447	435.094409
8	Genipin	$C_{11}H_{14}O_5$	11.7112	209.080969099999
9	Carvone	$C_{10}H_{14}O$	13.5809	133.1013854
10	Kahweol	$C_{20}H_{26}O_3$	19.5627	332.2196618000
Flavonoids				
11	Cynaroside	$C_{21}H_{20}O_{11}$	7.0215	449.1077437
12	Catechin	$C_{15}H_{14}O_6$	7.7130	291.0863623
13	Hesperetin	$C_{16}H_{14}O_6$	8.2874	303.0868847
14	Kaempferol	$C_{15}H_{10}O_6$	8.9881	287.054886
15	Orientin	$C_{21}H_{20}O_{11}$	9.6627	493.0997219
16	Myricetin	$C_{15}H_{10}O_8$	11.1222	319.0452683
17	Luteolin	$C_{15}H_{10}O_6$	12.8466	285.0411301
18	Fisetin	$C_{15}H_{10}O_6$	14.4979	285.0411181
19	Liquiritigenin	$C_{15}H_{12}O_4$	17.2008	257.0810664
20	Quercetin	$C_{15}H_{10}O_7$	21.5714	303.0499775

Table 1. *Cont.*

ID.	Identified Compound	Formula	Rt (min)	M/Z
Phenylpropanoids				
21	Melilotoside	$C_{15}H_{18}O_8$	7.3099	325.0939562
22	Sinapic acid	$C_{11}H_{12}O_5$	7.5178	225.07579959999
23	Coniferin	$C_{16}H_{22}O_8$	8.4912	341.1246012
24	Clemaphenol A	$C_{20}H_{22}O_6$	8.5585	341.1384034
25	Arctiin	$C_{27}H_{34}O_{11}$	8.5684	579.2101222
26	Caffeic acid	$C_9H_8O_4$	8.7172	181.0495659
27	Ferulic acid	$C_{10}H_{10}O_4$	10.4062	193.050046
28	Daphnetin	$C_9H_6O_4$	6.6184	179.0342196
29	Matairesinol	$C_{20}H_{22}O_6$	12.3796	357.1353564
30	Coumarin	$C_9H_6O_2$	15.2106	147.0441273
Alkaloids				
31	Aminophylline	$C_7H_8N_4O_2$	2.0131	225.0613935
32	Trigonelline	$C_7H_7NO_2$	2.1357	138.0550452
33	Niacinamide	$C_6H_6N_2O$	2.1357	123.0554621
34	Nicotinic acid	$C_6H_5NO_2$	2.2493	124.0395691
35	Picolinic acid	$C_6H_5NO_2$	3.0782	124.0396142
36	Pipecolic acid	$C_6H_{11}NO_2$	3.0782	130.0864943
37	Xanthosine	$C_{10}H_{12}N_4O_6$	3.4114	283.069145
38	Dopamine	$C_8H_{11}NO_2$	9.9235	118.0654293
39	Cepharanthine	$C_{37}H_{38}N_2O_6$	12.6136	611.2462267
40	Irinotecan	$C_{33}H_{38}N_4O_6$	26.3161	609.271034799999
Polyketides				
41	Gentiacaulein	$C_{15}H_{12}O_6$	7.2492	287.05699489999
42	Isogentisin	$C_{14}H_{10}O_5$	8.0218	303.0518434
43	Emodin 8-glucoside	$C_{21}H_{20}O_{10}$	11.8486	455.095751599999
44	Chrysophanein	$C_{21}H_{20}O_9$	12.0973	415.1043764
45	Franguloside	$C_{21}H_{20}O_9$	14.1133	461.1099776
46	Aloe-emodin	$C_{15}H_{10}O_5$	14.2320	269.0461515
47	Rheic acid	$C_{15}H_8O_6$	14.4979	283.0254713999
48	Chrysophanic acid	$C_{15}H_{10}O_4$	15.2399	313.0726244
49	Kavain	$C_{14}H_{14}O_3$	16.9331	231.1017323
Shikimate/acetate-malonate pathway derived compounds				
50	Trans-Piceid	$C_{20}H_{22}O_8$	9.6816	411.1068254
51	Yakuchinone-A	$C_{20}H_{24}O_3$	10.8562	347.1407132
52	Batatasin I	$C_{17}H_{16}O_4$	11.2297	343.119330399999
53	Resveratrol	$C_{14}H_{12}O_3$	11.5252	273.0776406999
54	Curcumin	$C_{21}H_{20}O_6$	13.3306	349.1072668
55	6-paradol	$C_{17}H_{26}O_3$	14.1811	279.193054

Table 1. *Cont.*

ID.	Identified Compound	Formula	Rt (min)	M/Z
56	Pinosylvin	$C_{14}H_{12}O_2$	14.8899	213.0909792
57	6-gingerol	$C_{17}H_{26}O_4$	19.0101	295.1906158
58	Gingerol	$C_{17}H_{26}O_4$	22.1175	349.199659
Amino acid related compounds				
59	Linustatin	$C_{16}H_{27}NO_{11}$	7.8120	464.1763025
60	Amygdalin	$C_{20}H_{27}NO_{11}$	9.1630	475.194189
61	Glucoerucin	$C_{12}H_{23}NO_9S_3$	10.3185	439.0846983
62	Triglochinin	$C_{14}H_{17}NO_{10}$	11.8486	401.1208912
63	Glucoberteroin	$C_{13}H_{24}NO_9S_{3-}$	12.1166	415.0458546
64	Lucuminoside	$C_{19}H_{25}NO_{10}$	12.9959	445.1834607
65	Betanin	$C_{24}H_{26}N_2O_{13}$	15.8566	595.1469962
Fatty acids related compounds				
66	Panaxytriol	$C_{17}H_{26}O_3$	17.3533	323.1871353
67	Caprylic acid	$C_8H_{16}O_2$	18.5133	287.2234452
68	Gamma-Linolenic acid	$C_{18}H_{30}O_2$	20.0594	323.2235911
69	Jasmonic acid	$C_{12}H_{18}O_3$	20.5980	211.132915
70	Palmitoleic acid	$C_{16}H_{30}O_2$	21.9555	255.2319082
71	Palmitic acid	$C_{16}H_{32}O_2$	22.3487	255.2330876
72	Vaccenic acid	$C_{18}H_{34}O_2$	24.7196	283.26346639999
Others				
73	Pyrogallol	$C_6H_6O_3$	0.6018	127.03927209999
74	Gallic acid	$C_7H_6O_5$	1.5681	169.0135405
75	Juglone	$C_{10}H_6O_3$	6.9224	175.0392134
76	Ptaquiloside	$C_{20}H_{30}O_8$	7.1493	443.1933204

Table 2. Quantification of major identified flavonoids compounds in the CFE.

ID.	Identified Compound	Concentration (ng/mL, Mean ± SD)
1	Luteolin	10,796.3674 ± 65.53
2	Kaempferol	3082.77 ± 110.12
3	Orientin	339.54 ± 22.03
4	Hesperetin	336.42 ± 12.40
5	Liquiritigenin	182.71 ± 31.67
6	Myricetin	170.84 ± 2.74
7	Catechin	65.67 ± 2.60
8	Cynaroside	62.76 ± 8.91
9	Fisetin	15.73 ± 5.60
10	Quercetin	4.60 ± 0.61

3.3. CFE Attenuated Cognitive Decline in HNF Mice

To evaluate the potential of CFE in mitigating LPS-induced HNF and cognitive decline, mice were administered CFE for four weeks (Figure 2A). No significant differences in body weight were observed among groups prior to LPS challenge. Following LPS administration, mice in the LPS group exhibited significant weight loss, confirming successful model induction. Notably, CFE pretreatment significantly attenuated this LPS-induced weight reduction ($p < 0.05$), indicating its ability to counteract inflammation-associated metabolic changes (Figure 2B).

Spatial learning and memory were assessed using the MWM (Figure 2C–F). Compared with the Control group, LPS-treated mice showed significant decreases in the number of platform crossings ($p < 0.05$), time spent in the target quadrant ($p < 0.01$), and distance traveled in the target quadrant ($p < 0.001$), indicating marked spatial memory deficits. CFE pretreatment significantly improved these parameters, increasing platform crossings ($p < 0.05$), time in the target quadrant ($p < 0.05$), and distance traveled in the target quadrant ($p < 0.01$) relative to the LPS group, demonstrating that CFE alleviates spatial memory impairment.

These findings were further supported by the NOR test (Figure 2G,H). Mice pretreated with CFE displayed a significantly higher recognition index than LPS-treated mice ($p < 0.001$), reflecting enhanced exploratory behavior and novel-object discrimination. Collectively, these results indicate that CFE pretreatment effectively ameliorates the severe cognitive decline associated with HNF in mice.

3.4. CFE Alleviated Hippocampal Damage in HNF Mice

Hippocampal histopathological changes are presented in Figure 2I–K. The LPS group showed a disrupted cytoarchitecture characterized by disorganized neuronal arrangement, widened intercellular spaces, and irregular morphology. Nucleolar condensation, dissolution, or loss was also evident. Quantitative analysis revealed a significant reduction in neuronal density ($p < 0.01$) and in the proportion of eosinophilic neurons ($p < 0.05$) compared to the Control group. In contrast, CFE intervention effectively restored hippocampal histology, significantly increasing both neuronal density ($p < 0.05$) and the percentage of eosinophilic neurons ($p < 0.05$) relative to the LPS group. Together, these results demonstrate that CFE pretreatment confers substantial protection against HNF-induced structural damage in the hippocampus.

3.5. CFE Modulated Inflammatory Cytokine Levels in Serum and Hippocampus of HNF Mice

ELISA analysis of serum (Figure 2L–O) showed that LPS administration significantly increased the levels of the pro-inflammatory cytokines IL-1β ($p < 0.05$), TNF-α ($p < 0.001$), and IL-33 ($p < 0.05$), while reducing the anti-inflammatory cytokine IL-10 ($p < 0.001$). In contrast, CFE pretreatment significantly lowered serum IL-1β ($p < 0.05$), TNF-α ($p < 0.001$), and IL-33 ($p < 0.05$), and elevated IL-10 ($p < 0.05$) compared to the LPS group. Similarly, RT-qPCR analysis of hippocampal tissue (Figure 2P–S) indicated that LPS challenge markedly upregulated mRNA expression of IL-1β ($p < 0.01$), TNF-α ($p < 0.05$), and IL-33 ($p < 0.05$), and downregulated IL-10 ($p < 0.01$). CFE intervention significantly reversed these changes, reducing IL-1β, TNF-α, and IL-33 expression and enhancing IL-10 levels (all $p < 0.05$). Together, these data demonstrate that CFE effectively mitigates systemic and hippocampal inflammation in HNF mice.

3.6. CFE Alleviated the Expression of Aβ1–42 Protein in the Hippocampus of HNF Mice

To assess the impact of CFE on Aβ1–42 levels, IHC (Figure 3A,B) and WB (Figure 3C,D) were performed. IHC analysis confirmed that the LPS group exhibited significantly ele-

vated AOD values for Aβ1–42 compared to the Control group ($p < 0.001$), as evidenced by widespread brown-yellow deposition throughout the hippocampus. CFE intervention markedly reduced Aβ1–42 AOD relative to the LPS group ($p < 0.001$). WB analysis confirmed this reduction ($p < 0.05$). The results suggested that the amelioration of cognitive decline by CFE in HNF mice is associated with reduced hippocampal Aβ1–42 deposition and subsequent improvement in the brain microenvironment.

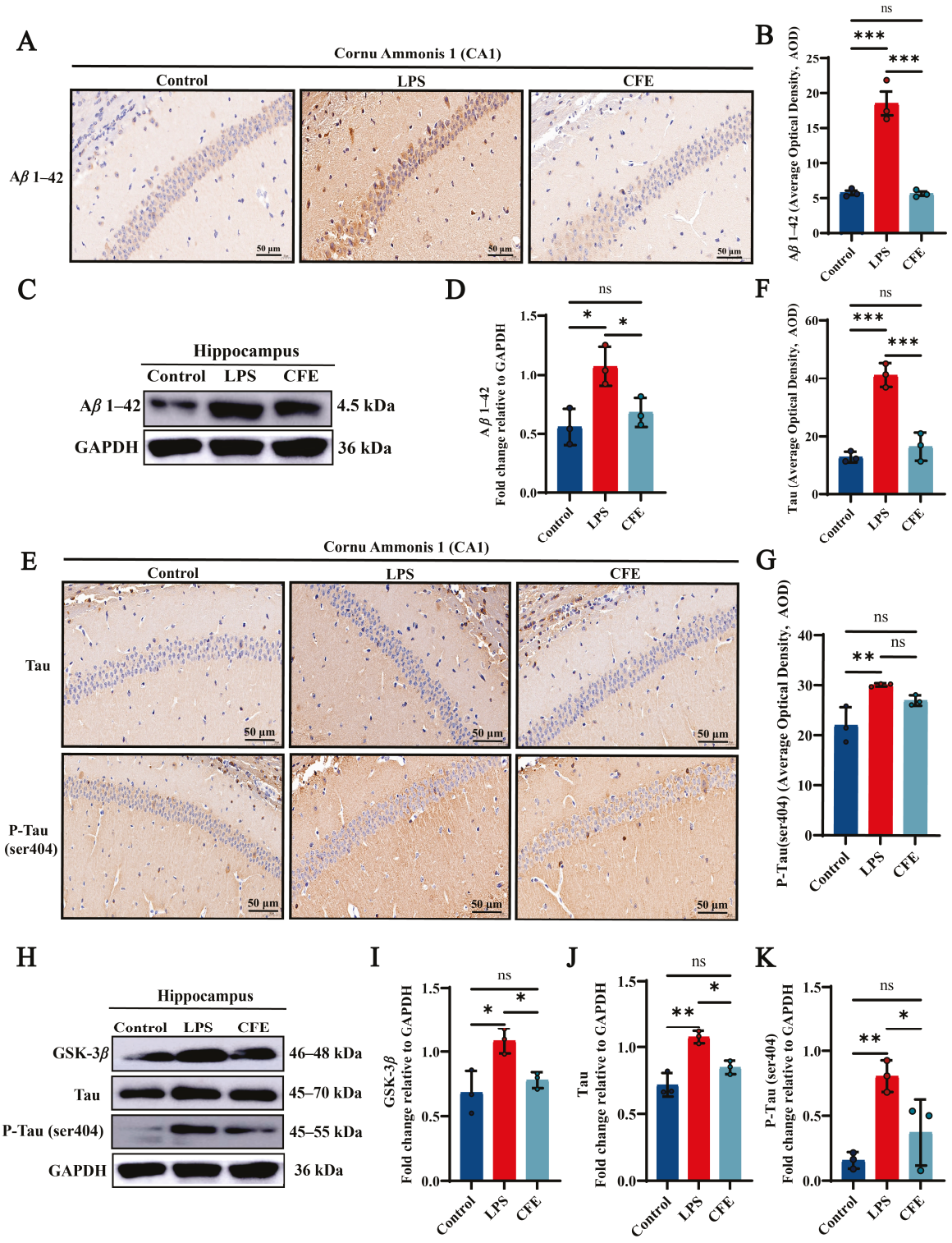

Figure 3. CFE downregulated hippocampal levels of Aβ1–42, GSK-3β, Tau and P-Tau in HNF mice. The colored dots represent data points from different sample groups. (**A**) Representative immunohistochemical

(IHC) staining images of Aβ1–42 (40× magnification). (**B**) Quantification of Aβ1–42 IHC staining intensity expressed as average optical density (AOD). (**C**) Representative Western blot images of hippocampal Aβ1–42. (**D**) Quantitative analysis of Aβ1–42 protein levels from Western blot, normalized to GAPDH. (**E**) Representative IHC staining images of total Tau and P-Tau (Ser404) (40×). (**F**,**G**) Quantification of Tau and P-Tau (Ser404) IHC staining intensity (AOD). (**H**) Representative Western blot images of GSK-3β, total Tau and P-Tau (Ser404). (**I**–**K**) Quantitative analysis of GSK-3β, total Tau and P-Tau (Ser404) protein levels from Western blot, normalized to GAPDH. Data are presented as the mean ± SEM (N = 3). Statistically significant differences were indicated: * $p < 0.05$, ** $p < 0.01$, *** $p < 0.001$, ns $p > 0.05$, compared to the LPS group.

3.7. CFE Alleviated the Expressions of GSK-3β, Tau and P-Tau Protein in the Hippocampus of HNF Mice

IHC and WB analysis of CA1 hippocampal regions quantified GSK-3β, Tau and P-Tau (ser404) immunoreactivity (Figure 3E–K). Compared to the Control group, the LPS group demonstrated a marked increase in AOD values for Tau ($p < 0.001$) and P-Tau (ser404) ($p < 0.01$), characterized by extensive brown-yellow deposits diffusely distributed across the hippocampal formation. CFE intervention significantly lowered Tau ($p < 0.001$) and P-Tau (ser404) AOD value compared to the LPS group. Furthermore, WB analysis revealed a decrease in GSK-3β, Tau and P-Tau (ser404) (all $p < 0.05$) expression which is consistent with the IHC results. Our results show that CFE reduces hippocampal GSK-3β, Tau and P-Tau (ser404) expression, suggesting a potential mechanism for neuronal cytoskeletal stabilization.

3.8. CFE Enhanced the Expressions of BDNF and MAP2 Protein in the Hippocampus of HNF Mice

IHC examination of CA1 hippocampal subfields was performed to quantify BDNF and MAP2 expression (Figure 4A–C). In the Control group, BDNF and MAP2 high expressions were a brown-yellow sediment, which was widely distributed in the hippocampus. CFE supplementation significantly increased BDNF and MAP2 AOD value compared to the LPS group ($p < 0.01$). Notably, WB analysis (Figure 4D–F) revealed enhanced expression of both BDNF and MAP2 in the CFE group compared to the LPS group ($p < 0.05$). Our findings indicated that CFE enhanced neuronal synaptic plasticity by modulating the BDNF signaling pathway.

3.9. CFE Inhibited the Abnormal Activation of Microglia and Astrocytes in the Hippocampus of HNF Mice

IF analysis revealed that the activation of microglia and astrocytes, as indicated by Iba1 and GFAP labeling, respectively, was significantly attenuated in the CFE group compared to the LPS group (all $p < 0.05$) (Figure 5A–D). Additionally, IHC analysis demonstrated that CFE intervention markedly reduced CD11b AOD compared to the LPS group ($p < 0.0001$) (Figure 5E,F). Concordantly, WB analysis (Figure 5G,H) confirmed decreased CD11b protein expression in the CFE group ($p < 0.01$). These data collectively indicated that CFE inhibited microglial and astrocyte activation.

3.10. CFE Increased SCFAs in Fecal of HNF Mice

Given the established role of SCFAs in microbiota-gut-brain axis signaling, we measured fecal SCFAs levels to evaluate the effect of CFE on gut microbiota metabolism (Figure 6A–D). Notably, CFE intervention elevated total SCFAs ($p < 0.01$), acetic acid ($p < 0.01$), propanoic acid and butanoic acid compared to the LPS group. The results indicated that CFE reversed the reduction in fecal SCFAs levels induced by HNF.

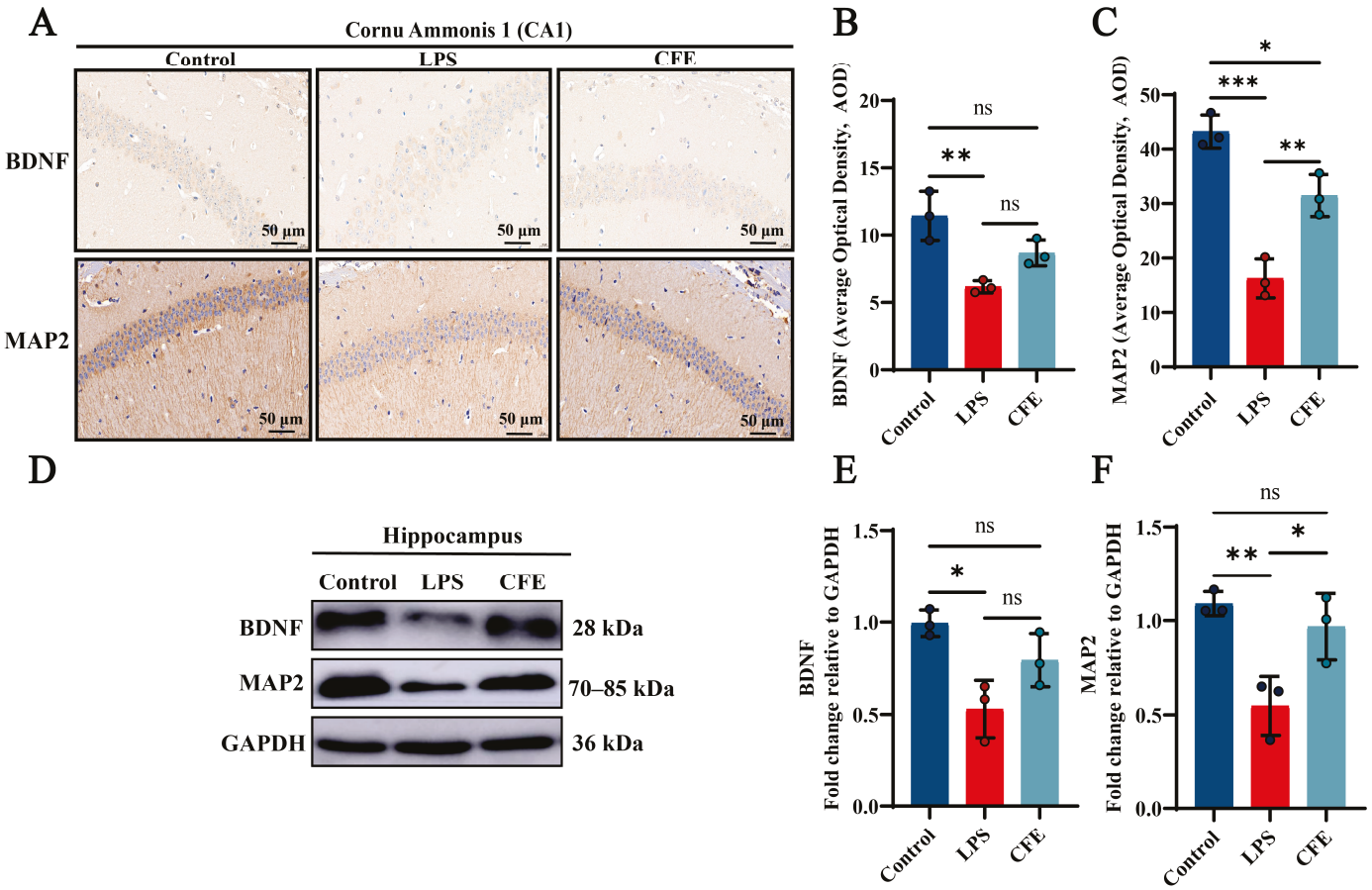

Figure 4. CFE increased hippocampal levels of BDNF and MAP2 in HNF mice. The colored dots represent data points from different sample groups. (**A**) Representative immunohistochemical (IHC) staining images of BDNF and MAP2. (**B**,**C**) Quantification of BDNF and MAP2 IHC staining intensity expressed as AOD. (**D**) Representative Western blot images of hippocampal BDNF and MAP2. (**E**,**F**) Quantitative analysis of BDNF and MAP2 protein levels from Western blot, normalized to GAPDH. Data are presented as the mean ± SEM (N = 3). Statistically significant differences were indicated: * $p < 0.05$, ** $p < 0.01$, *** $p < 0.001$, ns $p > 0.05$, compared to the LPS group.

3.11. CFE Reshaped the Gut Microbiota of HNF Mice

Fecal 16S rRNA gene sequencing was performed to evaluate CFE's impact on gut microbiota in HNF mice. PCoA based on Bray-Curtis distances (Figure 6E) revealed distinct inter-group clustering. PC1 and PC2 accounted for 33.68% and 21.97% of variance, respectively. Notably, reduced compositional overlap between the LPS and CFE groups indicated microbiota restructuring. At the genus level (Figure 6F), CFE administration shifted dominant bacterial flora from *Lactobacillus* and *Staphylococcus* (LPS group) to *norank_f__Muribaculaceae* and *unclassified_f__Lachnospiraceae* (CFE group). Wilcoxon tests (Figure 6G–K) confirmed CFE significantly increased *norank_f__Muribaculaceae* ($p < 0.05$) and *norank_f__Lachnospiraceae* ($p < 0.05$), while decreasing *Staphylococcus* ($p < 0.01$) and *Helicobacter* ($p < 0.05$) compared to the LPS group. Collectively, the findings proved that CFE supplementation renovated LPS-induced gut microbiota disturbances.

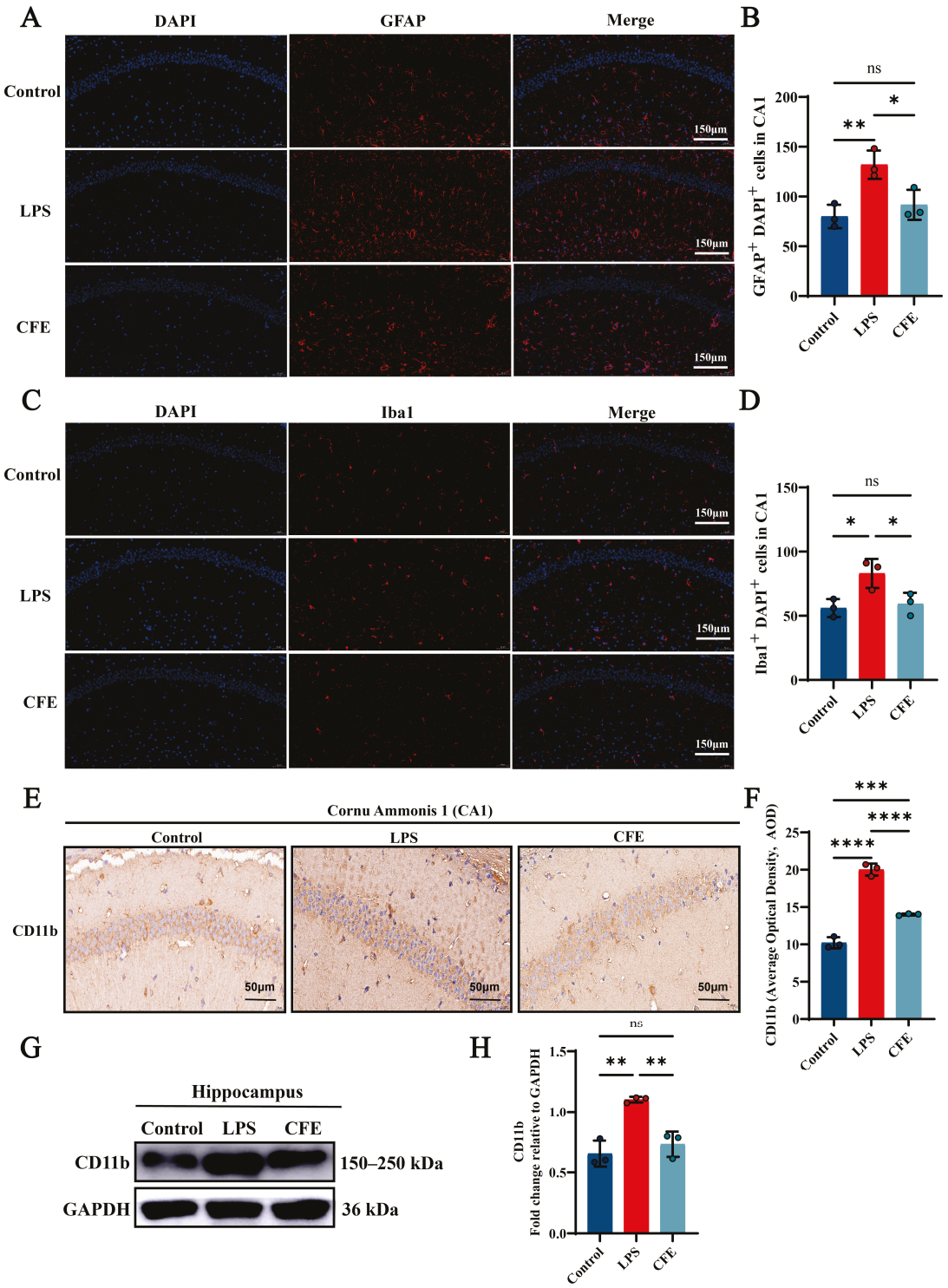

Figure 5. CFE suppressed glial cell activation in the hippocampus of HNF mice. The colored dots represent data points from different sample groups. (**A**) Representative immunofluorescence (IF) image of GFAP (astrocyte marker) in the hippocampal CA1 region. (**B**) Quantitative analysis of GFAP immunofluorescence intensity. (**C**) Representative immunofluorescence image of Iba1 (microglial marker) in the hippocampal CA1 region. (**D**) Quantitative analysis of Iba1 immunofluorescence intensity. (**E**) Representative immunohistochemical (IHC) staining of CD11b. (**F**) Quantification of CD11b IHC intensity expressed as AOD. (**G**) Representative Western blot images of hippocampal CD11b. (**H**) Quantitative analysis of CD11b protein levels from Western blot, normalized to GAPDH. Data are presented as the mean ± SEM (N = 3). Statistically significant differences were indicated: * $p < 0.05$, ** $p < 0.01$, *** $p < 0.001$, **** $p < 0.0001$, ns $p > 0.05$, compared to the LPS group.

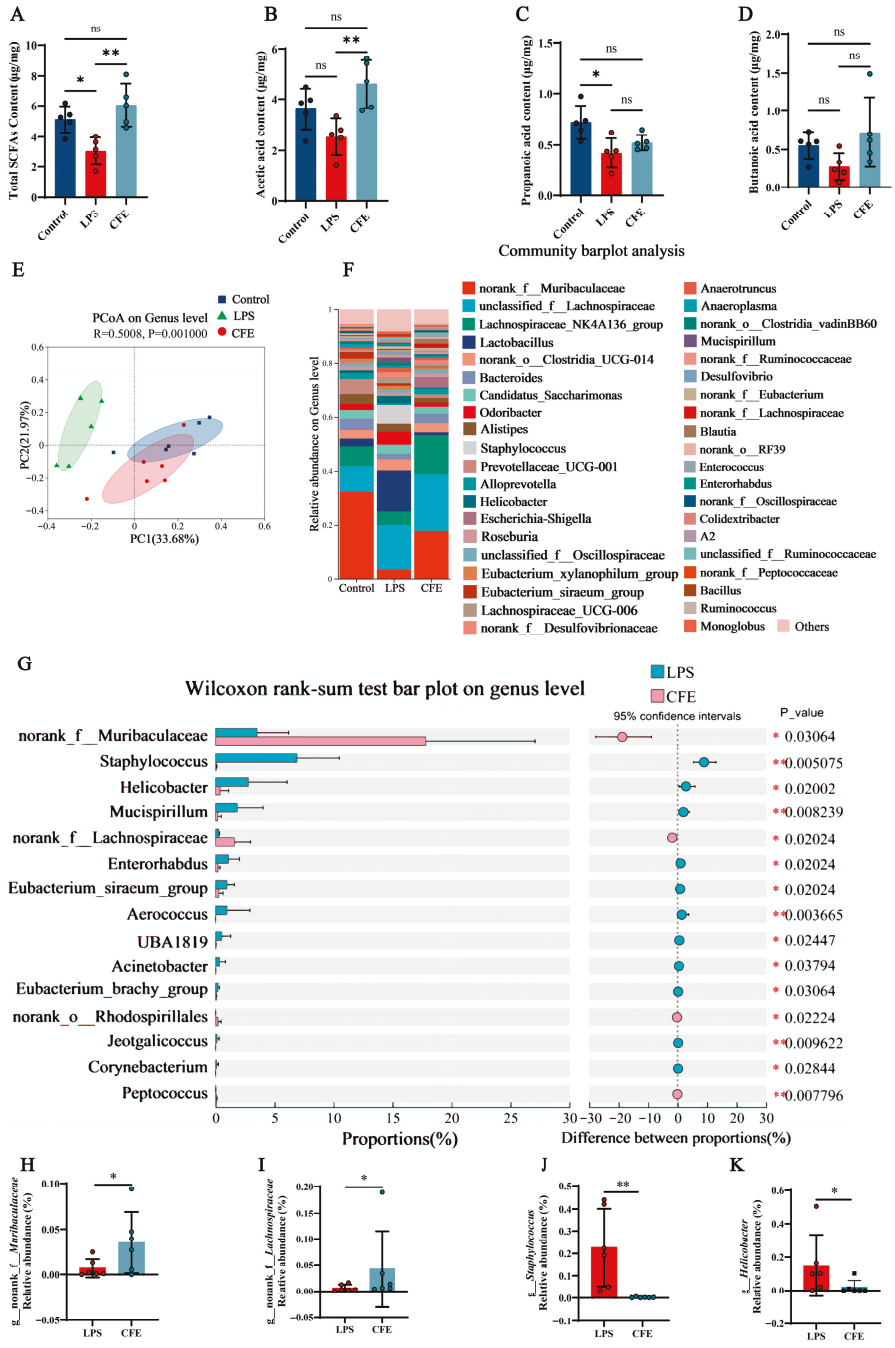

Figure 6. CFE modulates the gut microbiome and enhances SCFAs production in HNF mice. The colored dots represent data points from different sample groups. (**A**) Fecal concentration of total SCFAs (N = 5). (**B**) Fecal concentration of acetic acid (N = 5). (**C**) Fecal concentration of propionic acid (N = 5). (**D**) Fecal concentration of butyric acid (N = 5). (**E**) Beta diversity of the gut microbiota visualized by PCoA based on Bray-Curtis distances at the genus level. The plot shows the microbial community composition of samples from the Control (blue), LPS (green), and CFE (red) groups. Each dot represents an individual sample. The background color illustrates the clustering of samples within the ordination space. (**F**) Bar plot showing the relative abundance of bacterial genera. (**G**) Differential abundance analysis between the CFE and LPS groups (Wilcoxon rank-sum test). (**H**) Relative abundance of the genus *Muribaculaceae* across groups. (**I**) Relative abundance of the genus *Lachnospiraceae* across groups. (**J**) Relative abundance of the genus *Staphylococcus* across groups. (**K**) Relative abundance of the genus *Helicobacter* across groups. Data are presented as the mean ± SEM (N = 6). Statistically significant differences were indicated: * $p < 0.05$, ** $p < 0.01$, ns $p > 0.05$, compared to the LPS group.

3.12. CFE Regulated Serum Metabolites in HNF Mice

Serum untargeted metabolomic profiling was employed to characterize systemic metabolic alterations during HNF progression. The clear separation between the LPS and control groups in the PCA score plot (Figure 7A) confirmed distinct metabolic profiles and verified successful model induction. Differential metabolites were identified using dual thresholds of variable importance in projection (VIP) > 1 and statistical significance ($p < 0.05$), with fold-change (FC) values determining regulation directionality (FC < 1: downregulation; FC > 1: upregulation; Figure 7B). 475 metabolites exhibited significant abundance changes between the LPS and CFE groups (304 upregulated, 171 downregulated). Hierarchical clustering analysis revealed that the CFE group substantially increased concentrations of phosphatidylserine [PS (20:5 (5Z,8Z,11Z,14Z,17Z)/22:1 (13Z))], phosphatidylcholines [PC (18:0/20:3 (8Z,11Z,14Z), PC (20:0/18:2)], phosphatidylethanolamine [PE (20:2 (11Z,14Z)/20:3 (8Z,11Z,14Z))], lysophosphatidylcholines [LPC (15:0), LPC (P-18:0/0:0)], choline, ALA, stearidonic acid (SDA), and 5-HT compared to the LPS group (Figure 7C). KEGG Topological analysis further identified 20 significantly enriched metabolic routes, notably encompassing glycerophospholipid metabolism, α-linolenic acid metabolism, tryptophan metabolism, and glycine-serine-threonine metabolism (Figure 7D). Metabolomic interaction networks revealed the pathway interconnections and underlying mechanisms (Figure 7E). ELISA quantification confirmed CFE group elevations of 5-HT ($p < 0.05$) and ALA ($p < 0.05$) in both serum and hippocampal tissues compared to the LPS group (Figure 7F–I). For establishing gut-microbiota-metabolite crosstalk, Pearson correlation-based networks were generated and genus-level networks demonstrated significant associations (Figure 7J): g__norank_f__*Muribaculaceae* and g__norank_f__*Lachnospiraceae* abundances showed positive correlations with PC (15:0/18:2), PC (20:0/18:2), PE (20:2/20:3), PS (20:5/22:1), 5-HT, ALA, SDA, acetate, and isobutyrate, while *Staphylococcus* abundance was inversely correlated with these metabolites. Similarly, *Helicobacter* exhibited negative correlations specifically with PC (18:0/20:3), PE (20:2/20:3), PS (20:5/22:1), ALA, and SDA. Collectively, CFE mediated microbiota remodeling characterized by enrichment of *Muribaculaceae* and *Lachnospiraceae* alongside suppression of *Staphylococcus* and *Helicobacter* potentiated beneficial metabolite production.

3.13. CFE, Luteolin, and Kaempferol Significantly Improved Cell Viability and Reduced ROS Levels in BV2 Cells

We evaluated the impact of CFE, luteolin and kaempferol on cell viability and ROS levels in BV2 cells. The CCK-8 assay revealed that CFE significantly attenuated LPS-induced cytotoxicity in a concentration-dependent manner, with the most pronounced improvement in BV2 cell viability observed at 400 μg/mL ($p < 0.01$), prompting the selection of this concentration for further experiments (Figure 8A). Both luteolin (14 μM) and kaempferol (10 μM) also enhanced BV2 cells viability ($p < 0.001$, Figure 8B). Moreover, CFE, luteolin, and kaempferol significantly suppressed ROS generation (Figure 8C, $p < 0.05$, $p < 0.01$, and $p < 0.01$, respectively). The findings indicated that CFE, Luteolin, and Kaempferol confer protection against inflammatory and oxidative stress in BV2 cells.

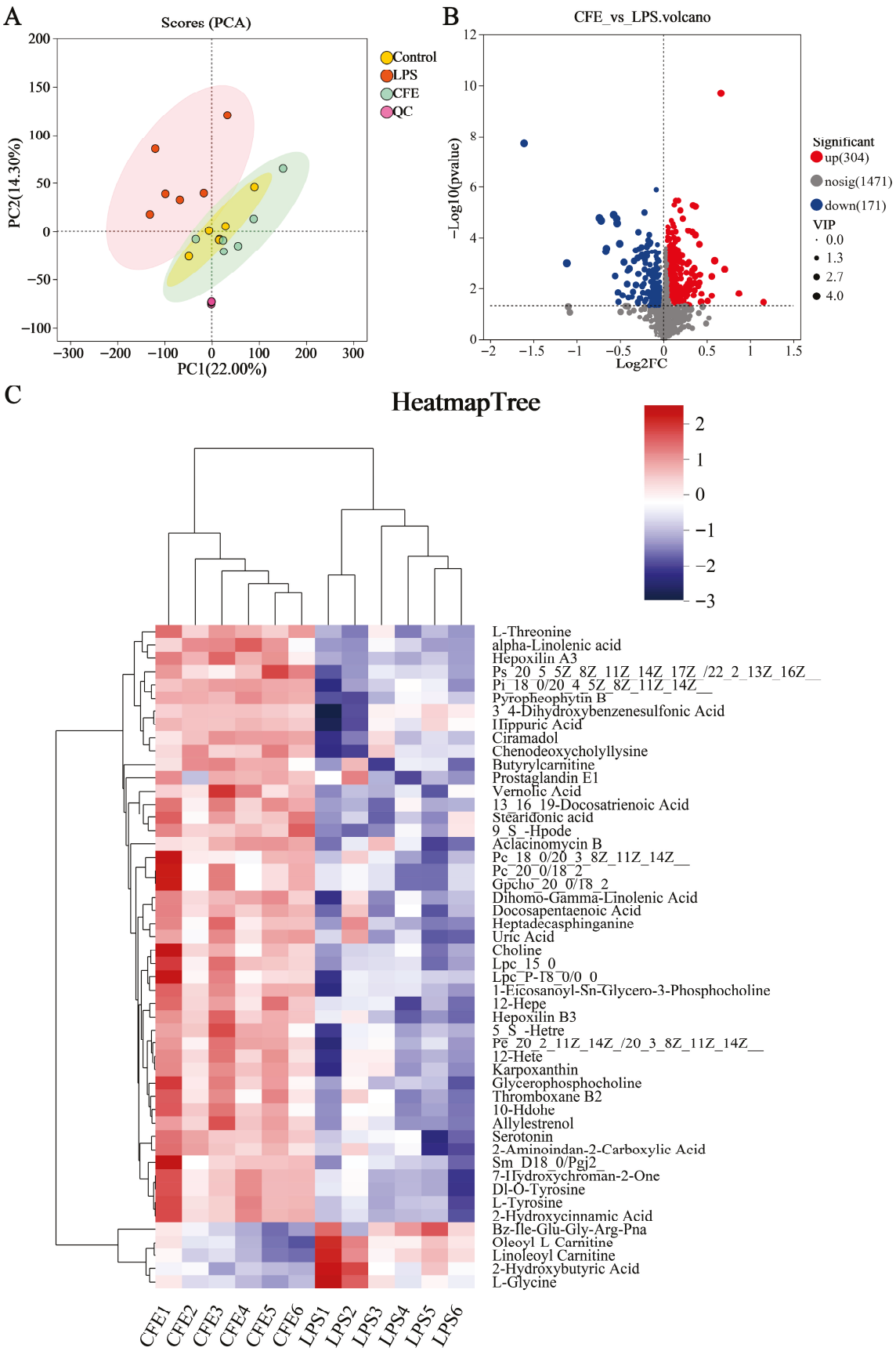

Figure 7. *Cont.*

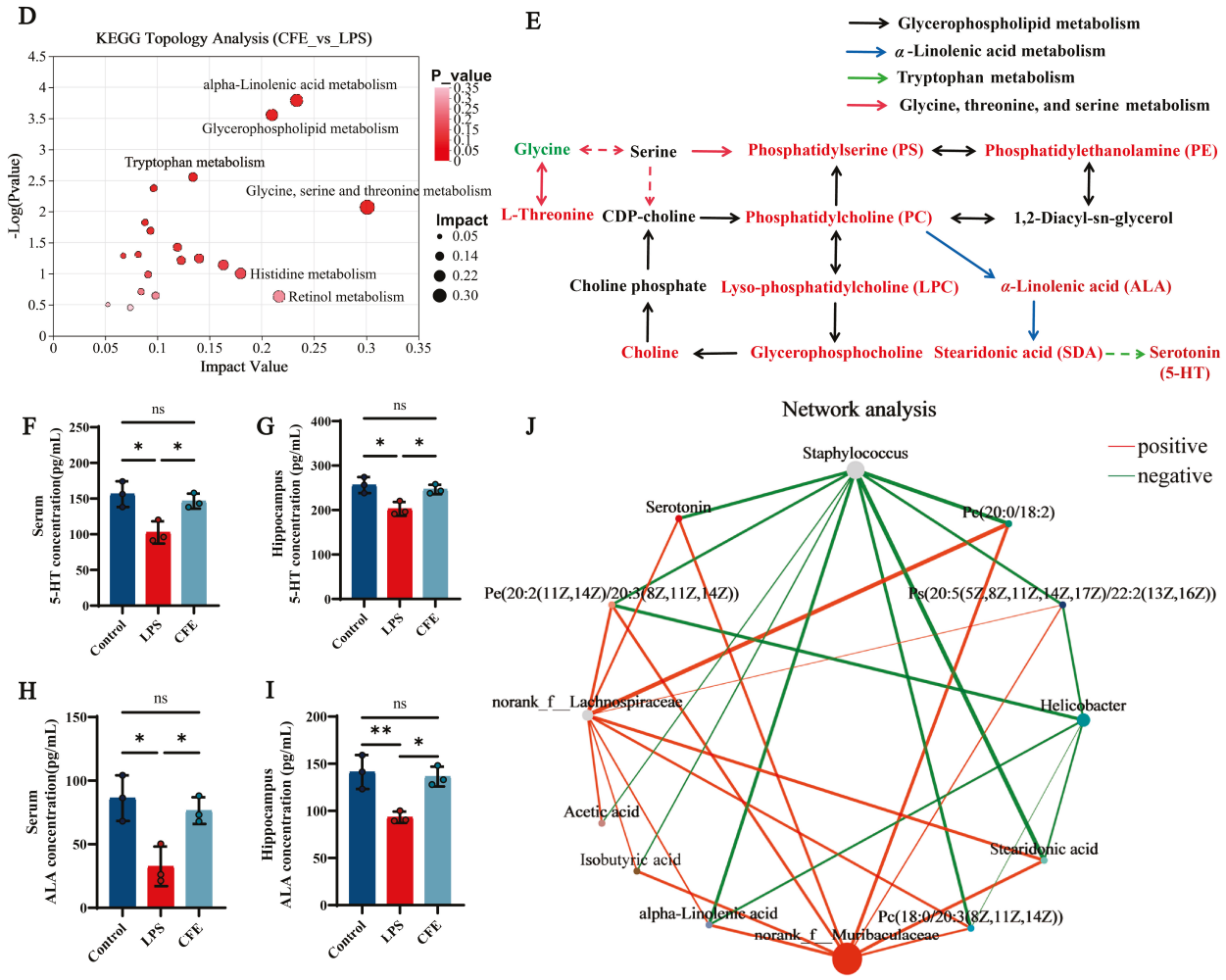

Figure 7. CFE modulated host systemic metabolism. The colored dots represent data points from different sample groups. (**A**) Principal component analysis (PCA) score chart. (**B**) The volcano plots of significantly differential metabolic components in the CFE group compared to the LPS group ($p < 0.05$). (**C**) Hierarchical cluster analysis of differential metabolites between the CFE group and the LPS group. (**D**) Potential target metabolic pathways of CFE in the pretreatment of HNF mice. (**E**) A schematic map depicting the enriched key pathways and the targeted compounds regulated by CFE in HNF mice; Red represents the upregulation of metabolites and green represents the downregulation of metabolites. (**F**,**G**) 5-HT concentrations in serum and hippocampus (N = 3). (**H**,**I**) ALA concentrations in serum and hippocampus (N = 3). (**J**) Integrated analysis reveals that the gut microbiome is associated with changes in metabolites. Red edges indicate a positive correlation and green edges indicate a negative correlation. Data are presented as the means ± SEM (N = 6). Statistically significant differences were indicated: * $p < 0.05$, ** $p < 0.01$, ns $p > 0.05$, compared to the LPS group.

3.14. CFE, Luteolin and Kaempferol Suppressed M1 Polarization and Promoted M2 Polarization in BV2 Microglial Cells

RT-qPCR analysis showed that CFE, luteolin and kaempferol significantly suppressed M1 marker expression (Figure 8D–F) while elevating M2 marker expression (Figure 8G–I). Specifically, CFE downregulated iNOS, CD86, and TNF-α (all $p < 0.05$) while concurrently upregulating Arg-1, CD206, and IL-10 (all $p < 0.05$). Luteolin significantly decreased iNOS ($p < 0.01$), CD86 ($p < 0.001$), and TNF-α ($p < 0.01$), and increased Arg-1 ($p < 0.01$), CD206 ($p < 0.001$), and IL-10 ($p < 0.01$). Kaempferol downregulated iNOS ($p < 0.01$), CD86 ($p < 0.001$), and TNF-α ($p < 0.01$), and upregulated Arg-1 ($p < 0.01$), CD206 ($p < 0.001$), and IL-10 ($p < 0.001$). Compared to the CFE group, the Luteolin and Kaempferol groups

demonstrated superior regulatory effects on M1/M2 polarization of BV2 microglial cells. The results showed that the CFE, Luteolin and Kaempferol attenuated macrophage inflammatory responses in BV2 macrophages by suppressing M1 polarization and promoting M2 polarization.

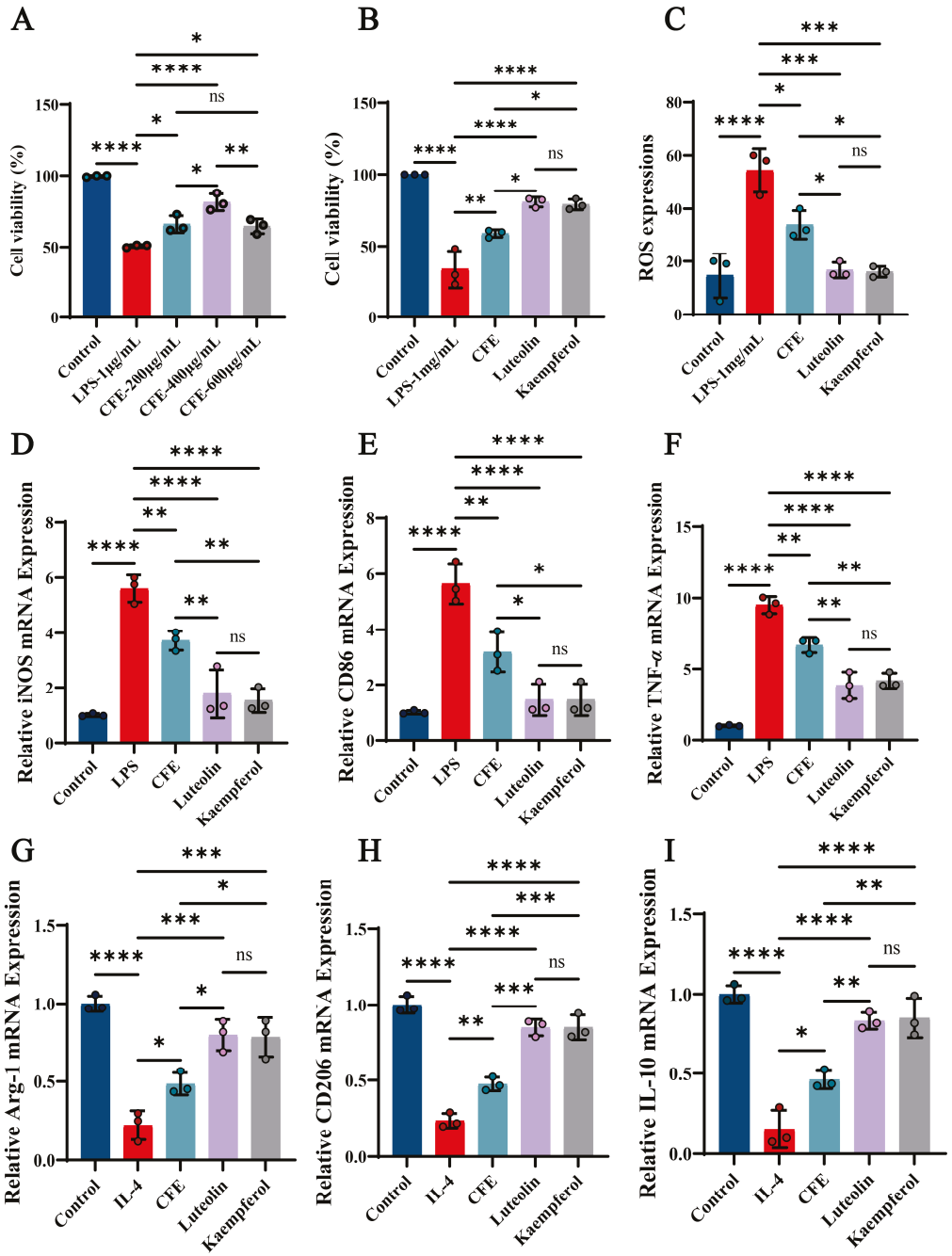

Figure 8. CFE regulated microglial polarization in LPS-induced BV2 cells. The colored dots represent data points from different sample groups. (**A**) Cell viability assessed by CCK-8 assay following pretreatment with increasing concentrations of CFE. (**B**) Cell viability measured by CCK-8 after pretreatment with CFE, luteolin or kaempferol. (**C**) Quantitative analysis of intracellular ROS levels. (**D**–**F**) mRNA expression of M1 polarization markers (iNOS, CD86, TNF-α) determined by qPCR. (**G**–**I**) mRNA expression of M2 polarization markers (Arg-1, CD206, IL-10) determined by qPCR. Data are presented as the means ± SEM (N = 3). Statistically significant differences were indicated: * $p < 0.05$, ** $p < 0.01$, *** $p < 0.001$, **** $p < 0.0001$, ns $p > 0.05$, compared to the LPS group.

4. Discussion

The rising incidence of cognitive decline, which increasingly affects younger demographics and severely compromises quality of life, identifies HNF as a central driver in its pathogenesis and progression [46–48]. However, the development of therapeutics specifically targeting HNF remains limited. In this context, the growing recognition of plant-derived natural products as potential treatments for neurological disorders has opened a new avenue for HNF intervention [26,49]. Our study demonstrated that CFE confers significant protection against cognitive decline in a mouse model of HNF. This protective efficacy is underpinned by a multi-faceted mechanism involving direct anti-neuroinflammatory action, remodeling of the gut microbiota and associated metabolites, modulation of microglial polarization, and subsequent activation of the BDNF/5-HT pathway. Phytochemical analysis further revealed that CFE possesses a rich flavonoid profile, with luteolin and kaempferol identified as the predominant constituents, which are considered primary contributors to its observed therapeutic effects.

Our initial experiments used in vitro models to assess the neuroprotective and antioxidant potential of CFE. Pretreatment with CFE demonstrated substantial efficacy in protecting HT22 cells against HNF, with the solvent C extract (chloroform-methanol, 6:4, v/v) exhibiting the strongest activity and therefore being selected for subsequent investigation. The marked recovery in cell viability and pronounced reduction in ROS levels confirmed that CFE confers protection against the intertwined pathologies of inflammatory and oxidative stress in HNF [50]. To identify the active constituents responsible for these effects, we characterized the chemical composition of CFE. HPLC-MS analysis revealed a complex profile with multiple identified compounds. Based on their established bioavailability, BBB permeability, and documented anti-inflammatory and neuroimmunomodulatory properties [51], flavonoids were prioritized as the likely active fraction. Among these, luteolin and kaempferol were the most abundant, quantified at concentrations of 10,796.37 ng/mL and 3082.77 ng/mL, respectively.

The neuroprotective potential of CFE observed in cellular models was further validated in a mouse model of LPS-induced HNF and cognitive decline. As reported in previous studies [52], HNF mice in our model exhibited significant cognitive impairment. Following CFE intervention, behavioral performance improved notably: in the Morris water maze test, increased platform crossings, longer time spent, and greater distance traveled in the target quadrant indicated enhanced spatial learning and memory. In the novel object recognition test, an elevated recognition index reflected improved exploratory behavior and discrimination of novel objects. These behavioral benefits were accompanied by amelioration of hippocampal histopathology. CFE intervention effectively reversed key LPS-induced structural alterations in the CA1 region, including disorganized neuronal arrangement, widened intercellular spaces, nucleolar condensation, and significant reductions in neuronal density and eosinophilic proportion. Together, these histopathological findings demonstrate that CFE effectively preserves hippocampal structural integrity under neuroinflammatory conditions.

As key pathological drivers in HNF, both the accumulation of Aβ1–42 and the aberrant hyperphosphorylation of Tau protein are directly promoted by the inflammatory process. Consequently, strategies aimed at inhibiting Aβ1–42 accumulation and P-Tau formation, while mitigating their neurotoxicity, are crucial for preventing and treating HNF [5]. Accumulating evidence suggests that certain plant-derived natural products and their bioactive components can counteract HNF by suppressing Aβ1–42 aggregation and Tau hyperphosphorylation. For instance, *Scrophularia buergeriana* extract was shown to reduce Aβ1–42 deposition and Tau hyperphosphorylation in a mouse model of cognitive decline [53]. In line with this, our data from IHC and Western blot analyses demonstrated that CFE

significantly suppressed the expression of Aβ1–42, the kinase GSK-3β, total Tau, and Tau phosphorylated at Ser404. GSK-3β is a pivotal kinase that, upon activation, potently drives Tau phosphorylation, leading to neurofibrillary tangle formation and subsequent neuronal dysfunction [7]. Our results suggest that CFE reduces the expression of Aβ1–42 and GSK-3β, thereby inhibiting p-Tau (Ser404) formation by blocking Aβ1–42-mediated aggregation. This mechanism likely contributes to the protection of neuronal and synaptic structure, ultimately improving HNF and cognitive decline, which is consistent with previous research [54].

Synaptic plasticity, which underlies learning and memory, depends critically on neurotrophic support and the maintenance of neuronal structural integrity; thus, enhancing synaptic function represents a promising therapeutic strategy for HNF [55]. BDNF acts as a master regulator of neuronal survival, differentiation, and synaptic function, and its expression in the hippocampus is particularly vital for cognitive processes [56]. Similarly, MAP2 is essential for dendritic arborization and stability, which are fundamental for synaptic connectivity and information integration [57]. Previous studies have shown that luteolin significantly restored the BDNF-TrkB signaling axis and increased MAP2 protein levels, thereby attenuating HNF in mice [58]. In the present study, we found that CFE significantly upregulated hippocampal levels of both BDNF and MAP2, indicating its role in promoting a neuroplastic milieu. This enhancement of neurotrophic signaling and structural support likely represents a key mechanism through which CFE facilitates the recovery of cognitive function, as observed in our behavioral tests.

The neuroprotective and synaptoprotective effects of CFE were accompanied by a marked suppression of HNF. Neuroinflammatory responses are typically driven by aberrant activation of glial cells [59]. Pathological activation of microglia and astrocytes triggers the release of pro-inflammatory cytokines, ultimately contributing to neuronal damage and synaptic loss [14]. In our study, CFE significantly reduced both the protein and mRNA levels of key pro-inflammatory cytokines in the hippocampus and in systemic circulation. Furthermore, CFE markedly downregulated hippocampal expression of the surface receptor CD11b, a marker of microglial activation that is upregulated during HNF and contributes to pro-inflammatory signaling [4]. Immunofluorescence analysis further demonstrated that CFE reduced the activation of both microglia (Iba1+) and astrocytes (GFAP+), indicating that CFE exerts an anti-inflammatory effect on hippocampal glial cells.

The microbiota-gut-brain axis functions as a key bidirectional communication network, linking the gut microbiota with the central nervous system and maintaining a dynamic equilibrium among the gut, brain, and microbial communities [60]. Homeostasis of the gut microbiota, characterized by balanced composition and diversity, is essential for overall health [61]. Studies on the therapeutic application of natural products have shown that plant-derived floral extracts can modulate intestinal microecology and exert prebiotic effects. For example, flavonoids from *Dendrobium officinale* flowers alleviated cognitive decline by reshaping the gut microbiota and suppressing microglial activation, which in turn upregulated BDNF and synaptic proteins and improved synaptic plasticity [49]. In the present study, 16S rRNA sequencing revealed that CFE effectively counteracted LPS-induced gut dysbiosis. It significantly increased the abundance of beneficial bacterial families with known SCFAs-producing capabilities, such as *Muribaculaceae* and *Lachnospiraceae*, while suppressing potential pathobionts like *Staphylococcus* and *Helicobacter*. These microbial changes are functionally important: *Muribaculaceae* and *Lachnospiraceae* are consistently associated with anti-inflammatory activity, gut barrier integrity, and SCFAs production [62,63], whereas *Staphylococcus* and *Helicobacter* have been positively correlated with systemic inflammation, increased gut permeability, and risk for hippocampal neuroinflammation and cognitive decline [64,65]. These results confirm that CFE can restore

intestinal microbial health by modulating gut flora structure. The regulatory influence of gut microbiota metabolites on the gut-brain axis is largely mediated by SCFAs. Produced through microbial fermentation of dietary fiber, major SCFAs-acetate, propionate, and butyrate-cross the BBB and perform critical functions such as modulating microglial activity, suppressing HNF, and supporting cognitive processes [66]. Our targeted metabolomics data showed that CFE significantly restored fecal SCFAs levels, with acetate exhibiting a particularly marked increase. This rise in SCFAs provides a mechanistic link between CFE-induced gut microbiota remodeling and the alleviation of brain pathology, likely through microglial modulation and reinforcement of the BBB.

To characterize the systemic metabolic changes induced by CFE, we performed untargeted metabolomic profiling of serum. The analysis indicated that CFE administration altered the host metabolome, upregulating key metabolites involved in glycerophospholipid metabolism, α-linolenic acid (ALA) metabolism, and tryptophan metabolism. ELISA confirmed a central finding: elevated levels of ALA and 5-HT in both serum and hippocampal tissues. ALA, a plant-derived omega-3 fatty acid, exhibits multiple neuroprotective properties, including direct inhibition of Tau aggregation, attenuation of Aβ-induced neurotoxicity, and potent anti-inflammatory and antioxidant activities [67,68]. 5-HT, a key monoamine neurotransmitter, is integral not only to regulating mood, sleep, and cognition but also to modulating neuroimmune responses, as its receptors are expressed on microglia and other immune cells [69]. A Pearson correlation-based network further reinforced the gut-brain link. It showed that the abundances of beneficial bacteria (*Lachnospiraceae*, *Muribaculaceae*) were positively correlated with ALA, 5-HT, and SCFAs, whereas pathogenic genera (*Staphylococcus*, *Helicobacter*) exhibited strong negative correlations. These results suggest that CFE facilitates a coherent gut microbiota-metabolite-brain signaling axis, whereby the restructured gut microbial community enhances the production of beneficial systemic metabolites that can cross the BBB to support brain health and function.

Luteolin treatment has been shown to shift microglial polarization toward the anti-inflammatory M2 phenotype in both in vitro and in vivo studies [17]. Kaempferol, a major flavonoid in edible plants, has been shown to modulate microglial M1/M2 polarization, thereby alleviating neuroinflammatory dyshomeostasis [18]. To determine how the phytochemical profile of CFE influences brain immunity, we examined its direct effects on microglia, the principal cellular mediators of HNF. In BV2 microglial cells, a key finding was that both CFE and its principal flavonoid constituents, luteolin and kaempferol, significantly shifted polarization from the pro-inflammatory M1 phenotype toward the anti-inflammatory M2 state. At the mRNA level, this shift was characterized by downregulation of M1 markers (iNOS, CD86, TNF-α) and upregulation of M2 markers (Arg-1, CD206, IL-10). Notably, luteolin and kaempferol alone induced these changes more potently than the complete CFE extract. These results establish a direct link between the chemical constituents of CFE and the suppression of HNF and glial activation in vitro. We conclude that luteolin and kaempferol mediate the effects of CFE by driving microglial phenotype switching, which in turn disrupts persistent neuroinflammatory signaling and helps establish a microenvironment conducive to neural repair and plasticity.

5. Conclusions

In summary, this study demonstrates that CFE is a promising therapeutic candidate for mitigating HNF and cognitive decline. The protective efficacy of CFE is mediated through a multi-level mechanism: it provides direct neuroprotection against oxidative and inflammatory stress; inhibits core neuropathology by reducing Aβ1–42 and P-Tau levels; promotes neuroplasticity via upregulation of BDNF and MAP2; attenuates neuroinflammation by suppressing microglial and astrocyte activation while modulating cytokine

networks; remodels the microbiota-gut-brain axis to enhance production of beneficial metabolites such as SCFAs, ALA and 5-HT; and facilitates microglial polarization toward the anti-inflammatory M2 phenotype, an effect likely attributable to its flavonoid constituents, especially luteolin and kaempferol. Collectively, these findings validate the neuroprotective role of CFE via the microbiota-gut-brain axis and provide novel perspectives for preventing and managing cognitive decline with natural compounds. A limitation of the current study lies in its reliance on animal models, which may not fully recapitulate human disease. Thus, these promising preclinical results warrant further validation in clinical trials.

Supplementary Materials: The following supporting information can be downloaded at: https://www.mdpi.com/article/10.3390/nu17243958/s1, Table S1: Primer sequence.

Author Contributions: Conceptualization, H.G. and H.H.; methodology, H.G. and L.L.; software, Y.L.; validation, W.L., Y.L. and X.L.; formal analysis, W.L.; investigation, Y.L.; resources, H.G. and B.Z.; data curation, W.L.; writing—original draft preparation, W.L.; writing—review and editing, Y.L.; visualization, H.H.; supervision, Y.L.; project administration, H.G.; funding acquisition, H.G. All authors have read and agreed to the published version of the manuscript.

Funding: This research was funded by the National Key R&D Program of China, grant number 2022YFD1600404-04; the National Natural Science Foundation of China, grant number 32201951; the National Center of Technology Innovation for Dairy, grant number 2024-QNJJ-014.

Institutional Review Board Statement: The animal study protocol was approved by the Animal Experimentation Ethics Committee of China Agricultural University (Protocol Aw71705202-6-04, 17 July 2025).

Informed Consent Statement: Not applicable.

Data Availability Statement: We permit unrestricted use, distribution, and reproduction in any medium, provided the original work is properly cited. Sequencing data generated in this study were deposited in the Sequence Read Archive (SRA) (https://www.ncbi.nlm.nih.gov/sra/, accessed on 19 November 2025) with the BioProject ID: PRJNA1366079 and MTBLS12026.

Conflicts of Interest: The authors declare no conflicts of interest.

Abbreviations

The following abbreviations are used in this manuscript:

HNF	Hippocampal Neuroinflammation
CFE	*Corylus heterophylla* Fisch. Male Flower Extract
LPS	Lipopolysaccharide
Aβ1–42	Amyloid-beta 1–42
P-Tau	Phosphorylated Tau Protein
GSK-3β	Glycogen Synthase Kinase-3β
IL-33	Interleukin-33
BDNF	Brain-derived Neurotrophic Factor
MAP2	Microtubule-associated Protein 2
ALA	α-linolenic Acid
5-HT	Serotonin
NFTs	Neurofibrillary Tangles
BBB	Blood-Brain Barrier
CD11b	Cluster of Differentiation 11b
ROS	Reactive Oxygen Species
SCFAs	Short-chain Fatty Acids
DMEM	Dulbecco's Modified Eagle Medium
FBS	Fetal Bovine Serum

P/S	Penicillin-streptomycin
CA1	Cornu Ammonis 1
OTUs	Operational Taxonomic Units
DCFH-DA	2′,7′-dichlorofluorescin Diacetate

References

1. Hampshire, A.; Trender, W.; Chamberlain, S.R.; Jolly, A.E.; Grant, J.E.; Patrick, F.; Mazibuko, N.; Williams, S.C.; Barnby, J.M.; Hellyer, P.; et al. Cognitive deficits in people who have recovered from COVID-19. *eClinicalMedicine* **2021**, *39*, 101044. [CrossRef] [PubMed]
2. Tran, N.B.; Lee, H.; Ji, M.G.; Ngo Hoang, L.; Lee, S.J. The synergistic extract of *Zophobas atratus* and *Tenebrio molitor* regulates neuroplasticity and oxidative stress in a scopolamine-induced cognitive impairment model. *Front. Aging Neurosci.* **2025**, *17*, 1566621. [CrossRef]
3. Zhang, W.; Xiao, D.; Mao, Q.; Xia, H. Role of neuroinflammation in neurodegeneration development. *Signal Transduct. Target. Ther.* **2023**, *8*, 267. [CrossRef]
4. Qin, L.; Wu, X.; Block, M.L.; Liu, Y.; Breese, G.R.; Hong, J.S.; Knapp, D.J.; Crews, F.T. Systemic LPS causes chronic neuroinflammation and progressive neurodegeneration. *Glia* **2007**, *55*, 453–462. [CrossRef]
5. Lee, J.W.; Lee, Y.K.; Yuk, D.Y.; Choi, D.Y.; Ban, S.B.; Oh, K.W.; Hong, J.T. Neuro-inflammation induced by lipopolysaccharide causes cognitive impairment through enhancement of beta-amyloid generation. *J. Neuroinflamm.* **2008**, *5*, 37. [CrossRef]
6. Thapa, A.; Jett, S.D.; Chi, E.Y. Curcumin Attenuates Amyloid-β Aggregate Toxicity and Modulates Amyloid-β Aggregation Pathway. *ACS Chem. Neurosci.* **2016**, *7*, 56–68. [CrossRef]
7. Fan, X.; Zhao, Z.; Wang, D.; Xiao, J. Glycogen synthase kinase-3 as a key regulator of cognitive function. *Acta Biochim. Biophys. Sin.* **2020**, *52*, 219–230. [CrossRef]
8. Decandia, D.; Gelfo, F.; Landolfo, E.; Balsamo, F.; Petrosini, L.; Cutuli, D. Dietary Protection against Cognitive Impairment, Neuroinflammation and Oxidative Stress in Alzheimer's Disease Animal Models of Lipopolysaccharide-Induced Inflammation. *Int. J. Mol. Sci.* **2023**, *24*, 5921. [CrossRef]
9. Fu, Y.; Jie, J.; Lei, L.; Liu, M.; Wang, J.; Lei, L.; Liu, H. Exploring the destructive synergy between IL-33 and Suilysin hemolysis on blood-brain barrier stability. *Microbiol. Spectr.* **2024**, *12*, e0061224. [CrossRef] [PubMed]
10. Geng, Z.; Peng, F.; Cheng, Z.; Su, J.; Song, J.; Han, X.; Li, R.; Li, X.; Cui, R.; Li, B. Astrocytic FABP7 Alleviates Depression-Like Behaviors of Chronic Unpredictable Mild Stress Mice by Regulating Neuroinflammation and Hippocampal Spinogenesis. *FASEB J* **2025**, *39*, e70606. [CrossRef] [PubMed]
11. Lima Giacobbo, B.; Doorduin, J.; Klein, H.C.; Dierckx, R.A.J.O.; Bromberg, E.; de Vries, E.F.J. Brain-Derived Neurotrophic Factor in Brain Disorders: Focus on Neuroinflammation. *Mol. Neurobiol.* **2019**, *56*, 3295–3312. [CrossRef] [PubMed]
12. Fontanella, R.A.; Ghosh, P.; Pesapane, A.; Taktaz, F.; Puocci, A.; Franzese, M.; Feliciano, M.F.; Tortorella, G.; Scisciola, L.; Sommella, E.; et al. Tirzepatide prevents neurodegeneration through multiple molecular pathways. *J. Transl. Med.* **2024**, *22*, 114. [CrossRef] [PubMed]
13. Wang, X.-H.; Zuo, Z.-F.; Meng, L.; Yang, Q.; Lv, P.; Zhao, L.-P.; Wang, X.-B.; Wang, Y.-F.; Huang, Y.; Fu, C.; et al. Neuroprotective effect of salidroside on hippocampal neurons in diabetic mice via PI3K/Akt/GSK-3β signaling pathway. *Psychopharmacology* **2023**, *240*, 1865–1876. [CrossRef]
14. Barbati, S.A.; D'Amelio, C.; Feroleto, C.; Morotti, M.; Sarrapochiello, I.N.; Natale, F.; Puma, D.D.L.; Gomez-Galvez, Y.; Blanco-Suarez, E.; Iacovitti, L.; et al. Intranasal delivery of extracellular vesicles derived from human bone marrow mesenchymal stem cells dampens neuroinflammation and ameliorates motor deficits in a mouse model of cortical stroke. *Exp. Neurol.* **2025**, *396*, 115540. [CrossRef]
15. Nam, H.Y.; Nam, J.H.; Yoon, G.; Lee, J.-Y.; Nam, Y.; Kang, H.-J.; Cho, H.-J.; Kim, J.; Hoe, H.-S. Ibrutinib suppresses LPS-induced neuroinflammatory responses in BV2 microglial cells and wild-type mice. *J. Neuroinflamm.* **2018**, *15*, 271. [CrossRef] [PubMed]
16. Yang, T.; Tang, S.; Feng, W.; Li, Z.; Liu, X.; Cheng, C.; Wei, F.; Ding, G. Dental pulp stem cells promote the recovery of spinal cord injury by regulating microglia polarization via JAK2/STAT3 signaling pathway. *Int. Immunopharmacol.* **2025**, *164*, 115395. [CrossRef]
17. Xie, Y.; Zhang, H.; Chen, J.; Xu, S.; Luo, Y. Luteolin Mitigates Dopaminergic Neuron Degeneration and Restrains Microglial M1 Polarization by Inhibiting Toll Like Receptor 4. *J. Integr. Neurosci.* **2024**, *23*, 185. [CrossRef]
18. Su, P.; Liu, L.; Gong, Y.; Peng, S.; Yan, X.; Bai, M.; Xu, E.; Li, Y. Kaempferol improves depression-like behaviors through shifting microglia polarization and suppressing NLRP3 via tilting the balance of PPARγ and STAT1 signaling. *Int. Immunopharmacol.* **2024**, *143*, 113538. [CrossRef]
19. Liu, Q.; Xi, Y.; Wang, Q.; Liu, J.; Li, P.; Meng, X.; Liu, K.; Chen, W.; Liu, X.; Liu, Z. Mannan oligosaccharide attenuates cognitive and behavioral disorders in the 5xFAD Alzheimer's disease mouse model via regulating the gut microbiota-brain axis. *Brain Behav. Immun.* **2021**, *95*, 330–343. [CrossRef]

20. Zeyneb, H.; Song, Y.; Wang, L.; Zheng, J.; Wang, W.; Pei, H.; Cao, X. Preventive effect of quinoa polysaccharides on lipopolysaccharide-induced inflammation in mice through gut microbiota regulation. *Int. J. Biol. Macromol.* **2025**, *307*, 141899. [CrossRef]
21. Izzy, S.; Yahya, T.; Albastaki, O.; Cao, T.; Schwerdtfeger, L.A.; Abou-El-Hassan, H.; Chopra, K.; Ekwudo, M.N.; Kurdeikaite, U.; Verissimo, I.M.; et al. High-salt diet induces microbiome dysregulation, neuroinflammation and anxiety in the chronic period after mild repetitive closed head injury in adolescent mice. *Brain Commun.* **2024**, *6*, fcae147. [CrossRef]
22. Zou, J.; Gao, J.; Shang, W.; Fan, X. Minocycline Ameliorates *Staphylococcus aureus*-Induced Neuroinflammation and Anxiety-like Behaviors by Regulating the TLR2 and STAT3 Pathways in Microglia. *Brain Sci.* **2025**, *15*, 128. [CrossRef] [PubMed]
23. Liu, J.J.; Wei, F.; Wang, Y.D.; Liu, J.; Xu, B.L.; Ma, S.C.; Yang, J.B. Ginseng and *Polygonum multiflorum* formula protects brain function in Alzheimer's disease. *Front. Pharmacol.* **2025**, *16*, 1461177. [CrossRef] [PubMed]
24. Dalile, B.; Van Oudenhove, L.; Vervliet, B.; Verbeke, K. The role of short-chain fatty acids in microbiota-gut-brain communication. *Nat. Rev. Gastroenterol. Hepatol.* **2019**, *16*, 461–478. [CrossRef] [PubMed]
25. Knox, E.G.; Aburto, M.R.; Clarke, G.; Cryan, J.F.; O'Driscoll, C.M. The blood-brain barrier in aging and neurodegeneration. *Mol. Psychiatry* **2022**, *27*, 2659–2673. [CrossRef]
26. Gupta, D.P.; Park, S.H.; Lee, Y.S.; Lee, S.; Lim, S.; Byun, J.; Cho, I.H.; Song, G.J. *Daphne genkwa* flower extract promotes the neuroprotective effects of microglia. *Phytomedicine* **2023**, *108*, 154486. [CrossRef]
27. Zhou, H.R.; Wu, J.R.; Bei, L.; Wang, B.X.; Xu, H.; Wang, J.T.; Ma, S.X. Hydroalcoholic extract from *Abelmoschus manihot* (Linn.) Medicus flower reverses sleep deprivation-evoked learning and memory deficit. *Food Funct.* **2020**, *11*, 8978–8986. [CrossRef]
28. Olasehinde, T.A.; Ekundayo, T.C.; Okaiyeto, K.; Olaniran, A.O. *Hibiscus sabdariffa* (Roselle) calyx: A systematic and meta-analytic review of memory-enhancing, anti-neuroinflammatory and antioxidative activities. *Inflammopharmacology* **2023**, *31*, 231–240. [CrossRef]
29. Wang, J.; Zhou, M.; Wu, T.; Fang, L.; Liu, C.; Min, W. Novel anti-obesity peptide (RLLPH) derived from hazelnut (*Corylus heterophylla* Fisch) protein hydrolysates inhibits adipogenesis in 3T3-L1 adipocytes by regulating adipogenic transcription factors and adenosine monophosphate-activated protein kinase (AMPK) activation. *J. Biosci. Bioeng.* **2020**, *129*, 259–268. [CrossRef]
30. Zhao, T.; Ma, W.; Yang, Z.; Liang, L.; Chen, X.; Wang, G.; Ma, Q.; Wang, L. A chromosome-level reference genome of the hazelnut, *Corylus heterophylla* Fisch. *GigaScience* **2021**, *10*, giab027. [CrossRef]
31. Talebi, S.; Khodagholi, F.; Bahaeddin, Z.; Ansari Dezfouli, M.; Zeinaddini-Meymand, A.; Berchi Kankam, S.; Foolad, F.; Alijaniha, F.; Fayazi Piranghar, F. Does hazelnut consumption affect brain health and function against neurodegenerative diseases? *Nutr. Neurosci.* **2024**, *27*, 1008–1024. [CrossRef]
32. Nikolaieva, N.; Kačániová, M.; González, J.C.; Grygorieva, O.; Nôžková, J. Determination of microbiological contamination, antibacterial and antioxidant activities of natural plant hazelnut (*Corylus avellana* L.) pollen. *J. Environ. Sci. Health B* **2019**, *54*, 525–532. [CrossRef] [PubMed]
33. Gao, J. Study on Chemical Constituents and Hepatoprotective Activity of Male Flowers of *Corylus heterophylla*. Master's Thesis, Yanbian University, Yanji, China, 2018. [CrossRef]
34. Wu, S.B.; Pu, H.; Cao, Z.D.; Zhang, W.; Qi, Q.Q. Therapeutic Effect of Total Flavones from Hazel's Flower on Chronic Ischemic Nephropathy Rats Models. *Mod. J. Integr. Tradit. Chin. West. Med.* **2012**, *21*, 1164–1166. [CrossRef]
35. Ibrahim, R.M.; Abdel-Baki, P.M.; El-Rashedy, A.A.; Mahdy, N.E. LC-MS/MS profiling of *Tipuana tipu* flower, HPLC-DAD quantification of its bioactive components, and interrelationships with antioxidant, and anti-inflammatory activity: In vitro and in silico approaches. *BMC Complement. Med. Ther.* **2024**, *24*, 176. [CrossRef]
36. Akkol, E.K.; Süntar, I.; Keles, H.; Yesilada, E. The potential role of female flowers inflorescence of *Typha domingensis* Pers. in wound management. *J. Ethnopharmacol.* **2011**, *133*, 1027–1032. [CrossRef] [PubMed]
37. Wang, X.; Wang, Z.; Cao, J.; Dong, Y.; Chen, Y. Melatonin Alleviates Acute Sleep Deprivation-Induced Memory Loss in Mice by Suppressing Hippocampal Ferroptosis. *Front. Pharmacol.* **2021**, *12*, 708645. [CrossRef]
38. Bui, T.T.; Nguyen, H.T. Ethanolic extract of *Sophora japonica* flower buds alleviates cognitive deficits induced by scopolamine in mice. *Orient. Pharm. Exp. Med.* **2017**, *17*, 337–344. [CrossRef]
39. Jiao, Q.; Dong, X.; Guo, C.; Wu, T.; Chen, F.; Zhang, K.; Ma, Z.; Sun, Y.; Cao, H.; Tian, C.; et al. Effects of sleep deprivation of various durations on novelty-related object recognition memory and object location memory in mice. *Behav. Brain Res.* **2022**, *418*, 113621. [CrossRef]
40. Hilvering, B.; Koenderman, L. Quality over quantity; eosinophil activation status will deepen the insight into eosinophilic diseases. *Respir. Med.* **2023**, *207*, 107094. [CrossRef]
41. Park, S.H.; Jang, S.; An, J.E.; Choo, B.k.; Kim, H.K. *I. inflexus* (Thunb.) Kudo extract improves atopic dermatitis and depressive-like behavior in DfE-induced atopic dermatitis-like disease. *Phytomedicine* **2020**, *67*, 153137. [CrossRef]
42. Oliveros, E.; Ramirez, M.; Vazquez, E.; Barranco, A.; Gruart, A.; Delgado-Garcia, J.M.; Buck, R.; Rueda, R.; Martin, M.J. Oral supplementation of 2′-fucosyllactose during lactation improves memory and learning in rats. *J. Nutr. Biochem.* **2016**, *31*, 20–27. [CrossRef] [PubMed]

43. Wang, W.; Zhou, Q.; Jiang, T.; Li, S.; Ye, J.; Zheng, J.; Wang, X.; Liu, Y.; Deng, M.; Ke, D.; et al. A novel small-molecule PROTAC selectively promotes tau clearance to improve cognitive functions in Alzheimer-like models. *Theranostics* **2021**, *11*, 5279–5295. [CrossRef] [PubMed]
44. Jing, Y.; Yang, D.; Bai, F.; Wang, Q.; Zhang, C.; Yan, Y.; Li, Z.; Li, Y.; Chen, Z.; Li, J.; et al. Spinal cord injury-induced gut dysbiosis influences neurological recovery partly through short-chain fatty acids. *npj Biofilms Microbiomes* **2023**, *9*, 99. [CrossRef] [PubMed]
45. Ji, W.; Zhao, W.; Xu, Y.; Wang, Y.; Meng, X.; Xiao, H.; Zhuang, X.; Pan, C.; Mo, T.; Wang, B.; et al. Shenling Kaixin granules attenuate depression via multi-target mechanisms: Evidence from CSDS model and cellular studies. *Phytomedicine* **2025**, *149*, 157547. [CrossRef]
46. Chun, C.T.; Seward, K.; Patterson, A.; Melton, A.; MacDonald-Wicks, L. Evaluation of Available Cognitive Tools Used to Measure Mild Cognitive Decline: A Scoping Review. *Nutrients* **2021**, *13*, 3974. [CrossRef]
47. Fu, J.; Li, J.; Sun, Y.; Liu, S.; Song, F.; Liu, Z. In-depth investigation of the mechanisms of *Schisandra chinensis* polysaccharide mitigating Alzheimer's disease rat via gut microbiota and feces metabolomics. *Int. J. Biol. Macromol.* **2023**, *232*, 123488. [CrossRef]
48. Li, Z.; Zhu, Y.; Kang, Y.; Qin, S.; Chai, J. Neuroinflammation as the Underlying Mechanism of Postoperative Cognitive Dysfunction and Therapeutic Strategies. *Front. Cell. Neurosci.* **2022**, *16*, 843069. [CrossRef]
49. Hu, N.; Wang, K.; Ge, X.; Zhang, X.; Zheng, X.; Sun, S. Effects of Dendrobium officinale Kimura & Migo flower flavonoids on cognitive function by regulating gut microbiota. *Front. Pharmacol.* **2025**, *16*, 1562775. [CrossRef]
50. Wu, Y.; Zhang, Y.; Xie, B.; Abdelgawad, A.; Chen, X.; Han, M.; Shang, Y.; Yuan, S.; Zhang, J. RhANP attenuates endotoxin-derived cognitive dysfunction through subdiaphragmatic vagus nerve-mediated gut microbiota-brain axis. *J. Neuroinflamm.* **2021**, *18*, 300. [CrossRef]
51. Cheng, S.; Gao, H.; Yang, Y.; Zhang, M.; Wang, J.; Li, N.; Ji, Y.; Wang, H.; Zhou, Y. Pharmacological Diversity of Flavonoids and Their Clinical Application Prospects in Neurological Disorders. *Phytother. Res.* **2025**, *39*, 5222–5248. [CrossRef]
52. Mohamed Yusof, N.I.S.; Ramasamy, K.; Mohd Fauzi, F. Elucidating the Neuroprotective Mechanism of 5,7-Dimethoxyflavone and 5,7′,4′-Trimethoxyflavone Through In Silico Target Prediction and in Memory-Impaired Mice. *Neurochem. Res.* **2025**, *50*, 274. [CrossRef]
53. Kim, H.L.; Lee, S.K.; Min, D.E.; Bastola, T.; Chang, B.Y.; Bae, J.H.; Lee, D.R. Effects of *Scrophularia buergeriana* Extract (Brainon®) on Aging-Induced Memory Impairment in SAMP8 Mice. *Curr. Issues Mol. Biol.* **2023**, *45*, 1287–1305. [CrossRef]
54. Gao, H.; Fang, B.; Sun, Z.; Du, X.; Guo, H.; Zhao, L.; Zhang, M. Effect of Human Milk Oligosaccharides on Learning and Memory in Mice with Alzheimer's Disease. *J. Agric. Food Chem.* **2024**, *72*, 1067–1081. [CrossRef] [PubMed]
55. Qi, Z.; Peng, J.; Wang, H.; Wang, L.; Su, Y.; Ding, L.; Cao, B.; Zhao, Y.; Xing, Q.; Yang, J.J. Modulating neuroinflammation and cognitive function in postoperative cognitive dysfunction via CCR5-GPCRs-Ras-MAPK pathway targeting with microglial EVs. *CNS Neurosci. Ther.* **2024**, *30*, e14924. [CrossRef]
56. Kang, E.J.; Cha, M.G.; Kwon, G.H.; Han, S.H.; Yoon, S.J.; Lee, S.K.; Ahn, M.E.; Won, S.M.; Ahn, E.H.; Suk, K.T. *Akkermansia muciniphila* improve cognitive dysfunction by regulating BDNF and serotonin pathway in gut-liver-brain axis. *Microbiome* **2024**, *12*, 181. [CrossRef] [PubMed]
57. Lyu, J.; DeMarco, A.G.; Sweet, R.A.; Grubisha, M.J. MAP2 phosphorylation: Mechanisms, functional consequences, and emerging insights. *Front. Cell. Neurosci.* **2025**, *19*, 1610371. [CrossRef] [PubMed]
58. Zhao, M.; Zeng, L.; Zhou, Y.; Yang, C.; Sheng, R.; Liu, X.; Wen, W.; Yang, S.; Zhang, S.; Xu, S. Ethyl Acetate Fraction of *Zanthoxylum bungeanum* Ameliorates Cognitive Deficit by Facilitating the PHGDH-Dependent Astrocyte-Neuron Serine Shuttle in Aging Mice. *J. Agric. Food Chem.* **2025**, *73*, 16301–16316. [CrossRef]
59. Ge, T.; Chen, X.; Liu, C.; Huang, S. Involvement of CXCR2 in chronic postsurgical pain occurrence through ERK/p38 activation. *Neurosci. Lett.* **2025**, *870*, 138440. [CrossRef]
60. Loh, J.S.; Mak, W.Q.; Tan, L.K.S.; Ng, C.X.; Chan, H.H.; Yeow, S.H.; Foo, J.B.; Ong, Y.S.; How, C.W.; Khaw, K.Y. Microbiota-gut-brain axis and its therapeutic applications in neurodegenerative diseases. *Signal Transduct. Target. Ther.* **2024**, *9*, 37. [CrossRef]
61. Sharma, V.K. Microbiota-Derived SCFAs in Multiple Sclerosis: From Immune Priming to Neurodegeneration. *Mol. Neurobiol.* **2025**, *63*, 31. [CrossRef]
62. Smith, B.J.; Miller, R.A.; Ericsson, A.C.; Harrison, D.C.; Strong, R.; Schmidt, T.M. Changes in the gut microbiome and fermentation products concurrent with enhanced longevity in acarbose-treated mice. *BMC Microbiol.* **2019**, *19*, 130. [CrossRef]
63. Gu, X.; Fan, M.; Zhou, Y.; Zhang, Y.; Wang, L.; Gao, W.; Li, T.; Wang, H.; Si, N.; Wei, X.; et al. Intestinal endogenous metabolites affect neuroinflammation in 5×FAD mice by mediating "gut-brain" axis and the intervention with Chinese Medicine. *Alzheimer's Res. Ther.* **2024**, *16*, 222. [CrossRef]
64. Zou, J.; Shang, W.; Yang, L.; Liu, T.; Wang, L.; Li, X.; Zhao, J.; Rao, X.; Gao, J.; Fan, X. Microglia activation in the mPFC mediates anxiety-like behaviors caused by *Staphylococcus aureus* strain USA300. *Brain Behav.* **2022**, *12*, e2715. [CrossRef]
65. Wang, D.; Wang, L.; Han, L.; Wang, B.; Shi, R.; Ye, J.; Xia, B.; Zhao, Z.; Zhao, B.; Liu, X. Leucine-Restricted Diet Ameliorates Obesity-Linked Cognitive Deficits: Involvement of the Microbiota–Gut–Brain Axis. *J. Agric. Food Chem.* **2023**, *71*, 9404–9418. [CrossRef]

66. Cheng, J.; Hu, H.; Ju, Y.; Liu, J.; Wang, M.; Liu, B.; Zhang, Y. Gut microbiota-derived short-chain fatty acids and depression: Deep insight into biological mechanisms and potential applications. *Gen. Psychiatr.* **2024**, *37*, e101374. [CrossRef]
67. Desale, S.E.; Dubey, T.; Chinnathambi, S. α-Linolenic acid inhibits Tau aggregation and modulates Tau conformation. *Int. J. Biol. Macromol.* **2021**, *166*, 687–693. [CrossRef]
68. Wang, T.; Liu, S.; Shen, W.; Liu, J.; Liu, Y.; Li, Y.; Zhang, F.; Li, T.; Zhang, X.; Tian, W.; et al. α-linolenic acid mitigates microglia-mediated neuroinflammation of schizophrenia in mice by suppressing the NF-κB/NLRP3 pathway via binding GPR120-β-arrestin 2. *Int. Immunopharmacol.* **2024**, *142*, 113047. [CrossRef]
69. Wang, Y.; Li, N.; Yang, J.J.; Zhao, D.M.; Chen, B.; Zhang, G.Q.; Chen, S.; Cao, R.F.; Yu, H.; Zhao, C.Y.; et al. Probiotics and fructo-oligosaccharide intervention modulate the microbiota-gut brain axis to improve autism spectrum reducing also the hyper-serotonergic state and the dopamine metabolism disorder. *Pharmacol. Res.* **2020**, *157*, 104784. [CrossRef]

Disclaimer/Publisher's Note: The statements, opinions and data contained in all publications are solely those of the individual author(s) and contributor(s) and not of MDPI and/or the editor(s). MDPI and/or the editor(s) disclaim responsibility for any injury to people or property resulting from any ideas, methods, instructions or products referred to in the content.

nutrients

MDPI

Article

The Hypoglycaemic Effects of the New Zealand Pine Bark Extract on Sucrose Uptake and Glycaemic Responses in Healthy Adults—A Single-Blind, Randomised, Placebo-Controlled, Crossover Trial

Wen Xin Janice Lim [1,*], Rachel A. Page [2], Cheryl S. Gammon [3] and Paul J. Moughan [1]

[1] Riddet Institute, Massey University, Palmerston North 4442, New Zealand; p.j.moughan@massey.ac.nz
[2] School of Health Sciences, Massey University, Wellington 6021, New Zealand; r.a.page@massey.ac.nz
[3] School of Health Sciences, Massey University, Auckland 0632, New Zealand; c.gammon@massey.ac.nz
* Correspondence: w.x.j.lim@massey.ac.nz

Abstract

Background: The New Zealand pine bark has been demonstrated in vitro to inhibit digestive enzymes involved in carbohydrate digestion (alpha-amylase, alpha-glucosidase, and dipeptidyl-peptidase 4 (DPP-4)). Objective: This study aims to investigate the inhibitory effects of the New Zealand pine bark on sucrose uptake and glycaemic responses in humans. Methods: A single-blind, randomised, placebo-controlled, crossover trial was carried out involving healthy adults (n = 40 (M: 12, F: 28), 30.1 ± 1.3 years, BMI 23.4 ± 0.5 kg/m^2, HbA1c 32.5 ± 0.6 mmol/mol, FBG 4.7 ± 0.1 mmol/L). A control (75 g of sucrose powder only), and two doses of the pine bark extract (50 and 400 mg) were provided on separate occasions, with 75 g of sucrose mixed in 250 mL of water. Blood samples were collected at −10, 0, 15, 30, 45, 60, 90, and 120 min via a finger prick test. A linear mixed model for repeated measures (SPSS v30, IBM) was applied, and data presented as model-adjusted mean ± SEM. Results: Compared to control (247.5 ± 14.0 mmol/L·min), the iAUCglucose was significantly reduced with the 400 mg dose (211.8 ± 13.9 mmol/L·min, 14.4% reduction, and $p = 0.037$), but not with 50 mg dose (220.8 ± 14.2 mmol/L·min, 10.8% reduction, and $p = 0.184$). Compared to control (9.1 ± 0.2 mmol/L), glucose peak value was significantly reduced with the 50 mg dose (8.6 ± 0.2 mmol/L, 5.5% reduction, and $p = 0.016$) but not with the 400 mg dose (8.7 ± 0.2 mmol/L, 4.4% reduction, and $p = 0.093$). There were no statistically significant changes in postprandial insulin levels with the pine bark extract compared to control. Conclusions: The New Zealand pine bark extract attenuated sucrose uptake with improved glycaemic responses, and may therefore be useful as a hypoglycaemic adjunct to the diet.

Keywords: bioactives; hyperglycaemia; glucose intolerance; plant extract; postprandial glucose; postprandial insulin; proanthocyanin; sucrose inhibition; type 2 diabetes

1. Introduction

Worldwide, there is currently an increasing prevalence of prediabetes (impaired glucose tolerance, IGT) and similarly for diabetes [1]. Presently, 589 million adults (20–79 years), equivalent to 1 in 9, are living with diabetes, and this is predicted to rise to 853 million by 2050 (45% increase) [1]. Approximately 75% of all foods and beverages contain added sugars in various forms [2]. Habitual overconsumption of dietary sugars,

such as glucose and sucrose (which is the predominant sugar in the modern diet), and starches increases energy intake and this coupled with a sedentary lifestyle contributes to obesity risk and the development of cardiometabolic diseases such as type 2 diabetes (T2D) [2,3].

A range of plant-derived, antioxidant-rich extracts including pine bark extracts has been shown to improve glycaemia in both healthy individuals and those with impaired glycaemic control or T2D [4–8]. As such, these extracts including pine bark may have potential to improve glycaemic control within at-risk populations, either as a dietary adjunct or incorporated into a functional food product.

The New Zealand pine bark extract is obtained from 15–30 year old Pinus radiata trees grown in New Zealand [9]. The Pinus radiata belongs to the family Pinaceae which is a fast-growing evergreen conifer [9,10]. The pine bark undergoes an extensive water-based extraction process that involves grinding, washing, extraction with deionized hot water (95–99 °C for 30 min), the removal of extracted solids, the cooling of raw liquor by heat exchanger, the concentration of raw liquor by reverse osmosis to approximately 25% dissolved solids whilst continuously removing undissolved solids, freeze drying, further grinding, and lastly blending [9]. The pine bark extract then undergoes a quality control check, where physical, chemical, microbiological, heavy metal, herbicide, and pesticide analyses are carried out to ensure consistent conformity with its product specifications [9]. The dry powder contains greater than 80% proanthocyanidins, 1–2% taxifolin, other flavonoids and phenolic acids (approximately 8%), and some carbohydrates (5–10%) [9]. The extract reportedly contains a higher concentration of proanthocyanidins than the French Maritime pine bark (Pycnogenol®), which contains 65–75% total procyanidins [11]. The New Zealand pine bark extract has been shown to reduce postprandial glucose in normoglycaemic, healthy participants at doses of 50 and 400 mg [7]. A recent in vitro study on the New Zealand pine bark extract has further provided supporting evidence of its glucose-lowering effects by its ability to inhibit alpha-amylase, alpha-glucosidase, and dipeptidyl-peptidase 4 (DPP-4) enzymes [12]. The enzymatic inhibition attributes of the pine bark extract may play a relevant role in reducing or slowing postprandial glucose absorption [13–15], or enhancing the incretin effect [16,17], potentially improving glycaemic responses in humans.

The hypoglycaemic effect of New Zealand pine bark may result from its high concentration of oligomeric proanthocyanidins in varying degrees of polymerisation [9], and unique structural properties such as hydrogen moieties (e.g., OH) and double bonds that determine its effective interaction with digestive enzymes, trans-membrane glycoproteins such as DPP-4, and apically located transporters and receptors involved in glucose absorption [11,18,19].

The present study investigates if the New Zealand pine bark is able to reduce postprandial glycaemia with sucrose as the carbohydrate load instead of glucose. We hypothesise that the New Zealand pine bark has the potential to inhibit the enzyme sucrase leading to a delayed or reduced digestion of sucrose (table sugar, also known as disaccharide composing glucose and fructose linked by an alpha-1,2-glycosidic bond), thereby improving postprandial glycaemic responses. This hypothesis is in line with the action of Acarbose, a known alpha-glucosidase inhibitor (antidiabetic drug), and other plant extracts, such as mulberry leaf extract, which have demonstrated inhibitory actions on enzymes that digest various types of carbohydrates including maltose, maltodextrin, and sucrose [20–22]. This suggests that the New Zealand pine bark may influence glucose absorption from sucrose by both reducing glucose absorption [7] and/or inhibiting sucrose digestion, thus improving the overall glycaemic responses.

To date there has been no study examining the effects of the New Zealand pine bark on sucrose and its impact on postprandial glucose and insulin responses in healthy humans.

This study aimed to determine if the New Zealand pine bark extract of two doses (50 and 400 mg) were able to improve glycaemic and insulinaemic postprandial responses in healthy participants when co-administered with 75 g of sucrose solution.

2. Materials and Methods

2.1. Study Population

This study was approved in March 2024 by the Central Health and Disability Ethics Committee (HDEC) (2024 EXP 19678). The clinical trial was registered prospectively at anzctr.org.au (Australia New Zealand Clinical Trials Registry Number: ACTRN12624000491561). This study was conducted in accordance with the Declaration of Helsinki and all participants gave their informed consent prior to participating in the study.

Participants were recruited from Auckland, New Zealand using poster advertisements within the local university and community (May–November 2024). They were selected according to the following inclusion criteria: (i) Body Mass Index (BMI) of 18.5–29.9 kg/m^2, (ii) aged 18–60 years, (iii) not suffering from any impaired glycaemic control ((fasting blood glucose (FBG) < 5.6 mmol/L) and glycated haemoglobin A1c (HbA1c) < 40 mmol/mol (Cobas b 101 HbA1c test, CV 0.8–1.7%, Roche Diagnostics)), (iv) not taking any forms of glucose-lowering medications or medications that may affect glucose metabolism, and (v) free from any form of illnesses or chronic diseases. Participants were excluded from the study if they had any form of cardiovascular or metabolic diseases, digestive ailments, if they smoked, were pregnant or lactating, and if they had any known allergies to pine bark. Participants were also required to complete the International Physical Activity Questionnaire (IPAQ) and The Eating Attitudes Testing (EAT-26) to determine the general physical activity level of the participants, and to ensure they did not have any eating disorders that might confound with the study data collected.

2.2. Study Design

This was an acute, randomised, single-blind, crossover, placebo-controlled study conducted at the nutrition research facility at Massey University, Auckland, New Zealand. The order of intervention of treatment assigned to each participant was randomised using a computer-generated random allocation sequence.

Participants attended the study visits in the morning in a fasted condition (no food for at least 12 h, except water). A baseline sample was taken at 10 min prior to the start of intervention. The participants were then told to consume the treatment within five minutes. Further blood samples were taken at time points 15, 30, 45, 60, 90, and 120 min. Blood samples were obtained via the finger prick test.

Glucose readings were obtained using a single-use disposable lancet (Accu-Chek Safe T-Pro Plus, Roche Diagnostics, Indianapolis, USA) and glucose meter (MediSense, Optium, Abbott, Auckland, New Zealand, 2.7–4.0% CV). Blood samples (300 µL) were collected into microvette capillary blood collection tubes (Sarstedt Microvette CB300 Lithium Heparin, Nümbrecht, Germany) treated with heparin for plasma insulin analysis. The samples were centrifuged at 2000× g for 5 min according to the manufacturer's instructions to obtain 200 µL supernatant, which was then stored in 200 µL aliquot and kept in −80 °C freezer until the plasma insulin analysis. Plasma insulin was measured by a two-site sandwich immunoassay using direct chemiluminescent technology (Atellica IM Analyzer, CV 1.4–1.8%, Siemens Healthcare Limited, Auckland, New Zealand) [23].

At each study visit, all participants were checked for dietary and lifestyle compliance, such as having fasted at least 12 h prior to each study visit, having a consistent diet, refraining from strenuous physical activity, alcohol, caffeinated tea or coffee formulations, health supplements 24 h prior to visit, any supplements or medications that may influence

glucose levels, and no consumption of pine bark throughout the duration of the study. Research has demonstrated that pine bark extract undergoes extensive metabolism and is typically eliminated from the human body within 24 h [11]. Therefore, a washout period consisting of at least a 48–72 h gap to a week was observed between each study visit to minimise carry-over effects.

2.3. Intervention Treatments

Three intervention treatments were given to each participant at separate visits: control using a placebo (75 g of sucrose powder only), and two doses of the New Zealand pine bark extract (50 and 400 mg). Each intervention extract was prepared with 75 g of sucrose powder dissolved in 250 mL of water with 3.75 mL of artificial lemon flavour, and served to participants in an opaque, black cup (to conceal contents). All intervention treatments were of similar taste, flavour, and consistency to mask the contents given. Each intervention treatment was prepared fresh on the day of the study visit.

The New Zealand pine bark extract doses (50 and 400 mg) chosen for this study were based on our previous work on glucose metabolism in healthy participants demonstrating that both doses were effective in improving acute glycaemic control [7]. This was supported by other studies investigating the impact of pine bark (French Maritime) using doses ranging from 50 to 300 mg on longer-term (3 to 12 weeks) glycaemic control in people with T2D [24–26]. The pine bark extract has been vigorously tested for its safety for human consumption. Two human studies involving the consumption of 480 mg/day of the pine bark extract for 6 months and 960 mg/day for 5 weeks demonstrated no adverse effects on liver and kidney function, and haematology in the participants tested [9].The doses selected represented concentrations with no known toxicity [9]. The New Zealand pine bark extract (Enzogenol®) was supplied by ENZO Nutraceutical Limited (Paeroa, New Zealand), and was produced to the standards of dietary supplement preparations and quality control in New Zealand [9].

2.4. Sample Size

Following a similar study protocol that was used for the study examining mulberry leaf extract [22], it was estimated that n = 34 participants in each treatment group were required to detect a statistically significant difference ($p \leq 0.05$) in incremental area under the curve (iAUC) between treatments of 43.1 mmol/L/min with a SD of 53.02 mmol/L/min. A total of n = 44 participants were recruited to factor in recruitment attrition and dropouts.

2.5. Statistical Analysis

Primary outcomes such as fasting and postprandial plasma glucose and insulin concentrations were measured at time points −10, 0, 15, 30, 45, 60, 90, and 120 min. The iAUC of both glucose and insulin were geometrically calculated using the trapezoidal rule and compared amongst the intervention treatments [27,28]. Secondary measures including the peak glucose, peak insulin, 1 h glucose, 1 h insulin, time of peak glucose, and time of peak insulin were calculated, similar to the study parameters measured in the mulberry leaf extract study [22]. IBM SPSS statistics version 30 (IBM corporation, New York, NY, USA) was used for statistical analysis. A linear mixed model for repeated-measures was performed suitable for a crossover study that also accounted for missing data values, and a Bonferroni post-hoc test for pairwise comparisons. Prior to statistical analysis, data normality was tested using the Kolmogorov–Smirnov and Shapiro–Wilks statistics. A p value of $\leq$0.05 was considered to be significant (95% confidence level), based on 80% power with alpha = 0.05 and beta = 0.10. The data were expressed as model-adjusted mean ± standard error of the mean (SEM).

3. Results

3.1. Participant Demographics

A total of 44 participants were recruited for the study (Figure 1), and 40 participants (M: 12, F: 28) completed the study. Data from participants who did not complete or withdrew from the study were included in the data analysis. One participant was detected to be an outlier (significantly elevated iAUCglucose values compared to other participants) and was removed from the data analysis. There were three participants who were non-respondents in the study (with iAUCglucose of control significantly lower than other participants and compared to all treatments tested) and they were also removed from the data analysis. The removal of the outlier and non-respondents improved the normality of the data. The participants who completed the study and data from withdrawn participants were included in the data analysis were healthy adults (n = 40 (M: 12, F: 28), 30.1 ± 1.3 years, BMI 23.4 ± 0.5 kg/m^2, HbA1c 32.5 ± 0.6 mmol/mol, FBG 4.7 ± 0.1 mmol/L), and their blood pressure and lipid profile were within normal ranges (Table 1). The ethnicity distribution of the participants was 62% Asian (total n = 25, 24% South Asian (n = 6), 36% Southeast Asian (n = 9), 40% East Asian (n = 10)), 27% Caucasian (n = 11), 8% Middle Eastern (n = 3), and 3% African (East African (n = 1)). The IPAQ obtained at screening indicated that n = 3 (7%) participants had a low physical activity level, n = 19 (48%) had a moderate level of physical activity level, while n = 18 (45%) participants had a high physical activity level. The EAT-26 questionnaire given at screening did not detect any propensity for any eating disorder in participants recruited for the study. There were no adverse events reported during the course of the study.

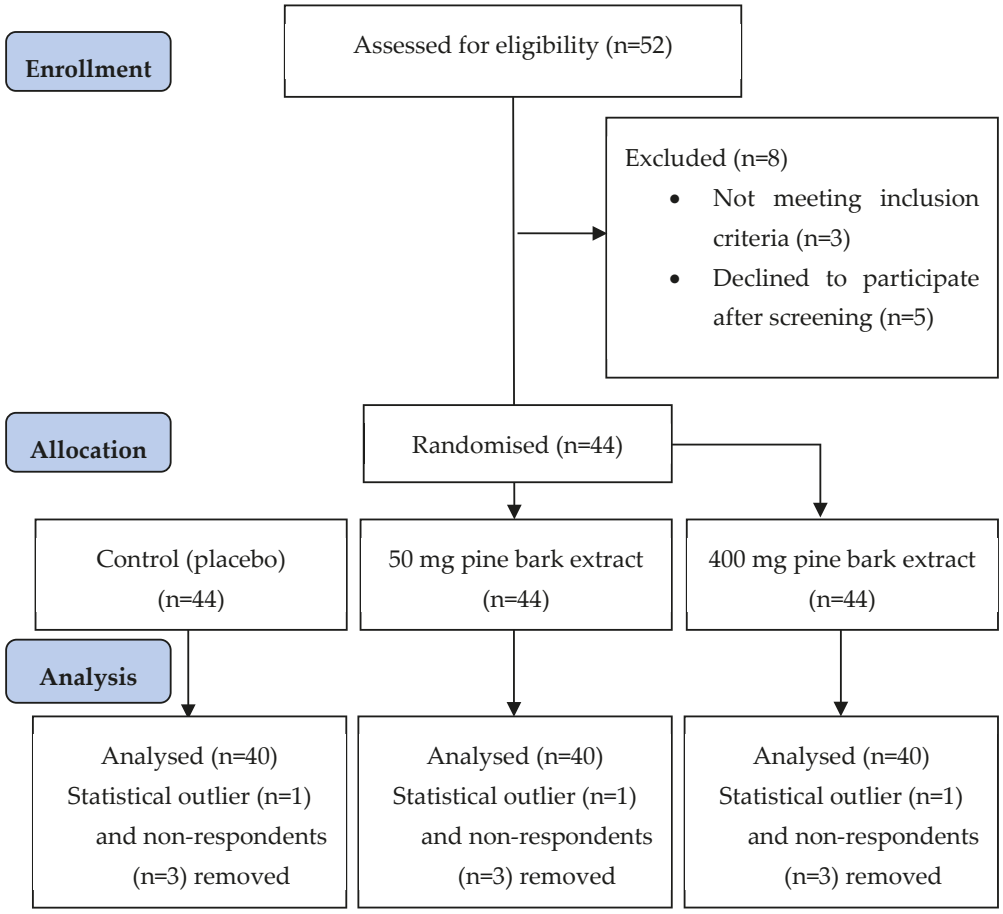

Figure 1. CONSORT diagram for the pine bark Study.

Table 1. Baseline characteristics of participants (n = 40) ± SEM.

Characteristics	Male (n = 12)	Female (n = 28)	Mean (n = 40)
Age (year)	33.8 ± 2.2	30.1 ± 1.6	30.1 ± 1.3
Body Mass Index (BMI, kg/m^2)	23.8 ± 0.8	23.2 ± 0.6	23.4 ± 0.5
Waist circumference (cm)	83.0 ± 2.2	74.5 ± 1.7	77.0 ± 1.5
Hip circumference (cm)	99.5 ± 2.3	98.7 ± 1.5	98.9 ± 1.2
Systolic blood pressure (mmHg)	113 ± 3.3	106 ± 1.7	108 ± 1.6
Diastolic blood pressure (mmHg)	74 ± 2.0	68 ± 1.1	70 ± 1.0
Fasting glucose (mmol/L)	4.5 ± 0.2	4.7 ± 0.1	4.7 ± 0.1
Glycated haemoglobin A1c (HbA1c, mmol/mol)	32.8 ± 1.0	32.3 ± 0.7	32.5 ± 0.6
Total cholesterol (TC, mmol/L)	4.7 ± 0.3	4.6 ± 0.2	4.7 ± 0.1
Triglyceride (TG, mmol/L)	1.2 ± 0.1	1.3 ± 0.1	1.3 ± 0.1
High density lipoprotein (HDL, mmol/L)	1.5 ± 0.1	1.7 ± 0.1	1.6 ± 0.1
Low density lipoprotein (LDL, mmol/L)	2.7 ± 0.2	2.3 ± 0.2	2.4 ± 0.1
Non-high-density lipoprotein (non-HDL, mmol/L)	3.2 ± 0.3	2.9 ± 0.2	3.0 ± 0.1
TC/HDL ratio	3.1 ± 0.2	2.9 ± 0.2	3.0 ± 0.1

3.2. Changes in Postprandial Glucose

Compared to control (247.5 ± 14.0 mmol/L·min), the iAUCglucose was significantly reduced with 400 mg of pine bark extract (211.8 ± 13.9 mmol/L·min, 14.4% reduction, and p = 0.037), but no significant change was detected with 50 mg of pine bark extract (220.8 ± 14.2 mmol/L·min, 10.8% reduction, and p = 0.184). Referring to Table 2, the significant reduction in iAUCglucose with 400 mg of pine bark extract could be seen at 90 min (p = 0.029) and 120 min (p = 0.037). Compared to the control (9.1 ± 0.2 mmol/L), there was also a significant reduction in the glucose peak value with 50 mg but not 400 mg of pine bark extract (8.6 ± 0.2 mmol/L, 5.5% reduction, p = 0.016, and 8.7 ± 0.2 mmol/L, 4.4% reduction, p = 0.093, respectively) (Table 2). Postprandial glucose was also significantly lower at 45 min with 400 mg of pine bark extract (p = 0.010), and at 90 min with 50 mg of pine bark extract (p = 0.023) compared to the control (Table 3 and Figure 2). There was only a statistical dose differences in the glucose peak time between 50 mg (36.7 ± 1.9 min) and 400 mg (31.3 ± 1.8 min) of the pine bark extract, p = 0.05 (Table 2).

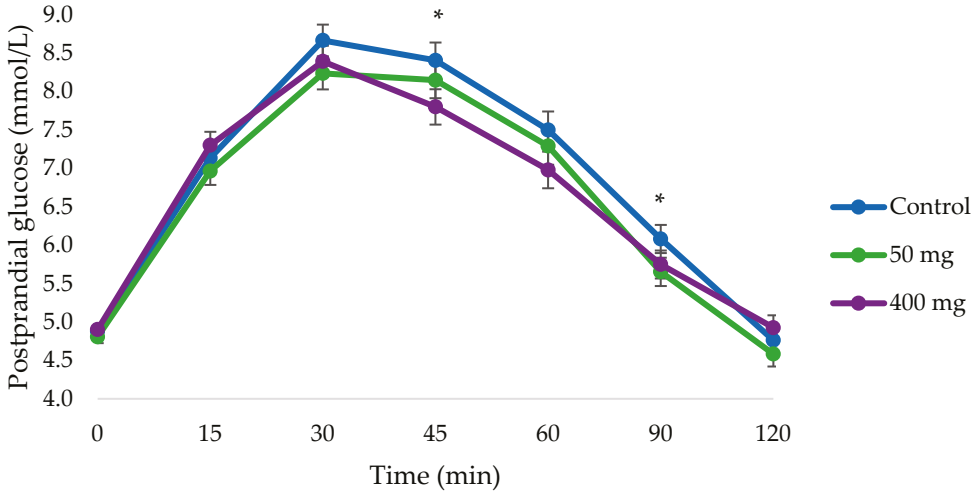

Figure 2. Changes in mean postprandial glucose (mmol/L) (± SEM) from 0 to 120 min of participants (n = 40) in each intervention (50 and 400 mg of pine bark extract compared to control). * Statistically significant differences were detected at 45 min with 400 mg of pine bark extract and 90 min with 50 mg of pine bark extract compared to control (p < 0.05).

Table 2. Results of incremental area under the curve (iAUC) of postprandial glucose (mmol/L·min) (± SEM) at 30, 60, 90, and 120 min (which is also the iAUC mean), 1 h glucose (mmol/L) (± SEM), glucose peak value (mmol/L) (± SEM), and glucose peak time (min) (± SEM) of participants (n = 40) in each intervention (50 and 400 mg of pine bark extract compared to control). * Statistically significant difference detected compared to control ($p < 0.05$).

	Control (Only Sucrose Solution)	50 mg Pine Bark Extract	400 mg Pine Bark Extract
iAUC 30	62.2 ± 3.4	58.1 ± 3.5	62.3 ± 3.4
iAUC 60	163.4 ± 8.1	152.7 ± 8.1	147.5 ± 8.0
iAUC 90	223.1 ± 12.0	203.1 ± 12.1	192.3 ± 11.9 *
iAUC 120	247.5 ± 14.0	220.8 ± 14.2	211.8 ± 13.9 *
1 h glucose	7.5 ± 0.2	7.3 ± 0.2	7.0 ± 0.2
Glucose peak	9.1 ± 0.2	8.6 ± 0.2 *	8.7 ± 0.2
Glucose peak time	35.8 ± 1.8	36.7 ± 1.9	31.3 ± 1.8

Table 3. Mean postprandial glucose (mmol/L) (± SEM) of participants (n = 40) with time in each intervention (50 and 400 mg of pine bark extract compared to control). * Statistically significant difference detected compared to control ($p < 0.05$).

Time (min)	Control (Only Sucrose Solution)	50 mg Pine Bark Extract	400 mg Pine Bark Extract
0	4.9 ± 0.1	4.8 ± 0.1	4.9 ± 0.1
15	7.1 ± 0.2	7.0 ± 0.2	7.3 ± 0.2
30	8.7 ± 0.2	8.2 ± 0.2	8.4 ± 0.2
45	8.4 ± 0.2	8.1 ± 0.2	7.8 ± 0.2 *
60	7.5 ± 0.2	7.3 ± 0.2	7.0 ± 0.2
90	6.1 ± 0.2	5.7 ± 0.2 *	5.7 ± 0.2
120	4.8 ± 0.2	4.6 ± 0.2	4.9 ± 0.2

3.3. Changes in Postprandial Insulin

There were no statistically significant changes detected with either 50 mg of pine bark extract (4874.0 ± 504.5 mU/L·min, $p = 1.000$) or 400 mg of pine bark extract (4231.9 ± 498.3 mU/L·min, $p = 0.949$) compared to the control (4601.9 ± 499.4 mU/L·min) (Table 4 and Figure 3). There were also no statistically significant changes in 1 h insulin, peak insulin, and insulin peak time with the pine bark treatments compared to control, $p > 0.05$ (Tables 4 and 5). There was only a significant dose difference in 1 h insulin concentrations between 50 and 400 mg of the extract (67.77 ± 6.70 mU/L vs. 50.66 ± 6.69 mU/L, respectively, $p = 0.019$).

Table 4. Results of incremental area under the curve (iAUC) of postprandial insulin (mU/L·min) (± SEM) at 30, 60, 90, and 120 min (which is also the iAUC mean), 1 h insulin (mU/L) (± SEM), insulin peak value (mmol/L) (± SEM), and insulin peak time (min) (± SEM) of participants (n = 40) in each intervention (50 and 400 mg of pine bark extract compared to control).

	Control (Only Sucrose Solution)	50 mg Pine Bark Extract	400 mg Pine Bark Extract
iAUC 30	1094.11 ± 122.67	939.31 ± 124.86	1001.49 ± 123.54
iAUC 60	2787.52 ± 288.11	2797.96 ± 290.89	2547.35 ± 287.53
iAUC 90	4021.70 ± 413.63	4059.75 ± 417.78	3629.88 ± 412.78
iAUC 120	4601.86 ± 499.39	4873.98 ± 504.54	4231.87 ± 498.35
1 h insulin	60.26 ± 6.76	67.77 ± 6.70	50.65 ± 6.69
Insulin peak	81.74 ± 7.59	77.99 ± 7.63	76.19 ± 7.54
Insulin peak time	37.2 ± 2.8	35.6 ± 2.8	37.8 ± 2.8

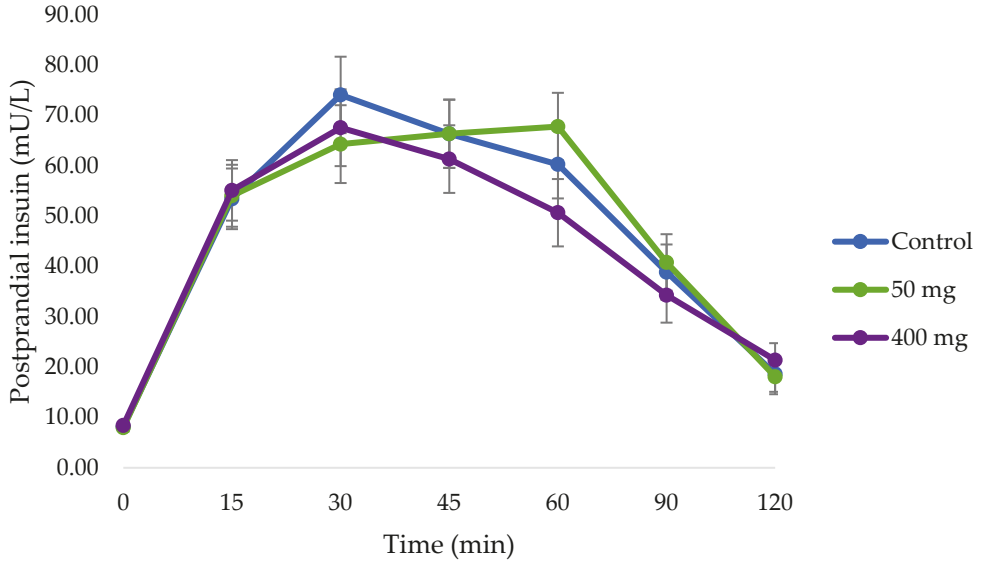

Figure 3. Changes in mean postprandial insulin (mU/L) (±SEM) from 0 to 120 min of participants (n = 40) in each intervention (50 and 400 mg of pine bark extract compared to control).

Table 5. Mean postprandial insulin (mU/L) (± SEM) of participants (n = 40) with time in each intervention (50 and 400 mg of pine bark extract compared to control).

Time (min)	Control (Only Sucrose Solution)	50 mg Pine Bark Extract	400 mg Pine Bark Extract
0	8.12 ± 0.79	7.97 ± 0.80	8.41 ± 0.79
15	53.42 ± 6.02	54.03 ± 6.15	55.10 ± 6.01
30	74.06 ± 7.59	64.29 ± 7.73	67.54 ± 7.63
45	66.34 ± 6.76	66.35 ± 6.80	61.32 ± 6.72
60	60.26 ± 6.76	67.77 ± 6.70	50.66 ± 6.69
90	38.86 ± 5.50	40.79 ± 5.61	34.28 ± 5.45
120	18.66 ± 3.57	18.08 ± 3.47	21.39 ± 3.36

4. Discussion

The New Zealand pine bark (*Pinus radiata*) extract and other similar pine bark extracts have been extensively studied for their hypoglycaemic effects in both healthy humans and individuals with T2D [9,10,24–26,29,30]. To the best of our knowledge, this is the first study that examines the effect of the New Zealand pine bark on sucrose digestion in improving glycaemic responses in human subjects. The current findings demonstrate that a higher dose of the pine bark extract (400 mg) significantly reduced overall mean iAUC of blood glucose with sucrose consumption. The pine bark extract was postulated to inhibit the sucrase enzyme leading to an attenuation in sucrose digestion. Equally, the pine bark extract may have attenuated glucose absorption. As the New Zealand pine bark extract mainly comprises large molecular structures of proanthocyanidins with varying degrees of polymerisation typically from 3 to 11, it was potentially able to inhibit both the digestive enzymes and glucose transporters in the small intestine via steric hindrance thus hindering the digestion of carbohydrates and glucose absorption [11,18,19], as observed in the current study. Even though 50 mg of pine bark dose showed no statistically significant reduction in iAUCglucose, it did significantly reduce the glucose peak value compared to the control ($p = 0.016$), and thus may be associated with potential reduction in oxidative stress and cardiometabolic (T2D and cardiovascular disease) risk [31,32]. Although the higher dose of pine bark (400 mg) tended to have a lower glucose peak compared to the control ($p = 0.093$), it did not reach statistical significance. An explanation might be, that at

a 400 mg dose, there was a significantly delayed attenuation of overall postprandial glucose, notably only from 90 min onwards (Table 2), which was later than when the glucose peaked at approximately 30 min. However, 400 mg of pine bark extract had an earlier glucose peak time (31.3 ± 1.8 min) compared to the 50 mg dose (36.7 ± 1.9 min) and the control (35.8 ± 1.8 min), where the glucose peak time of 400 mg dose was significantly shorter than the 50 mg dose ($p = 0.05$). A shorter time to glucose peak has been associated with better glycaemic control and beta-cell function, and reduced T2D risk [33].

Whilst there was a statistically significant reduction in postprandial glucose with 400 mg of pine bark extract, the blood glucose reductions or pine bark concentration given did not appear to have been sufficient to elicit a change in overall postprandial insulin levels or to down-regulate insulin secretion via insulin-signalling pathways [29]. This finding concurs with a previous study (2004) conducted on participants with T2D who were given doses of the French Maritime pine bark (Pcynogenol®) ranging from 50 to 300 mg on separate occasions and reported significant improvements in fasting and postprandial glucose, and HbA1c without any statistically significant changes in insulin levels, thus excluding the possibility of insulin secretion enhancement as one of the mechanistic actions of pine bark in improving glycaemia [25]. Another 2020 study concluded that, depending on the composition of plant extracts and their relative bioactivity, some extracts were only able to demonstrate reductions in postprandial glucose without improvements in postprandial insulin levels in healthy adults, whilst others only influenced changes in postprandial insulin [34]. Nevertheless, there was an indication that postprandial blood glucose was reduced with 400 mg of the pine bark extract without the need to increase insulin secretion for the enhanced disposal of glucose, which may be protective against beta-cell dysfunction [35]. The finding is in contrast to an animal study (2014) that demonstrated reductions in HbA1c, insulin, and glucagon levels when pine bark extract (Enzogenol®) was administered to a diabetic mice model [36]. A larger variability in insulin levels was also observed within treatments in the current study, leading to the inability to detect potential statistical differences between the treatments. For future work, the measurement of *C*-peptide levels instead of insulin would provide more accurate readings of true portal insulin secretion and eliminate variability in the pulsative nature and hepatic clearance of insulin [37], in order to ascertain if indeed postprandial insulin secretion was not impacted by the co-administration of the pine bark extract with sucrose.

Postprandial glucose curve shapes deriving from the oral glucose tolerance test (OGTT) have been shown to be useful indicators of future T2D risk even in healthy individuals [38,39]. A monophasic glucose curve shape is defined by having only one peak in the glucose curve, and is associated with heightened T2D risk [40,41]. In contrast, both the biphasic and triphasic glucose curves shapes (complex) are defined as having at least two or more peaks, respectively, and are associated with better glycaemic outcomes and lower T2D risk [40,41]. A persistence in monophasic glucose curve shape and the shift from biphasic to monophasic glucose curve shape was associated with an increased risk of impaired glucose metabolism [42]. Interestingly, the current study showed that 86.8% of the participants exhibited monophasic glucose curve shapes with the control, 83.8% with 50 mg of the pine bark extract, and a lower 66.7% with 400 mg of the extract. Biphasic glucose curve shapes were observed in 13.2% of the participants with the control, 13.5% with 50 mg of the pine bark extract, and 30.8% with 400 mg of the extract. There was also 2.7% of the participants exhibiting triphasic glucose curve shapes with 50 mg of the pine bark extract and 2.6% with 400 mg of the extract. This indicates that the New Zealand pine bark, particularly with a higher dose (400 mg), was able to improve glucose curve shapes in healthy individuals in an acute manner.

Compared with our previous study on the New Zealand pine bark with glucose consumption in an OGTT [7], 400 mg of the pine bark extract was able to significantly reduce iAUCglucose compared to the control with the glucose solution (235.7 ± 16.5 vs. 299.5 ± 26.9 mmol/L·min, 21.3% reduction, and p = 0.016). The current study demonstrated that the pine bark extract was also able to significantly reduce iAUCglucose compared to the control with a sucrose solution (211.8 ± 13.9 vs. 247.5 ± 14.0 mmol/L·min, 14.4% reduction, and p = 0.037). This suggests that the New Zealand pine bark works via multiple pathways to regulate postprandial blood glucose, as it was shown in both studies that the pine bark extract was able to attenuate and reduce overall postprandial glucose via its inhibitory actions on the digestion and absorption of sucrose and glucose, two common carbohydrate sources in the diet. Nonetheless, further work is required to determine the exact mechanistic actions of the pine bark extract to determine why it was able to reduce glucose absorption to a greater extent than for sucrose. One explanation may be that as sucrose breaks down into glucose and fructose for absorption, the pine bark compounds might be active at the site of action for both the inhibition of sucrose digestion and glucose absorption in the small intestine, thus reducing its maximal effects in inhibiting sucrose digestion. The pine bark extract might also be potentially active on the fructose-specific transporter (glucose transporter 5, GLUT5) for fructose uptake during sucrose digestion [43], thus further limiting its enzymatic inhibitory capacity on sucrase. Another explanation might be that the structural inhibition of the pine bark polyphenols, predominantly high in proanthocyanidins, are more specific to the structure of glucose transporters rather than the sucrase enzyme, thus leading to a more fitting inhibition and greater improved glycaemic responses with glucose than with sucrose consumption. More recent reviews suggest that plant extracts high in proanthocyanidins could have differential inhibitory effects on carbohydrate digestion enzymes depending on their respective phenolic compositions, complexity, and polymerisation [19,44], such that proanthocyanidin oligomers may be preferred over longer-chain polymers as better alpha-glucosidase inhibitors for diabetes prevention and management [45]. Additionally, dependent on the structure, active sites, and composition of phenolic compounds present in plant extracts, the extracts could exhibit more efficacious inhibitory intensities towards specific glucose transporters (e.g., sodium-glucose cotransporter (SGLT1) or glucose transporter 2 (GLUT2)), leading to reduced glucose uptake across the intestinal brush border membrane and into the bloodstream [43,46].

One study done by Wang and co-workers (2018) concluded that the actions of mulberry leaf plant extract on maltose, maltodextrin, and sucrose produced lower postprandial glucose levels in healthy participants than when mulberry leaf extract was consumed with glucose alone [21]. However, the study did not compare intervention treatments with their respective carbohydrate sources, as also noted by the authors, such as comparing sucrose combined with Reducose® and sucrose (control) only, rather than with glucose, as carbohydrates may raise blood glucose by different magnitudes (e.g., dietary glucose raises blood glucose and insulin levels to a greater extent than sucrose) [47]. Therefore, it remains inconclusive as to whether mulberry leaf extract was able to inhibit sucrose digestion better than glucose absorption. A merit of the current study was that sucrose, in combination with the pine bark extract, was compared to a control (sucrose only), in order to accurately quantify the glycaemic improvements.

Although it is generally accepted that a 20% or more reduction in postprandial iAUCglucose would be considered as clinically significant for the management of glycaemia [48,49], a 14.4% reduction in iAUCglucose with 400 mg of pine bark extract as demonstrated in the present study would still provide a useful means to optimise glycaemic control, if taken on a consistent basis. This is especially so when hyperglycaemic

excursions after a meal and daily fluctuating blood glucose contribute to increased oxidative stress and endothelial dysfunction, leading to increased T2D and cardiovascular risk [50]. Therefore, even a small but consistent improvement in postprandial glycaemic responses may be beneficial for healthy individuals without diabetes [51]. The effect could potentially be more pronounced in individuals with prediabetes with elevated fasting glucose or impaired glucose tolerance, or T2D. Further studies should investigate the longer-term effects of the New Zealand pine bark on glycaemic measures such as HbA1c, glycaemic variability, beta-cell function, and cardiovascular risk factors such as blood lipids and blood pressure, in order to determine the overall clinical significance of the New Zealand pine bark on postprandial glycaemia.

Further merits of this study include the use of a crossover design which minimised interindividual variation amongst treatments, and a larger sample size to determine the efficacy of the New Zealand pine bark on postprandial glycaemic responses in humans.

Nevertheless, this study is not without limitations. Although this study was conducted using sucrose solution to provide insights into the potential inhibitory effect of the pine bark extract on sucrose digestion by sucrase enzyme, we did not quantify the degree of undigested sucrose such as through hydrogen breath tests to ascertain that sucrose has indeed not been digested, resulting in reduced postprandial blood glucose levels [34,52].

The clinical impacts of the New Zealand pine bark on glycaemic responses may be attributed to its inhibitory effects on digestive enzymes, such as sucrase. Notwithstanding, further mechanisms might have also acted in concert, by the phenolic compounds improving glycaemia, such as the enhancement of incretin levels that stimulate insulin secretion towards increased glucose uptake, the inhibition of glucose transport and uptake [53], the activation of hepatic glucokinase, glycogen synthase activity, and AMP-activated protein kinase (AMPK), and the suppression of glucose-6-phosphatase (G-6-Pase) and phosphoenolpyruvate carboxykinase (PEPCK) expressions leading to a decrease in gluconeogenic enzyme activity [36], which have been previously demonstrated with pine bark extracts using in vitro and rat models. Further work is warranted to determine other mechanistic actions of the pine bark extract that might be involved in reducing glucose absorption to support the improvement in glycaemic responses seen in the present study.

Future clinical studies should therefore examine other physiological parameters, such as incretin glucose-dependent insulinotropic polypeptide (GIP) and glucagon-like peptide-1 (GLP-1) levels to ascertain their impact on glycaemic responses upon pine bark extract administration. The improvements in incretin levels have recently been demonstrated in other plant extracts with similar inhibitory functions to the New Zealand pine bark [54,55]. The New Zealand pine bark may also be examined in composite meals to determine its effectiveness in regulating postprandial glycaemia after meals, which are more representative of what is normally consumed. Longer-term consumption of the pine bark extract should be tested to examine its efficacy and safety in regulating glycaemic responses. Further research should also examine the impact of the New Zealand pine bark in a cohort of individuals with prediabetes or T2D to determine its effectiveness in improving glycaemic control in this population group.

5. Conclusions

The current study demonstrated that the New Zealand pine bark leads to better postprandial glycaemic responses in participants fed a sucrose solution. The results suggest an inhibitory effect of the New Zealand pine bark on sucrose digestion and uptake, potentially via sucrase enzyme inhibition. This adds to the current knowledge of plant-based extracts such as pine bark extract that may potentially be useful adjuncts to the diet for the healthy maintenance of postprandial glycaemia.

Author Contributions: Conceptualisation, W.X.J.L.; Methodology, W.X.J.L., C.S.G., R.A.P. and P.J.M.; Investigation, W.X.J.L.; Data Curation, W.X.J.L.; Writing—Original Draft Preparation, W.X.J.L.; and Writing—Review and Editing, W.X.J.L., C.S.G., R.A.P. and P.J.M. All authors have read and agreed to the published version of the manuscript.

Funding: This research was funded by ENZO Nutraceuticals Limited, Paeroa, New Zealand.

Institutional Review Board Statement: This study was conducted in accordance with the Declaration of Helsinki, and approved by the Central Health and Disability Ethics Committee (HDEC), New Zealand (2024 EXP 19678, 28 March 2024). The clinical trial was registered prospectively at anzctr.org.au (Australia New Zealand Clinical Trials Registry Number: ACTRN12624000491561).

Informed Consent Statement: Informed consent was obtained from all subjects involved in the study.

Data Availability Statement: The original contributions presented in this study are included in the article. Further inquiries can be directed to the corresponding author.

Acknowledgments: We would like to thank ENZO Nutraceuticals Limited, Paeroa, New Zealand, for providing the pine bark extract (Enzogenol®) for the study. We would also like to thank the Waitemata District Health Board North Shore Hospital Laboratory, Auckland, New Zealand, for analysing the insulin levels in blood samples.

Conflicts of Interest: The authors declare no conflicts of interest. The authors declare that this study received funding from ENZO Nutraceuticals Limited, Paeroa, New Zealand. The funder had no role in the design of the study; in the collection, analyses, or interpretation of data; in the writing of the manuscript; or in the decision to publish the results.

Abbreviations

BMI	Body Mass Index
DBP	Diastolic blood pressure
EAT-26	The Eating Attitudes Testing (questionnaire)
FBG	Fasting blood glucose
HbA1c	Glycated haemoglobin A1c
HDL	High-density lipoprotein cholesterol
LDL	Low-density lipoprotein cholesterol
iAUC	Incremental area under the curve
iAUCglucose	Incremental area under the curve of postprandial glucose
IPAQ	International Physical Activity Questionnaire
OGTT	Oral glucose tolerance test
SBP	Systolic blood pressure
TC	Total cholesterol
TG	Triglyceride
1hPG	1 h postprandial glucose
2hPG	2 h postprandial glucose

References

1. International Diabetes Federation. *IDF Diabetes Atlas*; International Diabetes Federation: Brussels, Belgium, 2025.
2. Bray, G.A.; Popkin, B.M. Dietary sugar and body weight: Have we reached a crisis in the epidemic of obesity and diabetes? Health be damned! Pour on the sugar. *Diabetes Care* **2014**, *37*, 950–956. [CrossRef] [PubMed]
3. Ludwig, D.S.; Hu, F.B.; Tappy, L.; Brand-Miller, J. Dietary carbohydrates: Role of quality and quantity in chronic disease. *BMJ* **2018**, *361*, k2340. [CrossRef] [PubMed]
4. Williamson, G. Possible effects of dietary polyphenols on sugar absorption and digestion. *Mol. Nutr. Food Res.* **2013**, *57*, 48–57. [CrossRef]
5. Hanhineva, K.; Torronen, R.; Bondia-Pons, I.; Pekkinen, J.; Kolehmainen, M.; Mykkanan, H.; Poutanen, K. Impact of Dietary Polyphenols on Carbohydrate Metabolism. *Int. J. Mol. Sci.* **2010**, *11*, 1365–1402. [CrossRef]

6. Zhao, C.; Yang, C.F.; Wai, S.T.C.; Zhang, Y.B.; Portillo, M.P.; Paoli, P.; Wu, Y.J.; San Cheang, W.; Liu, B.; Carpene, C.; et al. Regulation of glucose metabolism by bioactive phytochemicals for the management of type 2 diabetes mellitus. *Crit. Rev. Food Sci. Nutr.* **2019**, *59*, 830–847. [CrossRef] [PubMed]
7. Lim, W.X.J.; Chepulis, L.; von Hurst, P.; Gammon, C.S.; Page, R.A. An Acute, Placebo-Controlled, Single-Blind, Crossover, Dose-Response, Exploratory Study to Assess the Effects of New Zealand Pine Bark Extract (Enzogenol®) on Glycaemic Responses in Healthy Participants. *Nutrients* **2020**, *12*, 497. [CrossRef]
8. Lim, W.X.J.; Gammon, C.S.; von Hurst, P.R.; Chepulis, L.; Mugridge, O.; Page, R.A. Hypoglycemic effects of antioxidant-rich plant extracts on postprandial glycemic responses in participants with prediabetes (GLARE study). *Funct. Foods Health Dis.* **2021**, *11*, 604–626. [CrossRef]
9. Frevel, M.A.; Pipingas, A.; Grigsby, W.J.; Frampton, C.M.; Gilchrist, N.L. Production, composition and toxicology studies of Enzogenol® Pinus radiata bark extract. *Food Chem. Toxicol.* **2012**, *50*, 4316–4324. [CrossRef]
10. Li, Y.-Y.; Feng, J.; Zhang, X.-L.; Cui, Y.-Y. Pine bark extracts: Nutraceutical, pharmacological, and toxicological evaluation. *J. Pharmacol. Exp. Ther.* **2015**, *353*, 9–16. [CrossRef]
11. Bayer, J.; Högger, P. Review of the pharmacokinetics of French maritime pine bark extract (Pycnogenol®) in humans. *Front. Nutr.* **2024**, *11*, 1389422. [CrossRef]
12. Lim, W.X.J.; Gammon, C.S.; von Hurst, P.; Chepulis, L.; Page, R.A. The Inhibitory Effects of New Zealand Pine Bark (Enzogenol (R)) on alpha-Amylase, alpha-Glucosidase, and Dipeptidyl Peptidase-4 (DPP-4) Enzymes. *Nutrients* **2022**, *14*, 1596. [CrossRef] [PubMed]
13. Tundis, R.; Loizzo, M.R.; Menichini, F. Natural Products as alpha-Amylase and alpha-Glucosidase Inhibitors and their Hypoglycaemic Potential in the Treatment of Diabetes: An Update. *Mini-Rev. Med. Chem.* **2010**, *10*, 315–331. [CrossRef]
14. Sun, L.; Miao, M. Dietary polyphenols modulate starch digestion and glycaemic level: A review. *Crit. Rev. Food Sci. Nutr.* **2019**, *60*, 541–555. [CrossRef]
15. Nyambe-Silavwe, H.; Villa-Rodriguez, J.A.; Ifie, I.; Holmes, M.; Aydin, E.; Jensen, J.M.; Williamson, G. Inhibition of human alpha-amylase by dietary polyphenols. *J. Funct. Foods* **2015**, *19*, 723–732. [CrossRef]
16. Lin, S.R.; Chang, C.H.; Tsai, M.J.; Cheng, H.; Chen, J.C.; Leong, M.K.; Weng, C.F. The perceptions of natural compounds against dipeptidyl peptidase 4 in diabetes: From in silico to in vivo. *Ther. Adv. Chronic Dis.* **2019**, *10*, 16. [CrossRef]
17. Huang, P.K.; Lin, S.R.; Chang, C.H.; Tsai, M.J.; Lee, D.N.; Weng, C.F. Natural phenolic compounds potentiate hypoglycemia via inhibition of Dipeptidyl peptidase IV. *Sci. Rep.* **2019**, *9*, 11. [CrossRef] [PubMed]
18. Xiao, J.B.; Högger, P. Dietary polyphenols and type 2 diabetes: Current insights and future perspectives. *Curr. Med. Chem.* **2015**, *22*, 23–38. [CrossRef] [PubMed]
19. Cires, M.J.; Wong, X.; Carrasco-Pozo, C.; Gotteland, M. The gastrointestinal tract as a key target organ for the health-promoting effects of dietary proanthocyanidins. *Front. Nutr.* **2017**, *3*, 57. [CrossRef]
20. Lown, M.; Fuller, R.; Lightowler, H.; Fraser, A.; Gallagher, A.; Stuart, B.; Byrne, C.; Lewith, G. Mulberry-extract improves glucose tolerance and decreases insulin concentrations in normoglycaemic adults: Results of a randomised double-blind placebo-controlled study. *PLoS ONE* **2017**, *12*, e0172239. [CrossRef]
21. Wang, R.H.; Li, Y.F.; Mu, W.; Li, Z.Q.; Sun, J.X.; Mi, B.; Wang, B.H.; Zhong, Z.; Luo, X.Z.; Xie, C.; et al. Mulberry leaf extract reduces the glycemic indexes of four common dietary carbohydrates. *Medicine* **2018**, *97*, e11996. [CrossRef]
22. Thondre, P.S.; Lightowler, H.; Ahlstrom, L.; Gallagher, A. Mulberry leaf extract improves glycaemic response and insulaemic response to sucrose in healthy subjects: Results of a randomized, double blind, placebo-controlled study. *Nutr. Metab.* **2021**, *18*, 41. [CrossRef] [PubMed]
23. El Kenz, H.; Bergmann, P. Evaluation of immunochemiluminometric assays for the measurement of insulin and C-peptide using the ADVIA Centaur®. *Clin. Lab.* **2004**, *50*, 171–174. [PubMed]
24. Liu, X.; Wei, J.; Tan, F.; Zhou, S.; Würthwein, G.; Rohdewald, P. Antidiabetic effect of Pycnogenol® French maritime pine bark extract in patients with diabetes type II. *Life Sci.* **2004**, *75*, 2505–2513. [CrossRef] [PubMed]
25. Liu, X.; Zhou, H.-J.; Rohdewald, P. French maritime pine bark extract Pycnogenol dose-dependently lowers glucose in type 2 diabetic patients. *Diabetes Care* **2004**, *27*, 839–840. [CrossRef]
26. Zibadi, S.; Rohdewald, P.J.; Park, D.; Watson, R.R. Reduction of cardiovascular risk factors in subjects with type 2 diabetes by Pycnogenol supplementation. *Nutr. Res.* **2008**, *28*, 315–320. [CrossRef]
27. Wolever, T.M.S.; Jenkins, D.J.A. The use of the glycemic index in predicting the blood glucose response to mixed meals. *Am. J. Clin. Nutr.* **1986**, *43*, 167–172. [CrossRef]
28. Lefloch, J.P.; Escuyer, P.; Baudin, E.; Baudon, D.; Perlemuter, L. Blood glucose area under the curve: Methodological aspects. *Diabetes Care* **1990**, *13*, 172–175. [CrossRef]
29. Yang, K.; Chan, C.B. Proposed mechanisms of the effects of proanthocyanidins on glucose homeostasis. *Nutr. Rev.* **2017**, *75*, 642–657. [CrossRef]

30. Jerez, M.; Selga, A.; Sineiro, J.; Torres, J.L.; Núñez, M.J. A comparison between bark extracts from Pinus pinaster and Pinus radiata: Antioxidant activity and procyanidin composition. *Food Chem.* **2007**, *100*, 439–444. [CrossRef]
31. Hulman, A.; Simmons, R.K.; Vistisen, D.; Tabák, A.G.; Dekker, J.M.; Alssema, M.; Rutters, F.; Koopman, A.D.; Solomon, T.P.; Kirwan, J.P. Heterogeneity in glucose response curves during an oral glucose tolerance test and associated cardiometabolic risk. *Endocrine* **2017**, *55*, 427–434. [CrossRef]
32. Ceriello, A.; Esposito, K.; Piconi, L.; Ihnat, M.; Thorpe, J.; Testa, R.; Bonfigli, A.R.; Giugliano, D. Glucose "peak" and glucose "spike": Impact on endothelial function and oxidative stress. *Diabetes Res. Clin. Pract.* **2008**, *82*, 262–267. [CrossRef] [PubMed]
33. Kramer, C.K.; Vuksan, V.; Choi, H.; Zinman, B.; Retnakaran, R. Emerging parameters of the insulin and glucose response on the oral glucose tolerance test: Reproducibility and implications for glucose homeostasis in individuals with and without diabetes. *Diabetes Res. Clin. Pract.* **2014**, *105*, 88–95. [CrossRef]
34. Mela, D.J.; Cao, X.-Z.; Dobriyal, R.; Fowler, M.I.; Lin, L.; Joshi, M.; Mulder, T.J.; Murray, P.G.; Peters, H.P.; Vermeer, M.A. The effect of 8 plant extracts and combinations on post-prandial blood glucose and insulin responses in healthy adults: A randomized controlled trial. *Nutr. Metab.* **2020**, *17*, 51. [CrossRef]
35. Aston-Mourney, K.; Proietto, J.; Morahan, G.; Andrikopoulos, S. Too much of a good thing: Why it is bad to stimulate the beta cell to secrete insulin. *Diabetologia* **2008**, *51*, 540–545. [CrossRef] [PubMed]
36. Bang, C.-Y.; Choung, S.-Y. Enzogenol improves diabetes-related metabolic change in C57BL/KsJ-db/db mice, a model of type 2 diabetes mellitus. *J. Pharm. Pharmacol.* **2014**, *66*, 875–885. [CrossRef]
37. Janssen, J.A.M.J.L. Hyperinsulinemia and its pivotal role in aging, obesity, type 2 diabetes, cardiovascular disease and cancer. *Int. J. Mol. Sci.* **2021**, *22*, 7797. [CrossRef]
38. Abdul-Ghani, M.A.; Williams, K.; DeFronzo, R.; Stern, M. Risk of progression to type 2 diabetes based on relationship between postload plasma glucose and fasting plasma glucose. *Diabetes Care* **2006**, *29*, 1613–1618. [CrossRef] [PubMed]
39. Abdul-Ghani, M.A.; Lyssenko, V.; Tuomi, T.; DeFronzo, R.A.; Groop, L. The shape of plasma glucose concentration curve during OGTT predicts future risk of type 2 diabetes. *Diabetes/Metab. Res. Rev.* **2010**, *26*, 280–286. [CrossRef]
40. Tschritter, O.; Fritsche, A.; Shirkavand, F.; Machicao, F.; Haring, H.; Stumvoll, M. Assessing the shape of the glucose curve during an oral glucose tolerance test. *Diabetes Care* **2003**, *26*, 1026–1033. [CrossRef]
41. Kaga, H.; Tamura, Y.; Takeno, K.; Kakehi, S.; Someya, Y.; Suzuki, R.; Kadowaki, S.; Sugimoto, D.; Furukawa, Y.; Funayama, T.; et al. The shape of the glucose response curve during an oral glucose tolerance test was associated with muscle insulin sensitivity and visceral fat accumulation in nonobese healthy men. *J. Diabetes Investig.* **2020**, *11*, 874–877. [CrossRef]
42. Manco, M.; Nolfe, G.; Pataky, Z.; Monti, L.; Porcellati, F.; Gabriel, R.; Mitrakou, A.; Mingrone, G. Shape of the OGTT glucose curve and risk of impaired glucose metabolism in the EGIR-RISC cohort. *Metabolism* **2017**, *70*, 42–50. [CrossRef] [PubMed]
43. Loureiro, G.; Martel, F. The effect of dietary polyphenols on intestinal absorption of glucose and fructose: Relation with obesity and type 2 diabetes. *Food Rev. Int.* **2019**, *35*, 390–406. [CrossRef]
44. Barrett, A.H.; Farhadi, N.F.; Smith, T.J. Slowing starch digestion and inhibiting digestive enzyme activity using plant flavanols/tannins—A review of efficacy and mechanisms. *LWT* **2018**, *87*, 394–399. [CrossRef]
45. Lee, Y.A.; Cho, E.J.; Tanaka, T.; Yokozawa, T. Inhibitory activities of proanthocyanidins from persimmon against oxidative stress and digestive enzymes related to diabetes. *J. Nutr. Sci. Vitaminol.* **2007**, *53*, 287–292. [CrossRef]
46. Williamson, G. Effects of Polyphenols on Glucose-Induced Metabolic Changes in Healthy Human Subjects and on Glucose Transporters. *Mol. Nutr. Food Res.* **2022**, *66*, 2101113. [CrossRef]
47. Lee, B.; Woleve, T. Effect of glucose, sucrose and fructose on plasma glucose and insulin responses in normal humans: Comparison with white bread. *Eur. J. Clin. Nutr.* **1998**, *52*, 924–928. [CrossRef] [PubMed]
48. Ramdath, D.D.; Renwick, S.; Hawke, A.; Ramdath, D.G.; Wolever, T.M. Minimal Effective Dose of Beans Required to Elicit a Significantly Lower Glycemic Response Than Commonly Consumed Starchy Foods: Predictions Based on In Vitro Digestion and Carbohydrate Analysis. *Nutrients* **2023**, *15*, 4495. [CrossRef]
49. Chang, C.R.; Francois, M.E.; Little, J.P. Restricting carbohydrates at breakfast is sufficient to reduce 24-hour exposure to postprandial hyperglycemia and improve glycemic variability. *Am. J. Clin. Nutr.* **2019**, *109*, 1302–1309. [CrossRef] [PubMed]
50. Ajjan, R. The clinical importance of measuring glycaemic variability: Utilising new metrics to optimise glycaemic control. *Diabetes Obes. Metab.* **2024**, *26*, 3–16. [CrossRef]
51. Bermingham, K.M.; Smith, H.A.; Gonzalez, J.T.; Duncan, E.L.; Valdes, A.M.; Franks, P.W.; Delahanty, L.; Dashti, H.S.; Davies, R.; Hadjigeorgiou, G. Glycaemic variability, assessed with continuous glucose monitors, is associated with diet, lifestyle and health in people without diabetes. *Res. Sq.* **2023**, *3*, rs-3469475.
52. Mudra, M.; Ercan-Fang, N.; Zhong, L.; Furne, J.; Levitt, M. Influence of mulberry leaf extract on the blood glucose and breath hydrogen response to ingestion of 75g sucrose by type 2 diabetic and control subjects. *Diabetes Care* **2007**, *30*, 1272–1275. [CrossRef] [PubMed]
53. El-Zein, O.; Kreydiyyeh, S.I. Pine bark extract inhibits glucose transport in enterocytes via mitogen-activated kinase and phosphoinositol 3-kinase. *Nutrition* **2011**, *27*, 707–712. [CrossRef] [PubMed]

54. Mohamed, M.; Zagury, R.L.; Bhaskaran, K.; Neutel, J.; Mohd Yusof, B.N.; Mooney, L.; Yeo, L.; Kirwan, B.-A.; Aprikian, O.; von Eynatten, M. A Randomized, Placebo-Controlled Crossover Study to Evaluate Postprandial Glucometabolic Effects of Mulberry Leaf Extract, Vitamin D, Chromium, and Fiber in People with Type 2 Diabetes. *Diabetes Ther.* **2023**, *14*, 749–766. [CrossRef] [PubMed]
55. Ríos, J.-L.; Andújar, I.; Schinella, G.R.; Francini, F. Modulation of diabetes by natural products and medicinal plants via incretins. *Planta Medica* **2019**, *85*, 825–839. [CrossRef]

Disclaimer/Publisher's Note: The statements, opinions and data contained in all publications are solely those of the individual author(s) and contributor(s) and not of MDPI and/or the editor(s). MDPI and/or the editor(s) disclaim responsibility for any injury to people or property resulting from any ideas, methods, instructions or products referred to in the content.

nutrients

MDPI

Article

Bioactive Phenolics from Vinegar–Egg Accelerates Acute Wound Healing by Activation of Focal Adhesion and Mitogen-Activated Protein Kinase Signaling

Taehoon Oh [1,2,†], Chan Hee Cho [3,†], Su Cheol Baek [3], Mun Seok Jo [3], Woo Bong Kang [4], Yun Seok Kang [4], Sung-Kyun Ko [1,5,*] and Ki Hyun Kim [3,*]

[1] Chemical Biology Research Center, Korea Research Institute of Bioscience and Biotechnology (KRIBB), Cheongju 28116, Republic of Korea; dhxogns10@kribb.re.kr
[2] College of Pharmacy, Chungbuk National University, Cheongju 28160, Republic of Korea
[3] School of Pharmacy, Sungkyunkwan University, Suwon 16419, Republic of Korea; whckswhcks@g.skku.edu (C.H.C.); schii513@daum.net (S.C.B.); anstjr920827@gmail.com (M.S.J.)
[4] Crystal Insul Bio, Paju 10930, Republic of Korea; sjcbkemp@gmail.com (W.B.K.); ko2niyiru@naver.com (Y.S.K.)
[5] KRIBB School of Bioscience, Korea University of Science and Technology (UST), Daejeon 34141, Republic of Korea
* Correspondence: ksk1230@kribb.re.kr (S.-K.K.); khkim83@skku.edu (K.H.K.); Tel.: +82-31-290-7700 (K.H.K.)
† These authors contributed equally to this study.

Abstract

Background/Objectives: Vinegar–egg is a traditional health-promoting beverage prepared by soaking eggs in vinegar. While both eggs and vinegar are common dietary components with well-documented nutritional and pharmacological activities, eggs treated with vinegar have been rarely studied. This study aims to identify and characterize bioactive compounds in vinegar–egg and investigate their potential wound-healing activities. Methods: The vinegar–egg extract was analyzed using liquid chromatography–mass spectrometry (LC–MS) and column chromatography, including HPLC purification, which led to the isolation of four phenolic compounds. Results: These compounds were identified as 4-hydroxybenzoic acid (**1**), vanillic acid (**2**), methyl syringate (**3**), and leptosperin (**4**) using ESI-MS, UV, and NMR spectroscopic data. Among the isolates, 4-hydroxybenzoic acid (**1**) and vanillic acid (**2**) demonstrated wound-healing properties in mouse embryonic fibroblast (MEF) cells. None of the compounds, 4-hydroxybenzoic acid (**1**), vanillic acid (**2**), methyl syringate (**3**), or leptosperin (**4**), exhibited cytotoxicity in PC12, AGS, MEF, or MDA-MB-231 cells. Notably, 4-hydroxybenzoic acid (**1**) enhanced cell motility by 2.59-fold and cell invasion by 1.20-fold, while vanillic acid (**2**) increased cell motility by 2.69-fold and cell invasion by 1.23-fold. Western blot analysis revealed that treatment with 4-hydroxybenzoic acid (**1**) and vanillic acid (**2**) increased the phosphorylation of focal adhesion kinase (p-FAK) and matrix metalloproteinase 2 (MMP-2). Furthermore, both compounds elevated the phosphorylation of p38, a key regulator in wound-healing pathways. Conclusions: These findings demonstrate that 4-hydroxybenzoic acid (**1**) and vanillic acid (**2**) accelerate wound healing through the activation of focal adhesion and mitogen-activated protein kinase (MAPK) signaling pathways. These results highlight vinegar–egg as a promising therapeutic candidate for wound healing.

Keywords: vinegar–egg; 4-hydroxy-benzoic acid; vanillic acid; wound healing; focal adhesion kinase (FAK); mitogen-activated protein kinase (MAPK)

1. Introduction

Wound healing involves coordinated interactions among diverse cell types, signaling molecules, and the extracellular matrix [1,2]. It proceeds by primary intention, which involves closure of wound edges by suturing, fibroblast driven proliferation, collagen deposition, angiogenesis, and epithelialization [3–10], and by secondary intention, in which open wounds are repaired through chemotactic recruitment of immune cells for debris clearance, growth factor secretion, and epidermal migration [3,11–15]. Together, these mechanisms restore tissue integrity [16,17].

The mitogen-activated protein kinase (MAPK) pathway is central to wound healing, being activated by growth factors and cytokines such as epidermal growth factor (EGF) and tumor necrosis factor-alpha (TNF-α) [12,18–22]. During the inflammatory stage, MAPK signaling regulates cell proliferation, differentiation, and survival by phosphorylating downstream targets in fibroblasts, endothelial cells, and other repair-related cell types [9,13,23–26]. Matrix metalloproteinase 2 (MMP2; gelatinase A), which is also induced early in healing, degrades collagen, elastin, and fibronectin to enable matrix remodeling [27–30]. Moreover, MAPK and MMP2 pathways are tightly interconnected: MAPK controls MMP2 expression and activity, while MMP2 supports MAPK-mediated cell migration and proliferation [8,31–33]. Together, these coordinated mechanisms underscore the therapeutic potential of targeting MAPK signaling and MMP2 modulation in chronic-wound treatment.

Eggs are one of the few foods consumed universally across the globe. They are rich in nutrients, with high protein content and amino acid compositions similar to those of human proteins. Eggs are considered a source of high-quality (complete) protein and contain numerous biologically active ingredients. Numerous studies have demonstrated that eggs possess a variety of health-promoting and medicinal properties, including antifungal, antihypertensive, antitumor, antioxidant, brain-enhancing, and immune-regulating effects [34–39]. Vinegar, a food product derived from microbial fermentation, is a common, widely used, and economical item in daily life. It is not only utilized to enhance the flavor of food and prevent spoilage but is also consumed in some countries as a health-promoting beverage [40]. With increasing research on vinegar, it has been shown to provide numerous health benefits. Its applications have expanded from a traditional condiment to a component in various food types, such as meals, beverages, and healthcare products [40]. While eggs are often consumed after thermal processing, a traditional health-promoting beverage known as vinegar–egg is produced in some Asian countries, including China and Korea, by soaking eggs in vinegar. The history of vinegar–egg dates back to the Han Dynasty, where it was used as a remedy for throat inflammation and voice loss. It continues to be consumed as a health-promoting beverage in these regions [38]. This unique beverage exhibits several pharmacological activities including antioxidant, immunomodulatory, and anti-inflammatory effects, as well as angiotensin-converting enzyme (ACE) inhibitory activity [38,41–43], indicating that treating eggs with vinegar holds significant potential as a non-thermal processing method that maximizes the nutritional preservation of eggs.

Previous studies have suggested some potential bioactivities of vinegar–egg; however, its wound-healing effects have not yet been explored. As part of our ongoing efforts in natural product discovery to identify bioactive ingredients from diverse natural resources [44–48], we conducted a chemical analysis to isolate and characterize potent bioactive compounds from vinegar–egg and evaluate its potential wound-healing properties. Although vinegar–egg comprises a complex mixture of proteins, peptides, amino acids, and other organic acids, the present study aimed to explore the bioactive potential of small molecules, particularly phenolic compounds—given their well-documented wound-healing and related biological activities [49]. The chemical investigation of vinegar–egg,

utilizing liquid chromatography–mass spectrometry (LC–MS) and column chromatography, including HPLC purification, resulted in the isolation of four phenolic compounds (**1**–**4**). The chemical structures of these compounds were elucidated through nuclear magnetic resonance (NMR) spectroscopy, as well as UV and MS data obtained from LC–MS analysis. The wound-healing properties of the isolated compounds were assessed in mouse embryonic fibroblast (MEF) cells. In this study, we detail the process of isolating and structurally characterizing compounds **1**–**4** from vinegar–egg and investigate the molecular mechanisms underlying their wound-healing activities.

2. Materials and Methods

2.1. General Experimental Procedures

The detailed information is available in Supplementary Materials.

2.2. Preparation of Vinegar–Egg

Fresh chicken eggs (average mass: 45–55 g) and rice vinegar (9°) were purchased from a local market in Korea and used within 24 h of purchase. The eggs were washed with water, sterilized by wiping the shell with 95% ethanol, and then air-dried. The prepared egg samples were mixed with rice vinegar at a 1:1 weight ratio (eggs/vinegar) and kept at room temperature for 7 days. After the eggshell was completely dissolved, the solution was filtered through sterile gauze. The resulting filtrate was further incubated at room temperature for an additional 3 days. The final vinegar–egg solution was stored at −20 °C in a freezer until use.

2.3. Extraction and Isolation

The vinegar–egg solution was first suspended in 700 mL of distilled water and then sequentially partitioned with *n*-hexane, dichloromethane (CH_2Cl_2), ethyl acetate (EtOAc), and *n*-butanol (*n*-BuOH), using three 700 mL extractions for each solvent. This process yielded 0.6 g, 0.6 g, 0.7 g, and 2.8 g of the respective fractions. LC/MS analysis indicated that the major phenolic compounds were primarily distributed in the CH_2Cl_2, EtOAc, and *n*-BuOH-soluble fractions. The CH_2Cl_2-soluble fraction (0.6 g) was subjected to silica gel chromatography (230–400 mesh) using a CH_2Cl_2-MeOH-H_2O solvent gradient (50:1–1:1:0.2, *v*/*v*), yielding four subfractions (OTC1–OTC4). From OTC1 (25 mg), compound **3** (0.7 mg, t_R = 26.0 min, 0.117%) was isolated via semi-preparative reversed-phase HPLC (Phenomenex Luna Phenyl-hexyl 100 Å column, 250 × 10 mm i.d., 10 μm) under an isocratic solvent system of 29% CH_3CN/H_2O at a flow rate of 2 mL/min. The EtOAc-soluble fraction (0.7 g) was subjected to silica gel chromatography (230–400 mesh) using a CH_2Cl_2-MeOH solvent gradient (50:1–1:1, *v*/*v*), yielding five subfractions (OTE1–OTE5). From OTE2 (56 mg), compound **1** (1.8 mg, t_R = 20.0 min, 0.257%) and compound **2** (0.8 mg, t_R = 23.0 min, 0.114%) were purified using semi-preparative reversed-phase HPLC on Phenomenex Luna Phenyl-hexyl 100 Å column (250 × 10 mm i.d., 10 μm particle size) under an isocratic mobile phase of 17% CH_3CN/H_2O at a flow rate of 2 mL/min. The *n*-BuOH-soluble fraction (2.8 g) was fractionated over silica gel (230–400 mesh) using a methanol–water gradient system (2:8–8:2, *v*/*v*), yielding five subfractions (OTB1–OTB5). From OTB4 (24 mg), compound **4** (0.6 mg, t_R = 19.0 min, 0.021%) was isolated via semi-preparative reversed-phase HPLC (Phenomenex Luna Phenyl-hexyl 100 Å column, 250 × 10 mm i.d., 10 μm) under an isocratic solvent system of 15% CH_3CN/H_2O at a flow rate of 2 mL/min. The isolated phenolic compounds (**1**–**4**) were used without any chemical modification in all subsequent in vitro biological assays.

2.4. Reagents and Antibodies

The HaCaT cell line (immortalized human keratinocytes, #300493) and MDA-MB-231 (human breast cancer, #300275) were acquired from Cytion (Eppelheim, Germany). The AGS (human gastric adenocarcinoma, #CRL-1739), HCT116 (human colorectal carcinoma, #CCL-247), A549 (human lung carcinoma, #CCL-185), MRC-5 (human lung fibroblasts, #CCL-171), MEF (mouse embryonic fibroblasts, #SCRC-1040), and PC12 (rat adrenal medulla pheochromocytoma, #CRL-1721) cell lines were acquired from the ATCC (American Type Culture Collection, Manassas, VA, USA). FBS (fetal bovine serum, S001-01) was sourced from Welgene (Gyeongsangbuk-do, Republic of Korea). Penicillin-streptomycin (P4333), paraformaldehyde (P6148), DMEM (Dulbecco's modified Eagle's medium, 10-013-CVRC), crystal violet (C6158), mitomycin C (M7949), phosphatase inhibitor cocktail 3 (P0044), epidermal growth factor (EGF; SRP6253), dimethyl sulfoxide (DMSO; 472301), and protease inhibitor cocktail (5056489001) were supplied by Sigma-Aldrich (St. Louis, MO, USA). M-PER buffer (#78501), chemiluminescent detection reagents used in this study, including SuperSignal West Pico (#34080) and SuperSignal West Femto Maximum Sensitivity substrate (#34095), were obtained from Thermo Fisher Scientific (Waltham, MA, USA). Matrigel (354234) and Transwell® membranes (3422) were obtained from Corning (New York, NY, USA). The CytoX colorimetric assay (CYT3000) was obtained from LPS Solution (Deajeon, Republic of Korea). Primary antibodies against p-p38 MAPK(#4511), MMP2 (matrix metallopeptidase 2, #13132), and p38 MAPK (#9212) were supplied by Cell Signaling Technology (CST, Danvers, MA, USA), whereas antibodies against β-actin (#sc-47778), phosphorylated focal adhesion kinase (p-FAK, #sc-81493), and focal adhesion kinase (FAK, #sc-1688) were supplied by Santa Cruz Biotechnology (SCB, Dallas, TX, USA). The HRP-linked secondary antibodies, consisting of anti-mouse IgG (#7076) and anti-rabbit IgG (#7074), were acquired from CST.

2.5. Cell Culture

MEF, HaCaT, PC-12, AGS, MDA-MB-231, HCT116, A549, and MRC5 cells were grown at 37 °C with 5% CO_2 in a humidified chamber. The culture medium consisted of DMEM supplemented with 10% FBS, along with penicillin (100 U/mL) and streptomycin (100 μg/mL).

2.6. Cell Viability and Cell Proliferation Assay

To evaluate cytotoxic effects, MEF, HaCaT, PC12, AGS, MDA-MB-231, HCT116, A549, and MRC5 cells were seeded at a density of 1.0×10^4 cells per well in 96-well plates and incubated for 12 h. The cells were subsequently treated with compounds **1**–**4** at concentrations of up to 100 μM for 24 h. For proliferation analysis, MEF and HaCaT cells were plated at a density of 3.0×10^3 cells per well and treated with compounds **1**–**4** at defined concentrations of 25, 50, and 100 μM for 24, 48, and 72 h. At each time point, the culture medium was replaced with CytoX reagent, followed by a 1 h incubation. Absorbance was recorded at 450 nm using a microplate reader (SpectraMax 190, Molecular Devices, San Jose, CA, USA), and cell viability and proliferation rates were calculated relative to untreated controls.

2.7. Scratch Wound Healing Assay

For the scratch wound healing assay, MEF and HaCaT cells were seeded into 24-well plates at a density of 6.0×10^4 cells per well and incubated for 12 h to allow adherence. A uniform linear wound was generated at the center of each well using a sterile 200 μL pipette tip. To suppress cell proliferation, 10 μg/mL mitomycin C was applied for 3 h prior to compound treatment. Cells were then exposed to compounds **1**–**4** at final concentrations

of 50 and 100 μM for 24 h. Following incubation, cells were fixed in 4% paraformaldehyde for 15 min and stained with 0.2% crystal violet. Images were acquired using a ZEISS microscope (Jena, Germany), and wound closure was quantitatively analyzed using ImageJ software (v1.53k, NIH, Bethesda, MD, USA).

2.8. Transwell Chamber Invasion Assay

Cell invasion was assessed using a Transwell® system equipped with 6.5 mm inserts containing 8.0 μm pores (Corning, #3422, USA). MEF cells were seeded at a density of 6.0×10^4 cells per well onto the Matrigel-coated upper chamber in 200 μL of serum-free medium supplemented with compounds **1**–**4**. The lower chamber was filled with DMEM containing FBS to serve as a chemoattractant. After a 24 h incubation period, non-invading cells on the upper membrane surface were carefully removed. The cells that had migrated through the membrane were fixed in 4% paraformaldehyde for 15 min, stained with 0.2% crystal violet, and visualized using a ZEISS microscope (Germany).

2.9. Time-Lapse Cell Tracking Analysis

For live cell migration tracking, MEF cells were seeded at a density of 9.0×10^3 cells per 100 μL in DMEM lacking fetal bovine serum and supplemented with 2% Matrigel, using μ-Slide I chambers (Ibidi, #80106). After a 3 h pre-incubation period, 900 μL of DMEM containing 10% FBS was gently added to each well, followed by overnight incubation. Cells were subsequently treated with 100 μM of compounds **1**–**4** and immediately transferred to a HoloMonitor M4 imaging system (phase-holographic cytometry) maintained at 37 °C. Time-lapse images were acquired at 15 min intervals over a 12 h period, and cell motility was quantified using HoloStudio M4 analysis software (v2.6.4; Hstudio M4, Sun Valley, CA, USA).

2.10. Western Blot Analysis

Total protein extracts from MEF cells were prepared by lysing the cells on ice using cold M-PER buffer supplemented with both protease and phosphatase inhibitors. Lysates were clarified by centrifugation at 13,500 rpm for 15 min at 4 °C, and the supernatants were subjected to separation on 10% SDS-polyacrylamide gels. Proteins were subsequently transferred to nitrocellulose membranes with a pore size of 0.2 μm (Bio-Rad, #162-0112). Membranes were incubated with a blocking solution of 5% non-fat dry milk in tris-buffered saline containing 0.1% Tween-20 for 1 h at ambient temperature. Following blocking, membranes were incubated with the relevant primary antibodies overnight at 4 °C, then washed and treated with HRP-linked secondary antibodies (anti-mouse or anti-rabbit IgG, diluted 1:5000) for 2 h. Visualization of immunoreactive bands was performed using chemiluminescent substrates (SuperSignal West Pico or West Femto, Thermo Fisher Scientific).

2.11. Statistical Analysis

All results are expressed as the mean ± standard error of the mean (SEM), based on a minimum of three biologically independent replicates. Statistical analysis was conducted using GraphPad Prism software (v9.5.1; GraphPad Software, San Diego, CA, USA). Comparisons with the DMSO-treated control group were considered statistically significant at * $p < 0.05$, ** $p < 0.01$.

3. Results and Discussion

3.1. Isolation and Structure Elucidation of Compounds

The prepared vinegar–egg solutions were suspended in distilled water and sequentially partitioned with four organic solvents of increasing polarity: *n*-hexane, CH_2Cl_2,

EtOAc, and *n*-BuOH, yielding four respective fractions (Figure 1). LC–MS analysis, supported by a custom-built UV spectral library, revealed that the major phenolic constituents were concentrated in the CH_2Cl_2-, EtOAc-, and *n*-BuOH-soluble fractions. These fractions were further purified using a combination of open column chromatography and semi-preparative HPLC, resulting in the isolation of four phenolic compounds, designated as compounds **1**–**4** (Figure 1). Structural identification of these compounds was achieved by comparing their NMR spectroscopic data with literature values and LC–MS analysis (Figures S1–S8), confirming them as 4-hydroxybenzoic acid (**1**) [50], vanillic acid (**2**) [51], methyl syringate (**3**) [52], and leptosperin (**4**) [53] (Figure 2).

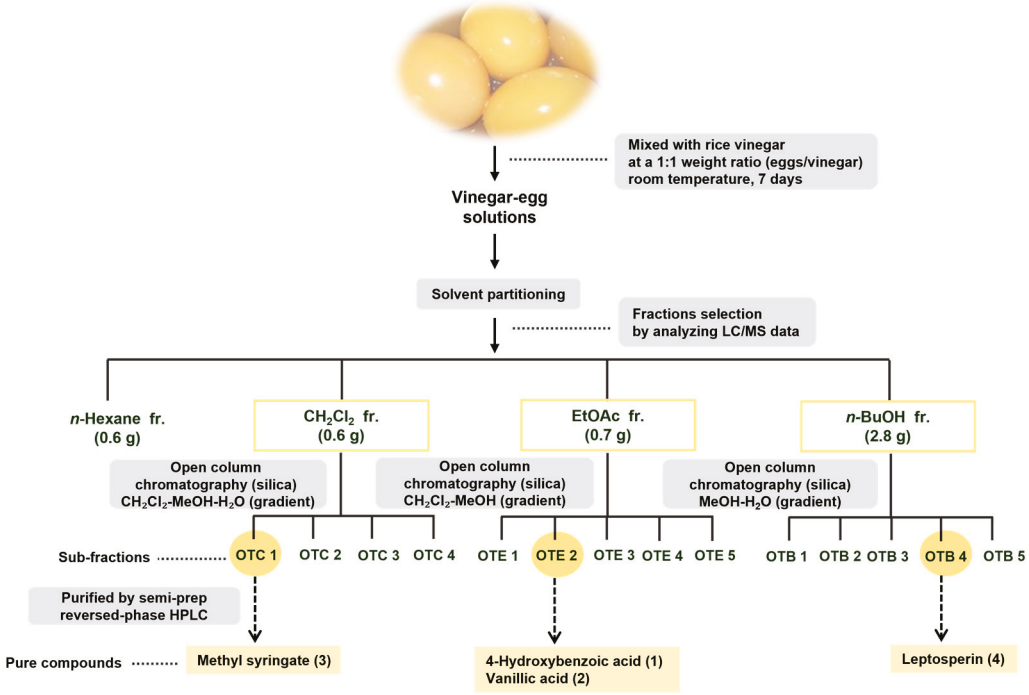

Figure 1. The separation scheme of compounds **1**–**4**.

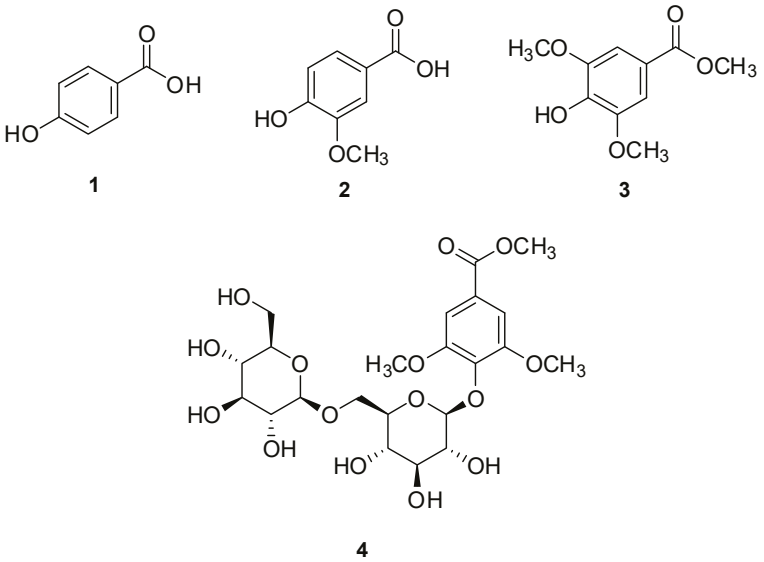

Figure 2. Structures of compounds **1**–**4** isolated from vinegar–egg. 4-Hydroxybenzoic acid (**1**), vanillic acid (**2**), methyl syringate (**3**), and leptosperin (**4**).

3.2. Effects of Compounds **1–4** *on Cytotoxicity*

To investigate the potential cytotoxicity of compounds **1–4** in the context of wound healing, eight cell lines (PC-12, AGS, MDA-MB-231, HCT116, A549, MRC5, HaCaT, and MEF) were treated with the compounds at concentrations ranging from low doses up to 100 μM for 24 h. Cell viability was assessed using the CytoX colorimetric assay following treatment with compounds **1–4** at concentrations up to 100 μM, and no apparent cytotoxic effects were observed in AGS, MDA-MB-231, HCT116, A549, MRC5, HaCaT, MEF, and PC12 cells under the tested conditions. To further examine whether compounds **1–4** influence cellular proliferation, MEF and HaCaT cells were treated with 25, 50, and 100 μM of each compound and monitored over 24, 48, and 72 h. No significant changes in proliferation were detected compared to the DMSO control, indicating that the compounds did not adversely affect cell growth at the tested concentrations (Figure 3).

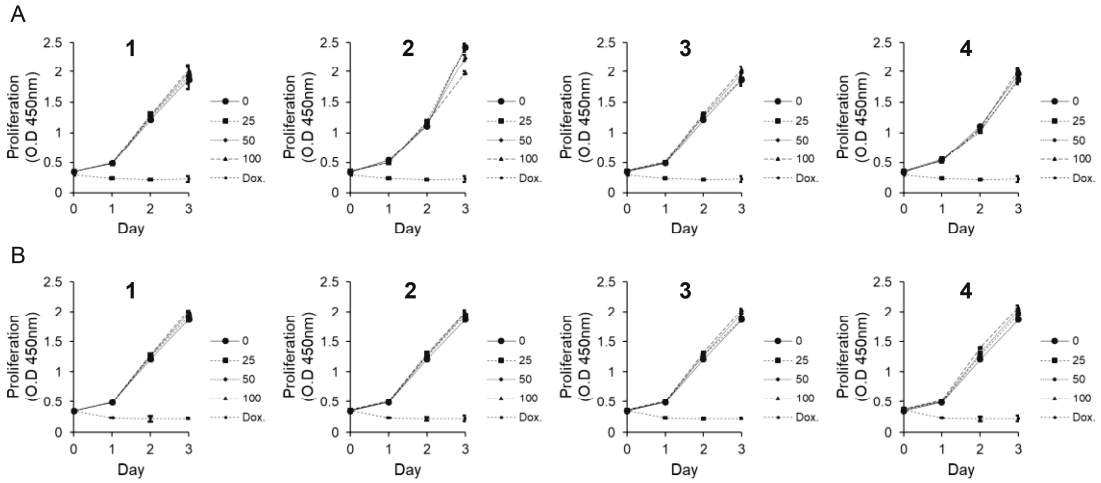

Figure 3. Effects of compounds **1–4** on the proliferation. Cell proliferation was evaluated in (**A**) MEF and (**B**) HaCaT cells following treatment with compounds **1–4** at concentrations of 0, 25, 50, and 100 μM for 24, 48, and 72 h. Cells were seeded in 96-well plates (3×10^3 cells/well). Doxorubicin (5 μM) served as a positive control. Data are presented as mean ± SEM ($n = 3$). Abbreviations: OD, optical density; Dox, doxorubicin.

3.3. Effect of Compounds **1–4** *on MEF Cells Motility*

We performed a scratch wound healing assay to evaluate the wound closure effects of compounds **1–4**. Treatment with 100 μM of compounds **1–4** and EGF enhanced wound closure in MEF cells by 2.59-, 2.69-, 1.05-, 0.93-, and 2.72-fold, respectively, compared to DMSO-treated cells (Figure 4A). Treatment with 100 μM of compounds **1–4** and EGF enhanced wound closure in HaCaT cells by 1.76-, 3.27-, 1.07-, 1.02-, and 3.51-fold, respectively, compared to DMSO-treated cells (Figure 4B). Live cell analysis using the HoloMonitor M4, which tracks individual cells to monitor movement and migration patterns, confirmed that cells treated with compounds **1–4** exhibited enhanced motility. Cell migration was assessed to determine the distance and direction of cell movement. Matrigel was placed inside the chamber of a μ-Slide I to prevent medium circulation, while medium containing FBS was placed outside the chamber. Compared to DMSO, compounds **1** and **2** exhibited an increased tendency to move in different directions (Figure 5A). Compounds **1–4** moved 1.23-, 1.15-, 1.00-, and 0.94-fold faster than the DMSO-treated control group, respectively (Figure 5B). The complete cell motility video is provided in Supplementary Data (Videos S1–S5). These results suggest that the compounds **1–4** may influence cell migration and wound healing by promoting cell motility without increasing cell numbers.

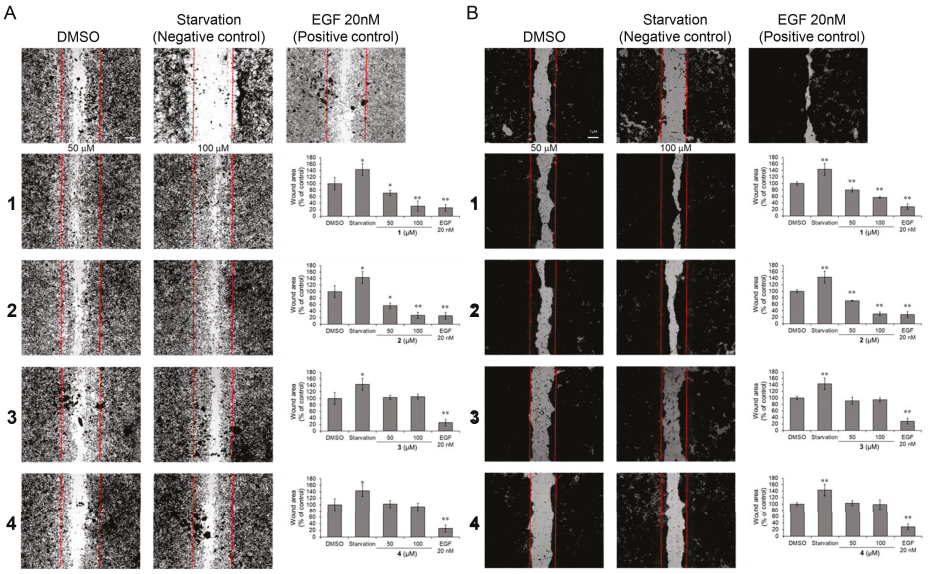

Figure 4. Effects of compounds **1–4** on cell migration in MEF cells. (**A**) MEF and (**B**) HaCaT cells were seeded in 24-well plate (6.0×10^4 cells/well) and incubated with compounds **1–4** at 50 and 100 μM for 24 h. Epidermal growth factor (EGF, 20 nM) was used as a positive control. Cell migration was quantified using a scratch wound healing assay by measuring the area and width of the wound gap. Images were captured using a 4× objective lens, and scale bars indicate 1 mm. Data are expressed as mean ± SEM from three independent experiments (n = 3; * $p < 0.05$, ** $p < 0.01$ vs. DMSO-treated group).

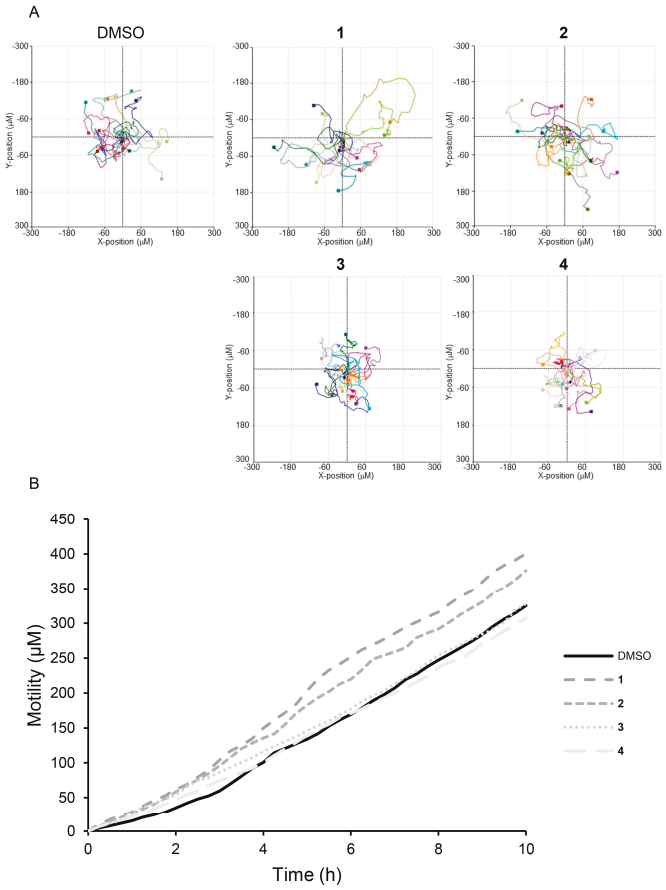

Figure 5. Effects of compounds **1–4** on the acceleration of cell migration in MEF cells. (**A**) The holographic recordings of live MEF cells treated with 100 μM compounds **1–4** were monitored every 15 min for 12 h. (**B**) The average of motility (μm) was analyzed using the HoloStudio software.

*3.4. Effect of 4-Hydroxy-Benzoic Acid (**1**) and Vanillic Acid (**2**) on MEF Cells Invasion*

To confirm the effects of 4-hydroxybenzoic acid (**1**) and vanillic acid (**2**) on cell invasion, we performed a Transwell chamber invasion assay. Based on the assay results, treatment with 100 μM of 4-hydroxybenzoic acid (**1**) and vanillic acid (**2**), and EGF enhanced MEF cell invasion by 1.20-, 1.23-, and 1.32-fold, respectively, compared to DMSO-treated cells (Figure 6). These results indicate that while cell mobility was enhanced, there was no increase in cell number, suggesting that the tested compounds **1** and **2** may influence cell migration and wound healing processes. Specifically, 4-hydroxybenzoic acid (**1**) and vanillic acid (**2**) may enhance cell mobility by promoting invasion ability, thereby facilitating wound closure.

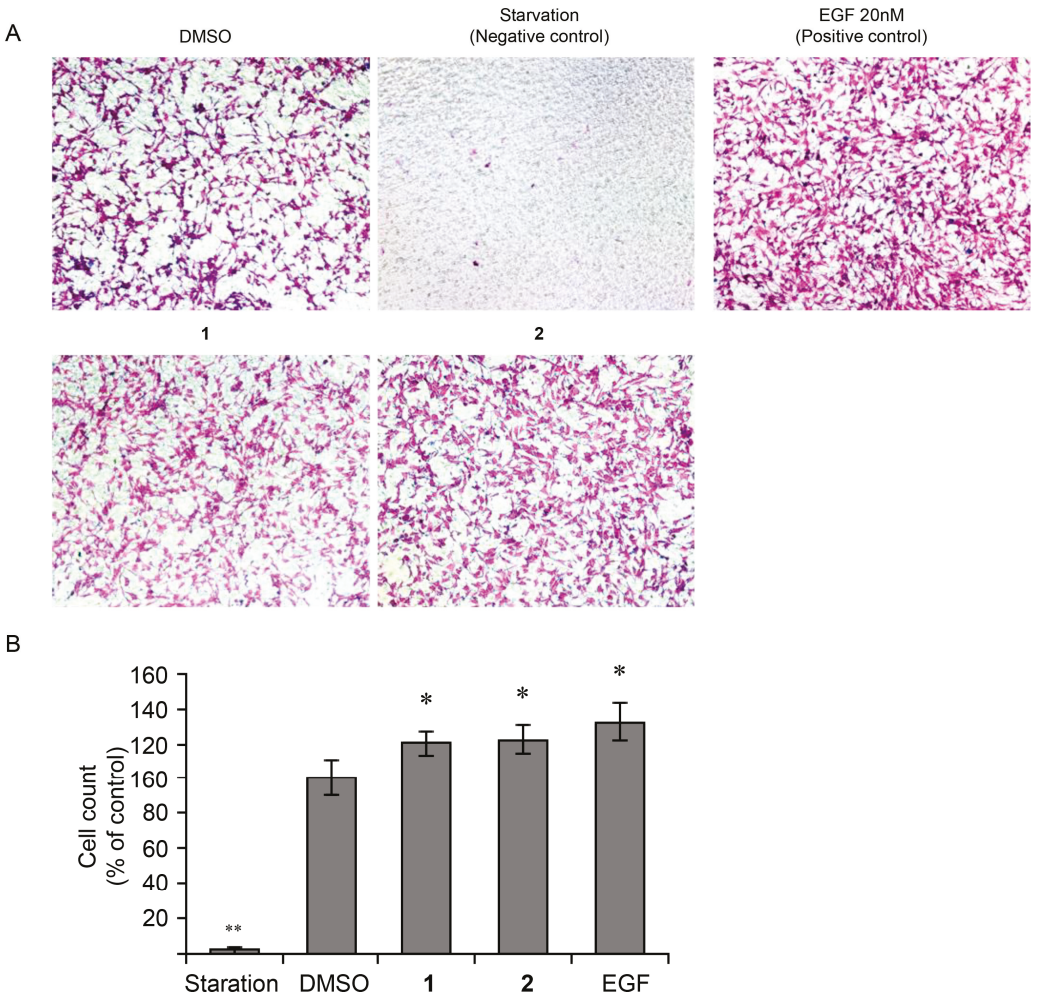

Figure 6. Matrigel invasion assay of MEF cells using a Transwell system. (**A**) Cells were seeded on a Transwell insert plate (2.5×10^4 cells/well) and treated with 100 μM compounds **1** and **2** for 24 h. (**B**) Graph showing the invasion assay, including the measurement of cell numbers. Data are expressed as mean ± SEM from three independent experiments ($n = 3$; * $p < 0.05$, ** $p < 0.01$ vs. DMSO-treated group).

*3.5. Acceleration of FAK and MAPK Phosphorylation in MEF Cells Following Treatment with 4-Hydroxy-Benzoic Acid (**1**) and Vanillic Acid (**2**)*

To further elucidate the potential mechanisms of action of 4-hydroxy-benzoic acid (**1**) and va-nillic acid (**2**), we examined their effects on MAPK phosphorylation. Our findings indicate that treatment with these compounds increased the phosphorylation of FAK and p38 in MEF cells (Figure 7). Additionally, MMP2 expression was upregulated

in MEF cells. Collectively, these results suggest that the activation of MAPK signaling by 4-hydroxy-benzoic acid (**1**) and vanil-lic acid (**2**) may promote the movement of MEF cells.

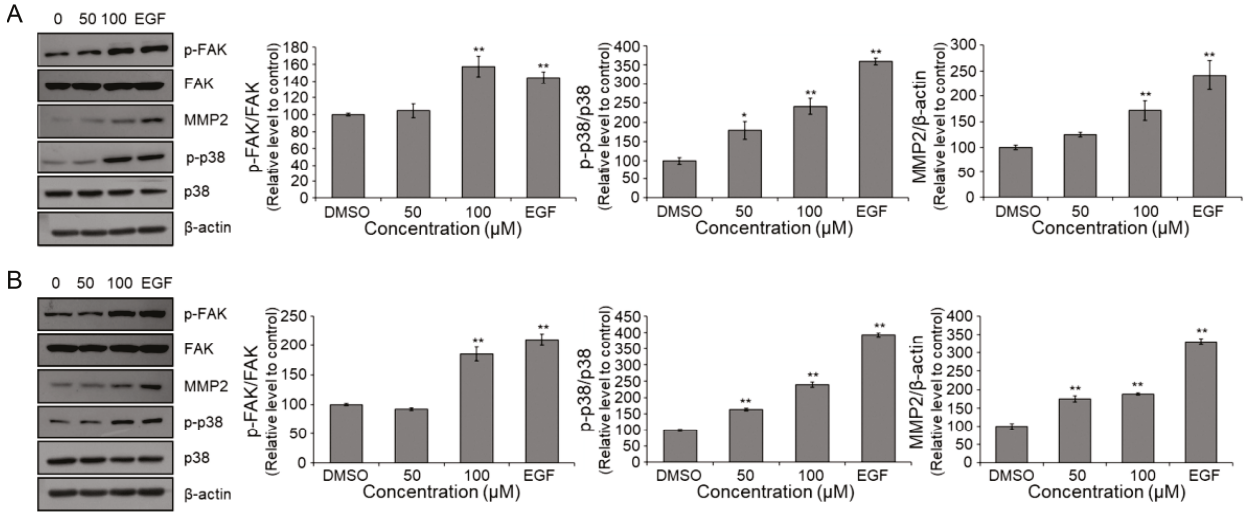

Figure 7. Involvement of the FAK pathway in MMP2 and MAPK expression and promotion of cell migration. MEF Cells were seeded in 6-well plates (1.5×10^5 cells/well) and treated for 24 h with DMSO (0.1%, *v*/*v*), (**A**) 4-hydroxy-benzoic acid (**1**) or (**B**) vanillic acid (**2**) at 50 and 100 μM for 24 h. The protein levels of phosphorylated and total FAK and p38 MAPK (p-FAK/FAK and p-p38/p38 MAPK) were analyzed by Western blotting. To confirm equivalent protein amounts, β-actin was employed as a reference protein. All values are expressed as mean ± SEM ($n = 3$; * $p < 0.05$, ** $p < 0.01$ compared with the DMSO control group).

In the present study, we aimed to evaluate the wound-healing properties of the isolated compounds from vinegar–egg. Our findings suggest that these compounds effectively promote the epithelialization stage of wound healing, the second stage in the four-phase wound-healing process, which includes inflammation, epithelialization, proliferation, and maturation [28]. The examined compounds facilitated wound healing by enhancing cell mobility and invasion without affecting cell proliferation, thereby playing a crucial role in barrier maintenance and re-epithelialization following injury.

To repair damaged skin, intercellular junctions must be loosened, and the activation of FAK and MMPs plays a crucial role in this process [54,55]. In this study, we observed that the tested compounds increased cell migration in a concentration-dependent manner by inducing FAK phosphorylation. The activation of FAK triggers downstream signaling pathways, such as MAPK. MAPKs are serine-threonine protein kinases that play a critical role in signal transduction from the cytoplasm to the nucleus and regulate various cellular functions, including differentiation, proliferation, development, inflammatory responses, apoptosis, and oxidative stress [18,19,28]. Similarly to EGF treatment, the tested compounds significantly enhanced p38 phosphorylation, leading to increased migration of MEF cell [56,57]. Furthermore, our results suggest that the tested compounds promote cell migration by modulating MMP2 expression. These findings imply that vinegar treatment, a simple and non-thermal process, can enhance the functional properties of egg-based products while preserving their nutritional composition. This strategy is consistent with current trends in the food industry that emphasize the development of minimally processed, health-promoting functional foods. Furthermore, the identification of safe, cost-effective, and biologically active compounds from widely consumed food materials opens new avenues for the formulation of value-added products, functional ingredients, and nutraceuticals. Leveraging readily available raw materials in such innovative ways holds significant poten-

tial to improve production efficiency and diversify product offerings within the functional food sector.

4. Conclusions

Natural products have long been used as relatively inexpensive and generally safe options for the prevention and treatment of diseases. In this context, this work set out to identify and characterize the bioactive phenolic compounds present in vinegar–egg and to evaluate their wound-healing potential. As a result, we investigated the effects of 4-hydroxy-benzoic acid (**1**) and vanillic acid (**2**) on wound healing in MEF cells. In our comparative in vitro assays, compounds **3** (methyl syringate) and **4** (leptosperin) were also tested at identical concentrations but demonstrated only limited wound-healing activity. This differential efficacy underscores the superior potency of 4-hydroxybenzoic acid and vanillic acid in promoting cell migration, and justifies our emphasis on these two phenolics for further evaluation. The active compounds, 4-hydroxy-benzoic acid (**1**) and vanillic acid (**2**), evaluated in this study were significantly more cost-effective than EGF while exhibiting similar effects. Cell viability assays demonstrated that concentrations of up to 100 μM of these compounds did not significantly affect cell viability or proliferation. However, scratch wound healing assays revealed that both compounds enhanced MEF cell wound closure. Live cell analysis using HoloMonitor further confirmed that individual cells treated with these compounds exhibited increased motility compared to the DMSO-treated control group. Transwell chamber invasion assays also demonstrated that 4-hydroxy-benzoic acid (**1**) and vanillic acid (**2**) enhanced the invasion ability of MEF cells, thereby facilitating wound closure. Additionally, we evaluated MMP2 expression and MAPK phosphorylation levels in the presence and absence of 4-hydroxy-benzoic acid (**1**) and vanillic acid (**2**). Our data indicate that treatment with these compounds increased the phosphorylation levels of FAK and p38. Collectively, these findings suggest that 4-hydroxy-benzoic acid (**1**) and vanillic acid (**2**) may serve as promising agents for accelerating wound healing by promoting cell migration and invasion through FAK-MAPK signaling and MMP2 modulation. To the best of our knowledge, this is the first report to isolate and characterize phenolic compounds from vinegar–egg and to demonstrate their wound-healing efficacy via modulation of focal adhesion and MAPK signaling pathways. This work not only provides a mechanistic explanation for the traditional use of vinegar–egg but also introduces a novel strategy for generating functional ingredients from safe and widely available food matrices.

Supplementary Materials: The following are available online at https://www.mdpi.com/article/10.3390/nu17162584/s1; Figure S1: The ^{1}H NMR spectrum of **1** (CD_3OD, 850 MHz); Figure S2: The ESI-MS data of **1**; Figure S3: The ^{1}H NMR spectrum of **2** (CD_3OD, 850 MHz); Figure S4: The ESI-MS data of **2**; Figure S5: The ^{1}H NMR spectrum of **3** (CD_3OD, 850 MHz); Figure S6: The ESI-MS data of **3**; Figure S7: The ^{1}H NMR spectrum of **4** (CD_3OD, 850 MHz); Figure S8: The ESI-MS data of **4**; General Experimental Procedures; Cell motility videos for compounds **1**–**4**; Video File S1: Effects of DMSO on the motility of MEF cells in time-lapse cell tracking videos; Video File S2: Effects of **4**-Hydroxy-benzoic acid on the motility of MEF cells in time-lapse cell tracking videos; Video File S3: Effects of vanillic acid on the motility of MEF cells in time-lapse cell tracking videos; Video File S4: Effects of methyl syringate on the motility of MEF cells in time-lapse cell tracking videos; Video File S5: Effects of leptosperin on the motility of MEF cells in time-lapse cell tracking videos.

Author Contributions: Conceptualization, S.-K.K. and K.H.K.; methodology, T.O., C.H.C., S.C.B. and M.S.J.; formal analysis, T.O., C.H.C., S.C.B., M.S.J., W.B.K. and Y.S.K.; writing—original draft preparation, T.O., C.H.C., S.-K.K. and K.H.K.; writing—review and editing, S.-K.K. and K.H.K.; supervision, K.H.K.; funding acquisition, S.-K.K. and K.H.K. All authors have read and agreed to the published version of the manuscript.

Funding: This work was supported by a grant from KRIBB Research Initiative Program (KGM1272511 and KGM1462511), and the National Research Council of Science and Technology grant (CAP23011-300) funded by the Ministry of Science ICT (MSIT). This work was also supported by National Research Foundation of Korea (NRF) grants funded by the Korean government (MSIT; grant numbers RS-2019-NR040057 and RS-2021-NR059240). This research was supported by the National Research Foundation of Korea (NRF) grant funded by the Korea government (MSIT) (RS-2024-00440614).

Institutional Review Board Statement: Not applicable.

Informed Consent Statement: Not applicable.

Data Availability Statement: The original contributions presented in this study are included in the article/Supplementary Materials. Further inquiries can be directed to the corresponding authors.

Conflicts of Interest: The authors declare no conflicts of interest.

References

1. Schneider, A.; Wang, X.Y.; Kaplan, D.L.; Garlick, J.A.; Egles, C. Biofunctionalized electrospun silk mats as a topical bioactive dressing for accelerated wound healing. *Acta Biomater.* **2009**, *5*, 2570–2578. [CrossRef]
2. Silva, S.S.; Popa, E.G.; Gomes, M.E.; Cerqueira, M.; Marques, A.P.; Caridade, S.G.; Teixeira, P.; Sousa, C.; Mano, J.F.; Reis, R.L. An investigation of the potential application of chitosan/aloe-based membranes for regenerative medicine. *Acta Biomater.* **2013**, *9*, 6790–6797. [CrossRef]
3. Chhabra, S.; Chhabra, N.; Kaur, A.; Gupta, N. Wound Healing Concepts in Clinical Practice of OMFS. *J. Maxillofac. Oral. Surg.* **2017**, *16*, 403–423. [CrossRef]
4. Guo, S.; Dipietro, L.A. Factors affecting wound healing. *J. Dent. Res.* **2010**, *89*, 219–229. [CrossRef]
5. Velnar, T.; Bailey, T.; Smrkolj, V. The wound healing process: An overview of the cellular and molecular mechanisms. *J. Int. Med. Res.* **2009**, *37*, 1528–1542. [CrossRef]
6. Schmitt, S.; Safferling, K.; Westphal, K.; Hrabowski, M.; Müller, U.; Angel, P.; Wiechert, L.; Ehemann, V.; Müller, B.; Holland-Cunz, S.; et al. Stathmin regulates keratinocyte proliferation and migration during cutaneous regeneration. *PLoS ONE* **2013**, *8*, e75075. [CrossRef]
7. Shimabukuro, Y.; Ueda, M.; Ozasa, M.; Anzai, J.; Takedachi, M.; Yanagita, M.; Ito, M.; Hashikawa, T.; Yamada, S.; Murakami, S. Fibroblast growth factor-2 regulates the cell function of human dental pulp cells. *J. Endod.* **2009**, *35*, 1529–1535. [CrossRef] [PubMed]
8. Gomes, R.N.; Manuel, F.; Nascimento, D.S. The bright side of fibroblasts: Molecular signature and regenerative cues in major organs. *NPJ Regen. Med.* **2021**, *6*, 43. [CrossRef] [PubMed]
9. Landén, N.X.; Li, D.; Ståhle, M. Transition from inflammation to proliferation: A critical step during wound healing. *Cell. Mol. Life Sci.* **2016**, *73*, 3861–3885. [CrossRef] [PubMed]
10. Shams, F.; Moravvej, H.; Hosseinzadeh, S.; Mostafavi, E.; Bayat, H.; Kazemi, B.; Bandehpour, M.; Rostami, E.; Rahimpour, A.; Moosavian, H. Overexpression of VEGF in dermal fibroblast cells accelerates the angiogenesis and wound healing function: In vitro and in vivo studies. *Sci. Rep.* **2022**, *12*, 18529. [CrossRef]
11. Schultz, G.S.; Chin, G.A.; Moldawer, L.; Diegelmann, R.F. *Principles of Wound Healing*; University of Adelaide Press: Adelaide, Australia, 2011.
12. Nourian Dehkordi, A.; Mirahmadi Babaheydari, F.; Chehelgerdi, M.; Raeisi Dehkordi, S. Skin tissue engineering: Wound healing based on stem-cell-based therapeutic strategies. *Stem Cell Res. Ther.* **2019**, *10*, 111. [CrossRef]
13. Piipponen, M.; Li, D.; Landén, N.X. The Immune Functions of Keratinocytes in Skin Wound Healing. *Int. J. Mol. Sci.* **2020**, *21*, 8790. [CrossRef]
14. Diller, R.B.; Tabor, A.J. The Role of the Extracellular Matrix (ECM) in Wound Healing: A Review. *Biomimetics* **2022**, *7*, 87. [CrossRef]
15. El Ghalbzouri, A.; Hensbergen, P.; Gibbs, S.; Kempenaar, J.; van der Schors, R.; Ponec, M. Fibroblasts facilitate re-epithelialization in wounded human skin equivalents. *Lab. Investig.* **2004**, *84*, 102–112. [CrossRef]
16. Gonzalez, A.C.; Costa, T.F.; Andrade, Z.A.; Medrado, A.R. Wound healing—A literature review. *An. Bras. Dermatol.* **2016**, *91*, 614–620. [CrossRef]
17. Tottoli, E.M.; Dorati, R.; Genta, I.; Chiesa, E.; Pisani, S.; Conti, B. Skin Wound Healing Process and New Emerging Technologies for Skin Wound Care and Regeneration. *Pharmaceutics* **2020**, *12*, 735. [CrossRef]
18. Cargnello, M.; Roux, P.P. Activation and function of the MAPKs and their substrates, the MAPK-activated protein kinases. *Microbiol. Mol. Biol. Rev.* **2011**, *75*, 50–83. [CrossRef]
19. Li, T.; Sun, Y.; Wang, J.; Zhang, C.; Sun, Y. Promoted Skin Wound Healing by Tail-Amputated Eisenia foetida Proteins via the Ras/Raf/MEK/ERK Signaling Pathway. *ACS Omega* **2023**, *8*, 13935–13943. [CrossRef]

20. Zhang, W.; Liu, H.T. MAPK signal pathways in the regulation of cell proliferation in mammalian cells. *Cell Res.* **2002**, *12*, 9–18. [CrossRef]
21. Hu, X.; Li, J.; Fu, M.; Zhao, X.; Wang, W. The JAK/STAT signaling pathway: From bench to clinic. *Signal Transduct. Target. Ther.* **2021**, *6*, 402. [CrossRef]
22. Katz, M.; Amit, I.; Yarden, Y. Regulation of MAPKs by growth factors and receptor tyrosine kinases. *Biochim. Biophys. Acta* **2007**, *1773*, 1161–1176. [CrossRef]
23. Kong, T.; Liu, M.; Ji, B.; Bai, B.; Cheng, B.; Wang, C. Role of the Extracellular Signal-Regulated Kinase 1/2 Signaling Pathway in Ischemia-Reperfusion Injury. *Front. Physiol.* **2019**, *10*, 1038. [CrossRef]
24. Kurtzeborn, K.; Kwon, H.N.; Kuure, S. MAPK/ERK Signaling in Regulation of Renal Differentiation. *Int. J. Mol. Sci.* **2019**, *20*, 1779. [CrossRef]
25. Plotnikov, A.; Zehorai, E.; Procaccia, S.; Seger, R. The MAPK cascades: Signaling components, nuclear roles and mechanisms of nuclear translocation. *Biochim. Biophys. Acta* **2011**, *1813*, 1619–1633. [CrossRef]
26. Farooq, M.; Khan, A.W.; Kim, M.S.; Choi, S. The Role of Fibroblast Growth Factor (FGF) Signaling in Tissue Repair and Regeneration. *Cells* **2021**, *10*, 3242. [CrossRef]
27. Jabłońska-Trypuć, A.; Matejczyk, M.; Rosochacki, S. Matrix metalloproteinases (MMPs), the main extracellular matrix (ECM) enzymes in collagen degradation, as a target for anticancer drugs. *J. Enzyme. Inhib. Med. Chem.* **2016**, *31*, 177–183. [CrossRef]
28. Kandhwal, M.; Behl, T.; Singh, S.; Sharma, N.; Arora, S.; Bhatia, S.; Al-Harrasi, A.; Sachdeva, M.; Bungau, S. Role of matrix metalloproteinase in wound healing. *Am. J. Transl. Res.* **2022**, *14*, 4391–4405.
29. Sang, Q.X. Complex role of matrix metalloproteinases in angiogenesis. *Cell Res.* **1998**, *8*, 171–177. [CrossRef]
30. Siméon, A.; Monier, F.; Emonard, H.; Gillery, P.; Birembaut, P.; Hornebeck, W.; Maquart, F.X. Expression and activation of matrix metalloproteinases in wounds: Modulation by the tripeptide-copper complex glycyl-L-histidyl-L-lysine-Cu2+. *J. Investig. Dermatol.* **1999**, *112*, 957–964. [CrossRef]
31. Cabral-Pacheco, G.A.; Garza-Veloz, I.; Castruita-De la Rosa, C.; Ramirez-Acuña, J.M.; Perez-Romero, B.A.; Guerrero-Rodriguez, J.F.; Martinez-Avila, N.; Martinez-Fierro, M.L. The Roles of Matrix Metalloproteinases and Their Inhibitors in Human Diseases. *Int. J. Mol. Sci.* **2020**, *21*, 9739. [CrossRef]
32. Chen, P.C.; Tang, C.H.; Lin, L.W.; Tsai, C.H.; Chu, C.Y.; Lin, T.H.; Huang, Y.L. Thrombospondin-2 promotes prostate cancer bone metastasis by the up-regulation of matrix metalloproteinase-2 through down-regulating miR-376c expression. *J. Hematol. Oncol.* **2017**, *10*, 33. [CrossRef]
33. Hong, I.K.; Kim, Y.M.; Jeoung, D.I.; Kim, K.C.; Lee, H. Tetraspanin CD9 induces MMP-2 expression by activating p38 MAPK, JNK and c-Jun pathways in human melanoma cells. *Exp. Mol. Med.* **2005**, *37*, 230–239. [CrossRef]
34. Je, J.-Y.; Park, P.-J.; Kim, S.-K. Antioxidant activity of a peptide isolated from Alaska pollack (*Theragra chalcogramma*) frame protein hydrolysate. *Food Res. Int.* **2005**, *38*, 45–50. [CrossRef]
35. Lee, W.; Chen, T. Functional characteristics of egg white solids obtained from papain treated albumen. *J. Food Eng.* **2002**, *51*, 263–266. [CrossRef]
36. Liu, J.; Yu, Z.; Zhao, W.; Lin, S.; Wang, E.; Zhang, Y.; Hao, H.; Wang, Z.; Chen, F. Isolation and identification of angiotensin-converting enzyme inhibitory peptides from egg white protein hydrolysates. *Food Chem.* **2010**, *122*, 1159–1163. [CrossRef]
37. Mine, Y.; Ma, F.; Lauriau, S. Antimicrobial peptides released by enzymatic hydrolysis of hen egg white lysozyme. *J. Agric. Food Chem.* **2004**, *52*, 1088–1094. [CrossRef]
38. Qing, M.; Zang, J.; Ma, Y.; Chi, Y.; Chi, Y. Effects of rice vinegar treatment on the antioxidant activities and protein structures of whole egg liquid before and after gastrointestinal digestion. *Food Chem.* **2023**, *404*, 134574. [CrossRef]
39. You, S.-J.; Udenigwe, C.C.; Aluko, R.E.; Wu, J. Multifunctional peptides from egg white lysozyme. *Food Res. Int.* **2010**, *43*, 848–855. [CrossRef]
40. Solieri, L.; Giudici, P. *Vinegars of the World*; Springer: Berlin/Heidelberg, Germany, 2009; pp. 1–16.
41. Chen, Y.J.; Ma, M.H.; Fu, X. Changes in physicochemical properties of protein in vinegar-egg emulsion processing. *Mod. Food Sci. Technol.* **2019**, *35*, 80–86.
42. Wang, S.-Y.; Chang, C.-Y.; Chen, C.-W. Effects of vinegar–egg on growth inhibition, differentiation human leukemic U937 cells and its immunomodulatory activity. *J. Food. Drug. Anal.* **2018**, *26*, 731–740. [CrossRef]
43. Zeng, Q.; Cai, Z.-X.; Liu, Y.-P.; Jin, Y.-G. A comprehensive review on bioactive peptides derived from egg proteins. *Food Sci.* **2021**, *42*, 272–287.
44. Cho, C.H.; Chae, S.H.; Kim, S.H.; Kim, K.H. Phenolic compounds isolated from Juncus decipiens and their effects on osteoblast differentiation in the mouse mesenchymal stem cell line C3H10T1/2. *Nat. Prod. Sci.* **2024**, *30*, 135–142. [CrossRef]
45. Glick, V.J.; Webber, C.A.; Simmons, L.E.; Martin, M.C.; Ahmad, M.; Kim, C.H.; Adams, A.N.; Bang, S.; Chao, M.C.; Howard, N.C. Vaginal lactobacilli produce anti-inflammatory β-carboline compounds. *Cell Host Microbe* **2024**, *32*, 1897–1909. [CrossRef] [PubMed]

46. Lee, D.E.; Park, K.H.; Hong, J.-H.; Kim, S.H.; Park, K.-M.; Kim, K.H. Anti-osteoporosis effects of triterpenoids from the fruit of sea buckthorn (*Hippophae rhamnoides*) through the promotion of osteoblast differentiation in mesenchymal stem cells, C3H10T1/2. *Arch. Pharm. Res.* **2023**, *46*, 771–781. [CrossRef]
47. Lee, J.-E.; Jeong, S.Y.; Li, Z.; Kim, H.-Y.; Kim, H.-W.; Yoo, M.J.; Jang, H.J.; Kim, D.-K.; Cho, N.; Yoo, H.M. Development of a screening platform to discover natural products active against SARS-CoV-2 infection using lung organoid models. *Biomater. Res.* **2023**, *27*, 18. [CrossRef]
48. Lee, S.; Jang, M.; Ryoo, R.; Roh, J.; Ko, S.-K.; Kim, K.H. New autophagy-modulating lanostane-type triterpenoids from a hallucinogenic poisonous mushroom Gymnopilus orientispectabilis. *Arch. Pharm. Res.* **2024**, *47*, 272–287. [CrossRef] [PubMed]
49. Amrati, F.E.-Z.; Chebaibi, M.; Galvao de Azevedo, R.; Conte, R.; Slighoua, M.; Mssillou, I.; Kiokias, S.; de Freitas Gomes, A.; Soares Pontes, G.; Bousta, D. Phenolic composition, wound healing, antinociceptive, and anticancer effects of *Caralluma europaea* extracts. *Molecules* **2023**, *28*, 1780. [CrossRef]
50. Badaoui, M.I.; Chabani, S.; Magid, A.A.; Voutquenne-Nazabadioko, L.; Sayagh, C.; Harakat, D.; Haba, H. Chemical constituents of Centaurea dissecta Ten. and sesquiterpenes chemotaxonomic significance. *Biochem. Syst. Ecol.* **2024**, *114*, 104808. [CrossRef]
51. Curir, P.; Dolci, M.; Dolci, P.; Lanzotti, V.; Cooman, L.D. Fungitoxic phenols from carnation (*Dianthus caryophyllus*) effective against *Fusarium oxysporum* f. sp. dianthi. *Int. J. Plant Chem. Biochem. Tech.* **2003**, *14*, 8–12. [CrossRef]
52. Jermnak, U.; Yoshinari, T.; Sugiyama, Y.; Tsuyuki, R.; Nagasawa, H.; Sakuda, S. Isolation of methyl syringate as a specific aflatoxin production inhibitor from the essential oil of Betula alba and aflatoxin production inhibitory activities of its related compounds. *Int. J. Food Microbiol.* **2012**, *153*, 339–344. [CrossRef]
53. Aitken, H.R.; Johannes, M.; Loomes, K.M.; Brimble, M.A. Synthesis of leptosin, a glycoside isolated from mānuka honey. *Tetrahedron Lett.* **2013**, *54*, 6916–6919. [CrossRef]
54. D'Onofrio, P.M.; Shabanzadeh, A.P.; Choi, B.K.; Bähr, M.; Koeberle, P.D. MMP Inhibition Preserves Integrin Ligation and FAK Activation to Induce Survival and Regeneration in RGCs Following Optic Nerve Damage. *Investig. Ophthalmol. Vis. Sci.* **2019**, *60*, 634–649. [CrossRef] [PubMed]
55. Shutova, M.S.; Boehncke, W.H. Mechanotransduction in Skin Inflammation. *Cells* **2022**, *11*, 2026. [CrossRef]
56. Frey, M.R.; Golovin, A.; Polk, D.B. Epidermal growth factor-stimulated intestinal epithelial cell migration requires Src family kinase-dependent p38 MAPK signaling. *J. Biol. Chem.* **2004**, *279*, 44513–44521. [CrossRef]
57. Yang, D.J.; Moh, S.H.; Son, D.H.; You, S.; Kinyua, A.W.; Ko, C.M.; Song, M.; Yeo, J.; Choi, Y.H.; Kim, K.W. Gallic Acid Promotes Wound Healing in Normal and Hyperglucidic Conditions. *Molecules* **2016**, *21*, 899. [CrossRef] [PubMed]

Disclaimer/Publisher's Note: The statements, opinions and data contained in all publications are solely those of the individual author(s) and contributor(s) and not of MDPI and/or the editor(s). MDPI and/or the editor(s) disclaim responsibility for any injury to people or property resulting from any ideas, methods, instructions or products referred to in the content.

nutrients

MDPI

Article

Maternal Dietary Anthocyanidin, Dietary Inflammatory Potential, and Risk of Small-for-Gestational-Age in China

Binyan Zhang [1,2], Kun Xu [2,3], Baibing Mi [2], Hong Yan [2], Duolao Wang [4], Shaonong Dang [2,*] and Ke Men [1,*]

[1] School of Public Health, Xi'an Medical University, Xi'an 710021, China; zhangbinyan@stu.xjtu.edu.cn
[2] Department of Epidemiology and Biostatistics, School of Public Health, Xi'an Jiaotong University Health Science Center, Xi'an 710061, China; xukun_728@hust.edu.cn (K.X.); xjtu.mi@xjtu.edu.cn (B.M.); yanhonge@mail.xjtu.edu.cn (H.Y.)
[3] Department of Nutrition and Food Hygiene, School of Public Health, Tongji Medical College, Huazhong University of Science and Technology, Wuhan 430030, China
[4] Department of Clinical Sciences, Liverpool School of Tropical Medicine, Liverpool L7 8XZ, UK; duolao.wang@liverpool.ac.uk
* Correspondence: tjdshn@xjtu.edu.cn (S.D.); menke@xiyi.edu.cn (K.M.); Tel.: +86-29-8265-5104 (S.D.); +86-29-8617-7494 (K.M.)

Abstract

Background: The interaction between anthocyanidin intake and dietary inflammatory potential might influence small-for-gestational-age (SGA), but the available evidence has been limited. This study aims to examine the associations of anthocyanidin with SGA and whether these associations change with dietary inflammatory potential. **Methods:** Data were derived from 2244 pregnant women enrolled in a community-based, randomized controlled trial between 2015 and 2019 in China. Anthocyanidin intake was calculated with the use of validated food-frequency questionnaires. The energy-adjusted dietary inflammatory index (EDII) was determined by aggregating data from 33 food parameters. Infant birth outcome measurements were obtained from hospital records. Associations were assessed by generalized estimating equations with adjustment for confounding factors. **Results:** During 39.7 gestational weeks of follow-up, 234 SGA cases occurred. The median intake of anthocyanidin was 28.7 mg/d. Higher consumption of total anthocyanidins (OR: 0.96, 95% CI: 0.95 to 0.97), cyanidin (OR: 0.96, 95% CI: 0.95 to 0.97), and peonidin (OR: 0.96, 95% CI: 0.96 to 0.97) subclasses was associated with a reduced risk of SGA. EDII was associated with an increased risk of SGA (OR: 1.08, 95% CI: 1.03 to 1.12). In addition, we observed that higher anthocyanidin intake was inversely associated with EDII (β: −0.40, 95% CI: −0.46 to −0.34). The inverse anthocyanidin-SGA association was mostly greater among women in the highest tertile of EDII (OR: 0.67, 95% CI: 0.65 to 0.68) compared with the lowest tertile. **Conclusions:** Higher anthocyanidin intake was inversely associated with SGA, especially among women with higher EDII scores.

Keywords: pregnancy; anthocyanidin; dietary inflammatory index; small-for-gestational-age

1. Introduction

The phenotypic small-for-gestational-age (SGA) was defined as failure to achieve its genetic growth potential based on international standards [1,2]. It remained a critical global health issue, with an estimated 23.3 million infants born SGA in 2012 and 23.4 million in 2020 [3,4], accounting for 22.4% of the 2.4 million annual neonatal deaths [4]. Beyond mortality, SGA survivors were at increased risk for lifetime health and developmental problems, leading to loss of human capital and vulnerable societies [5,6]. Evidence-based antenatal interventions

to reduce the incidence of SGA, such as multiple micronutrient and protein-energy supplements, had been proven effective [7]. However, WHO recommendations regarding these interventions were restricted to undernourished populations [7,8]. To date, timely termination of pregnancy was the definitive intervention but carried an increased risk of preterm birth, highlighting the urgent need for more effective and safer interventions.

As a simple and practicable non-pharmacological intervention, dietary modification has been well-established to have many health benefits [9,10]. An adequate maternal diet during pregnancy might be an important modifiable risk factor for SGA prevention [10,11]. Evidence indicated that higher consumption of vegetables, fruits, and whole grains was associated with a reduced risk of SGA [11–13], yet the underlying bioactive compounds had not been fully elucidated [14–16]. An anti-inflammatory state of pregnancy was acknowledged to be associated with fetal growth [17]. The potential role of diet in preventing SGA might be partly attributed to the intake of dietary phytochemicals with anti-inflammatory properties, such as anthocyanidins [18–20].

Anthocyanidins, a member of the flavonoid class of secondary metabolite, were water-soluble plant pigments. Structurally, they were flavylium cations, characterized by a C_6-C_3-C_6 carbon skeleton. Owing to their poor stability, anthocyanidins most commonly occurred in nature in their glycosylated forms, known as anthocyanins [21]. More than 600 anthocyanins derived from anthocyanidins have been identified in nature [22]. Among these anthocyanidins, delphinidin, cyanidin, and peonidin occurred ubiquitously and had dietary importance. These compounds were commonly consumed in the human diet, especially in red, blue, or purple fruits and vegetables, as well as in certain cereals [23]. A randomized, double-blind, placebo-controlled trial further confirmed that anthocyanin supplementation improved anti-inflammatory capacity [24]. Epidemiological evidence suggested that maternal consumption of a more pro-inflammatory diet during pregnancy had been associated with an increased risk of SGA births [25], suggesting that dietary inflammatory potential might have an important moderating role on the anthocyanin-SGA associations. However, it remained unclear whether dietary anthocyanidins could protect against SGA and to what extent this association was modified by dietary inflammatory potential.

We hypothesized that anthocyanidin intake would protect against SGA births and that women who consumed higher levels of a pro-inflammatory diet during pregnancy would benefit more. The current study aimed to investigate the associations of maternal dietary anthocyanidin and its subclasses with SGA and to examine the extent to which dietary inflammatory potential may modify these associations in a cohort of pregnant women in China.

2. Materials and Methods

2.1. Study Population

This prospective population-based study analyzed data from a community-based, randomized controlled trial (RCT) assessing maternal multivitamin supplementation effects on birth outcomes (ClinicalTrials.gov NCT02537392). The trial methodology had been previously described in detail [26]. In brief, this community-based intervention was conducted across three rural counties (Bin, Xunyi, and Changwu) in western China from July 2015 to December 2019. Eligible participants were pregnant women aged 15–47 years with a gestational age of <20 weeks at enrollment. Participants were randomly allocated at the township level in a 1:1:1 ratio to receive either 400 μg folic acid alone, 400 μg folic acid plus 60 mg iron, or 400 μg folic acid combined with a B-complex vitamin containing 2 mg vitamin B_1 (thiamine), 2 mg vitamin B_2 (riboflavin), 2 mg vitamin B_6 (pyridoxine), 2 μg vitamin B_{12} (cobalamin), 5 mg calcium pantothenate, and 15 mg nicotinamide. The present analysis initially included 2438 eligible participants with complete dietary data. Based on

predefined exclusion criteria, we subsequently excluded 70 participants lost to follow-up, 16 who voluntarily withdrew, 20 cases of fetal loss, 4 stillbirths, 24 with hypertension or diabetes, 17 with missing birthweight data, and 43 reporting implausible energy intake (<500 or >5000 kcal/day), yielding a final analytical sample of 2244 participants (Figure S1).

Written informed consent was obtained from all participants, and ethical approval for the study was obtained from the Ethics Review Committee of Xi'an Jiaotong University Health Science Center (No. 20120008, approved on 6 March 2012).

2.2. Assessment of Dietary Anthocyanidin

Maternal dietary intake during pregnancy was assessed through face-to-face interviews using a validated 107-item Food Frequency Questionnaire (FFQ) during follow-up visits after enrollment [27,28]. The FFQ was designed to capture foods commonly consumed by rural populations in western China. Specifically, participants were asked to report both the frequency (8-tier frequency scale ranging from "almost never' to "$\geq$2 times/day") and portion sizes of each food item during the most recent pregnancy. Based on these responses, the average daily intake for each food item was calculated.

The estimation of dietary anthocyanidin intake and its subclasses of delphinidin, cyanidin, and peonidin was based on FFQ data by referencing the China Food Composition Table (Standard Edition) [29]. This database included anthocyanidin content for 346 food items. We could not assume that foods that were not in the reference database did not contain anthocyanidins. Therefore, anthocyanidin intake estimation accounted for database limitations by incorporating three data treatment strategies. First, we assigned logical zeros (71.0% of items in FFQ) to animal products and non-pigmented plants where anthocyanidins were biologically absent. Second, we estimated values (12.1%) through nutritional equivalency modeling from analogous foods in both the FFQ and the reference database. Therefore, 83.2% of food items were assigned estimated values. Only processed foods (16.8%) without reference data received conservative zero assignments. The intake of anthocyanidin subclasses was calculated as Σ[consumed amount (g/day) $\times$ anthocyanidin content (mg/100 g)] for all foods. Total anthocyanidin intake was calculated by summing the intake of anthocyanidin subclasses. To analyze the association between anthocyanidins and SGA, we classified individuals based on quartile cut-off points of anthocyanidin intake.

2.3. Assessment of Dietary Inflammatory Index

The Dietary Inflammatory Index (DII) was developed to evaluate an individual's dietary inflammatory potential [30]. Briefly, the DII was derived from a systematic review of 1943 articles (1950–2010) to account for the effects of 45 food parameters on six inflammatory biomarkers (IL-1β, IL-4, IL-6, IL-10, TNF-α, and CRP) that were upregulated in non-specific immune responses. In our analysis, 33 of the original 45 food parameters were available to calculate the DII. Pro-inflammatory parameters included energy, carbohydrates, cholesterol, protein, total fat, saturated fat, vitamin B_{12}, and iron, and anti-inflammatory parameters included monounsaturated fatty acids (MUFA), polyunsaturated fatty acids (PUFA), *n*-3 fatty acids, *n*-6 fatty acids, fiber, vitamin A, β-carotene, thiamin, riboflavin, niacin, vitamin B_6, folic acid, vitamin C, vitamin D, vitamin E, magnesium, zinc, selenium, caffeine, alcohol, isoflavones, anthocyanidins, green/black tea, onion, and garlic. To calculate the DII score, the pregnant women's daily intake of each food parameter was transformed into z-scores by subtracting the global daily mean intake and dividing by the standard deviation. These z-scores were then converted to a percentile score to minimize the effect of right skewing. Each percentile value was subsequently doubled and centered by subtracting 1. The centered values were then multiplied by their corresponding inflammatory effect scores and aggregated to generate the composite DII score. Finally, the energy-adjusted DII

(EDII) was derived using the residual method [31]. To explore the association between anthocyanidins and SGA at different degrees of EDII, we classified individuals based on tertile cut-off points of EDII.

2.4. Assessment of Small-for-Gestational-Age

Infant birth outcome measurements, including birth weight and gestational age at delivery, were obtained from hospital records. Gestational age- and sex-specific birthweight z-scores were derived using the INTERGROWTH-21st standards [1], and neonates with z-scores below the 10th percentile were classified as SGAs.

2.5. Assessment of Covariates

According to expert consensus regarding the pathogenic mechanisms of SGA and previous epidemiological studies [10,32,33], we identified and collected a set of potential covariates. These included maternal age, socioeconomic status, season of birth, parity, passive smoking, multivitamin supplements, maternal body mass index (BMI) at enrollment, pregnancy-induced hypertension or gestational diabetes mellitus, and total energy intake. Maternal age was analyzed as a continuous variable. Socioeconomic status was derived via principal component analysis of five indicators, including household wealth index, parental education, and parental occupation, and categorized into tertiles (lower, medium, and upper). Season of birth was classified as spring, summer, autumn, and winter. Parity was dichotomized into nulliparous or multiparous. Passive smoking was defined as exposure to secondhand smoke for more than 15 min daily during pregnancy. Multivitamin supplements were classified as folic acid alone, folic acid plus iron, or folic acid with B-complex vitamins. Maternal BMI at enrollment (kg/m^2) was derived by dividing weight (kg) by height squared (m^2).

2.6. Statistical Analyses

We conducted statistical analyses using SAS version 9.4 (SAS Institute, Cary, NC, USA). Descriptive analyses were performed to characterize the study population and food parameters across quartiles of anthocyanidin intake (Q1–Q4), presenting continuous variables as either median (interquartile range, IQR) or mean ± standard deviation (SD) depending on distribution normality or not, and categorical variables as frequencies (percentages). We employed generalized estimating equations (GEE) with adjustment for country-level clustering to assess differences across quartiles of total anthocyanidin intake [34]. Anthocyanidin and food parameters were standardized to mitigate skewness. Pearson correlation analysis was used to assess the associations between total anthocyanidin intake and food parameters. To assess the relative contribution of different dietary sources to variation in anthocyanidin intake among pregnant women, forward linear regression was employed. GEE was used to assess the odds ratios (ORs) with 95% confidence intervals (95%CIs) for the associations of dietary anthocyanidin intake and EDII with the risk of SGA. To explore the relationships of dietary anthocyanidin intake with EDII, GEE was also used to estimate the coefficient (β) and 95%CI. For all analyses, we modeled anthocyanidin intake and EDII both as continuous variables and in quartiles. We developed two hierarchical regression models to account for potential confounding factors. Model 1 adjusted for country-level clustering, while Model 2 was additionally adjusted for maternal age, socioeconomic status, season of birth, parity, passive smoking, multivitamin supplements, maternal BMI at enrollment, pregnancy-induced hypertension or gestational diabetes mellitus, and total energy intake. To assess potential effect modification by dietary inflammatory potential, interactions between the dietary anthocyanidin intake and EDII on SGA were evaluated by adding the interaction term (anthocyanidins × EDII) to the final adjusted model. Accordingly, we further performed stratified analyses by the tertiles of EDII to evaluate how

anthocyanidin–SGA associations varied across EDII levels. A two-sided p value < 0.05 was considered statistically significant.

3. Results

3.1. Population Characteristics

During 39.7 gestational weeks of follow-up among the 2244 pregnant women, we documented 234 incident cases of SGA. Baseline characteristics of the participants according to quartiles of anthocyanidin intake were shown in Table 1. Dietary assessment was conducted at a mean gestational age of 26.2 ± 12.4 weeks. The median daily intake of anthocyanidin was 28.7 mg, with an intake range of 0.0–990.7 mg/d. Compared to women in the lowest quartile of anthocyanidin intake, those in the highest quartile were more likely to deliver in autumn, were multiparous, and had a lower incidence of pregnancy complications and SGA, as well as lower EDII scores ($p < 0.05$). The distributions of multivitamin supplements, maternal age, socioeconomic status, BMI, passive smoking, birth weight, and gestational age were similar across quartiles of anthocyanidin intake ($p > 0.05$). Anthocyanidin intake was most strongly correlated with the intake of fiber, vitamin C, and vitamin B_6 (r ranging from 0.31 to 0.35, $p < 0.001$). However, no significant association was observed between anthocyanidin intake and the intake of caffeine, alcohol, green/black tea, or garlic ($p > 0.05$) (Table 2).

Table 1. Characteristics of the study participants across quartiles of dietary anthocyanidin intake during pregnancy in China during 2015–2019.

Baseline Characteristics	*n* = 2244	Quartiles of Anthocyanidins, mg/d				*p*
		Q1 (*n* = 561)	Q2 (*n* = 561)	Q3 (*n* = 561)	Q4 (*n* = 561)	
Anthocyanidin, range, mg/d	(0, 990.7)	(0, 13.3)	(13.3, 28.7)	(28.7, 67.8)	(67.8, 990.7)	
Anthocyanidin, median (P_{25}, P_{75})	28.7 (13.3, 67.8)	6.2 (3.7, 9.9)	20.5 (16.7, 24.2)	39.4 (34.3, 52.7)	131.8 (103.1, 198.6)	
Season of birth						<0.001
Spring (March-May), *n* (%)	467 (20.8)	114 (25.7)	144 (25.7)	77 (13.7)	48 (8.56)	
Summer (June-August), *n* (%)	509 (22.7)	114 (20.3)	114 (20.3)	137 (24.4)	133 (23.7)	
Autumn (September-November), *n* (%)	661 (29.5)	149 (26.6)	149 (26.6)	194 (34.6)	223 (39.8)	
Winter (December-February), *n* (%)	607 (27.1)	154 (27.5)	154 (27.5)	153 (27.3)	157 (28.0)	
Multivitamin supplement, *n* (%)						0.931
Folic acid	814 (36.3)	201 (35.8)	214 (38.2)	206 (36.7)	193 (34.4)	
Folic acid plus iron	704 (31.4)	176 (31.4)	158 (28.2)	177 (31.6)	193 (34.4)	
Folic acid plus B-complex vitamins	726 (32.4)	184 (32.8)	189 (33.7)	178 (31.7)	175 (31.2)	
Maternal age (years), mean ± SD	25.8 ± 4.1	26.0 ± 4.4	25.8 ± 4.2	25.5 ± 3.6	25.9 ± 4.1	0.193
Parity, *n* (%)						<0.001
Nulliparous	1095 (48.8)	279 (49.7)	296 (52.8)	265 (47.2)	255 (45.5)	
Multiparous	1149 (51.2)	282 (50.3)	365 (47.2)	296 (52.8)	306 (54.6)	
Socioeconomic status [a], *n* (%)						0.800
Lower	747 (33.3)	190 (33.9)	178 (31.7)	183 (32.6)	196 (34.9)	
Medium	747 (33.3)	195 (34.8)	184 (32.8)	198 (35.3)	170 (30.3)	
Upper	750 (33.4)	176 (31.4)	199 (35.5)	180 (32.1)	195 (34.8)	
Body mass index (kg/m^2), mean ± SD	21.4 ± 2.7	21.4 ± 2.8	21.5 ± 2.7	21.5 ± 2.7	21.4 ± 2.5	0.631
Passive smoking [b], *n* (%)	248 (11.1)	67 (11.9)	61 (10.9)	54 (9.6)	66 (11.8)	0.354
Pregnancy complication [c], *n* (%)	70 (3.1)	29 (5.2)	17 (3.0)	7 (1.3)	17 (3.0)	<0.001
Birthweight, gram, mean ± SD	3240.2 ± 430.3	3234.8 ± 428.5	3219.0 ± 435.6	3251.9 ± 427.5	3255.1 ± 429.8	0.114
Gestational age, weeks, mean ± SD	39.7 ± 1.2	39.7 ± 1.2	39.6 ± 1.3	39.7 ± 1.2	39.7 ± 1.3	0.210
Small-for-gestational-age, *n* (%)	234 (10.4)	62 (11.1)	57 (10.2)	64 (11.4)	51 (9.1)	0.033
EDII, mean ± SD	−0.002 ± 1.805	0.63 ± 1.77	0.21 ± 1.74	−0.11 ± 1.74	0.75 ± 1.69	<0.001

Q, quartile. EDII, energy-adjusted dietary inflammatory index. Values are mean ± standard deviations or *n* (%). Tests of significance are adjusted for clustering by county using a generalized estimating equation. [a] Socioeconomic status was assessed using principal component analysis to derive a composite score from five indicators: family wealth index, maternal and paternal education levels, and maternal and paternal occupations. Socioeconomic status was then categorized into lower, medium, and higher groups based on tertiles of the composite score. [b] Passive smoking was defined as exposure to secondhand smoke for more than 15 min daily during pregnancy. [c] Pregnancy complications included pregnancy-induced hypertension syndrome and gestational diabetes mellitus.

Table 2. Correlation of food parameters with anthocyanidin intake and their distribution across anthocyanidin intake quartiles.

Food Parameters	Correlation with Anthocyanidin		Quartiles of Anthocyanidin, mg/d			
	Pearson's *r*	*p*	Q1	Q2	Q3	Q4
Energy (kcal/d)	0.24	<0.001	2041.2 ± 678.8	2231.1 ± 675.6	2373.4 ± 678.6	2534.8 ± 719.3
Carbohydrate (g/d)	0.22	<0.001	322.1 ± 126.3	355.3 ± 125.6	383.3 ± 124	407.1 ± 132.5
Protein (g/d)	0.18	<0.001	58.1 ± 22.1	64.6 ± 22.3	67.7 ± 22.7	72.2 ± 24.1
Total fat (g/d)	0.18	<0.001	64.4 ± 21.9	68.7 ± 22.1	71.2 ± 24.7	76.9 ± 24.6
Saturated fat (g/d)	0.13	<0.001	13.8 ± 6.6	15.2 ± 6.7	15.7 ± 7.0	16.9 ± 7.5
MUFA (g/d)	0.14	<0.001	27.6 ± 7.0	29.3 ± 7.0	30.1 ± 8.0	31.3 ± 8.0
PUFA (g/d)	0.17	<0.001	17.6 ± 10.1	18.8 ± 10.4	19.8 ± 12.3	22.6 ± 11.9
n-3 fatty acids (g/d)	0.15	<0.001	5.2 ± 3.9	5.4 ± 4.0	5.7 ± 4.8	6.7 ± 4.7
n-6 fatty acids (g/d)	0.17	<0.001	17.7 ± 10.1	18.8 ± 10.5	19.9 ± 12.4	22.7 ± 12.0
Cholesterol (mg/d)	0.04	0.064	197.8 ± 144.9	218.2 ± 142.3	217.7 ± 143.9	223.7 ± 152.9
Fiber (g/d)	0.31	<0.001	8.6 ± 4.8	10.1 ± 5.0	11.1 ± 5.4	13.6 ± 6.3
Vitamin A (μg/d, RAE)	0.15	<0.001	294.6 ± 259.5	336.8 ± 207.6	359.0 ± 219.2	435.3 ± 371.7
β-Carotene (μg/d)	0.27	<0.001	1613.5 ± 1166.4	1989.1 ± 1309.2	2246.2 ± 1431	2755.7 ± 1481.8
Thiamin (mg/d)	0.29	<0.001	0.7 ± 0.3	0.8 ± 0.3	0.9 ± 0.3	1.0 ± 0.3
Riboflavin (mg/d)	0.25	<0.001	0.9 ± 0.6	1.0 ± 0.5	1.1 ± 0.5	1.3 ± 0.6
Niacin (mg/d)	0.29	<0.001	11.3 ± 4.2	12.9 ± 4.3	13.8 ± 4.9	15.5 ± 5.3
Vitamin B6 (mg/d)	0.35	<0.001	1.1 ± 0.5	1.2 ± 0.5	1.4 ± 0.6	1.7 ± 0.6
Vitamin B12 (μg/d)	0.004	0.842	4.0 ± 4.5	4.5 ± 4.3	4.8 ± 4.0	4.7 ± 5.0
Folic acid (μg/d)	0.26	<0.001	234.4 ± 119.6	270.8 ± 125.3	295.2 ± 142.4	351.5 ± 152.8
Vitamin C (mg/d)	0.34	<0.001	89.4 ± 56.7	103.3 ± 54.3	116.6 ± 58.4	148.7 ± 67
Vitamin D (μg/d)	0.08	<0.001	1.8 ± 1.5	2.0 ± 1.5	1.9 ± 1.4	2.2 ± 1.5
Vitamin E (mg/d)	0.18	<0.001	35.4 ± 18.8	37.6 ± 19.2	39.7 ± 23	45.1 ± 22.7
Mg (mg/d)	0.23	<0.001	369 ± 157.9	411.2 ± 159.6	442.6 ± 156.2	488.1 ± 168.1
Fe (mg/d)	0.25	<0.001	16.7 ± 6.3	18.7 ± 6.3	20.2 ± 7.6	22.7 ± 8.4
Zn (mg/d)	0.21	<0.001	5.8 ± 2.4	6.6 ± 2.4	6.9 ± 2.8	7.7 ± 3
Se (μg/d)	0.14	<0.001	26.9 ± 12.3	29.9 ± 12.9	32.1 ± 14.7	33.7 ± 15.2
Isoflavones (mg/d)	0.12	<0.001	0.8 ± 0.5	0.9 ± 0.5	0.9 ± 0.9	1.0 ± 0.8
Caffeine (g/d)	0.04	0.070	1.0 ± 7.0	1.3 ± 8.0	1.2 ± 4.3	1.3 ± 4.7
Alcohol (g/d)	0.02	0.449	0.01 ± 0.10	0.01 ± 0.08	0.003 ± 0.047	0.02 ± 0.34
Green/black tea (g/d)	0.003	0.903	3.5 ± 34.7	3.9 ± 39.1	3.7 ± 20.5	3.3 ± 20.5
Onion (g/d)	0.14	<0.001	4.0 ± 9.6	5.1 ± 8.4	7.2 ± 12.2	8.9 ± 16.7
Garlic (g/d)	0.02	0.336	3.7 ± 10.7	3.3 ± 5.5	4.8 ± 12.5	4.1 ± 5.7

Q, quartile. Values are means ± standard deviations.

3.2. Anthocyanidin and Its Food Source

Table 3 presented the primary dietary contributors to total anthocyanidin intake and its subclasses. Watermelon accounted for the majority (98.6%) of the variation in total anthocyanidin intake among pregnant women, followed by sweet potato (0.6%) and grapes (0.4%). For delphinidin intake, the top three contributing foods were eggplant (49.5%), sweet potato (30.7%), and grapes (16.6%). In the case of cyanidin, watermelon was the predominant source, explaining 99.5% of the observed variation, with minimal contributions from plum/apricot (0.3%) and eggplant (0.1%). Regarding peonidin, sweet potatoes and grapes were the primary sources, accounting for 58.4% and 41.7% of the variation, respectively.

Table 3. Explained interindividual variance in the anthocyanidins by food sources among pregnant women in China during 2015–2019.

Food Source	R^2	Model R^2
Anthocyanidins		
Watermelon	0.986	0.986
Sweet potato	0.006	0.991
Grapes	0.004	0.995
Plum/apricot	0.003	0.999
Eggplant	0.001	1.000
Delphinidin		
Eggplant	0.495	0.495
Sweet potato	0.307	0.802
Grapes	0.166	0.968
Persimmon	0.031	0.999
Banana	0.001	1.000
Cyanidin		
Watermelon	0.995	0.995
Plum/apricot	0.003	0.999
Eggplant	0.001	1.000
Peonidin		
Sweet potato	0.584	0.584
Grapes	0.417	1.000

Forward linear regression was used to calculate the R^2 and model R^2. Food groups that explain 0.1% of the interindividual variation are shown.

3.3. Anthocyanidin, Dietary Inflammatory Potential, and Small-for-Gestational-Age

The median daily intakes of total anthocyanidin and its subclasses were as follows: 28.67 mg for total anthocyanidins (IQR: 13.29–67.78 mg), 0.83 mg for delphinidin (IQR: 0.44–1.69 mg), 23.56 mg for cyanidin (IQR: 8.40–62.56 mg), and 2.20 mg for peonidin (IQR: 0.88–4.64 mg). The mean EDII score was -0.002 (SD 1.805). Our multivariable-adjusted analysis demonstrated inverse associations between dietary anthocyanidin intake and SGA risk, with a consistent 4% risk reduction per SD increase for total anthocyanidins (OR: 0.96, 95% CI: 0.95 to 0.97), cyanidin (OR: 0.96, 95% CI: 0.95 to 0.97), and peonidin (OR: 0.96, 95% CI: 0.96 to 0.97). However, delphinidin intake showed no significant association (OR: 1.03, 95% CI: 0.99 to 1.07) (Table 4).

In multivariable-adjusted models, participants in the highest quartile of total anthocyanidin intake, with a median of 131.88 mg/d, had a 19% lower risk of SGA (OR: 0.81, 95% CI: 0.66 to 0.98) compared to those in the lowest quartile. Similarly, participants in the highest quartile of cyanidin intake, with a median daily consumption of 125.08 mg/d, had a 17% lower risk of SGA (OR: 0.83, 95% CI: 0.71 to 0.97) compared to the lowest quartile. Those in the highest quartile of peonidin intake, who consumed a median of 9.85 mg/d, demonstrated an 11% risk reduction in SGA (OR: 0.89, 95% CI: 0.79 to 1.00). Conversely, a positive association was observed between EDII and SGA risk (OR: 1.08, 95% CI: 1.03 to 1.12), with a 50% greater risk of SGA when comparing the highest versus lowest quartile of EDII (Table 4).

Table 5 displayed the associations of dietary anthocyanidin with the EDII. Per SD increase in the intake of anthocyanidin, the EDII decreased by 0.40 (β: −0.40, 95% CI: −0.46 to −0.34) in the multivariate model. Participants in the highest quartile of anthocyanidin intake had a 1.56−unit lower EDII (β: −1.56, 95% CI: −1.98 to −1.14) compared to those in the lowest quartile. Similar inverse associations were also observed for anthocyanidin subclasses. Our findings suggested that dietary anthocyanidin intake may mitigate the overall inflammatory potential of diet.

Table 4. Associations of anthocyanidin and dietary inflammatory index with the risk of small-for-gestational-age in China during 2015–2019.

	Continuous	Quartile of Anthocyanidin or EDII			
		Q1	Q2	Q3	Q4
Total anthocyanidin					
Cases/subjects	234/2244	62/561	57/561	64/561	51/561
Median (25th, 75th), mg/d	28.67 (13.29, 67.78)	6.21 (3.68, 9.86)	20.45 (16.65, 24.18)	39.43 (34.32, 52.73)	131.82 (103.12, 198.56)
Model 1, OR (95%CI)	0.96 (0.95, 0.97)	referent	0.91 (0.69, 1.19)	1.04 (0.88, 1.23)	0.80 (0.66, 0.97)
Model 2, OR (95%CI)	0.96 (0.95, 0.97)	referent	0.91 (0.70, 1.18)	1.04 (0.89, 1.21)	0.81 (0.66, 0.98)
Individual anthocyanidin					
Delphinidin					
Cases/subjects	234/2244	60/561	58/561	58/561	58/561
Median (25th, 75th), mg/d	0.83 (0.44, 1.69)	0.24 (0.15, 0.35)	0.60 (0.51, 0.71)	1.14 (0.99, 1.35)	2.75 (2.26, 3.62)
Model 1, OR (95%CI)	1.02 (0.98, 1.06)	referent	0.96 (0.85, 1.09)	0.96 (0.84, 1.10)	0.96 (0.88, 1.06)
Model 2, OR (95%CI)	1.03 (0.99, 1.07)	referent	0.97 (0.85, 1.10)	0.96 (0.84, 1.11)	0.99 (0.93, 1.07)
Cyanidin					
Cases/subjects	234/2244	60/561	57/561	66/561	51/561
Median (25th, 75th), mg/d	23.56 (8.40, 62.56)	3.53 (1.96, 5.40)	15.30 (12.29, 19.99)	33.89 (28.93, 45.81)	125.08 (95.01, 188.15)
Model 1, OR (95%CI)	0.96 (0.95, 0.97)	referent	0.94 (0.78, 1.14)	1.11 (0.91, 1.36)	0.84 (0.72, 0.97)
Model 2, OR (95%CI)	0.96 (0.95, 0.97)	referent	0.93 (0.77, 1.12)	1.10 (0.97, 1.34)	0.83 (0.71, 0.97)
Peonidin					
Cases/subjects	234/2244	65/554	55/566	56/571	58/553
Median (25th, 75th), mg/d	2.20 (0.88, 4.64)	0.27 (0.00, 0.53)	1.51 (1.14, 1.85)	3.06 (2.64, 3.65)	9.85 (6.75, 13.40)
Model 1, OR (95%CI)	0.96 (0.94, 0.97)	referent	0.81 (0.75, 0.87)	0.81 (0.69, 0.95)	0.88 (0.80, 0.97)
Model 2, OR (95%CI)	0.96 (0.96, 0.97)	referent	0.81 (0.74, 0.89)	0.80 (0.67, 0.95)	0.89 (0.79, 1.00)
EDII					
Cases/subjects	234/2244	42/561	68/561	63/561	61/561
Means ± SD	−0.002 ± 1.805	0.63 ± 1.77	0.21 ± 1.74	−0.11 ± 1.74	0.75 ± 1.69
Model 1, OR (95%CI)	1.08 (1.03, 1.12)	referent	1.70 (1.43, 2.03)	1.56 (1.22, 2.00)	1.51 (1.11, 2.04)
Model 2, OR (95%CI)	1.08 (1.03, 1.12)	referent	1.73 (1.43, 2.10)	1.56 (1.19, 2.05)	1.50 (1.08, 2.08)

EDII, energy-adjusted dietary inflammatory index; Q, quartile; SD, standard deviations. Analysis using generalized estimating equations. Odds ratios (ORs) with 95% confidence intervals (95% CIs) were estimated for a 1-SD increment in continuous dietary anthocyanidins. Model 1 adjusted for clustering by country using generalized estimating equations. Model 2 adjusted for multivitamin supplement (folic acid, folic acid plus iron, and folic acid plus B-complex vitamins), intake of total energy, birth season (spring, summer, autumn, and winter), maternal age (continuous), nulliparity status (nulliparity or multiparity), socioeconomic situation (lower, medium, and upper), passive smoking (yes or no), maternal body mass index at enrollment (continuous), and pregnancy complication (hypertension or gestational diabetes). For the effect of peonidin in model 2, the OR (95%CI) was 0.886 (0.786, 0.997).

Table 5. Associations of dietary anthocyanidin with the dietary inflammatory index in China during 2015–2019.

	Continuous	Quartile of Anthocyanidin, mg/d			
		Q1	Q2	Q3	Q4
Total anthocyanidin					
Median (25th, 75th), mg/d	28.67 (13.29, 67.78)	6.21 (3.68, 9.86)	20.45 (16.65, 24.18)	39.43 (34.32, 52.73)	131.82 (103.12, 198.56)
Model 1, β (95%CI)	−0.36 (−0.41, −0.33)	referent	−0.42 (−0.58, −0.26)	−0.74 (−1.03, −0.45)	−1.39 (−1.76, −1.02)
Model 2, β (95%CI)	−0.40 (−0.46, −0.34)	referent	−0.48 (−0.62, −0.34)	−0.88 (−1.17, −0.59)	−1.56 (−1.98, −1.14)
Individual anthocyanidin					
Delphinidin					
Median (25th, 75th), mg/d	0.44 (0.83, 1.69)	0.24 (0.15, 0.35)	0.60 (0.51, 0.71)	1.14 (0.99, 1.35)	2.75 (2.26, 3.62)
Model 1, β (95%CI)	−0.65 (−0.70, −0.60)	referent	−0.56 (−0.65, −0.47)	−1.42 (−1.54, −1.30)	−1.94 (−2.04, −1.84)
Model 2, β (95%CI)	−0.74 (−0.78, −0.69)	referent	−0.66 (−0.78, −0.55)	−1.56 (−1.72, −1.41)	−2.20 (−2.35, −2.05)
Cyanidin					
Median (25th, 75th), mg/d	8.40 (23.56, 62.56)	3.53 (1.96, 5.40)	15.30 (12.29, 19.99)	33.89 (28.93, 45.81)	125.08 (95.01, 188.15)
Model 1, β (95%CI)	−0.33 (−0.37, −0.29)	referent	−0.01 (−0.26, 0.24)	−0.44 (−0.66, −0.23)	−1.07 (−1.56, −0.59)
Model 2, β (95%CI)	−0.36 (−0.41, −0.30)	referent	−0.07 (−0.27, 0.14)	−0.55 (−0.72, −0.39)	−1.21 (−1.70, −0.71)

Table 5. *Cont.*

	Continuous	Quartile of Anthocyanidin, mg/d			
		Q1	Q2	Q3	Q4
Peonidin					
Median (25th, 75th), mg/d	0.88 (2.20, 4.64)	0.27 (0.00, 0.53)	1.51 (1.14, 1.85)	3.06 (2.64, 3.65)	9.85 (6.75, 13.40)
Model 1, β (95%CI)	−0.53 (−0.57, −0.51)	referent	−0.36 (−0.53, −0.18)	−1.06 (−1.13, −0.98)	−1.67 (−1.71, −1.63)
Model 2, β (95%CI)	−0.58 (−0.61, −0.54)	referent	−0.37 (−0.57, −0.18)	−1.12 (−1.21, −1.02)	−1.78 (−1.87, −1.70)

Q, quartile. Analysis using generalized estimating equations. Model 1 adjusted for clustering by country using generalized estimating equations. Model 2 adjusted for multivitamin supplement (folic acid, folic acid plus iron, and folic acid plus B-complex vitamins), intake of total energy, birth season (spring, summer, autumn, and winter), maternal age (continuous), nulliparity status (nulliparity or multiparity), socioeconomic situation (lower, medium, and upper), passive smoking (yes or no), maternal body mass index at enrollment (continuous), and pregnancy complication (hypertension or gestational diabetes).

Table 6 showed a significant interaction between dietary anthocyanidin intake (including its subclasses) and dietary inflammatory potential on the risk of SGA (p interaction < 0.05). The associations between total anthocyanidin and anthocyanidin subclass intakes with SGA, stratified by EDII tertiles, were presented in Table 7. Higher intakes of total anthocyanidin (OR: 0.67, 95% CI: 0.65 to 0.68) and peonidin (OR: 0.93, 95% CI: 0.87 to 0.99) were associated with a reduced risk of SGA among participants in the highest tertile of EDII.

Table 6. Interaction effect of dietary anthocyanidin and dietary inflammatory potential on small-for-gestational-age in China during 2015–2019.

	OR (95%CI)	*p*
EDII	1.08 (1.03, 1.12)	<0.001
Total anthocyanidin		
Anthocyanidin	0.97 (0.97, 0.98)	<0.001
EDII	1.10 (1.04, 1.17)	0.002
Anthocyanidin × EDII	0.96 (0.94, 0.98)	<0.001
Individual anthocyanidin		
Delphinidin	1.05 (1.02, 1.09)	0.005
EDII	1.15 (1.12, 1.19)	<0.001
Delphinidin × EDII	0.95 (0.93, 0.96)	<0.001
Cyanidin	0.97 (0.97, 0.98)	<0.001
EDII	1.10 (1.03, 1.17)	0.004
Cyanidin × EDII	0.97 (0.94, 0.99)	0.010
Peonidin	0.96 (0.92, 1.01)	0.093
EDII	1.11 (1.09, 1.14)	<0.001
Peonidin × EDII	0.95 (0.92, 0.98)	0.004

EDII, energy-adjusted dietary inflammatory index. Odds ratios (ORs) with 95% confidence intervals (95% CIs) were estimated using generalized estimating equations adjusted for clustering, multivitamin supplements (folic acid, folic acid plus iron, and folic acid plus B-complex vitamins), intake of total energy, birth season (spring, summer, autumn, and winter), maternal age (continuous), nulliparity status (nulliparity or multiparity), socioeconomic situation (lower, medium, and upper), passive smoking (yes or no), maternal body mass index at enrollment (continuous), and pregnancy complications (hypertension or gestational diabetes).

Table 7. Stratified analysis of the association between dietary anthocyanidin and small-for-gestational-age by tertiles of energy-adjusted dietary inflammatory index in China during 2015–2019.

	Tertiles of Energy-Adjusted Dietary Inflammatory Index		
	T_1	T_2	T_3
Total anthocyanidin			
Median (25th, 75th), mg/d	41.24 (18.92, 112.50)	30.66 (13.85, 67.83)	21.12 (8.40, 36.39)
OR (95%CI)	1.08 (0.96, 1.21)	1.04 (0.89, 1.22)	0.67 (0.65, 0.68)
Individual anthocyanidin			
Delphinidin			
Median (25th, 75th), mg/d	1.35 (0.77, 2.61)	0.84 (0.49, 1.52)	0.49 (0.25, 0.91)
OR (95%CI)	1.10 (1.00, 1.45)	1.02 (0.88, 1.18)	0.88 (0.69, 1.10)

Table 7. *Cont.*

	Tertiles of Energy-Adjusted Dietary Inflammatory Index		
	T_1	T_2	T_3
Cyanidin			
Median (25th, 75th), mg/d	32.95 (13.23, 107.22)	25.10 (8.96, 63.72)	17.03 (5.47, 33.31)
OR (95%CI)	1.10 (0.94, 1.29)	0.95 (0.81, 1.11)	0.91 (0.82, 1.02)
Peonidin			
Median (25th, 75th), mg/d	3.45 (1.57, 7.74)	2.28 (1.05, 4.64)	1.23 (0.53, 2.55)
OR (95%CI)	1.06 (0.97, 1.15)	0.97 (0.90, 1.06)	0.93 (0.87, 0.99)

T, tertiles. Odds ratios (ORs) with 95% confidence intervals (95% CIs) were estimated using generalized estimating equation adjusted for clustering, multivitamin supplements (folic acid, folic acid plus iron, and folic acid plus B-complex vitamins), intake of total energy, birth season (spring, summer, autumn, and winter), maternal age (continuous), nulliparity status (nulliparity or multiparity), socioeconomic situation (lower, medium, and upper), passive smoking (yes or no), maternal body mass index at enrollment (continuous), and pregnancy complications (hypertension or gestational diabetes).

4. Discussion

To our knowledge, this was the first prospective population-based study to examine the associations between dietary intake of total anthocyanidin as well as its individual subclasses and the risk of SGA. We found that higher intake of total anthocyanidins, as well as of the cyanidin and peonidin subclasses, was inversely associated with the risk of SGA. In addition, we confirmed that a higher EDII score was associated with an increased risk of SGA, whereas higher anthocyanidin intake was inversely associated with EDII scores. The inverse association between anthocyanidin intake and SGA risk was greater among women with higher EDII scores.

In the current study, cyanidin (80.3%) and peonidin (14.6%) subclasses accounted for the majority (94.9%) of total anthocyanidin intake, with delphinidin contributing 5.1%. The primary dietary source was watermelon (98.6%), followed by sweet potato (0.6%) and grapes (0.4%). These findings aligned with previous reports identifying these foods as rich anthocyanin sources [19,35–37]. Notably, our findings contrasted with previous epidemiological studies identifying red wine and berries as primary anthocyanidin or anthocyanin sources in general populations [23,38–40]. This divergence might stem from both significantly lower red wine consumption (0.01 ± 0.27 g/day) and limited berry intake assessment via FFQ in our pregnant women. Of particular interest, we identified watermelon as a substantial contributor to anthocyanidin intake (accounting for 98.6% of total and 99.5% of cyanidin intake). This biological plausibility was supported by the verified presence of anthocyanin in watermelon rind extracts [41]. Human daily anthocyanidin intake varied considerably across diets, typically ranging from several milligrams to hundreds of milligrams. Our reported median anthocyanidin intake (28.7 mg/day) was consistent with estimates from other Asian populations, including Chinese adults (27.6 mg/day) [42] and Korean women (27.7 mg/day) [43]. Beyond this regional consistency, however, our findings highlighted substantial global geographic disparities. Anthocyanin intake varied worldwide, ranging from 12.5 mg/day in U.S. adults [44] to 24.2 mg/day in Australians [45] and 44.1 mg/day in Italians [46]. A likely explanation for the higher intake among Italians was the Mediterranean diet, which was rich in anthocyanin-containing foods such as berries and red wine. Despite being non-essential nutrients, anthocyanins had been recommended by the Chinese Nutrition Society at 50 mg/day in order to reduce oxidative stress and the risk of multiple chronic diseases [19].

To date, epidemiological evidence has found that higher consumption of anthocyanin was associated with a lower risk of several chronic diseases [47–50]. There was no evidence, to our knowledge, for a beneficial effect of anthocyanidin intake for SGA. Our findings highlighted the importance of consuming anthocyanidin for the prevention of SGA risk, which, from a public health perspective, provided support for consuming a variety of

anthocyanidin-rich foods such as watermelon, sweet potatoes and grapes. This fits with our current understanding that anthocyanin could exert potential biological benefits for human health [19]. In addition, our findings confirmed that the relationship between EDII and SGA was consistent with other studies [25,51,52]. Furthermore, we found that anthocyanidin had an inverse association with EDII, and the positive EDII–SGA association was mostly apparent among women with higher EDII scores. Taken together, anthocyanidin might provide a non-pharmacological beneficial effect against SGA by reducing dietary inflammatory potential.

However, the mechanisms behind the beneficial effects of anthocyanidin at risk for SGA were poorly revealed. As well established, oxidative-antioxidative balance was crucial for implantation and embryonic development. Notably, excessive oxygen peroxidation products could induce placental degeneration and subsequent fetal growth impairment [53], while evidence further confirmed that fetal growth restriction might be associated with antioxidant deficiency [54]. Importantly, pregnancy progresses through three immunological states that align with fetal development, where an anti-inflammatory state supports fetal growth while inflammation is associated with adverse outcomes [17]. In this context, recent studies demonstrated that anthocyanins could neutralize reactive oxygen species (ROS) and activate antioxidant genes, contributing to antioxidant effects reducing inflammation [55]. Moreover, experimental and epidemiological evidence demonstrated that anthocyanins exerted anti-inflammatory effects by decreasing C-reactive protein, IL-6, TNF-α, IL-1β, and IL-8 levels [56–58]. At the molecular level, in vitro studies revealed that both free anthocyanin compounds (FAC) and protein-bound anthocyanin compounds (p-BAC) from purple sweet potato might exert anti-inflammatory effects via inhibition of the JNK/AP-1 signaling pathway, thereby inhibiting their downstream pro-inflammatory responses [35]. Additionally, anthocyanins extracted from a novel hybrid sweet potato peel could alleviate oxidative stress through mitigation of LPS-induced inflammation [55]. Collectively, current evidence supported that anthocyanidin might exert protective effects against SGA through comprehensive regulation of oxidative stress and inflammation.

To our knowledge, this was the first prospective population-based study to evaluate the protective role of anthocyanidin and its subclasses against SGA risk, as well as the potential modifying effect of dietary inflammatory potential. Nevertheless, several limitations should be acknowledged. First, the original research design was RCT, in which all women received multivitamins. This could potentially attenuate the influence of maternal dietary anthocyanidin on SGA, despite multivariable adjustment for multivitamins, thereby limiting the generalizability of our findings on this specific exposure. Second, anthocyanidin intake estimates likely represented conservative values due to incomplete food composition data for certain items, so we could not assume foods that were not in the reference databases did not contain anthocyanidins. Third, the current study was conducted in a rural area of China; the ethnic homogeneity of the study population might limit the generalizability of our findings, highlighting the need for confirmation in diverse ethnic groups.

5. Conclusions

In this prospective population-based study, we demonstrated that higher intake of anthocyanidin was protective against SGA risk. This protective effect was greater among pregnant women with higher dietary inflammatory potential. Further intervention studies in diverse populations were warranted to validate these findings.

Supplementary Materials: The following supporting information can be downloaded at: https://www.mdpi.com/article/10.3390/nu17203187/s1, Figure S1: Study participant flow chart in China.

Author Contributions: Conceptualization, S.D. and H.Y.; methodology, B.Z., K.X., B.M., D.W. and K.M.; software, K.X. and B.M.; validation, S.D. and H.Y.; formal analysis, B.Z.; investigation, B.M. and B.Z.; resources, S.D.; data curation, S.D.; writing—original draft preparation, B.Z.; writing—review and editing, B.Z.; visualization, B.Z.; supervision, S.D. and H.Y.; project administration, S.D. and H.Y.; funding acquisition, K.M. All authors have read and agreed to the published version of the manuscript.

Funding: This research was funded by the Special Program for Scientific and Technological Capacity Enhancement, Xi'an Medical University, grant number 2024NLTS001, and the National Natural Science Foundation of China, grant number 81230016.

Institutional Review Board Statement: The study was conducted according to the guidelines of the Declaration of Helsinki and approved by the Human Research Ethics Committee of the Xi'an Jiaotong University Health Science Center (No. 20120008, approved on 6 March 2012).

Informed Consent Statement: Written informed consent was obtained from all participants prior to their inclusion in the study.

Data Availability Statement: The original contributions presented in the study are included in the article Further inquiries can be directed to the corresponding author S.D. (tjdshn@xjtu.edu.cn).

Acknowledgments: We gratefully acknowledge all participants, the management team, and the study group members for their contributions to this prospective population-based study.

Conflicts of Interest: The authors declared no conflicts of interest.

References

1. Villar, J.; Cheikh Ismail, L.; Victora, C.G.; Ohuma, E.O.; Bertino, E.; Altman, D.G.; Lambert, A.; Papageorghiou, A.T.; Carvalho, M.; Jaffer, Y.A.; et al. International standards for newborn weight, length, and head circumference by gestational age and sex: The Newborn Cross-Sectional Study of the INTERGROWTH-21st Project. *Lancet* **2014**, *384*, 857–868. [CrossRef]
2. Villar, J.; Giuliani, F.; Fenton, T.R.; Ohuma, E.O.; Ismail, L.C.; Kennedy, S.H. INTERGROWTH-21st very preterm size at birth reference charts. *Lancet* **2016**, *387*, 844–845. [CrossRef]
3. Lee, A.C.; Kozuki, N.; Cousens, S.; Stevens, G.A.; Blencowe, H.; Silveira, M.F.; Sania, A.; Rosen, H.E.; Schmiegelow, C.; Adair, L.S.; et al. Estimates of burden and consequences of infants born small for gestational age in low and middle income countries with INTERGROWTH-21(st) standard: Analysis of CHERG datasets. *BMJ* **2017**, *358*, j3677. [CrossRef]
4. Lawn, J.E.; Ohuma, E.O.; Bradley, E.; Idueta, L.S.; Hazel, E.; Okwaraji, Y.B.; Erchick, D.J.; Yargawa, J.; Katz, J.; Lee, A.C.C.; et al. Small babies, big risks: Global estimates of prevalence and mortality for vulnerable newborns to accelerate change and improve counting. *Lancet* **2023**, *401*, 1707–1719. [CrossRef]
5. Ashorn, P.; Ashorn, U.; Muthiani, Y.; Aboubaker, S.; Askari, S.; Bahl, R.; Black, R.E.; Dalmiya, N.; Duggan, C.P.; Hofmeyr, G.J.; et al. Small vulnerable newborns-big potential for impact. *Lancet* **2023**, *401*, 1692–1706. [CrossRef]
6. Mohiddin, A.; Semrau, K.E.A.; Simon, J.; Langlois, E.V.; Shiffman, J.; Nabwera, H.; Hofmeyr, G.J.; Lawn, J.E.; Black, R.E.; Askari, S.; et al. The ethical, economic, and developmental imperative to prevent small vulnerable newborns and stillbirths: Essential actions to improve the country and global response. *Lancet* **2023**, *401*, 1636–1638. [CrossRef] [PubMed]
7. Hofmeyr, G.J.; Black, R.E.; Rogozińska, E.; Heuer, A.; Walker, N.; Ashorn, P.; Ashorn, U.; Bhandari, N.; Bhutta, Z.A.; Koivu, A.; et al. Evidence-based antenatal interventions to reduce the incidence of small vulnerable newborns and their associated poor outcomes. *Lancet* **2023**, *401*, 1733–1744. [CrossRef] [PubMed]
8. Hewison, M.; Wagner, C.L.; Hollis, B.W. Vitamin D Supplementation in Pregnancy and Lactation and Infant Growth. *N. Engl. J. Med.* **2018**, *379*, 1880–1881. [CrossRef]
9. Longo, V.D.; Anderson, R.M. Nutrition, longevity and disease: From molecular mechanisms to interventions. *Cell* **2022**, *185*, 1455–1470. [CrossRef] [PubMed]
10. Raghavan, R.; Dreibelbis, C.; Kingshipp, B.L.; Wong, Y.P.; Abrams, B.; Gernand, A.D.; Rasmussen, K.M.; Siega-Riz, A.M.; Stang, J.; Casavale, K.O.; et al. Dietary patterns before and during pregnancy and birth outcomes: A systematic review. *Am. J. Clin. Nutr.* **2019**, *109*, 729s–756s. [CrossRef]
11. Hwang, J.; Shin, D.; Kim, H.; Kwon, O. Association of maternal dietary patterns during pregnancy with small-for-gestational-age infants: Korean Mothers and Children's Environmental Health (MOCEH) study. *Am. J. Clin. Nutr.* **2022**, *115*, 471–481. [CrossRef]

12. Emond, J.A.; Karagas, M.R.; Baker, E.R.; Gilbert-Diamond, D. Better Diet Quality during Pregnancy Is Associated with a Reduced Likelihood of an Infant Born Small for Gestational Age: An Analysis of the Prospective New Hampshire Birth Cohort Study. *J. Nutr.* **2018**, *148*, 22–30. [CrossRef] [PubMed]
13. Crovetto, F.; Crispi, F.; Casas, R.; Martín-Asuero, A.; Borràs, R.; Vieta, E.; Estruch, R.; Gratacós, E. Effects of Mediterranean Diet or Mindfulness-Based Stress Reduction on Prevention of Small-for-Gestational Age Birth Weights in Newborns Born to At-Risk Pregnant Individuals: The IMPACT BCN Randomized Clinical Trial. *JAMA* **2021**, *326*, 2150–2160. [CrossRef]
14. Lash, G.; MacPherson, A.; Liu, D.; Smith, D.; Charnock-Jones, S.; Baker, P. Abnormal fetal growth is not associated with altered chorionic villous expression of vascular endothelial growth factor mRNA. *Mol. Hum. Reprod.* **2001**, *7*, 1093–1098. [CrossRef]
15. Witkamp, R.F. Bioactive Components in Traditional Foods Aimed at Health Promotion: A Route to Novel Mechanistic Insights and Lead Molecules? *Annu. Rev. Food Sci. Technol.* **2022**, *13*, 315–336. [CrossRef]
16. Tapsell, L.C.; Neale, E.P.; Satija, A.; Hu, F.B. Foods, Nutrients, and Dietary Patterns: Interconnections and Implications for Dietary Guidelines. *Adv. Nutr.* **2016**, *7*, 445–454. [CrossRef]
17. Mor, G.; Aldo, P.; Alvero, A.B. The unique immunological and microbial aspects of pregnancy. *Nat. Rev. Immunol.* **2017**, *17*, 469–482. [CrossRef] [PubMed]
18. Prior, R.L.; Wu, X. Anthocyanins: Structural characteristics that result in unique metabolic patterns and biological activities. *Free Radic. Res.* **2006**, *40*, 1014–1028. [CrossRef]
19. Gonçalves, A.C.; Nunes, A.R.; Falcão, A.; Alves, G.; Silva, L.R. Dietary Effects of Anthocyanins in Human Health: A Comprehensive Review. *Pharmaceuticals* **2021**, *14*, 690. [CrossRef] [PubMed]
20. Zafra-Stone, S.; Yasmin, T.; Bagchi, M.; Chatterjee, A.; Vinson, J.A.; Bagchi, D. Berry anthocyanins as novel antioxidants in human health and disease prevention. *Mol. Nutr. Food Res.* **2007**, *51*, 675–683. [CrossRef]
21. Glover, B.J.; Martin, C. Anthocyanins. *Curr. Biol.* **2012**, *22*, R147–R150. [CrossRef]
22. Smeriglio, A.; Barreca, D.; Bellocco, E.; Trombetta, D. Chemistry, Pharmacology and Health Benefits of Anthocyanins. *Phytother. Res.* **2016**, *30*, 1265–1286. [CrossRef]
23. Zamora-Ros, R.; Knaze, V.; Luján-Barroso, L.; Slimani, N.; Romieu, I.; Touillaud, M.; Kaaks, R.; Teucher, B.; Mattiello, A.; Grioni, S.; et al. Estimation of the intake of anthocyanidins and their food sources in the European Prospective Investigation into Cancer and Nutrition (EPIC) study. *Br. J. Nutr.* **2011**, *106*, 1090–1099. [CrossRef]
24. Zhang, H.; Xu, Z.; Zhao, H.; Wang, X.; Pang, J.; Li, Q.; Yang, Y.; Ling, W. Anthocyanin supplementation improves anti-oxidative and anti-inflammatory capacity in a dose-response manner in subjects with dyslipidemia. *Redox Biol.* **2020**, *32*, 101474. [CrossRef]
25. Chen, L.W.; Aubert, A.M.; Shivappa, N.; Bernard, J.Y.; Mensink-Bout, S.M.; Geraghty, A.A.; Mehegan, J.; Suderman, M.; Polanska, K.; Hanke, W.; et al. Associations of maternal dietary inflammatory potential and quality with offspring birth outcomes: An individual participant data pooled analysis of 7 European cohorts in the ALPHABET consortium. *PLoS Med.* **2021**, *18*, e1003491. [CrossRef]
26. Zhang, B.; Men, K.; Li, C.; Xu, K.; Mi, B.; Cai, J.; Pei, L.; Zhang, S.; Ma, Y.; Li, Y.; et al. Association Between Anti-Inflammatory Diet, Dietary Diversity, and Depressive Symptoms Among Chinese Pregnant Women. *Nutrients* **2025**, *17*, 2823. [CrossRef]
27. Cheng, Y.; Yan, H.; Dibley, M.J.; Shen, Y.; Li, Q.; Zeng, L. Validity and reproducibility of a semi-quantitative food frequency questionnaire for use among pregnant women in rural China. *Asia Pac. J. Clin. Nutr.* **2008**, *17*, 166–177.
28. Zhang, B.; Xu, K.; Mi, B.; Liu, H.; Wang, Y.; Huo, Y.; Ma, L.; Liu, D.; Jing, H.; Liu, J.; et al. Maternal Dietary Inflammatory Potential and Offspring Birth Outcomes in a Chinese Population. *J. Nutr.* **2023**, *153*, 1512–1523. [CrossRef] [PubMed]
29. Institute of Nutrition and Food Safety; China Center for Disease Control and Prevention. *China Food Composition Book 1*, 6th ed.; Peking University Medical Press: Beijing, China, 2018.
30. Shivappa, N.; Steck, S.E.; Hurley, T.G.; Hussey, J.R.; Hébert, J.R. Designing and developing a literature-derived, population-based dietary inflammatory index. *Public Health Nutr.* **2014**, *17*, 1689–1696. [CrossRef] [PubMed]
31. Willett, W.; Stampfer, M.J. Total energy intake: Implications for epidemiologic analyses. *Am. J. Epidemiol.* **1986**, *124*, 17–27. [CrossRef] [PubMed]
32. Hinkle, S.N.; Albert, P.S.; Mendola, P.; Sjaarda, L.A.; Boghossian, N.S.; Yeung, E.; Laughon, S.K. Differences in risk factors for incident and recurrent small-for-gestational-age birthweight: A hospital-based cohort study. *BJOG* **2014**, *121*, 1080–1088, discussion 1089. [CrossRef] [PubMed]
33. Li, X.; Ma, J.; Cheng, Y.; Feng, L.; Wang, S.; Dong, G. The relationship between extreme ambient temperature and small for gestational age: A cohort study of 1,436,480 singleton term births in China. *Environ. Res.* **2023**, *232*, 116412. [CrossRef]
34. LIANG, K.-Y.; ZEGER, S.L. Longitudinal data analysis using generalized linear models. *Biometrika* **1986**, *73*, 13–22. [CrossRef]
35. Jiang, T.; Zhou, J.; Liu, W.; Tao, W.; He, J.; Jin, W.; Guo, H.; Yang, N.; Li, Y. The anti-inflammatory potential of protein-bound anthocyanin compounds from purple sweet potato in LPS-induced RAW264.7 macrophages. *Food Res. Int.* **2020**, *137*, 109647. [CrossRef]

36. Frond, A.D.; Iuhas, C.I.; Stirbu, I.; Leopold, L.; Socaci, S.; Andreea, S.; Ayvaz, H.; Andreea, S.; Mihai, S.; Diaconeasa, Z.; et al. Phytochemical Characterization of Five Edible Purple-Reddish Vegetables: Anthocyanins, Flavonoids, and Phenolic Acid Derivatives. *Molecules* **2019**, *24*, 1536. [CrossRef]
37. Jennings, A.; Welch, A.A.; Fairweather-Tait, S.J.; Kay, C.; Minihane, A.M.; Chowienczyk, P.; Jiang, B.; Cecelja, M.; Spector, T.; Macgregor, A.; et al. Higher anthocyanin intake is associated with lower arterial stiffness and central blood pressure in women. *Am. J. Clin. Nutr.* **2012**, *96*, 781–788. [CrossRef]
38. Parmenter, B.H.; Thompson, A.S.; Bondonno, N.P.; Jennings, A.; Murray, K.; Perez-Cornago, A.; Hodgson, J.M.; Tresserra-Rimbau, A.; Kühn, T.; Cassidy, A. High diversity of dietary flavonoid intake is associated with a lower risk of all-cause mortality and major chronic diseases. *Nat. Food* **2025**, *6*, 668–680. [CrossRef]
39. Bondonno, N.P.; Lewis, J.R.; Blekkenhorst, L.C.; Bondonno, C.P.; Shin, J.H.; Croft, K.D.; Woodman, R.J.; Wong, G.; Lim, W.H.; Gopinath, B.; et al. Association of flavonoids and flavonoid-rich foods with all-cause mortality: The Blue Mountains Eye Study. *Clin. Nutr.* **2020**, *39*, 141–150. [CrossRef]
40. Goetz, M.E.; Judd, S.E.; Safford, M.M.; Hartman, T.J.; McClellan, W.M.; Vaccarino, V. Dietary flavonoid intake and incident coronary heart disease: The REasons for Geographic and Racial Differences in Stroke (REGARDS) study. *Am. J. Clin. Nutr.* **2016**, *104*, 1236–1244. [CrossRef] [PubMed]
41. Augustia, V.A.S.; Oktaviani, I.; Setyati, W. Anthocyanin and Flavonoid Extracted from Watermelon Rind (*Citrullus lanatus*) with Two Different Colors of Watermelon Flesh: Yellow and Red. *Mater. Sci. Forum* **2020**, *998*, 261–265. [CrossRef]
42. Li, G.; Zhu, Y.; Zhang, Y.; Lang, J.; Chen, Y.; Ling, W. Estimated daily flavonoid and stilbene intake from fruits, vegetables, and nuts and associations with lipid profiles in Chinese adults. *J. Acad. Nutr. Diet.* **2013**, *113*, 786–794. [CrossRef]
43. Oh, J.S.; Kim, H.; Vijayakumar, A.; Kwon, O.; Kim, Y.; Chang, N. Association of Dietary Flavonoid Intake with Prevalence of Type 2 Diabetes Mellitus and Cardiovascular Disease Risk Factors in Korean Women Aged $\geq$ 30 Years. *J. Nutr. Sci. Vitaminol.* **2017**, *63*, 51–58. [CrossRef]
44. Wu, X.; Beecher, G.R.; Holden, J.M.; Haytowitz, D.B.; Gebhardt, S.E.; Prior, R.L. Concentrations of anthocyanins in common foods in the United States and estimation of normal consumption. *J. Agric. Food Chem.* **2006**, *54*, 4069–4075. [CrossRef]
45. Igwe, E.O.; Charlton, K.E.; Probst, Y.C. Usual dietary anthocyanin intake, sources and their association with blood pressure in a representative sample of Australian adults. *J. Hum. Nutr. Diet.* **2019**, *32*, 578–590. [CrossRef]
46. Pojer, E.; Mattivi, F.; Johnson, D.; Stockley, C.S. The Case for Anthocyanin Consumption to Promote Human Health: A Review. *Compr. Rev. Food Sci. Food Saf.* **2013**, *12*, 483–508. [CrossRef] [PubMed]
47. Kent, K.; Yousefi, M.; do Rosario, V.A.; Fitzgerald, Z.; Broyd, S.; Visentin, D.; Roodenrys, S.; Walton, K.; Charlton, K.E. Anthocyanin intake is associated with improved memory in older adults with mild cognitive impairment. *Nutr. Res.* **2022**, *104*, 36–43. [CrossRef]
48. Cassidy, A.; Mukamal, K.J.; Liu, L.; Franz, M.; Eliassen, A.H.; Rimm, E.B. High anthocyanin intake is associated with a reduced risk of myocardial infarction in young and middle-aged women. *Circulation* **2013**, *127*, 188–196. [CrossRef] [PubMed]
49. Mohan, A.; Dummi Mahadevan, G.; Anand Iyer, V.; Mukherjee, T.K.; Haribhai Patel, V.; Kumar, R.; Siddiqui, N.; Nayak, M.; Maurya, P.K.; Kumar, P. Dietary flavonoids in health and diseases: A concise review of their role in homeostasis and therapeutics. *Food Chem.* **2025**, *487*, 144674. [CrossRef] [PubMed]
50. Bell, W.; Thompson, A.S.; Bondonno, N.P.; Jennings, A.; Gaggl, M.; Kühn, T.; Cassidy, A. A flavonoid-rich diet is associated with a lower risk of chronic kidney disease: A prospective cohort study. *Clin. Nutr.* **2025**, *51*, 126–135. [CrossRef]
51. Sen, S.; Rifas-Shiman, S.L.; Shivappa, N.; Wirth, M.D.; Hébert, J.R.; Gold, D.R.; Gillman, M.W.; Oken, E. Dietary Inflammatory Potential during Pregnancy Is Associated with Lower Fetal Growth and Breastfeeding Failure: Results from Project Viva. *J. Nutr.* **2016**, *146*, 728–736. [CrossRef]
52. de Freitas, N.P.A.; Carvalho, T.R.; Gonçalves, C.; da Silva, P.H.A.; de Melo Romão, L.G.; Kwak-Kim, J.; Cavalcante, M.B. The Dietary Inflammatory Index as a predictor of pregnancy outcomes: Systematic review and meta-analysis. *J. Reprod. Immunol.* **2022**, *152*, 103651. [CrossRef]
53. Toboła-Wróbel, K.; Pietryga, M.; Dydowicz, P.; Napierała, M.; Brązert, J.; Florek, E. Association of Oxidative Stress on Pregnancy. *Oxid. Med. Cell. Longev.* **2020**, *2020*, 6398520. [CrossRef]
54. Marseglia, L.; D'Angelo, G.; Manti, S.; Arrigo, T.; Barberi, I.; Reiter, R.J.; Gitto, E. Oxidative stress-mediated aging during the fetal and perinatal periods. *Oxid. Med. Cell. Longev.* **2014**, *2014*, 358375. [CrossRef]
55. Saenjum, C.; Thim-Uam, A.; Khonthun, C.; Oonlao, P.; Nuntaboon, P.; Surh, Y.J.; Phromnoi, K. Anthocyanins from a new hybrid sweet potato peel cultivated in Northern Thailand mitigate LPS-induced inflammation and RANKL-induced osteoporosis by regulating ROS-mediated pathways. *Inflammopharmacology* **2025**, *33*, 381–399. [CrossRef] [PubMed]
56. Jang, B.K.; Lee, J.W.; Choi, H.; Yim, S.V. Aronia melanocarpa Fruit Bioactive Fraction Attenuates LPS-Induced Inflammatory Response in Human Bronchial Epithelial Cells. *Antioxidants* **2020**, *9*, 816. [CrossRef]

57. do Rosario, V.A.; Chang, C.; Spencer, J.; Alahakone, T.; Roodenrys, S.; Francois, M.; Weston-Green, K.; Hölzel, N.; Nichols, D.S.; Kent, K.; et al. Anthocyanins attenuate vascular and inflammatory responses to a high fat high energy meal challenge in overweight older adults: A cross-over, randomized, double-blind clinical trial. *Clin. Nutr.* **2021**, *40*, 879–889. [CrossRef] [PubMed]
58. Li, L.; Wang, L.; Wu, Z.; Yao, L.; Wu, Y.; Huang, L.; Liu, K.; Zhou, X.; Gou, D. Anthocyanin-rich fractions from red raspberries attenuate inflammation in both RAW264.7 macrophages and a mouse model of colitis. *Sci. Rep.* **2014**, *4*, 6234. [CrossRef] [PubMed]

Disclaimer/Publisher's Note: The statements, opinions and data contained in all publications are solely those of the individual author(s) and contributor(s) and not of MDPI and/or the editor(s). MDPI and/or the editor(s) disclaim responsibility for any injury to people or property resulting from any ideas, methods, instructions or products referred to in the content.

nutrients

MDPI

Article

Purified Anthocyanins Indicated No Significant Effect on Arterial Stiffness, Four-Limb Blood Pressures and Cardiovascular Risk—A 12-Week Dose–Response Trial in Chinese Middle-Aged and Elderly Adults with Hyperglycemia

Zhaomin Liu [1,*,†], Minmin Li [1,†], Yuming Chen [1], Cheng Wang [2], Jianyin Chen [3], Huanhuan Long [1], Ruqing Liu [4], Jiachi Chiou [5] and Chaogang Chen [2]

[1] Department of Nutrition, School of Public Health, Sun Yat-sen University (North Campus), Guangzhou 510080, China
[2] Department of Clinical Nutrition, Sun Yat-Sen Memorial Hospital, Guangzhou 510080, China
[3] Guangzhou Bai-Yun District Community Health-Care Center, Guangzhou 510080, China
[4] Faculty of Preventive Medicine, School of Public Health, Sun Yat-sen University, Guangzhou 510080, China
[5] Department of Food Science and Nutrition, The Hong Kong Polytechnic University, Hung Hom, Kowloon, Hong Kong 999077, China
* Correspondence: liuzhm8@mail.sysu.edu.cn; Tel.: +86-20-87335516; Fax: +86-20-87335498
† These authors contributed equally to this work.

Abstract

Background: Diabetes is associated with sub-optimal vascular function. Current evidence suggested purified anthocyanins (ACNs) could improve cardio-metabolic health, but the dose–response effects on arterial stiffness have not been verified. **Objectives:** To assess the dose-responsiveness of purified ACNs on vascular stiffness and cardiovascular risk among Chinese middle-aged and elderly patients with either prediabetes or early diabetes. **Methods:** This was a secondary analysis based on a 12-week double-blind, randomized and placebo-controlled trial. Eligible participants were randomly assigned to placebo, 160, 320 and 640 mg/d ACNs groups (n = 46/group). Information on dietary intakes and lifestyle habits and blood samples were collected at baseline and at week 12. Arterial stiffness and vascular function were measured by brachial-ankle pulse wave velocity (baPWV), ankle-brachial index (ABI) and four-limb blood pressures. Composite cardiovascular indices were estimated based on lipids and anthropometric data. **Results:** Total 184 eligible participants were recruited and 19 withdrew during the intervention. Baseline characteristics were generally comparable among groups. No significant effects or dose–response relationships were observed by ACNs supplementation on arterial stiffness and cardiovascular risk factors. **Conclusions:** The 12-week randomized controlled trial among Chinese middle-aged and elderly adults with dysglycemia showed multiple dosages of anthocyanins had no significant impacts on arterial stiffness and cardiovascular risk.

Keywords: randomized controlled trial; anthocyanins; dose–response effect; pulse wave velocity; ankle-brachial index; cardiovascular risk

1. Introduction

Diabetes is a major risk factor for atherosclerosis and associated with compromised vascular function and dysregulated lipids, contributing to significant increase in cardiovascular morbidity and all-cause mortality. Compared with pharmaceutical therapies,

phytochemicals are safer and more cost-effective in management of cardiometabolic conditions. Anthocyanins (ACNs) are one major subclass of flavonoids and natural plant pigments conferring purple, blue and red hues to plants. In vitro and animal experiments suggested that ACNs and their metabolites may improve vascular function through enhancing antioxidant defense, reducing oxidative stress and inflammation, augmenting nitric oxide production and bioavailability or modulating gut microbiota [1,2]. Observational studies also suggested higher intake of flavonoid or ACN-rich foods were associated with improved arterial stiffness and lowered risk of cardiovascular diseases (CVD) [3–5].

Despite the favorable roles suggested by laboratory and observational studies, randomized controlled trials (RCTs) by ACN intervention have reported equivocal findings on vascular health [2,6–8]. A recent meta-analysis of RCTs suggests that chronic berry consumption benefits endothelial function (flow-mediated dilation, FMD) but is less certain on arterial stiffness including pulse wave velocity (PWV) and augmentation index (AIx) [8]. A systematic review supported an improvement on arterial stiffness by flavonoids intake [4], but another found null improvement by chronic ACNs supplementation [6]. The inconsistencies might be due to the wide heterogeneity in ACNs formula and dosage, the food matrix, durations and participants' features. More clinical trials are required to clarify the efficacy and determine the optimal dosage of ACNs on vascular distensibility.

PWV has been established as a gold standard tool for arterial stiffness and a promising biomarker in cardiovascular diagnostics [9]. Studies confirmed that both PWV [10] and ankle-brachial index (ABI) [11] independently predict all-cause mortality or major cardiovascular events in diabetic patients. A combination of high PWV and low ABI exhibited superior associations with health outcomes in diabetic patients [12] and all-cause mortality in the elder population [13]. Furthermore, four-limb blood pressures are recommended for early detection and diagnosis of hypertension. Increased systolic inter-arm (sIAD) and inter-ankle (sIAND) differences in blood pressure are thought to be associated with atherosclerotic vascular damage in the systemic arterial tree [14]. In addition, both sIAD and sIAND are well-correlated with arterial stiffness and considered as the valid measures for vascular function to assess preclinical vascular diseases [15] and predict CVD events [16] and all-cause mortality [17].

There was considerable inconsistency in the evidence on the efficacy of ACNs with vascular function. No study has testified the dose-responsiveness of ACN on arterial stiffness and four-limb BPs, and its optimal dosage on vascular function has not been determined especially in at-risk populations. We thus conducted secondary analysis on the basis of a 12-week RCT which was conducted among 184 Chinese middle-aged and elderly adults with either prediabetes or early diabetes to testify the dose–response effects of purified ACNs (0, 160, 320 and 640 mg/d) on vascular function and composite CVD variables. We hypothesized that patients with dysglycemia under higher dosages of ACNs supplementation would have better improved arterial elasticity and CVD health.

2. Materials and Methods

2.1. Participants Recruitment

The study was based on a 12-week randomized, double-blind, placebo-controlled, dose–response trial which was conducted from October 2021 to February 2024 with the original purpose to testify the dose–response effects of ACNs on glycemic control and insulin sensitivity. Participants were recruited from health check-up center or local communities. Potential participants were screened for their initial eligibility by questionnaire via either telephone or in person interview. Persons who were identified at high risk of type 2 diabetes (i.e., a recent medical record of hyperglycemia, metabolic syndromes, medical or family history of diabetes, etc.) were invited to receive a standard 75 g oral

https://doi.org/10.3390/nu18010112

glucose tolerance test (OGTT) for diabetes determination. For prediabetes, impaired fasting glucose was defined as fasting glucose (FG) within 5.6 to 6.9 mmol/L and impaired glucose tolerance was defined as 2 h post-load glucose (2 h PG) within 7.8 to 11.0 mmol/L. Diabetes was defined as FG level $\geq$ 7.0 mmol/L or 2 h PG level $\geq$ 11.1 mmol/L [18].

The Biomedical Ethics Committee of School of Public Health, Sun Yat-sen University approved the study protocol (No. 042 on 30 March 2020). Written informed consents have been obtained from all participants before enrollment. The trial has been registered at Chinese Clinical Trial Registry (ChiCTR2100041743) before initiation of recruitment.

2.2. Inclusion and Exclusion Criteria

Participants were eligible if they were aged 45 to 75 years; with a fasting glucose (FG) $\geq$ 5.6 mmol/L or a 2 h post-load glucose (PG) $\geq$ 7.8 mmol/L by standard OGTT; a body mass index (BMI) within 18.5 to 35 kg/m^2. They were excluded if they had severe cardiovascular, endocrinal, hepatic or renal dysfunction in the prior 6 months; any malignancies in the last 5 years; abnormal vaginal bleeding for postmenopausal women; were a heavy smoker (>1 cigarette/d) or a heavy alcohol drinker (>30 g alcohol/d); taking medications for losing weight or long-term antibiotic users; mental or cognitive disorders; allergic to berries. Patients of clinically diagnosed type 2 diabetes or hyperlipidemia were allowed if they were undertaking a stable dosage and mono-therapy managed by a physician in the prior 3 months and across the intervention. All the eligible participants were asked to attend an orientation talk during which detailed study information and requirements were introduced.

2.3. Supplements, Randomization and Allocation

Both ACN (Medox) and placebo (maltodextrin) capsules were provided by Medpalett AS (Biolink Group, Sandnes, Norway). Treatment identity was masked by providing all interventions in capsules identical in weight, appearance and packaging. Each Medox capsule contains 80 mg anthocyanin citrate, which are concentrated extracts from wild bilberries (*Vaccinium myrtillus*) and blackcurrant (*Ribes nigrum*) comprising a mixture of 32% cyanidin, 58% delphinidin, 2.5% petunidin, 2.5% peonidin and 3.0% malvidin. ACN capsules also contained pullulan, maltodextrin and citric acid to maintain its stability. All capsules were packed into vacuumed blister and stored in cool, dark and dry place.

Before randomization, participants were required to take a two-week run-in exercise with intake of placebo capsules in order to familiarize them with the study requirements. Participants who consumed at least 90% assigned dosages and complied with all lifestyle instructions during the run-in phase, were randomly allocated into 4 treatment groups (0, 160, 320 and 640 mg/d ACNs) by a block randomization strategy in a block size of 8. The random numbers were computer-generated and performed by personnel not involved in the investigation. To secure blinding, participants in all the groups took the same number of 8 capsules daily. For example, participants in the 320 mg/d ACN group consumed 4 capsules of Medox and 4 capsules of placebos, while in the 160 mg/d group, they took 2 Medox and 6 placebo capsules. Total 184 eligible participants were randomized. Series numbers (1–184) were labeled in the cardboard boxes which contained a monthly dosage. Supplements were assigned to participants according to their sequence of enrollment. The group allocation was blinded to all the participants and study investigators. Allocation disclosure was allowed only if serious adverse events occurred with approval from the principle investigator. Blinding efficacy was tested at the end of the trial by asking participants to guess their assignment and comparing the correct rates among groups.

2.4. Instructions to Participants and Compliance Assessment

Participants were free living. They were asked to reduce ACN- or polyphenol-rich foods intake (i.e., purple potatoes, blue strawberries, brassicas, mulberries, cherries, waxberries, red or black rice, red wine and strong tea, etc.) to less than 2 times per week and to refrain from phytochemical supplements and usages of antioxidants or probiotics (i.e., sesame, flax seeds, resveratrol, vitamin E and C, fish oil, berries or berry products, etc.) since the run-in phase. Alcohol drinking was restricted to no more than 30 g alcohol/week. Participants were asked to maintain their habitual lifestyles and medications unchanged during the study course. Both telephone and personal interviews were conducted monthly by research staff to investigate the supplements' consumption, adverse events, medication usages and lifestyle changes. Compliance was evaluated by counting the leftover capsules to estimate the percentage of intake. Good compliance was defined as intake of at least 80% of expected dosages and attendance of three clinical visits for specimens' collection.

2.5. Data Collection

2.5.1. Questionnaire Survey and Anthropometric Measures

Socio-demographics were investigated at baseline via face-to-face or telephone interviews using a pre-tested questionnaire. Anthropometrics including body weight, height and waist circumference were measured at baseline and at week 12 by standard protocols. Dietary intakes were evaluated by a validated 79-item food frequency questionnaire (FFQ) at baseline and at the end of trial [19]. Dietary energy and nutrients intakes were calculated using the 2018 Chinese Food Composition Table [20]. Consumption of major nutrients and food groups as well as the changes across intervention were compared among different groups. Physical activities (PAs) were evaluated by a short form of the International Physical Activity Questionnaire (IPAQ) to investigate the weekly time spent on sedentary, walking, moderate and intensive activities [21]. Total PA energy expenditure was expressed as MET-h per week (metabolic equivalent of task hours per week) according to an established compendium PA coding scheme [22]. Basal and final PA as well as their pre–post changes were compared among groups.

2.5.2. Arterial Stiffness and Four-Limb Blood Pressures

Brachial-ankle PWV (baPWV) and ABI were measured in both upper and lower limbs by trained research staff using a non-invasive vascular screening device of Omron Colin BP-203RPEIII (Omron Healthcare, Kyoto, Japan) based on a standard protocol [23]. The measures were made with participants in supine position after a 10 min rest. Participants were asked to refrain from coffee, alcohol and intensive exercise for at least 12 h and to empty their bladder before testing. They were asked to keep calm and remain immobile during measurement. Standard cuffs with oscillometric sensors were attached to their upper arms and ankles. One heart sound detector was placed at the left edge of the sternum. Pulse waves of bilateral brachial and posterior tibial arteries were recorded simultaneously over 10–15 consecutive heartbeats. BaPWV was estimated by dividing the transmission distance (cm) with the time interval (s) from brachium to ankle. The system automatically and simultaneously measured BPs in all four limbs. ABI was calculated as the SBP ratio in the ankle to the brachial artery. Maximum PWV (the higher lateral baPWV) and minimum ABI (the ratio of lower ankle SBP to higher brachial SBP) were further estimated. Systolic inter-arm and inter-ankle blood pressures (sIAD and sIAND) were calculated accordingly.

2.5.3. Specimens Collection and Biochemical Testing

Blood collection was made at the start of run-in, week 0 and week 12 of intervention. Overnight fasting venous samples were collected in both NaF, EDTA and blank tubes.

https://doi.org/10.3390/nu18010112

Plasma and serum were separated within 2 h after blood collection and centrifuged at 3000 r/min for 15 min at 4 °C. Samples were allocated into several vials and stored at −80 °C in a freezer until analysis. Blood samples which were collected at baseline and at the end of the trial were analyzed simultaneously in the same run of the auto-analyzer. Lipids including total cholesterol (TC), triglycerides (TG), HDL and LDL-cholesterol were tested by enzymatic methods on Beckman Coulter AU5821 (Brea, CA, USA). All the intra- and inter-CVs were less than 5%. Remnant cholesterol (RC) was calculated by subtracting HDL-c and LDL-c from TC. Non-HDL was estimated by the formula of (LDL-c + 1/5 × TG). The Framingham risk score (FRS) was estimated on the basis of several common coronary risk factors (age, sex, TC, HDL-c, smoking and SBP) to assess individual's risk of developing coronary heart disease (CHD) [24].

2.6. Sample Size and Power Estimation

Sample size estimation was made for the original study outcome of HbA1c using the formula of $2[(Z_{\alpha/2} + Z_{\beta}) \times SD/\delta]^2$] for two-arm RCT, with SD of 0.35% for the change in HbA1c [25]. Based on the conventional two-tailed α of 0.05 and 90% power ($\beta = 0.10$), and accounting for a 10% drop-out, 38 subjects per group are appropriate to obtain a significant change in HbA1c ($\delta = 0.2\%$). Post hoc power estimation was made for current main outcomes according to their SD and mean differences at the 3-month changes by 320 mg/d ACNs supplementation, which were 94% for max-baPWV, 95% for min-ABI, 91% for sIAD and 93% for sIAND.

2.7. Statistical Analysis

All statistical analyses were performed using IBM SPSS 25.0 software. Statistical significance was defined at an adjusted p value of 0.017 (0.05/3 due to 3 ACNs groups being compared with the placebo). Baseline characteristics were compared to examine the initial comparability among different dosage groups. A carry-forward strategy was applied for complementing the missing data at week 12 due to withdrawals. Normality was tested by Kolmogorov–Smirnov approach. Data of heterogenous variance were logarithmically transformed or analyzed by non-parametric approach. The primary analytical approach was intention-to-treat (ITT) analysis for all the participants who were randomized ($n = 184$). Per-protocol analysis was furthermore performed as sensitivity analysis among participants of good compliance ($n = 161$). Pre-post changes and change percentages were compared among groups by one-way ANOVA for ITT analysis, or analysis of covariance (ANCOVA) for per-protocol analysis with controlling for baseline variables and possible confounders. Trend analysis across different dosage groups was conducted by either parametric (ANOVA, linear trend) or non-parametric (Jonckheere–Terpstra) approach when applicable.

Further sensitivity analyses were made to testify the results' robustness by (1) exclusion of patients who were under medications for lowering glucose, lipids and thyroid dysfunction; (2) multivariable linear mixed model (LMM) with individual participants as random factors and adjustment for baseline data to compare the 3-month change and change% among treatment groups [26]. Subgroup analyses by gender (male vs. female), age (<65 vs. ≥65 yrs), baseline BMI (<24 vs. ≥24 kg/m^2), hyperglycemia (prediabetes vs. diabetes), hypertension (yes vs. no) and hyperlipidemia (yes vs. no) were conducted to explore possible effect modifications of ACNs treatment on the outcomes. Interactions were testified before stratification with inclusion of a product term (subgroup variable*treatment group) into the general linear models (GLM). Results by stratification were presented only for those with p for interactions less than 0.15 with at least one of the main outcomes.

https://doi.org/10.3390/nu18010112

3. Results

The study flow was shown in Figure 1. A total of 184 participants were randomized and 19 withdrew during follow-up. The major reasons for the dropouts were discomfort or medical conditions (n = 6, two for abdominal pain, one for edema in foot, one for visual blur, one for diagnosis of breast cancer and one for knee operation), too busy (n = 3) or far distance (n = 3). The dropout rates were similar among different dosage groups (p = 0.561). In total, 161 participants (87.5%) were defined as having good compliance. The blinding tests at the final visit suggested a general good blinding efficacy (p = 0.865 for kappa agreement test).

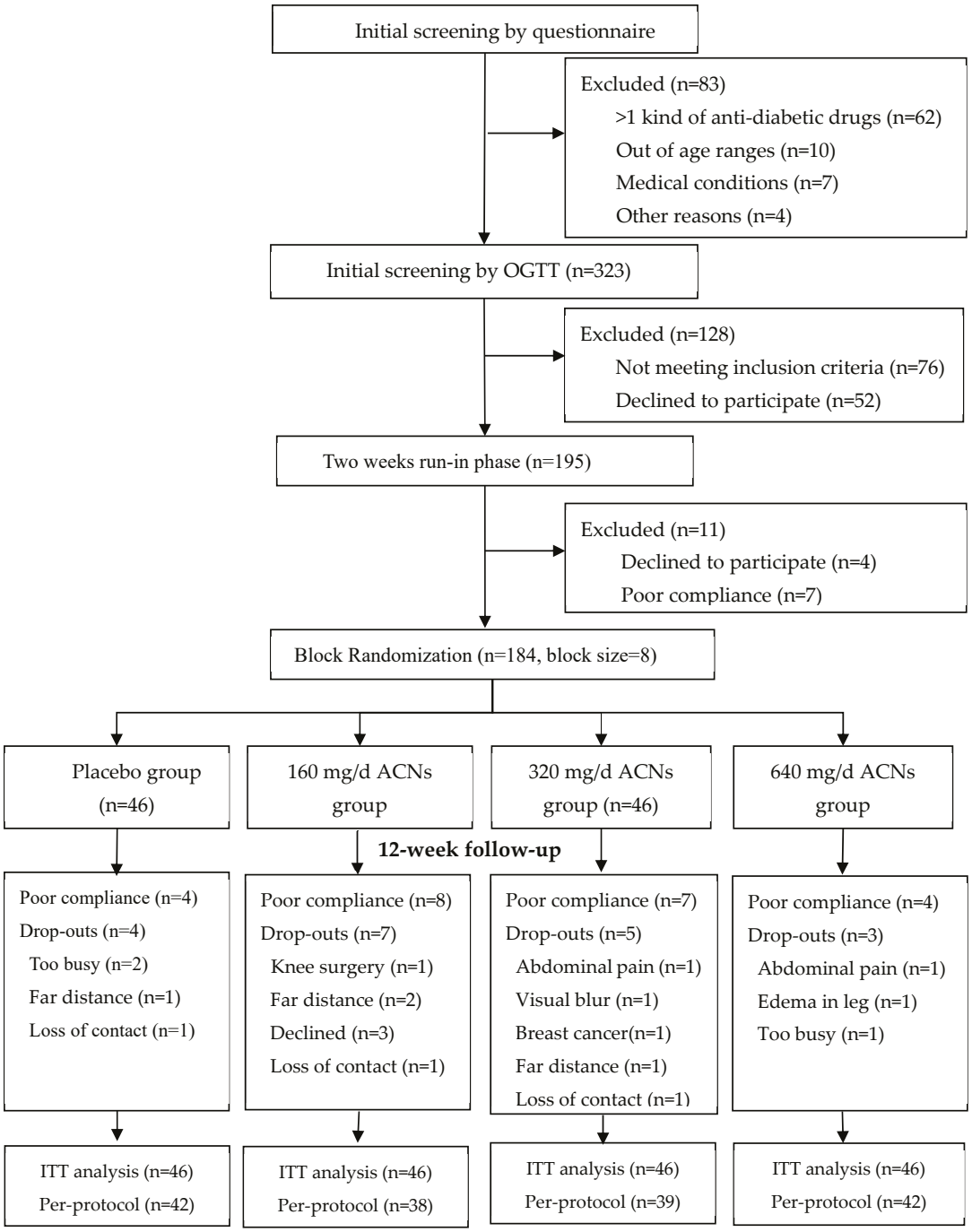

Figure 1. Study flow chart. **Abbreviations:** OGTT, oral glucose tolerance test; ACNs, anthocyanins; ITT, intention to treat analysis; Per-protocol, per-protocol analysis was conducted among participants who had good compliance.

Baseline features of participants were generally comparable among different dosage groups in terms of age, gender, education attainment, marital status, medication usages, weight, BMI, smoking, alcohol, and tea and coffee drinking (Table 1). Dietary intakes, sedentary time and total PA energy expenditure at baseline and at week 12 and their changes across intervention did not differ significantly among the four treatment groups (Table 2). Results by ITT analysis among 184 randomized participants demonstrated generally non-significant differences among four groups in both change and change% for variables of arterial stiffness including bilateral baPWV and ABI, the max-baPWV and the min-ABI (Table 3). Different dosages of ACNs had no significant impact on four limbs systolic and diastolic BP, mean arterial BP (MAP), sIAN and sIAND (Table 4). Neither significant effect was found on the composite CVD markers including TG/HDL-c, triglycerides-glucose index (TyG-index), TyG-BMI, visceral adiposity index (VAI) and FRS (Table 5).

Table 1. Baseline characteristics of participants by different dosages of anthocyanins (n = 184).

	Anthocyanins Supplementation by Different Dosages (n = 46/Group)				
	Placebo	**160 mg/d**	**320 mg/d**	**640 mg/d**	***p***
Age, years	62.9 ± 8.0	63.8 ± 8.7	62.8 ± 8.9	60.2 ± 9.4	0.218
Female, %	37 (29.8%)	27 (21.6%)	28 (22.4%)	33 (26.4%)	0.091
Diabetes, %	26 (27.4%)	23 (24.2%)	23 (24.2%)	23 (24.2%)	0.899
Prediabetes (sIFG/sIGT/both), %	7/5/8	5/9/9	4/7/12	5/8/10	0.832
Education, college and above, %	9 (19.6%)	13 (28.3%)	12 (26.1%)	15 (32.6%)	0.607
Marriage, singled, %	11 (23.9%)	5 (10.9%)	10 (21.7%)	5 (10.9%)	0.110
Baseline hyperlipidemia, %	26 (28.6%)	16 (17.6%)	26 (28.6%)	23 (25.3%)	0.121
Baseline hypertension, %	19 (26.4%)	18 (25.0%)	20 (27.8%)	15 (20.8%)	0.734
Baseline overweight, %	30 (30.9%)	24 (24.8%)	23 (23.7%)	20 (20.6%)	0.203
Medications at baseline, %					
Diabetes	3 (6.5%)	8 (17.4%)	4 (8.7%)	4 (8.7%)	0.326
Hypertension	13 (28.3%)	13 (28.3%)	16 (34.8%)	8 (17.4%)	0.074
Hyperlipidemia	1 (2.2%)	1 (2.2%)	0	1 (2.2%)	1.000
Thyroid dysfunction	5 (10.9%)	0	3 (6.5%)	5 (10.9%)	0.146
Smoking, %	3 (6.5%)	3 (6.5%)	2 (4.3%)	2 (4.3%)	0.935
Alcohol drinking, %	20 (43.5%)	11 (23.9%)	14 (30.4%)	21 (45.7%)	0.089
Tea drinking, %	39 (84.8%)	39 (84.8%)	38 (82.6%)	40 (87.0%)	0.953
Coffee drinking, %	16 (34.8%)	7 (15.2%)	15 (32.6%)	11 (23.9%)	0.130
Anthropometrics					
Weight, kg	64.0 ± 9.5	61.5 ± 10.0	64.8 ± 11.6	60.5 ± 12.8	0.205
BMI, kg/m^2	25.1 ± 2.9	23.9 ± 2.9	24.5 ± 3.3	23.6 ± 3.6	0.120
WHR	0.890 ± 0.058	0.897 ± 0.058	0.900 ± 0.057	0.880 ± 0.062	0.417
SBP, mmHg	129.5 ± 16.5	128.2 ± 17.4	131.3 ± 17.8	130.0 ± 18.8	0.865
DBP, mmHg	80.7 ± 11.5	77.9 ± 10.8	81.1 ± 10.4	82.2 ± 10.2	0.277
Max baPWV > 1800 cm/s, %	13 (30.2%)	11 (25.6%)	12 (27.9%)	7 (16.3%)	0.501
Min ABI < 0.9	0	0	0	0	NA
sIAD > 15 mmHg, %	0	2 (33.3%)	2 (33.3%)	2 (33.3%)	0.613
sIAND > 15 mmHg, %	0	4 (44.4%)	3 (33.3%)	2 (22.2%)	0.233

Data were presented as mean ± SD for continuous variables and compared by ANOVA, or n (%) for categorical variables and compared by chi-square test. Abbreviations: sIFG, sole impaired fasting glucose; sIGT, sole impaired glucose tolerance; both, having both IFG and IGT; WHR: waist-to-hip ratio; BMI, body mass index; SBP/DBP: systolic/diastolic blood pressure; baPWV, brachial-ankle pulse wave velocity; ABI, ankle brachial index; sIAD, systolic inter-arm difference; sIAND, systolic inter-ankle difference. The maximum baPWV was determined by the higher either left or right PWV. The minimal ABI was estimated by dividing the lower one of ankle SBP with the higher one of brachial SBP.

https://doi.org/10.3390/nu18010112

Table 2. Dietary intakes of major nutrients and food groups, sedentary time and total physical activities across intervention by different treatment groups, intention to treat analysis (n = 184).

	Anthocyanins Supplementation by Different Dosages (n = 46/Group)				
	0 mg/d (Placebo)	**160 mg/d**	**320 mg/d**	**640 mg/d**	***p***
Nutrients					
Total energy, kcal/d					
baseline	1884 ± 709	1913 ± 681	2042 ± 741	1963 ± 927	0.179
week 12	1774 ± 787	1927 ± 702	1907 ± 699	1839 ± 731	0.257
change	−109 ± 564	10 ± 782	−136 ± 654	−131 ± 748	0.920
Protein, % total energy					
baseline	21.2 ± 4.1	21.6 ± 5.4	21.1 ± 4.4	22.4 ± 4.5	0.531
week 12	20.4 ± 4.3	21.7 ± 3.7	20.8 ± 4.4	22.7 ± 4.1	0.036
change	−0.8 ± 4.2	0.1 ± 5.5	−0.3 ± 3.9	0.4 ± 5.3	0.666
Total fat, % total energy					
baseline *	23.2 (20.1, 29.4)	22.6 (17.3, 28.2)	22.0 (18.2, 26.7)	22.5 (18.4, 24.4)	0.707
week 12	23.5 ± 8.8	22.9 ± 7.5	24.7 ± 6.6	23.9 ± 8.1	0.752
change	−0.7 ± 6.7	−0.8 ± 6.5	1.1 ± 9.7	1.5 ± 8.0	0.362
Carbohydrate, % total energy					
baseline	58.7 ± 10.4	58.3 ± 12.0	58.3 ± 11.9	59.2 ± 9.6	0.975
week 12	60.0 ± 12.0	58.4 ± 9.7	56.5 ± 9.6	56.8 ± 11.0	0.358
change	1.3 ± 9.2	0.1 ± 10.6	−1.8 ± 14.3	−2.5 ± 11.1	0.376
Total cholesterol, mg/d					
baseline	558.0 ± 342.0	535.9 ± 183.1	579.8 ± 365.8	564.0 ± 301.2	0.921
week 12	502.6 ± 349.7	546.9 ± 199.3	623.1 ± 352.6	543.4 ± 285.8	0.289
change *	−22.1 (−118.3, 24.3)	0 (−71.5, 99.0)	0 (−87.7, 132.4)	10.4 (−132.3, 99.2)	0.174
Food groups, g/d					
Total grains, g/d					
baseline *	481.8 (384.1, 574.8)	480.8 (359.6, 664.2)	499.5 (316.8, 649.2)	478.4 (333.5, 662.7)	0.459
week 12 *	490.0 (382.4, 573.3)	498.8 (302.3, 703.4)	465.2 (328.9, 610.2)	467.0 (286.3, 558.5)	0.953
change	1.4 ± 156.8	6.6 ± 229.9	−20.8 ± 241.7	−56.5 ± 202.0	0.465
Vegetables, g/d					
baseline	600.0 ± 608.8	597.2 ± 266.4	615.0 ± 393.8	595.4 ± 457.9	0.892
week 12	609.3 ± 624.6	620.0 ± 246.9	526.6 ± 251.3	582.6 ± 390.3	0.695
change	−50.7 ± 275.1	22.9 ± 274.2	−88.4 ± 319.8	−12.8 ± 426.4	0.406
Fruits, g/d					
baseline	245.6 ± 273.5	214.8 ± 255.2	222.2 ± 177.3	247.2 ± 350.1	0.918
week 12	192.6 ± 149.8	261.8 ± 239.5	220.1 ± 135.4	245.7 ± 324.4	0.479
change	−52.9 ± 260.8	46.9 ± 254.5	−2.1 ± 202.8	−1.4 ± 211.5	0.244
Red and processed meat, g/d					
baseline	108.9 ± 78.9	96.8 ± 92.4	113.5 ± 100.0	105.5 ± 99.0	0.850
week 12	93.9 ± 68.4	102.4 ± 102.1	108.8 ± 94.7	99.4 ± 69.1	0.864
change	−15.0 ± 72.29	5.6 ± 102.2	−4.7 ± 122.0	−6.1 ± 78.5	0.784
Sedentary time, hrs/d					
baseline	2.348 ± 2.063	2.500 ± 1.880	2.326 ± 1.898	2.576 ± 2.119	0.918
week 12	2.435 ± 2.177	2.526 ± 2.400	2.630 ± 2.339	2.614 ± 2.703	0.979
change	0.087 ± 2.140	0.026 ± 2.111	0.304 ± 1.618	0.038 ± 2.313	0.909
Total PA, Met/h/week					
baseline	87.7 ± 66.7	67.6 ± 62.7	65.6 ± 58.0	67.6 ± 52.4	0.251
week 12 *	62.1 (34.6, 140.9)	44.5 (26.1, 112.0)	49.0 (28.6, 75.3)	49.0 (25.9, 84.5)	0.385
change	−0.741 ± 64.457	6.905 ± 41.632	−6.325 ± 55.652	−4.049 ± 54.275	0.678

Data were presented as mean ± SD with comparison by ANOVA or median (P_{25}–P_{75}) with comparison by Kruskal–Wallis test if unequal variance was identified. * p value by Kruskal–Wallis test. Trend analysis across different dosage groups was conducted by either parametric (ANOVA, linear trend) or non-parametric (Jonckheere-Terpstra) approach when applicable. For dietary total energy intake, 5 cases (3 at baseline and 2 at week 12) had more than 5000 kcal/d. They were replaced with 5000 kcal/d. The macro-nutrients were expressed as percentages of total energy (% total energy). Abbreviations: PA, physical activity; SD, standard deviation; ANOVA, analysis of variance. Energy expenditure for total physical activity were estimated by adding mild, moderate and intensive PA energy expenditures (Met/h/week).

https://doi.org/10.3390/nu18010112

Table 3. Effects of different dosages of purified anthocyanins on bilateral brachial-ankle pulse wave velocity (baPWV) and ankle brachial index (ABI) by intention to treat analysis (n = 184).

	Supplementation of Purified Anthocyanins					
	Placebo (n = 46)	**160 mg/d (n = 46)**	**320 mg/d (n = 46)**	**640 mg/d (n = 46)**	$P_{overall}$	P_{trend}
Right PWV, cm/s						
baseline	1587.3 ± 312.8	1559.8 ± 335.9	1560.3 ± 333.2	1486.6 ± 298.9	0.490	
week 12	1552.6 ± 300.1	1563.8 ± 317.3	1519.8 ± 263.2	1468.7 ± 283.4	0.401	
change	−34.6 ± 193.1	5.26 ± 233.6	−40.4 ± 230.1	−23.5 ± 156.6	0.719	0.514
change%	−1.64 ± 10.85	1.40 ± 14.49	−0.42 ± 18.71	−1.00 ± 10.21	0.751	0.547
Left PWV, cm/s						
baseline	1586.0 ± 314.3	1590.5 ± 352.7	1532.3 ± 326.7	1481.0 ± 287.7	0.325	
week 12	1523.1 ± 287.2	1565.5 ± 339.0	1506.0 ± 287.6	1451.1 ± 273.1	0.325	
change	−62.9 ± 210.9	−24.3 ± 251.1	−26.3 ± 205.0	−30.4 ± 168.6	0.796	0.760
change%	−3.14 ± 12.22	−0.43 ± 14.75	−0.22 ± 14.95	−1.45 ± 10.91	0.711	0.602
Max-PWV, cm/s						
baseline	1620.5 ± 317.4	1601.1 ± 353.9	1580.0 ± 333.3	1510.6 ± 296.5	0.405	
week 12	1575.8 ± 300.6	1605.4 ± 332.3	1550.8 ± 266.4	1492.5 ± 280.5	0.309	
change	−44.7 ± 192.5	5.4 ± 247.6	−29.3 ± 212.8	−18.4 ± 161.3	0.699	0.747
change%	−2.21 ± 10.53	1.53 ± 14.47	0.02 ± 16.64	−0.63 ± 10.17	0.601	0.715
Right ABI						
baseline	1.143 ± 0.067	1.155 ± 0.079	1.153 ± 0.087	1.144 ± 0.082	0.866	0.981
week 12	1.147 ± 0.088	1.153 ± 0.093	1.154 ± 0.082	1.135 ± 0.092	0.713	0.604
change	0.003 ± 0.081	0.004 ± 0.083	0.001 ± 0.072	−0.011 ± 0.082	0.798	0.870
change%	0.419 ± 7.185	0.506 ± 6.894	0.282 ± 6.121	−0.787 ± 7.094	0.785	0.843
Left ABI						
baseline	1.137 ± 0.071	1.158 ± 0.088	1.137 ± 0.086	1.130 ± 0.084	0.420	0.466
week 12	1.132 ± 0.071	1.145 ± 0.092	1.136 ± 0.094	1.126 ± 0.084	0.757	0.618
change	−0.004 ± 0.062	−0.007 ± 0.092	−0.000 ± 0.065	−0.003 ± 0.100	0.985	0.942
change%	−0.237 ± 5.496	−0.274 ± 7.704	0.085 ± 5.811	0.095 ± 9.140	0.991	0.988
Min-ABI						
baseline	1.119 ± 0.069	1.126 ± 0.077	1.120 ± 0.076	1.114 ± 0.077	0.893	
week 12	1.117 ± 0.085	1.123 ± 0.088	1.122 ± 0.084	1.109 ± 0.085	0.858	
change	−0.001 ± 0.082	−0.003 ± 0.069	0.002 ± 0.059	−0.005 ± 0.088	0.976	0.883
change%	0.051 ± 7.311	−0.172 ± 5.952	0.228 ± 5.256	−0.226 ± 8.196	0.988	0.924

The analysis was made by analysis of variance (ANOVA) with results being presented as mean ± SD. Abbreviations: PWV: pulse wave velocity; ABI: ankle brachial index. The max-PWV was the higher baPWV at either the left or right side. The min-ABI was estimated by dividing the lower side of the ankle SBP with the higher side of brachial SBP. Change = data at 3-month − data at baseline. Change% = (data at 3-month − data at baseline) × 100/data at baseline.

Table 4. Effects of different dosages of purified anthocyanins on brachial and ankle systolic and diastolic blood pressures by intention to treat analysis (n = 184).

	Supplementation of Purified Anthocyanins					
	Placebo (n = 46)	**160 mg/d (n = 46)**	**320 mg/d (n = 46)**	**640 mg/d (n = 46)**	$P_{overall}$	P_{trend}
Left-brachial SBP, mmHg						
baseline	129.2 ± 13.2	125.7 ± 13.3	127.4 ± 13.3	127.1 ± 19.2	0.693	
week 12	125.1 ± 11.1	122.7 ± 12.8	123.8 ± 11.4	122.0 ± 18.1	0.742	
change	−4.2 ± 10.5	−2.9 ± 11.2	−3.6 ± 10.4	−5.0 ± 10.6	0.749	0.609
change%	−2.8 ± 8.1	−2.0 ± 8.5	−2.4 ± 7.7	−3.6 ± 8.3	0.752	0.572
Left-brachial DBP, mmHg						
baseline	73.8 ± 8.7	71.7 ± 9.5	73.7 ± 9.4	74.1 ± 11.7	0.562	
week 12	71.8 ± 8.0	70.9 ± 9.6	71.9 ± 9.3	72.4 ± 11.2	0.885	
change	−2.00 ± 7.15	−0.89 ± 7.72	−1.78 ± 8.46	−1.70 ± 7.52	0.841	0.965
change%	−2.18 ± 9.65	−0.71 ± 10.45	−1.75 ± 11.88	−1.76 ± 10.12	0.865	0.992

https://doi.org/10.3390/nu18010112

Table 4. *Cont.*

	Supplementation of Purified Anthocyanins					
	Placebo (*n* = 46)	**160 mg/d (*n* = 46)**	**320 mg/d (*n* = 46)**	**640 mg/d (*n* = 46)**	$P_{overall}$	P_{trend}
Left-brachial MAP, mmHg						
baseline	97.0 ± 12.2	95.0 ± 11.5	95.7 ± 11.2	95.5 ± 15.5	0.849	
week 12	94.4 ± 10.0	92.0 ± 11.4	93.5 ± 10.1	93.3 ± 15.0	0.828	
change	−2.63 ± 10.23	−3.02 ± 9.33	−2.15 ± 10.17	−2.24 ± 8.27	0.993	0.795
change%	−1.94 ± 10.88	−2.77 ± 9.52	−1.62 ± 10.19	−1.96 ± 8.62	0.986	0.912
Right-brachial SBP, mmHg						
baseline	129.3 ± 13.8	125.4 ± 13.4	125.6 ± 13.9	126.1 ± 19.8	0.561	
week 12	125.3 ± 12.7	123.9 ± 13.3	124.2 ± 11.8	121.5 ± 17.3	0.626	
change	−4.0 ± 11.5	−1.5 ± 10.9	−1.3 ± 11.9	−4.6 ± 9.2	0.297	0.785
change%	−2.7 ± 8.8	−0.8 ± 8.7	−0.5 ± 9.4	−3.0 ± 8.3	0.353	0.862
Right-brachial DBP, mmHg						
baseline	74.4 ± 9.5	71.9 ± 9.5	72.4 ± 9.2	73.0 ± 14.5	0.661	
week 12	71.8 ± 9.2	70.7 ± 9.3	72.1 ± 9.1	71.0 ± 11.7	0.902	
change	−2.6 ± 8.6	−1.2 ± 6.5	−0.3 ± 7.4	−2.1 ± 8.1	0.449	0.670
change%	−2.8 ± 11.9	−1.2 ± 9.3	0.1 ± 10.6	−0.1 ± 24.7	0.789	0.368
Right-brachial MAP, mmHg						
baseline	97.8 ± 12.3	94.9 ± 11.1	94.5 ± 11.9	94.8 ± 17.5	0.579	
week 12	94.6 ± 10.6	93.3 ± 10.8	94.8 ± 10.4	92.6 ± 14.4	0.785	
change	−3.2 ± 10.7	−1.6 ± 8.2	0.3 ± 11.4	−2.1 ± 9.4	0.386	0.485
change%	−2.5 ± 11.4	−1.3 ± 8.9	1.1 ± 12.1	−0.6 ± 16.2	0.573	0.355
Left-ankle SBP, mmHg						
baseline	149.5 ± 20.3	146.8 ± 18.1	146.7 ± 21.0	145.9 ± 26.3	0.872	
week 12	144.4 ± 16.8	143.8 ± 17.3	143.4 ± 17.9	139.6 ± 23.0	0.621	
Change	−5.1 ± 15.2	−3.0 ± 14.1	−3.3 ± 12.4	−6.3 ± 16.1	0.665	0.685
change%	−2.7 ± 9.7	−1.6 ± 9.6	−1.7 ± 7.9	−3.5 ± 10.7	0.739	0.693
Right-ankle SBP, mmHg						
baseline	150.4 ± 19.1	146.5 ± 18.3	148.8 ± 20.8	147.9 ± 25.4	0.851	
week 12	146.0 ± 17.7	144.5 ± 16.7	145.8 ± 18.4	140.7 ± 23.4	0.525	
Change	−4.3 ± 14.8	−2.0 ± 12.9	−3.0 ± 14.2	−7.1 ± 13.4	0.325	0.307
change%	−2.4 ± 9.4	−0.9 ± 8.5	−1.4 ± 9.6	−4.4 ± 8.6	0.276	0.276
sIAD, mmHg						
baseline	4.130 ± 3.110	4.370 ± 4.255	4.935 ± 4.459	4.348 ± 5.551	0.842	
week 12	4.326 ± 3.590	4.544 ± 4.722	4.544 ± 5.184	4.239 ± 4.100	0.983	
Change	0.196 ± 4.612	0.174 ± 2.719	−0.391 ± 4.674	−0.109 ± 7.024	0.935	0.654
change% *	0 (−60.0, 100.0)	0 (−50.0, 76.7)	0 (−60.0, 50.0)	0 (−58.3, 200.0)	0.479	0.710
sIAND, mmHg						
baseline	5.500 ± 3.494	6.174 ± 6.819	6.283 ± 6.473	6.044 ± 4.477	0.907	
week 12	5.783 ± 6.401	6.609 ± 6.923	5.739 ± 5.277	5.196 ± 5.171	0.728	
change	0.283 ± 7.638	0.435 ± 7.562	−0.544 ± 6.706	−0.848 ± 6.606	0.788	0.355
change%	80.4 ± 356.2	55.2 ± 272.7	74.7 ± 288.2	38.7 ± 188.9	0.896	0.872

The analysis was made by analysis of variance (ANOVA) with results being presented as mean ± SD. * Results of heterogenous variance were presented as median (inter-quartile range P_{25}–P_{75}) and compared by Kruskal–Wallis ANOVA with trend analysis by Jonckheere–Terpstra approach. Abbreviations: sIAD, systolic inter-arm difference; sIAND, systolic inter-ankle difference; SBP, systolic blood pressure; DBP, diastolic blood pressure; MAP, mean arterial blood pressure. Change = final value − baseline value; change% = (final value − baseline value) × 100%/baseline value.

Only marginal differences were suggested in the 3-month change and change% for RC (p = 0.048 and 0.034) and non-HDL-c (p = 0.037 and 0.033) yet lacking a dose–response trend. Compared with the 160 mg ACN group, RC in the 320 mg group exhibited a significant reduction in the 3-month change with a mean difference of −0.158 ± 0.618 mmol/L (p = 0.011 by LSD approach). Compared with the 320 mg group, a marginal increase in RC was observed in the 640 mg group in the 3-month change and change% with a mean difference

of −0.131 ± 0.061 (p = 0.034) mmol/L and 56.6 ± 23.3% (p = 0.016), respectively. For non-HDL-c, compared with placebo, an increase was observed in the 160 mg ACN group with a mean difference of 0.292 ± 0.107 mmol/L in the 3 m change (p = 0.007) or 7.711% ± 2.910% for change% (p = 0.009). In addition, patients in the 640 mg group had a marginal decrease in non-HDL-c in comparison with those of the 160 mg group, with a mean difference of −0.249 ± 0.107 mmol/L in the 3 m change (p = 0.021) or −7.242% ± 2.910% in change% (p = 0.014).

Table 5. Effects of different dosages of purified anthocyanins on composite cardiovascular variables by intention to treat analysis, (n = 184).

	Supplementation of Purified Anthocyanins					
	Placebo (n = 46)	**160 mg/d (n = 46)**	**320 mg/d (n = 46)**	**640 mg/d (n = 46)**	$P_{overall}$	P_{trend}
RC, mmol/L						
baseline	0.599 ± 0.522	0.476 ± 0.328	0.650 ± 0.527	0.615 ± 0.560	0.367	
week 12	0.564 ± 0.438	0.541 ± 0.388	0.556 ± 0.465	0.652 ± 0.642	0.705	
change	−0.035 ± 0.374	0.064 ± 0.273	−0.094 ± 0.243	0.037 ± 0.271	0.048	0.773
change% *	2.7 (−31.0, 39.9)	0 (−18.4, 47.8)	−6.8 (−32.2, 10.8)	13.2 (−17.6, 75.1)	0.034	0.746
Non-HDL-c, mmol/L						
baseline	4.000 ± 1.001	3.764 ± 1.067	3.899 ± 1.081	3.926 ± 0.964	0.742	
week 12	3.933 ± 0.965	3.992 ± 1.065	3.944 ± 1.084	3.905 ± 0.988	0.982	
change	−0.065 ± 0.520	0.228 ± 0.570	0.044 ± 0.489	−0.021 ± 0.468	0.037	0.877
change%	−0.340 ± 13.471	7.371 ± 16.567	1.747 ± 13.070	0.128 ± 12.340	0.033	0.647
TG/HDL-c						
baseline	1.609 ± 2.256	1.081 ± 0.851	1.616 ± 1.406	1.814 ± 3.120	0.379	
week 12	1.341 ± 1.320	1.187 ± 1.485	1.333 ± 0.892	1.686 ± 3.312	0.666	
change	−0.269 ± 1.316	0.106 ± 0.854	−0.283 ± 1.005	−0.128 ± 1.346	0.338	0.965
change%	7.381 ± 56.469	7.292 ± 44.389	−4.429 ± 32.179	−0.310 ± 30.692	0.451	0.213
TyG-index						
baseline	8.989 ± 0.548	8.779 ± 0.475	9.044 ± 0.662	8.976 ± 0.626	0.144	
week 12	8.988 ± 0.498	8.816 ± 0.552	8.966 ± 0.560	8.930 ± 0.595	0.452	
change	−0.001 ± 0.378	0.038 ± 0.325	−0.078 ± 0.346	−0.046 ± 0.302	0.382	0.262
change%	0.100 ± 4.185	0.447 ± 3.700	−0.728 ± 3.651	−0.439 ± 3.366	0.433	0.259
TyG-BMI						
baseline	225.7 ± 29.1	210.3 ± 31.0	221.3 ± 33.7	212.6 ± 39.4	0.097	
week 12	225.7 ± 32.8	211.5 ± 32.0	219.1 ± 30.9	210.9 ± 39.8	0.126	
change	−0.047 ± 12.368	1.200 ± 9.679	−2.238 ± 11.054	−1.712 ± 9.066	0.390	0.230
change%	−0.098 ± 5.426	0.627 ± 4.655	−0.704 ± 4.825	−0.739 ± 4.222	0.484	0.306
VAI						
baseline *	1.608 (1.151, 2.385)	1.318 (0.878, 2.086)	1.731 (1.209, 3.516)	1.425 (1.065, 2.477)	0.206	
week 12	2.400 ± 2.418	1.876 ± 2.036	2.186 ± 1.442	2.998 ± 6.596	0.533	
change	−0.454 ± 2.411	0.095 ± 1.198	−0.530 ± 1.760	−0.292 ± 2.504	0.473	0.919
change%	8.504 ± 57.948	6.017 ± 44.244	−6.004 ± 31.911	−2.144 ± 30.090	0.321	0.119
FRS						
baseline	14.4 ± 3.3	13.5 ± 4.1	14.0 ± 3.7	13.2 ± 4.4	0.482	
week 12	14.1 ± 3.4	13.9 ± 4.1	13.9 ± 3.9	13.0 ± 4.2	0.507	
change	−0.3 ± 1.7	0.3 ± 1.8	−0.04 ± 1.5	−0.2 ± 2.0	0.359	0.953
change%	−1.7 ± 13.4	5.9 ± 26.2	−0.2 ± 11.1	4.0 ± 31.9	0.335	0.460

Data were presented as mean ± SD with comparison by ANOVA. * If unequal variance was identified, data were presented as median (P_{25}–P_{75}) with group comparison by Kruskal–Wallis and trend analysis by Jonckheere–Terpstra approach. Formulas: RC = TC-HDL-c-LDL-c; Non-HDL-c = LDL-c + 1/5 × TG; TyG-index = ln(TG(mg/dL) × FG(mg/dL)/2); TyG-BMI = TyG-index × BMI; Visceral adiposity index (VAI) = WC/(39.68 + 1.88 × BMI) × (TG/1.03) × (1.31/HDL-c) (for males); and WC/(36.58 + 1.89 × BMI) × (TG/0.81) × (1.52/HDL-c) for females. Change = final value − baseline value; change% = (final value − baseline value) × 100%/baseline value. Abbreviations: RC, remnant cholesterol; TG, triglycerides; TC, total cholesterol; TyG-index, triglycerides-glucose index; TyG-BMI, triglycerides-glucose body mass index; Non-HDL-c, non-high density lipoprotein cholesterol; VAI, visceral adiposity index; FRS: Framingham risk score; WC, waist circumference.

https://doi.org/10.3390/nu18010112

Similar findings were observed by per-protocol (Table S1 and Figures S1–S13) and LMM (Table S2) analyses; neither dosages of ACNs significantly affected vascular and CVD risk variables, although a relatively low level of RC was observed in the 320 mg group at 3 m change% while an elevated level was observed in the 640 mg group with marginal significance ($P_{overall}$ = 0.018~0.051). Exclusion of patients who were taking medications for hyperglycemia, hyperlipidemia or thyroid dysfunction suggested similar findings with those of whole participants (Supplemental Table S3). Subgroup analyses stratified by different groups of gender, age, basal BMI, hyperglycemia, hypertension and hyperlipidemia exhibited generally non-significant findings and a lack of dose-effectiveness (Supplemental Tables S4–S9). Marginal differences among the four groups were observed in RC at the 3-month change% in the female ($P_{overall}$ = 0.026) and per-diabetes ($P_{overall}$ = 0.040) subgroups, with a reduced RC in the 320 mg group.

4. Discussion

4.1. Summary of Current Findings

The 12-week RCT among Chinese middle-aged and elderly men and women with hyperglycemia examined the dose–response effects of ACNs (0, 160, 320 and 640 mg/d) and failed to find their positive effects on the improvement of arterial stiffness, four-limb BP and CVD risk. No dose–response relationship was identified either. ACNs were generally safe even in a high dosage of 640 mg/d; however, the study did not support their anti-arthrosclerosis benefits. Although marginal improvement was suggested by 320 mg/d ACNs supplementation on RC, the one or two significant exploratory findings among the dozens of comparisons should be treated with caution and require confirmation with further research. To our knowledge, this trial was the first testifying the dose–response effects of purified ACNs on arterial stiffness and four-limb BPs. Further studies exploring the mechanisms on treatment response variability by intestinal microbiome and targeted metabolome are warranted to untangle the controversial evidence.

4.2. Results Explanation

Reviews on ACNs with vascular function and elasticity reported inconsistent findings [2,4,6,8,27]. Our findings align with a range of trials demonstrating non-significant changes in PWV or BPs by ACNs supplementation [28–36] but not all [37–40]. The contradictory findings are hard to interpret by different ACNs formulas, duration, dosages or health status of participants. This is because there were studies with longer duration than ours [32], including different ACNs dosages [32,36], ACNs contained in polyphenol-rich foods [28–36] or among at-risk populations [28–36], that still reported non-significant findings in vascular stiffness. In line with our findings, a 6-month RCT [32] examined the effect of blueberry intake (1, 0.5 and 0 cup/d, containing 364, 182 and 0 mg anthocyanin and 879, 439 and 0 mg phenolics, respectively) among 115 patients of metabolic syndromes showed that, although one cup of blueberries daily improved FMD and AIx, insulin resistance, PWV, BP, NO and overall plasma thiol status were unaffected. A 12-week RCT [35] comparing aronia whole fruit (12 mg polyphenol, 10 g berries) and extract powder (116 mg polyphenol, 75 g berries) found a significant increase in FMD over the control (maltodextrin), but no significant difference in peripheral and central BP, arterial stiffness and lipids. A 3-month RCT [28] with 60 mL tart montmorency cherries (MC) concentrate (equivalent to 68–73.5 mg ACNs and 160.8–178.8 mg total phenolics) on adults at high risk of type 2 diabetes reported null effects of MC on vascular function (PWV, FMD and BP) and metabolic variables. Another randomized, open label, cross-over trial [30] on adults with central obesity also showed, consumption of ACN-rich (50 mg ACNs/500 mL)

https://doi.org/10.3390/nu18010112

blood-orange juice for four weeks did not affect lipoproteins, aortic BPs, carotid-femoral and brachial-ankle PWV.

In contrast, several trials reported favorable improvement on arterial stiffness by ACN-rich foods or extracts [37–40]. A 12-week RCT [37] on overweight participants reported that daily dietary intakes of 293.6 mg anthocyanins and 1370 mg total polyphenols were effective in protecting against arterial stiffness, although they had no benefit on weight loss. Another study [39] among prehypertensive participants found that 12-week Aronia berry consumption improved PWV and Aix, although there were no changes in BP, endothelial function and blood lipids. The favorable changes were possibly via modulation of gut microbiome composition and richness. Evidence suggested the intricate interplay of ACNs with other constituents in the food matrix (i.e., glucose, protein, fibers, organic acids and other polyphenolic compounds) might favor improved bioavailability, leaning benefits towards whole foods over purified foods or extracts [41,42]. The food matrix may exert a protective effect against the degradation of anthocyanins by enhancing its stability, antioxidant property and bioactivity relative to its isolated counterpart [41]. In addition, different flavonoids may generate common groups of metabolites exerting synergistic or additive impacts on vascular health [41]. Further investigations on supplement processing techniques, gut microbiota interactions, inter-individual differences in genetics, ACNs in combination with lifestyle factors or medications for enhanced efficacy might help explain the results [41].

We observed a marginal difference among groups in remnant lipoproteins at the 3-month change or change% with a relative lower level of RC in the 320 mg/d ACNs group while elevated levels were found in the 640 mg/d group. Recent evidence suggested RC [43,44] and non-HDL-c [24] might actually have stronger associations with major adverse CVD events or mortality than LDL-c did. Remnant lipoproteins are deemed as the strongest candidates among triglycerides for targeting CHD risk reduction [24]. A recent systematic review and meta-analysis [45] including 28 cohort studies showed that each 1 SD increase in RC was associated with a 67% (HR 95% CI: 1.39, 2.01) increase in risk of major adverse cardiovascular events (MACE) in a notable dose–response manner. Mendelian randomization results reinforced the existence of causal relationship, suggesting the atherosclerotic risk may be majorly driven by the direct effect of RC [46]. This is because RC has a smaller particle size than LDL-c, favoring its penetration to the endothelial barrier and contributing to the progression of atherosclerosis [47]. Non-HDL-c has been confirmed to highly correlate with atherogenic remnant lipoproteins to enhance CV risk prediction when serum triglycerides are high [24]. Our study was the first RCT examining the effects of ACNs on RC; however, contrary to our expectation, we observed a paradoxical effect on RC, non-HDL-c and triglycerides-related markers (null effect) by ACNs supplementation even if these lipid variables were highly correlated. The reasons are unclear and the paradoxical findings warrant further investigation. Future studies are required with inclusion of a larger sample size and direct measurement of RC and subclasses of HDL-c to confirm the role of ACNs on lipids metabolism.

We did not observe the obvious dose–response effects of ACNs on cardiometabolic markers as other ACNs trials did [48–50]. Similar to our findings, studies with higher doses of ACNs-rich foods did not exhibit greater impacts on vascular function than those of lower doses [32,36]. Inadequate sample size, insufficient dosages of ACNs and short duration of intervention might contribute to the null effect. However, compared with trials that reported the significant effects of ACNs on vascular stiffness [37,38,40], our study had relatively large sample size and long enough duration. Post hoc power estimation suggested adequate power (all > 90%) for PWV-, ABI- and peripheral BP-related variables. In addition, our trial included a wide range of ACNs dosages from 0 to 640 mg/d. The

https://doi.org/10.3390/nu18010112

insufficient dosage and duration as well as the small sample size thus seem unlikely to be driving the non-significant findings on vascular stiffness.

The health status of participants or their use of medications might confound the results. Although the current study was specifically conducted among patients with either prediabetes or early diabetes, they had generally normal vascular stiffness and BP levels and much lower rates of lipid-lowering therapy among participants. Concurrent medication therapies for metabolic conditions might affect the intervention efficacy. However, all the participants who were undertaking medications for metabolic disorders kept stable dosages and monotherapy across the intervention. Sensitivity analysis with exclusion of patients under medications and subgroup analyses by different metabolic conditions revealed similar findings to those of whole participants. We did not observe significant impacts on lipids other than RC. It is therefore unlikely participants' health status or medications could explain the non-significant findings.

The null findings could also be explained as the varied responsiveness to ACNs treatment among participants. However, we did not investigate the factors affecting the interindividual variability in response to the intervention. Studies showed participants' heterogeneities in their biological responses, including gut microbiome composition and (epi)-genetic profiles as well as the differences in the absorption, distribution, metabolism and excretion of bioactive compounds, might play an important role in the contradictory findings [51]. Identifying the main determinants of inter-individual differences and responsiveness profiles, remains essential to target specific populations and optimize the beneficial health effects of bioactive plant food [51].

4.3. Study Strengths and Limitations

The double-blinded, block randomized and placebo-controlled trial designed with multi-dose ACNs were the major strengths of this study. This study was the first to evaluate the dose–response effect of purified ACNs on arterial stiffness among Chinese adults with hyperglycemia. The study had strength in adequate sample size, generally good compliance, low drop-out, effective blinding and use of non-invasive measures for arterial stiffness. In addition, we allowed medication treatment for chronic metabolic conditions which was a common circumstance in the elderly population and this might facilitate the generalizability of the study and its findings. The data regarding the medication history and changes in prescriptions were fully investigated and followed across the intervention, which effectively limited the impact from medications on the outcomes. In addition, all the participants were instructed to restrict their ACNs/polyphenol-rich foods intake to no more than two times per weeks, terminate any phytochemicals or antioxidants supplements since the run-in phase and keep lifestyles unchanged throughout the intervention. Both per-protocol, subgroup and sensitivity analyses suggested robust findings. Although the study was conducted during the COVID pandemic period, which resulted in a relatively slow recruitment progress, no participants withdrew or were hospitalized due to virus infection or quarantine. Lifestyle changes and psychological stress might be brought about during the virus spread [52,53]. However, dietary intakes and physical activities investigated before and after intervention suggested their changes were comparable among different dosage groups.

The study's limitations should be acknowledged. First, although we applied block randomization for participant assignment, the influence of different genders and BMI levels was not pre-specified. However, post hoc stratification suggested similar findings among subgroups. Second, due to resource limitation, ACNs' bioavailability and participants' compliance were not assessed by objective biomarkers. As most of previous ACNs trials did, compliance was not objectively evaluated by ACNs metabolites due to their low

https://doi.org/10.3390/nu18010112

bioavailability, short half shelf-life and limited specificity in circulation. Third, arterial stiffness was assessed by baPWV not carotid-femoral PWV (cfPWV). Ba-PWV was an alternative technique for aortic PWV which was measured directly by oscillometry over the arm and ankle [54]. Longitudinal studies have revealed baPWV showed better predictivity for CVD events in Asian diabetic patients [10,55], as baPWV assesses the mechanical property covering both the large-sized central elastic and medium-sized peripheral muscular arteries [56]. In addition, compared with cfPWV, baPWV requires a simpler and faster recording procedure that is less traumatic for the patients and more practical and cost-effective [57].

5. Conclusions

This first dose–response trial among Chinese middle-aged and elder adults with dysglycemia suggested ACNs supplementation for 12 weeks had no significant effects on vascular stiffness, four-limb BP and CVD risk. Although the findings were generally non-significant, ACNs were shown to be safe, well-tolerated and had no deleterious effects on vascular health. Further investigations exploring the mechanisms of individual variability in response to ACNs by gut metabolites and targeted metabolomics are necessary.

Supplementary Materials: The following supporting information can be downloaded at: https://www.mdpi.com/article/10.3390/nu18010112/s1. Reference [58] is cited in the supplementary materials. **Table S1.** Per-protocol analysis for the effects (change and change%) of anthocyanins on arterial stiffness, four-limb blood pressures and composite cardiovascular markers among participants who had good compliance by multivariable general linear model (n = 161); **Table S2.** Sensitivity analyses by linear mixed model (LMM) with individual participants as random factor and adjustment for baseline data on the week-12 change and change% of arterial stiffness, four-limb blood pressures and composite cardiovascular markers (n = 184); **Table S3.** Sensitivity analyses by exclusion of patients under medications for lowering glucose, lipids, or thyroid conditions for the effects of anthocyanins (3-month change and change%) on arterial stiffness, four-limb blood pressures and composite cardiovascular markers by ANCOVA; **Table S4.** Subgroup analyses by gender (female and male) for the effects of anthocyanins on the pre-post change% of arterial stiffness, four-limb blood pressure and composite cardiovascular markers by ANCOVA; **Table S5.** Subgroup analyses by age (<65 and ≥65 yrs) for the effects of anthocyanins on the pre-post change% of arterial stiffness, four-limb blood pressure and composite cardiovascular markers by ANCOVA; **Table S6.** Subgroup analyses by body mass index (BMI < 24 vs. ≥24 kg/m^2) for the effects of anthocyanins on the pre-post change% of arterial stiffness, four-limb blood pressures and composite cardiovascular markers by ANCOVA; **Table S7.** Subgroup analyses by severity of hyperglycemia (pre-diabetes vs. diabetes) for the effects of anthocyanins on the pre-post change% of arterial stiffness, four-limb blood pressures and composite cardiovascular markers by ANCOVA; **Table S8.** Subgroup analyses by baseline hypertension for the effects of anthocyanins on the pre-post change% of arterial stiffness, four-limb blood pressure and composite cardiovascular markers by ANCOVA; **Table S9.** Subgroup analyses by baseline hyperlipidemia for the effects of anthocyanins on the pre-post change% of arterial stiffness, four-limb blood pressures and composite cardiovascular markers by ANCOVA; **Table S10.** CONSORT 2025 checklist item description; **Figure S1.** Max-PWV change and change% by different dosages of ACNs; **Figure S2.** Min-ABI change and change% by different dosages of ACNs; **Figure S3.** Left brachial SBP change and change% by different dosages of ACNs; **Figure S4.** Left brachial DBP change and change% by different dosages of ACNs; **Figure S5.** sIAD change and change% by different dosages of ACNs; **Figure S6.** sIAND change and change% by different dosages of ACNs; **Figure S7.** RC change and change% by different dosages of ACNs; **Figure S8.** Non-HDL change and change% by different dosages of ACNs; **Figure S9.** TG/HDL-c change and change% by different dosages of ACNs; **Figure S10.** TyG-BMI change and change% by different dosages of ACNs; **Figure S11.** VAI change and change% by different dosages of ACNs; **Figure S12.** FRS change and change% by different dosages of ACN; **Figure S13.** TyG-index change and change% by different dosages of ACN.

https://doi.org/10.3390/nu18010112

Author Contributions: Z.L., R.L. and J.C. (Jiachi Chiou) conceptualized the topic and obtained funding support; Z.L. and M.L. made data curation and analysis, results explanation and drafted the manuscript; Y.C. conducted randomization and allocation concealment and offered professional consultation on the project. M.L. and H.L. made field investigation and data collection and analysis; C.C., C.W. and J.C. (Jianyin Chen) helped in participants recruitment, coordinated the study investigation and provided professional advice. All authors have read and agreed to the published version of the manuscript.

Funding: The study was funded by the Natural Science of Funding of China (Grant No: 82073533).

Institutional Review Board Statement: The study was conducted according to the guidelines of the Declaration of Helsinki and approved by the Ethics Committees of School of Public Health, Sun Yat-sen University (North Campus) with protocol code of 2020042 (date of approval: 30 March 2020) and registered on Chinese Clinical Trial with the registry no of ChiCTR2100041743 (date of registration: 3 January 2021; in website of https://www.chictr.org.cn/hvshowproject.html?id=81960&v=1.7, accessed on 1 December 2025).

Informed Consent Statement: Informed consent was obtained from all participants before enrolment.

Data Availability Statement: The original datasets are not publicly available due to ethical limitations on publishing medical record data, but are available from the corresponding author on reasonable request under a strict confidential process.

Acknowledgments: We are grateful to the Medox Norway company for their generous sponsorship, for providing supplements and for their preparation of placebo capsules. We are grateful to all the research members for their keen efforts in field investigation and data collection. We greatly appreciate the doctors and nurses in the Sun Yat-sen Memorial Hospital for their keen assistance in facilitating participants' recruitment, blood collection and data coordination. We acknowledge the Department of Clinical Laboratory of Sun Yat-sen Memorial Hospital for analyzing the bio-specimens. We would like to thank all the participants for their good compliance and for so generously making their data available for research. We acknowledge Wen-hua Ling (Sun Yat-sen University) provided keen assistance for seeking sponsorship of supplements.

Conflicts of Interest: All the authors had no conflicts of interest to be claimed. The funder and sponsor had no role in the design of the study; the data collection, analyses or interpretation of data; in the writing of the manuscript; or in the decision to publish the results.

References

1. Tang, Z. Cyanidin-3-glucoside: Targeting atherosclerosis through gut microbiota and anti-inflammation. *Front. Nutr.* **2025**, *12*, 1627868. [CrossRef] [PubMed]
2. Woolf, E.K.; Lee, S.Y.; Ghanem, N.; Vazquez, A.R.; Johnson, S.A. Protective effects of blueberries on vascular function: A narrative review of preclinical and clinical evidence. *Nutr. Res.* **2023**, *120*, 20–57. [CrossRef] [PubMed]
3. Wood, E.; Hein, S.; Heiss, C.; Williams, C.; Rodriguez-Mateos, A. Blueberries and cardiovascular disease prevention. *Food Funct.* **2019**, *10*, 7621–7633. [CrossRef] [PubMed]
4. Lilamand, M.; Kelaiditi, E.; Guyonnet, S.; Antonelli Incalzi, R.; Raynaud-Simon, A.; Vellas, B.; Cesari, M. Flavonoids and arterial stiffness: Promising perspectives. *Nutr. Metab. Cardiovasc. Dis.* **2014**, *24*, 698–704. [CrossRef]
5. Jennings, A.; Welch, A.A.; Fairweather-Tait, S.J.; Kay, C.; Minihane, A.M.; Chowienczyk, P.; Jiang, B.; Cecelja, M.; Spector, T.; Macgregor, A.; et al. Higher anthocyanin intake is associated with lower arterial stiffness and central blood pressure in women. *Am. J. Clin. Nutr.* **2012**, *96*, 781–788. [CrossRef]
6. Fairlie-Jones, L.; Davison, K.; Fromentin, E.; Hill, A.M. The Effect of Anthocyanin-Rich Foods or Extracts on Vascular Function in Adults: A Systematic Review and Meta-Analysis of Randomised Controlled Trials. *Nutrients* **2017**, *9*, 908. [CrossRef]
7. Wallace, T.C.; Slavin, M.; Frankenfeld, C.L. Systematic Review of Anthocyanins and Markers of Cardiovascular Disease. *Nutrients* **2016**, *8*, 32. [CrossRef]
8. Talebi, S.; Shirani, M.; Shokri-Mashhadi, N.; Sadeghi, O.; Karav, S.; Bagherniya, M.; Sahebkar, A. The long-term and post-prandial effects of berry consumption on endothelial dysfunction in adults: A systematic review and meta-analysis of randomised controlled trials. *Int. J. Food Sci. Nutr.* **2025**, *76*, 134–164. [CrossRef]

9. Pilz, N.; Heinz, V.; Ax, T.; Fesseler, L.; Patzak, A.; Bothe, T.L. Pulse Wave Velocity: Methodology, Clinical Applications, and Interplay with Heart Rate Variability. *Rev. Cardiovasc. Med.* **2024**, *25*, 266. [CrossRef]
10. Kim, J.M.; Kim, S.S.; Kim, I.J.; Kim, J.H.; Kim, B.H.; Kim, M.K.; Lee, S.H.; Lee, C.W.; Kim, M.C.; Ahn, J.H.; et al. Arterial stiffness is an independent predictor for risk of mortality in patients with type 2 diabetes mellitus: The REBOUND study. *Cardiovasc. Diabetol.* **2020**, *19*, 143. [CrossRef]
11. Nie, F.; He, J.; Cao, H.; Hu, X. Predictive value of abnormal ankle-brachial index in patients with diabetes: A meta-analysis. *Diabetes Res. Clin. Pract.* **2021**, *174*, 108723. [CrossRef]
12. Chang, L.H.; Lin, H.D.; Kwok, C.F.; Won, J.G.; Chen, H.S.; Chu, C.H.; Hwu, C.M.; Kuo, C.S.; Jap, T.S.; Shih, K.C.; et al. The combination of the ankle brachial index and brachial ankle pulse wave velocity exhibits a superior association with outcomes in diabetic patients. *Intern. Med.* **2014**, *53*, 2425–2431. [CrossRef]
13. Zhang, A.; Liu, Y.; Ma, S.; Bao, Q.; Sun, J.; Su, Y.; Cai, S.; Cheng, B.; Li, M.; Zhang, Y.; et al. Effects of ankle-brachial index and brachial-ankle pulse wave velocity on all-cause mortality in a community-based elderly population. *Front. Cardiovasc. Med.* **2022**, *9*, 883651. [CrossRef] [PubMed]
14. Tomiyama, H.; Ohkuma, T.; Ninomiya, T.; Mastumoto, C.; Kario, K.; Hoshide, S.; Kita, Y.; Inoguchi, T.; Maeda, Y.; Kohara, K.; et al. Simultaneously Measured Interarm Blood Pressure Difference and Stroke: An Individual Participants Data Meta-Analysis. *Hypertension* **2018**, *71*, 1030–1038. [CrossRef] [PubMed]
15. Liu, S.; Li, P.; Su, H. Four-Limb Blood Pressure Measurement with an Oscillometric Device: A Tool for Diagnosing Peripheral Vascular Disease. *Curr. Hypertens. Rep.* **2019**, *21*, 15. [CrossRef] [PubMed]
16. Yang, W.; Sun, L.; He, Y.; Xu, X.; Gan, L.; Guo, T.; Yang, L. Association between four-limb blood pressure differences and arterial stiffness: A cross-sectional study. *Postgrad. Med.* **2022**, *134*, 309–315. [CrossRef]
17. Clark, C.E.; Warren, F.C.; Boddy, K.; McDonagh, S.T.J.; Moore, S.F.; Goddard, J.; Reed, N.; Turner, M.; Alzamora, M.T.; Ramos Blanes, R.; et al. Associations Between Systolic Interarm Differences in Blood Pressure and Cardiovascular Disease Outcomes and Mortality: Individual Participant Data Meta-Analysis, Development and Validation of a Prognostic Algorithm: The INTERPRESS-IPD Collaboration. *Hypertension* **2021**, *77*, 650–661. [CrossRef]
18. American Diabetes Association Professional Practice Committee; ElSayed, N.A.; Aleppo, G.; Bannuru, R.R.; Bruemmer, D.; Collins, B.S.; Ekhlaspour, L.; Gaglia, J.L.; Hilliard, M.E.; Johnson, E.L.; et al. 2. Diagnosis and Classification of Diabetes: Standards of Care in Diabetes-2024. *Diabetes Care* **2024**, *47*, S20–S42. [CrossRef]
19. Zhang, C.X.; Ho, S.C. Validity and reproducibility of a food frequency Questionnaire among Chinese women in Guangdong province. *Asia Pac. J. Clin. Nutr.* **2009**, *18*, 240–250.
20. Yang, Y.X. *China Food Composition Tables*, 6th ed.; Peking University Medical Press: Beijing, China, 2018.
21. Craig, C.L.; Marshall, A.L.; Sjöström, M.; Bauman, A.E.; Booth, M.L.; Ainsworth, B.E.; Pratt, M.; Ekelund, U.; Yngve, A.; Sallis, J.F.; et al. International physical activity questionnaire: 12-country reliability and validity. *Med. Sci. Sports Exerc.* **2003**, *35*, 1381–1395. [CrossRef]
22. Ainsworth, B.E.; Haskell, W.L.; Whitt, M.C.; Irwin, M.L.; Swartz, A.M.; Strath, S.J.; O'Brien, W.L.; Bassett, D.R., Jr.; Schmitz, K.H.; Emplaincourt, P.O.; et al. Compendium of physical activities: An update of activity codes and MET intensities. *Med. Sci. Sports Exerc.* **2000**, *32*, S498–S504. [CrossRef] [PubMed]
23. Zheng, M.; Xu, X.; Wang, X.; Huo, Y.; Xu, X.; Qin, X.; Tang, G.; Xing, H.; Fan, F.; Cui, W.; et al. Age, arterial stiffness, and components of blood pressure in Chinese adults. *Medicine* **2014**, *93*, e262. [CrossRef] [PubMed]
24. National Cholesterol Education Program (NCEP) Expert Panel on Detection, Evaluation, and Treatment of High Blood Cholesterol in Adults (Adult Treatment Panel III). Third Report of the National Cholesterol Education Program (NCEP) Expert Panel on Detection, Evaluation, and Treatment of High Blood Cholesterol in Adults (Adult Treatment Panel III) final report. *Circulation* **2002**, *106*, 3143–3421.
25. Yang, L.; Ling, W.; Yang, Y.; Chen, Y.; Tian, Z.; Du, Z.; Chen, J.; Xie, Y.; Liu, Z.; Yang, L. Role of Purified Anthocyanins in Improving Cardiometabolic Risk Factors in Chinese Men and Women with Prediabetes or Early Untreated Diabetes-A Randomized Controlled Trial. *Nutrients* **2017**, *9*, 1104. [CrossRef] [PubMed]
26. Schielzeth, H.; Dingemanse, N.J.; Nakagawa, S.; Westneat, D.F.; Allegue, H.; Teplitsky, C.; Réale, D.; Dochtermann, N.A.; Garamszegi, L.Z.; Araya-Ajoy, Y.G. Robustness of Linear Mixed-Effects Models to Violations of Distributional Assumptions. *Methods in Ecology and Evolution* **2020**, *11*, 1141–1152. [CrossRef]
27. Mozos, I.; Flangea, C.; Vlad, D.C.; Gug, C.; Mozos, C.; Stoian, D.; Luca, C.T.; Horbańczuk, J.O.; Horbańczuk, O.K.; Atanasov, A.G. Effects of Anthocyanins on Vascular Health. *Biomolecules* **2021**, *11*, 811. [CrossRef]
28. Kimble, R.; Keane, K.M.; Lodge, J.K.; Howatson, G. The Influence of Tart Cherry (*Prunus cerasus*, cv Montmorency) Concentrate Supplementation for 3 Months on Cardiometabolic Risk Factors in Middle-Aged Adults: A Randomised, Placebo-Controlled Trial. *Nutrients* **2021**, *13*, 1417. [CrossRef]

29. Lynn, A.; Mathew, S.; Moore, C.T.; Russell, J.; Robinson, E.; Soumpasi, V.; Barker, M.E. Effect of a tart cherry juice supplement on arterial stiffness and inflammation in healthy adults: A randomised controlled trial. *Plant Foods Hum. Nutr.* **2014**, *69*, 122–127. [CrossRef]
30. Hollands, W.J.; Armah, C.N.; Doleman, J.F.; Perez-Moral, N.; Winterbone, M.S.; Kroon, P.A. 4-Week consumption of anthocyanin-rich blood orange juice does not affect LDL-cholesterol or other biomarkers of CVD risk and glycaemia compared with standard orange juice: A randomised controlled trial. *Br. J. Nutr.* **2018**, *119*, 415–421. [CrossRef]
31. Johnson, S.A.; Navaei, N.; Pourafshar, S.; Jaime, S.J.; Akhavan, N.S.; Alvarez-Alvarado, S.; Proaño, G.V.; Litwin, N.S.; Clark, E.A.; Foley, E.M.; et al. Effects of Montmorency Tart Cherry Juice Consumption on Cardiometabolic Biomarkers in Adults with Metabolic Syndrome: A Randomized Controlled Pilot Trial. *J. Med. Food* **2020**, *23*, 1238–1247. [CrossRef]
32. Curtis, P.J.; van der Velpen, V.; Berends, L.; Jennings, A.; Feelisch, M.; Umpleby, A.M.; Evans, M.; Fernandez, B.O.; Meiss, M.S.; Minnion, M.; et al. Blueberries improve biomarkers of cardiometabolic function in participants with metabolic syndrome-results from a 6-month, double-blind, randomized controlled trial. *Am. J. Clin. Nutr.* **2019**, *109*, 1535–1545. [CrossRef]
33. Woolf, E.K.; Terwoord, J.D.; Litwin, N.S.; Vazquez, A.R.; Lee, S.Y.; Ghanem, N.; Michell, K.A.; Smith, B.T.; Grabos, L.E.; Ketelhut, N.B.; et al. Daily blueberry consumption for 12 weeks improves endothelial function in postmenopausal women with above-normal blood pressure through reductions in oxidative stress: A randomized controlled trial. *Food Funct.* **2023**, *14*, 2621–2641. [CrossRef] [PubMed]
34. Wood, E.; Hein, S.; Mesnage, R.; Fernandes, F.; Abhayaratne, N.; Xu, Y.; Zhang, Z.; Bell, L.; Williams, C.; Rodriguez-Mateos, A. Wild blueberry (poly)phenols can improve vascular function and cognitive performance in healthy older individuals: A double-blind randomized controlled trial. *Am. J. Clin. Nutr.* **2023**, *117*, 1306–1319. [CrossRef] [PubMed]
35. Istas, G.; Wood, E.; Le Sayec, M.; Rawlings, C.; Yoon, J.; Dandavate, V.; Cera, D.; Rampelli, S.; Costabile, A.; Fromentin, E.; et al. Effects of aronia berry (poly)phenols on vascular function and gut microbiota: A double-blind randomized controlled trial in adult men. *Am. J. Clin. Nutr.* **2019**, *110*, 316–329. [CrossRef] [PubMed]
36. Feresin, R.G.; Johnson, S.A.; Pourafshar, S.; Campbell, J.C.; Jaime, S.J.; Navaei, N.; Elam, M.L.; Akhavan, N.S.; Alvarez-Alvarado, S.; Tenenbaum, G.; et al. Impact of daily strawberry consumption on blood pressure and arterial stiffness in pre- and stage 1-hypertensive postmenopausal women: A randomized controlled trial. *Food Funct.* **2017**, *8*, 4139–4149. [CrossRef]
37. Arisi, T.O.P.; Gorski, F.; Eibel, B.; Barbosa, E.; Boll, L.; Waclawovsky, G.; Lehnen, A.M. Dietary intake of anthocyanins improves arterial stiffness, but not endothelial function, in volunteers with excess weight: A randomized clinical trial. *Phytother. Res.* **2023**, *37*, 798–808. [CrossRef]
38. Dohadwala, M.M.; Holbrook, M.; Hamburg, N.M.; Shenouda, S.M.; Chung, W.B.; Titas, M.; Kluge, M.A.; Wang, N.; Palmisano, J.; Milbury, P.E.; et al. Effects of cranberry juice consumption on vascular function in patients with coronary artery disease. *Am. J. Clin. Nutr.* **2011**, *93*, 934–940. [CrossRef]
39. Le Sayec, M.; Xu, Y.; Laiola, M.; Gallego, F.A.; Katsikioti, D.; Durbidge, C.; Kivisild, U.; Armes, S.; Lecomte, M.; Fança-Berthon, P.; et al. The effects of Aronia berry (poly)phenol supplementation on arterial function and the gut microbiome in middle aged men and women: Results from a randomized controlled trial. *Clin. Nutr.* **2022**, *41*, 2549–2561. [CrossRef]
40. Johnson, S.A.; Figueroa, A.; Navaei, N.; Wong, A.; Kalfon, R.; Ormsbee, L.T.; Feresin, R.G.; Elam, M.L.; Hooshmand, S.; Payton, M.E.; et al. Daily blueberry consumption improves blood pressure and arterial stiffness in postmenopausal women with pre- and stage 1-hypertension: A randomized, double-blind, placebo-controlled clinical trial. *J. Acad. Nutr. Diet.* **2015**, *115*, 369–377. [CrossRef]
41. Kumkum, R.; Aston-Mourney, K.; McNeill, B.A.; Hernández, D.; Rivera, L.R. Bioavailability of Anthocyanins: Whole Foods versus Extracts. *Nutrients* **2024**, *16*, 1403. [CrossRef]
42. Mao, T.; Akshit, F.N.U.; Mohan, M.S. Effects of anthocyanin supplementation in diet on glycemic and related cardiovascular biomarkers in patients with type 2 diabetes: A systematic review and meta-analysis of randomized controlled trials. *Front. Nutr.* **2023**, *10*, 1199815. [CrossRef]
43. Castañer, O.; Pintó, X.; Subirana, I.; Amor, A.J.; Ros, E.; Hernáez, Á.; Martínez-González, M.; Corella, D.; Salas-Salvadó, J.; Estruch, R.; et al. Remnant Cholesterol, Not LDL Cholesterol, Is Associated with Incident Cardiovascular Disease. *J. Am. Coll. Cardiol.* **2020**, *76*, 2712–2724. [CrossRef] [PubMed]
44. Proctor, S.D.; Wang, M.; Vine, D.F.; Raggi, P. Predictive utility of remnant cholesterol in atherosclerotic cardiovascular disease. *Curr. Opin. Cardiol.* **2024**, *39*, 300–307. [CrossRef] [PubMed]
45. Bian, X.; Zhang, Y.; Shao, M.; Li, J.; Ge, J.; Li, Z.; Peng, H.; Zhang, M. Remnant cholesterol and risk of major adverse cardiovascular events: A systematic review and dose-response meta-analysis of cohort studies. *Coron. Artery Dis.* **2024**, *35*, 413–421. [CrossRef] [PubMed]
46. Raggi, P.; Becciu, M.L.; Navarese, E.P. Remnant cholesterol as a new lipid-lowering target to reduce cardiovascular events. *Curr. Opin. Lipidol.* **2024**, *35*, 110–116. [CrossRef]

47. Zhao, Y.; Zhuang, Z.; Li, Y.; Xiao, W.; Song, Z.; Huang, N.; Wang, W.; Dong, X.; Jia, J.; Clarke, R.; et al. Elevated blood remnant cholesterol and triglycerides are causally related to the risks of cardiometabolic multimorbidity. *Nat. Commun.* **2024**, *15*, 2451. [CrossRef]
48. Guo, Y.; Zhang, P.; Liu, Y.; Zha, L.; Ling, W.; Guo, H. A dose-response evaluation of purified anthocyanins on inflammatory and oxidative biomarkers and metabolic risk factors in healthy young adults: A randomized controlled trial. *Nutrition* **2020**, *74*, 110745. [CrossRef]
49. Xu, Z.; Xie, J.; Zhang, H.; Pang, J.; Li, Q.; Wang, X.; Xu, H.; Sun, X.; Zhao, H.; Yang, Y.; et al. Anthocyanin supplementation at different doses improves cholesterol efflux capacity in subjects with dyslipidemia-a randomized controlled trial. *Eur. J. Clin. Nutr.* **2021**, *75*, 345–354. [CrossRef]
50. Zhang, H.; Xu, Z.; Zhao, H.; Wang, X.; Pang, J.; Li, Q.; Yang, Y.; Ling, W. Anthocyanin supplementation improves anti-oxidative and anti-inflammatory capacity in a dose-response manner in subjects with dyslipidemia. *Redox Biol.* **2020**, *32*, 101474. [CrossRef]
51. Manach, C.; Milenkovic, D.; Van de Wiele, T.; Rodriguez-Mateos, A.; de Roos, B.; Garcia-Conesa, M.T.; Landberg, R.; Gibney, E.R.; Heinonen, M.; Tomás-Barberán, F.; et al. Addressing the inter-individual variation in response to consumption of plant food bioactives: Towards a better understanding of their role in healthy aging and cardiometabolic risk reduction. *Mol. Nutr. Food Res.* **2017**, *61*, 1600557. [CrossRef]
52. Wang, J.; Yeoh, E.K.; Yung, T.K.C.; Wong, M.C.S.; Dong, D.; Chen, X.; Chan, M.K.Y.; Wong, E.L.Y.; Wu, Y.; Guo, Z.; et al. Change in eating habits and physical activities before and during the COVID-19 pandemic in Hong Kong: A cross-sectional study via random telephone survey. *J. Int. Soc. Sports Nutr.* **2021**, *18*, 33. [CrossRef]
53. Wang, X.; Lei, S.M.; Le, S.; Yang, Y.; Zhang, B.; Yao, W.; Gao, Z.; Cheng, S. Bidirectional Influence of the COVID-19 Pandemic Lockdowns on Health Behaviors and Quality of Life among Chinese Adults. *Int. J. Environ. Res. Public Health* **2020**, *17*, 5575. [CrossRef] [PubMed]
54. Kang, J.; Jeon, K.H.; Choi, K.U.; Choi, H.I.; Sung, K.C. Brachial-Ankle Pulse Wave Velocity as a Predictor of Diabetes Development: Elevated Risk Within Normal Range Values in a Low-Risk Population. *J. Am. Heart Assoc.* **2024**, *13*, e037705. [CrossRef]
55. Townsend, R.R.; Wilkinson, I.B.; Schiffrin, E.L.; Avolio, A.P.; Chirinos, J.A.; Cockcroft, J.R.; Heffernan, K.S.; Lakatta, E.G.; McEniery, C.M.; Mitchell, G.F.; et al. Recommendations for Improving and Standardizing Vascular Research on Arterial Stiffness: A Scientific Statement from the American Heart Association. *Hypertension* **2015**, *66*, 698–722. [CrossRef]
56. Najjar, S.S.; Scuteri, A.; Shetty, V.; Wright, J.G.; Muller, D.C.; Fleg, J.L.; Spurgeon, H.P.; Ferrucci, L.; Lakatta, E.G. Pulse wave velocity is an independent predictor of the longitudinal increase in systolic blood pressure and of incident hypertension in the Baltimore Longitudinal Study of Aging. *J. Am. Coll. Cardiol.* **2008**, *51*, 1377–1383. [CrossRef]
57. Vlachopoulos, C.; Aznaouridis, K.; Terentes-Printzios, D.; Ioakeimidis, N.; Stefanadis, C. Prediction of cardiovascular events and all-cause mortality with brachial-ankle elasticity index: A systematic review and meta-analysis. *Hypertension* **2012**, *60*, 556–562. [CrossRef]
58. Hopewell, S.; Chan, A.-W.; Collins, G.S.; Hróbjartsson, A.; Moher, D.; Schulz, K.F.; Tunn, R.; Aggarwal, R.; Berkwits, M.; A Berlin, J.; et al. CONSORT 2025 Statement: Updated guideline for reporting randomised trials. *BMJ* **2025**, *388*, e081123. [CrossRef]

Disclaimer/Publisher's Note: The statements, opinions and data contained in all publications are solely those of the individual author(s) and contributor(s) and not of MDPI and/or the editor(s). MDPI and/or the editor(s) disclaim responsibility for any injury to people or property resulting from any ideas, methods, instructions or products referred to in the content.

MDPI AG
Grosspeteranlage 5
4052 Basel
Switzerland
Tel.: +41 61 683 77 34

Nutrients Editorial Office
E-mail: nutrients@mdpi.com
www.mdpi.com/journal/nutrients

Disclaimer/Publisher's Note: The title and front matter of this reprint are at the discretion of the Guest Editors. The publisher is not responsible for their content or any associated concerns. The statements, opinions and data contained in all individual articles are solely those of the individual Editors and contributors and not of MDPI. MDPI disclaims responsibility for any injury to people or property resulting from any ideas, methods, instructions or products referred to in the content.

Academic Open
Access Publishing

mdpi.com

ISBN 978-3-7258-7263-3